THE APPLICATION OF STATE OBSERVER TECHNIQUES TO PROBLEMS OF SYSTEM DESIGN AND INTEGRITY IN HELICOPTER FLIGHT CONTROL

A THESIS

SUBMITTED TO THE FACULTY OF ENGINEERING

OF THE UNIVERSITY OF GLASGOW

FOR THE DEGREE OF

DOCTOR OF PHILOSOPHY

BY

CHARLES STEWART PATERSON

APRIL 1990

ProQuest LLC.
789 East Eisenhower Parkway
P.O. Box 1346
Ann Arbor, MI 48106 – 1346

THIS THESIS IS DEDICATED TO
MY PARENTS AND MY AUNT

ACKNOWLEDGEMENTS

I am indebted to my supervisor Professor D. J. Murray–Smith for his support and many useful suggestions throughout this project. I would also like to express my thanks to P. Smith and S. Winter of the Royal Aerospace Establishment, Bedford, for their technical guidance.

I am grateful to Professor J. Lamb for the provision of research and computing facilities for the duration of this research and I acknowledge the financial support of the Science and Engineering Research Council and the Royal Aerospace Establishment.

Thanks are also due to L. McCormick and C. Carmichael for their encouragement and invaluable advice and assistance with all aspects of computer hardware and software.

Finally, I would like to express my appreciation to my parents whose moral and financial support enabled me to undertake this research.

CONTENTS

SUMMARY

Automatic flight control systems of modern aircraft, whether fixed wing or rotorcraft, have become increasingly complex and often involve the use of control activity which goes beyond the levels normally associated with human pilot operation. The sophisticated control laws employed frequently utilise the complete state vector, however, in practice not every state variable is available, either owing to the failure of its sensor or because it is impracticable to measure. The most feasible solution to the problem is therefore to use an estimate of the state vector produced from an observer.

This thesis is concerned with the application of deterministic, continuous–time, linear, time–invariant system theory in the design of 'Luenberger' state observers for state estimation in the flight control systems of the single main rotor helicopter. Observer design and system simulation were facilitated by using a complicated mathematical model of the helicopter. This model, which was provided by the Royal Aerospace Establishment, Bedford, is examined in detail and its limitations are discussed.

Observer design methods are reviewed and two approaches, a method proposed by Gopinath and an observable canonical form method, are examined in detail. Due to numerical problems the Gopinath method is shown to be unsuitable, however it is demonstrated that the observable canonical form method is capable of producing accurate designs. Details of the software implementation of the canonical form technique are given and the results obtained and problems encountered, are analysed.

Using this software, full and reduced order observers are designed for both eighth and fourteenth order system models. The performance of these observers are thoroughly assessed and it is shown that good estimates can be produced if the system states are 'clean', but that noise corrupted states result in poor estimates. To solve this problem a new form of observer – the twin observer – is introduced and it is demonstrated that with a precise model of the system, the twin observer can produce accurate, relatively noise free estimates of the system state.

A review of instrument fault detection techniques is given and an observer based scheme, known as the Dedicated Observer Scheme, is selected for analysis with the twin observer and a fourth order, longitudinal system model. The advantages and disadvantages of this scheme are examined and possible solutions to some of the problems are proposed.

CHAPTER ONE

INTRODUCTION

1.1 HISTORY OF HELICOPTER DEVELOPMENT

The principles of helicopter flight have been known for many centuries: some aviation historians have even claimed to have traced experiments with rotary wing models back to the fourth Century BC in China. What is certain, however, is that in 1490, after having spent some years trying to develop flying machines, Leonardo da Vinci designed a lifting screw made of starched linen. After this there was a gap of almost three hundred years until early flight pioneers, such as Sir George Cayley, started to design and construct helicopter models. Despite this, it was not until 1907 that the first helicopter capable of carrying a pilot was built and flown by Paul Cornu of France, although only for a few seconds and to a maximum height of one foot.

In the following thirty years many of the problems were overcome. In 1922, Juan de la Cierva, who perhaps influenced the progress of helicopters more than any other man, solved the problem of asymmetry of flow This is the rolling couple which occurs when a rotary wing aircraft moves forward: the advancing blade has more airspeed than the retreating blade and hence gains more lift. His solution, which is still in use today, was to use flapping hinges which allow each rotor blade to flap up and down. [Flapping hinge introduced by Renard in 1904]

Using this system, the advancing blade will, with increased airflow, lift itself up about the flapping hinge, thereby decreasing its angle of attack, while the retreating blade will flap down, thereby increasing its angle of attack; thus the net lifting effect on each blade is the same. De la Cierva was also responsible for the introduction of the lead/lag hinge which is used to alleviate bending moments caused by the tendency of each individual blade to move to and fro in the horizontal plane in relation to the hub or the other blades.

In 1939 Igor Sikorsky (who had previously built two unsuccessful helicopters in 1910) flew his VS−300, which was unique because not only was it the first aircraft using the main/tail rotor configuration to fly successfully, but in 1942 its production version, the R.4, marked the commencement of the helicopter industry in the USA.

Since then helicopter development has continued, but has always lagged behind that of the conventional aircraft due to frequent insurmountable stability and engineering problems. For example, the first helicopter crossing of the English Channel did not occur until 1945 − compare this with the performance and range of fixed−wing aircraft at that time. To understand these problems it is necessary to first consider the principles of helicopter control.

1.2 PRINCIPLES OF HELICOPTER CONTROL

Conventional helicopters are controlled in flight by *feathering* the blades: constantly adjusting the *pitch angle* (ie. the angle of the leading edge with respect to the horizontal plane of the rotor system) as the blades revolve. This feathering pattern, the *cyclic pitch*, varies sinusoidally and compensates for the sinusoidal variation in apparent airflow induced by the combination of rotor revolution and forward flight. In addition, momentarily changing the cyclic pitch causes the helicopter to change direction and speed, or both. This is because the craft will tilt and accelerate until its new speed and heading match the new amplitude and phase of the cyclic pitch. The average value of the cyclic pitch, the *collective pitch*, determines the average lift of the rotor and hence whether the helicopter moves vertically or hovers.

The pilot, therefore, has three sets of controls: the collective lever (or stick), the cyclic stick and two rudder pedals. Movement of the rudder pedals changes the collective pitch of the tail rotor blades, thus increasing/decreasing tail rotor thrust and causing the helicopter to rotate about a vertical axis for heading control in hover and low speed flight. As their names suggest, the collective lever alters the collective pitch of the main rotor and the cyclic stick varies the cyclic pitch; the variations in pitch being transmitted to the blades via a mechanism called a *swash plate*.

The cyclic stick can be moved fore and aft and sideways, or any combination of the two and the rotor will be tilted in the direction it is moved. When the stick is pushed forward, the helicopter will move forward, or, if already doing so, will accelerate. Similarly, if the stick is moved backwards or sideways the helicopter will proceed in these directions. The stick works in a natural sense and the degree of tilt of the rotor in relationship to the drive shaft depends mainly on the degree of stick movement.

At first sight these controls appear relatively straightforward, but compared to fixed wing aircraft, the flight controls of a helicopter interact in strange ways. For example, to ascend at an angle requires a certain collective and cyclic pitch setting; but as the craft gathers speed, the rotor lift increases, thereby requiring less collective pitch which in turn reduces the necessary engine power. This then requires less compensating thrust from the tail rotor. Learning these complex control interactions is not easy and executing flight manoeuvres requires the pilot's constant attention. In addition, helicopters are at best only neutrally stable, and usually unstable in at least one axis, even though the frequencies involved are fairly low. For these reasons an autostabilizer function is looked upon as essential.

1.3 AUTOMATIC FLIGHT CONTROL SYSTEMS

Automatic stabilisation equipment was developed in the 1950's and with this the helicopter can be flown without the pilot touching the controls, but he can use the controls at any time to carry out manoeuvres. In control terms, these stability augmentation systems are relatively simple and generally involve three separate functions corresponding to the three axes.

In the pitch axis the primary requirement is for stabilising attitude and therefore most systems are based on a pilot's stick position change demanding an attitude change. The operation of the roll axis autostabilisation function is substantially the same as the pitch axis, with a combination of roll attitude and roll rate feedback required for stabilisation. Similarly the yaw axis autostabiliser utilises yaw attitude and yaw rate, but in addition usually incorporates a heading hold facility.

Design of manual flight control systems for high performance helicopters such as the Lynx has also shown that it is possible to obtain alleviation of failure effects in the pitch channel and improved stability in normal operation by the inclusion of a vertical autostabiliser based upon feedback of normal acceleration to normal pitch.

Initially these systems were implemented using electromechanical devices, however with the advent of digital computers there has been an ever increasing use of digital control. This has led to the use of more sophisticated control laws and the proliferation of *Automatic Flight Control Systems* (AFCS). In these systems, flight control computers transmit cyclic and collective pitch commands to actuators mounted on the swash plate via electronic or optical cable instead of the present metal rods.

The control signals may be electronic signals transmitted via copper cable (*fly–by–wire*) or optical signals transmitted by fibre optic cable (*fly–by–light*). Existing helicopters with such systems include the DFVLR BO–105, MD LHX Apache, Bell Arti AH–1 and Boeing ADOCS.

Most recently, research has concentrated on *Active Control Technology* (ACT), which is defined as a full–authority manoeuvre demand flight control system, or, in other words, a full authority AFCS.

The specification for a military ACT helicopter system (which is necessarily more stringent than that for a civil helicopter) can be summarised as,

- A control system which provides decoupled, stable and rapidly acting vehicle response to command inputs, enabling safe flight to the extremes of the flight envelope.

- Ability to fly in bad weather, at night, low level (nap–of–the–earth, NOE) and at high speeds.

- Reduced pilot workload level so that he can concentrate on the primary mission and not on piloting the helicopter.

- Integrity of the system to failures and damage.

- Immunity from failures caused by electromagnetic radiations or electromagnetic pulse (eg. a lightning strike).

- Catastrophic failure rate of less than 10^{-7} per flight hour. (10^{-9} for the civil case).

These requirements can basically be divided into two subjects: control system design and failure detection/accommodation of faults in the control system and associated hardware, eg. communication lines, actuators, sensors.

ACT CONTROL SYSTEMS

ACT control system design involves two related areas of research – the elimination of adverse rotor effects and the improvement of handling qualities. In investigations of rotor effects the application of ACT has shown promise in reducing response to atmospheric turbulence, retreating blade stall, vibration suppression, blade–fuselage interference and flap–lag modal damping analysis.

All these applications use the method of active pitch control to produce counteracting aerodynamic forces on the rotor blades, however the method of control actuation can be divided into two fundamentally different approaches: *Higher Harmonic Control* (HHC) and *Individual Blade Control* (IBC). HHC has mainly been used for vibration reduction (eg. Wood, 1983; Shaw and Albion, 1980), where rotor rotational frequency is used to generate pitch commands that approximately cancel the harmonics of vibration passed down from the rotor to the fuselage.

IBC is a more sophisticated approach since it involves the use of actuators and sensors on each blade to control the pitch individually in the rotating frame of reference (eg. McKillip. Jr, 1985; Ham, 1983; Ham and McKillip. Jr, 1980 and Kretz, 1976). In addition, because this method is essentially a 'broad band' control of the rotor blade dynamics, in contrast to the HHC limitation of discrete frequency disturbance suppression, it is capable of modifying each blades aeroelastic stability, modal damping and modal frequencies.

The criteria used to assess rotor effects are relatively easy to define since they can be judged in purely analytical terms, but the task of defining handling quality criterion is altogether more esoteric and ultimately the final judgement rests upon the subjective interpretation of the pilot (see Padfield, 1988 for an overview of the problem). This has not, however, had any effect on the amount of research in this area, eg. Wyatt, 1984; Winter, Padfield and Buckingham, 1984; Tischler, 1987; Charlton and Houston, 1988; Charlton, Padfield and Horton, 1987.

In developing control laws to meet these handling qualities there are many issues to be faced by the control law designer. A summary of these are given by Padfield, 1988,

- Relationship of control law design to handling criteria
- Suitability of various optimisation schemes, eg. Linear Quadratic Gaussian (LQG), H– Infinity (H^{∞})
- Blending of response types throughout the flight envelope
- Robustness to changes in operating conditions and dynamic uncertainties
- Development of tuning algorithms
- Impact of system constraints
- Requirements for degraded reversionary modes

It will require considerable effort before these functional design issues can be considered as a mature design methodology.

In this quest for improved handling qualities the ergonomics of the pilot's controls have also been considered. One idea, now being explored by several helicopter

makers, is to replace the conventional controls with a joystick on the pilot's armrest – *sidearm control* (Baillie, 1988, for example). A four–axis stick controls roll, pitch, vertical motion and yaw, by sideways, forward–backward, up–down and twisting movements, respectively.

The position of the stick is monitored, through pressure sensitive or displacement sensitive transducers, by a computer which determines the appropriate main and tail rotor pitch settings, which are then transmitted to the actuators at the rotor head. A three–axis control stick, which would replace the cyclic and collective sticks, but leave the floor pedals in place, has also been investigated. In both cases pilot reaction was reported to be favourable.

An essential feature of all these control systems is that their control laws invariably utilise the complete state vector. In practice, however, not every state variable is available, either owing to the failure of its sensor or because it cannot be measured. The most practicable solution to the problem is therefore to use an estimate of the state vector produced from an *observer*.

An observer is a dynamic element that produces an estimate of the system state vector based on information received from the measurement of the input and the output of the system, and was first proposed by Luenberger in 1964. Its main element is an accurate model of the system being observed. This is driven by the system control input and an error term derived from the difference between the system output and the output of the observer.

Provided that the model is accurate and the inputs and the outputs are the same as those of the system, then the intermediate state variables must also be the same. Furthermore, the eigenvalues of the observer (ie. the error dynamics) can be arbitrarily assigned and are independent of the eigenvalues of the controlled system. Consequently, the design of a state feedback controller and the design of a state estimator can be carried out independently of each other.

In stochastic systems, an alternative form of estimator is often employed – the Kalman Filter. This has the same basic configuration as the Luenberger observer, but it also uses knowledge of the structure of the noise corrupting the measurements in order to reduce the effects of noise on the estimate of the state. The Kalman Filter was not investigated for three reasons. Firstly, a–priori information about the noise is not always available; secondly, it introduces additional constraints and problems; and thirdly because a method of adapting the Luenberger observer to provide noise free estimates from noise corrupted inputs, was developed.

FAULT DETECTION

The use of high gain, high bandwidth, active control systems with control activity which goes beyond the levels normally associated with human pilot operation, offers many benefits, but it also results in higher risks for mission completion and flight safety due to flight control component failure. In recognition of these higher risks a proliferation of redundant components has evolved; namely sensors, computers and servo– actuation systems.

These *Hardware Redundancy* systems are generally four lane (*Quadruplex*) or triple lane (*Triplex*) with self monitoring, the redundant components being dispersed around the aircraft for additional safety. This provides a precise and robust method: failures being identified by some form of *majority vote* logic system, but has the disadvantages of increased cost and weight and the utilisation of valuable space.

In recent years attention has therefore concentrated on analytical techniques, or *Software Redundancy*, the advantages of which lie in the trade– off of redundant hardware against computer processing of signals from dissimilar (non– redundant) sensors. In other words, the redundant information required to identify a fault, is generated by software rather than duplicated hardware.

There are two fundamentally different approaches to software redundancy – time series analysis, which, due to long delays between the occurrence and detection of a fault, is impracticable for most aerospace applications; and state estimation which can detect even small faults almost instantaneously.

The state estimation approach can be divided into four methods: the *Dedicated Observer Scheme*, the *Failure Detection Filter*, the *Unknown Input Observer* and the *Disturbance Rejection Filter*, all of which rely on the same basic principle. Only one set of sensors is required and each sensor is used to drive an observer especially designed for that sensor.

With the dedicated observer scheme, if each sensor is perfect and the dynamic parameters of the system are known exactly, then the estimated state vectors will all be identical. However, if one of the sensors develops a fault, then the estimate produced by that sensors observer will be in error and so a comparison between the estimated states will identify the faulty sensor. With the other three methods it is not the state vector, but rather the magnitude or direction of the error vector, which is monitored.

With the advancing complexity of AFCS and the use of techniques such as ACT and fault detection/accommodation, there has been increasing concern in the inability to guarantee the absence of *common–mode* latent faults in systems which utilise identical subsystems, eg. context dependent software errors and hardware deficiencies which are triggered by environmental changes (lightning strikes, power transients, etc).

Both Wyatt, 1984 and Richards, 1983, for example, recommend complete dissimilarity in processing, including software and the software design tools – assemblers, compilers, etc. With a system based on hardware redundancy, each flight control computer would be designed, developed and tested by separate teams of engineers working in isolation and employing different methodologies and components.
However, even then there could still be problems since each flight control computer would be designed to a common control law specification, would have common timing requirements and would operate in a common dynamic system environment. With software redundancy techniques the problems are very similar except that the main area of concern is the fidelity of the software.

The best solution to these problems would appear to be a balanced approach, with extreme care being taken to ensure simplicity, clarity and correctness of those high level requirements and designs which are common to each hardware/software sub– system.

1.4 OBJECTIVES

The main objective of this research was to investigate the application of deterministic, continuous– time, linear, time– invariant system theory in the design of 'Luenberger' state observers for state estimation in the single main rotor helicopter. The use of Luenberger state observers in this harsh environment (sources of noise include such things as electromagnetic pick– up, inadequate power supply filtering and in particular, mechanical vibration from the main and tail rotors resulting in electrical disturbances) is unusual, since in stochastic systems an alternative form of estimator is usually employed – the Kalman filter.

This has the same basic configuration as the Luenberger observer, but it also uses knowledge of the structure of the noise corrupting the measurements in order to reduce the effects of noise on the estimate of the state. The Kalman filter was not investigated for three reasons. Firstly, *a–priori* information about the noise is not always available; secondly, it introduces additional constraints and problems; and

thirdly, because a major objective was to determine whether a method of adapting the Luenberger observer to provide noise free estimates from noise corrupted inputs, could be developed.

As indicated in the previous section an observer requires an accurate model of the system that is being observed and therefore the first objective was to select and evaluate an appropriate mathematical model. The model selected was developed at the Royal Aircraft Establishment, Bedford, for use in the prediction of rigid body, fuselage dynamic motions throughout the flight envelope, and is described in detail in Chapter two.

Once the model had been chosen the next step was to evaluate existing observer design techniques. The necessary theory is contained in Chapter three and a review of the literature is presented in Chapter four. Two design methods were initially selected for consideration : a method proposed by Gopinath and an observable canonical form method. After consideration of basic observer performance, the Gopinath method is shown to be unsuitable for the design of helicopter state observers.

In chapter five the computer implementation of the canonical form method is described. This consists of an observability test, transformation of the system state space equation to observable canonical form and the determination of the elements of the observer matrix. It is demonstrated that this is a robust and accurate method and an observer is designed and successfully tested with a feedback controller. The use of flight data is explained and an analytical method of evaluating observer performance is defined.

The next objective was to investigate the performance of observable canonical form observers, and this is covered in Chapter six. Observer performance with eighth and fourteenth order system models is considered and several numerical problems are examined. It is shown that canonical form observers can produce accurate estimates if the system states are 'clean', but that noise corrupted states result in noise corrupted estimates. To solve this problem a new form of observer — the twin observer — is introduced and it is demonstrated that with an accurate model of the system, the twin observer can produce accurate, relatively noise free estimates of the system state.

The final objective of this research was to determine whether the twin observer was suitable for use in an instrument fault detection scheme. This question is considered in Chapter seven, which begins with a literature review of fault detection techniques.

From this review it is apparent that the most appropriate technique to use with the twin observer is the dedicated observer scheme. The advantages and disadvantages of this method are examined using a longitudinal model of the system and possible solutions to some of the problems are proposed.

Finally, Chapter eight summarises the main findings of the thesis and makes suggestions for further research.

1.5 STATEMENT OF ORIGINALITY

In general it is thought that an extensive investigation of the 'Luenberger' form of observer, for use in helicopter flight control systems, is original work. In particular the 'Twin observer' developed in chapter six is believed to be new and presents a possible solution to the problem of noise corrupted states.

The analysis of an observer based instrument fault detection scheme : the Dedicated Observer Scheme, using this form of observer, is also considered to be original work.

CHAPTER TWO

HELISTAB

A MATHEMATICAL MODEL

OF THE

SINGLE ROTOR HELICOPTER

2.1 INTRODUCTION

The heart of an observer is an accurate model of the system that is being observed and therefore the first requirement when considering the use of observers for state estimation and/or sensor fault detection, is the selection of a suitable mathematical model. Fundamental concepts required to establish the model are considered in sections 2.2 to 2.4 and include the basic aerodynamics of the helicopter rotor, axes systems and transformations, the fundamental equations of motion and procedures for linearizing non– linear equations about a steady state operating point. (The equations of motion are explicitly linearized in Appendix 1). Mathematical models in general, are discussed in section 2.5 and the reasons for using the model chosen for this research are given.

The ability to vary the order of the system is discussed and the choice of relevant axes for analysis of the external forces and moments is examined. External forces and moments are established in section 2.6 and the individual components from the main rotor (section 2.6.1), fuselage, empennage and tail rotor (section 2.6.2) are then derived.

Limitations of the model are discussed in section 2.7 and the use of the model to produce linearized equations of motion at any particular flight condition (section 2.8) and to produce time– responses of the system when subjected to control inputs (section 2.9), are considered.

2.2 BASIC CONCEPTS

There are four major forces acting on any aircraft, namely *lift, drag, thrust* and *gravity* (*fig 2.1*). Lift is the force which in general counteracts gravity. It is the useful reaction obtained from the flow of air over an aerofoil and acts from the *aerodynamic centre* (or *centre of pressure*) and perpendicular to the *relative wind.* The aerodynamic centre is that point on an aerofoil section through which all aerodynamic forces may be considered as acting and about which the aerodynamic moments are substantially constant. The relative wind is the oncoming air flowing parallel and opposite to the flight path of the aircraft.

Drag is the force which tends to retard or resist the forward motion of a body through the air and acts from the aerodynamic centre and is parallel to the relative wind. The force which overcomes drag and propels the aircraft forward or, as in the case of the helicopter, in any direction, is called thrust.

Any part of an aircraft designed to produce lift may be called an aerofoil. In a fixed–wing aircraft the wings and tailplane act as aerofoils, but in a helicopter lift is generated by the rotor. A rotor generates lift by accelerating a mass of air downwards through its blades and is proportional to the downwash mass and velocity. In flight, the blades bend upwards until gravity, lift and centrifugal force balance : a process called *coning* (*fig 2.2*). There is a fourth force acting on the blades – drag, and this is overcome by the torque from the engine.

In forward flight, blades advancing to the nose will encounter faster *apparent airflow* (the vector sum of forward, translational velocity of the helicopter and the rotational velocity of the rotor) than blades retreating towards the tail. As a result, advancing blades will generate greater lift than retreating blades, unbalancing the aircraft unless compensating measures are taken.

To assure stability, most helicopters employ two such measures : *flapping* and *feathering*. With flapping (*fig 2.3*), the blades respond to increased lift on the advancing side of the rotor by rising to a maximum angle over the nose, while falling to a minimum angle over the tail. This changes the apparent angle that the blades attack the air, thereby compensating for the airflow variations.

With feathering, the pitch of the rotor blades is varied sinusoidally as the rotor spins to compensate for the sinusoidal airflow variations. These pitch variations are transmitted from the pilot's control inputs to the individual blades via a device called a *swashplate.*

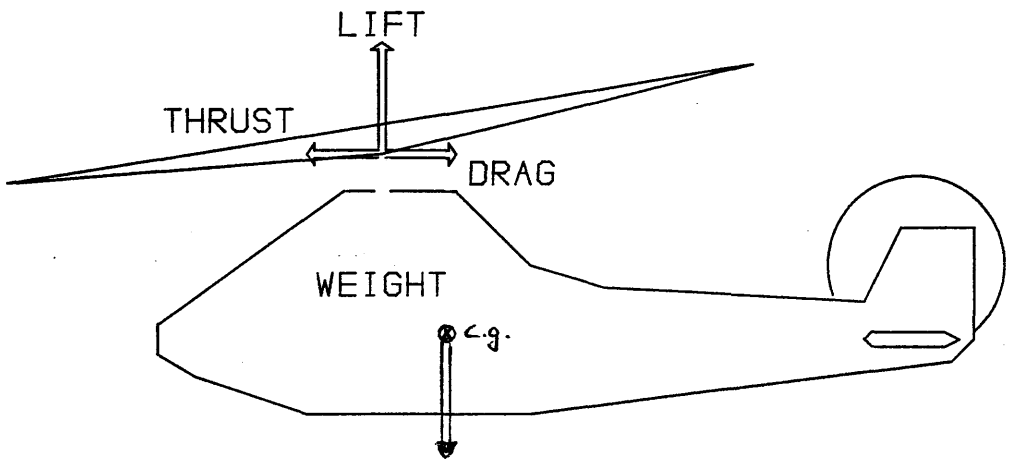

FIG 2.1 BALANCE OF FOUR FORCES DURING STEADY FLIGHT

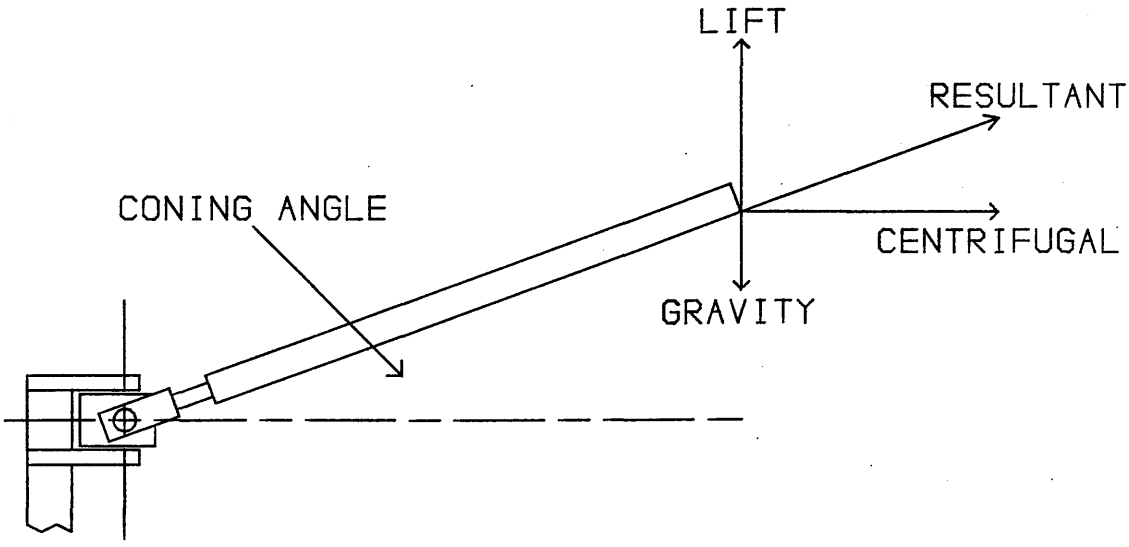

FIG 2.2 ROTOR BLADE CONING

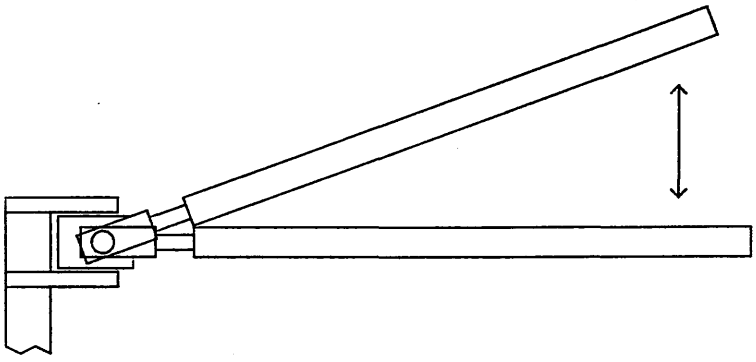

FIG 2.3 ROTOR BLADE FLAPPING ABOUT A HINGE

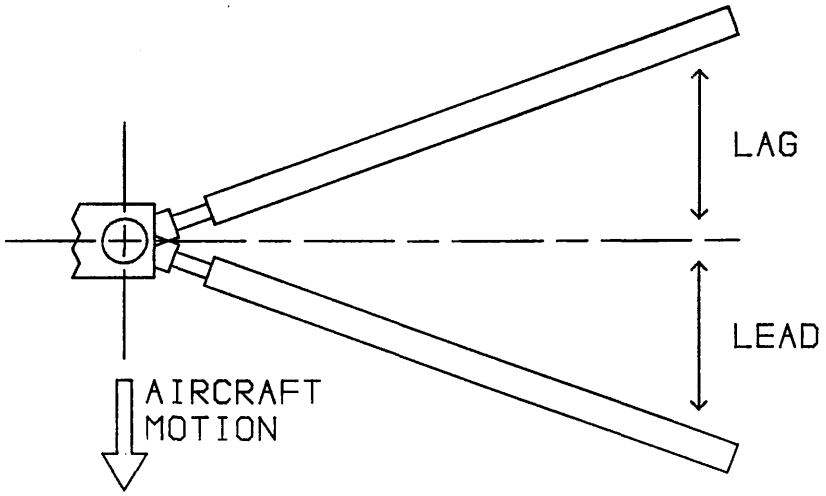

FIG 2.4 LEAD/LAG MOTIONS OF A ROTOR BLADE

To allow flapping and feathering, blades are typically hinged or made flexible at the hub. If there are also hinges to permit *lead* and *lag* motions induced by drag variations (*fig 2.4*), then the rotor is said to be *fully articulated.*

In addition to stabilizing the helicopter, cyclic pitch variations are used for control purposes. The average value of the *cyclic pitch*, the *collective pitch*, determines the average lift of the rotor blades. Varying the collective pitch can thus be used to make the helicopter ascend, descend or hover. Direction of travel is primarily controlled by cyclic pitch – changing the amplitude and phase of the pitch cycle temporarily unbalances the rotor, causing it to tilt in a specific direction. The helicopter then accelerates in that direction, until it regains a stable position corresponding to the new velocity.

The control motions are transmitted by the pilot via two sticks : a *collective stick* which pushes the swashplate up and down on the rotor mast, thereby changing the collective pitch; and a *cyclic stick* that tilts the swashplate, thereby changing the amplitude and phase of the cyclic pitch (fig 2.5).

2.3 AXES SYSTEMS AND TRANSFORMATIONS

In order to analyse an aircraft in flight it is necessary to first define a set of axes which will act as a reference frame around which the relevant equations of motion may be developed. Since the aircraft is a free body in space, its position and flight path may be defined with respect to a set of *earth fixed axes*, which remain fixed relative to the earth. These earth axes assume a flat, non–rotating earth and arbitrary origin, with the x–axis pointing Northward, y–axis Eastward and the z–axis pointing down to the centre of the earth (*fig 2.6b*).

However, this axis system is inconvenient for some analyses and therefore a set of axes which remain fixed relative to the airframe can be used. This axis set is called the *body fixed axes* and the origin is located at the aircraft's centre of gravity with the x–axis pointing forward, y–axis to starboard and z–axis downwards (Duncan, 1952). It is conventional to define the nomenclature associated with the body fixed axis system in a standard form and this is summarised in *table 2.1* and *fig 2.6a.*

The body fixed axis system may be related to the earth fixed axis system by a series of rotations. Consider *fig 2.7a* where OX_E, OY_E, OZ_E is the earth fixed axis system and OX_i, OY_i, OZ_i is an intermediate axis system, initially coincident with OX_E, OY_E, OZ_E.

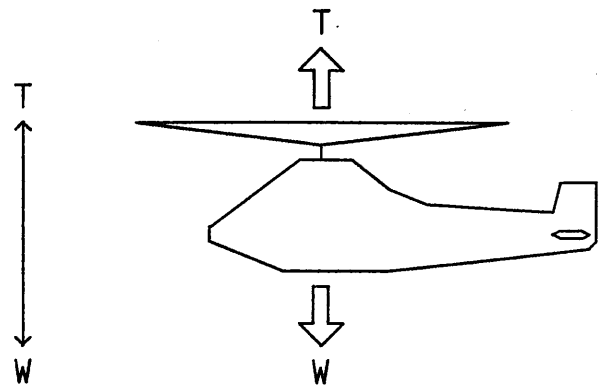

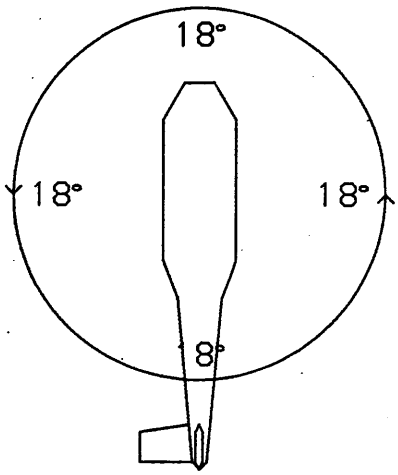

COLLECTIVE PITCH : 18°
CYCLIC PITCH : 18°
CYCLIC PHASE : 0°

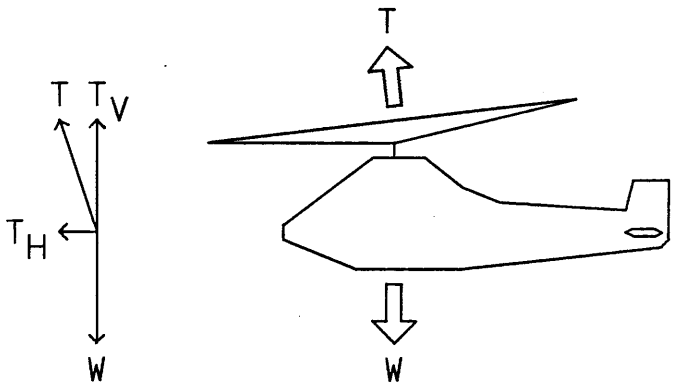

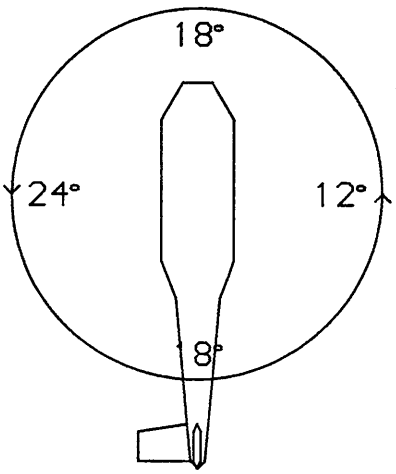

COLLECTIVE PITCH : 18°
CYCLIC PITCH : 6°
CYCLIC PHASE : 0°

NOTE THAT THE PITCH CHANGES OCCUR NINETY DEGREES OF ROTATION (ANGLE OF PRECESSION) BEFORE THE EFFECT OF THE CHANGE IS TO TAKE PLACE.

FIG 2.5 COLLECTIVE AND CYCLIC PITCH

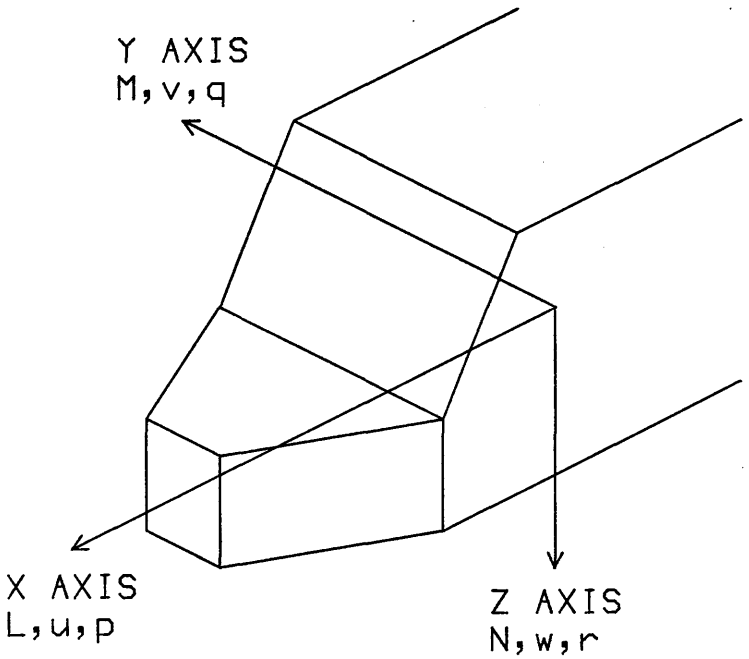

(a) BODY AXES
Origin at Centre
of Gravity

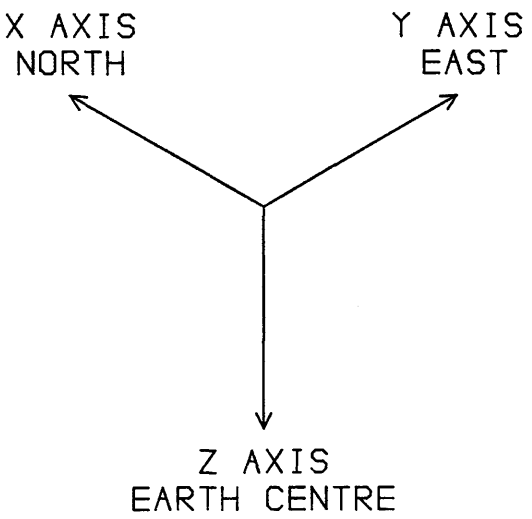

(b) EARTH AXES

FIG 2.6 BODY AND EARTH AXES SYSTEMS
Both systems are orthogonal
right-handed triads

AXIS	OX	OY	OZ
NAME	LONGITUDINAL	LATERAL	NORMAL
LINEAR DISPLACEMENT (m)	x	y	z
STEADY STATE VELOCITY (ms^{-1})	U	V	W
INCREMENTAL VELOCITY (ms^{-1})	u	v	w
FORCE COMPONENT (N)	X	Y	Z
ROLLING VELOCITY COMPONENT ($rads\ s^{-1}$)	ROLL p	PITCH q	YAW r
ANGULAR DISPLACEMENT (rads)	φ	θ	ψ
ROLLING MOMENT (Nm)	L	M	N

NOTES

(1) Linear displacements, velocities and forces are positive in the direction of the axis.

(2) Agular displacements, rolling velocities and moments are positive in the clockwise sense, looking along the axis from the origin.

TABLE 2.1 : BODY AXES DEFINITIONS

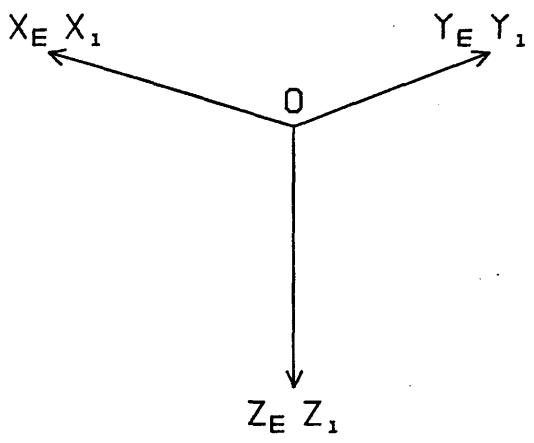

(a) EARTH AXES

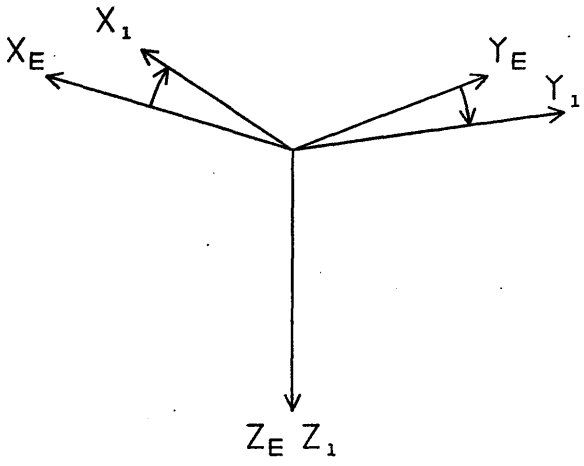

(b) ROTATION OF ψ ABOUT Z_E

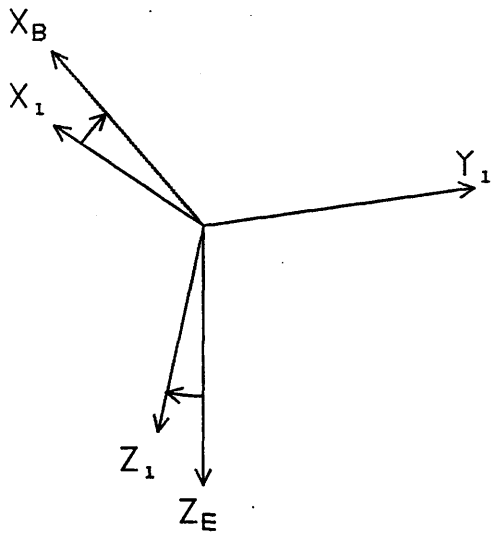

(c) ROTATION OF θ ABOUT Y_1

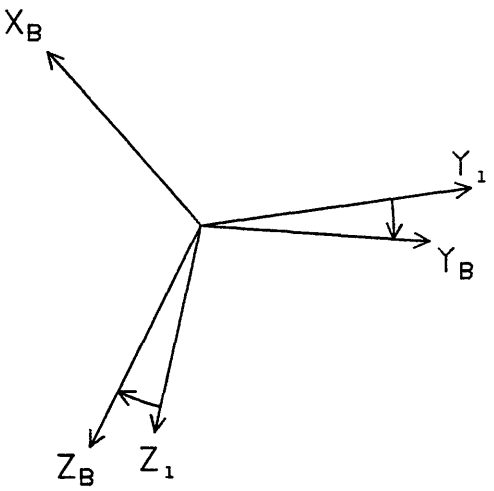

(d) ROTATION OF φ ABOUT X_B

FIG 2.7 TRANSFORMATION BETWEEN EARTH AND BODY AXES

The orientation of OX_B, OY_B, OZ_B with respect to OX_E, OY_E, OZ_E can then be determined as follows.

(1) Rotate OX_i, OY_i, OZ_i about the OZ_i axis by angle ψ, *fig 2.7b*

(2) Rotate OX_i, OY_i, OZ_i about the OY_i axis by angle θ, *fig 2.7c*

(3) Rotate OX_i, OY_i, OZ_i about the OX_i axis by angle φ, *fig 2.7d*

OX_i, OY_i, OZ_i are now coincident with OX_B, OY_B, OZ_B and the helicopter's *attitude*, ie. the orientation of its body fixed axes with respect to the earth fixed axes, is defined by the *Euler angles* ψ, θ and φ.

If each of the above rotations are considered separately, it is possible to derive a transformation matrix T, called the *direction cosine matrix* (Hopkin, 1966). For example, body axes velocities are found from earth axes velocities by,

$$\begin{bmatrix} u_b \\ v_b \\ w_b \end{bmatrix} = \begin{bmatrix} t_{11} & t_{12} & t_{13} \\ t_{21} & t_{22} & t_{23} \\ t_{31} & t_{32} & t_{33} \end{bmatrix} \begin{bmatrix} u_e \\ v_e \\ w_e \end{bmatrix} \qquad (2.1)$$

where

$$\begin{aligned}
t_{11} &= \cos\theta\cos\psi \\
t_{12} &= \cos\theta\sin\psi \\
t_{13} &= -\sin\theta \\
t_{21} &= \sin\varphi\sin\theta\cos\psi - \cos\varphi\sin\psi \\
t_{22} &= \sin\varphi\sin\theta\sin\psi + \cos\varphi\cos\psi \\
t_{23} &= \sin\varphi\cos\theta \\
t_{31} &= \cos\varphi\sin\theta\cos\psi + \sin\varphi\sin\psi \\
t_{32} &= \cos\varphi\sin\theta\sin\psi - \sin\varphi\cos\psi \\
t_{33} &= \cos\varphi\cos\theta
\end{aligned}$$

The transformation matrix is orthogonal and therefore its transpose is equivalent to its inverse, and can be used to transform a set of variables from body axes to earth axes.

Accelerations can be provided by differentiating equation 2.1,

$$\begin{bmatrix} \dot{u}_b \\ \dot{v}_b \\ \dot{w}_b \end{bmatrix} = \begin{bmatrix} t_{11} & t_{12} & t_{13} \\ t_{21} & t_{22} & t_{23} \\ t_{31} & t_{32} & t_{33} \end{bmatrix} \begin{bmatrix} \dot{u}_e \\ \dot{v}_e \\ \dot{w}_e \end{bmatrix} + \begin{bmatrix} \dot{t}_{11} & \dot{t}_{12} & \dot{t}_{13} \\ \dot{t}_{21} & \dot{t}_{22} & \dot{t}_{23} \\ \dot{t}_{31} & \dot{t}_{32} & \dot{t}_{33} \end{bmatrix} \begin{bmatrix} u_e \\ v_e \\ w_e \end{bmatrix} \quad (2.2)$$

Where

$$\dot{t}_{11} = \dot{\theta} t_{13} \cos\psi - \dot{\psi} t_{12}$$

$$\dot{t}_{12} = \dot{\theta} t_{13} \sin\psi + \dot{\psi} t_{11}$$

$$\dot{t}_{13} = -\dot{\theta} \cos\theta$$

$$\dot{t}_{21} = \dot{\varphi} t_{31} + \dot{\theta} t_{23} \cos\psi - \dot{\psi} t_{22}$$

$$\dot{t}_{22} = \dot{\varphi} t_{32} + \dot{\theta} t_{23} \sin\psi + \dot{\psi} t_{21}$$

$$\dot{t}_{23} = \dot{\varphi} t_{33} + \dot{\theta} t_{13} \sin\varphi$$

$$\dot{t}_{31} = -\dot{\varphi} t_{21} + \dot{\theta} t_{33} \cos\psi - \dot{\psi} t_{32}$$

$$\dot{t}_{32} = -\dot{\varphi} t_{22} + \dot{\theta} t_{33} \sin\psi + \dot{\psi} t_{31}$$

$$\dot{t}_{33} = -\dot{\varphi} t_{23} + \dot{\theta} t_{13} \cos\varphi$$

The velocity components of the body fixed axis system, u, v and w, can be resolved into a single total velocity vector V,

$$V = (u^2 + v^2 + w^2)^{\frac{1}{2}} \quad (2.3)$$

and the aircraft's angles of *sideslip* β, and *incidence* α, are as shown in *fig 2.8*, and are defined as:

$$\alpha = \tan^{-1}(w/u) \quad (2.4)$$

$$\beta = \sin^{-1}(v/V) \quad (2.5)$$

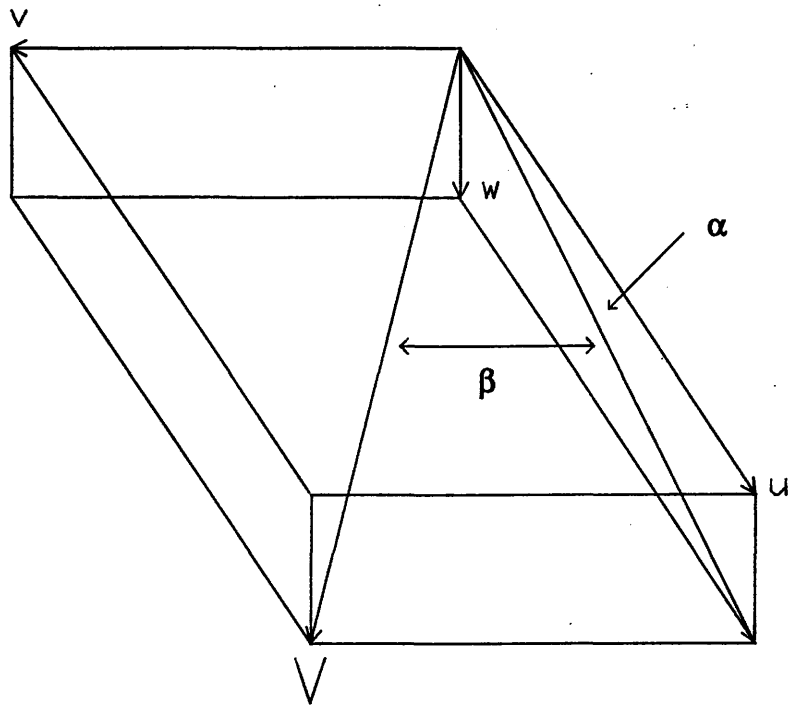

FIG 2.8 TOTAL VELOCITY(V), INCIDENCE(α) AND SIDESLIP(β)

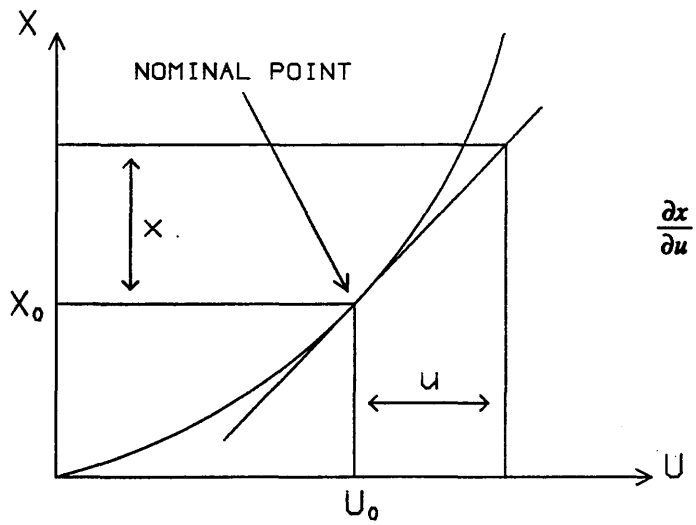

$$\left.\frac{\partial x}{\partial u}\right|_{U_0} = \left.\frac{\partial X}{\partial U}\right|_{U_0}$$

FIG 2.9 LINEARIZATION OF SIMPLE NONLINEAR FUNCTION

2.4 FUNDAMENTAL EQUATIONS OF MOTION

The next step in the development of the dynamics of the aircraft is to consider the aerodynamic forces and moments which act on the airframe and result in changes in the aircraft's body velocities and accelerations. These may then be translated to earth fixed axes using equations 2.1 and 2.2 and the resulting dynamic behaviour of the aircraft deduced.

In standard form (eg. Duncan, 1952) the fundamental equations of translational and rotational motion and the Euler angle rates can be written as,

Translational Motion

$$\left.\begin{aligned} \dot{u} &= (vr - wq) + \frac{X}{m} - g\sin\theta \\ \dot{v} &= (wp - ur) + \frac{Y}{m} + g\cos\theta\sin\varphi \\ \dot{w} &= (uq - vp) + \frac{Z}{m} + g\cos\theta\cos\varphi \end{aligned}\right\} \qquad (2.6)$$

Rotational Motion

$$\left.\begin{aligned} I_{xx}\dot{p} &= (I_{yy} - I_{zz})qr + I_{xz}(\dot{r} + pq) + L \\ I_{yy}\dot{q} &= (I_{zz} - I_{xx})rp + I_{xz}(r^2 - p^2) + M \\ I_{zz}\dot{r} &= (I_{xx} - I_{yy})pq + I_{xz}(\dot{p} - qr) + N \end{aligned}\right\} \qquad (2.7)$$

Euler Angle Rates

$$\left.\begin{aligned} \dot{\varphi} &= p + q\sin\varphi\tan\theta + r\cos\varphi\tan\theta \\ \dot{\theta} &= q\cos\varphi - r\sin\varphi \\ \dot{\psi} &= q\sin\varphi\sec\theta + r\cos\varphi\sec\theta \end{aligned}\right\} \qquad (2.8)$$

where I_{xx}, I_{yy}, I_{zz} and I_{xz} are the moments and product of inertia and m is the mass of the aircraft. The external forces (X,Y,Z) and moments (L,M,N) are considered to be the sum of contributions from all dynamic and aerodynamic sources. The importance of the above *Euler equations*, which are derived from a consideration of Newton's second law of motion, is that they allow the body velocities and accelerations to be defined in terms of the forces and moments acting on the aircraft.

In order to solve the fundamental equations of motion it is necessary to first select a set of axes. As discussed in the previous section there are two main axis sets: body fixed axes and earth fixed axes. The disadvantage of body fixed axes is that they produce a rotating frame of reference with the result that expressions for translational accelerations include angular velocity terms eg. equations 2.6.

However, by a suitable choice of axes, it is possible to uncouple translational motion from rotational motion. Since rotational motion is more rapid than translational, solution of the rotational equations can then be executed more frequently than the translational equations, thus resulting in a more efficient (and simpler) computer implementation. For solution of rotational equations, body–fixed axes are chosen and have the advantage of constant moments of inertia. Earth–based axes are used for the translational equations of motion.

To simplify the analysis of the main rotor a further three further axes systems are employed. The *blade system* (subscript B) is fixed in the flapping blade whilst the *hub system* (subscript H) is aligned along the shaft and centred at the rotor hub. The *hub/wind system* (subscript Hw) has the hub x–axis aligned with the resultant aircraft velocity in the hub xy–plane. Details of the transformation matrices between these systems and between these and body axes are derived and stated by Padfield, 1981.

The fundamental equations of motion are non–linear since superposition, the fundamental property of linear systems (and the property on which they may be defined) does not hold. However, it is often advantageous to represent the dynamic behaviour of a system by linear equations, perhaps the most important benefit being that the solution of linear equations is, in most cases, comparatively simple. Also, and of particular relevance to this thesis, it facilitates the use of linear matrix algebra which has many advantages in the study of control systems.

In general, there are very few real linear systems, and taken to the limits of their performance, it is probably true to say that there are no real full–range linear systems. However, in most cases, and provided the system is stable, when inputs are limited the system at least approximates to linear behaviour. In such cases it is possible to consider deviations about some desired set of steady–operating conditions. A change in input, desired or otherwise, then causes a change in output. Thus it is obvious that zero change in input will produce no change in output and that the initial steady operating conditions are zero. This process is known as linearization (*fig 2.9*, page 25). The general procedure for linearizing a system is outlined next, whilst the linearization of the Euler equations is presented in section 2.8.

The starting point for the linearization is to consider that any variable is composed of two distinct parts. Firstly, a component which constitutes an average steady–state or trimmed condition and secondly, a perturbation component about this nominal operating point, eg.

$$u = U_0 + u \qquad X = X_0 + X$$

where the subscript 'o' denotes the steady–state condition. The relevant dynamic equations of motion due to small perturbations can then be formulated by evaluating the trimmed equations and the perturbed equations independently, then subtracting the trimmed from the perturbed. In doing so, products of perturbations are neglected and small angle assumptions (ie. for general small angle ζ, $\cos\zeta = 1$; $\sin\zeta = \zeta$) are made.

Finally, the external forces and moments can be expanded as a standard Taylor series, neglecting second order and higher derivatives since these will be negligible for small perturbations, eg.

$$X = X_0 + \frac{\partial X}{\partial u} u + \frac{\partial X}{\partial w} w + \frac{\partial X}{\partial q} q + \ldots\ldots$$

Note that the equations derived are only valid for small excursions from the operating point and if a different operating point is used then the above process must be applied to the new operating point to produce a different set of linear equations.

2.5 MATHEMATICAL MODELS

To study the dynamics and control of a helicopter, or any system, it is necessary to establish a mathematical model which comprises (non–linear) differential (ordinary or partial) equations. If these equations have, or can be suitably reduced to, a linear form then the Laplace Transform or linear matrix algebra or a combination of both can be used in solving these equations and hence assisting in the determination of controllers and/or observers for the system.

The nature of the model depends largely on the use for which it is required and the complexity of the system being modelled. It may be a very detailed representation or it may be very simple, indicating approximate behaviour or behaviour within a limited operating condition. In many cases, either through necessity or for simplicity, and particularly in large, complex systems, the model will

be based on both theoretical and empirical knowledge. The advantages of a fully theoretical model are its reliability and flexibility in allowing for major changes in system and control, and its ability to predict behaviour in a wide operating range. However, this ideal situation is rarely achieved due to a lack of precise knowledge about the system and the need to make assumptions which require verification.

Although empirical results are essential for confirming basic theory, indicating deviations due to omitted or unknown factors and for determining parts of the model on a *black box* basis, it is important to remember the method has limitations. The relationships established are particular to the unit under test, will generally only be valid in a narrow operating range and require good test techniques and facilities. Nonetheless, in the absence of other knowledge or for a system which is difficult to define, this method is normally the most practical choice (See for example, Astrom and Eykhoff, 1971).

Once the model has been designed and 'created', it is crucial that it is verified : this is usually accomplished by a comparison of simulation results and empirical data from the actual system, and will indicate any deficiences in the model. This development cycle of adjustment and testing continues until the desired degree of correlation between the model and the system is achieved.

For this research the choice of mathematical model was influenced by the basic premise, according to the literature, that an accurate model is required for satisfactory observer performance. The model selected was developed by the Royal Aerospace Establishment (RAE) at Bedford, for general use in the prediction of the important, rigid body, fuselage dynamic motions, throughout the flight envelope. In order to obtain satisfactory simulation results, the model is extensive and complicated. This is because of the number of degrees of freedom required, the complexity of the rotor wake and its interference effects, and the non-linearities present.

Despite this, the model has proved to be accurate for limited manoeuvres associated with procedural or navigational flying tasks and although it is not yet able to portray the full character of stability, response and handling characteristics during the applied flying involved in nap-of-the-earth operations, it is still of immense use in the study of helicopter control system design.

The model is implemented as a digital computer program, written in Fortran, and contained within a software package known as HELISTAB (Padfield, 1981; Smith, 1984), which can be run with solutions, updated every 50mS, generated by a fourth

order Runge–Kutta numerical integration algorithm. The elements of the model : fuselage, a main and tail rotor, tailplane, fin and pilot controls are shown diagramatically in *fig 2.10*. It is a non–linear model and the system order is user selectable : eighth–order (six degrees of freedom), eleventh–order (nine degrees of freedom) or fourteenth–order (twelve degrees of freedom). The differences are a function of the modelling of the main rotor only.

In the eighth order model the rotor is assumed to have quasi–steady flapping and coning i.e the coning angle and the longitudinal and lateral flapping angles are determined purely through algebraic relationships. If the coning angle, longitudinal and lateral flapping angles are considered as degrees of freedom then the system becomes eleventh order, whilst the fourteenth order model also includes the derivatives of the coning and flapping angles as degrees of freedom.

Three other types of model were considered, but rejected. *Reduced order dynamic models* have the problem of inadequate prediction of coupling effects when simulating hingeless rotor helicopters and in severe manoeuvres, coupling between rotor collective pitch and fuselage pitch attitude can be excessive. The limitations of *kinematic models*, as shown by Curtiss and Price (1984), are insufficient prediction of dynamic behaviour at low speed, and since the rotor is not modelled, the significant aerodynamic effects of the rotor and its downwash are not considered. *Linearized models* are also of limited use since they only predict the helicopter's flight state for small perturbations from its trim condition.

In the interests of simplicity and illustration, the remaining sections of this chapter deal with the eighth order model only, however the relevant order–reducing assumptions are clearly stated in section 2.6.1, which discusses the modelling of the main rotor. For a full discourse on the derivation of the model, the reader is refered to the documentation on HELISTAB.

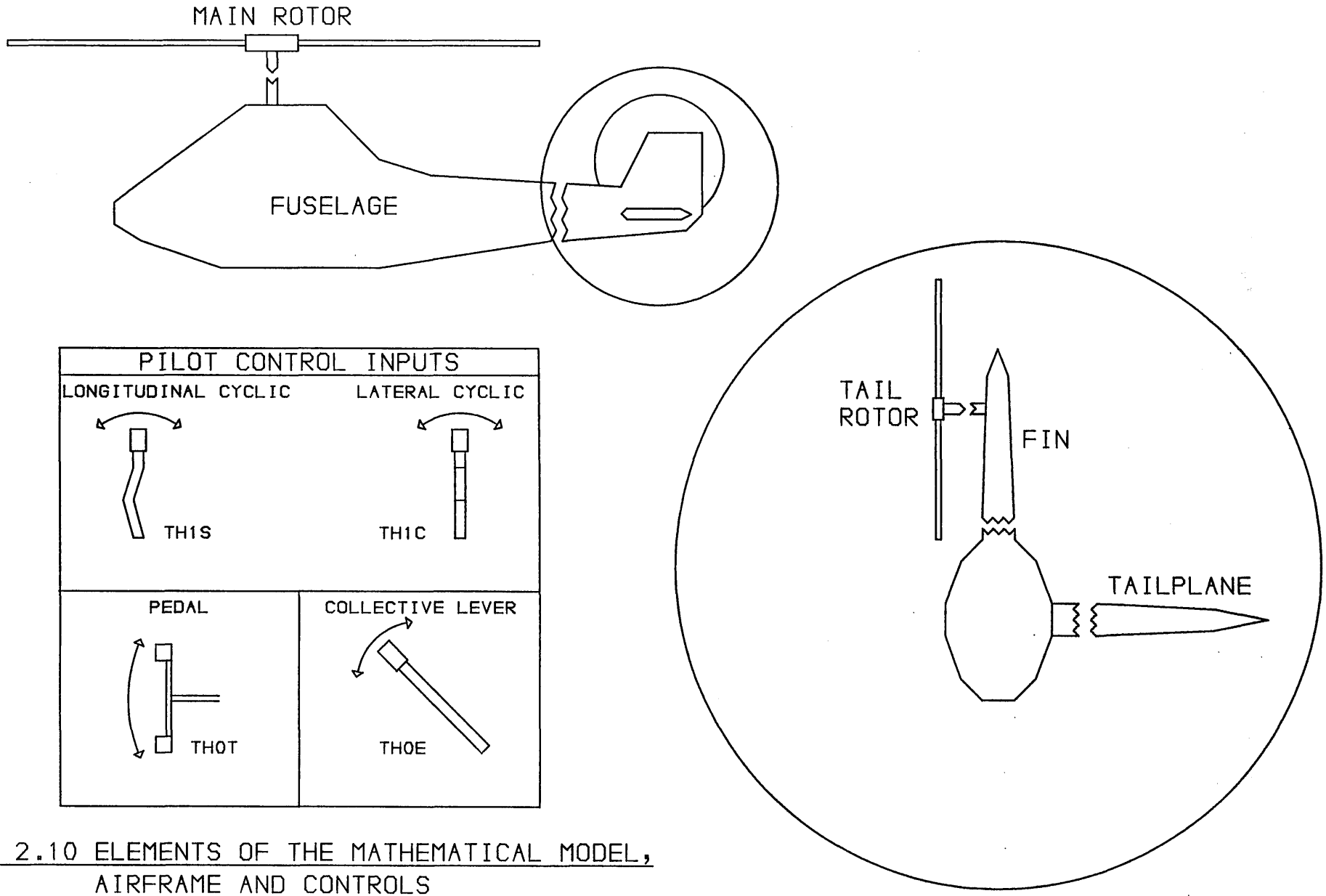

FIG 2.10 ELEMENTS OF THE MATHEMATICAL MODEL, AIRFRAME AND CONTROLS

2.6 EXTERNAL FORCES AND MOMENTS

To solve the nine differential equations 2.6, 2.7 and 2.8 it is necessary to first determine the external forces (X,Y,Z) and moments (L,M,N). These are considered to be a sum of the contributions from the main rotor (suffix R), tail rotor (suffix T), tailplane (suffix TP), fin (suffix FN) and fuselage (suffix F). Thus the forces and moments can be written as,

$$\left.\begin{aligned} X &= X_R + X_T + X_{TP} + X_{FN} + X_F \\ Y &= Y_R + Y_T + Y_{TP} + Y_{FN} + Y_F \\ Z &= Z_R + Z_T + Z_{TP} + Z_{FN} + Z_F \end{aligned}\right\} \qquad (2.9)$$

$$\left.\begin{aligned} L &= L_R + L_T + L_{TP} + L_{FN} + L_F \\ M &= M_R + M_T + M_{TP} + M_{FN} + M_F \\ N &= N_R + N_T + N_{TP} + N_{FN} + N_F \end{aligned}\right\} \qquad (2.10)$$

For a full account of the derivations of forces and moments used in this model the reader is refered to the documentation for HELISTAB (Padfield, 1981; Smith, 1984), however a brief description is given here, and should be read in conjunction with *fig 2.11*, which defines the forces and moment arms, and *fig 2.12* which is a block diagram of the complete helicopter flight dynamic simulation model. Expressions stated assume an anti-clockwise rotating rotor (as viewed from above), with $\psi = 0$ at the back of the disc and β positive up. Symbols used are defined in Appendix four.

2.6.1 FORCES AND MOMENTS OF THE MAIN ROTOR

The main rotor consists of rigid, constant chord blades, hinged with stiffness in flap at the centre of rotation. Linearly varying twist, θ_{tw}, can be defined and the pitch of the blades can be altered collectively and cyclically, once per revolution of the rotor. The lag degree of freedom is not included. A constant main rotor speed is assumed and therefore expressions for engine torque, Q_E, and main rotor speed, Ω, can be written as,

$$\left.\begin{aligned} Q_E &= Q_R + G_{TR}Q_{TR} \\ \Omega &= \frac{Q_E}{K_3} + \Omega_i \end{aligned}\right\} \qquad (2.11)$$

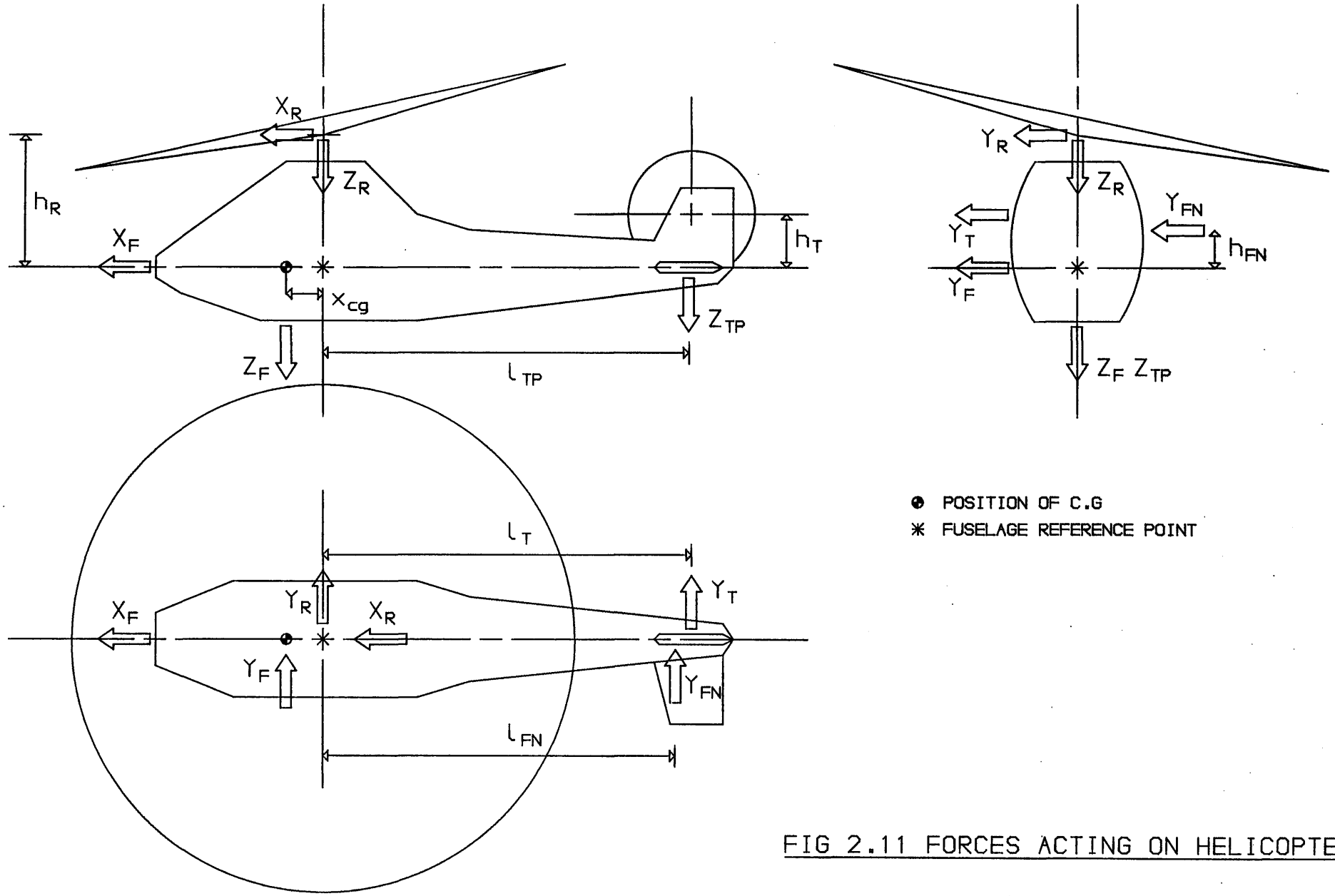

FIG 2.11 FORCES ACTING ON HELICOPTER

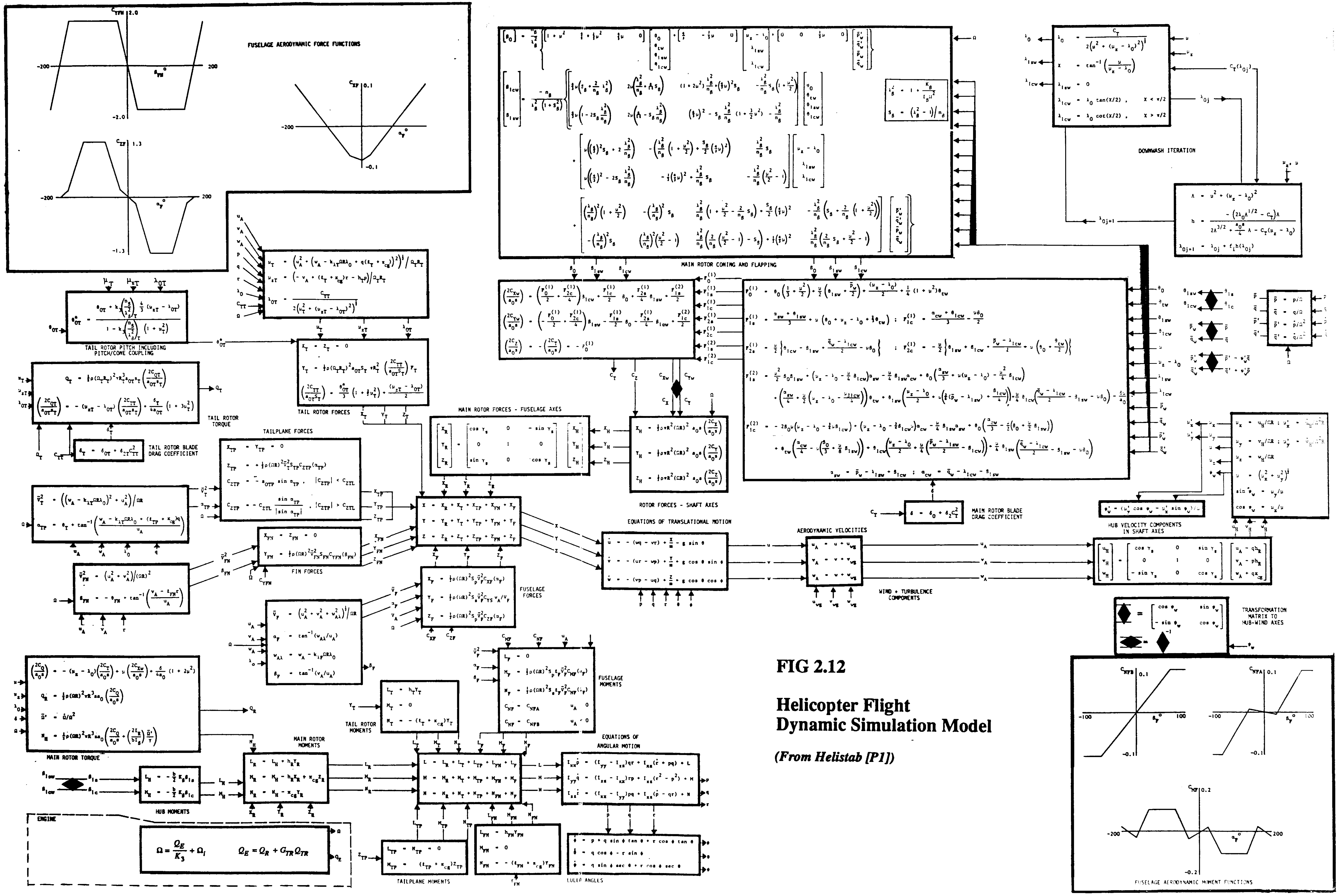

FIG 2.12

Helicopter Flight Dynamic Simulation Model

(From Helistab [P1])

Analysis of the rotor can be divided into three, related categories: kinematics, dynamics and aerodynamics, and these are examined below.

BLADE KINEMATICS

Inertial components of velocity and acceleration of a blade element are derived using several assumptions. Flapping angles are assumed to be small so that linearity assumptions can be invoked and the overall acceleration of the fuselage and blade weight– effects are neglected. Furthermore, yaw and sideslip rates are assumed to be small in comparison with the rotor angular rate Ω. Rotor rotation relative to the fuselage, and pitch, roll and yaw rates are, of course, superimposed on this basic flapping.

BLADE AERODYNAMICS

A number of assumptions are made to make it possible to integrate the aerodynamic loading analytically and hence produce closed form expressions for the rotor forces and moments. These are,

- A constant, two–dimensional, lift curve slope is assumed in calculating the lift of a blade, and its profile drag, δ, is found from a quadratic function of rotor–thrust coefficient.
- The local airflow is assumed to be steady and incompressible.
- Stall and reversed flow effects are ignored.
- The induced velocity distribution, normal to the rotor disc, includes linear lateral and longitudinal variations, the value at the centre satisfying simple momentum considerations.

The induced flow through the rotor is approximated by a simple, uniform distribution with a longitudinal variation produced by the rotor wake. The uniform component, normal to the rotor disc is given, from momentum theory, by the expression:

$$\lambda_0 = \frac{C_T}{2(\mu^2 + (\mu_Z - \lambda_0)^2)^{\frac{1}{2}}} \qquad (2.12)$$

which is solved for λ_0 (the non–dimensional downwash at the rotor centre) by an iterative process. However, it should be noted that this expression is not valid when the rotor is in the vortex ring state. This is the intermediate region between helicopter and windmill modes, where a ring of air is formed round the rotor blades. The helicopter will encounter turbulence and the pilot will experience vibration, a high rate of sink and some partial loss of control due to the fact that the helicopter is descending into its own slipstream (*fig 2.13*).

BLADE DYNAMICS

System order, as mentioned in section 2.5, is dependent on the modelling of the main rotor dynamics. In the eighth order, six degrees of freedom model, the important assumption is that quasi–steady flapping and coning are used in the derivation of the reaction forces and moments on the fuselage. This means that interaction of disc tilt modes with fuselage modes is neglected and the coning angle (β_0), longitudinal flapping angle (β_{1C}) and lateral flapping angle (β_{1S}) are determined solely through algebraic relationships.

The justification for this simplification is that blade flapping dynamics have a negligible effect on stability, control and handling qualities since the frequency separation between the rotor modes and overall fuselage rigid body modes is high and that the coupling between them is small.

For an eleventh order model, β_0, β_{1C} and β_{1S} are retained as degrees of freedom while the fourteenth order model also includes their derivatives $\dot{\beta}_0$, $\dot{\beta}_{1C}$ and $\dot{\beta}_{1S}$ as degrees of freedom. The other two main assumptions used in modelling the blade dynamics are that coupling effects from blade pitch and lag dynamics into flapping motion are neglected and that blade flapping is simulated by using a centre–spring equivalent rotor with flapping stiffness spring constant K_β, the value of which is chosen to give the same rotating and non–rotating flapping frequencies as those of the true blade.

In Padfield, 1981, the validity of this centre–spring approximation for articulated and hingeless rotors is discussed and it is established that an equivalent centre–spring model can be defined for both types of rotor through stiffness and inertia matching.

These assumptions, along with those for blade kinematics and aerodynamics, facilitate expressions to be formulated for the main rotor forces and moments which can be stated as:

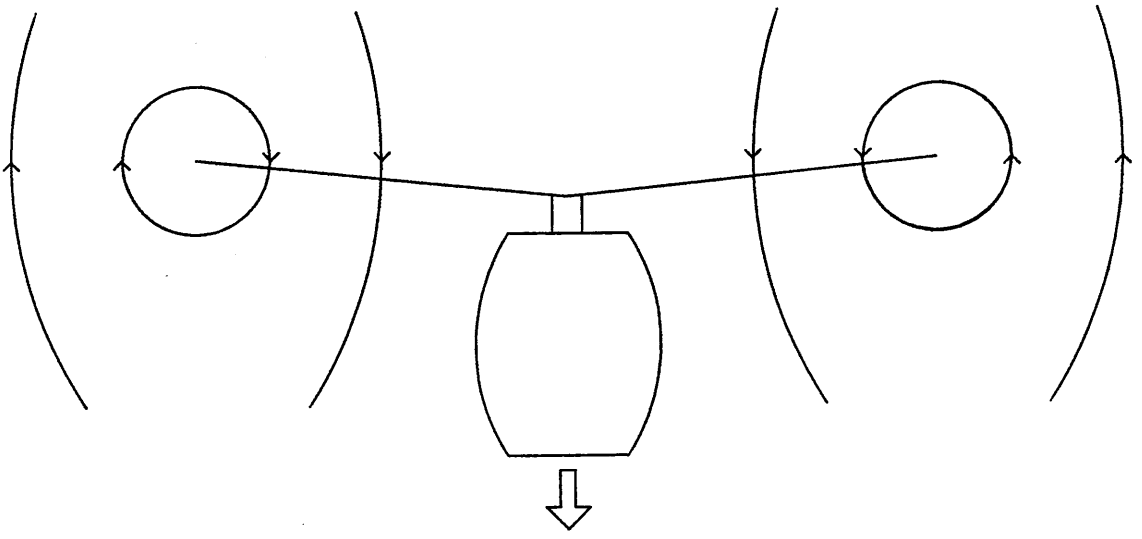

FIG 2.13 AIRFLOW PATTERN IN VORTEX RING STATE

$$\begin{bmatrix} X_R \\ Y_R \\ Z_R \end{bmatrix} = \begin{bmatrix} \cos\gamma_s & 0 & -\sin\gamma_s \\ 0 & 1 & 0 \\ \sin\gamma_s & 0 & \cos\gamma_s \end{bmatrix} \begin{bmatrix} \frac{1}{2}\rho\pi R^2(\Omega R)^2 a_0 s\left[\frac{2C_X}{a_0 s}\right] \\ \frac{1}{2}\rho\pi R^2(\Omega R)^2 a_0 s\left[\frac{2C_Y}{a_0 s}\right] \\ \frac{1}{2}\rho\pi R^2(\Omega R)^2 a_0 s\left[\frac{2C_Z}{a_0 s}\right] \end{bmatrix} \quad (2.13)$$

where the first matrix on the right–hand side of the equation is a transformation matrix which transforms the rotor forces from shaft–hub axes to body axes.

$$\left.\begin{aligned} L_R &= -\frac{b}{2} K_\beta \beta_{1s} + h_R Y_R \\ M_R &= -\frac{b}{2} K_\beta \beta_{1c} + x_{cg} Z_R - h_R X_R \\ N_R &= \tfrac{1}{2}\rho(\Omega R)^2 \pi R^3 a_0 s\left[\frac{2C_Q}{a_0 s} + \left[\frac{2I_R}{bI_\beta}\right]\frac{\bar{\Omega}'}{\gamma}\right] - x_{cg} Y_R \\ \text{Where} \quad \bar{\Omega}' &= \frac{\dot{\Omega}}{\Omega^2} \quad \text{and} \quad \gamma = \frac{\rho c a_0 R^4}{I_\beta} \end{aligned}\right\} \quad (2.14)$$

2.6.2 FORCES AND MOMENTS OF FUSELAGE, EMPENNAGE AND TAIL ROTOR

Due to the interaction of the main rotor wake with the fuselage, fin and tailplane and the complex flow patterns around them, it proved difficult to formulate analytic expressions for force and moment contributions from these elements. For these reasons, empirical wind tunnel data has been used to formulate piece–wise, linear relationships between aerodynamic coefficients and angles of attack and sideslip.

Fuselage aerodynamic force functions $C_{YFN}(\beta_{FN})$, $C_{XF}(\alpha_F)$, $C_{ZF}(\alpha_F)$ and fuselage aerodynamic moment functions $C_{NFA}(\beta_F)$, $C_{NFB}(\beta_F)$, $C_{MF}(\alpha_F)$ are shown in *fig 2.12* in the top–left hand corner and the bottom–right hand corner, respectively. α_F and β_F are the fuselage angles of incidence and sideslip and β_{FN} is the fin sideslip angle. The segmented appearance of these is due, in general, to distinct changes in the character of the flow field, eg. 'lift' forces associated with attached flow at low incidence producing destabilising moments followed by flow breakdown and separation at moderate incidences with stabilising moments.

FUSELAGE FORCES AND MOMENTS

Force and moment coefficients of the fuselage are referred to rotor disc area and radius, whilst those of the fin and tailplane are referred to their respective areas, S_{TP} and S_{FN}, and their distances to the centre of gravity : $(l_{TP}+x_{cg})$ and $(l_{FN}+x_{cg})$. The fuselage rolling moment L_F, is assumed to be zero.

$$\left.\begin{aligned} X_F &= \tfrac{1}{2}\rho(\Omega R)^2 S_p \bar{V}_F^2 [\, C_{XF}(\alpha_F)\,] \\ Y_F &= \tfrac{1}{2}\rho(\Omega R)^2 S_s \bar{V}_F^2 C_{YS} \frac{v_A}{V_F} \\ Z_F &= \tfrac{1}{2}\rho(\Omega R)^2 S_p \bar{V}_F^2 [\, C_{ZF}(\alpha_F)\,] \end{aligned}\right\} \qquad (2.15)$$

$$\left.\begin{aligned} L_F &= 0 \\ M_F &= \tfrac{1}{2}\rho(\Omega R)^2 S_p l_F \bar{V}_F^2 [\, C_{MF}(\alpha_F)\,] \\ N_F &= \tfrac{1}{2}\rho(\Omega R)^2 S_s l_F \bar{V}_F^2 [\, C_{NF}(\beta_F)\,] \end{aligned}\right\} \qquad (2.16)$$

where, in the expression for N_F, $C_{NFA}(\beta_F)$ is used for forward flight and $C_{NFB}(\beta_F)$ is used for rearward flight.

TAILPLANE FORCES AND MOMENTS

The tailplane is assumed to contribute a normal force along the body z– axis only, therefore the external forces are,

$$Z_{TP} = \tfrac{1}{2}\rho(\Omega R)^2 \bar{V}_T^2 S_{TP} [\, C_{ZTP}(\alpha_{TP})\,] \qquad (2.17)$$

and

$$X_{TP} = Y_{TP} = 0 \qquad (2.18)$$

where the coefficient $C_{ZTP}(\alpha_{TP})$ is effectively a function of the lift curve slope and the effect of the main rotor wake impinging on the tailplane is incorporated in terms $\bar{V}_T$ and α_{TP}.

The moment produced by force Z_{TP} is,

$$M_{TP} = (l_{TP} + x_{cg})Z_{TP} \tag{2.19}$$

and

$$L_{TP} = N_{TP} = 0 \tag{2.20}$$

FIN FORCES AND MOMENTS

A normal force only along the body y– axis is assumed and can be written as,

$$Y_{FN} = \tfrac{1}{2}\rho(\Omega R)^2 \bar{V}_{FN}^2 S_{FN}[\, C_{YFN}(\beta_{FN})\,] \tag{2.21}$$

and

$$X_{FN} = Z_{FN} = 0 \tag{2.22}$$

The moments produced by force Y_{FN} are given by,

$$\left.\begin{aligned} L_{FN} &= h_{FN} Y_{FN} \\ M_{FN} &= 0 \\ N_{FN} &= -(l_{FN} + x_{cg})Y_{FN} \end{aligned}\right\} \tag{2.23}$$

TAIL ROTOR FORCES AND MOMENTS

The thrust of the tail rotor is calculated in a similar manner to the main rotor, but without the inclusion of flapping terms, since rotor thrust is assumed to be independent of blade flapping. It is also small compared to the thrust produced by the main rotor and therefore drag and sideforce from the tail rotor blades is neglected.

The induced downwash at the tail rotor from the main rotor is taken to be the uniform induced velocity, λ_0, multiplied by a set factor $K_{\lambda T}$. An empirical fin blockage factor, F_T, is included to account for the presence of the fin and results in a decrease in the achieved tail rotor thrust. Reduction in tail rotor collective pitch due to coning is also modelled.

A sideforce on the helicopter is produced by the tail rotor thrust, and is given by,

$$Y_T = \tfrac{1}{2}\rho(\Omega_T R_T)^2 a_{0T} s_T \pi R_T^2 \left[\frac{2C_{TT}}{a_{0T} s_T} \right] F_T \tag{2.24}$$

and this produces two moments,

$$\left.\begin{aligned} L_T &= h_T Y_T \\ N_T &= -(l_T + x_{cg}) Y_T \end{aligned}\right\} \tag{2.25}$$

All other tail rotor forces and moments are assumed to be zero:

$$X_T = Z_T = 0 \tag{2.26}$$

$$M_T = 0 \tag{2.27}$$

2.6.3 EXTERNAL FORCES AND MOMENTS USED BY HELISTAB

From the above analysis of the external forces (X,Y,Z) and moments (L,M,N) of the main rotor (R), tail totor (T), tailplane (TP), fin (FN) and fuselage (F), it is obvious that equations 2.9 and 2.10 can be rewritten to take account of the forces and moments which are assumed to be zero. Thus,

$$\left.\begin{aligned} X &= X_R + X_F \\ Y &= Y_R + Y_T + Y_{FN} + Y_F \\ Z &= Z_R + Z_{TP} + Z_F \end{aligned}\right\} \tag{2.28}$$

$$\left.\begin{aligned} L &= L_R + L_T + L_{FN} \\ M &= M_R + M_{TP} + M_F \\ N &= N_R + N_T + N_{FN} + N_F \end{aligned}\right\} \tag{2.29}$$

2.7 MODEL LIMITATIONS

The theoretical model contained within the software package HELISTAB was derived for flight mechanics studies, and in particular, for the investigation of handling qualities using a real–time, piloted, ground based simulator. Although confidence in the model, over a range of flight conditions, has been encouraged by comparison with actual flight data, limitations have been identified: notably in the deficient modelling of hingeless rotors, and fuselage and empennage aerodynamic characteristics.

Aerodynamic force and moment coefficients of the fuselage are given as empirical functions of the incidence angles and are determined from wind tunnel data, whilst those of the tailplane and fin are derived using two–dimensional aerodynamic theory. In both these cases the coefficients are only accurate over a limited range :

$$-20° < \alpha, \beta < +20°$$

Outside these limits the functions increase or decrease rapidly – behaviour which is not consistent with a real helicopter where the flow would be expected to separate from the fuselage. The flow pattern in these circumstances is obviously extremely difficult to predict due to the downwash from the main rotor. The fin and tailplane coefficients are also likely to be inaccurate outside the above limits since their surfaces will probably have entered the stall region. In addition, the downwash effects on the tailplane from the main rotor are not modelled and this leads to poor prediction of the tailplane pitching moment and thus inaccuracies in the calculation of the pitch attitude.

Other factors requiring attention include,

- Inability to model vortex ring conditions at low speed and steep descent angles: an area of the flight envelope in which all types of helicopter could potentially be very effective.

- Effects of non–uniform inflow, derived from momentum theory, on rotor moment derivatives.

- Local non–linear aerodynamics determined on individual blades eg. blade stall effects, more complex representation of blade dynamics and improved modelling of the rotor wake and flow around the fuselage and empennage.

- Influence of engine/rotor dynamic couplings on flying qualities.

At present the model is being continually improved as studies of the aerodynamics and dynamics reveals new information which leads to a greater insight into the problems involved. In particular work by Black, Murray–Smith and Padfield, 1986; Black, 1987 and Black and Murray–Smith, 1989, into frequency domain parameter identification techniques has produced promising results. *Fig 2.14*, for example, gives a comparison of measured and predicted time responses for a pedal doublet input to the Puma at 100 Knots.

However, despite these improvements many problems remain which, as will be discussed in later chapters, causes serious problems in the application of observers for estimation and sensor fault detection. Nevertheless it has still proved invaluable in the course of this research.

2.8 LINEARIZING THE EQUATIONS OF MOTION

In order to apply the theory of chapter three it is first necessary to obtain the linearized state–space matrices A and B for any desired flight condition. The section of HELISTAB used for this purpose is the routine for calculating the helicopter's trim state. This routine calculates the trim attitude and rotor conditions for a given steady flight state by setting the acceleration terms in the equations of motion (2.6 and 2.7) to zero and solving the resultant six non–linear equations.

As discussed in section 2.4 the first step in the linearization process is the definition of a reference trim state and it is the rectilinear flight state (denoted by the subscript '$_0$') which is selected. Since the trimmed condition implies zero translational and rotational accelerations this gives –

$$p_0 = q_0 = r_0 \tag{2.30}$$

$$\left.\begin{aligned} \dot{u} = 0 &= X_0 - mg\sin\theta_0 \\ \dot{v} = 0 &= Y_0 + mg\cos\theta_0\sin\varphi_0 \\ \dot{w} = 0 &= Z_0 + mg\cos\theta_0\cos\varphi_0 \\ L_0 = M_0 &= N_0 = 0 \end{aligned}\right\} \tag{2.31}$$

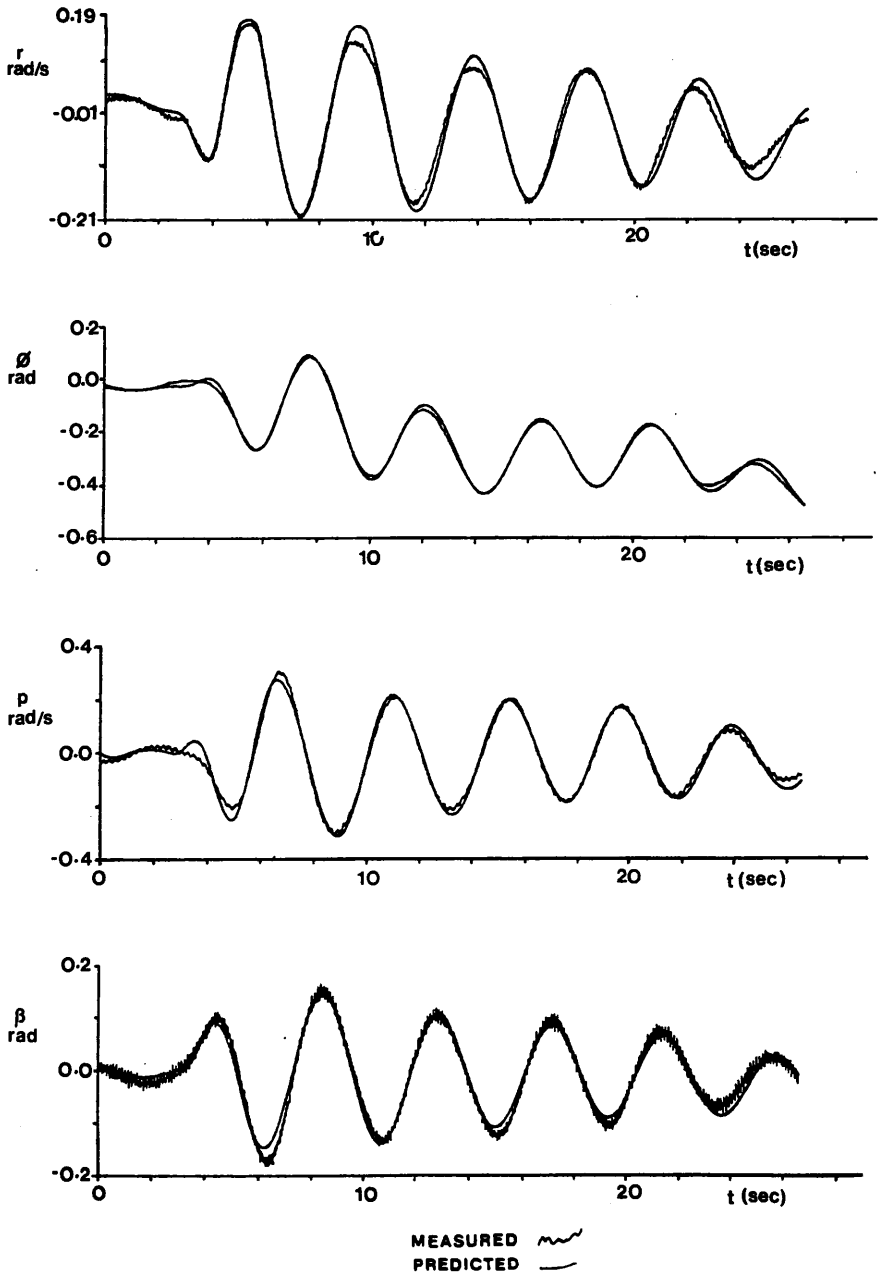

FIG 2.14 COMPARISON OF MEASURED AND PREDICTED TIME RESPONSES (FROM [B6])

The non-linear equations of motion (2.6, 2.7 and 2.8) can then be linearized as follows,

(1) Replace total values by a nominal value (subscript '$_0$' since this is the rectilinear trim state) plus a perturbation, eg

$$u = u_0 + u \qquad X = X_0 + X$$

(2) Expand resulting equations making small angle assumptions (ie. for general small angle ξ, $\cos\xi = 1$; $\sin\xi = \xi$) and neglecting products of perturbations.

(3) Express the external forces and moments as a standard Taylor series, eg.

$$X = X_0 + \frac{\partial X}{\partial u} u + \frac{\partial X}{\partial w} w + \ldots\ldots + \frac{\partial X}{\partial r} r + \frac{\partial X}{\partial \theta_{0e}} \theta_{0e} + \ldots\ldots + \frac{\partial X}{\partial \theta_{0t}} \theta_{0t}$$

and substitute using equations 2.31

Appendix 1 contains full details of this linearization process which results in the A and B state matrices shown at the end of this chapter.

If the state variables are then redefined as the perturbations from the reference state, then the linearized equations of motion can be written in the form,

$$\dot{\underline{x}} = A\underline{x} + B\underline{u}$$

where

$$\underline{x} = \begin{bmatrix} u \\ w \\ q \\ \theta \\ v \\ p \\ \varphi \\ r \end{bmatrix} \qquad \underline{u} = \begin{bmatrix} \theta_{0e} \\ \theta_{1s} \\ \theta_{1c} \\ \theta_{0t} \end{bmatrix}$$

A : System Matrix

B : Control Matrix

A MATRIX

	u	w	q	θ	v	p	φ	r
X	$\frac{\partial X}{\partial u}$	$\frac{\partial X}{\partial w}$	$\frac{\partial X}{\partial q} - w_0$	$\frac{\partial X}{\partial \theta} - g\cos\theta_0$	$\frac{\partial X}{\partial v}$	$\frac{\partial X}{\partial p}$	$\frac{\partial X}{\partial \varphi}$	$\frac{\partial X}{\partial r} + v_0$
Z	$\frac{\partial Z}{\partial u}$	$\frac{\partial Z}{\partial w}$	$\frac{\partial Z}{\partial q} + u_0$	$\frac{\partial Z}{\partial \theta} - g\cos\varphi_0\sin\theta_0$	$\frac{\partial Z}{\partial v}$	$\frac{\partial Z}{\partial p} - v_0$	$\frac{\partial Z}{\partial \varphi} - g\sin\varphi_0\cos\theta_0$	$\frac{\partial Z}{\partial r}$
M	$\frac{\partial M}{\partial u}$	$\frac{\partial M}{\partial w}$	$\frac{\partial M}{\partial q}$	$\frac{\partial M}{\partial \theta}$	$\frac{\partial M}{\partial v}$	$\frac{\partial M}{\partial p}$	$\frac{\partial M}{\partial \varphi}$	$\frac{\partial M}{\partial r}$
θ	0	0	$\cos\varphi_0$	0	0	0	0	$-\sin\varphi_0$
Y	$\frac{\partial Y}{\partial u}$	$\frac{\partial Y}{\partial w}$	$\frac{\partial Y}{\partial q}$	$\frac{\partial Y}{\partial \theta} - g\sin\varphi_0\sin\theta_0$	$\frac{\partial Y}{\partial v}$	$\frac{\partial Y}{\partial p} + w_0$	$\frac{\partial Y}{\partial \varphi} + g\cos\varphi_0\cos\theta_0$	$\frac{\partial Y}{\partial r} - u_0$
L	$\frac{\partial L}{\partial u} + i\frac{\partial N}{\partial u}$	$\frac{\partial L}{\partial w} + i\frac{\partial N}{\partial w}$	$\frac{\partial L}{\partial q} + i\frac{\partial N}{\partial q}$	$\frac{\partial L}{\partial \theta} + i\frac{\partial N}{\partial \theta}$	$\frac{\partial L}{\partial v} + i\frac{\partial N}{\partial v}$	$\frac{\partial L}{\partial p} + i\frac{\partial N}{\partial p}$	$\frac{\partial L}{\partial \varphi} + i\frac{\partial N}{\partial \varphi}$	$\frac{\partial L}{\partial r} + i\frac{\partial N}{\partial r}$
φ	0	0	$\sin\varphi_0\tan\theta_0$	0	0	1	0	$\cos\varphi_0\tan\theta_0$
N	$\frac{\partial N}{\partial u} + j\frac{\partial L}{\partial u}$	$\frac{\partial N}{\partial w} + j\frac{\partial L}{\partial w}$	$\frac{\partial N}{\partial q} + j\frac{\partial L}{\partial q}$	$\frac{\partial N}{\partial \theta} + j\frac{\partial L}{\partial \theta}$	$\frac{\partial N}{\partial v} + j\frac{\partial L}{\partial v}$	$\frac{\partial N}{\partial p} + j\frac{\partial L}{\partial p}$	$\frac{\partial N}{\partial \varphi} + j\frac{\partial L}{\partial \varphi}$	$\frac{\partial N}{\partial r} + j\frac{\partial L}{\partial r}$

B MATRIX

$$
\begin{array}{c}
 \\
X \\
Z \\
M \\
\theta \\
Y \\
L \\
\varphi \\
N
\end{array}
\begin{bmatrix}
\theta_{0e} & \theta_{1s} & \theta_{1c} & \theta_{0t} \\
\frac{\partial X}{\partial \theta_{0e}} & \frac{\partial X}{\partial \theta_{1s}} & \frac{\partial X}{\partial \theta_{1c}} & \frac{\partial X}{\partial \theta_{0t}} \\
\frac{\partial Z}{\partial \theta_{0e}} & \frac{\partial Z}{\partial \theta_{1s}} & \frac{\partial Z}{\partial \theta_{1c}} & \frac{\partial Z}{\partial \theta_{0t}} \\
\frac{\partial M}{\partial \theta_{0e}} & \frac{\partial M}{\partial \theta_{1s}} & \frac{\partial M}{\partial \theta_{1c}} & \frac{\partial M}{\partial \theta_{0t}} \\
0 & 0 & 0 & 0 \\
\frac{\partial Y}{\partial \theta_{0e}} & \frac{\partial Y}{\partial \theta_{1s}} & \frac{\partial Y}{\partial \theta_{1c}} & \frac{\partial Y}{\partial \theta_{0t}} \\
\frac{\partial L}{\partial \theta_{0e}} + i\frac{\partial N}{\partial \theta_{0e}} & \frac{\partial L}{\partial \theta_{1s}} + i\frac{\partial N}{\partial \theta_{1s}} & \frac{\partial L}{\partial \theta_{1c}} + i\frac{\partial N}{\partial \theta_{1c}} & \frac{\partial L}{\partial \theta_{0t}} + i\frac{\partial N}{\partial \theta_{0t}} \\
0 & 0 & 0 & 0 \\
\frac{\partial N}{\partial \theta_{0e}} + j\frac{\partial L}{\partial \theta_{0e}} & \frac{\partial N}{\partial \theta_{1s}} + j\frac{\partial L}{\partial \theta_{1s}} & \frac{\partial N}{\partial \theta_{1c}} + j\frac{\partial L}{\partial \theta_{1c}} & \frac{\partial N}{\partial \theta_{0t}} + j\frac{\partial L}{\partial \theta_{0t}}
\end{bmatrix}
$$

NOTES

The following points relate to both the A and B matrices.

(1) The partial derivatives in rows X,Y and Z should be multiplied by the factor : $\frac{1}{m}$

(2) Row M should be multiplied by the factor : $\frac{1}{I_{yy}}$

(3) $i = \frac{I_{xz}}{Izz}$

(4) $j = \frac{I_{xz}}{I_{xx}}$

In Helistab the partial derivatives are calculated by numerical differentiation which has the added advantage of simplifying the task of changing the model since only the expressions for forces and moments require alteration.

2.9 TIME RESPONSES

HELISTAB enables the user to define a control input from which it will determine the helicopter's time response. This is accomplished as follows,

(1) Pilot control inputs θ_{0e}, θ_{1s}, θ_{1c} and θ_{0t} are defined as functions of time.

(2) External forces and moments and the gravitational force components are calculated at time t.

(3) The resulting nine simultaneous non–linear, ordinary, differential equations (2.6, 2.7 and 2.8) are solved from time t to $t+\delta$, to obtain the helicopter's body axis, translational and rotational velocities and attitude

$$[\ u\ w\ q\ \theta\ v\ p\ \varphi\ r\ \psi\ ]^T$$

(4) Component velocities in earth–fixed axes can then be determined by transformation through the Euler angles.

(5) Finally position in earth–fixed axes are calculated by integration of the earth–axis velocities.

CHAPTER THREE

THEORY

3.1 MULTIVARIABLE STATE SPACE DESCRIPTION

In keeping with modern control theory, time–domain techniques provide one widely used approach to the analysis and design of helicopter flight control systems since they may be utilised for non–linear, time varying, multivariable systems. In standard form, the linearised, dynamic equation for the helicopter is of the form,

$$\dot{\underset{\sim}{x}} = A\underset{\sim}{x} + B\underset{\sim}{u} \tag{3.1}$$

where A is the system matrix and of dimension (n×n); B the distribution matrix (n×m); $\underset{\sim}{x}$ the state vector (n×1) and $\underset{\sim}{u}$ (m×1) the input vector. For the time invariant case the solution of the state equation is (see for example CHEN, 1984)

$$\underset{\sim}{x}(t) = e^{At}\underset{\sim}{x}(0) + \int_0^t e^{A(t-\tau)}B\underset{\sim}{u}(\tau)\, d\tau \tag{3.2}$$

the transition matrix e^{At} being given by

$$e^{At} = L^{-1}[(sI - A)^{-1}] \tag{3.3}$$

where L is the Laplace operator; and hence $\underset{\sim}{x}(t)$ can be written as

$$\underset{\sim}{x}(t) = L^{-1}[(sI - A)^{-1}\underset{\sim}{x}(0)] + L^{-1}[(sI - A)^{-1}B\underset{\sim}{u}(s)] \tag{3.4}$$

The dynamics of the system, ie the eigenvalues, are therefore determined by the roots of the characteristic equation of matrix A,

$$|\lambda I - A| = 0 \tag{3.5}$$

eigenvalues with negative real parts giving rise to stable systems, whilst those with positive real parts lead to instability.

The output equation for the system of equation 3.1 can be defined as

$$\underset{\sim}{y} = C\underset{\sim}{x} \tag{3.6}$$

where C is the output matrix of dimension (p×n) and $\underset{\sim}{y}$ is the output vector of dimension (p×1). The resulting system is shown diagramatically in *fig 3.1.*

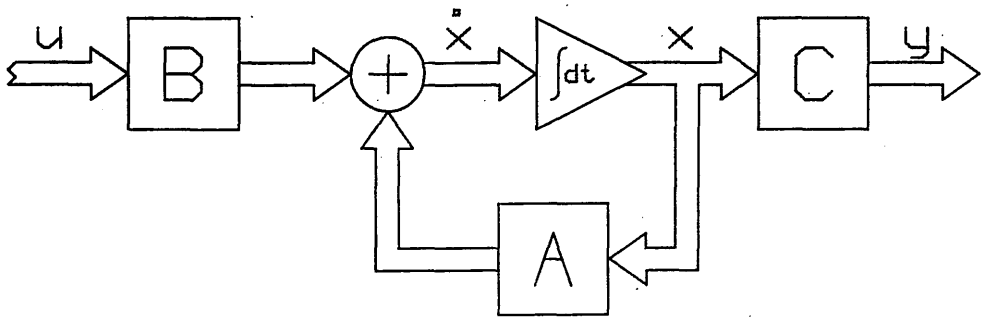

FIG 3.1 MULTIVARIABLE STATE SPACE DESCRIPTION

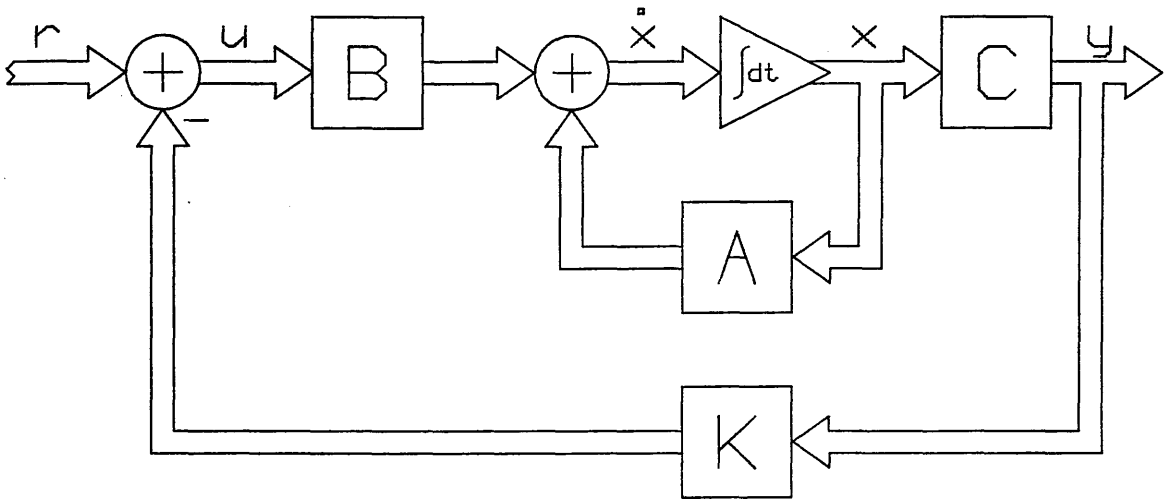

FIG 3.2 ADDITION OF FEEDBACK CONTROL LAW, K

NOTATION

x	STATE VECTOR	nx1
A	SYSTEM MATRIX	nxn
B	DISTRIBUTION MATRIX	nxm
u	INPUT/CONTROL VECTOR	mx1
y	OUTPUT VECTOR	px1
C	OUTPUT MATRIX	pxn
K	CONTROL MATRIX	mxp

3.2 WHY USE OBSERVERS ?

If a feedback control law K (m×n) is being used for an automatic flight control system (AFCS), then this may be represented by

$$\underset{\sim}{u} = -K\underset{\sim}{x} \tag{3.7}$$

however $\underset{\sim}{x}$ is not normally directly available and consequently the practical synthesis of the control law requires the use of (*fig 3.2*),

$$\underset{\sim}{u} = \underset{\sim}{f}-K\underset{\sim}{y} = \underset{\sim}{f}-KC\underset{\sim}{x} \tag{3.8}$$

Thus the entire state vector is usually required if the deduced control law is to be implemented. In practice however, not every state variable is accessible, either owing to failure of its sensor or because it cannot be measured. This is often the case in multi– lane systems where physical constraints often mean that it is not possible to have the same number of sensors as channels.

There are two possible solutions to the problem : use a control law design method which directly accounts for the unavailability of certain states or, more simply, to use an estimate of the state vector. A subsystem performing such observation of the state vector based on information received from the measurement of the input and the output of the system, is called a *state observer* or a *state estimator* and was first proposed by Luenberger, 1964 for deterministic systems; and by Kalman, 1960 for stochastic systems. (See also, for example, Aoki and Huddle, 1967; Newmann, 1970).

This thesis is concerned with the application of deterministic, continuous– time, linear, time– invariant system theory in the design of state observers and sensor fault detectors for a stochastic, non– linear, time– varying system: namely, the single rotor helicopter.

3.3 OBSERVABILITY OF LINEAR DYNAMICAL EQUATIONS

Rigid definitions for observability and controllability (which is the dual of observability), are comparatively recent, eg. Kalman, 1963; Gilbert, 1963. Simply stated a system is said to be observable if every state x(T) can be determined exactly from measurements of the outputs y(t), over a finite interval of time $0 \leqslant t \leqslant T$. The conditions for full observability may be stated mathematically as (Chen, 1984),

The n− dimensional linear, time invariant, dynamical equations of 3.1 and 3.6 are observable if and only if any of the following equivalent conditions is satisfied:

(1) All columns of Ce^{At} are linearly independent on $[0,\infty)$ over $\mathbb{C}$, the field of complex numbers.

All columns of $C(sI - A)^{-1}$ are linearly independent over $\mathbb{C}$.

(2) The *observability grammian*

$$W_{0t} \triangleq \int_0^t e^{A^*\tau} C^* C e^{A\tau} \, d\tau$$

where ' * ' indicates the complex conjugate transpose; is non− singular for all $t > 0$.

(3) The (np×n) *observability matrix*

$$V_2 = [\ C \ CA \ CA^2 \ \ldots\ldots \ CA^{n-1}\ ]^T \qquad (3.9)$$

has rank n.

(4) For every eigenvalue λ of A (and consequently for every λ in $\mathbb{C}$), the (n+ p×n) complex matrix

$$\begin{bmatrix} \lambda I - A \\ C \end{bmatrix}$$

has rank n, or equivalently, (sI− A) and C are right coprime.

The observability test given by (3) is the most common form and was the one used for this thesis. It is also used as a basis for canonical transformations as can be seen in section 3.7.

An important property of the observability and controllability of a linear, time invariant, dynamical equation is that they are invariant under any equivalence transformation.

3.3.1 OBSERVABILITY INDICES

Consider the observability matrix V_2, given by 3.9,

$$V_2 = \begin{bmatrix} C \\ CA \\ \vdots \\ CA^{n-1} \end{bmatrix} = \begin{bmatrix} C_1 \\ C_2 \\ \vdots \\ C_p \\ C_1A \\ C_2A \\ \vdots \\ C_pA \\ \vdots \\ C_1A^{n-1} \\ C_2A^{n-1} \\ \vdots \\ C_pA^{n-1} \end{bmatrix} \qquad (3.10)$$

Working from top to bottom, determine the linearly independent rows of V_2; that is, if a row can be written as a linear combination of the rows above it, the row is linearly dependent; otherwise, it is linearly independent. These independent rows are then arranged as,

$$[\ C_1\ C_1A\ \ldots\ C_1A^{\mu_1-1}\ C_2\ C_2A\ \ldots\ C_2A^{\mu_2-1}\ \ldots\ C_p\ \ldots\ C_pA^{\mu_p-1}\ ]^T \qquad (3.11)$$

The integer μ_i is the number of linearly independent rows associated with C_i, or the length of the *chain* associated with C_i. The *observability index* μ, of the pair [A,C] is then,

$$\mu = \max\ \{\ \mu_1, \mu_2, \ldots, \mu_p\ \} \qquad (3.12)$$

and

$$\mu_1 + \mu_2 + \ldots + \mu_p \leqslant n \qquad (3.13)$$

where the equality holds if pair [A,C] is observable. The set $\{\mu_1, \mu_2, \ldots, \mu_p\}$ are called the *observability indices* of [A,C] and their significance can be seen in section 3.7.

3.4 THE FULL ORDER OBSERVER

As shown by Luenberger, 1971, almost any system can be considered as an observer. If the available outputs of a free system S1, say, are used as inputs to drive another system S2, then the second system will almost always serve as an observer of the first system in the sense that its state will tend to track a linear transformation of the state of S1. This result forms the basis of observer theory and explains why there is a great deal of freedom in the design of an observer.

The heart of the observer is an accurate model of the system around which a feedback loop is added (*fig 3.3*). The aim is to subject this model to the same input as the plant and to make the model's output accurately follow the measured output of the plant. If,

- the model is accurate
- the inputs are the same, and
- the outputs are the same

then the intermediate state variables must also be the same.

Consider the system to be observed is in the form of linear equations 3.1 and 3.6,

$$\dot{\underset{\sim}{x}} = A\underset{\sim}{x} + B\underset{\sim}{u} \tag{3.1}$$

$$\underset{\sim}{y} = C\underset{\sim}{x} \tag{3.6}$$

where the system matrix A, distribution matrix B, output matrix C, input vector $\underset{\sim}{u}$, state vector $\underset{\sim}{x}$ and output vector $\underset{\sim}{y}$, are of dimensions (n×n), (n×m), (p×n), (m×1), (n×1) and (p×1), respectively. The equation governing the observer can then be written as:

$$\dot{\hat{\underset{\sim}{x}}} = A\hat{\underset{\sim}{x}} + B\underset{\sim}{u} + HC(\underset{\sim}{x} - \hat{\underset{\sim}{x}}) \tag{3.14}$$

where $\hat{\underset{\sim}{x}}$ is the state of the observer and hence the estimate of the system state $\underset{\sim}{x}$, and H is the (n×p) observer matrix. Define the error vector between the estimate of the state $\hat{\underset{\sim}{x}}$, and the true state $\underset{\sim}{x}$, as

$$\underset{\sim}{e} = \underset{\sim}{x} - \hat{\underset{\sim}{x}} \tag{3.15}$$

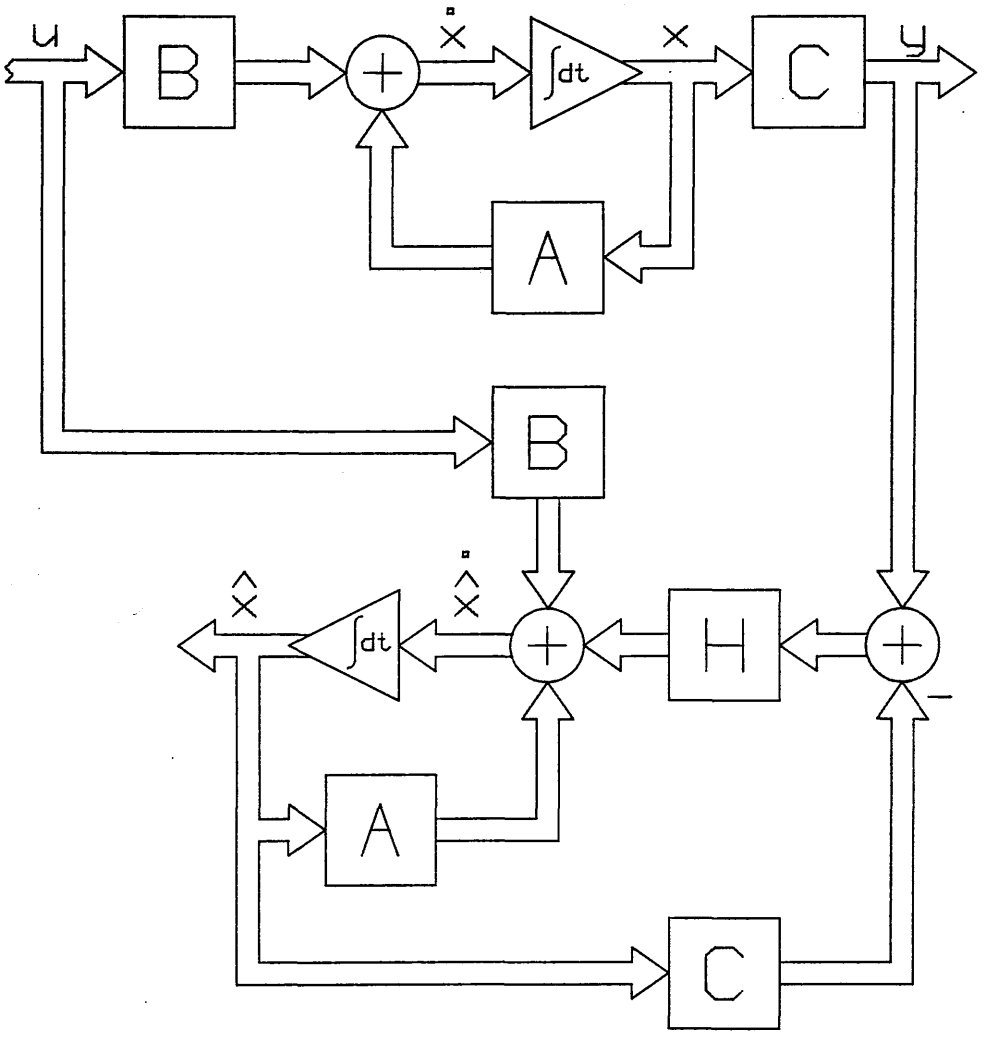

FIG 3.3 OBSERVER CONNECTED TO SYSTEM

and therefore the rate of change of this error is

$$\dot{\underset{\sim}{e}} = \dot{\underset{\sim}{x}} - \dot{\hat{\underset{\sim}{x}}} \tag{3.16}$$

Combining the system state equation 3.1, with the observer equation 3.14, yields,

$$\dot{\underset{\sim}{x}} - \dot{\hat{\underset{\sim}{x}}} = A\underset{\sim}{x} + B\underset{\sim}{u} - A\hat{\underset{\sim}{x}} - B\underset{\sim}{u} - HC(\underset{\sim}{x} - \hat{\underset{\sim}{x}})$$

$$= (A - HC)(\underset{\sim}{x} - \hat{\underset{\sim}{x}})$$

or

$$\dot{\underset{\sim}{e}} = (A - HC)\underset{\sim}{e} \tag{3.17}$$

This equation expresses the error dynamics $\dot{\underset{\sim}{e}}$, of the estimate in terms of the system matrix A, the output matrix C and the observer matrix H only, ie. the error dynamics are independent of the state $\underset{\sim}{x}$ and the input $\underset{\sim}{u}$.

Design of the observer therefore reduces to the problem of determining the matrix H, such that the composite matrix (A− HC) has some prescribed eigenvalues. Fortunately, as shown by O'Reilly, 1983, for example, given that [A,C] is observable the eigenvalues of (A− HC) can be arbitrarily assigned, provided complex conjugate eigenvalues appear in pairs.

Obviously the selection of H will be made such that the eigenvalues of the observer will be more negative than those of the system, so that the state of the observer will converge rapidly to the state of the observed system. Consequently, even if there is a large error between $\hat{\underset{\sim}{x}}(t_0)$ and $\underset{\sim}{x}(t_0)$ at initial time t_0, the vector $\hat{\underset{\sim}{x}}$ will approach $\underset{\sim}{x}$ rapidly.

Theoretically the eigenvalues can be moved arbitrarily towards minus infinity, yielding extremely rapid convergence, but in practice this tends to make the observer act like a differentiator and thereby become highly sensitive to noise, and to introduce other difficulties.

3.5 CLOSED LOOP PROPERTIES – USING A FEEDBACK CONTROLLER

Whatever the type of control employed, as far as the feedback of a measureable state vector is concerned, the closed loop properties of the system can be investigated, with particular emphasis on stability. However, if an observer is employed in order to obtain an estimate of the state vector, then the closed loop system is no longer dependent on the true state vector, but rather obtains characteristics from its estimated version (*fig 3.4*).

This raises three questions –

(1) In the state feedback $\underset{\sim}{u} = \underset{\sim}{r} + K\underset{\sim}{x}$, the eigenvalues of the resulting equation are given by the eigenvalues of $(A + BK)$. In the estimated state feedback $\underset{\sim}{u} = \underset{\sim}{r} + K\underset{\sim}{\hat{x}}$, are the eigenvalues the same?

(2) Will the eigenvalues of the state estimator be affected by the feedback $\underset{\sim}{u} = \underset{\sim}{r} + K\underset{\sim}{\hat{x}}$?

(3) What is the effect of the estimator on the transfer function matrix from $\underset{\sim}{r}$ to $\underset{\sim}{y}$?

To answer these questions consider the following system, with a controller using an observer to obtain an estimate of the state vector,

Control Law : $$\underset{\sim}{u} = \underset{\sim}{r} + K\underset{\sim}{\hat{x}} \tag{3.18}$$

System : $$\dot{\underset{\sim}{x}} = A\underset{\sim}{x} + B\underset{\sim}{u} \tag{3.1}$$

$$\underset{\sim}{y} = C\underset{\sim}{x} \tag{3.6}$$

Observer : $$\dot{\underset{\sim}{\hat{x}}} = A\underset{\sim}{\hat{x}} + B\underset{\sim}{u} + HC(\underset{\sim}{x} - \underset{\sim}{\hat{x}}) \tag{3.19}$$

Thus the closed loop system that results from the interconnection of the dynamic observer– based controller 3.18 and 3.19 to the open– loop system of 3.1 and 3.6, is described by the composite system

$$\dot{\underset{\sim}{x}} = A\underset{\sim}{x} + BK\underset{\sim}{\hat{x}} + B\underset{\sim}{r} \tag{3.20}$$

$$\dot{\underset{\sim}{\hat{x}}} = HC\underset{\sim}{x} + (A - HC + BK)\underset{\sim}{\hat{x}} + B\underset{\sim}{r} \tag{3.21}$$

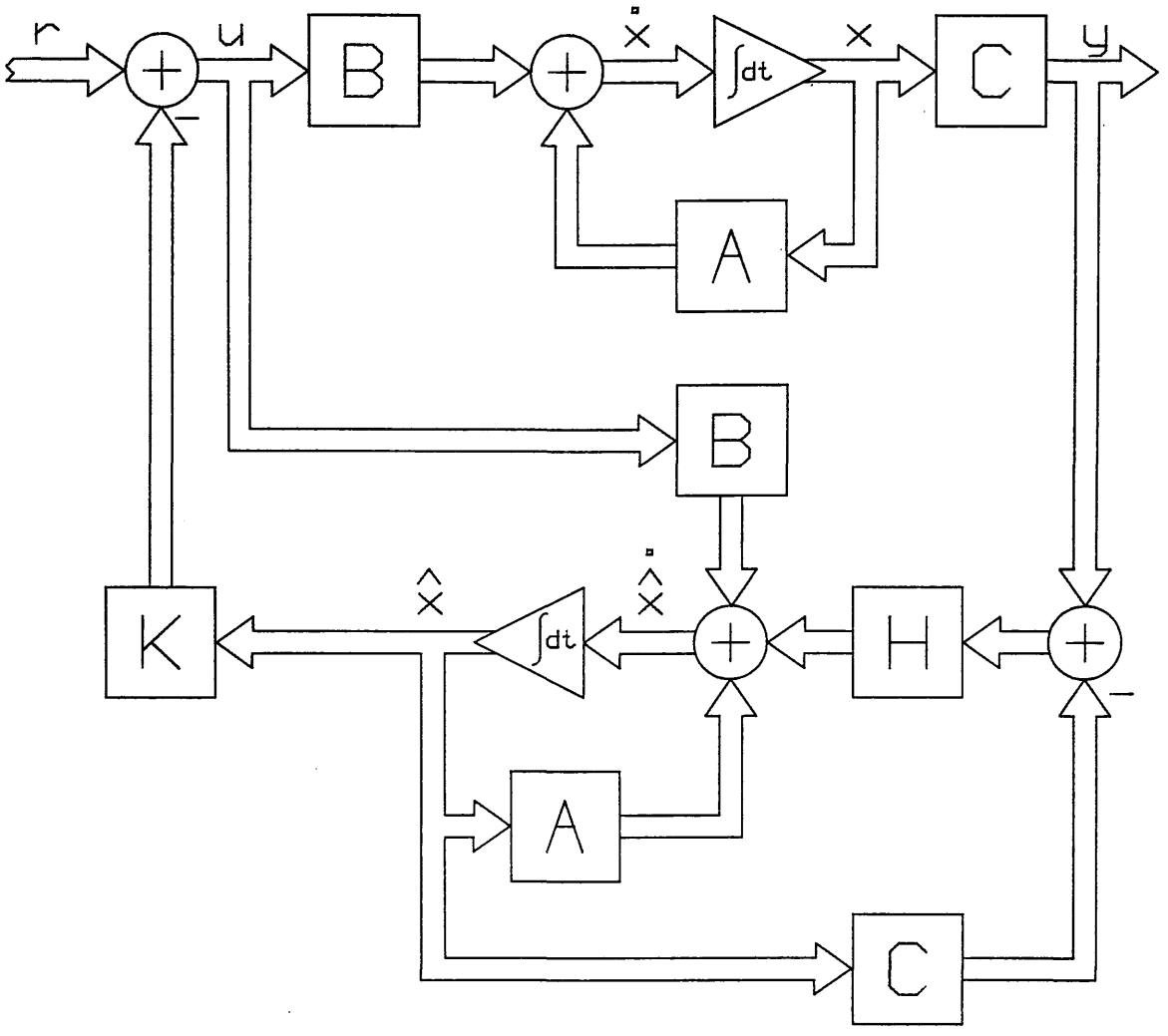

FIG 3.4 OBSERVER USED TO PROVIDE ESTIMATE OF STATE x FOR FEEDBACK CONTROL

or in matrix form,

$$\begin{bmatrix} \dot{\underset{\sim}{x}} \\ \dot{\hat{\underset{\sim}{x}}} \end{bmatrix} = \begin{bmatrix} A & BK \\ HC & A - HC + BK \end{bmatrix} \begin{bmatrix} \underset{\sim}{x} \\ \hat{\underset{\sim}{x}} \end{bmatrix} + \begin{bmatrix} B \\ B \end{bmatrix} \underset{\sim}{r} \tag{3.22}$$

By using the transformation

$$\begin{bmatrix} \underset{\sim}{x} \\ \underset{\sim}{e} \end{bmatrix} = \begin{bmatrix} I & 0 \\ I & -I \end{bmatrix} \begin{bmatrix} \underset{\sim}{x} \\ \hat{\underset{\sim}{x}} \end{bmatrix} \tag{3.23}$$

the system of 3.22 may be transformed to the composite system

$$\begin{bmatrix} \dot{\underset{\sim}{x}} \\ \dot{\underset{\sim}{e}} \end{bmatrix} = \begin{bmatrix} A + BK & -BK \\ 0 & A - HC \end{bmatrix} \begin{bmatrix} \underset{\sim}{x} \\ \underset{\sim}{e} \end{bmatrix} + \begin{bmatrix} B \\ 0 \end{bmatrix} \underset{\sim}{r} \tag{3.24}$$

The transformation between

$$\begin{bmatrix} \underset{\sim}{x} \\ \hat{\underset{\sim}{x}} \end{bmatrix} \text{ and } \begin{bmatrix} \underset{\sim}{x} \\ \underset{\sim}{e} \end{bmatrix}$$

is linear and non-singular so that the characteristic equation of the composite system 3.22, is exactly the same as that of 3.24, which is:

$$\det(\lambda I - A - BK) \times \det(\lambda I - A + HC) \tag{3.25}$$

Thus the eigenvalues of the total system 3.18, 3.1, 3.6 and 3.19 are the union of those of (A + BK) and those of (A − HC). The eigenvalues of the state are not affected by the feedback and, as far as the eigenvalues are concerned, there is no difference in state feedback from the estimated state $\hat{\underset{\sim}{x}}$ or from the actual state $\underset{\sim}{x}$.

Consequently, the design of a state feedback controller and the design of a state estimator can be carried out independently, the eigenvalues of the complete system being the union of those of state feedback and those of the state estimator. This is known as the *separation property*.

Finally, as shown by Chen, 1984, the transfer function matrix of the complete system is

$$G(s) = C(sI - A - BK)^{-1}B \tag{3.26}$$

which is the transfer function matrix of state feedback without the use of a state estimator. In other words, the estimator is completely cancelled and does not appear in the transfer function matrix from $\underset{\sim}{r}$ to $\underset{\sim}{y}$.

3.6 THE REDUCED ORDER OBSERVER

Section 3.4 dealt with observers of order n, ie of the same order as the system, however if C is assumed to be of full rank (this does not give any loss of generality) then it is clear that knowledge of $C\underset{\sim}{x}$ gives measurements on part of the state immediately; since

$$\underset{\sim}{y} = C\underset{\sim}{x} \tag{3.6}$$

gives the projection of $\underset{\sim}{x}$ on the row space of C. Hence it is possible to find the other component in the complement of the row space of C by making use of an observer of order $(n-p)$. This was first proved by Luenberger, 1964, and has been much published since, eg. Luenberger, 1971; Gopinath, 1971; O'Reilly, 1983.

Starting from the usual system equations

$$\dot{\underset{\sim}{x}} = A\underset{\sim}{x} + B\underset{\sim}{u} \tag{3.1}$$

$$\underset{\sim}{y} = C\underset{\sim}{x} \tag{3.6}$$

a change of basis is made ($\underset{\sim}{q} = R\underset{\sim}{x}$), such that C is of full rank and of the form

$$\tilde{C} = CR^{-1} = [0 \; I_p] \tag{3.27}$$

In the literature, the transformation is such that $\tilde{C}$ is of the form

$$\tilde{C} = [I_p \; 0] \tag{3.28}$$

However, if the canonical transformation of section 3.7.2 is used in designing an observer then the form of 3.27 is required. To obtain 3.28 Arbel and Tse, 1979 suggest the use of,

$$R = \left[\begin{array}{c:c} C_1 & C_2 \\ \hdashline 0 & I_{n-p} \end{array}\right] \tag{3.29}$$

where C_1, C_2, 0 and I_{n-p} are $(p\times p)$, $(p\times n-p)$, $(n-p\times p)$ and $(n-p\times n-p)$ matrices, respectively. It is a simple matter to demonstrate that the R matrix required to obtain 3.27 is,

$$R = \left[\begin{array}{c:c} 0 & I^*_{n-p} \\ \hdashline C_1 & C_2 \end{array}\right] \tag{3.30}$$

where the dimensions of C_1, C_2 and 0 are as above and I^*_{n-p} is the $(n-p\times n-p)$ matrix which has unity elements on the diagonal running from the bottom left-hand corner $(n-p,1)$ to the top right-hand corner $(1,n-p)$, and all other elements zero. I^*_1, ie the 1×1 matrix, is $[1]$.

The change of basis giving 3.27, transforms 3.1 and 3.6 to,

$$\dot{\underset{\sim}{q}} = \tilde{A}\underset{\sim}{q} + \tilde{B}\underset{\sim}{u} \tag{3.31}$$

$$\underset{\sim}{y} = \tilde{C}\underset{\sim}{q} \tag{3.32}$$

where $\underset{\sim}{q}$, $\tilde{A}$ and $\tilde{B}$ are partitioned as

$$\underset{\sim}{q} = \left[\begin{array}{c} \underset{\sim}{q}_1 \\ \hdashline \underset{\sim}{q}_2 \end{array}\right]\begin{array}{l} n-p\times 1 \\ p\times 1 \end{array} \tag{3.33}$$

$$\tilde{B} = RB = \left[\begin{array}{c} B_1 \\ \hdashline B_2 \end{array}\right]\begin{array}{l} n-p\times m \\ p\times m \end{array} \tag{3.34}$$

$$\tilde{A} = RAR^{-1} = \begin{array}{c} \begin{array}{cc} n-p\times n-p & \quad n-p\times p \end{array} \\ \left[\begin{array}{c:c} A_{11} & A_{12} \\ \hdashline A_{21} & A_{22} \end{array}\right] \\ \begin{array}{cc} p\times n-p & \quad p\times p \end{array} \end{array} \tag{3.35}$$

Equation 3.31 can then be written in the form

$$\left.\begin{aligned} \dot{\underset{\sim}{q}}_1 &= A_{11}\underset{\sim}{q}_1 + A_{12}\underset{\sim}{q}_2 + B_1\underset{\sim}{u} \\ \dot{\underset{\sim}{q}}_2 &= A_{21}\underset{\sim}{q}_1 + A_{22}\underset{\sim}{q}_2 + B_2\underset{\sim}{u} \end{aligned}\right\} \qquad (3.36)$$

$$\therefore \quad A_{21}\underset{\sim}{q}_1 = \dot{\underset{\sim}{q}}_2 - A_{22}\underset{\sim}{q}_2 - B_2\underset{\sim}{u} \qquad (3.37)$$

Defining the observer equation as

$$\dot{\underset{\sim}{z}} = A_{12}\underset{\sim}{q}_2 + A_{11}\underset{\sim}{z} + B_1\underset{\sim}{u} + HA_{21}(\underset{\sim}{q}_1 - \underset{\sim}{z}) \qquad (3.38)$$

and the error term

$$\underset{\sim}{e} = \underset{\sim}{q}_1 - \underset{\sim}{z} \qquad (3.39)$$

then

$$\dot{\underset{\sim}{e}} = (A_{11} - HA_{21})\underset{\sim}{e} \qquad (3.40)$$

Thus by choosing H appropriately, $\underset{\sim}{e}$ will rapidly tend to zero (c.f equation 3.17). The ability to arbitrarily place the eigenvalues is ensured by the observability of the pair $[A_{11},A_{21}]$ since the pair [A,C] is observable if and only if $[A_{11},A_{21}]$ is observable (Luenberger, 1971).

Now in equation 3.38, the term $(\underset{\sim}{q}_1 - \underset{\sim}{z})$ is not directly available and thus 3.37 is used and $H\dot{\underset{\sim}{q}}_2$ is subsequently replaced with $[A_{11} - HA_{21}]H\underset{\sim}{q}_2$ to obtain the final reduced order observer equations (shown diagramatically in *fig 3.5*):

$$\dot{\underset{\sim}{z}} = [A_{11}-HA_{21}]\underset{\sim}{z} + [A_{12}-HA_{22} + (A_{11}-HA_{21})H]\underset{\sim}{q}_2 + [B_1-HB_2]\underset{\sim}{u} \qquad (3.41)$$

$$\hat{\underset{\sim}{q}}_1 = \underset{\sim}{z} + H\underset{\sim}{q}_2 \qquad (3.42)$$

$$\hat{\underset{\sim}{q}} = \begin{bmatrix} \hat{\underset{\sim}{q}}_1 \\ \cdots \\ \underset{\sim}{q}_2 \end{bmatrix} \qquad (3.43) \qquad\qquad \hat{\underset{\sim}{x}} = R^{-1}\hat{\underset{\sim}{q}} \qquad (3.44)$$

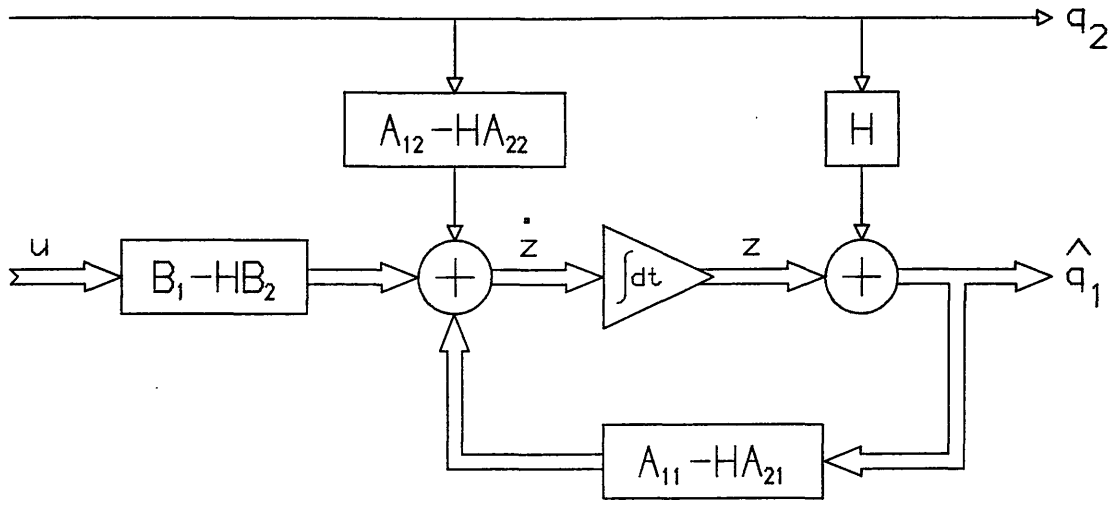

FIG 3.5 THE REDUCED ORDER OBSERVER

For instrument fault detection (chapter 7), the most frequently used C matrix is the row vector of dimension n, with only one non−zero (usually unity) element. However, in general, the transformation matrices given by 3.29 and 3.30 are singular for this form of C matrix. Fortunately, by a process of deduction, it was possible to deduce a relatively simple algorithm which produces transformation matrices R and R^{-1} for any C matrix which is a row vector of order n, ie. not just the specific case of only one non−zero element. This algorithm is given in Appendix 2 in the form of a FORTRAN computer program.

3.7 CANONICAL FORMS

Canonical forms for multivariable systems are, in general, not unique, but their structure can be controlled to some extent by their designer. There are many papers dealing with the problem of obtaining particular canonical forms (eg Luenberger, 1967; Jordan and Sridhar, 1973; Aplevich, 1974; Tuel, Chidambara, Rane, Mufti and Johnson, 1966), but the treatment given here deals with *observable canonical forms* (Chen, 1984; O'Reilly, 1983).

It was shown in section 3.3 that the observability of a system could be determined from the rank of

$$V_2 = [\ C\ CA\ \ldots\ CA^{n-1}\ ]^T \tag{3.9}$$

Equivalently, it can also be determined from

$$V = [\ C^T\ A^TC^T\ \ldots\ (A^T)^{n-1}C^T\ ] \tag{3.45}$$

The dimensions of V_2 and V are (np×n) and (n×np) and should be of rank n for observability.

Controllability of a system is dual to observability and a system is said to be controllable if either of the following two composite matrices are of rank n:

$$Q = [\ B\ AB\ \ldots\ A^{n-1}B\ ] \tag{3.46}$$

$$Q_2 = [\ B^T\ B^TA^T\ \ldots\ B^T(A^T)^{n-1}\ ]^T \tag{3.47}$$

Where Q and Q_2 have dimensions (n×nm) and (nm×n).

3.7.1 SELECTION OF LINEARLY INDEPENDENT VECTORS

The first step in the development of a canonical form of the class required is the selection of n linearly independent (LIN) vectors from the rows or columns of the defined observability (or controllability) matrices. The n LIN vectors chosen will form rows (V_2 and Q_2) or columns (V and Q) of a matrix P of form (stated here for V_2)

$$P = [\ C_1, C_1A, \ldots, C_1A^{\mu_1-1}, C_2, C_2A, \ldots, C_2A^{\mu_2-1}, C_3, \ldots, C_pA^{\mu_p-1}\ ]^T \qquad (3.48)$$

where the μ_i's are the observability indices defined in section 3.3.1

The essential restriction is that no vector of the form C_jA^k is selected unless all lower powers of A, multiplied by C_j are also selected, since if C_lA^m is linearly dependent then so are all vectors of form $C_lA^{m+\alpha}$, for $[\alpha = 1, 2, 3 \ldots]$. For the sake of simplicity and illustration, the following analysis assumes the use of observability matrix V_2.

Two methods of selection are of interest here,

(1) Select in the sequence

$$C_1,\ C_1A,\ C_1A^2, \ldots$$

where C_i is the i^{th} row of C; until either C_1A^{n-1} is obtained, in which case the system is completely observable from the first output alone, or until a dependency arises. If more independent vectors are required then select from:

$$C_2,\ C_2A,\ C_2A^2, \ldots$$

until a dependency arises. The procedure continues in this manner until a set of n LIN vectors are obtained, and the tendency is to develop a few long *chains*.

(2) Select in the sequence

$$C_1,\ C_2,\ \ldots\ C_p,\ C_1A,\ C_2A,\ \ldots\ C_pA,\ C_1A^2,\ \ldots.\ C_pA^{n-1}$$

The tendency with this method is to produce several chains of nearly equal length.

There are numerous other methods of selecting n LIN vectors, which is why canonical forms are not unique, but the above procedures are sufficient to produce two interesting and very useful forms. these are:

Observable Canonical Form

$$\tilde{A} = SAS^{-1} = \begin{bmatrix} \begin{matrix} 0 & 0 & \dots & x \\ 1 & 0 & \dots & x \\ 0 & 1 & \dots & x \\ \vdots & & & \vdots \\ 0 & \dots & 1 & x \end{matrix} & \begin{matrix} & & x \\ & & x \\ & & x \\ & & \vdots \\ & & x \end{matrix} & \begin{matrix} & & x \\ & & x \\ & & x \\ & & \vdots \\ & & x \end{matrix} \\ \begin{matrix} (\mu_1 \times \mu_1) & & x \\ & & x \\ & & x \\ & & \vdots \\ & & x \end{matrix} & \begin{matrix} 0 & 0 & \dots & x \\ 1 & 0 & \dots & x \\ 0 & 1 & \dots & x \\ \vdots & & & \vdots \\ 0 & \dots & 1 & x \end{matrix} & \begin{matrix} & & x \\ & & x \\ & & x \\ & & \vdots \\ & & x \end{matrix} \\ \begin{matrix} & & \\ & (\mu_2 \times \mu_2) & \\ & & \end{matrix} & & \begin{matrix} & & \\ & & \\ & & \\ & & \\ & & \end{matrix} \\ \begin{matrix} & & x \\ & & x \\ & & x \\ & & \vdots \\ & & x \end{matrix} & \begin{matrix} & & x \\ & & x \\ & & x \\ & & \vdots \\ & & x \end{matrix} & \begin{matrix} 0 & 0 & \dots & x \\ 1 & 0 & \dots & x \\ 0 & 1 & \dots & x \\ \vdots & & & \vdots \\ 0 & \dots & 1 & x \end{matrix} \\ & & (\mu_p \times \mu_p) \end{bmatrix} \qquad (3.49)$$

$$\tilde{C} = CS^{-1} = \begin{bmatrix} \begin{matrix} 0 & \dots & 1 \\ 0 & & x \\ \vdots & & \vdots \\ 0 & \dots & x \end{matrix} & \begin{matrix} 0 & \dots & 0 \\ 0 & \dots & 1 \\ \vdots & & \vdots \\ 0 & \dots & x \end{matrix} & \begin{matrix} & & 0 \\ & & 0 \\ & & \vdots \\ & & 1 \end{matrix} \end{bmatrix} \qquad (3.50)$$

$\tilde{B} = SB$ and has no special form.

The x's denote any number and in some circumstances are all zero.

Controllable Canonical Form

If the observable canonical form is denoted by the subscript 'o', then the controllable canonical form can be stated as,

$$\tilde{A} = [\ \tilde{A}_o\ ]^T \qquad \tilde{B} = [\ \tilde{C}_o\ ]^T \qquad \tilde{C} \text{ has no special form}$$

It is the observable canonical form which is most useful in the design of observers (see chapter 5) and the following algorithm was determined to produce this form from any observable pair [A,C].

3.7.2 ALGORITHM FOR OBSERVABLE CANONICAL FORM

(1) Select the n LIN vectors using method (2): this tends to produce several chains of nearly equal length. It also has the advantage (numerically) that it will involve smaller powers of A.

(2) Arrange these n LIN vectors to form the matrix P (equation 3.48). The observability indices μ_i, give the dimensions of the *blocks* on the main diagonal of the transformed A matrix.

$$P = [\ C_1, C_1A, \ldots, C_1A^{\mu_1-1}, C_2, C_2A, \ldots, C_2A^{\mu_2-1}, C_3, \ldots, C_pA^{\mu_p-1}\ ]^T$$

(3) Invert P to obtain P^{-1}.

(4) Consider the n columns of P^{-1} as the n column vectors

$$P^{-1} = [\ \underset{\sim}{e}_{11},\ \underset{\sim}{e}_{12},\ \cdots\ \underset{\sim}{e}_{1\mu_1},\ \underset{\sim}{e}_{21},\ \underset{\sim}{e}_{22},\ \cdots\ \underset{\sim}{e}_{2\mu_2},\ \underset{\sim}{e}_{31},\ \cdots\cdots\ \underset{\sim}{e}_{p\mu_p}\ ]$$

Only the last columns of each of the p blocks are required : thus let

$$\underset{\sim}{e}_i = \underset{\sim}{e}_{i\mu i}$$

(5) Construct matrix S^{-1} as

$$S^{-1} = [\ \underset{\sim}{e}_1,\ A\underset{\sim}{e}_1, \ldots\ A^{\mu_1-1}\underset{\sim}{e}_1,\ \underset{\sim}{e}_2,\ A\underset{\sim}{e}_2, \ldots\ A^{\mu_2-1}\underset{\sim}{e}_2,\ \underset{\sim}{e}_3, \ldots\ A^{\mu_p-1}\underset{\sim}{e}_p\ ]$$

(6) Invert S^{-1} to obtain S

(7) Calculate $\tilde{A}$, $\tilde{B}$ and $\tilde{C}$

3.7.3 NOTES ON OBSERVABLE CANONICAL FORM

(1) Each block of $\tilde{A}$ is also in observable canonical form.

(2) A block of dimension 1×1 is [x].

(3) The characteristic polynomial of

$$\begin{bmatrix} 0 & 0 & 0 & . & . & . & -\alpha_0 \\ 1 & 0 & 0 & . & . & . & -\alpha_1 \\ 0 & 1 & 0 & . & . & . & -\alpha_2 \\ . & . & . & & & & . \\ 0 & 0 & 0 & & . & 1 & -\alpha_{n-1} \end{bmatrix}$$

is

$$s^n + \alpha_{n-1}s^{n-1} + \ldots + \alpha_1 s + \alpha_0 \qquad (3.51)$$

Thus, if A_{ii} is an observable canonical form block, as above and

$$\tilde{A} = \begin{bmatrix} A_{11} & & & & \\ & A_{22} & & & \\ & & . & & \\ & & & . & \\ & & & & A_{pp} \end{bmatrix}$$

then the characteristic polynomial of $\tilde{A}$, $\tilde{A}(s)$ is

$$\tilde{A}(s) = A_{11}(s) \times A_{22}(s) \times \ldots\ldots \times A_{pp}(s) \qquad (3.52)$$

(4) The form of $\tilde{C}$ depends on the observability indices:

(a) The number of blocks in $\tilde{A}$ is p, the number of rows of $\tilde{C}$

(b) Working from left to right, top to bottom in $\tilde{A}$, the last column (column j of $\tilde{A}$) of block i (i= 1..p), corresponds to a 1 at position (i,j) in $\tilde{C}$. If i≠p then the remaining elements of column j of $\tilde{C}$ are given by,

$$\tilde{C}_{i+k,j} = 0 \text{ if } \mu_i \leqslant \mu_{i+k}$$

$$= x \text{ if } \mu_i > \mu_{i+k}$$

for k = 1,2,...p-i; all other elements of $\tilde{C}$ are zero

For example,

$$\tilde{A} = \left[\begin{array}{ccc:ccc:ccc:ccc} 0 & 0 & x & & & x & & x & & & x \\ 1 & 0 & x & & & x & & x & & & x \\ 0 & 1 & x & & & x & & x & & & x \\ \hdashline & & x & 0 & 0 & x & & x & & & x \\ & & x & 1 & 0 & x & & x & & & x \\ & & x & 0 & 1 & x & & x & & & x \\ \hdashline & & x & & & x & 0 & x & & & x \\ & & x & & & x & 1 & x & & & x \\ \hdashline & & x & & & x & & x & 0 & x \\ & & x & & & x & & x & 1 & x \end{array}\right]$$

$$\tilde{C} = \left[\begin{array}{ccc:ccc:cc:cc} 0 & 0 & 1 & 0 & 0 & 0 & 0 & 0 & 0 & 0 \\ 0 & 0 & 0 & 0 & 0 & 1 & 0 & 0 & 0 & 0 \\ 0 & 0 & x & 0 & 0 & x & 0 & 1 & 0 & 0 \\ 0 & 0 & x & 0 & 0 & x & 0 & 0 & 0 & 1 \end{array}\right]$$

(5) From (4), if $\mu_1 = \mu_2 = \ldots = \mu_p$; $\tilde{C}$ will only have p unity elements. Otherwise $\tilde{C}$ will be of form,

$$\tilde{C} = \left[\begin{array}{cccc:cccc:cccc:ccc:ccc} 0 & \cdots & & 1 & 0 & \cdots & & 0 & 0 & \cdots & & 0 & & \cdots & & 0 & \cdots & 0 \\ 0 & \cdots & & x & 0 & \cdots & & 1 & 0 & \cdots & & 0 & & \cdots & & 0 & \cdots & 0 \\ 0 & \cdots & & x & 0 & \cdots & & x & 0 & \cdots & & 1 & & \cdots & & 0 & \cdots & 0 \\ \vdots & & & \vdots & \vdots & & & \vdots & \vdots & & & \vdots & & & & \vdots & & \vdots \\ 0 & \cdots & & x & 0 & \cdots & & x & 0 & \cdots & & x & & \cdots & & 0 & \cdots & 1 \end{array}\right] \tag{3.53}$$

where at least one x is any number other than zero.

If F is defined as the (p×p) matrix constructed from the non−zero columns of $\tilde{C}$,

$$F = \left[\begin{array}{cccc} 1 & 0 & 0 & 0 \\ x & 1 & 0 & 0 \\ x & x & 1 & 0 \\ \vdots & \vdots & \vdots & \vdots \\ x & x & x & 1 \end{array}\right] \tag{3.54}$$

and C_o as

$$C_o = \left[\begin{array}{cccc:cccc:cccc:c:cccc} 0 & \cdots & 0 & 1 & 0 & \cdots & 0 & 0 & \cdots & 0 & 0 & \cdots & 0 & \cdots & 0 & \cdots & 0 \\ 0 & \cdots & 0 & 0 & 0 & \cdots & 1 & 0 & \cdots & 0 & 0 & \cdots & 0 & \cdots & 0 & \cdots & 0 \\ 0 & \cdots & 0 & 0 & 0 & \cdots & 0 & 0 & \cdots & 1 & 0 & \cdots & 0 & \cdots & 0 & \cdots & 0 \\ \vdots & & \vdots & \vdots & \vdots & & \vdots & \vdots & & \vdots & \vdots & & \vdots & & \vdots & & \vdots \\ 0 & \cdots & 0 & 0 & 0 & \cdots & 0 & 0 & \cdots & 0 & 0 & \cdots & 0 & \cdots & 0 & \cdots & 1 \end{array}\right] \qquad (3.55)$$

then it follows that

$$\tilde{C} = FC_o \Leftrightarrow C_o = F^{-1}\tilde{C} \qquad (3.56)$$

and furthermore, due to its form, F is always non-singular.

3.7.4 MORE CANONICAL FORMS

In determining an algorithm for the observable canonical form of 3.49 and 3.50, other possible algorithms, using V, V_2, Q and Q_2 as starting points, were investigated. Table 3.1 summarises the results.

3.8 EFFECT OF CANONICAL TRANSFORMATIONS ON OBSERVER EQUATIONS

If the state of the system

$$\dot{\underset{\sim}{x}} = A\underset{\sim}{x} + B\underset{\sim}{u} \qquad (3.1)$$

$$\underset{\sim}{y} = C\underset{\sim}{x} \qquad (3.6)$$

being observed by an observer of form

$$\dot{\hat{\underset{\sim}{x}}} = A\hat{\underset{\sim}{x}} + B\underset{\sim}{u} + HC(\underset{\sim}{x} - \hat{\underset{\sim}{x}}) \qquad (3.14)$$

is transformed to the observable canonical form (or any other canonical form)

$$\dot{\underset{\sim}{z}} = \tilde{A}\underset{\sim}{z} + \tilde{B}\underset{\sim}{u} \qquad (3.57)$$

$$\underset{\sim}{y} = \tilde{C}\underset{\sim}{z} \qquad (3.58)$$

SOURCE	LAST ROW	LAST COL	OBS	CON	$\tilde{C}$	$\tilde{B}$	S	R^{-1}
V	*			*			*	
V		*	*					*
V_2^*				*	[10...0]			*
V_2	*			*			*	
V_2		*	*		[0...01]			*
Q			*			$[10..0]^T$		*
Q	*			*		$[0..01]^T$	*	
Q		*	*					*
Q_2	*			*			*	
Q_2^*		*	*					*

TABLE 3.1 CANONICAL TRANSFORMATIONS

Notes

(1) **LAST ROW/LAST COL** – In the algorithm for observable canonical form the (n×n) matrix P^{-1} was considered to be formed from n column vectors divided into p blocks. The LAST COLumn of each block was then used to construct S^{-1}. Alternatively it is possible to consider P^{-1} as being n row vectors and selecting the LAST ROW of each of the p blocks. First rows and columns were also tried and gave an $\tilde{A}$ in observable or controllable canonical form, but no special forms for $\tilde{B}$ or $\tilde{C}$.

(2) **OBS/CON** – $\tilde{A}$ matrix in OBServable or CONtrollable canonical form.

(3) $\tilde{C}/\tilde{B}$ – $\tilde{C}$ or $\tilde{B}$ in canonical forms of 3.49, 3.50, with unity elements in either the first or last columns (for $\tilde{C}$) or rows (for $\tilde{B}$). No entry indicates no special form is produced.

(4) S/S^{-1} – Matrix produced from the $\underline{e}_i$'s (step 5, section 3.7.2) assumed to be either S or S^{-1}.

(5) V_2^*/Q_2^* – Miss out steps 3,4 and 5 and let V_2 or Q_2 be S or S^{-1}

with

$$\left.\begin{array}{ll} \tilde{A} = SAS^{-1} & \tilde{C} = CS^{-1} \\ \tilde{B} = SB & \underset{\sim}{z} = S\underset{\sim}{x} \end{array}\right\} \qquad (3.59)$$

then the observer equation of 3.14 must be changed to

$$\dot{\hat{\underset{\sim}{z}}} = \tilde{A}\underset{\sim}{z} + \tilde{B}\underset{\sim}{u} + H\tilde{C}(\underset{\sim}{z} - \hat{\underset{\sim}{z}}) \qquad (3.60)$$

Furthermore, if $\tilde{C}$ (3.53) is transformed to C_o (3.55) using matrix F (3.54) and equation 3.56, then the last term of 3.60 becomes,

$$HF^{-1}\tilde{C}(\underset{\sim}{z} - \hat{\underset{\sim}{z}}) = HC_o(\underset{\sim}{z} - \hat{\underset{\sim}{z}}) \qquad (3.61)$$

This is effectively applying a transformation to the outputs of both system and observer. Now since the term $C_o\underset{\sim}{z}$ is not directly available, $F^{-1}C\underset{\sim}{x}$ is used since,

$$F^{-1}\tilde{C}\underset{\sim}{z} = F^{-1}(CS^{-1})(S\underset{\sim}{x}) = F^{-1}C\underset{\sim}{x} \qquad (3.62)$$

Thus the final observer equation can be stated as,

$$\dot{\hat{\underset{\sim}{z}}} = \tilde{A}\underset{\sim}{z} + \tilde{B}\underset{\sim}{u} + H[F^{-1}(C\underset{\sim}{x}) - C_o\hat{\underset{\sim}{z}}] \qquad (3.63)$$

and the error dynamics can easily be shown to be given by

$$\dot{\underset{\sim}{e}} = (\tilde{A} - HC_o)\underset{\sim}{e} \qquad (3.64)$$

The observable canonical form observer is shown in *fig 3.6* and should be compared to the untransformed observer of *fig 3.3*.

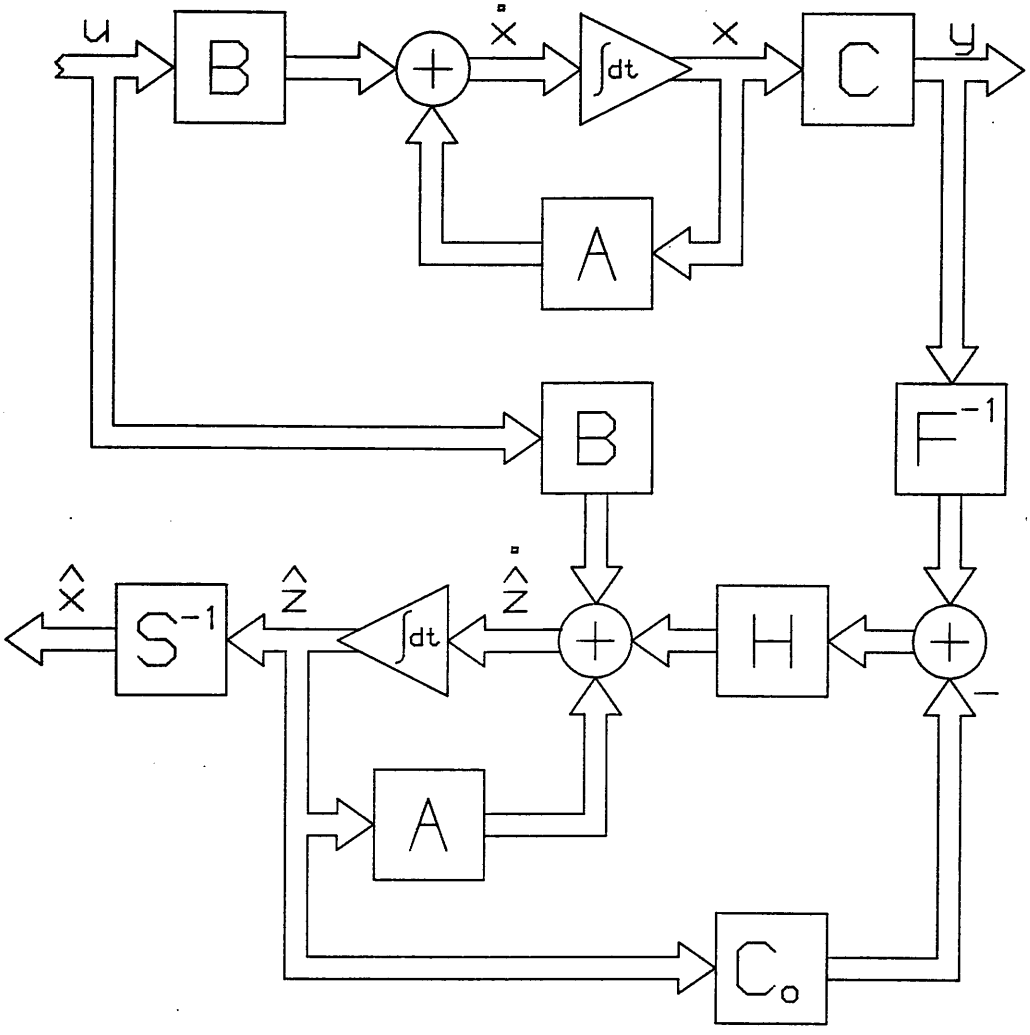

FIG 3.6 OBSERVABLE CANONICAL FORM OBSERVER

3.9 PARTITIONING OF SYSTEM IN OBSERVABLE CANONICAL FORM

As shown by Fortmann and Williamson, 1972, a system in observable canonical form can be considered as a set of subsystems, each being coupled to each other only through their outputs (*fig 3.7*).

For example, consider the following system in observable canonical form with n= 8, p= 3, m= 2 and observability indices $\mu_1 = 3$, $\mu_2 = 3$, $\mu_3 = 2$.

$$\begin{bmatrix} \dot{z}_1 \\ \dot{z}_2 \\ \dot{z}_3 \\ \dot{z}_4 \\ \dot{z}_5 \\ \dot{z}_6 \\ \dot{z}_7 \\ \dot{z}_8 \end{bmatrix} = \begin{bmatrix} 0 & 0 & x & : & & & x & : & & x \\ 1 & 0 & x & : & & & x & : & & x \\ 0 & 1 & x & : & & & x & : & & x \\ \cdots & \cdots & \cdots & \cdots & \cdots & \cdots & \cdots & \cdots & \cdots & \cdots \\ & & x & : & 0 & 0 & x & : & & x \\ & & x & : & 1 & 0 & x & : & & x \\ & & x & : & 0 & 1 & x & : & & x \\ \cdots & \cdots & \cdots & \cdots & \cdots & \cdots & \cdots & \cdots & \cdots & \cdots \\ & & x & : & & & x & : & 0 & x \\ & & x & : & & & x & : & 1 & x \end{bmatrix} \begin{bmatrix} z_1 \\ z_2 \\ z_3 \\ z_4 \\ z_5 \\ z_6 \\ z_7 \\ z_8 \end{bmatrix} + \begin{bmatrix} x & x \\ x & x \\ x & x \\ x & x \\ x & x \\ x & x \\ x & x \\ x & x \end{bmatrix} \begin{bmatrix} x \\ x \end{bmatrix}$$

$$\begin{bmatrix} y_1 \\ y_2 \\ y_3 \end{bmatrix} = \begin{bmatrix} 0 & 0 & 1 & : & & & : & & \\ \cdots & \cdots & \cdots & \cdots & \cdots & \cdots & \cdots & \cdots & \cdots \\ & & & : & 0 & 0 & 1 & : & \\ \cdots & \cdots & \cdots & \cdots & \cdots & \cdots & \cdots & \cdots & \cdots \\ & & & : & & & : & 0 & 1 \end{bmatrix} \begin{bmatrix} z_1 \\ z_2 \\ z_3 \\ \cdots \\ z_4 \\ z_5 \\ z_6 \\ \cdots \\ z_7 \\ z_8 \end{bmatrix} = \begin{bmatrix} z_3 \\ \cdots \\ z_6 \\ \cdots \\ z_8 \end{bmatrix} \qquad (3.65)$$

Re– writing as,

$$\begin{bmatrix} \dot{\underset{\sim}{Q}}_1 \\ \dot{\underset{\sim}{Q}}_2 \\ \dot{\underset{\sim}{Q}}_3 \end{bmatrix} = \begin{bmatrix} A_{11} & A_{12} & A_{13} \\ A_{21} & A_{22} & A_{23} \\ A_{31} & A_{32} & A_{33} \end{bmatrix} \begin{bmatrix} \underset{\sim}{Q}_1 \\ \underset{\sim}{Q}_2 \\ \underset{\sim}{Q}_3 \end{bmatrix} + \begin{bmatrix} B_1 \\ B_2 \\ B_3 \end{bmatrix} \underset{\sim}{u}$$

$$\begin{bmatrix} \tilde{y}_1 \\ \tilde{y}_2 \\ \tilde{y}_3 \end{bmatrix} = \begin{bmatrix} \underset{\sim}{C}_1 & 0 & 0 \\ 0 & \underset{\sim}{C}_2 & 0 \\ 0 & 0 & \underset{\sim}{C}_3 \end{bmatrix} \begin{bmatrix} \underset{\sim}{Q}_1 \\ \underset{\sim}{Q}_2 \\ \underset{\sim}{Q}_3 \end{bmatrix} \qquad (3.66)$$

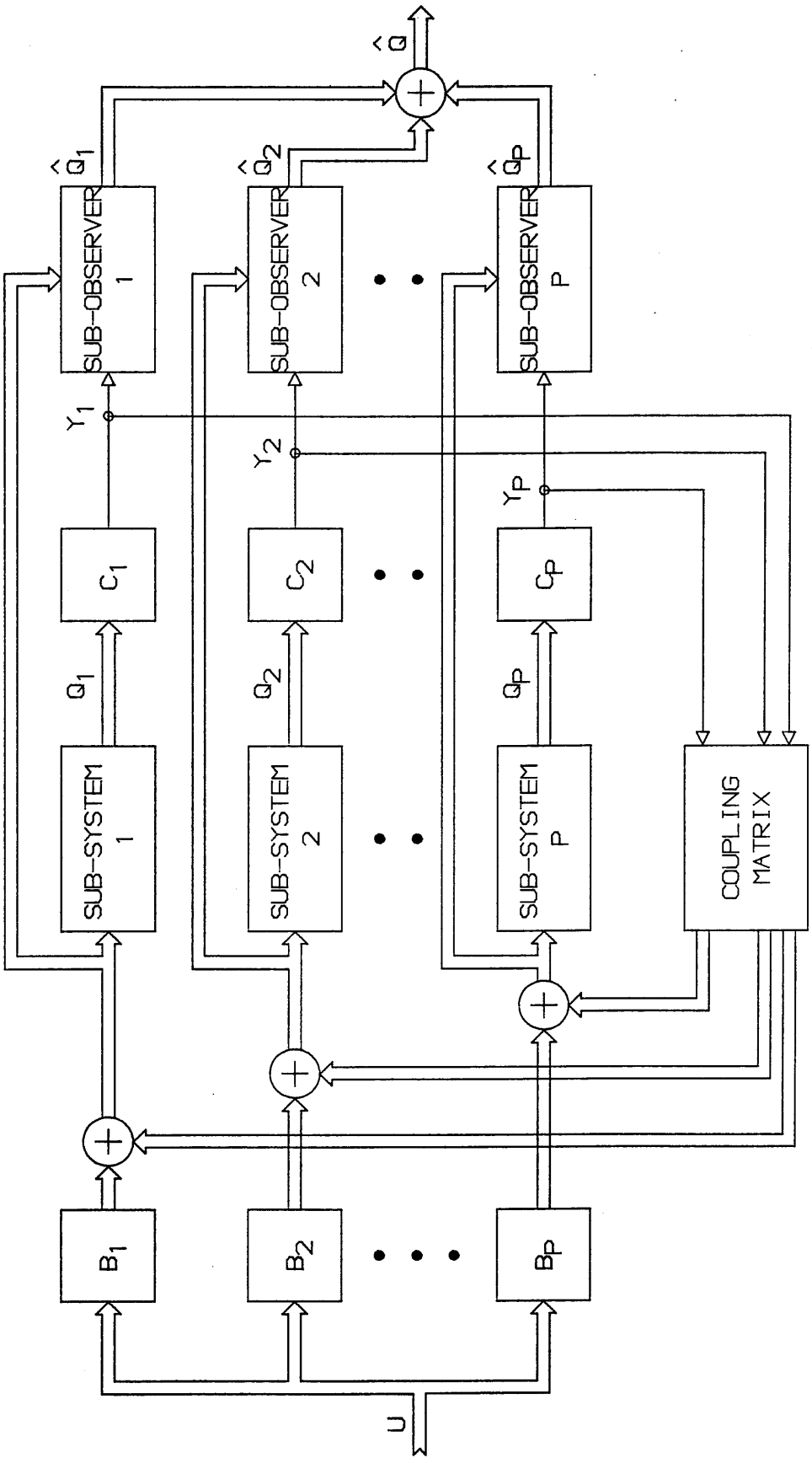

FIG 3.7 OBSERVER SCHEME FOR SYSTEM IN OBSERVABLE CANONICAL FORM CONSIDERED AS p SUBSYSTEMS

Then

$$\left.\begin{aligned} \dot{\underset{\sim}{Q}}_1 &= A_{11}\underset{\sim}{Q}_1 + A_{12}\underset{\sim}{Q}_2 + A_{13}\underset{\sim}{Q}_3 + B_1\underset{\sim}{u} \\ &= A_{11}\underset{\sim}{Q}_1 + A_{12}\tilde{\underset{\sim}{y}}_2 + A_{13}\tilde{\underset{\sim}{y}}_3 + B_1\underset{\sim}{u} \\ \tilde{\underset{\sim}{y}}_1 &= \underset{\sim}{C}_1\underset{\sim}{Q}_1 = z_3 \end{aligned}\right\} \; S_1 \qquad (3.67)$$

$$\left.\begin{aligned} \dot{\underset{\sim}{Q}}_2 &= A_{22}\underset{\sim}{Q}_2 + A_{21}\underset{\sim}{Q}_1 + A_{23}\underset{\sim}{Q}_3 + B_2\underset{\sim}{u} \\ &= A_{22}\underset{\sim}{Q}_2 + A_{21}\tilde{\underset{\sim}{y}}_1 + A_{23}\tilde{\underset{\sim}{y}}_3 + B_2\underset{\sim}{u} \\ \tilde{\underset{\sim}{y}}_2 &= \underset{\sim}{C}_2\underset{\sim}{Q}_2 = z_6 \end{aligned}\right\} \; S_2 \qquad (3.68)$$

$$\left.\begin{aligned} \dot{\underset{\sim}{Q}}_3 &= A_{33}\underset{\sim}{Q}_3 + A_{31}\underset{\sim}{Q}_1 + A_{32}\underset{\sim}{Q}_2 + B_3\underset{\sim}{u} \\ &= A_{33}\underset{\sim}{Q}_3 + A_{31}\tilde{\underset{\sim}{y}}_1 + A_{32}\tilde{\underset{\sim}{y}}_2 + B_3\underset{\sim}{u} \\ \tilde{\underset{\sim}{y}}_3 &= \underset{\sim}{C}_3\underset{\sim}{Q}_3 = z_8 \end{aligned}\right\} \; S_3 \qquad (3.69)$$

Now consider sub-system S_1 on its own, the output coupling between other subsystems being represented by a term $\underset{\sim}{D}_1$.

$$\left.\begin{aligned} \dot{\underset{\sim}{Q}}_1 &= A_{11}\underset{\sim}{Q}_1 + B_1\underset{\sim}{u} + \underset{\sim}{D}_1 \\ \tilde{\underset{\sim}{y}}_1 &= \underset{\sim}{C}_1\underset{\sim}{Q}_1 \end{aligned}\right\} \qquad (3.70)$$

or more explicity,

$$\begin{bmatrix} \dot{q}_1 \\ \dot{q}_2 \\ \dot{q}_3 \end{bmatrix} = \begin{bmatrix} 0 & 0 & x \\ 1 & 0 & x \\ 0 & 1 & x \end{bmatrix} \begin{bmatrix} q_1 \\ q_2 \\ q_3 \end{bmatrix} + \begin{bmatrix} x & x \\ x & x \\ x & x \end{bmatrix} \underset{\sim}{u} + \begin{bmatrix} x \\ x \\ x \end{bmatrix}$$

$$\tilde{y}_1 = \begin{bmatrix} 0 & 0 & 1 \end{bmatrix} \begin{bmatrix} q_1 \\ q_2 \\ q_3 \end{bmatrix} \qquad (3.71)$$

If a reduced order observer is to be designed for this sub-system and the others, it is necessary to first consider the effect term $\underset{\sim}{D}_1$ has on the reduced order observer equations:

$$\left.\begin{aligned} \dot{\underset{\sim}{q}} &= \tilde{A}\underset{\sim}{q} + \tilde{B}\underset{\sim}{u} + \underset{\sim}{D}_1 \\ \tilde{y} &= \tilde{C}\underset{\sim}{q} \end{aligned}\right\} \qquad (3.72)$$

The analysis is the same as that for the normal reduced order observer, except for the addition of term $\underset{\sim}{D}_1$ $(\mu_1 \times 1)$, which is partitioned as,

$$\underset{\sim}{D}_1 = \begin{bmatrix} \underset{\sim}{d}_1 \\ \cdots \\ d_2 \end{bmatrix} \begin{matrix} \mu_1 - 1 \times 1 \\ 1 \times 1 \end{matrix} \qquad (3.73)$$

The modified reduced order observer equations are thus,

$$\dot{\underset{\sim}{z}} = [A_{11} - HA_{21}]\underset{\sim}{z} + [A_{12} - HA_{22} + (A_{11} - HA_{21})H]q_2 + [B_1 - HB_2]\underset{\sim}{u} + [\underset{\sim}{d}_1 - Hd_2] \qquad (3.74)$$

and

$$\hat{\underset{\sim}{q}}_1 = \underset{\sim}{z} + Hq_2 \qquad (3.42)$$

$$\hat{\underset{\sim}{q}} = \begin{bmatrix} \hat{\underset{\sim}{q}}_1 \\ \cdots \\ q_2 \end{bmatrix} \qquad (3.43)$$

$$\hat{\underset{\sim}{x}} = R^{-1}\hat{\underset{\sim}{q}} \qquad (3.44)$$

$$\dot{\underset{\sim}{e}} = [A_{11} - HA_{21}]\underset{\sim}{e} \qquad (3.40)$$

as before.

An observable canonical form block or sub-system of dimension (1×1) does not require an observer.

3.10 SIMULATION

Computer simulation of helicopter motion and the response to control inputs was carried out using TSIM (Winter, Corbin and Murphy, 1983) which is a high level, interactive, computer–aided simulation package, originally written at the Royal Aerospace Establishment, Farnborough for use in flight control systems, but now available as a commercial software package. It incorporates facilities of particular relevance to the needs of the flight control systems engineer and was considered to be particularly suitable for this reason.

Within TSIM the system, in state–space form, is written as a set of differential equations and the time response of the system, plus any additional controller and/or observer scheme, when subjected to a control input, can then be generated by fourth–order Runge–Kutta numerical integration.

The package also includes a graphics facility so that the time response can be plotted to a graphics device (eg. screen, plotter), but for greater flexibility it can be written to a data file for future analysis/plotting.

DEFINITIONS AND NOMENCLATURE

The state vector $\underset{\sim}{x}$ of the full, fourteenth order, state space description, is defined as:

u	x–axis velocity	m/sec	
w	z–axis velocity	m/sec	LONGITUDINAL DYNAMICS
q	pitch rate	degs/sec	
θ	pitch attitude	degs	
v	y–axis velocity	m/sec	
p	roll rate	degs/sec	LATERAL DYNAMICS
φ	roll attitude	degs	
r	yaw rate	degs/sec	
β_0	coning angle	degs	
β_{1C}	longitudinal flapping	degs/sec	
β_{1S}	lateral flapping	degs/sec	ROTOR DYNAMICS
$\dot{\beta}_0$	derivative of β_0	degs/sec	
$\dot{\beta}_{1C}$	derivative of β_{1C}	degs/sec^2	
$\dot{\beta}_{1S}$	derivative of β_{1S}	degs/sec^2	

and since the model is often partitioned into longitudinal, lateral and rotor dynamics, it is shown in that form. The units stated are those which are used in this thesis. In addition to the eighth order (longitudinal / lateral dynamics) and fourteenth order (longitudinal / lateral / rotor dynamics) models which have already been discussed, two fourth order models were utilized. These were *longitudinal dynamics* and *lateral dynamics* models and were obtained by extracting the relevant portions of the appropiately partitioned A and B matrices and the input vector $\underset{\sim}{u}$.

The input or control vector $\underset{\sim}{u}$ is given by,

$$\left[\begin{array}{c} \theta_{0e} \\ \theta_{1s} \\ \hline \theta_{1c} \\ \theta_{0t} \end{array}\right] = \left[\begin{array}{l} \text{Main Rotor collective} \\ \text{longitudinal cyclic} \\ \hline \text{lateral cyclic} \\ \text{tail rotor collective} \end{array}\right] \begin{array}{l} \\ \\ \\ \text{LONGITUDINAL} \\ \\ \text{LATERAL} \end{array}$$

and the units are radians *at the rotor head.* Stick/pedal sign conventions for these inputs are given in Table 3.2 below

Pilot control inputs obtained from flight data were expressed as percentage stick positions, and therefore had to be converted to angles at the rotor head before being used for simulation.

+VE INPUT ON	EFFECT	STICK/PEDAL
θ_{0e}	ASCENDING	COLLECTIVE STICK UP
θ_{1s}	NOSE UP	CYCLIC STICK AFT
θ_{1c}	ROLL TO RIGHT	CYCLIC STICK RIGHT
θ_{0t}	YAW TO RIGHT	LEFT PEDAL

TABLE 3.2 : STICK/PEDAL SIGN CONVENTIONS

NOMENCLATURE FOR THE C MATRIX

In multivariable, state space form, the output vector $\underset{\sim}{y}$ is related to the state of the system $\underset{\sim}{x}$, through the output (or measurement) matrix C by:

$$\underset{\sim}{y} = C\underset{\sim}{x} \tag{3.6}$$

Ideally the states chosen for the state space form will all be readily available for independent measurement and this results in an (n×n) C matrix with only one non−zero element in each row. If, as is frequently the case in many systems, not all n states are accessible, then C will be of order (p×n); whilst any state which is not independently measurable will result in the corresponding row of C having more than one non−zero element. In this latter case the determinable sub−set of the state can be reconstructed from the output $\underset{\sim}{y}$ by premultiplying $\underset{\sim}{y}$ by C^{-1} (for C (n×n)) or the pseudoinverse of C (for C (p×n)).

For the purposes of this thesis it was assumed that the states q, θ, p, φ and r are monitored directly while u, w and v are derived from other measurements. It was also assumed that there are no sensors for the rotor states. Thus C was effectively an (8×8) Identity matrix for either the eighth or fourteenth order models; or a (4×4) Identity matrix for the longitudinal or lateral models.

However, in most cases only a small number of states (or even just a single state) were required to design an observer and therefore, in general, $p \ll n$. To avoid explicitly stating the C matrices, the following notation was used,

$$C(\alpha_1, \alpha_2, \ldots, \alpha_p) \quad \text{where } \alpha_i \in \{ 1, 2, \ldots, n \}$$

The α_i's denote which column has a unity element for each of the p rows. Thus, with n= 8 for example,

$$C(3,1) \equiv \begin{bmatrix} 0 & 0 & 1 & 0 & 0 & 0 & 0 & 0 \\ 1 & 0 & 0 & 0 & 0 & 0 & 0 & 0 \end{bmatrix}$$

$$C(2) \equiv \begin{bmatrix} 0 & 1 & 0 & 0 & 0 & 0 & 0 & 0 \end{bmatrix}$$

The above notation for C matrices is used throughout this thesis.

STANDARD CONTROL INPUTS

In the testing and development of helicopter flight control systems, three inputs which are relatively easily produced and replicated by the pilot, have evolved as being standard references. These are the *step, doublet* and *3–2–1–1*, and are defined as,

STEP : *fig 3.8a* – Magnitude K, starting at time T_1.
Expressed as K= , t= T_1

DOUBLET: *fig 3.8b* – Pulse of magnitude K, duration $(T_2 - T_1)$, followed by a pulse of magnitude $-K$, of the same duration. Normally $T_2 = T_3$.
Expressed as K= , t= $T_1/T_2/T_3/T_4$

3–2–1–1 : *fig 3.8c* – Four pulses of magnitude K, $-K$, K, $-K$ and durations in the ratio 3 : 2 : 1 : 1, respectively. Typically $T_2 = T_3$, $T_4 = T_5$ and $T_6 = T_7$.
Expressed as K= , t= $T_1/T_2/T_3/T_4/T_5/T_6/T_7/T_8$

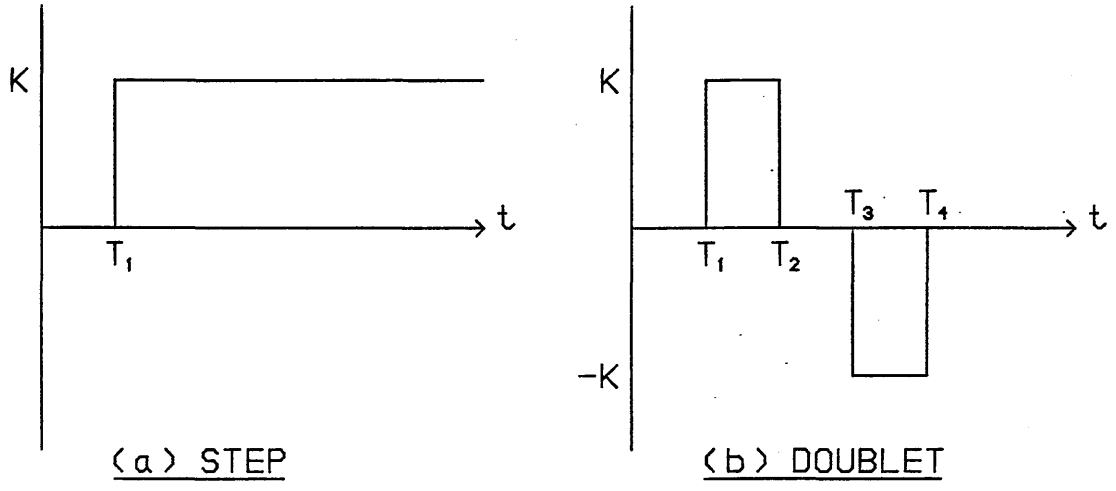

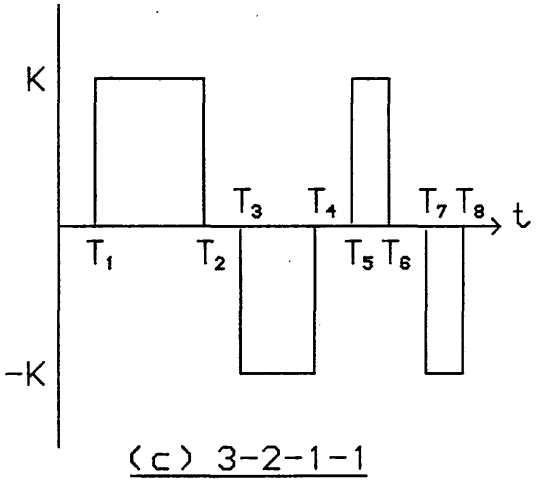

FIG 3.8 STANDARD CONTROL INPUTS

CHAPTER FOUR

OBSERVER DESIGN METHODS

AND BASIC PERFORMANCE

4.1 OBSERVER DESIGN METHODS

The possibility of a full order state reconstructor without feedback from the measurements was noted as early as 1958 by Kalman and Bertram. Subsequently Kalman, 1960b, developed a full order device which used measurement feedback for exactly reconstructing the state of a discrete–time system in a finite number of steps. However, it was the two seminal papers of Luenberger (1964, 1966) which marked the beginning of a fertile area of research.

Several fundamental results are established in these two papers; perhaps the most important being the ability to arbitrarily adjust the dynamics (i.e the eigenvalues) of the state reconstruction process: a central result in linear system theory. The *separation principle* describing the separation of controller and observer design is given and the closed–loop stability properties in linear or non–linear feedback designs are shown to be unaffected by the inclusion of an observer.

The 1966 paper also includes a lucid explanation of minimal (or reduced) order state observers (i.e of order (n– p)) for linear, time–invariant, continuous–time systems, where it is assumed that the A and D matrices have no common eigenvalues, thus assuring a unique T satisfying the equation TA– DT= EC. See also Luenberger, 1965. This restriction is removed in the time–invariant case by Newmann, 1970b, and in the time–variant case by Yuksel and Bongiorno, 1971, (see also Tse and Athans, 1970; Tse, 1973 and O'Reilly, 1983, for example).

4.1.1 TRANSFORMATIONS AND THE MULTIVARIABLE CANONICAL FORM

The advantages of transforming a linear system (by means of a similarity transformation) into a structurally simpler form has been reported by many authors. For example, see Dellon and Sarachik, 1968; Cumming, 1969; Newmann, 1969 and Gopinath, 1971. Transformation of the system into a more convenient form allows the minimal order state observer to be defined by a single explicit gain matrix (Dellon and Sarachik, 1968). Similar results are obtained by Cumming, 1969; Newmann, 1969 and Gopinath, 1971, for linear time–invariant systems.

More recently, an equivalent observer construction, based on the generalized matrix inverse, was introduced by Das and Ghoshal, 1981. The time–varying case for minimal order state observers, designed using a canonical transformation, is dealt with by Johnson, 1969; Yuksel and Bongiorno, 1971 and O'Reilly and Newmann, 1975, for example.

Since its introduction by Luenberger in 1966 (see also Luenberger, 1967), the *multivariable canonical form* has been widely used in observer design, system identification and realization theory because of the structural simplification it affords, eg. Wolovich, 1974; Chen, 1984; Munro, 1973. In this form the system effectively decomposes into p single output sub– systems for each of which a sub– observer may be designed. The composite observer is of dimension (n– p), as previously, but the observer eigenvalues may only be arbitrarily assigned within each of the p lower dimensional sub– observers.

Many so– called canonical forms are in fact *not* canonical in the strict mathematical sense; for a precise definition of canonical form see Wang and Davison, 1976. Wolovich, 1968, extends the theory of minimal order state observer design using the Luenberger companion form to time– varying systems and a time– varying generalization of the Tuel companion form is given by Yuksel and Bongiorno, 1971.

4.1.2 POLE PLACEMENT AND EIGENSTRUCTURE ASSIGNMENT

During these years of research into the various aspects and types of observers consideration has also been given to the dual problem of *pole placement* in the feedback equation, ie. the determination of a feedback gain matrix K, such that [A+ BK] has a prescribed set of eigenvalues, and the subject is pertinent to the design of observers since the determination of K in [A+ BK] is dual to the determination of H in [A– HC].

Modal control was first discussed by Rosenbrock, 1962, who considered the case where both matrices B and K in equations 3.1/3.7 could be chosen. Extension to the system where B is the defined vector $\underset{\sim}{b}$ and K is the vector $\underset{\sim}{k}$ to be chosen, was considered by Ellis and White, 1965, who describe a method for altering one eigenvalue at a time. In 1967, Wonham was the first to prove that if the state vector $\underset{\sim}{x}$ is perfectly accessible then the pair [A,B] is controllable if, and only if, K can be chosen to give [A+ BK] any desired set of eigenvalues.

Since then literally hundreds of papers dealing with pole placement have appeared and it is still an active area of research. See for example: Retallack and McFarlane, 1970; Porter and Crossley, 1972; Munro and Vardulakis, 1973; Davison and Wang, 1975; Djaferis, 1983 and Morse, Wolovich and Anderson, 1983.

Recently, attention has also been given to the problem of *eigenstructure assignment*, (or *modal control* when used to design feedback controllers), ie the selection of both

eigenvalues *and* eigenvectors. The choice of each closed–loop eigenvalue/eigenvector pair is not an arbitrary one since each eigenvector is limited to a subspace of the system subspace, but this still gives enough freedom to make suitable choices of those pairs.

A literature review of pole assignment and the broader question of eigenstructure assignment is given by Andry Jr, Shapiro and Chung, 1983. See also, for example, Moore, 1976; Klein and Moore, 1977; Srinathkumar, 1978; Shapiro and Chung, 1981 and Parry and Murray–Smith, 1985.

4.1.3 OTHER FORMS OF OBSERVER

The fundamental property of one system observing another can be applied in a reverse direction to obtain a special type of controller called a *dual observer* which can be thought of as supplying an approximation to the desired inputs. Since the notion of a dual observer was introduced by Brasch and subsequently discussed by Luenberger, 1971, it has been comparatively little studied, but see for example Blanvillian and Johnson, 1978.

As has been demonstrated already, reconstruction of the complete state vector of a linear system can be accomplished, regardless of the actual design method, by an observer of order (n–p) with arbitrary, stable dynamics. Frequently, however, only some linear function of the system state, usually a linear feedback control law of the form $K\underset{\sim}{x}$, is required to be estimated. This can be realized using an observer of further reduced dimension.

This type of observer was first explored by Bass and Gura, 1965 and Luenberger, 1966. Alternative design procedures for observing a *scalar linear function* of the state of a multiple–output system are presented in Wonham and Morse, 1972; Moore, 1972; Roman, Jones and Bullock, 1973 and Jameson and Rothschild, 1971.

Due to the greater complexities involved, progress on the general problem of reconstructing *vector linear functions* of the state has been relatively slow. The first significant contribution was due to Fortmann and Williamson, 1972, who obtain sufficient and necessary conditions for an observer of minimal order to reconstruct a vector linear function of the state for single–output systems. Subsequently, the multiple output case has been considered by Roman and Bullock, 1975; Moore and Ledwich, 1975; Sirisena, 1979 and Fairman and Gupta, 1980.

4.2 NUMERICAL CONSIDERATIONS

Despite the conceptual simplicity of the observer, the numerical problems associated with its design can be extremely demanding: particularly when dealing with a large–scale system. For an n–dimensional linear system, with p observation channels, the observer equation involves solving an $(n-p \times n)$ matrix equation. For a large n and small to moderate p, a solution to the observer equation requires an immense amount of computational effort, eg. if $n=100$ and $p=50$, there are a set of 5000 linear equations to be solved.

There have been some interesting attempts at reducing the complexity of the problem – for instance, Arbel and Tse, 1979, suggest an algorithm which, for a system with $p< n/2$, reduces the observer design to the solution of an $(n-2p \times n-p)$ matrix equation. However this constrains the eigenvalues since p eigenvalues must be placed together at a selected point while the remaining $(n-2p)$ can be arbitrarily placed.

Consideration has also been given to the problems caused by the use of computers, and in particular the difficulties associated with their finite precision. In most cases, in dealing with matrices and matrix operations, the technique best suited for the development of ideas and concepts is not that best suited for digital computer implementation. In fact, efficient computer–based algorithms seldom lend themselves well to conceptual understanding of the principles involved. Also, once a controller or observer has been synthesized, there remains the task of implementation.

Today the trend is towards digital implementation of control logic, principally through the use of microprocessors in one form or another. These processors make possible the realization of complex control logic, but the use of all–digital control logic introduces new concerns regarding precision, computational capability, interface speed and memory requirements, all of which must be established in the design process.

Many papers now give algorithms which are ideally suited for computer implementation: eg. Miminis and Paige, 1982, give a numerically stable algorithm for pole assignment in a single–input system. Goknar and Dervisoglu, 1977, give one for the determination of controllability and observability of linear, time–invariant systems using elementary row operations and similarly Aplevich, 1974, uses elementary matrix operations to compute canonical forms for linear systems. Jordan and Sridhar, 1973, achieve the same using an algorithm involving Gaussian techniques and Munro, 1971 / 1973, gives a procedure for reduced order observers.

4.3 THE GOPINATH METHOD

In this thesis two observer design methods were initially selected and examined in detail. The first of these is the method given by Gopinath, 1971, which avoids the use of complicated canonical forms and is applicable to the design of both controllers and observers (of full or reduced order).

Consider the system under consideration to have the characteristic equation given by,

$$s^n + \sum_{i=1}^{n} a_i s^{n-i} = 0 \tag{4.1}$$

and the desired characteristic equation of the observer (determined from the required eigenvalues) to be

$$[A - HC]_s = s^n + \sum_{i=1}^{n} \gamma_i s^{n-i} \tag{4.2}$$

In the paper it is then proven that

$$\begin{bmatrix} tr(HC) \\ tr(AHC) \\ tr(A^2HC) \\ \vdots \\ tr(A^{n-1}HC) \end{bmatrix} = F^{-1}(\underset{\sim}{\gamma} - \underset{\sim}{a}) \tag{4.3}$$

Where 'tr' denotes the trace of a matrix (ie. the sum of the elements on the main diagonal); H is *dyadic*, i.e of rank one (to satisfy the derivation) and γ, $\underset{\sim}{a}$ and F are the vectors and matrix given by,

$$\underset{\sim}{\gamma} = \begin{bmatrix} \gamma_1 \\ \vdots \\ \gamma_n \end{bmatrix} \qquad \underset{\sim}{a} = \begin{bmatrix} a_1 \\ \vdots \\ a_n \end{bmatrix} \tag{4.4}$$

$$F = \begin{bmatrix} 1 & 0 & 0 & \cdots & 0 \\ a_1 & 1 & 0 & & \vdots \\ a_2 & a_1 & 1 & & \vdots \\ \vdots & & & \ddots & 0 \\ a_{n-1} & \cdots & & a_1 & 1 \end{bmatrix} \tag{4.5}$$

Now any (n×p) H matrix which satisfies equation 4.3 will suffice and therefore the H matrix with p identical, non−zero columns (and hence of rank one) was selected for simplicity. Representing the H matrix as,

$$H = \begin{bmatrix} h_1 & h_1 & \cdot\cdot & h_1 \\ h_2 & h_2 & \cdot\cdot & h_2 \\ \vdots & \vdots & & \vdots \\ h_n & h_n & \cdot\cdot & h_n \end{bmatrix} \tag{4.6}$$

equation 4.3 can be re-written as

$$\begin{bmatrix} d_{11} & \cdot\cdot\cdot & d_{1n} \\ \cdot & & \cdot \\ \cdot & & \cdot \\ d_{n1} & \cdot\cdot\cdot & d_{nn} \end{bmatrix} \begin{bmatrix} h_1 \\ \cdot \\ \cdot \\ h_n \end{bmatrix} = \begin{bmatrix} e_1 \\ \cdot \\ \cdot \\ e_n \end{bmatrix} \tag{4.7}$$

where $\underset{\sim}{e}$ is the (n×1) vector produced from $F^{-1}(\underset{\sim}{\gamma}-\underset{\sim}{a})$ and d_{ij} are the elements of the (n×n) matrix defined by,

$$\left.\begin{aligned} & d_{ij} = \sum_{k=1}^{n} a_{kj} C_k \\ & \text{where} \\ & \quad a_{kj} \text{ is an element of matrix } A^{i-1} \\ & \quad C_k = \sum_{l=1}^{p} c_{lk} \\ & \quad c_{lk} \text{ is an element of matrix } C \end{aligned}\right\} \tag{4.8}$$

Equation 4.7 is in the form of a set of linear equations $A\underset{\sim}{x} = \underset{\sim}{b}$ and can thus be solved by numerical methods (eg. NAG routines [N4]) to give the required elements for the H matrix. Numerical problems with this method are discussed in section 4.6 and design results are presented in section 4.7.

4.4 CANONICAL FORM METHOD

In chapter three (section 3.6) it was shown that the system of equations 3.1/3.6,

$$\left.\begin{array}{l} \dot{\underset{\sim}{x}} = A\underset{\sim}{x} + B\underset{\sim}{u} \\ \underset{\sim}{y} = C\underset{\sim}{x} \end{array}\right] \tag{4.9}$$

can be transformed by a similarity transformation to the system of 3.31/3.32,

$$\left.\begin{array}{l} \dot{\underset{\sim}{q}} = A\tilde{\underset{\sim}{q}} + B\tilde{\underset{\sim}{u}} \\ \underset{\sim}{y} = \tilde{C}\underset{\sim}{q} \end{array}\right] \tag{4.10}$$

where $\tilde{A}$ and $\tilde{C}$ are in the observable canonical form of equations 3.49/3.55,

$$\tilde{A} = \left[\begin{array}{cccc|cccc|c|cccc}
0 & 0 & \cdots & x & & & & x & & & & & x \\
1 & 0 & \cdots & x & & & & x & & & & & x \\
0 & 1 & \cdots & x & & & & x & & & & & x \\
\vdots & & & \vdots & & & & \vdots & & & & & \vdots \\
0 & \cdots & 1 & x & & & & x & & & & & x \\
\hline
\multicolumn{3}{c}{(\mu_1\times\mu_1)} & x & 0 & 0 & \cdots & x & & & & & x \\
 & & & x & 1 & 0 & \cdots & x & & & & & x \\
 & & & x & 0 & 1 & \cdots & x & & & & & x \\
 & & & \vdots & \vdots & & & \vdots & & & & & \vdots \\
 & & & x & 0 & \cdots & 1 & x & & & & & x \\
\hline
 & & & \vdots & \multicolumn{3}{c}{(\mu_2\times\mu_2)} & \vdots & \ddots & & & & \vdots \\
\hline
 & & & x & & & & x & & 0 & 0 & \cdots & x \\
 & & & x & & & & x & & 1 & 0 & \cdots & x \\
 & & & x & & & & x & & 0 & 1 & \cdots & x \\
 & & & \vdots & & & & \vdots & & \vdots & & & \vdots \\
 & & & x & & & & x & & 0 & \cdots & 1 & x
\end{array}\right]_{(\mu_p\times\mu_p)} \tag{4.11}$$

$$\tilde{C} = \left[\begin{array}{ccc|ccc|c|c}
0 & \cdots & 1 & 0 & \cdots & 0 & & 0 \\
0 & & 0 & 0 & \cdots & 1 & & 0 \\
\vdots & & \vdots & \vdots & & \vdots & & \vdots \\
0 & \cdots & 0 & 0 & \cdots & 0 & & 1
\end{array}\right] \tag{4.12}$$

With the system in the above canonical form there are four different types of observer which can be designed, depending on whether the system is treated as a whole, or as a set of subsystems: each being coupled to each other only through

their outputs (section 3.9).

If the system is considered as one entity then either a full order observer of order n or a reduced order observer of order n−1 can be designed. When it is regarded as a set of subsystems, then for each subsystem a full order (μ_i) or reduced order (μ_{i-1}) observer can be designed. Thus in either case a total of n eigenvalues will be required for a full order observer design, but only n−p for a reduced order scheme.

In the case of the full order observer there is no advantage in the observer functioning as a set of subsystems since the elements of the separate H matrices, if taken together, would form the H matrix required for the full system. In fact it would actually be a retrograde measure in that the complexity of the observer would increase with the introduction of the cross−coupling terms. A full order observer will therefore henceforth refer to one which is designed from the full system in observable canonical form.

The situation with the reduced order observer is different because in its partitioned form the C matrices are in the required form to compute the necessary reduced order observers directly, whereas if the system is considered as a whole a further similarity transformation would be required to obtain the C matrix in the desired form, ie. $C = [\ I_{p\times p} \mid 0\ ]$. Thus henceforth a reduced order observer will refer to one which functions as a set of subobservers.

The simplicity of these designs is easily demonstrated by considering a sixth order $\tilde{A}$ matrix with three (2×2) canonical blocks and a requirement for a full order observer with eigenvalues at:

$$[\ -5,\ -5,\ -6,\ -7,\ -8,\ -8\ ]$$

then using *note 3* of section 3.7.3 the required form for $[\tilde{A}-H\tilde{C}]$ will be,

$$\begin{bmatrix} 0 & -25 & & & & \\ 1 & -10 & & & & \\ & & 0 & -42 & & \\ & & 1 & -13 & & \\ & & & & 0 & -64 \\ & & & & 1 & -16 \end{bmatrix} \qquad (4.13)$$

since

$$(S+5)(S+5) = S^2 + 10S + 25$$

$$(S+6)(S+7) = S^2 + 13S + 42$$

$$(S+8)(S+8) = S^2 + 16S + 64$$

If $[\tilde{A} - H\tilde{C}]$ is written out as,

$$\begin{bmatrix} 0 & a_{12} & 0 & a_{14} & 0 & a_{16} \\ 1 & a_{22} & 0 & a_{24} & 0 & a_{26} \\ 0 & a_{32} & 0 & a_{34} & 0 & a_{36} \\ 0 & a_{42} & 1 & a_{44} & 0 & a_{46} \\ 0 & a_{52} & 0 & a_{54} & 0 & a_{56} \\ 0 & a_{62} & 0 & a_{64} & 1 & a_{66} \end{bmatrix} - \begin{bmatrix} 0 & h_{11} & 0 & h_{12} & 0 & h_{13} \\ 0 & h_{21} & 0 & h_{22} & 0 & h_{23} \\ 0 & h_{31} & 0 & h_{32} & 0 & h_{33} \\ 0 & h_{41} & 0 & h_{42} & 0 & h_{43} \\ 0 & h_{61} & 0 & h_{52} & 0 & h_{53} \\ 0 & h_{71} & 0 & h_{62} & 0 & h_{63} \end{bmatrix} \qquad (4.14)$$

Then by equating 4.13 and 4.14 the elements of the (6×3) H matrix can be determined as,

$$h_{11} = a_{12} + 25 \qquad h_{12} = a_{14} \qquad h_{13} = a_{16}$$
$$h_{21} = a_{22} + 10 \qquad h_{22} = a_{24} \qquad h_{23} = a_{26}$$
$$h_{31} = a_{32} \qquad h_{32} = a_{34} + 42 \qquad h_{33} = a_{36}$$
$$h_{41} = a_{42} \qquad h_{42} = a_{44} + 13 \qquad h_{43} = a_{46}$$
$$h_{51} = a_{52} \qquad h_{52} = a_{54} \qquad h_{53} = a_{56} + 64$$
$$h_{61} = a_{62} \qquad h_{62} = a_{64} \qquad h_{63} = a_{66} + 16$$

If a reduced order observer was to be designed from the partitioned system then, since the system can be considered as consisting of three second order systems, the task is to determine a reduced order observer for each of the second order systems and the output coupling terms between them (Section 3.9).

The major computational process using this method is therefore in determining the similarity transformation required to obtain the system in observable canonical form, since in this form the determination of the required H matrix (or matrices), and the reduced order cross–coupling terms, is just simple arithmetic.

4.5 BASIC OBSERVER PERFORMANCE

Assuming an accurate model of the system which, as was discussed in chapter two, is not usually the case, observer performance is fundamentally determined by the two major design parameters: which system state variable(s) are used to reconstruct an estimate of the remaining state variables (ie. the choice of observer C matrix); and the selection of observer eigenvalues. For the eigenvalues, the larger the magnitudes of the negative real parts, the faster the estimate $\hat{x}(t)$ approaches the system state $x(t)$.

However, these larger eigenvalues will cause larger gains in H and generate larger magnitudes in transient – as is the case for feedback control. As the eigenvalues tend towards minus infinity, the observer will act as a differentiator and will therefore be susceptible to noise.

Hence there is no simple answer to the question of what are the ideal eigenvalues, but the literature suggests that the negative real parts of the eigenvalues of [A– HC] be chosen to be two or three times faster than those of [A+ BK]. Richards, 1979, advocates that they be an order of magnitude faster.

To illustrate the basic properties of observer performance, first consider the following second order system.

$$A = \begin{bmatrix} -3 & 1 \\ 0 & -1 \end{bmatrix} \qquad B = \begin{bmatrix} 0 \\ 1 \end{bmatrix} \qquad C = \begin{bmatrix} 1 & 0 \end{bmatrix} \tag{4.15}$$

Therefore, $n=2$, $m=1$, $p=1$ and the eigenvalues of the A matrix are $\lambda_1=-3$, $\lambda_2=-1$. ie. the system is stable. For a full order observer, the H matrix will be of form,

$$H = \begin{bmatrix} h_1 \\ h_2 \end{bmatrix}$$

and the characteristic equation of [A– HC] is,

$$|\lambda I - [A - HC]| = \lambda^2 + (4+h_1)\lambda + (3+h_1+h_2) \tag{4.16}$$

Thus for observer eigenvalues of $\lambda_1=\lambda_2=-15$ and $\lambda_1=-6$, $\lambda_2=-6.12$, the observers are given by,

Observer 1		Observer 2	
$\lambda_1 = -15$	$H = \begin{bmatrix} 26 \\ 196 \end{bmatrix}$	$\lambda_1 = -6$	$H = \begin{bmatrix} 8.12 \\ 25.6 \end{bmatrix}$
$\lambda_2 = -15$		$\lambda_2 = -6.12$	

Finally define two inputs:

U_1 : Step, $K = 0.1$, $t = 0$

U_2 : Doublet, $K = 0.1$, $t = 0/2/2/4$

4.5.1 INITIAL STATES

Firstly consider the situation where the observer and the system have identical states, ie. the observer estimate equals the state of the system. Now since the observer is governed by equation 3.14:

$$\dot{\hat{\underset{\sim}{x}}} = A\hat{\underset{\sim}{x}} + B\underset{\sim}{u} + HC(\underset{\sim}{x} - \hat{\underset{\sim}{x}}) \qquad (4.17)$$

and $\underset{\sim}{x} = \hat{\underset{\sim}{x}}$, the response of the observer will be identical to the response of the system. The state variable time-response of system and observer are shown in *fig 4.1a* (Observer-1 and step input U_1), *fig 4.2a* (Observer-1 and doublet input U_2) and *fig 4.3a* (Observer-2 and U_2).

When the observer and system have different states then $\underset{\sim}{x} \neq \hat{\underset{\sim}{x}}$ and the term $HC(\underset{\sim}{x}-\hat{\underset{\sim}{x}})$ is no longer zero. The error dynamics of the observer, given by equation 3.17,

$$\dot{\underset{\sim}{e}} = (A - HC)\underset{\sim}{e} \qquad (4.18)$$

will now act to reduce the error between system and observer state and the speed with which the error will reduce to zero, will be determined by the eigenvalues of (A-HC). *Figs 4.1b, 4.2b* and *4.3b* demonstrate this for observer-1 with input U_1; observer-1 with input U_2; and observer-2 with input U_2, respectively, for an initial observer error of 0.1

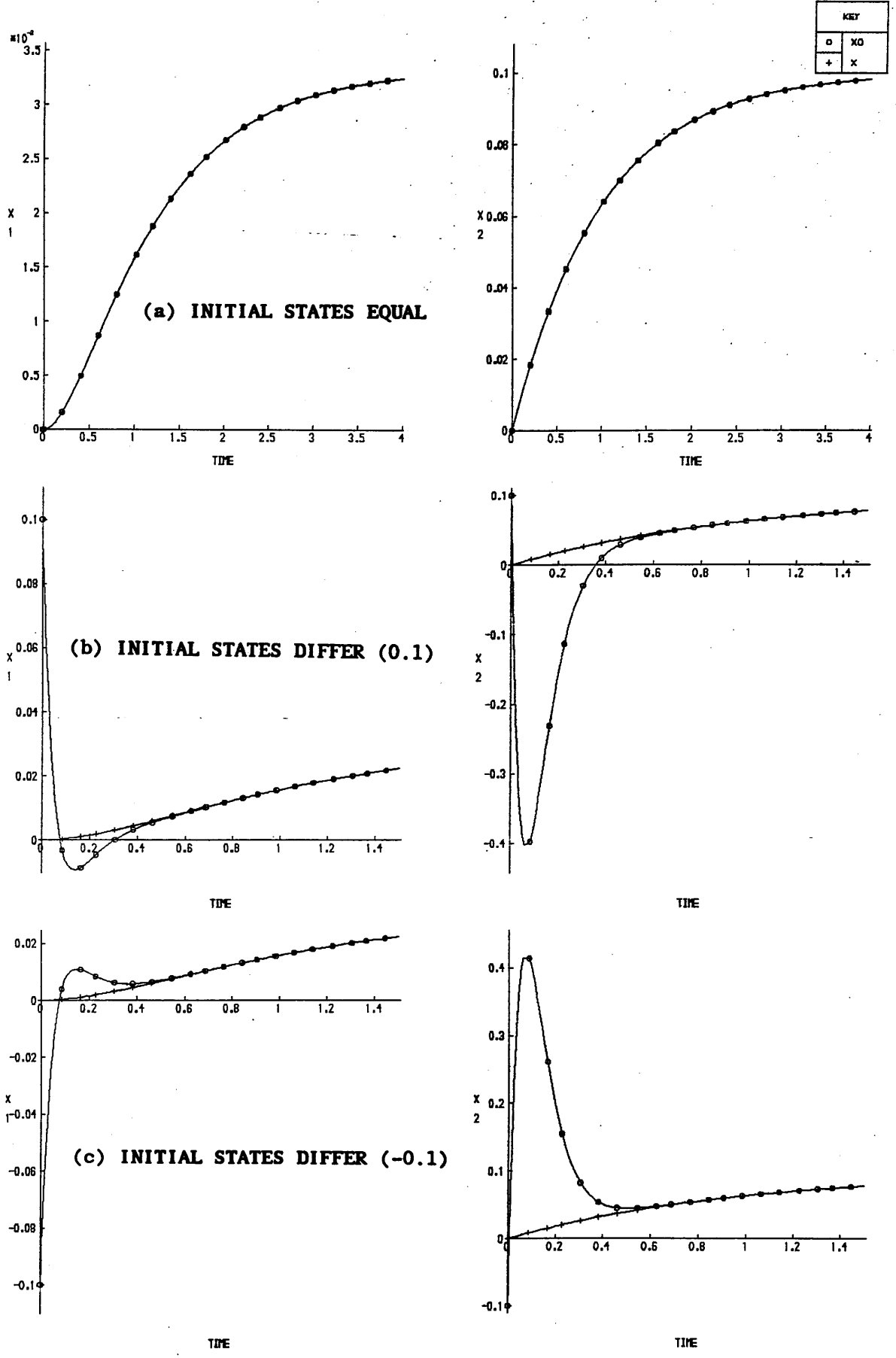

FIG 4.1 OBSERVER-1 RESPONSE TO STEP INPUT

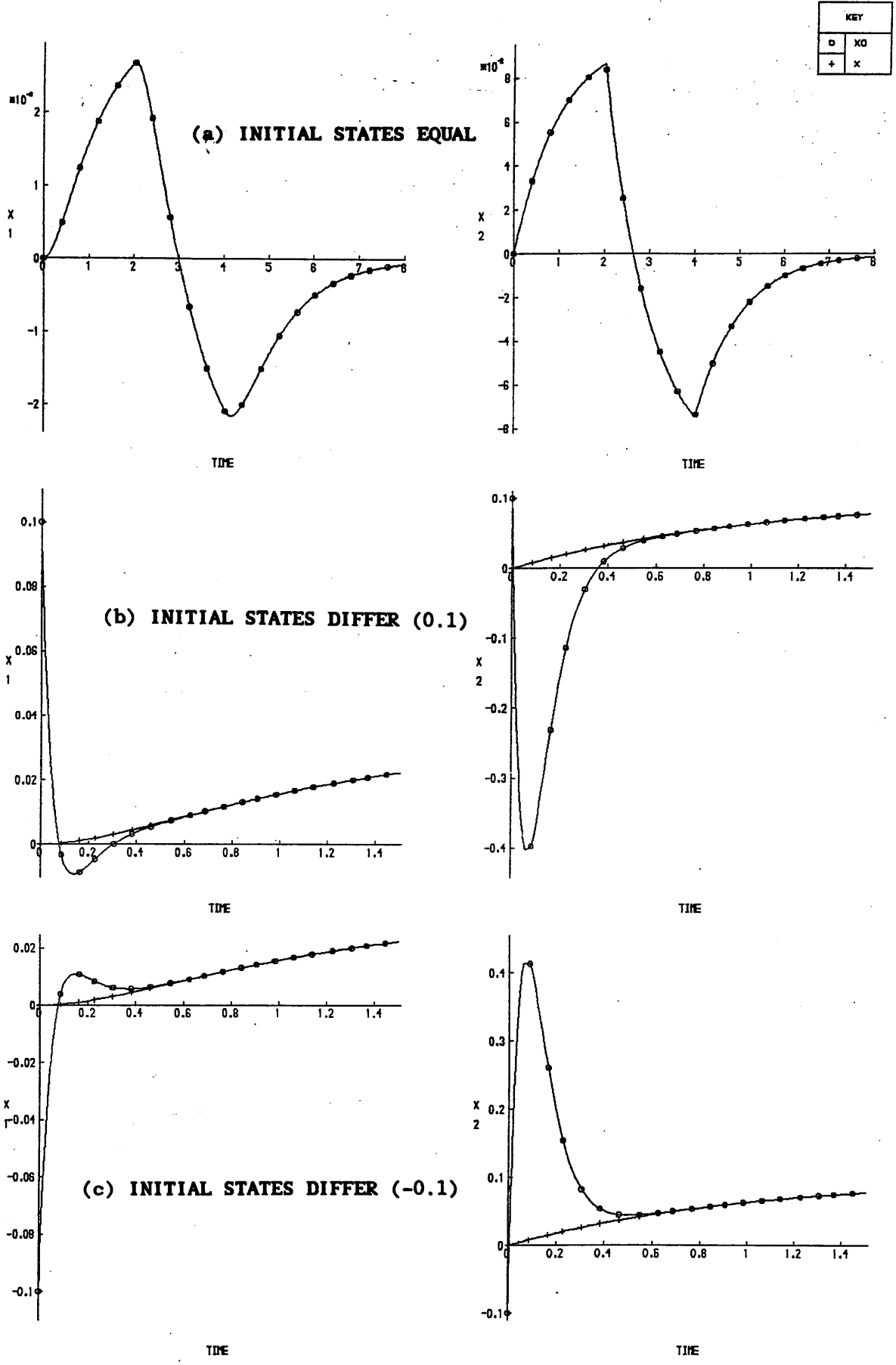

FIG 4.2 OBSERVER-1 RESPONSE TO DOUBLET INPUT

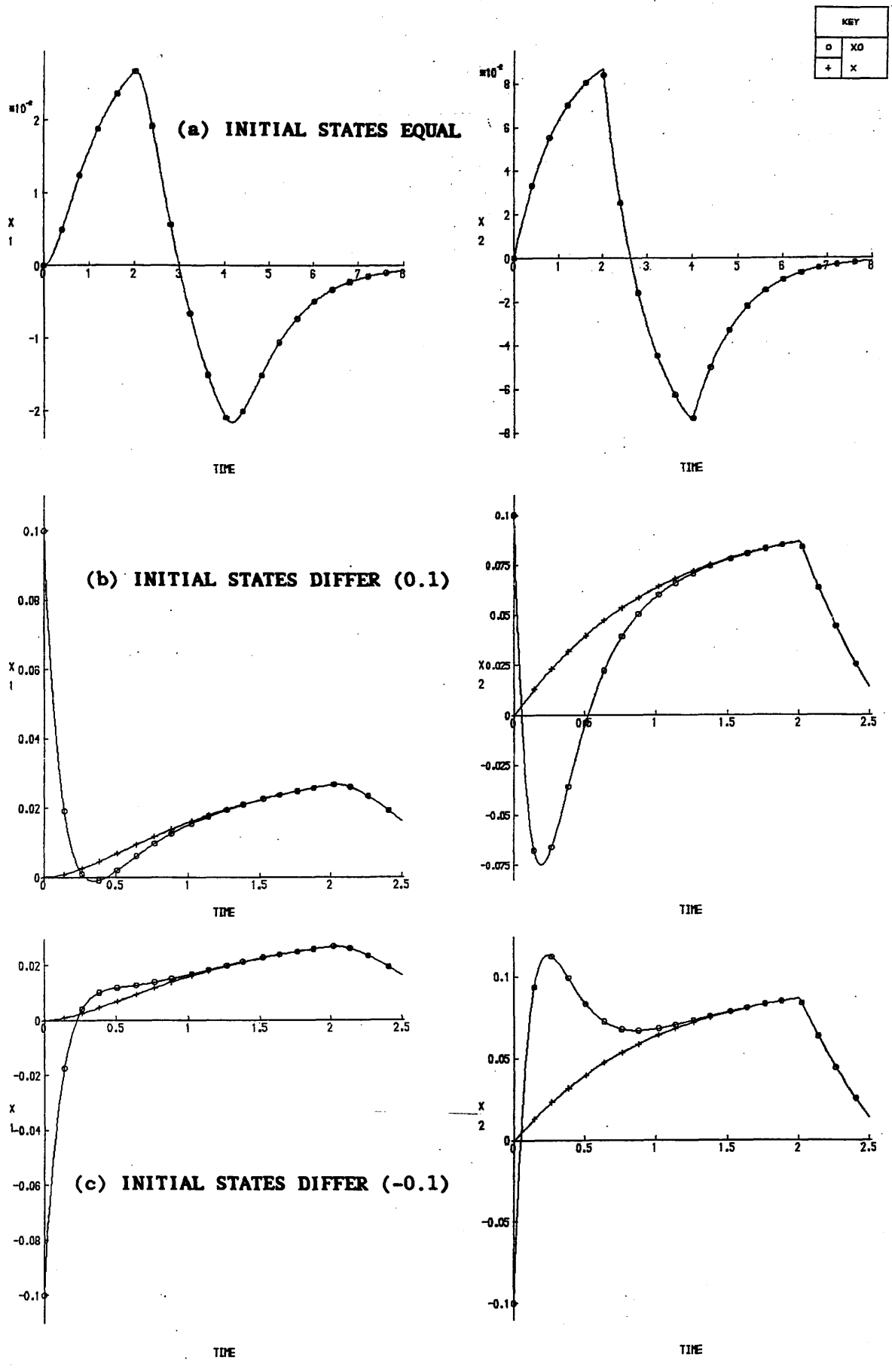

FIG 4.3 OBSERVER-2 RESPONSE TO DOUBLET INPUT

If the initial estimate of the system state is $\hat{\underset{\sim}{x}}_0$, then for an estimate $-\hat{\underset{\sim}{x}}_0$, the error dynamics of the observer, given by the time–response of $\underset{\sim}{e}$ ($=\underset{\sim}{x}-\hat{\underset{\sim}{x}}$ [eq 3.15]), will be the negative of those due to estimate $\hat{\underset{\sim}{x}}_0$. *Figs 4.1c, 4.2c* and *4.3c* give the state variable time–responses with $\hat{\underset{\sim}{x}}_0 = -0.1$, whilst a comparison of the error dynamics of observer–1 / U_2 for $\hat{\underset{\sim}{x}}_0 = 0.1$ and $\hat{\underset{\sim}{x}}_0 = -0.1$ is shown in *fig 4.4.* It can clearly be seen that the two time–responses are 'mirror images' of one another.

4.5.2 EFFECTS OF VARYING OBSERVER EIGENVALUES

As mentioned earlier there are three main consequences in increasing the magnitudes of the negative real parts of the observer eigenvalues: larger gains in H, larger magnitudes in transient and an increased susceptibility to noise. The latter will be dealt with in section 4.5.3.

Table 4.1, below, shows the values of the elements of the H matrix, h_1 and h_2, for required observer eigenvalues of -1 to -10. It is apparent that the value of h_2 rises as the square of the eigenvalues (plus one), whilst h_1 rises linearly.

EIGENVALUES	h_1	h_2
2 @ -1 + j0	-2	0
2 @ -2 + j0	0	1
2 @ -3 + j0	2	4
2 @ -4 + j0	4	9
2 @ -5 + j0	6	16
2 @ -6 + j0	8	25
2 @ -7 + j0	10	36
2 @ -8 + j0	12	49
2 @ -9 + j0	14	64
2 @ -10 + j0	16	81

TABLE 4.1

VALUES OF h_1 AND h_2

FOR DIFFERENT OBSERVER

EIGENVALUES

In general, for a (n×p) H matrix observing an n^{th} order system, several of the elements of H will tend to increase in proportion to the n^{th} power as the negative real parts of the required eigenvalues are increased.

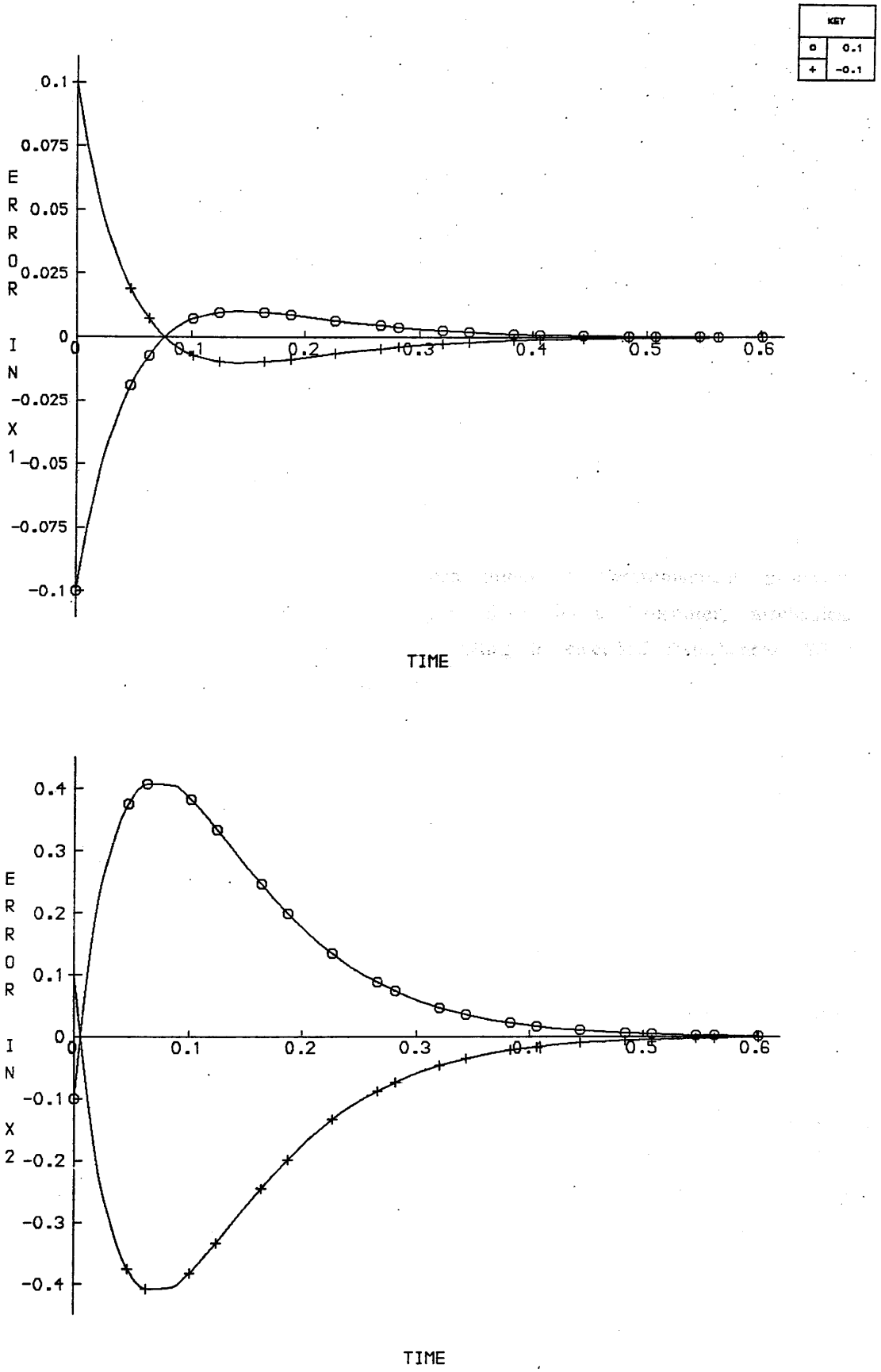

FIG 4.4 COMPARISON OF OBSERVER RESPONSE DUE TO $\hat{\underline{x}}_o$ = 0.1/-0.1

This has obvious implications on the numerical stability of design procedures and on the transient behaviour of the observer. The effect on the transient performance can clearly be seen in *figs 4.5a* and *4.5b*, which show the difference between observer−1 and observer−2 when subjected to input U_2. The larger eigenvalues of observer−1 have resulted in a faster response time (the time it takes the observer estimate $\hat{\underset{\sim}{x}}$ to converge to the true state $\underset{\sim}{x}$ or, alternatively, the error to reduce to zero), but the penalty is a greatly increased overshoot due to the larger gains.

4.5.3 EFFECTS OF NOISE

In a general sense, noise consists of any unwanted signals, random or deterministic, which interfere with the faithful reproduction of a desired signal in a system. Sources of interference (noise) include such things as electromagnetic pick−up, inadequate power supply filtering and, particularly in a helicopter, mechanical vibration (from the main and tail rotors) resulting in electrical disturbances. What effect does this noise have on the observer?

Consider the signals supplied to observer−1 to be as shown in *fig 4.6a*. These were generated by adding noise obtained from flight data, to the time−responses generated by TSIM for the doublet input U_2. The process and validity of adding noise obtained from flight data is examined in Section 5.2.5.

When the initial observer state $\hat{\underset{\sim}{x}}_0$ is equal to the system state $\underset{\sim}{x}$, the time−response is as shown in *fig 4.6b*. When $\hat{\underset{\sim}{x}}_0 \neq \underset{\sim}{x}$ ($\hat{\underset{\sim}{x}}_0 = 0.1$) the response is that of *fig 4.6c*. Clearly the observer is still following the state of the system, but the observer estimates are now corrupted by the noise on the inputs.

The effect of changing the eigenvalues can be seen from *fig 4.7* which shows a small section of the time−responses obtained from observer−1 and observer−2. The larger eigenvalues of observer−1 have resulted in the noise being amplified to a greater extent due to the faster dynamics. Thus as the system stands, when designing an observer it would be necessary to compromise between the speed of response and the level of acceptable noise on the estimates.

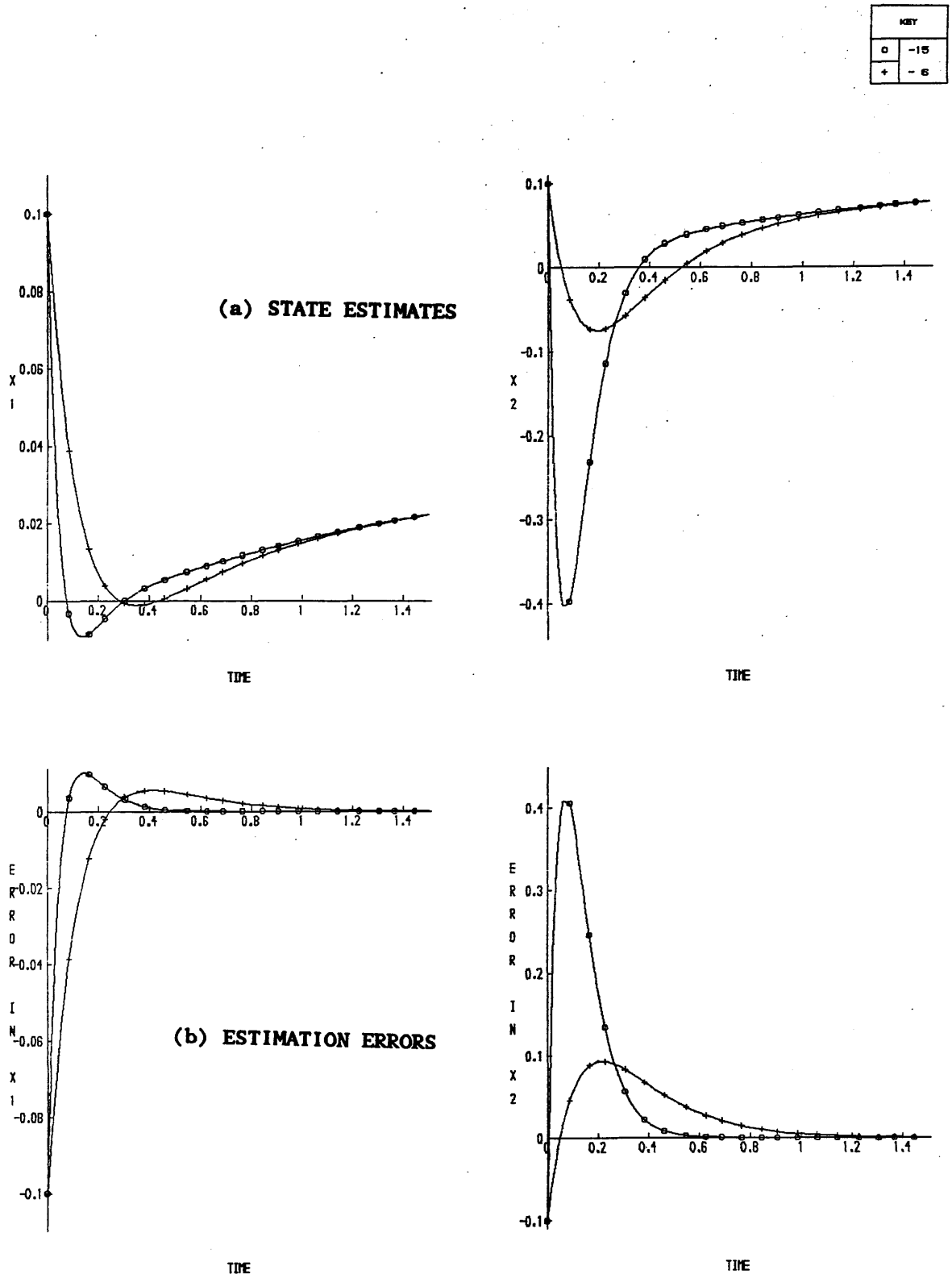

FIG 4.5 COMPARISON OF OBSERVER RESPONSE DUE TO DIFFERENT EIGENVALUES

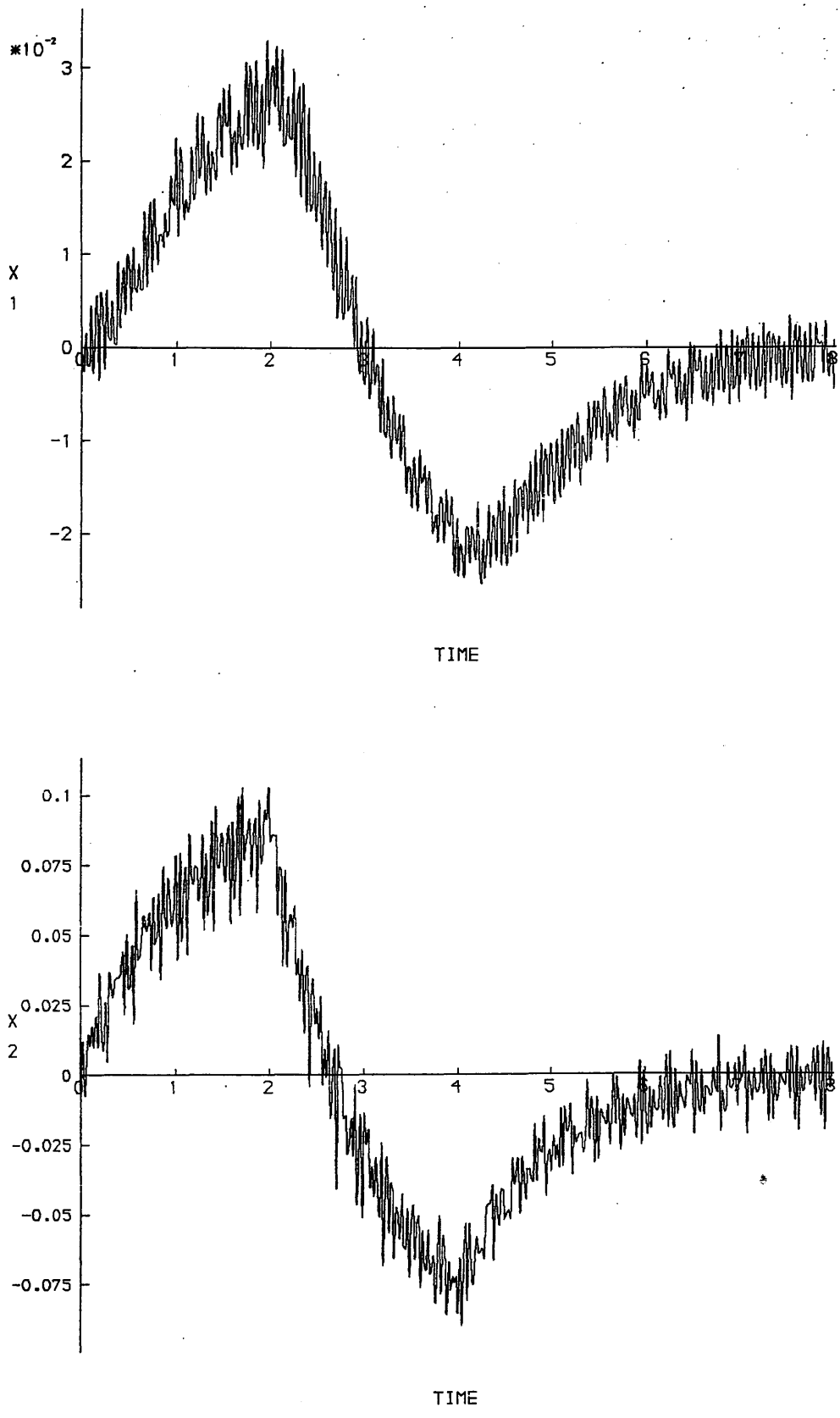

FIG 4.6A FLIGHT DATA NOISE ADDED TO SYSTEM STATE

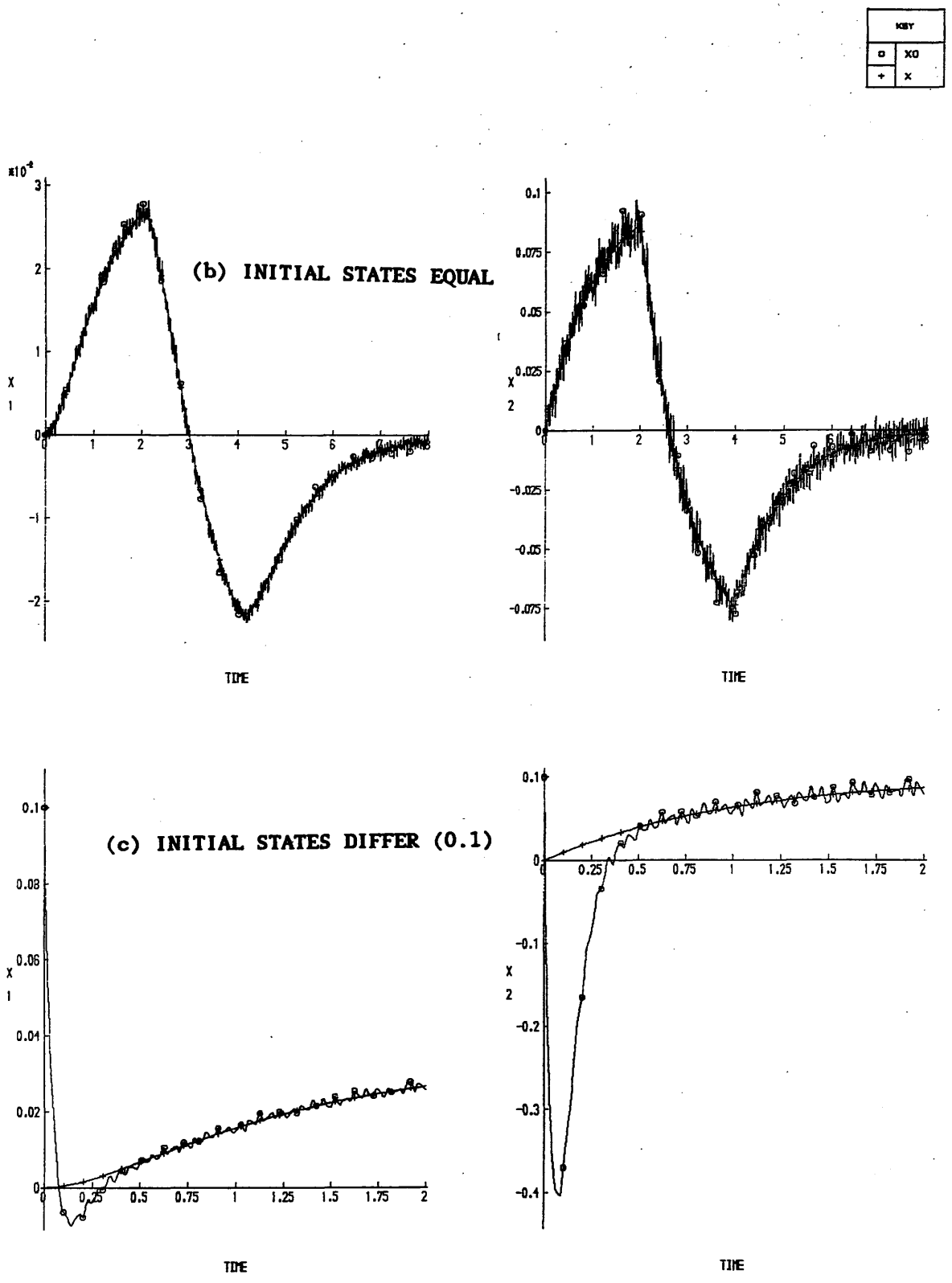

FIG 4.6B/C EFFECTS OF NOISE ON OBSERVER ESTIMATES

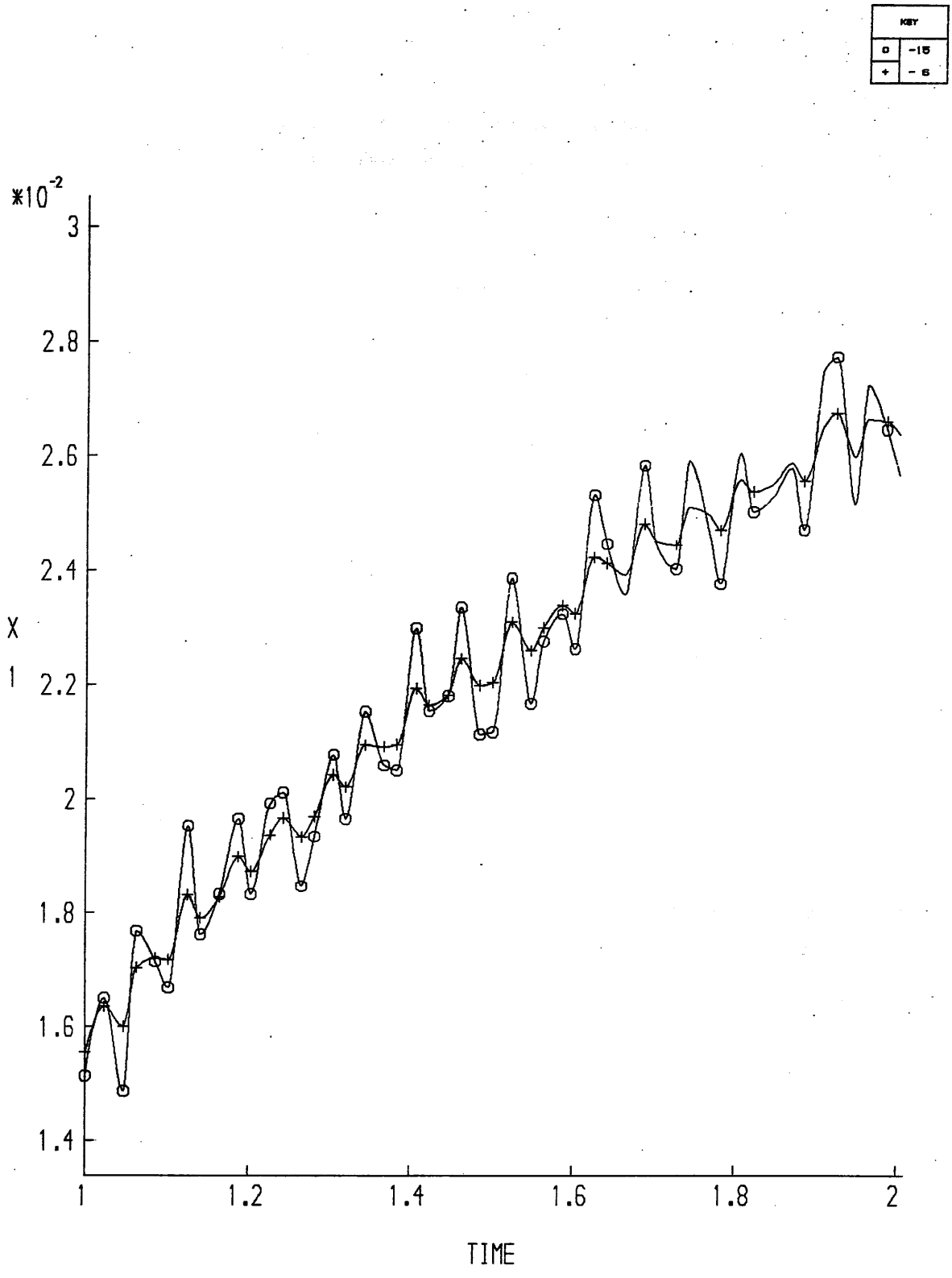

FIG 4.7 EFFECT OF DIFFERENT EIGENVALUES ON OBSERVER RESPONSE TO NOISY STATES

4.5.4 UNSTABLE SYSTEMS

When the system being observed is unstable, ie. has eigenvalues with positive real parts, the observer will still follow the state. This is easily demonstrated by altering the A matrix to:

$$A = \begin{bmatrix} -3 & 1 \\ 0 & 1 \end{bmatrix} \qquad \underset{\sim}{x} = \begin{bmatrix} x_1 \\ x_2 \end{bmatrix} \qquad \underset{\sim}{u} = [u_1]$$

which gives system eigenvalues of $\lambda_1 = -3$, $\lambda_2 = +1$. An H matrix can then be determined as previously and for a pair of eigenvalues at -15 this is given by,

$$H = \begin{bmatrix} 28 \\ 256 \end{bmatrix}$$

The time–responses of the system and observer when subjected to the doublet input (U_2), and with the initial observer state $\hat{\underset{\sim}{x}}_0 \neq \underset{\sim}{x}$ ($\hat{\underset{\sim}{x}}_0 = -1$), are shown in *fig 4.8.*

4.5.5 EFFECTS OF DIFFERENT C MATRICES

To examine the effects of changing the C matrix, in other words the system state(s) used in the estimation process, consider a fourth order longitudinal model of the Puma helicopter at 100 Knots, level flight. For this flight condition, the A and B matrices given by HELISTAB are,

$$A = \begin{bmatrix} -0.027 & 0.004 & 4.653 & -32.183 \\ -0.030 & -0.857 & 168.220 & 0.466 \\ 0.002 & -0.008 & -0.801 & 0.000 \\ 0.000 & 0.000 & 1.000 & 0.000 \end{bmatrix} \qquad B = \begin{bmatrix} -7.818 & -30.938 \\ -377.693 & -130.775 \\ 2.139 & 6.386 \\ 0.000 & 0.000 \end{bmatrix}$$

and the eigenvalues of A are complex conjugate pairs:

$-0.83 \pm j1.12$
$-0.02 \pm j0.18$

Flight data time–histories were used for inputs on θ_{0e} and θ_{1s}, the manoeuvre being a doublet on θ_{1s}. These input time–histories are shown in Appendix six. A

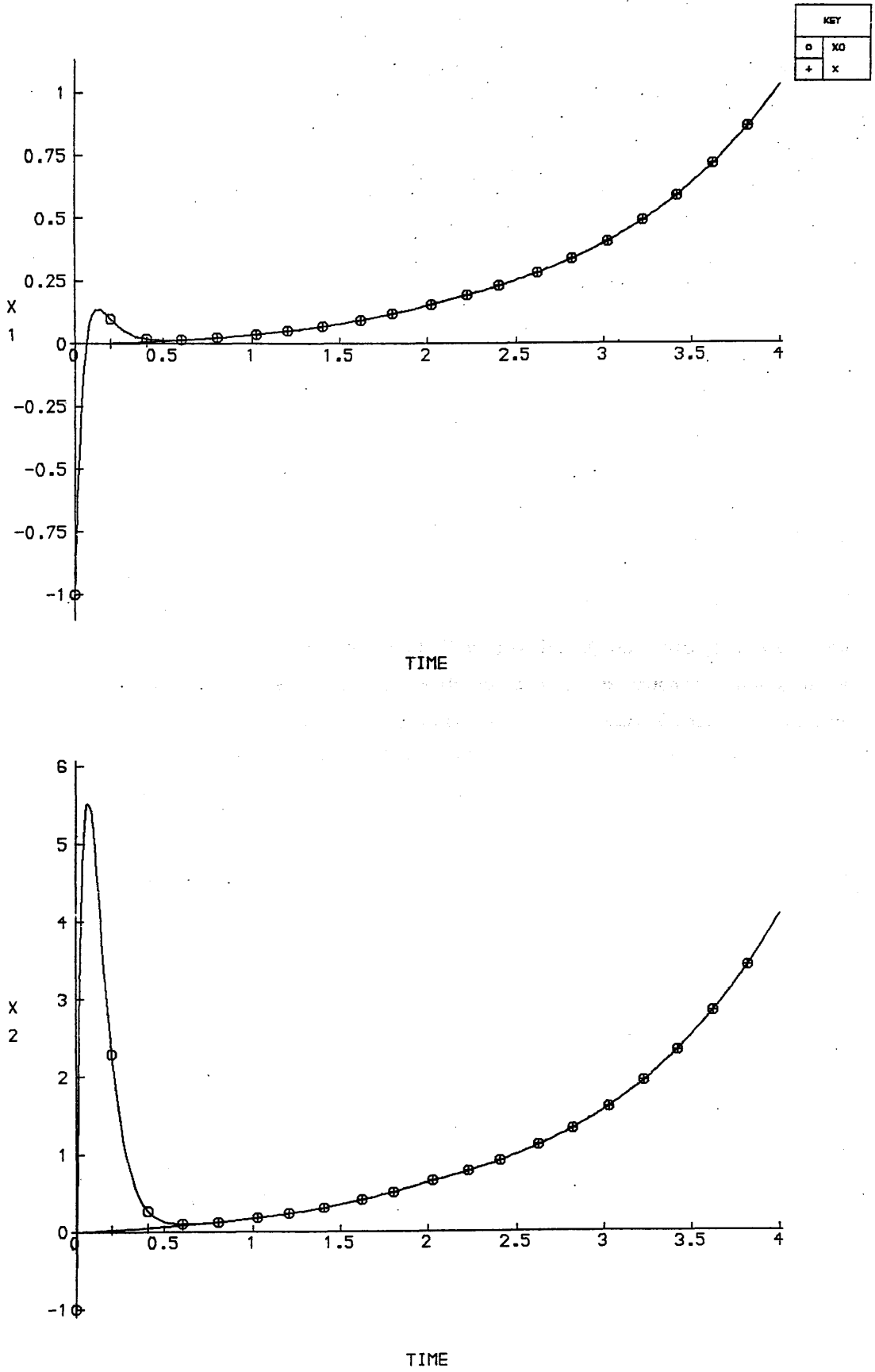

FIG 4.8 OBSERVER RESPONSE WITH AN UNSTABLE SYSTEM

full order, observable canonical form observer, with eigenvalues at

$$[\ -3.31,\ -3.38,\ -3.44,\ -3.51\ ]$$

was used and initial errors were introduced into the observer estimate. TSIM simulations were run for the following ten C matrices,

C(1)	C(1,2)	C(2,3)	C(3,4)
C(2)	C(1,3)	C(2,4)	
C(3)	C(1,4)		
C(4)			

and a comparison of their respective error time–responses, for forward velocity (u), are shown in *fig 4.9*.

It is immediately evident that the choice of C matrix has a very strong influence on the transient behaviour of the observer (overshoots vary by as much as two to three orders of magnitude) and this can be explained using the *Modal Expansion Theorem* [Andry Jr, Shapiro and Chung, 1983]. This demonstrates that every solution representing a free response of:

$$\dot{\underset{\sim}{x}}(t) = A\underset{\sim}{x}(t) \qquad \underset{\sim}{x}(0) = \underset{\sim}{x}_0 \tag{4.19}$$

depends on three quantities –

(1) eigenvalues, which determine the *decay/ growth rate* of the response,

(2) eigenvectors, which determine the *shape* of the response, and

(3) the initial condition, which determines the *degree* to which each mode will participate in the free response.

For the forced system of equation 4.9, there is a fourth quantity: namely the input vector $\underset{\sim}{u}$, however for two similar observers (ie. with the same eigenvalues and initial conditions, but different C matrices) it is the difference in eigenvectors which causes the dissimilar transient behaviour.

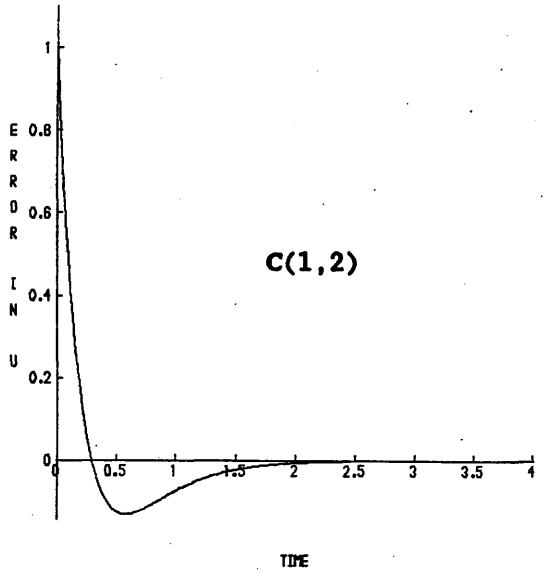

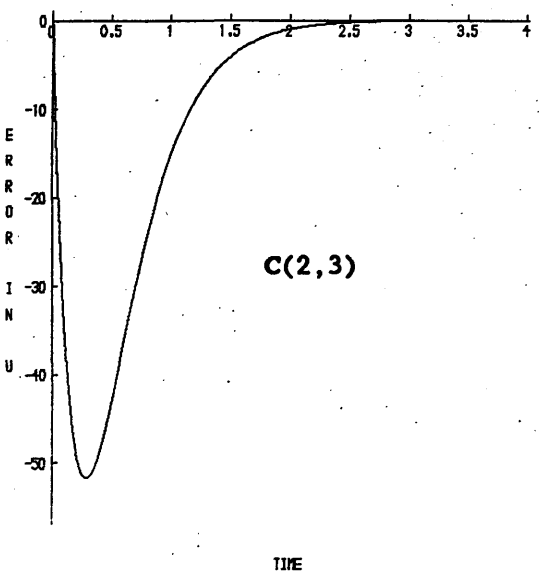

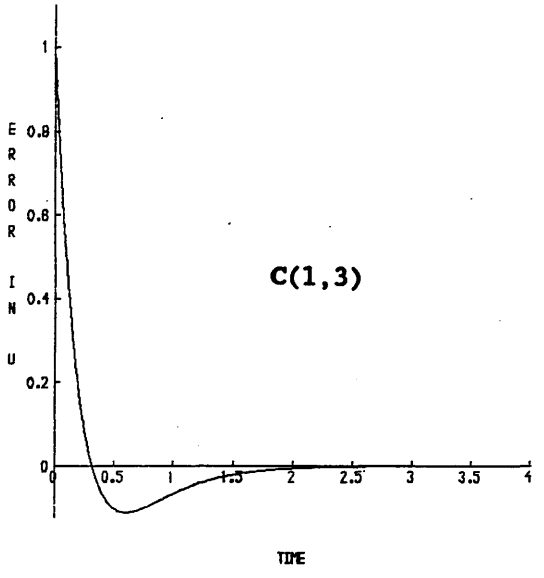

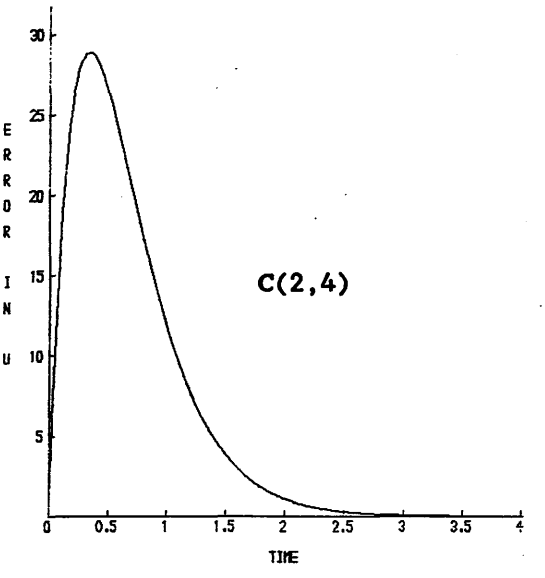

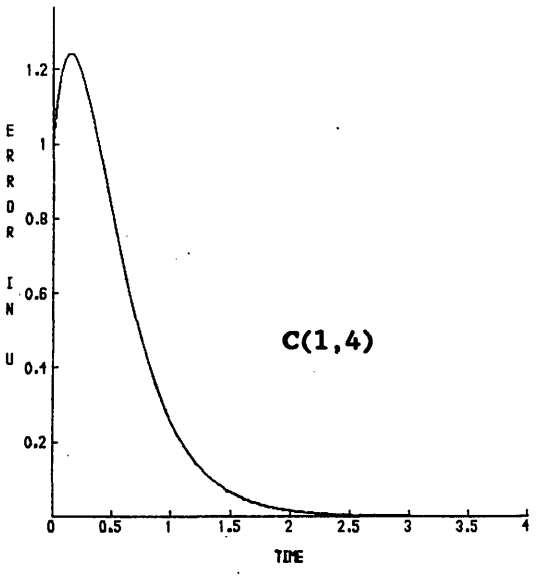

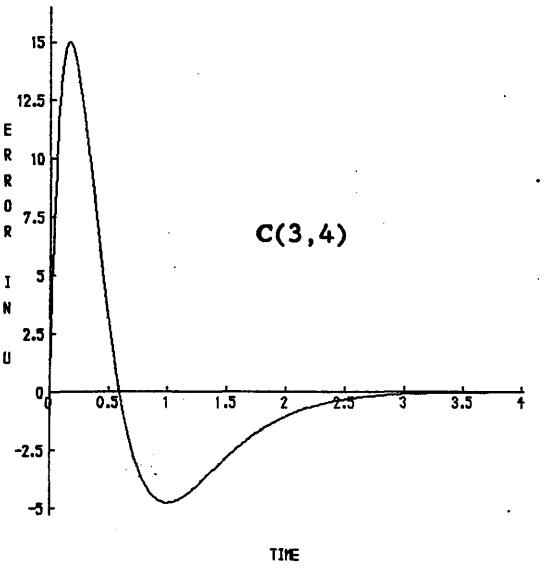

FIG 4.9 COMPARISON OF ERROR IN u FOR DIFFERENT C MATRICES

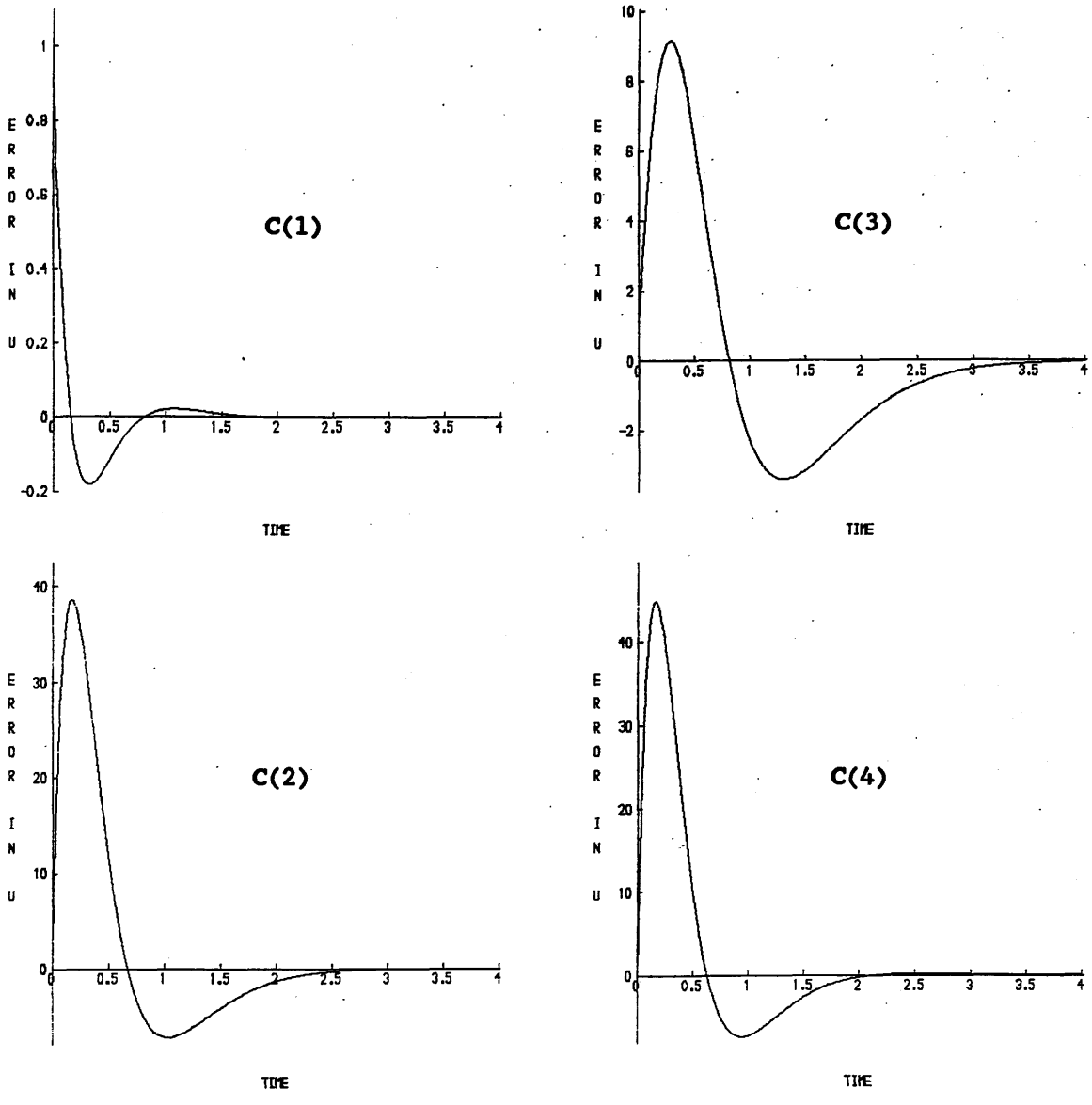

FIG 4.9 COMPARISON OF ERROR IN u FOR DIFFERENT C MATRICES

4.6 NUMERICAL PROBLEMS WITH THE GOPINATH METHOD

In any discussion of numerical problems it is important to understand the following terms,

- A problem is said to be *ill−conditioned* if small changes in data will lead to large changes in solutions; otherwise it is *well−conditioned.*

- A procedure for solving a problem is said to be *numerically stable* if numerical errors inside the procedure will not be amplified; otherwise the algorithm is *numerically unstable.*

The condition of a problem and the numerical stability of an algorithm are two independent concepts and clearly, whenever possible, a numerically stable method should be used to solve a problem. If a numerically stable method is used to solve a well− conditioned problem then the result will generally be good; however if the problem is ill− conditioned, even if a stable algorithm is used, there is no guarantee that the result will be correct.

With the Gopinath method the fundamental equation to be solved is that of equation 4.3 which, as was shown in section 4.3, requires to be manipulated into the form of equation 4.7 for a solution to be obtained. Although the solution of linear equations

$$A\underset{\sim}{x} = \underset{\sim}{b} \tag{4.20}$$

can be written as

$$\underset{\sim}{x} = A^{-1}\underset{\sim}{b} \tag{4.21}$$

the solution should never be computed by first inverting A and then computing $A^{-1}\underset{\sim}{b}$, since this is numerically unstable.

NAG routine F04ATF [N4] calculates the accurate solution of a set of real linear equations with a single right hand side by the numerically stable method of Crouts Factorisation (the solution is to full machine accuracy : Real*8 arithmetic on the VAX− 11/750 NAG implementation) and was therefore used to obtain the elements of H from equation 4.7. Unfortunately, in obtaining equation 4.7 there are several stages at which errors can be introduced.

One of these is in determining the coefficients of the characteristic equation of A (equation 4.1). To do this it is necessary to first determine the eigenvalues of A or, in other words, the roots of the characteristic equation. This is achieved by using a series of NAG routines [N4] in order to optimize the accuracy of the procedure. These are F01ATF which balances the matrix (the Euclidean norm of the matrix is reduced since most eigenvalue programs produce results with errors proportional to the Euclidean norm of the matrix), F01AKF which then reduces it to *upper Hessenberg* form and finally F02APF which calculates the eigenvalues using Francis' economical method for performing the QR algorithm without using complex arithmetic.

The first two routines are extremely accurate, however, although the QR algorithm is very stable, the accuracy of the eigenvalues determined by routine F02APF depends on how well–conditioned the original matrix is. An interesting example of the problem is given by Chen, 1984, where it is shown how two of the eigenvalues of the matrix:

$$\begin{bmatrix} 20 & 20 & & & & \\ & 19 & 20 & & & \\ & & 18 & 20 & & \\ & & & \ddots & & \\ & & & & 2 & \\ \alpha & & & & & 1 \end{bmatrix}$$

$\alpha = 7.8 \times 10^{-14}$	$10.5 \pm j0$
$\alpha = 10^{-10}$	$10.5 \pm j2.73$
$\alpha = 10^{-5}$	$10.5 \pm j8.05$
$\alpha = 1$	$10.5 \pm j16.26$

change as the value of α (the element at the $[20,1]^{th}$ position) varies. See also Crossley and Porter, 1969, who consider the more general problem of eigenvalue *and* eigenvector sensitivities.

Having determined the eigenvalues of A, or once the prescribed eigenvalues have been selected for the observer, the next task is to calculate the coefficients a_i and γ_i of the respective characteristic equations (equations 4.1 and 4.2). The algorithm used is given as a FORTRAN computer program in Appendix 3 and only involves the operations of addition and multiplication. Thus the sole source of errors at this stage would be through the introduction and propagation of round–off errors.

The final step is to form equation 4.7 using equations 4.3 to 4.6, inclusive. All operations, except in determining the inverse of F, involve only addition and multiplication, however the A matrix in particular is not usually well–conditioned since the elements tend to have large variations in magnitude. NAG routine F04AEF

[N4] is used to calculate the inverse of F and the solution is accurate to full machine accuracy.

The need to calculate the inverse of F can be eliminated by pre-multiplying both sides of equation 4.3 by F and therefore modifying equation 4.7 to,

$$F D \underset{\sim}{h} = \underset{\sim}{\gamma} - \underset{\sim}{a} \qquad (4.22)$$

where D is defined, as previously, by equation 4.8.

Finally note the range of magnitude of the numbers involved since a wide range tends to produce an ill-conditioned problem. This is particularly the case when an operation involves numbers at opposite ends of the range, eg. adding a small number to a large number. For instance, in an eighth order model requiring eight observer eigenvalues at -20, the coefficients of the characteristic equation would be:

$\alpha_1 = 1.6 \times 10^2$ $\qquad$ $\alpha_5 = 1.792 \times 10^8$

$\alpha_2 = 1.12 \times 10^4$ $\qquad$ $\alpha_6 = 1.792 \times 10^9$

$\alpha_3 = 4.48 \times 10^5$ $\qquad$ $\alpha_7 = 1.024 \times 10^{10}$

$\alpha_4 = 1.12 \times 10^7$ $\qquad$ $\alpha_8 = 2.56 \times 10^{10}$

For a fourteenth order model the range would be from $\alpha_1 = 2.8 \times 10^2$ to $\alpha_{14} = 1.6384 \times 10^{14}$. Similar differences in magnitude can be observed in the D matrix.

4.7 OBSERVER DESIGN RESULTS OBTAINED USING THE GOPINATH METHOD

The model used to test the FORTRAN computer program was of a Lynx helicopter at eighty knots level flight. The A and B matrices obtained from HELISTAB are shown in Appendix five and the eigenvalues of the A matrix are

-10.545	0.134 ± j0.376
-3.199	-0.406
-0.654 ± j2.255	-0.031

The required eigenvalues for the full order observer were arbitrarily stipulated to be:

[-20, -20, -18, -17, -16, -15, -15, -12]

and two C matrices of dimensions (1×8) and (2×8) were used,

$$C_1 = [\ 0\ 0\ 1\ 0\ 0\ 0\ 0\ 0\ ] \qquad C_2 = \begin{bmatrix} 1 & 1 & 0 & 1 & 1 & 0 & 1 & 1 \\ 0 & 1 & 1 & 0 & 1 & 1 & 0 & 1 \end{bmatrix}$$

Four versions of the program were tested and the differences between them were as follows,

(1) Real*8 arithmetic and equations 4.3/4.7, ie. the inverse of F is used on the right hand side of the equation.

(2) Real*16 arithmetic and equations 4.3/4.7 (Nb. NAG routines still in Real*8).

(3) Real*8 arithmetic and equation 4.22, ie. inverse of F not required.

(4) Real*16 arithmetic and equation 4.22.

The results obtained, in terms of the eigenvalues, are shown in Tables 4.2 and 4.3 for C_1 and C_2 respectively. For each of the eight required eigenvalues, the minimum, percentage magnitude error is indicated by a '*'. It should be noted that the previous comments concerning the accuracy of eigenvalues detremined by NAG routine F02APF, apply equally to the determination of the eigenvalues of [A− HC].

The obvious difference between the two sets of results is that those obtained from using C_1 are much more accurate than those obtained from C_2. This loss of accuracy is due to the increase in the number of calculations involved and hence an increased opportunity for errors to be introduced, accumulate and propagate. For example, with p=1: C is of dimension (1×8) and H is (8×1). Therefore the 64 elements of the product HC will each be produced by a single multiplication. However, when p=2: the product of H (8×2) and C (2×8) will require the addition of two multiplications for each of the 64 elements, eg.

$$HC_{11} = H_{11}*C_{11} + H_{12}*C_{21}$$

The second point that can be deduced, is that the best results are achieved using version four of the program. Unfortunately with C_2 the designs still contain unacceptable deviations from the required eigenvalues. Several other flight conditions were also examined and the same pattern of C_1 giving superior results to C_2 and version four of the program giving the fewest errors, was repeated.

VERS	REQ'D EV'S	DESIGNED EV'S		ERRORS		
		REAL	IMAG	REAL	IMAG	% MAG
1	-20	-20.00	.03	.75E-3	-.34E-1	.004
	-20	-20.00	-.03	.75E-3	.34E-1	.004
	-18	-17.99	0	-.70E-2	0	.039
	-17	-17.01	0	.12E-1	0	.071
	-16	-15.99	0	-.12E-1	0	.074
	-15	-15.05	0	.51E-1	0	.343
	-15	-14.95	0	-.46E-1	0	.307
	-12	-12.00	0	.41E-5	0	.000*
2	-20	-20.00	.05	.17E-2	-.51E-1	.009
	-20	-20.00	-.05	.17E-2	.51E-1	.009
	-18	-17.98	0	-.15E-1	0	.084
	-17	-17.02	0	.25E-1	0	.146
	-16	-15.98	0	-.23E-1	0	.146
	-15	-15.07	0	.72E-1	0	.477
	-15	-14.94	0	-.61E-1	0	.407
	-12	-12.00	0	.50E-5	0	.000*

VERS	REQ'D EV'S	DESIGNED EV'S		ERRORS		
		REAL	IMAG	REAL	IMAG	% MAG
3	-20	-20.00	.03	.81E-3	-.34E-1	.004
	-20	-20.00	-.03	.81E-3	.34E-1	.004
	-18	-17.99	0	-.83E-2	0	.046
	-17	-17.02	0	.15E-1	0	.090
	-16	-15.98	0	-.16E-1	0	.102
	-15	-15.06	0	.63E-1	0	.417
	-15	-14.94	0	-.55E-1	0	.365
	-12	-12.00	0	.66E-5	0	.000*
4	-20	-20.00	.02	.40E-3	-.25E-1	.002*
	-20	-20.00	-.02	.40E-3	.25E-1	.002*
	-18	-17.99	0	-.36E-2	0	.020*
	-17	-17.01	0	.62E-2	0	.036*
	-16	-15.99	0	-.60E-2	0	.038*
	-15	-15.04	0	.36E-1	0	.238*
	-15	-14.97	0	-.33E-1	0	.220*
	-12	-12.00	0	.20E-5	0	.000*

TABLE 4.2 : ERROR ANALYSIS FOR OBSERVERS DESIGNED WITH C1

VERS	REQ'D EV'S	DESIGNED EV'S		ERRORS		
		REAL	IMAG	REAL	IMAG	% MAG
1	-20	-29.17	9.18	.92E+1	-.92E+1	53.04
	-20	-29.17	-9.18	.92E+1	.92E+1	53.04
	-18	-15.38	9.99	-.26E+1	-.10E+2	1.92
	-17	-15.38	-9.99	-.16E+1	.10E+2	7.91
	-16	-11.15	4.44	-.48E+1	-.44E+1	24.99
	-15	-11.15	-4.44	-.38E+1	.44E+1	19.99
	-15	-10.76	0.72	-.42E+1	-.72E+0	28.11
	-12	-10.76	-0.72	-.12E+1	.72E+0	10.13
2	-20	-26.64	6.58	.66E+1	-.66E+1	37.20
	-20	-26.64	-6.58	.66E+1	.66E+1	37.20
	-18	-16.32	8.03	-.17E+1	-.80E+1	1.05*
	-17	-16.32	-8.03	-.68E+0	.80E+1	6.96*
	-16	-12.33	3.93	-.37E+1	-.39E+1	19.12
	-15	-12.33	-3.93	-.27E+1	.39E+1	13.73
	-15	-11.22	1.02	-.38E+1	-.10E+1	24.89
	-12	-11.22	-1.02	-.78E+0	.10E+1	6.16

VERS	REQ'D EV'S	DESIGNED EV'S		ERRORS		
		REAL	IMAG	REAL	IMAG	% MAG
3	-20	-32.12	0	.12E+2	0	60.50
	-20	-21.31	11.10	.13E+2	-.11E+2	74.56
	-18	-21.31	-11.10	.33E+1	.11E+2	33.49
	-17	-12.79	6.88	-.42E+1	-.69E+1	14.57
	-16	-12.79	- 6.88	-.32E+1	.69E+1	9.23*
	-15	-11.07	0	-.39E+1	0	26.20
	-15	-10.81	2.31	-.42E+1	-.23E+1	26.31
	-12	-10.81	- 2.31	-.12E+1	.23E+1	7.88
4	-20	-24.61	4.41	.46E+1	-.44E+1	25.01*
	-20	-24.61	- 4.41	.46E+1	.44E+1	25.01*
	-18	-17.07	6.59	-.93E+0	-.66E+1	1.66
	-17	-17.07	- 6.59	.71E-1	.66E+1	7.64
	-16	-12.82	3.37	-.32E+1	-.34E+1	17.15
	-15	-12.82	- 3.37	-.22E+1	.34E+1	11.63*
	-15	-12.44	0	-.26E+1	0	17.07*
	-12	-11.56	0	-.44E+0	0	3.71*

TABLE 4.3 : ERROR ANALYSIS FOR OBSERVERS DESIGNED WITH C2

4.8 CONCLUSIONS

From the above results, which demonstrate the difficulties in accurately designing an observer with a desired set of eigenvalues, it is apparent that the dyadic observer design algorithm proposed by Gopinath is unsuitable for systems of this order. The reasons for this are twofold. Firstly the system (A), distribution (B) and output (C) matrices are usually ill–conditioned, or tend to produce an ill–conditioned problem, and secondly the digital computer implementation of the algorithm is numerically unstable.

Fortunately, an alternative method was established in section 4.4 where it was shown that the determination of the observer matrix, H, was a trivial calculation once the system had been transformed into observable canonical form. An important consequence of this transformation is that it allows the system to be treated as a set of coupled subsystems, each of which is of lower order than the complete system.

For example, with $n=8$ and $p=2$, the subsystems are of order four and therefore two full order observers (with $n=4$) or two reduced order observers ($n=3$) are required. This is a numerically simpler task than determining an observer for the full order, untransformed system.

For these reasons, it was thus decided to reject the Gopinath design method and to continue investigation of the canonical form method.

CHAPTER FIVE

THE DESIGN OF AN OBSERVABLE CANONICAL FORM OBSERVER AND ITS USE WITH A FEEDBACK CONTROLLER

5.1 INTRODUCTION

In chapter four it was demonstrated that the design method of Gopinath, 1971), which avoids the use of canonical forms and is applicable to the design of both controllers and observers, was unsuitable for systems of this order. This was due to the fact that when the algorithm was implemented on a digital computer it tended to produce the undesirable combination of an ill–conditioned problem with an unstable algorithm.

It was also established that if the system is transformed to observable canonical form (ie. equations 4.11/4.12) then the determination of the observer matrix H becomes trivial. This transformattion can be accomplished using the algorithm given in section 3.7.2 and its effect on the observer equations was detailed in section 3.8.

An important consequence of the system being transformed into observable canonical form is that in this form it can be considered as a set of subsystems, each being coupled to each other only through their outputs. This leads to further modifications of the observer equations and the particulars of these are given in section 3.9.

This chapter covers the software implementation of full and reduced order observable canonical form observers, for both eighth and fourteenth order system models. Consideration is given to the selection of observer eigenvalues with respect to the accuracy of the design. The use of flight data is examined and the method for obtaining noise from the state variables, for use in simulations, is given. A method of evaluating observer performance by correlation methods is described and the use of an observer in a feedback control system is demonstrated. It is shown that the observer provides an estimate of the state $\underset{\sim}{x}$ without altering the dynamics of the controller. The system plus controller is then used to illustrate some further properties of observers: the effects of varying individual observer eigenvalues or of varying p; and the effect different sensor faults have on the state estimates.

5.2 COMPUTER IMPLEMENTATION OF THE DESIGN PROCEDURE

The transformation of a multivariable state space description of a system into observable canonical form by hand is, at best, a time–consuming, laborious, error–prone process. For large order systems it approaches the impossible. Fortunately, the use of modern digital computers and numerical methods makes the procedure a comparatively simple one although, as will be seen in chapter six, not without its own associated (numerical) problems.

During the course of the research a *Fortran* program was developed which automated the observer design procedure. The program was written such that it could be resident within a *Tsim* executable file and thus allowed design and simulation to be generated from a single program. The various sections of the program: observability test, transformation to observable canonical form, observer design and addition of noise, are dealt with in the following sections. Any, or all, of the subroutines can be run in batch mode.

5.2.1 THE OBSERVABILITY TEST

The first step in designing any observer, irrespective of the subsequent design algorithm, is to ascertain whether the pair [A,C] is observable. Four equivalent conditions for observability are stated in section 3.3 and the method selected was,

If the (np×n) *observability matrix*

$$V_2 = [\ C\ CA\ \ldots\ CA^{n-1}\ ]^T \tag{5.1}$$

is of full column rank n, the the pair [A,C] is observable

An equivalent statement, as shown in section 3.7, is

If the (n×np) observability matrix

$$V = [\ C^T\ A^TC^T\ \ldots\ (A^T)^{n-1}C^T\ ] \tag{5.2}$$

is of full row rank n, then the pair [A,C] is observable

Now since the algorithm given in section 3.7.2 to transform a system into observable canonical form involves the selection of n linearly independent (LIN) vectors in the sequence,

$$C_1,\ C_2,\ \ldots\ C_p,\ C_1A,\ C_2A,\ \ldots\ C_pA,\ C_1A^2,\ \ldots.\ C_pA^{n-1} \tag{5.3}$$

it is logical to use the form of equation 5.1 for the observability test. The reason for this follows directly from the definition of the rank of a matrix :

The rank of a matrix A, is the number of LIN rows (and columns) in A.

The rank is also equal to the order of the largest non−zero *minor* of A (a minor is the determinant of any square submatrix of A) or to the number of non−zero rows when the matrix is transformed into *row echelon form* (a matrix with an ever−increasing number of zeros in its rows until, possibly, all elements are zero).

To first evaluate V_2 and then calculate the rank would be improvident, since the composite matrix has n*p rows, but there can at most be only n linearly independent rows. It is more judicious to determine the m ($0 \leqslant m \leqslant n$) linearly independent rows by examining V_2 in the sequence given by 5.3. Often the first n rows are linearly independent and therefore much computation is saved and the accuracy improved since lower powers of A are involved. If a row of form C_jA^k is found to be linearly dependent then all rows of form $C_jA^{k+\alpha}$, for [$\alpha = 1,2,3,...$], are also linearly dependent and need not be examined (section 3.7.1). Thus it is obvious that an initial requirement is that C has linearly independent rows.

In order to determine whether the rows of a matrix are linearly independent, *NAG* routine F04JDF, [N4], is used. This routine returns the rank of a matrix by evaluating its *singular value decomposition* (the rank is equal to the number of singular values).

Therefore, to calculate the rank of V_2 a new matrix is formed from the p linearly independent rows of C and hence initially has rank equal to p. If the next row from sequence 5.3 is added to this matrix it will then have p+1 rows: if the rank of the matrix is now p+1, then these p+1 rows are linearly independent and the new row is retained. However, if the rank is still equal to p, the new row is linearly dependent and is rejected.

This procedure continues until n rows have been obtained, in which case V_2 is of rank n; or until the last row has been examined and rejected, in which case $m < n$ and the pair [A,C] is unobservable. This is a valid method for calculating the rank of V_2 due to the above and because *if a set of vectors is linearly dependent, then any larger set, containing this set, is also linearly dependent* (Bronson, 1969). The observability of pair [A,C] ensures the observability of pair $[A_{11},A_{21}]$ and hence the ability to construct a reduced order observer (section 3.6).

The observability test took approximately fifteen to thirty seconds of central processing unit (CPU) time for an eighth order system and approximately sixty to ninety seconds for a fourteenth order system: the minimum times occurring when the first n vectors are linearly independent.

If the complete system is unobservable with V_2 having rank m ($m < n$) as determined above, then there exists an equivalence transformation, $\underset{\sim}{z} = P\underset{\sim}{x}$ that transforms the system into,

$$\begin{bmatrix} \dot{z}_0 \\ \dot{z}_{\bar{0}} \end{bmatrix} = \begin{bmatrix} \tilde{A}_0 & 0 \\ \tilde{A}_{21} & \tilde{A}_{\bar{0}} \end{bmatrix} \begin{bmatrix} z_0 \\ z_{\bar{0}} \end{bmatrix} + \begin{bmatrix} \tilde{B}_0 \\ \tilde{B}_{\bar{0}} \end{bmatrix} \underset{\sim}{u} \tag{5.4}$$

$$y = \begin{bmatrix} \tilde{C}_0 & 0 \end{bmatrix} \begin{bmatrix} z_0 \\ z_{\bar{0}} \end{bmatrix} \tag{5.5}$$

where the subscripts '$_0$' and '$_{\bar{0}}$' signify observable and unobservable, respectively, and the m− dimensional subequation of the above,

$$\left.\begin{aligned} \dot{\underset{\sim}{z}}_0 &= \tilde{A}_0 \underset{\sim}{z}_0 + \tilde{B}_0 \underset{\sim}{u} \\ y &= \tilde{C}_0 z_0 \end{aligned}\right\} \tag{5.6}$$

is observable (the observability and controllability of a linear, time− invariant, dynamical equation are invariant under any equivalence transformation) and has the same transfer− function matrix as the original system. For a proof see Chen, 1984.

5.2.2 THE TRANSFORMATION TO OBSERVABLE CANONICAL FORM

From the previous section, if the pair [A,C] is observable then there will be n linearly independent vectors which can be arranged in the form of (3.11),

$$\begin{bmatrix} C_1 & C_1A & \dots & C_1A^{\mu_1-1} & C_2 & C_2A & \dots & C_2A^{\mu_2-1} & \dots & C_p & \dots & C_pA^{\mu_p-1} \end{bmatrix}^T$$

to determine the observability indices $\{\mu_1, \mu_2, \dots, \mu_p\}$. These are the dimensions of the blocks on the main diagonal of the transformed matrix $\tilde{A}$ or, in other words, the orders of the sub systems for which full order (μ_i) or reduced order ($\mu_i - 1$) observers can be designed.

Steps (3) to (7) of the transformation algorithm (section 3.7.2) were relatively straightforward to program, the inverses being determined by *NAG* routine F04AEF, [N4] and the solutions being to full machine accuracy. All calculations are executed in Real*16 arithmetic, except for *NAG* routines which operate in Real*8 arithmetic. Due to the finite precision of the computer the elements of $\tilde{A}$ and $\tilde{C}$ which should,

from theory, be zero or unity were, in general, not exact. Therefore a short routine converted elements (i,j) into integers if they met the following criterion,

$$(i,j) < 1 \times 10^{-10} \quad \text{Then } (i,j) = 0$$

$$|1-(i,j)| < 1 \times 10^{-8} \quad \text{Then } (i,j) = 1$$

The transformation to observable canonical form takes approximately one minute CPU time for an eighth order system and approximately three minutes CPU for a fourteenth order system. Because the processing times for the observability test and canonical transformation are relatively long, particularly in a multi-user computer system where the CPU times translate into much longer real times, the program was written such that the observability tests and canonical transformations could be carried out as batch jobs. Thus any number of flight conditions (ie. different A and B matrices) and C matrix combinations can be tested for observability, converted into observable canonical form and written to data files, without user intervention. When an observer is subsequently required, it is a simple matter to read the relative data file into the program.

5.2.3 DESIGNING THE OBSERVER

Once the system has been transformed into observable canonical form, there are two types of observer to be considered: full order or reduced order observer. The full order observer uses p out of n states to estimate the n states, whilst the reduced order observer uses p states to estimate the remaining (n-p) states. The question is which should be used?

As might be expected form the previous chapter, this depends to a large extent on numerical considerations. There are two aspects to this: firstly, the accuracy of the design in terms of the stipulated eigenvalues, and secondly, the fidelity of the designed observer's state estimation. The latter will be dealt with in chapter six.

The answer to the first question is easily addressed by using the program to design the two different types of observer for various eigenvalues and flight conditions. Extensive tests were carried out and from these it could clearly be seen that transforming the system into observable canonical form had resulted in a substantial increase in accuracy. Thus unless otherwise stated, all subsequent observer designs (whether reduced order or full order) are based on the system in this form.

It was also discovered that there are four major factors affecting the accuracy of a design. These can be stated as,

The accuracy of the design will be *increased* by,

- using a reduced order observer rather than a full order observer
- increasing p, ie. increasing the number of subsystems
- having well distributed, distinct observer eigenvalues
- positioning the observer eigenvalues with the largest magnitudes into the smallest blocks, and vice– versa.

In addition, for a fixed set of eigenvalues, C matrix and reduced or full order observer, the accuracy will vary with flight condition.

To illustrate the above points, consider the following observers. First examine *Table 5.1* (page 127) which shows, for a full order observer, the effect of increasing p. The designs were for a Lynx at eighty knots level and the C matrices were,

$$C_1 = C(1) \qquad C_2 = C(1,2) \qquad C_3 = C(1,2,3) \qquad C_4 = C(1,2,3,4)$$

It is immediately apparent that as p increases, the errors reduce until, at p= 4, the errors are zero; clearly demonstrating the numerical advantages of considering the system in canonical form. The reason for the reduction in errors as p increases is straightforward: the magnitude of the canonical blocks is decreasing and hence the order of the characteristic polynomials A_{ii} (Section 3.7.3, Note 3) are also decreasing. This gives numbers of smaller magnitude and variation which, as was noted in Chapter Four, leads to greater numerical accuracy.

Thus as p increases, and assuming no linear dependencies, the polynomials involved are,

p = 1 One 8^{th} order
p = 2 Two 4^{th} order
p = 3 Two 3^{rd} order and one 2^{nd} order
p = 4 Four 2^{nd} order

Table 5.2 gives details of the equivalent reduced order observers for this flight condition. Again it can be seen that as p increases the errors reduce; however the errors now reduce to zero with p= 3, where the design consists of one 1st order and two 2nd order observers. Comparing *Tables 5.1/ 5.2* demonstrates that reduced order observers are more accurate than full order observers since they involve lower order polynomials and hence the design involves numbers of smaller magnitude.

Now consider *Table 5.3* which shows, for the same flight condition, the effect of using distinct, well spaced out eigenvalues. The observers were full order and in each case the C matrix was C(1) and should therefore be compared with C_1 in *Tables 5.1* and *5.2*. It is evident that spacing out the eigenvalues reduces the errors, and that increasing the spacing further reduces the errors – contrast version–3 (spacing = one) with version–4 (spacing = two). However, at some point the trend is reversed as the effect of their magnitudes on accuracy becomes more significant than the rewards of spacing. The benefits of distinct eigenvalues is discernible from a comparison of versions–2 and 3: although the spacing is greater in version–2, the distinct eigenvalues of version–3 has produced the more accurate result.

Tables 5.4 and *5.5* indicate the consequences of placing the largest observer eigenvalues in the smallest blocks and the smallest eigenvalues in the largest blocks. The observers were designed for a fourteenth order model of the Lynx at eighty knots and the C matrix used was C(1,2,3,4) which gives blocks of size 4,4,3,3. *Table 5.4* is for full order observers and *Table 5.5* is for reduced order observers. In each table, version–1 is the observer where the largest eigenvalues are in the largest blocks, whilst version–2 is the observer with the largest eigenvalues in the smallest blocks.

Clearly, in each table, version–2 is the more accurate design and from a comparison of the two tables, the benefit of reduced order over full order is again apparent. The reason for the reduction in errors is simply that the magnitude of the polynomial coefficients in the largest blocks is reduced. For example, consider the difference in coefficients in each of the four blocks, between versions–1 and 2, for the reduced order observer:

	VERSION-1				VERSION-2			
	S^3	S^2	S^1	S^0	S^3	S^2	S^1	S^0
Block 1 :	1	120	4,800	64,000	1	75	1,800	14,000
2 :	1	110	4,025	49,000	1	105	3,675	42,875
3 :		1	70	1,225		1	80	1,600
4 :		1	40	400		1	80	1,600

Finally, look at *Table 5.6* which has the results for two full order observers, designed using C(1,7) and two different flight conditions, for a fourteenth order Puma model. Version−1 is one hundred knots with a descent angle of minus nine degrees and version−2 is for one hundred knots level. As expected, the accuracy of the design differs between the two flight conditions, due to the difference in the system A matrices.

Since the program gives the user the option of designing a full or reduced order observer the only error reducing feature from the above that could be built in, was the allocation of the largest eigenvalues to the smallest blocks (and vice−versa). Thus in all subsequent designs, unless otherwise stated, this procedure was carried out automatically by the program. The algorithm to achieve this was relatively straightforward, but allowance had to be made for the possibility of complex conjugate observer eigenvalues being stipulated.

For example, consider a design where the smallest block is of order three and, in descending order of magnitude, the first five observer eigenvalues are: $-10\pm j2$, $-9\pm j2$, -8. Since the first two largest eigenvalues are $-10\pm j2$, they will be allocated to the block first, leaving space for one more eigenvalue. The next largest eigenvalue is $-9+j2$ (or $-9-j2$), but because eigenvalues must appear as complex conjugate pairs it is the next largest *real* eigenvalue which is used, ie. -8. $-9\pm j2$ is then the first choice for the next block.

The subroutine to input the observer eigenvalues informs the user of the maximum number of permissible complex conjugate pairs (calculated from the block sizes for any given flight condition/C matrix combination) and prompts the user to reenter different eigenvalues if this number has been exceeded.

VERS	REQ'D EV'S	DESIGNED EV'S		ERRORS		
		REAL	IMAG	REAL	IMAG	% MAG
C1 ↑	-20	-20.40	0	.40E+0	0	1.982
	-20	-20.28	-.28	.28E+0	.28E+0	1.404
	-20	-20.28	.28	.28E+0	-.28E+0	1.404
	-20	-20.00	-.39	-.21E-2	.39E+0	.009
8	-20	-20.00	.39	-.21E-2	-.39E+0	.009
	-20	-19.72	-.28	-.28E+0	.28E+0	1.385
	-20	-19.72	.28	-.28E+0	-.28E+0	1.385
↓	-20	-19.61	0	-.39E+0	0	1.961
C2 ↑	-20	-20.00	0	.28E-2	0	.014
	-20	-20.00	0	.20E-2	0	.010
4	-20	-20.00	.00	-.14E-6	.20E-2	.000
↓	-20	-20.00	.00	-.14E-6	-.20E-2	.000
↑	-20	-20.00	.00	-.20E-6	.28E-2	.000
	-20	-20.00	.00	-.20E-6	-.28E-2	.000
4	-20	-20.00	0	-.20E-2	0	.010
↓	-20	-20.00	0	-.28E-2	0	.014

VERS	REQ'D EV'S	DESIGNED EV'S		ERRORS		
		REAL	IMAG	REAL	IMAG	% MAG
C3 ↑	-20	-20.00	0	.81E-4	0	.000
3	-20	-20.00	0	.62E-4	0	.000
↓	-20	-20	0	0	0	0
↑	-20	-20	0	0	0	0
3	-20	-20.00	.00	-.31E-4	.54E-4	.000
↓	-20	-20.00	.00	-.31E-4	-.54E-4	.000
↑	-20	-20.00	.00	-.41E-4	.70E-4	.000
2	-20	-20.00	.00	-.41E-4	-.70E-4	.000
↓						
C4 ↑	-20	-20	0	0	0	0
2	-20	-20	0	0	0	0
↓						
↑	-20	-20	0	0	0	0
2	-20	-20	0	0	0	0
↓						
↑	-20	-20	0	0	0	0
2	-20	-20	0	0	0	0
↓						
↑	-20	-20	0	0	0	0
2	-20	-20	0	0	0	0
↓						

TABLE 5.1 : EFFECT ON ACCURACY OF INCREASING p. FULL ORDER OBSERVER

VERS	REQ'D EV'S	DESIGNED EV'S		ERRORS		
		REAL	IMAG	REAL	IMAG	% MAG
C1 ↑	-20	-20.18	-.09	.18E+0	.88E-1	.916
	-20	-20.18	.09	.18E+0	-.88E-1	.916
	-20	-20.04	-.20	.44E-1	.20E+0	.227
7	-20	-20.04	.20	.44E-1	-.20E+0	.227
	-20	-19.87	-.16	-.13E+0	.16E+0	.630
	-20	-19.87	.16	-.13E+0	-.16E+0	.630
↓	-20	-19.80	0	-.20E+0	0	1.010
C2 ↑	-20	-20.00	0	.81E-4	0	.001
3	-20	-20.00	-.00	-.41E-4	.70E-4	.000
↓	-20	-20.00	.00	-.41E-4	-.70E-4	.000
↑	-20	-20.00	0	-.81E-4	0	.001
3	-20	-20.00	-.00	-.41E-4	.70E-4	.000
↓	-20	-20.00	.00	-.41E-4	-.70E-4	.000

VERS	REQ'D EV'S	DESIGNED EV'S		ERRORS		
		REAL	IMAG	REAL	IMAG	% MAG
C3 ↑	-20	-20	0	0	0	0
2 ↓	-20	-20	0	0	0	0
↑	-20	-20	0	0	0	0
2 ↓	-20	-20	0	0	0	0
1	-20	-20	0	0	0	0

TABLE 5.2 : EFFECT ON ACCURACY OF INCREASING p. REDUCED ORDER OBSERVER

VERS	REQ'D EV'S	DESIGNED EV'S		ERRORS		
		REAL	IMAG	REAL	IMAG	% MAG
1	-23	-23.01	0	.61E-2	0	.027
	-23	-22.99	0	-.63E-2	0	.027
	-22	-22.02	0	.17E-1	0	.077
	-22	-21.98	0	-.17E-1	0	.078
	-21	-21.02	0	.16E-1	0	.075
	-21	-20.98	0	-.15E-1	0	.074
	-20	-20.00	0	.48E-2	0	.024
	-20	-20.00	0	-.47E-2	0	.023
2	-26	-26.00	-.00	.33E-6	.62E-3	.000
	-26	-26.00	.00	.33E-6	-.62E-3	.000
	-24	-24.00	-.00	.54E-6	.17E-2	.000
	-24	-24.00	.00	.54E-6	-.17E-2	.000
	-22	-22.00	-.00	-.69E-6	.15E-2	.000
	-22	-22.00	.00	-.69E-6	-.15E-2	.000
	-20	-20.00	-.00	-.18E-6	.43E-3	.000
	-20	-20.00	.00	-.18E-6	-.43E-3	.000

VERS	REQ'D EV'S	DESIGNED EV'S		ERRORS		
		REAL	IMAG	REAL	IMAG	% MAG
3	-27	-27.00	0	.79E-6	0	.000
	-26	-26.00	0	-.49E-5	0	.000
	-25	-25.00	0	.13E-4	0	.000
	-24	-24.00	0	-.19E-4	0	.000
	-23	-23.00	0	.16E-4	0	.000
	-22	-22.00	0	-.84E-5	0	.000
	-21	-21.00	0	.24E-5	0	.000
	-20	-20.00	0	-.29E-6	0	.000
4	-34	-34.00	0	-.20E-8	0	.000
	-32	-32.00	0	.60E-8	0	.000
	-30	-30.00	0	.12E-9	0	.000
	-28	-28.00	0	-.22E-7	0	.000
	-26	-26.00	0	.36E-7	0	.000
	-24	-24.00	0	-.26E-7	0	.000
	-22	-22.00	0	.93E-8	0	.000
	-20	-20.00	0	-.13E-8	0	.000

TABLE 5.3 : EFFECT ON ACCURACY OF DISTINCT, WELL SPACED OUT EIGENVALUES. FULL ORDER OBSERVER

VERS	REQ'D EV'S	DESIGNED EV'S		ERRORS		
		REAL	IMAG	REAL	IMAG	% MAG
1	-40	-41.10	-1.1	.11E+1	.11E+1	2.790
↑	-40	-41.10	1.1	.11E+1	-.11E+1	2.790
4	-40	-38.90	-1.1	-.11E+1	.11E+1	2.699
↓	-40	-38.90	1.1	-.11E+1	-.11E+1	2.699
↑	-35	-36.65	0	.16E+1	0	4.716
4	-35	-35.00	-1.7	.30E-2	.17E+1	.122
↓	-35	-35.00	1.7	.30E-2	-.17E+1	.122
	-35	-33.33	0	-.17E+1	0	4.766
↑	-20	-20.43	0	.43E+0	0	2.165
3	-20	-19.78	-.38	-.22E+0	.38E+0	1.065
↓	-20	-19.78	.38	-.22E+0	-.38E+0	1.065
↑	-18	-18.08	0	.86E-1	0	.475
3	-18	-17.96	-.07	-.43E-1	.74E-1	.236
↓	-18	-17.96	.07	-.43E-1	-.74E-1	.236

VERS	REQ'D EV'S	DESIGNED EV'S		ERRORS		
		REAL	IMAG	REAL	IMAG	% MAG
2	-18	-17.65	-.51	-.35E+0	.51E+0	1.896
↑	-18	-17.65	.51	-.35E+0	-.51E+0	1.896
4	-18	-18.78	0	.78E+0	0	4.340
↓	-20	-19.82	0	-.18E+0	0	.899
↑	-20	-20.00	0	.10E-3	0	.000
4	-20	-20.10	0	.98E-1	0	.489
↓	-35	-34.87	0	-.13E+0	0	.359
	-35	-35.12	0	.12E+0	0	.353
↑	-35	-35.00	-.17	-.29E-2	.17E+0	.007
3	-35	-35.00	.17	-.29E-2	-.17E+0	.007
↓	-40	-40.00	0	.40E-3	0	.001
↑	-40	-39.93	-.13	-.71E-1	.13E+0	.178
3	-40	-39.93	.13	-.71E-1	-.13E+0	.178
↓	-40	-40.15	0	.15E+0	0	.369

TABLE 5.4 : EFFECT OF PLACING THE LARGEST EIGENVALUES IN THE SMALLEST BLOCKS.
FULL ORDER OBSERVER

VERS	REQ'D EV'S	DESIGNED EV'S		ERRORS		
		REAL	IMAG	REAL	IMAG	% MAG
1 ↑	-40	-40.48	0	.48E+0	0	1.196
3 ↕	-40	-39.76	-.41	-.24E+0	.41E+0	.592
↓	-40	-39.76	.41	-.24E+0	-.41E+0	.592
↑	-40	-39.99	0	-.73E-2	0	.018
3 ↕	-35	-35.19	0	.20E+0	0	.556
↓	-35	-34.81	0	-.19E+0	0	.535
↑	-35	-35.04	0	.45E-1	0	.127
2 ↓	-35	-34.96	0	-.45E-1	0	.127
↑	-20	-20	0	0	0	0
2 ↓	-20	-20	0	0	0	0

VERS	REQ'D EV'S	DESIGNED EV'S		ERRORS		
		REAL	IMAG	REAL	IMAG	% MAG
2 ↑	-20	-20.00	-.05	-.91E-4	.52E-1	.000
3 ↕	-20	-20.00	.05	-.91E-4	-.52E-1	.000
↓	-35	-35.00	0	.18E-3	0	.000
↑	-35	-35.28	-.48	.28E+0	.48E+0	.795
3 ↕	-35	-35.28	.48	.28E+0	-.48E+0	.795
↓	-35	-34.45	0	-.55E+0	0	1.571
↑	-40	-40.05	0	.48E-1	0	.119
2 ↓	-40	-39.95	0	-.48E-1	0	.119
↑	-40	-40	0	0	0	0
2 ↓	-40	-40	0	0	0	0

TABLE 5.5 : EFFECT OF PLACING THE LARGEST EIGENVALUES IN THE SMALLEST BLOCKS. REDUCED ORDER OBSERVER

VERS	REQ'D EV'S	DESIGNED EV'S		ERRORS		
		REAL	IMAG	REAL	IMAG	% MAG
1	-40	-40.05	-.05	.50E-1	.50E-1	.125
	-40	-40.05	.05	.50E-1	-.50E-1	.125
	-40	-39.95	-.05	-.50E-1	.51E-1	.125
7	-40	-39.95	.05	-.50E-1	-.51E-1	.125
	-35	-35.01	-.01	.74E-2	.13E-1	.021
	-35	-35.01	.01	.74E-2	-.13E-1	.021
	-35	-35.00	0	-.1E-10	0	.000
	-35	-34.98	0	-.15E-1	0	.042
	-20	-20.01	0	.62E-2	0	.031
	-20	-20.00	-.00	-.31E-2	.54E-2	.016
7	-20	-20.00	.00	-.31E-2	-.54E-2	.016
	-18	-18.00	-.00	.27E-2	.47E-2	.015
	-18	-18.00	.00	.27E-2	-.47E-2	.015
	-18	-17.99	0	-.54E-2	0	.030

VERS	REQ'D EV'S	DESIGNED EV'S		ERRORS		
		REAL	IMAG	REAL	IMAG	% MAG
2	-40	-40.06	0	.64E-1	0	.161
	-40	-40.00	-.06	.55E-3	.65E-1	.002
	-40	-40.00	.06	.55E-3	-.65E-1	.002
7	-40	-39.93	0	-.65E-1	0	.163
	-35	-35.01	0	.13E-1	0	.038
	-35	-34.99	-.01	-.66E-2	.11E-1	.019
	-35	-34.99	.01	-.66E-2	-.11E-1	.019
	-35	-35.00	0	-.8E-10	0	.000
	-20	-20.01	0	.12E-1	0	.062
	-20	-19.99	-.01	-.62E-2	.11E-1	.031
7	-20	-19.99	.01	-.62E-2	-.11E-1	.031
	-18	-18.00	-.01	.53E-2	.93E-2	.029
	-18	-18.00	.01	.53E-2	-.93E-2	.029
	-18	-17.99	0	.11E-1	0	.059

TABLE 5.6 : EFFECT OF DIFFERENT FLIGHT CONDITIONS. FULL ORDER OBSERVER

5.2.4 THE USE OF FLIGHT DATA

The *Helistab* software package has facilities to produce linear and non−linear time histories from an initial flight condition and input $\underset{\sim}{u}$. For example, consider *fig 5.1* which shows the linear and non−linear time responses of a Puma at one hundred knots, for a doublet input on θ_{1S} (k= 0.1, t= 0/2/2/4). There is good agreement between the time responses and, in general, this is true for the majority of 'easy' manoeuvres; but for more severe manoeuvres, the differences can be substantial, particularly in the lateral states. However, since this research concentrated on flight conditions and manoeuvres well within the flight envelope, the linear model was considered to be a satisfactory model for initial investigation into the feasibility of state estimation and instrument fault detection, in the single rotor helicopter.

As discussed in chapter two, *Helistab* will produce a linearized state−space description, for any given flight condition, in the form of a system matrix A and a distribution matrix B. If the model is perfect, then for any given control input vector $\underset{\sim}{u}$, the *Tsim* simulation of the state time histories should be identical to the actual response of the helicopter. Naturally, since it is a linearized model of a highly unlinear system, this only applies at reasonable excursions from the nominal point.

Unfortunately the model has many limitations (see section 2.7) and therefore cannot be considered as accurately portraying the true response. To illustrate this, first consider *figs 5.2* and *5.3* which are the pilot control inputs and state time histories, respectively, for a Puma initially at one hundred knots. The test input applied by the pilot is a doublet on θ_{1S}, after which no inputs are applied until corrective action is required. Note the degree to which the measurements of both control inputs and system states are corrupted by noise. The sampling rate is $1/64^{th}$ (0.015625) of a second.

Now in order to provide realistic control inputs for the simulation model and to facilitate the comparison of state time responses, it is necessary to *trim* the flight data: ie. the initial values of $\underset{\sim}{u}$ and $\underset{\sim}{x}$ should be zero. This is because the model is produced by a linearization about a nominal point and therefore the simulation deals with perturbations from this point.

To trim the data the user inspects the time histories and selects a period of time, before the test input, over which the values of $\underset{\sim}{u}$ and $\underset{\sim}{x}$ are relatively constant. The values over this range are averaged to give a set of trims which are then subtracted from each value in the time histories. Finally, the user selects the time period

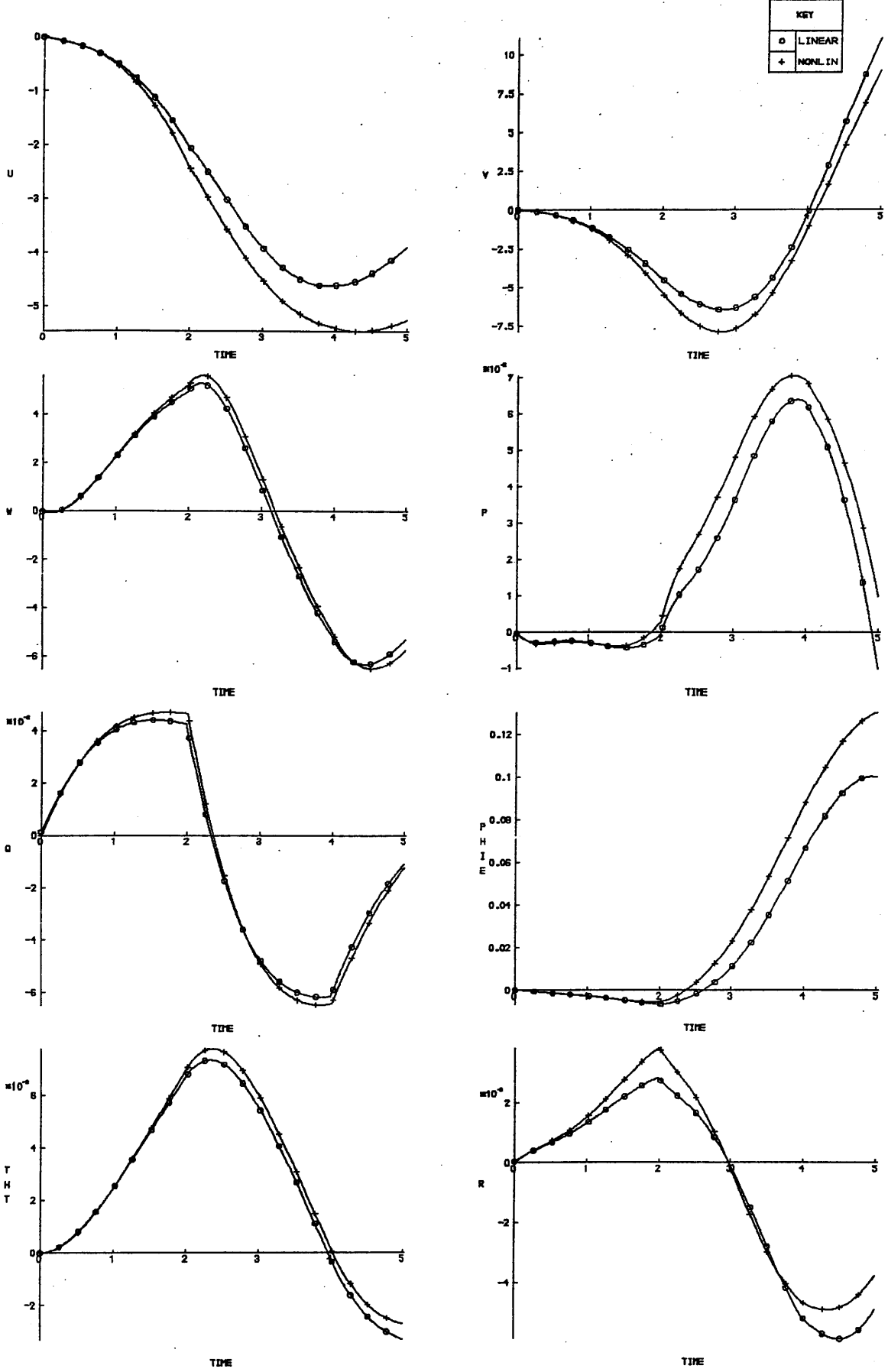

FIG 5.1 COMPARISON OF LINEAR AND NON-LINEAR TIME RESPONSES

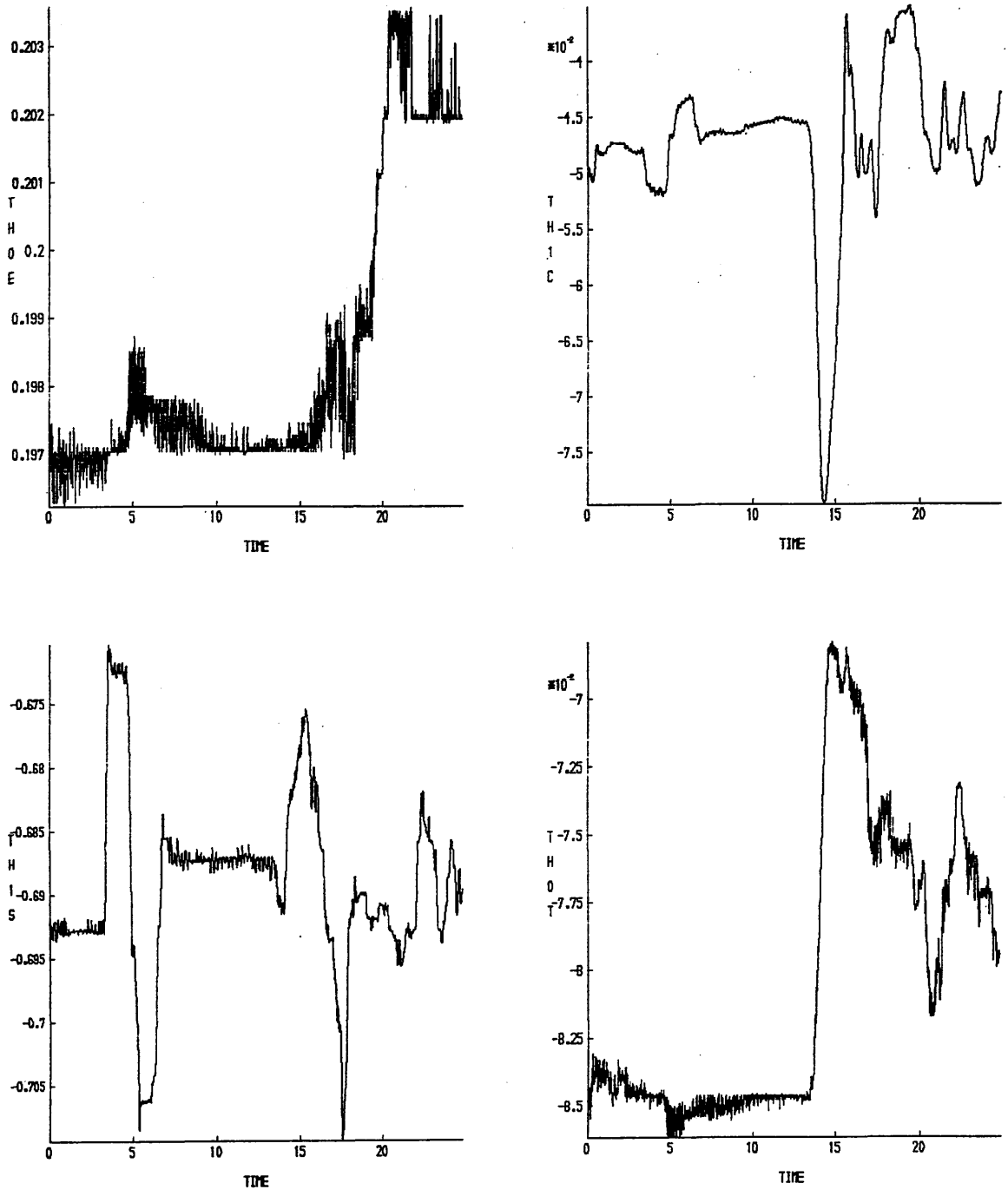

FIG 5.2 UNTRIMMED CONTROL INPUTS FOR A DOUBLET ON θ_{1s}

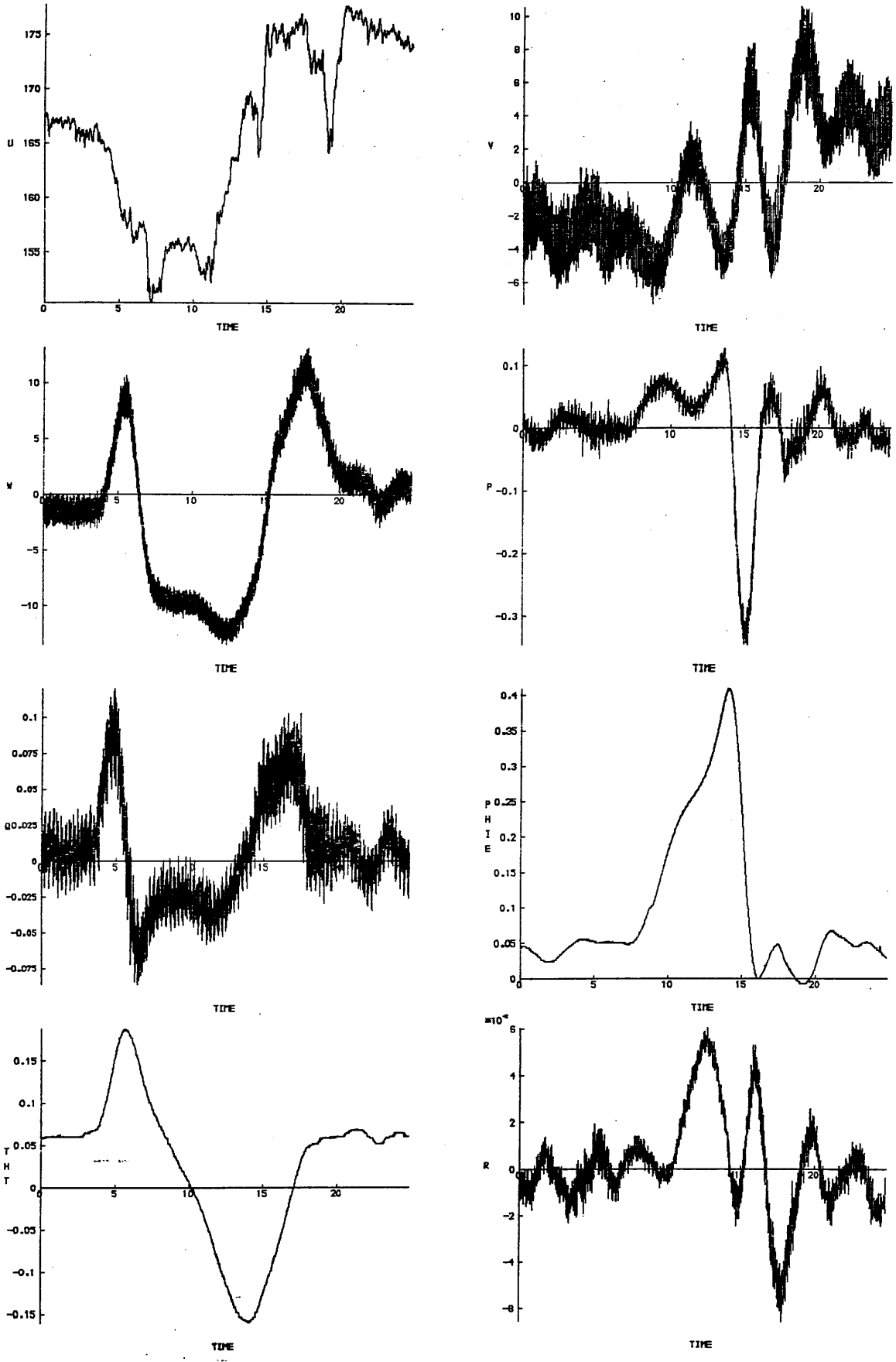

FIG 5.3 UNTRIMMED STATE TIME-HISTORY FOR A DOUBLET ON θ_{1s}

required (t_1 to t_2): normally the beginning of the test input is selected as $t_1 = 0$, and t_2 is taken to be several seconds after the input has been removed. *Figs 5.4* and *5.5* show the trimmed inputs and states. Once trimmed they can be used for simulation or stored in data files for future use.

The trimmed control vector $\underset{\sim}{u}$ was applied to the model and the subsequent state time response was plotted with the trimmed flight data state time history: *fig 5.6.* Estimates of states w, q and θ are reasonably accurate over the first four seconds and u exhibits the correct trend, but the estimates of the lateral states are very poorly correlated.

Now one major prerequisite for accurate state estimation is that the observer should be based on a precise model of the system: which, as can be seen from the above, *Helistab* does not provide. However, if the A and B matrices obtained from *Helistab* are used to model the system, as well as for designing an observer, then the state vector $\underset{\sim}{x}$ of this model can be used as input to the observer, whilst both system and observer are driven by the control vector $\underset{\sim}{u}$ attained from flight data. This effectively gives a perfect model and was used to investigate the various aspects of observer design and performance, and the feasibility of sensor fault detection schemes.

If the performance proves satisfactory under these 'ideal conditions' then the simulation can be made more realistic by firstly corrupting the system state vector $\underset{\sim}{x}$ by noise, and secondly, by varying the elements of the A and B matrices so that the observer is no longer a precise model of the system.

5.2.5 ADDITION OF NOISE TO SIGNALS

Since the noise on the signals is not *white* and therefore could not be easily simulated, it was decided to filter the noise from the flight data and then add this noise to the state vector $\underset{\sim}{x}$ going to the observer: *fig 5.7.*

A simple first order *High Pass* or *Lead* filter of form

$$W(s) = \frac{Y(s)}{u(s)} = \frac{s}{1 + s\tau} \qquad (5.7)$$

was used to filter off the noise and the *cut–off* frequency was set at sixteen hertz ($\tau = 0.01$). As s (ie. $j\omega$) increases, the magnitude of the transfer function tends

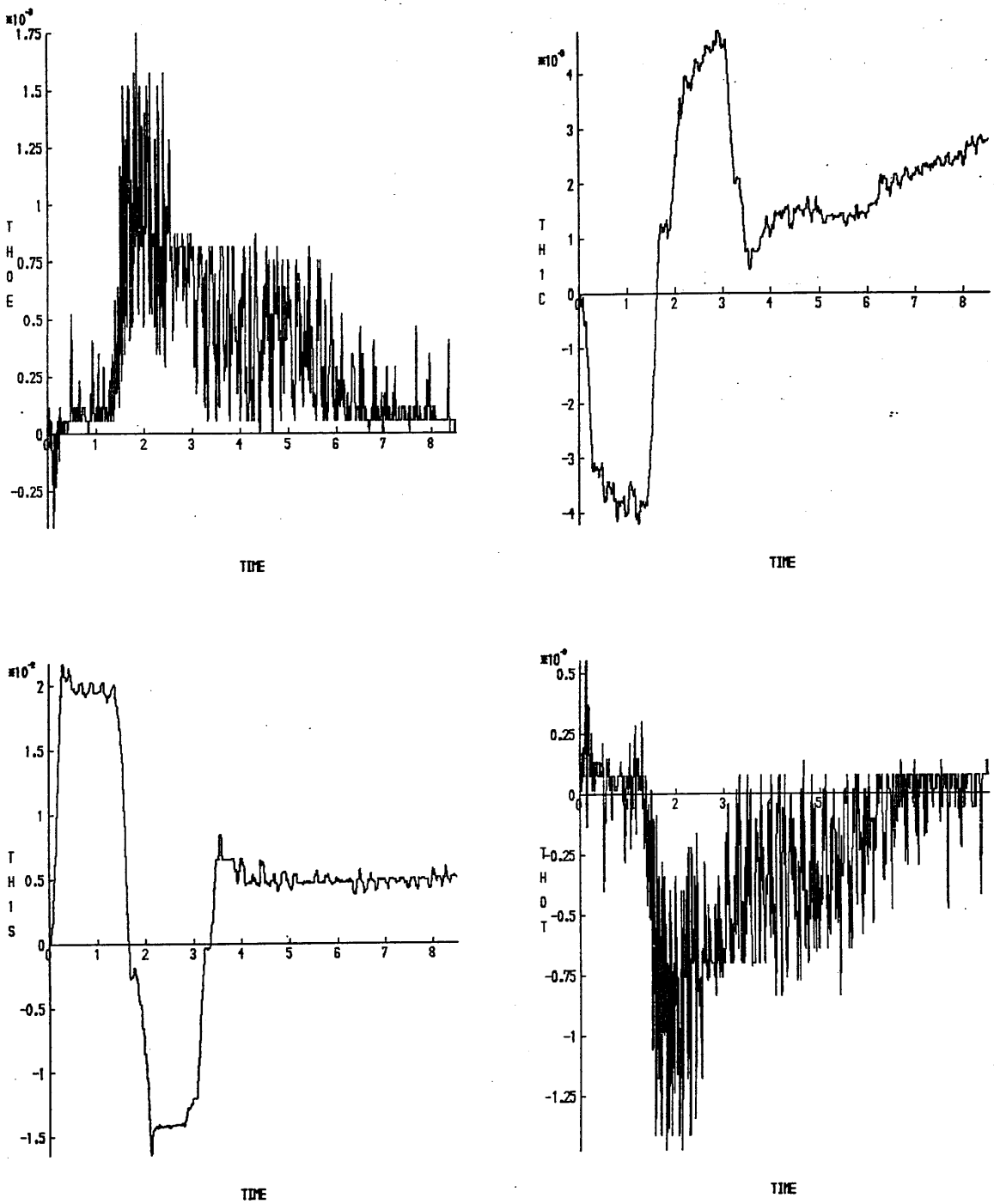

FIG 5.4 TRIMMED CONTROL INPUTS FOR A DOUBLET ON θ_{1s}

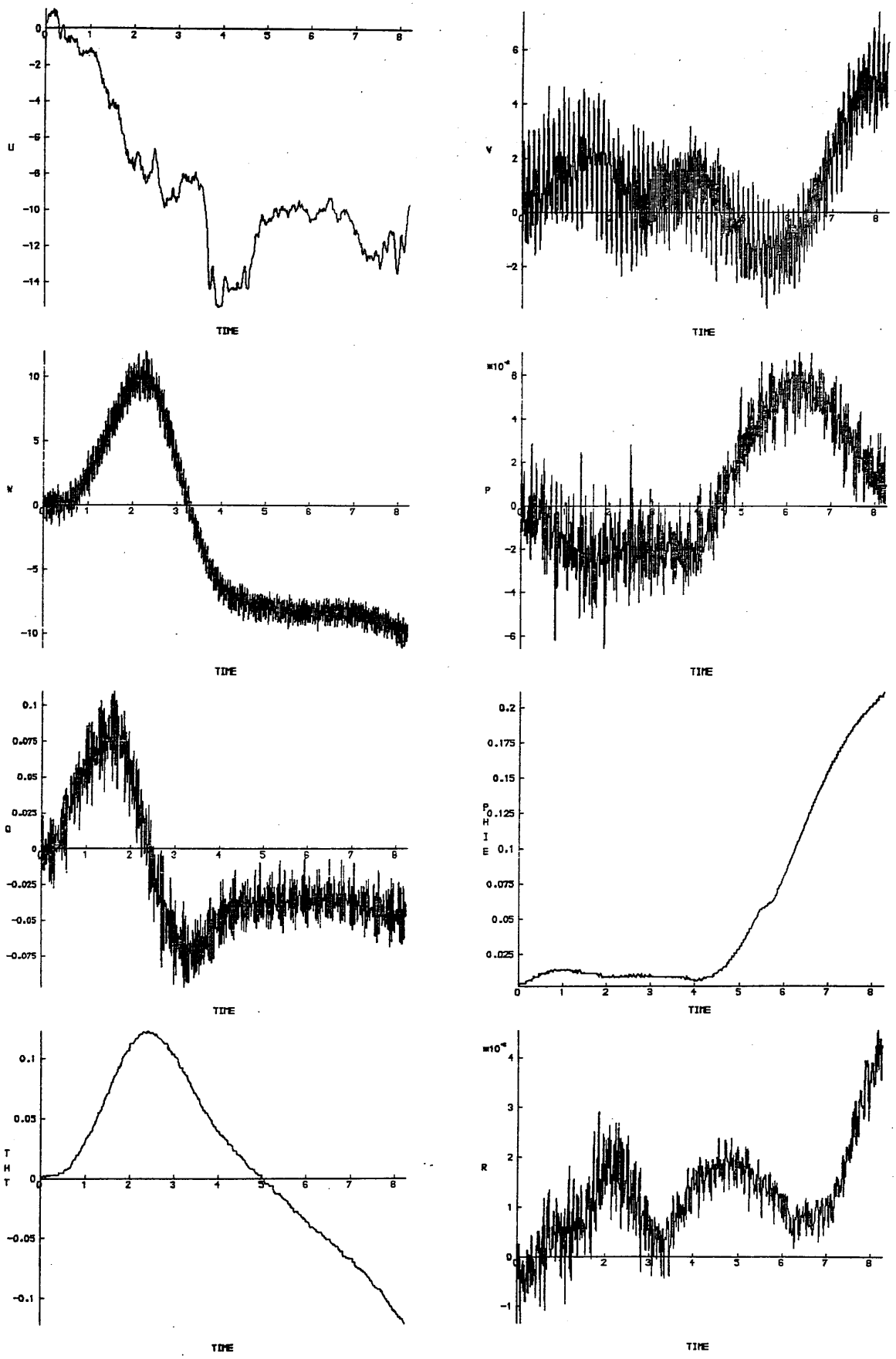

FIG 5.5 TRIMMED STATE TIME HISTORY FOR A DOUBLET ON θ_{1S}

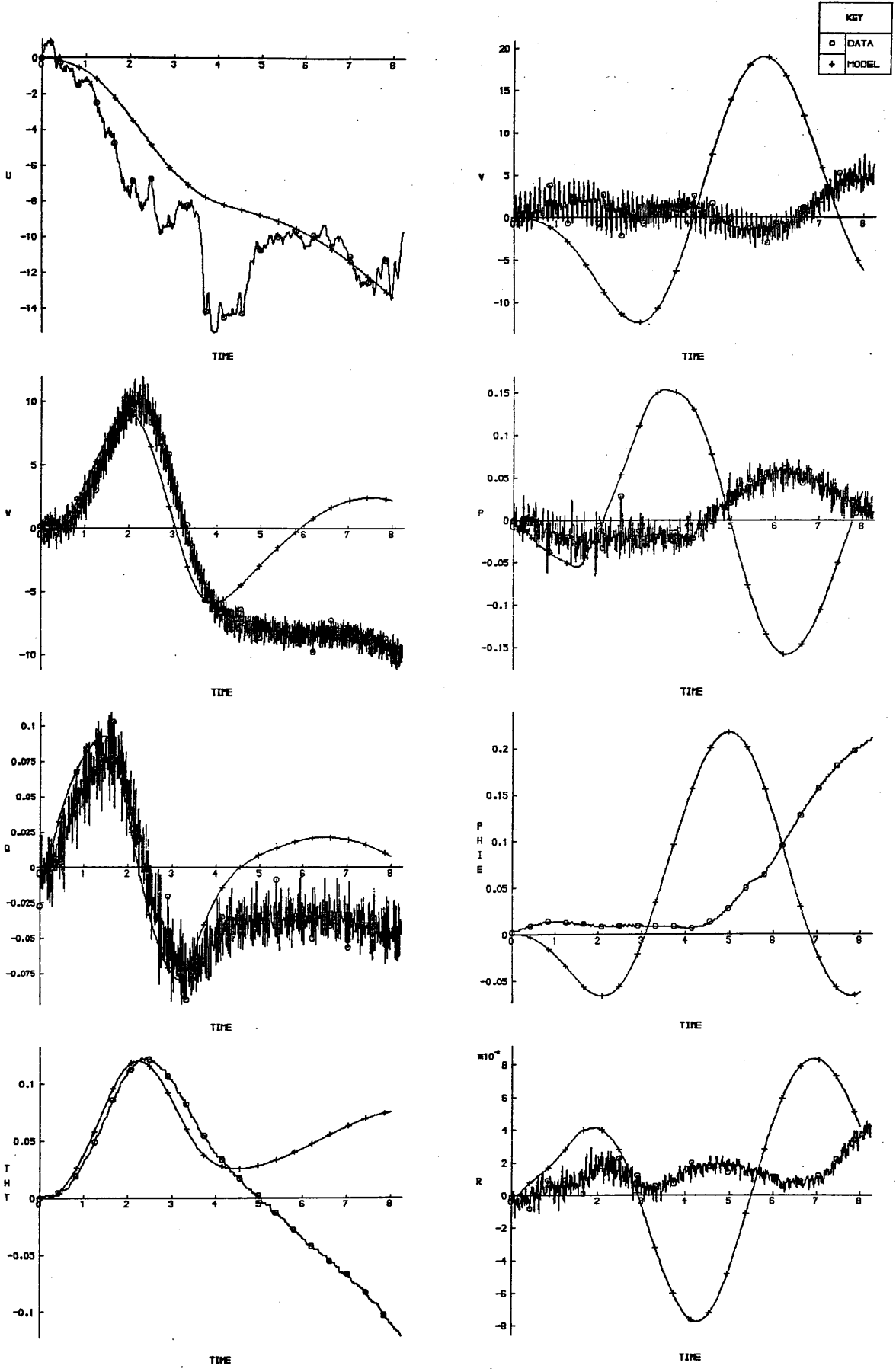

FIG 5.6 COMPARISON OF MODEL AND FLIGHT DATA

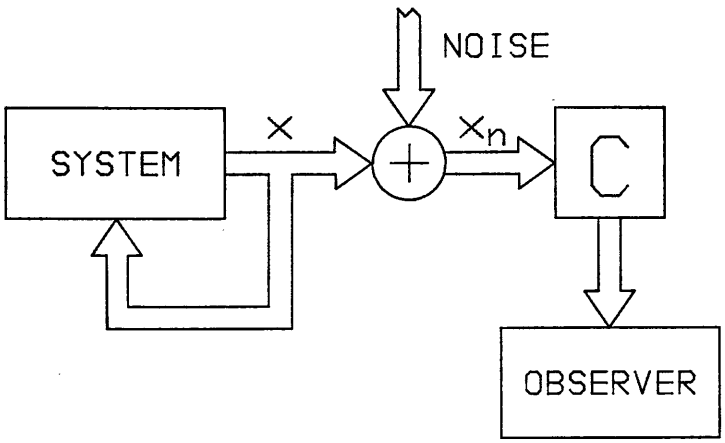

FIG 5.7 ADDITION OF NOISE TO STATE VECTOR x

towards $1/\tau$ (=100) and therefore the amplitude of the noise must be restored to its original levels before being used in a simulation. To accomplish this it was necessary to first determine the *Noise Power* P_n of the original signals, where P_n is given by,

$$P_n = \left[\frac{\sum_{i=1}^{N} f(i)^2}{N} \right]^{\frac{1}{2}} \qquad (5.8)$$

and f(i) is the value of noise at point i, in the finite time interval of N points. Therefore in order to establish f(i), the value of the signal x(i) must be known. However the true value of x(i) is not available and therefore must be estimated by using a curve fitting numerical method.

The *NAG* routines used were E02BAF and E02BBF, [N4], which calculate the value of a function at point i by computing a weighted least–squares approximation to an arbitrary set of data points, by a cubic spline with user prescribed *knots*. Since the noise was observed to be independent of signal amplitude the weights were all set to unity and the knots (the number of which determine the number of coefficients in the spline and hence the degree to which the spline 'follows' the data) were chosen by 'trial and error'. Knots were initially evenly spaced and the results examined graphically. Where the fit was poor extra knots were added – and this continued until a satisfactory fit was achieved. *Fig 5.8* gives the eight state variables computed using four knots – compare this *fig 5.9* which shows the results with sixteen knots: this was taken to be the best fit. Thus the noise is given by,

$$f(i) = x_n(i) - x(i) \qquad (5.9)$$

where $x_n(i)$ is the noisy flight data and x(i) is the cubic spline estimation of the true state.

The noise power was then calculated and *Table 5.7* (overleaf) gives the values of P_n as the number of knots used for the cubic spline increases. As expected, P_n decreases as the number of knots increase. The values obtained with sixteen knots will be referred to as *full noise power*.

Finally, P_n was determined (using equation 5.8) for the noise filtered from x_n and then the noise was scaled down to unity noise power by multiplying each point by $1/P_n$. The filtered and normalized noise noise is shown in *fig 5.10*. To obtain a given noise power each point is multiplied by that power. Thus the power of the

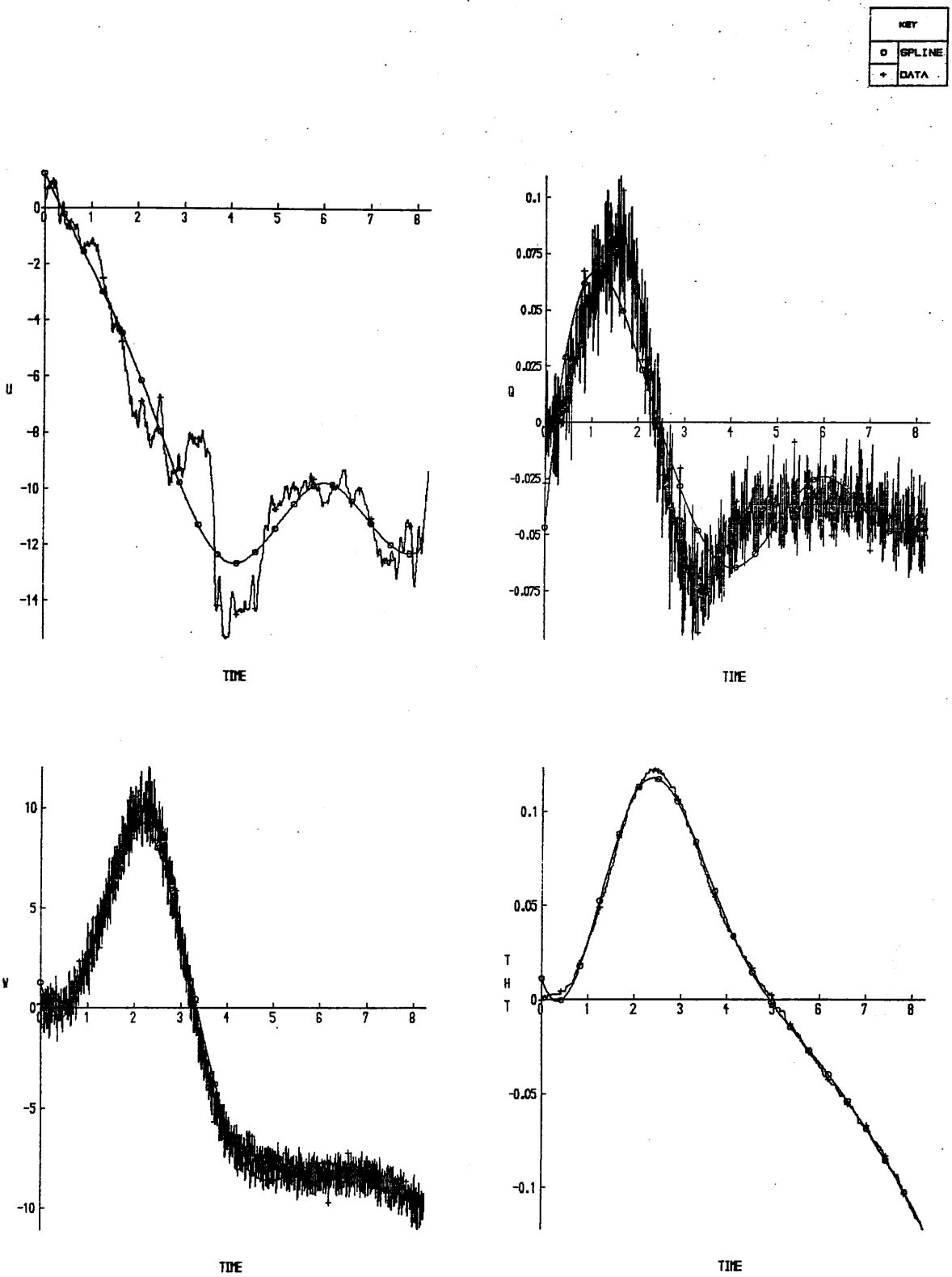

FIG 5.8 STATES COMPUTED USING A 4 KNOT CUBIC SPLINE

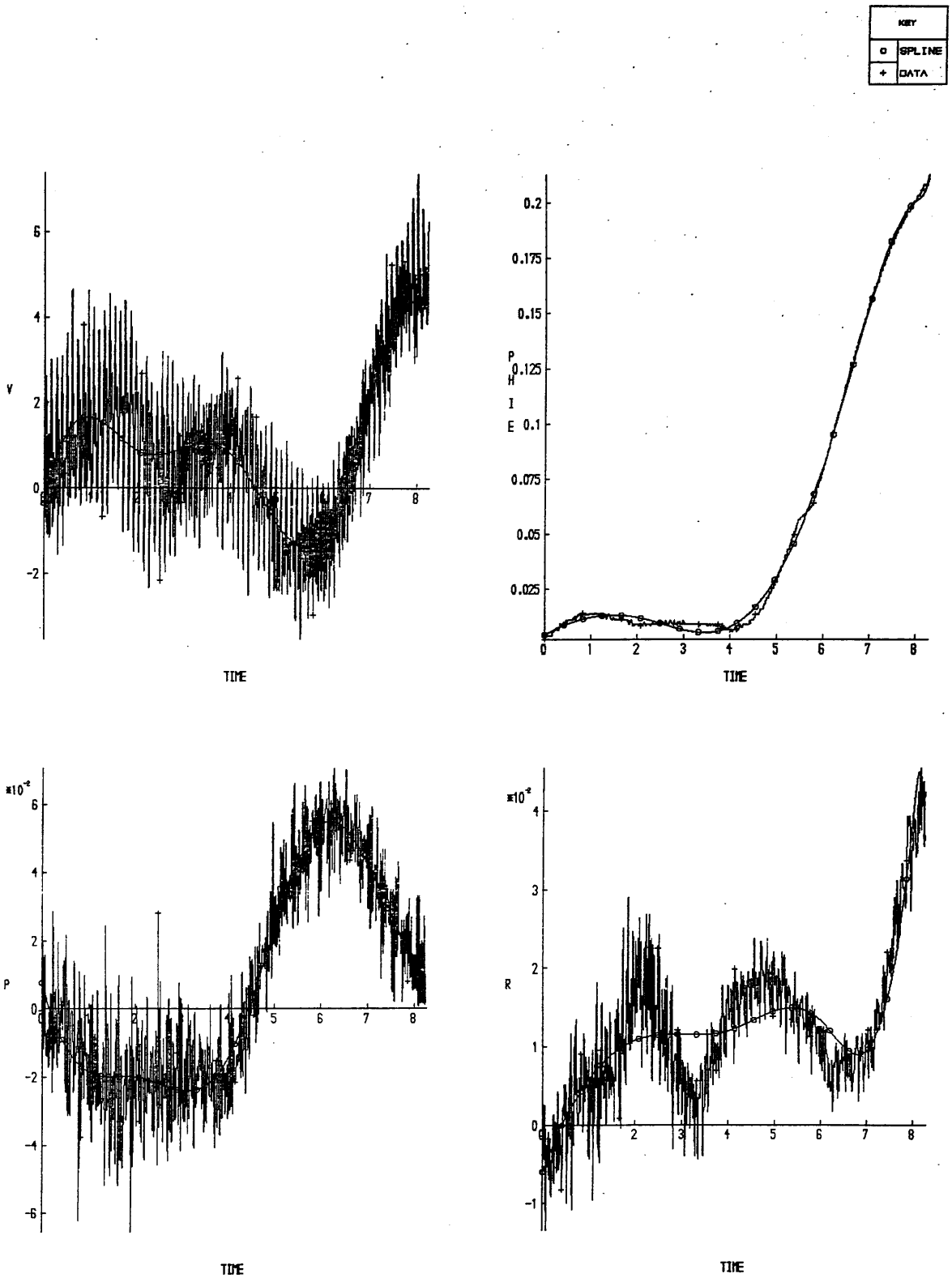

FIG 5.8 STATES COMPUTED USING A 4 KNOT CUBIC SPLINE

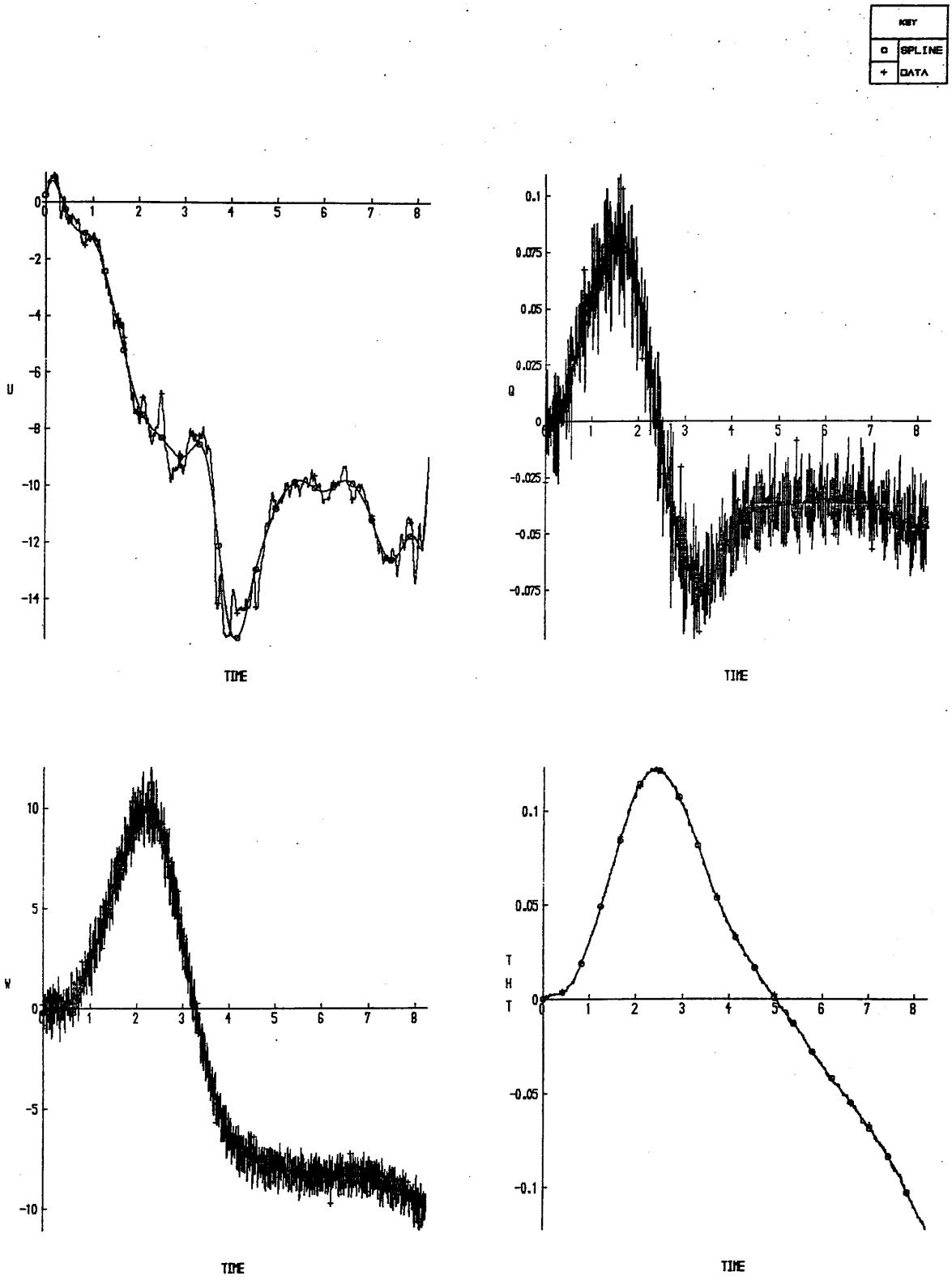

FIG 5.9 STATES COMPUTED USING A 16 KNOT CUBIC SPLINE

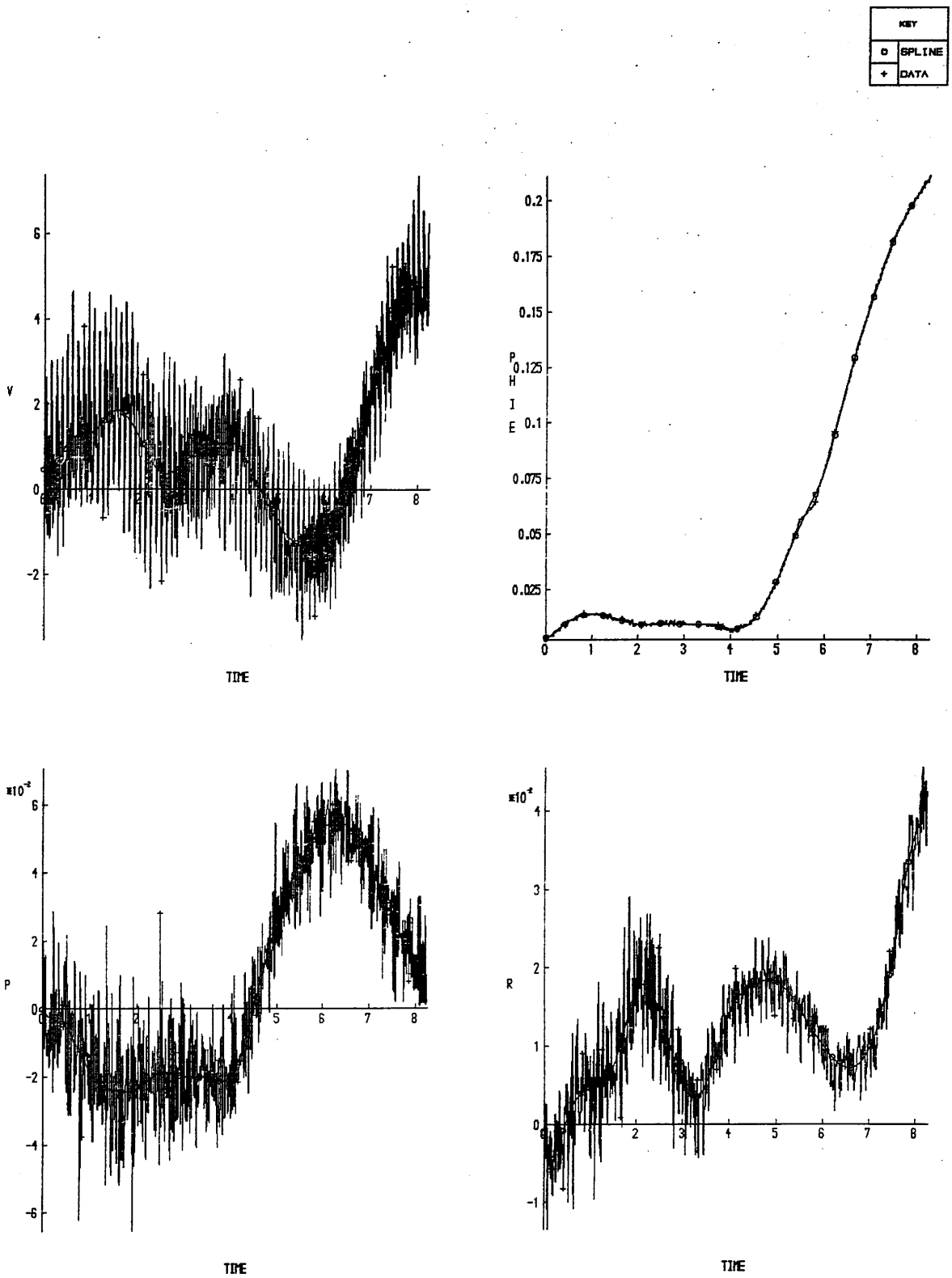

FIG 5.9 STATES COMPUTED USING A 16 KNOT CUBIC SPLINE

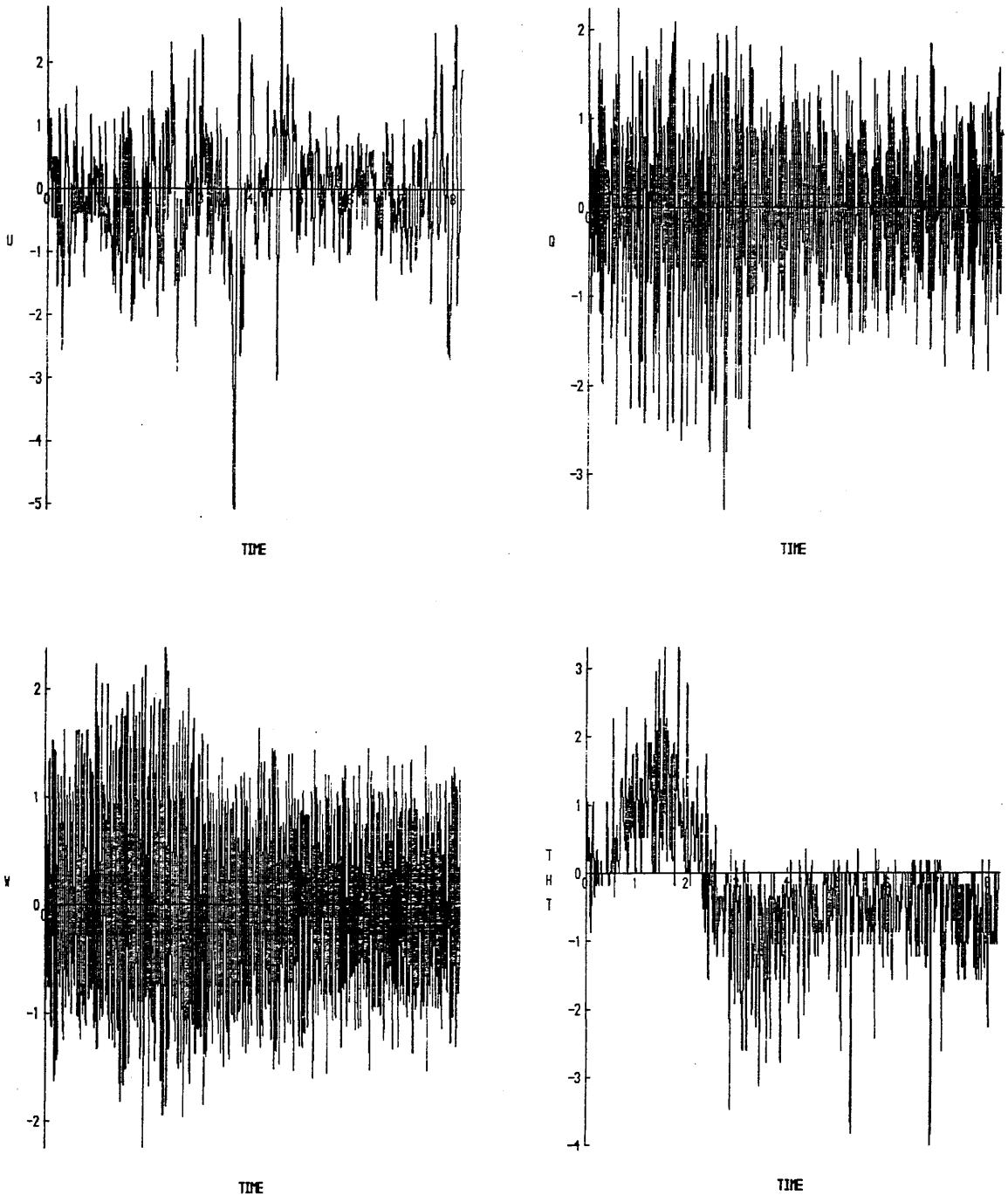

FIG 5.10 NOISE FILTERED FROM FLIGHT DATA AND NORMALISED

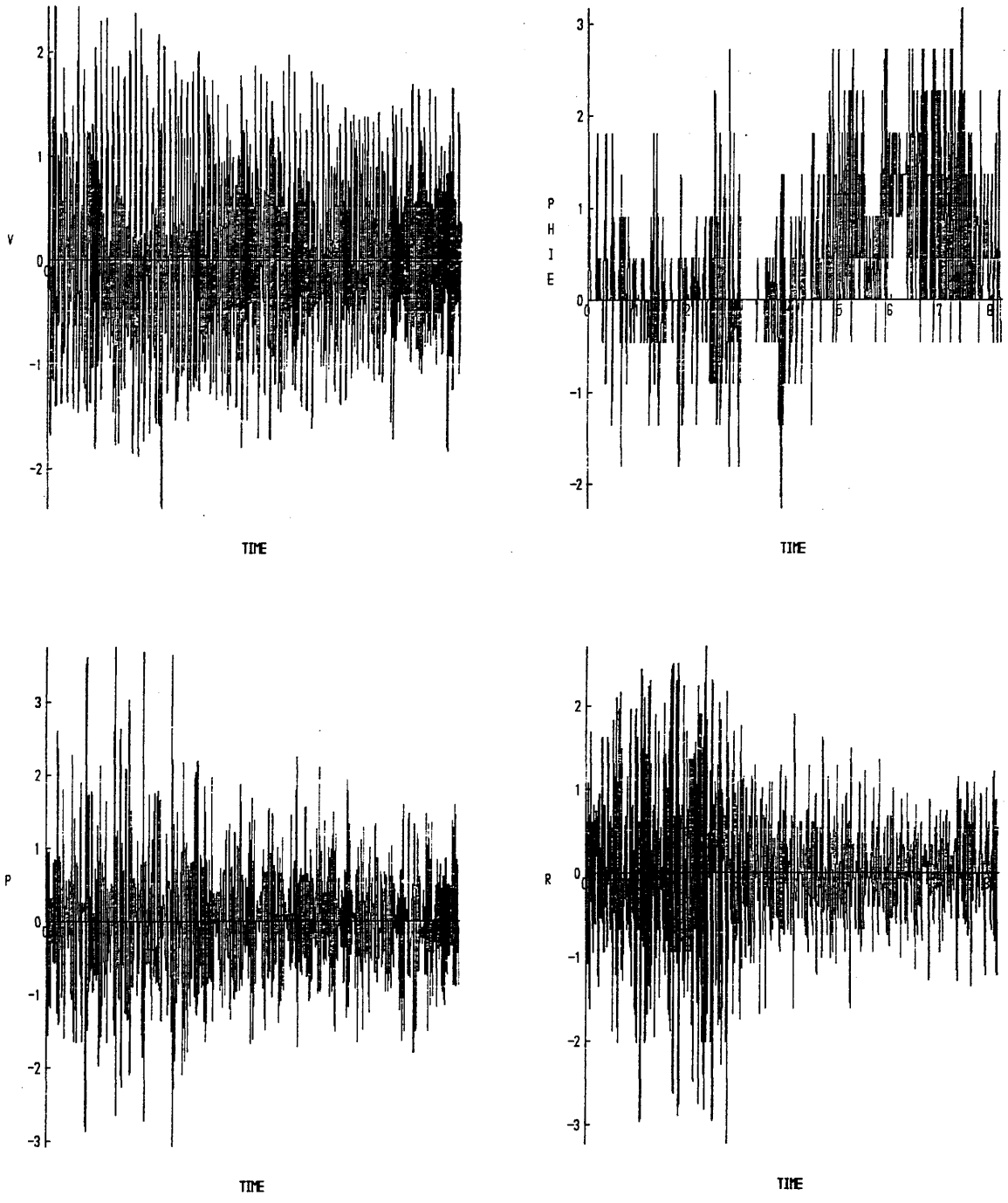

FIG 5.10 NOISE FILTERED FROM FLIGHT DATA AND NORMALISED

STATE	NUMBER OF KNOTS		
	4	8	16
u	1.16472	0.80084	0.53630
w	1.04035	0.91727	0.88705
q	0.02120	0.01469	0.01461
θ	0.00257	0.00124	0.00086
v	1.26718	1.24790	1.24242
p	0.01270	0.01239	0.01238
φ	0.00233	0.00149	0.00083
r	0.00538	0.00422	0.00399

TABLE 5.7
VARIATION OF NOISE POWER
WITH THE NUMBER OF KNOTS
USED FOR THE CUBIC SPLINE

noise can easily be altered to investigate the effect it has on observer performance. The program contains a subroutine which allows the normalized noise to be read in from a data file and the selection of the required noise power for each state. *Fig 5.11* shows the noise (at full noise power) added to the simulation generated states.

5.2.6 CORRELATION OF SIMULATION RESULTS

If the method of section 5.2.4 is used, whereby the system is modelled by the A and B matrices produced by *Helistab*, then the exact value of the state $\underset{\sim}{x}$, which the observer has to estimate, is known. Thus the time history of the estimated state vector $\hat{\underset{\sim}{x}}$, derived by an observer, can be *correlated* with the known time history of the state vector $\underset{\sim}{x}$, to produce n *correlation coefficients* (one per state) as a quantitative measure of observer performance.

The correlation method used was *Pearson (zero–order) Product–Moment correlation* and was provided by *NAG* routine G02BAF, [N4]. The correlation coefficient varies from -1.0 to $+1.0$. A coefficient of zero indicates that no linear relationship exists; a $+1.0$ coefficient implies a 'perfect' positive relationship (ie. an increase in one variable is always associated with a corresponding increase in the other variable); and a coefficient of -1.0 indicates a 'perfect' negative relationship (ie. an increase in one variable is always associated with a corresponding decrease in the other variable).

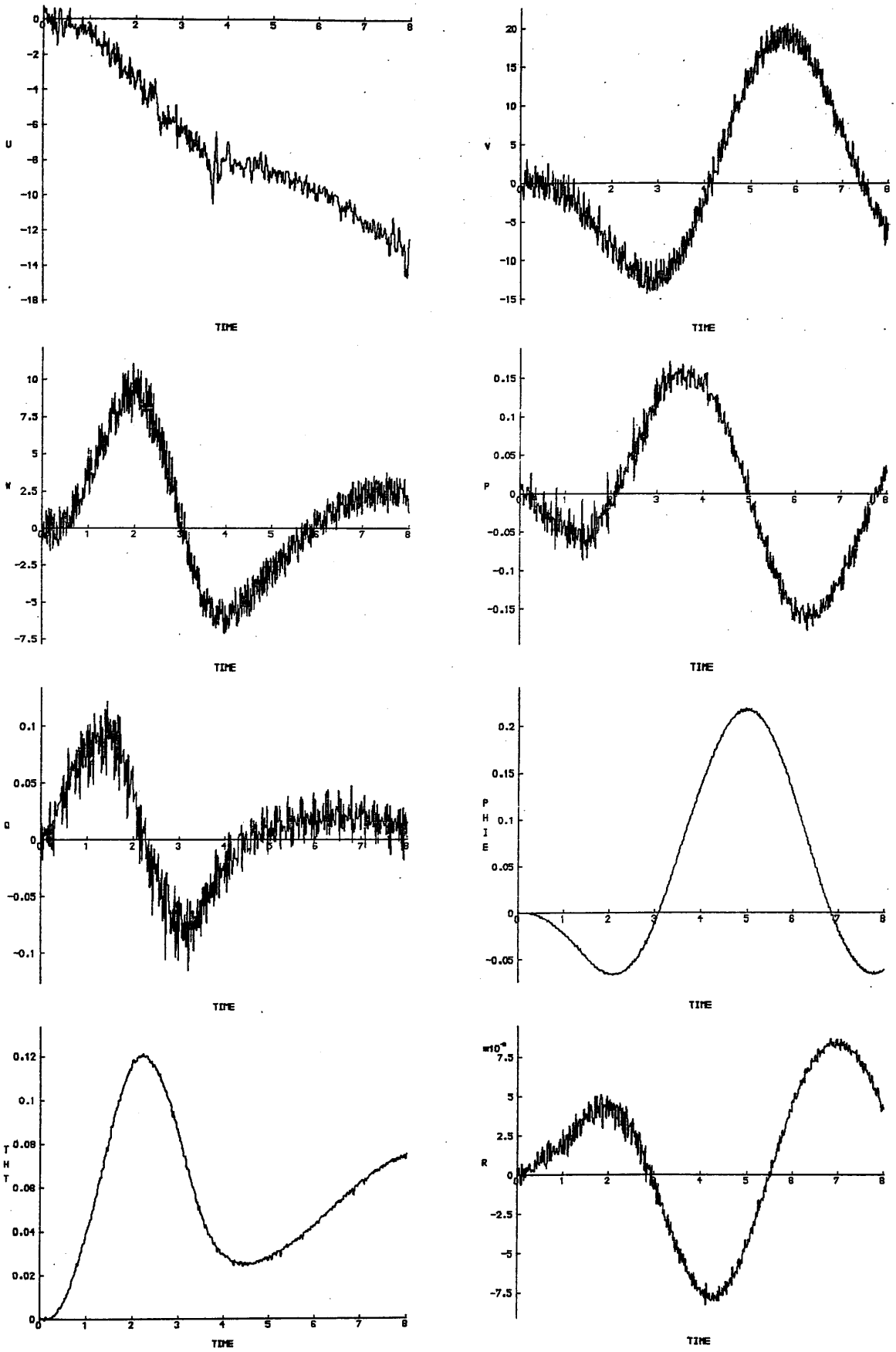

FIG 5.11 NOISE ADDED TO STATES PRODUCED BY SIMULATION

A program was written to calculate the correlation coefficients at the end of a simulation. The time histories are examined in two halves and the lower value of correlation coefficient is used to decide whether the estimate of each state is a 'pass' or 'fail': the pass criterion being,

$$\text{correlation} \geq 0.995$$

This value was determined by plotting one hundred time histories and visually deciding what was an acceptable estimate and what was not. The correlation coefficients of the 'fails' were then determined and the lowest value used to set the pass criterion. *Fig 5.12* shows examples of passes whilst *fig 5.13* gives examples of failures. The correlation coefficients are displayed for each plot.

5.3 STATE ESTIMATION WITH A FEEDBACK CONTROLLER

The most common application of a state estimator is to facilitate the provision of the complete state vector $\underset{\sim}{x}$ for use in a feedback control law. In the particular case of the helicopter, $\underset{\sim}{x}$ may not be completely accessible for a number of reasons: physical constraints may limit the number of sensors; sensors may fail 'naturally' or through damage sustained during combat; or some of the states may simply not be measurable. If an automatic flight control system (AFCS) or Active Control Technology (ACT) is being employed then the consequences of the sudden loss of the complete state vector could be catastrophic.

To investigate the use of a state estimator in a feedback control system it was necessary to select a pertinent design philosophy for the control system. Conveniently, previous research at Glasgow University had dealt with the design of automatic flight control systems, using *Modal Control Theory*, for the single rotor helicopter (Parry and Murray–Smith, 1985), and therefore this was the obvious choice.

The form of Modal control used by Parry and Murray–Smith utilizes *principal angles* (ie. angles between subspaces) in the design method to allow the selection of both the closed–loop eigenvalues and the corresponding eigenvectors (ie. eigenstructure assignment), and is a fast and visible method which can meet practical handling quality criteria. The allowance for selection of eigenvectors in addition to eigenvalues permits the decoupling of control inputs which result in a reduction in pilot workload, whilst still allowing fast responses to pilot demands. This is desirable because the inherent cross–coupling effects between pilot control inputs can cause

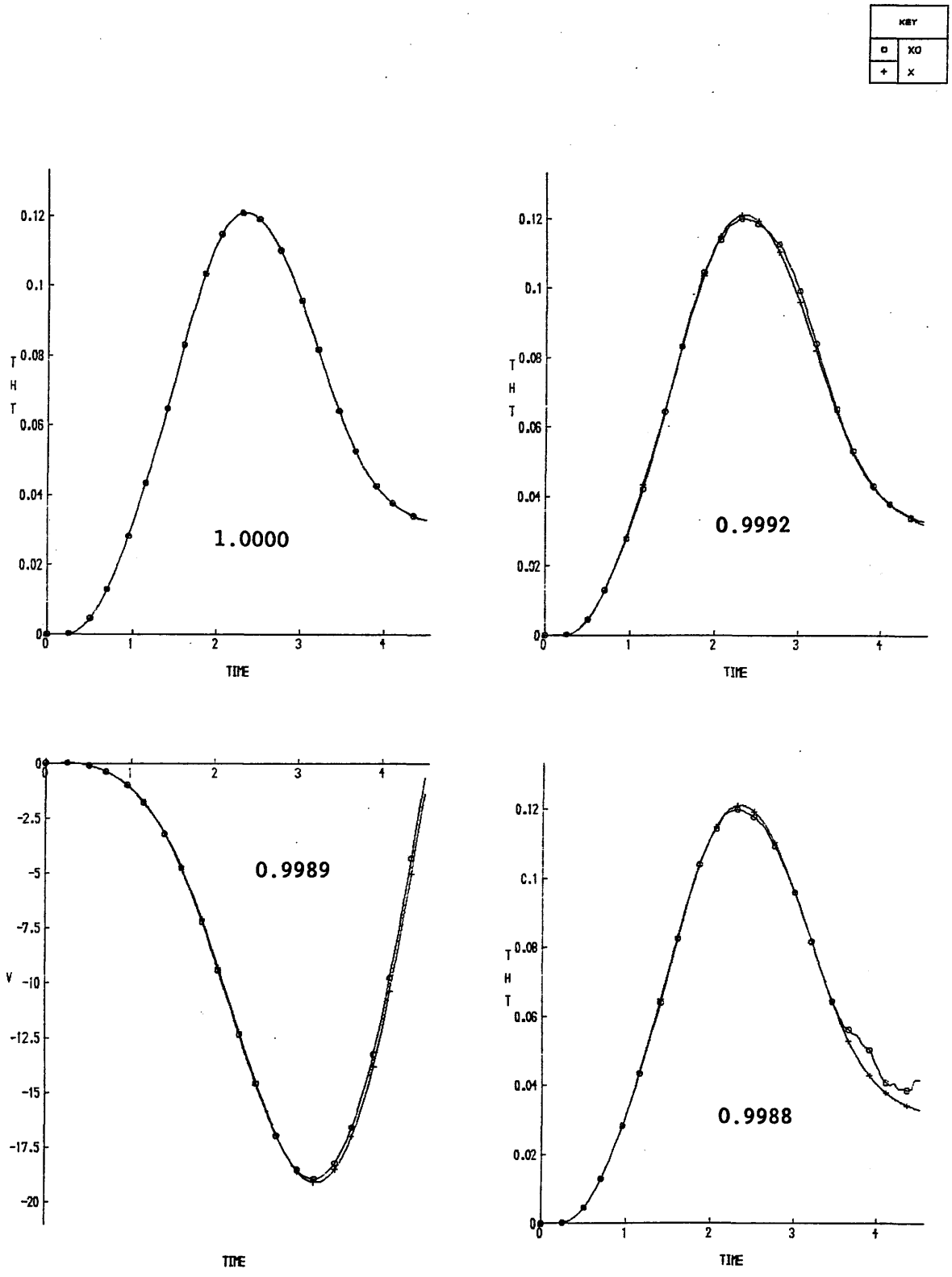

FIG 5.12 EXAMPLES OF CORRELATION PROGRAM PASSES

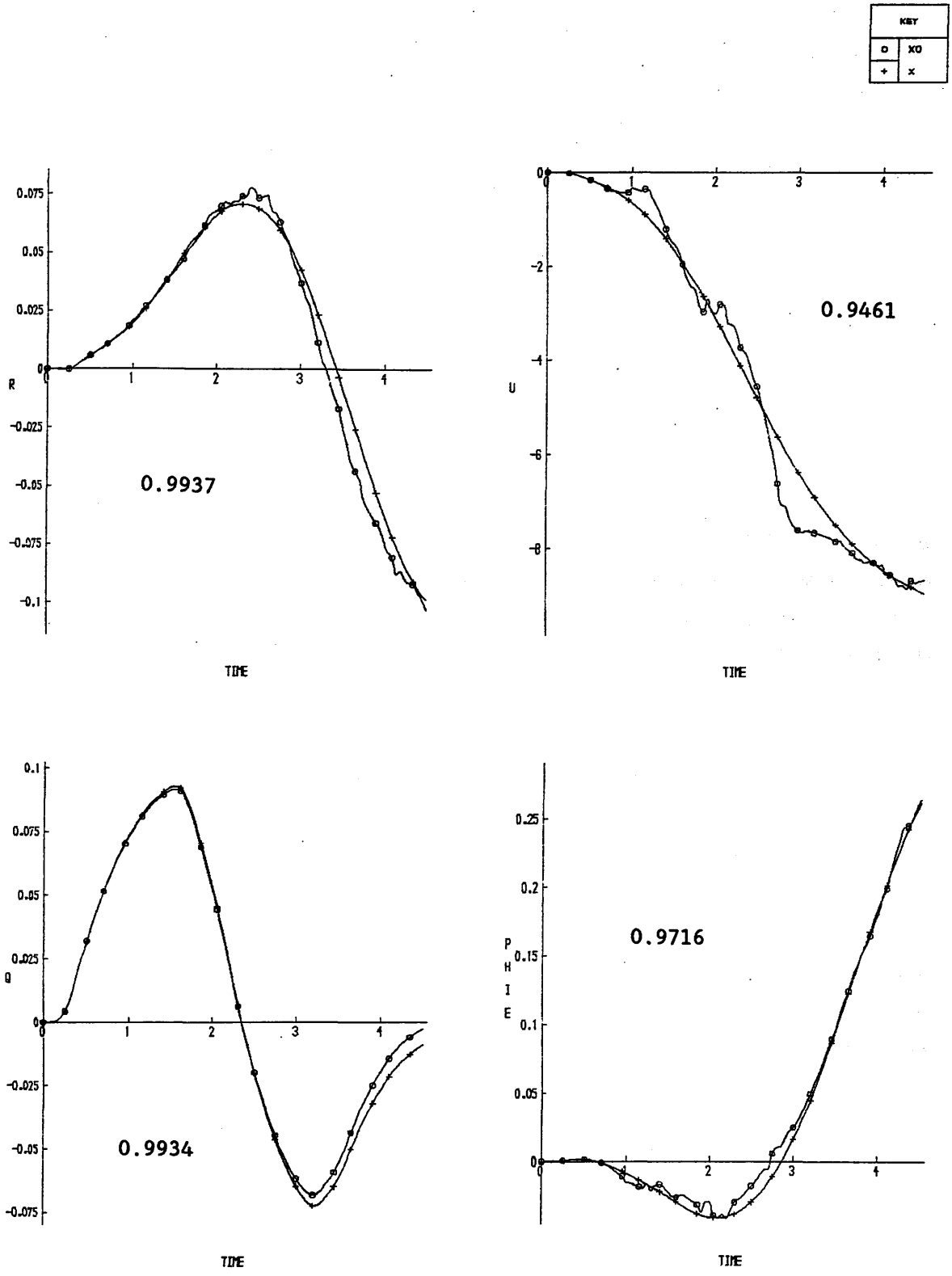

FIG 5.13 EXAMPLES OF CORRELATION PROGRAM FAILS

handling difficulties, and can limit the desired flight path.

In Parry and Murray–Smith's 1985 paper a controller is designed for a Lynx at eighty knots and is based on a *Helistab* generated, eighth order model. The A and B matrices are given in Appendix five and the eigenvalues of A (the open–loop dynamics) consist of three longitudinal and three lateral modes, namely

LONGITUDINAL	LATERAL
Fast Pitch = -3.199	Roll = -10.544
Slow pitch = -0.406	Spiral = -0.03
Phugoid = 0.134 ± j0.376	Dutch Roll = -0.654 ± j2.255

The design criteria for the controller are given in *Table 5.8* and the desired eigenvector or eigenvector subspace for each mode are shown in *Table 5.9*. Thus w is associated with fast pitch, φ with spiral, and so on. The paper gives the details of the design procedure and the resulting closed–loop eigenvalue/eigenvector pairs – these are shown in *Table 5.10*, but does not give the feedback matrix K. This was determined from the authors to be,

$$\begin{bmatrix} 0.71e\text{-}2 & -0.88e\text{-}2 & -0.44 & -0.28 & -0.49e\text{-}4 & 0.47e\text{-}3 & -0.33e\text{-}2 & -0.35e\text{-}3 \\ -0.27e\text{-}1 & 0.19e\text{-}2 & 0.36 & 0.11e{+}1 & 0.38e\text{-}3 & 0.13e\text{-}1 & 0.22e\text{-}2 & 0.14e\text{-}2 \\ 0.59e\text{-}2 & -0.26e\text{-}2 & -0.14 & -0.24 & 0.10e\text{-}3 & -0.62e\text{-}2 & -0.28e\text{-}2 & 0.66e\text{-}2 \\ 0.70e\text{-}2 & -0.33e\text{-}2 & -0.24 & -0.27 & 0.17e\text{-}1 & 0.12 & 0.15 & -0.57 \end{bmatrix}$$

Fig 5.14 shows the connection of the controller to the system: there are two additional elements when compared to the controller of *fig 3.2*. These are an actuator and P, the *precompensator matrix*. P (order (m×m) and of full rank, so as not to alter the orientation of the assignable subspaces) is designed to reduce the coupling effext of the input matrix B, and is derived in two steps,

(1) Form matrix T from the rows of matrix B:

$$T = \begin{bmatrix} \text{Row } 2 \\ 1 \\ 6 \\ 5 \end{bmatrix}$$

(2) $P = T^{-1}$

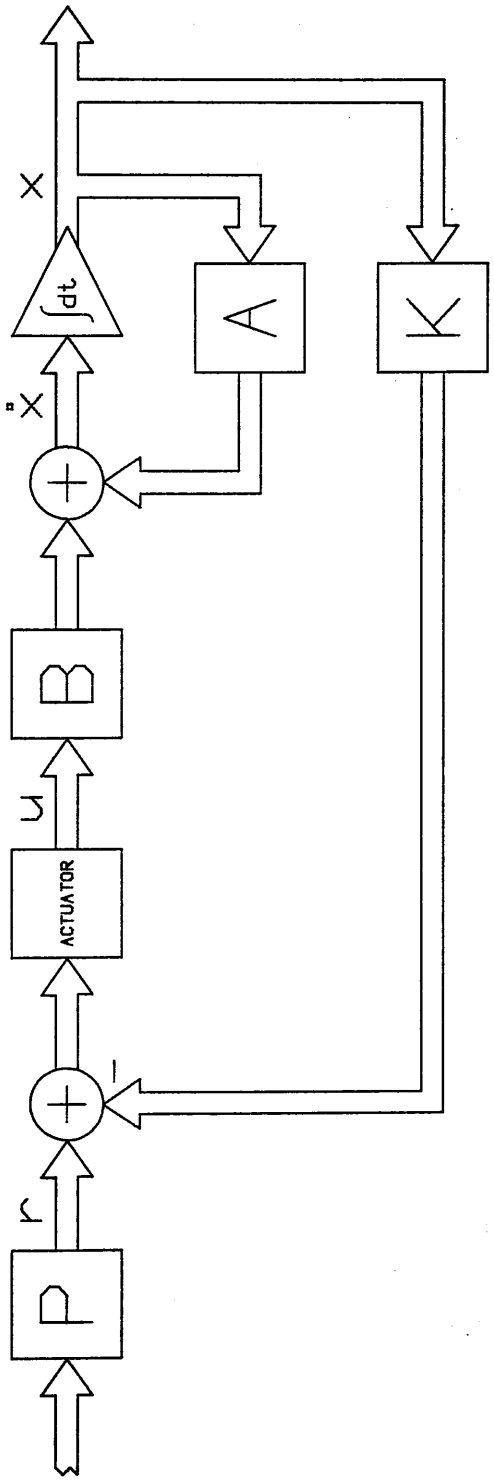

FIG 5.14 MODAL CONTROL

STATE	TIME CONSTANT	CROSS COUPLING
VERTICAL VELOCITY w	< 0.25 SECS	< 1 %
LONGITUDINAL VELOCITY u	< 1.00	< 10
ROLL RATE p	< 0.10	< 5
LATERAL VELOCITY v	< 0.20	< 5

TABLE 5.8 : DESIGN CRITERIA FOR CONTROLLER

	FAST PITCH	SLOW PITCH & PHUGOID	ROLL	SPIRAL	DUTCH ROLL
u	0	1 0 0	0	0	0 0
w	1	0 0 0	0	0	0 0
q	0	0 0 0	0	0	0 0
θ	0	0 1 0	0	0	0 0
v	0	0 0 1	0	0	1 0
p	0	0 0 0	1	0	0 0
φ	0	0 0 0	0	1	0 0
r	0	0 0 0	0	0	0 1

TABLE 5.9 : DESIRED EIGENVECTOR SUBSPACE FOR EACH MODE

LONGITUDINAL MODES

	FAST PITCH (-4)	SLOW PITCH (-2)	PHUGOID (-3±j1.73)
u	-0.0031	0.9963	0.9825±j0.0001
w	0.9999	0.0000	0.0000±j0.0000
q	-0.0146	-0.0768	-0.1404±j0.1107
θ	0.0037	0.0384	0.0511±j0.0074
v	0.0000	0.0000	0.0001±j0.0000
p	0.0000	-0.0002	-0.0001±j0.0003
φ	0.0000	0.0001	0.0001±j0.0001
r	0.0001	-0.0024	0.0042±j0.0040

LATERAL MODES

	ROLL (-11)	SPIRAL (0)	DUTCH ROLL (-6±j3.5)
u	0.0015	0.0000	-0.0001±j0.0001
w	-0.0001	-0.0011	0.0000±j0.0000
q	-0.0011	-0.0076	-0.0004±j0.0000
θ	-0.0002	0.0008	-0.0002±j0.0000
v	0.9960	-0.0032	0.9986±j0.0001
p	0.0034	-0.0050	0.0000±j0.0000
φ	-0.0005	0.9728	-0.0002±j0.0000
r	0.0892	0.2316	0.0451±j0.0289

TABLE 5.10 : CLOSED-LOOP EIGENVALUE/EIGENVECTOR PAIRS

PILOT INPUT	STATE EFFECTED
COLLECTIVE STICK θ_{0e}	NORM' VELOCITY w
LONG' CYCLIC STICK θ_{1s}	LONG' VELOCITY u
LAT' CYCLIC STICK θ_{1c}	ROLL RATE p
PEDAL θ_{0t}	LAT' VELOCITY v

TABLE 5.11 : RELATIONSHIP BETWEEN PILOT INPUT AND STATE VARIABLES

Corresponding rows of the modified input matrix B_c, where

$$B_c = B*P \tag{5.10}$$

will then approximate the identity matrix, yielding the relationships between pilot inputs and state variables given in *Table 5.11.* The m actuators are modelled as *first order lags* of form,

$$W(s) = \frac{Y(s)}{u(s)} = \frac{1}{1 + s\tau} \tag{5.11}$$

with a time constant of $\tau = 50$mS, and since the use of a state observer is assumed, C is taken to be the identity matrix and therefore not shown on *fig 5.14.*

For the above flight condition and controller a full order observer was designed with eight eigenvalues at -20 (the design of an observer can be carried out independently of the design of a controller: separation property – section 3.5) and the observer C matrix was C(1,2,3,4). The simulation was first run without the observer in the feedback loop, ie. $\underset{\sim}{x}$ was obtained directly from the controlled system. *Figs 5.15 – 5.18* show the state time responses for a doublet input of K= 0.1 rads, t= 0.0/2.5/3.5/6.0, applied to each of the four inputs: θ_{0e}, θ_{1s}, θ_{1c} and θ_{0t}; whilst *fig 5.19* shows the time response of the uncontrolled (open–loop) system with the doublet applied to θ_{0e}. Nb. angles and rates are shown in degrees and degrees/second, respectively.

It is evident from the time responses that modal control has resulted in a stable system with minimal interaction between the four controlled inputs w, u, p and v, and that the longitudinal and lateral dynamics are highly decoupled. Compare this to the open–loop system: *fig 5.19.*

Next, the simulation was run with the controller using the state vector $\hat{\underset{\sim}{x}}$, ie. the observer estimate of $\underset{\sim}{x}$. Visually, the time responses appear identical, however *fig 5.20* demonstrates that there are very small differences between $\hat{\underset{\sim}{x}}$ and $\underset{\sim}{x}$, but this is only due to numerical errors in the estimation process and therefore there is no difference in state feedback from the estimated state $\hat{\underset{\sim}{x}}$ or the actual state $\underset{\sim}{x}$: as predicted in section 3.5. The simulations were repeated using a reduced order observer with four eigenvalues at -20 and the results achieved were very similar to the full order case: ie. no practical difference between using $\hat{\underset{\sim}{x}}$ or $\underset{\sim}{x}$.

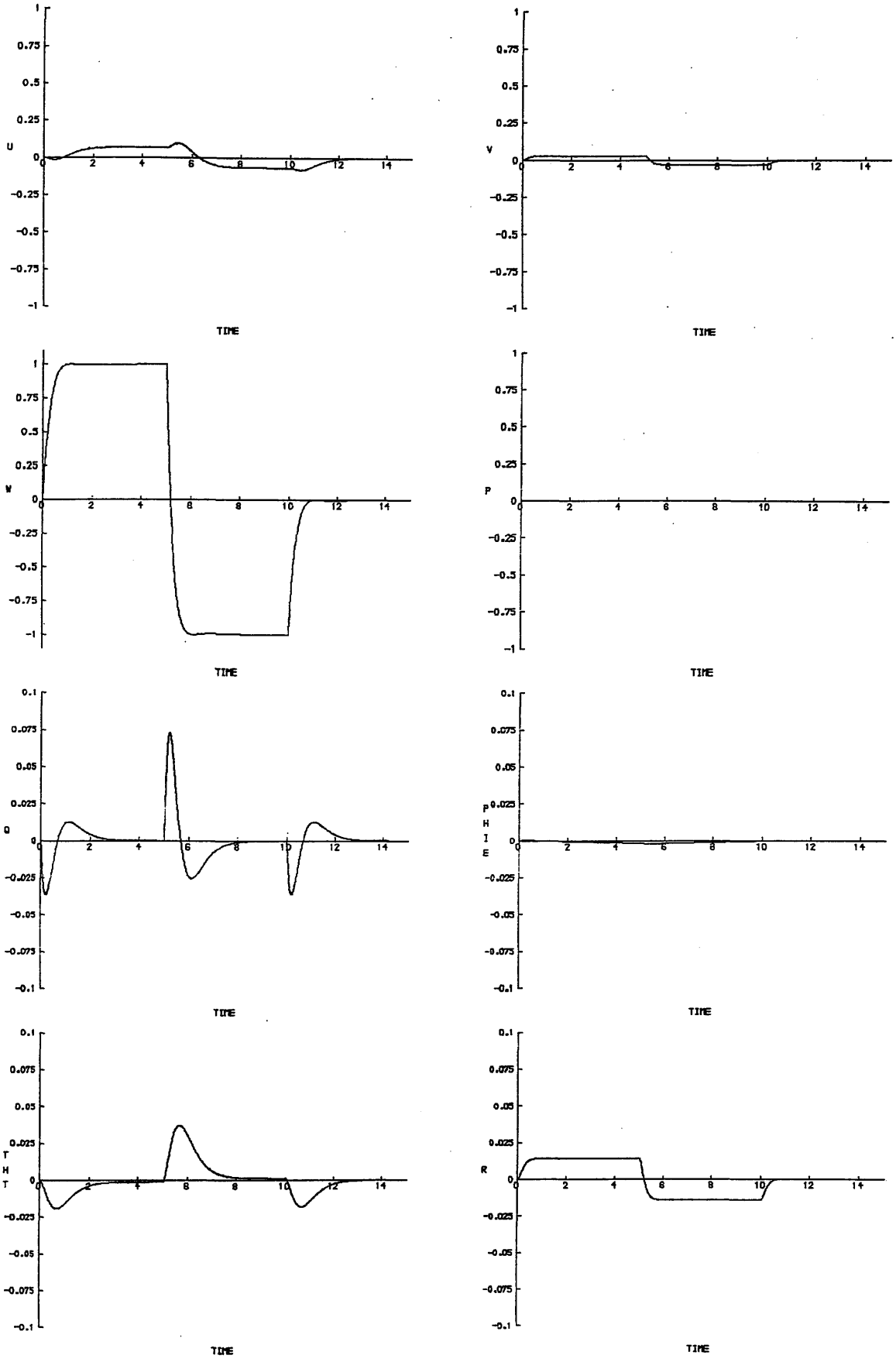

FIG 5.15 CLOSED-LOOP RESPONSE TO A DOUBLET ON θ_{0e}

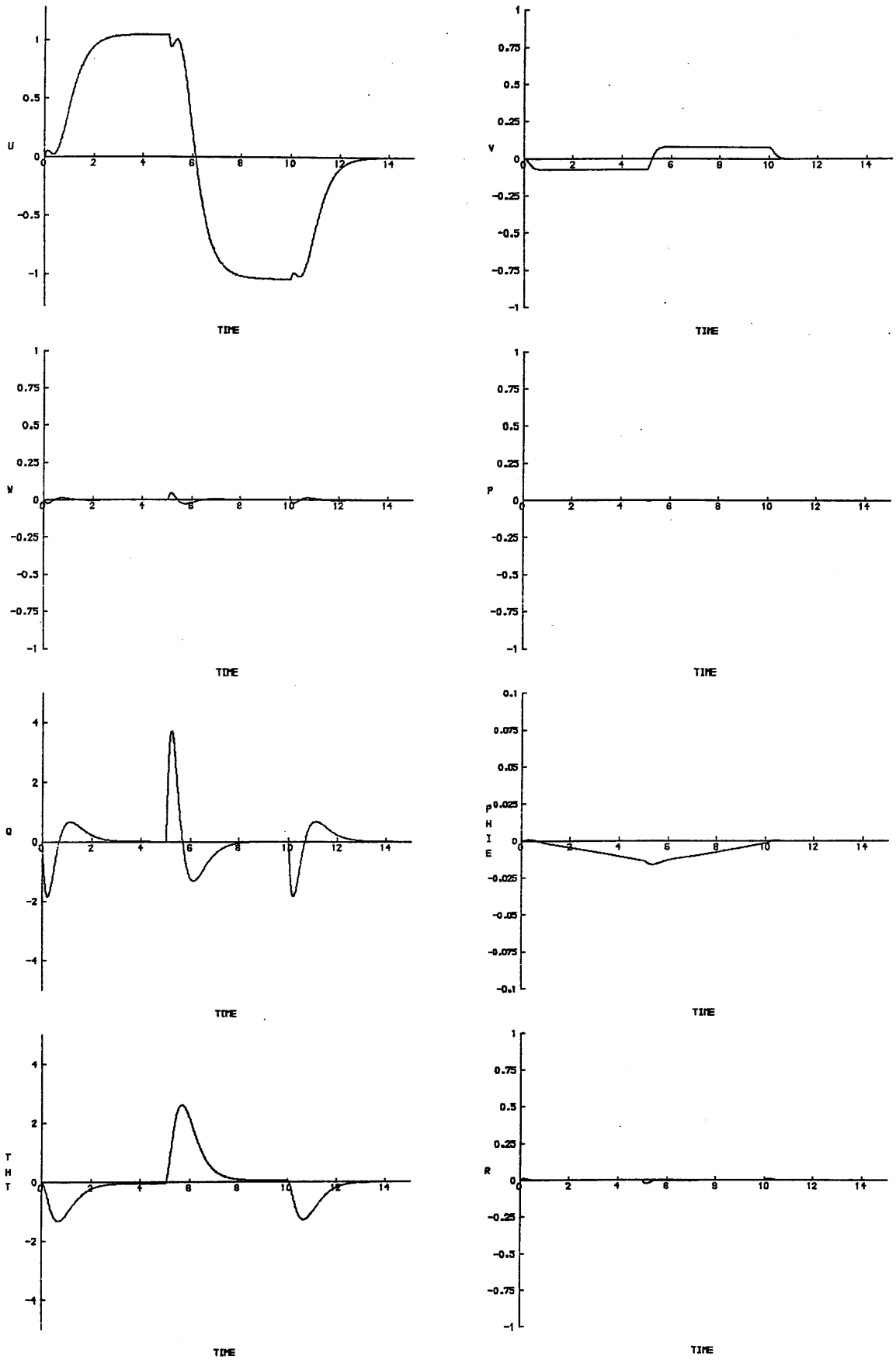

FIG 5.16 CLOSED-LOOP RESPONSE TO A DOUBLET ON θ_{1S}

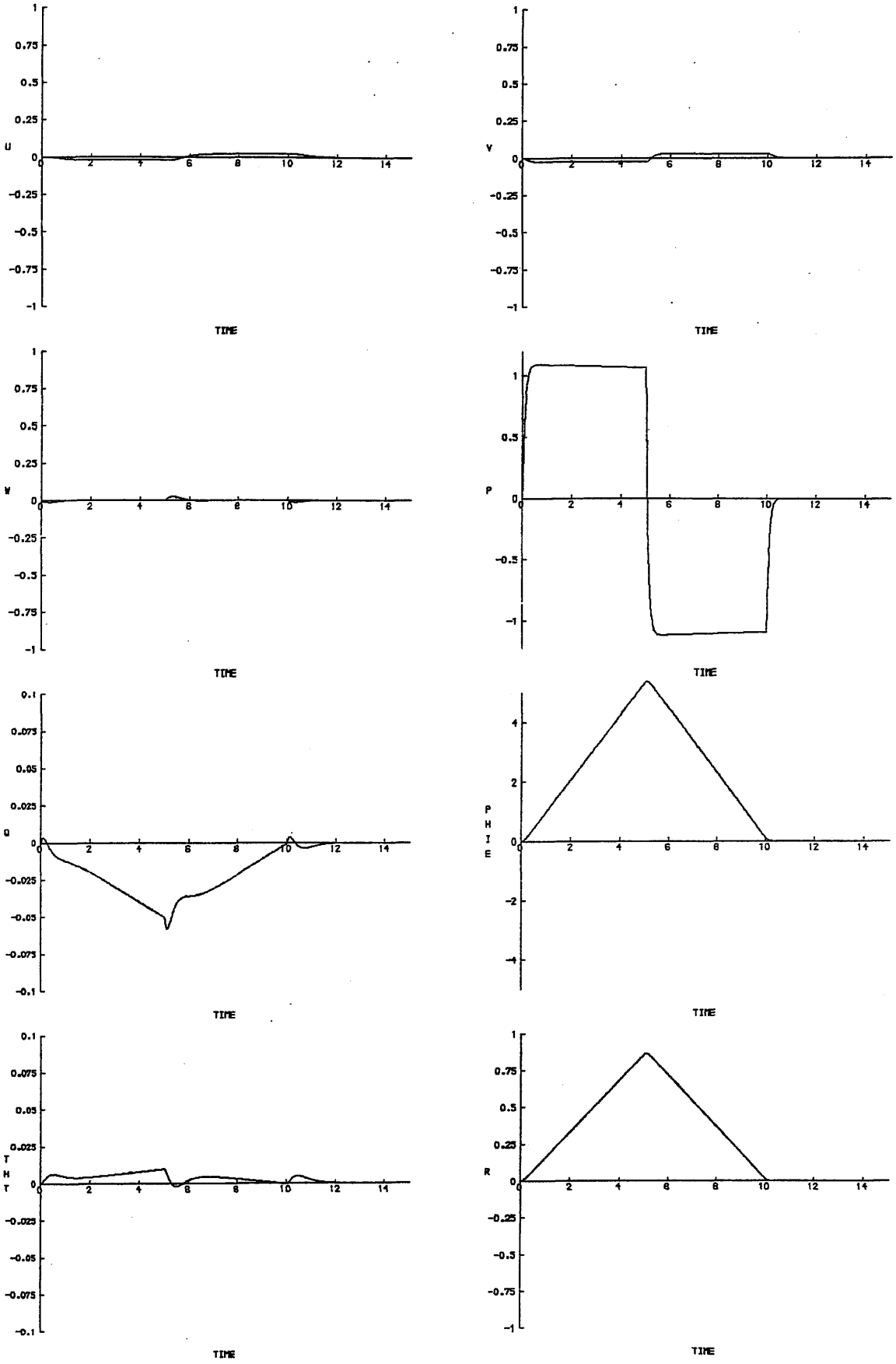

FIG 5.17 CLOSED-LOOP RESPONSE TO A DOUBLET ON θ_{1c}

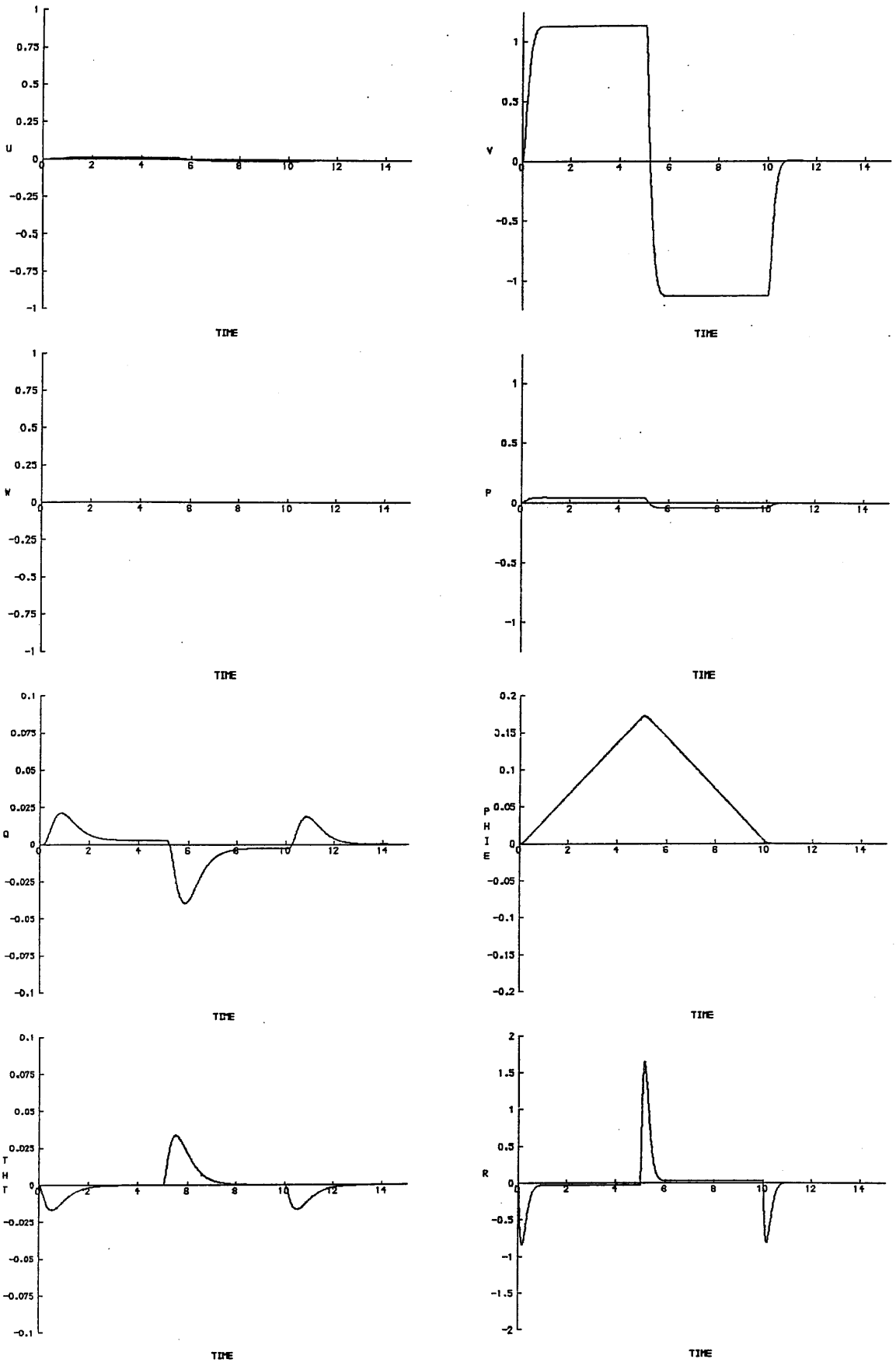

FIG 5.18 CLOSED-LOOP RESPONSE TO A DOUBLET ON θ_{0t}

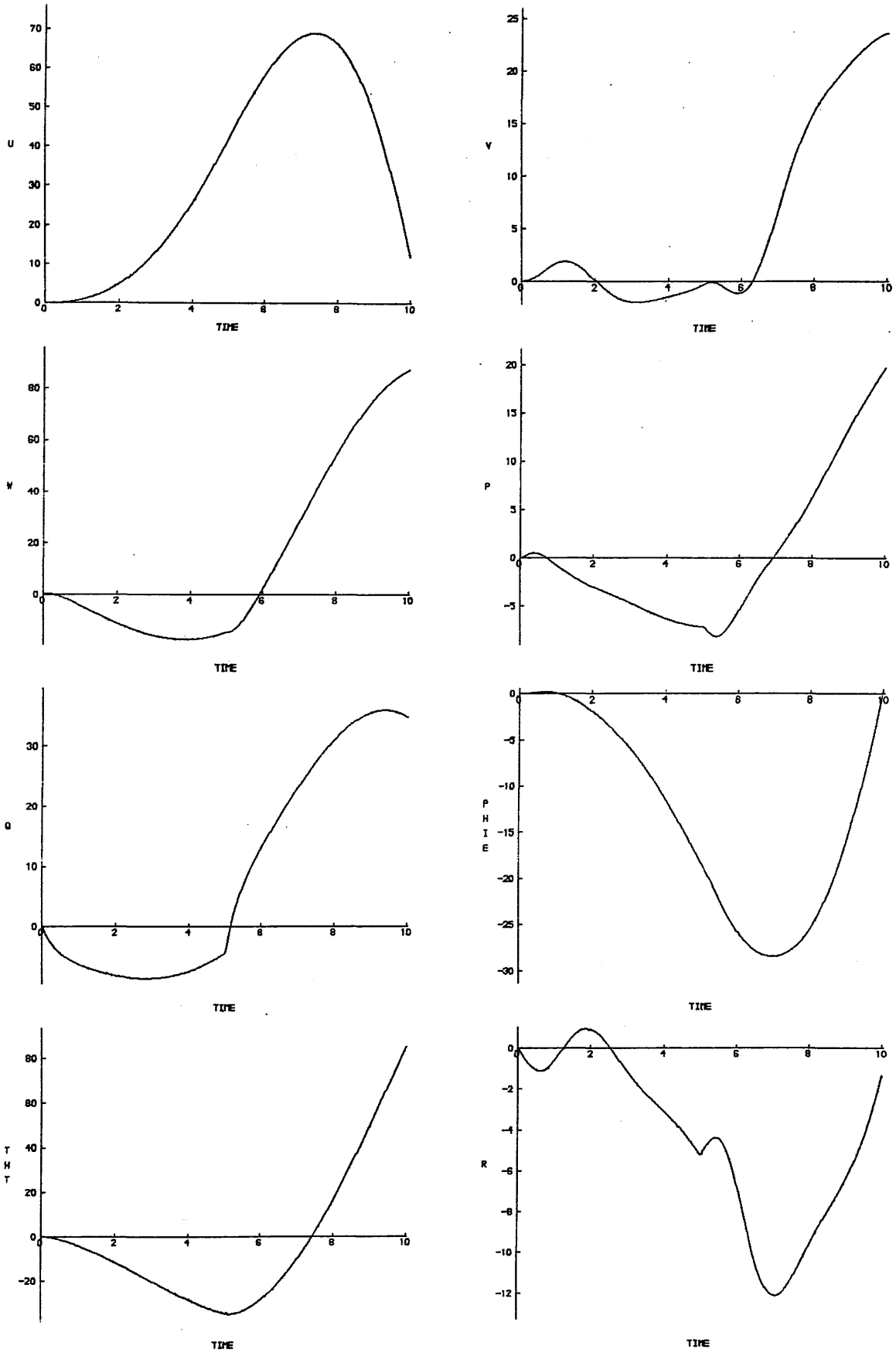

FIG 5.19 OPEN-LOOP RESPONSE TO A DOUBLET ON θ_{0e}

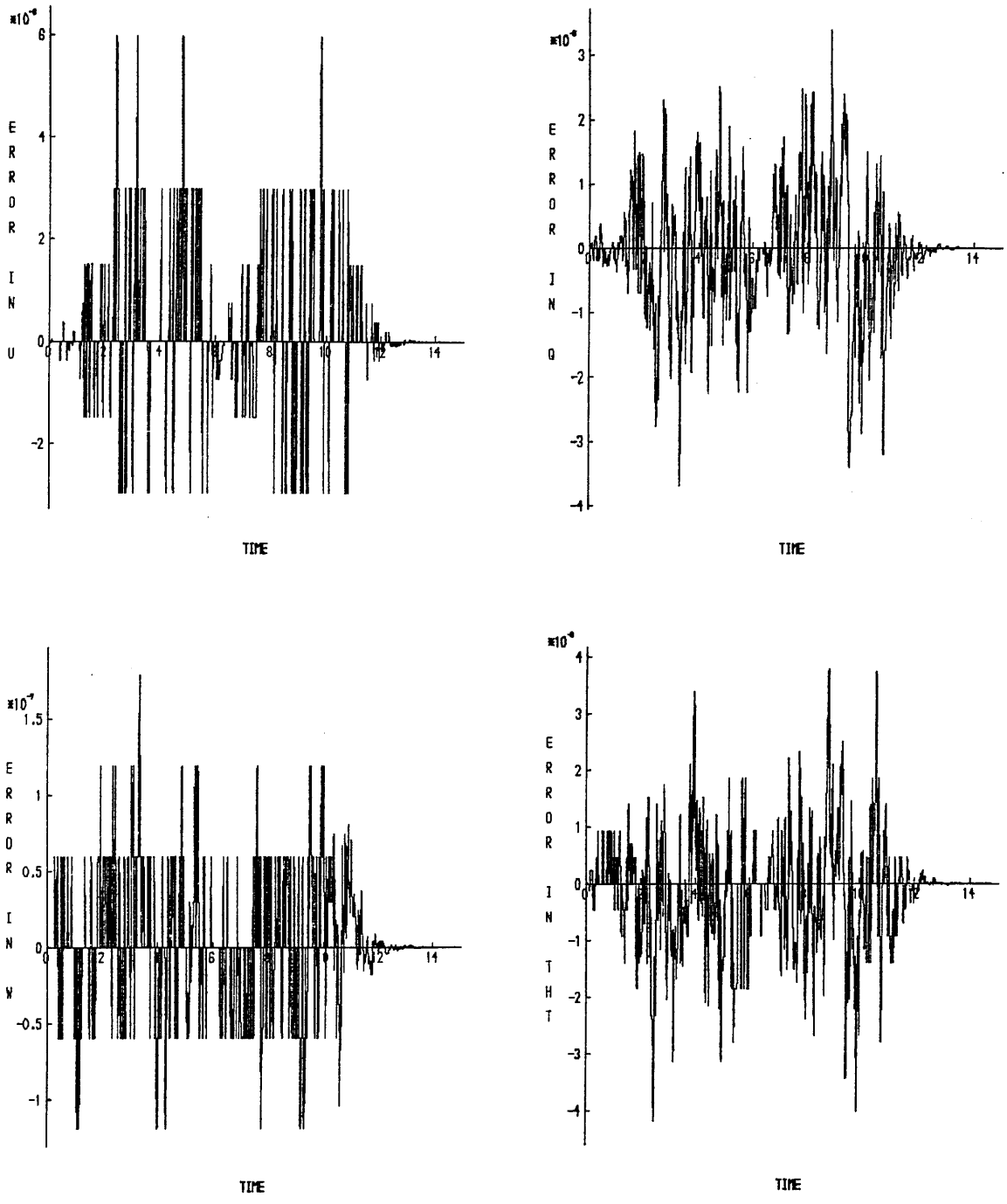

FIG 5.20 NUMERICAL ERRORS IN THE STATE ESTIMATION PROCESS

5.4 FURTHER OBSERVER CHARACTERISTICS

Now having demonstrated that using an observer in a state feedback control system does not alter the dynamics of the controller, the above combination of system and controller were used to demonstrate a further two characteristics of observers, namely: the effect changing individual observer eigenvalues has on the state estimates and the increase in magnitude of overshoots as p is decreased.

EFFECT OF CHANGING INDIVIDUAL OBSERVER EIGENVALUES

Much has already been said about the selection of suitable eigenvalues for the observer: both in terms of design accuracy and observer performance, but what effect does changing individual eigenvalues have on the state estimates? To answer this question each of the eight eigenvalues were individually changed to -40 and the simulation run for a doublet input on θ_{0e} and initial estimation errors introduced on each state. The time responses were then examined to see which state estimates had been effected.

Figs 5.21 and *5.22* show the observer error time histories for changing eigenvalues one and six respectively. It can be seen that not all the states are affected by a change in eigenvalue (eg, w, q and θ in *fig 5.21*) and that different states are effected by different eigenvalues (eg. q). The effect of changing any particular eigenvalue is difficult to forecast since the eigenvectors are also altered: it would require an observer design method which allowed the allocation of both eigenvalues and eigenvectors, analogous to the above modal control procedure. Fortunately, the ability to assign a set of eigenvalues without any knowledge of their associated eigenvectors, is adequate in the vast majority of practical applications, and providing the eigenvalues are all sufficiently fast, their individual contributions are irrelevant.

EFFECT OF VARYING p

The effect of varying p. ie. the number of rows in C, with respect to the accuracy of a design, was discussed in section 5.2.3; but it also has a significant effect on the magnitudes of overshoots during the state estimation process. Three observers were designed using C(1), C(1,2) and C(1,2,3), and each had eigenvalues at -20, -21, ..., -27. Simulations were run for each observer with a step input on θ_{1s} (K= 0.1 rads, t= 0.0) and a scale factor fault of 0.9 applied to the sensor measuring u, between three and four seconds. *Fig 5.23* demonstrates the dramatic differences

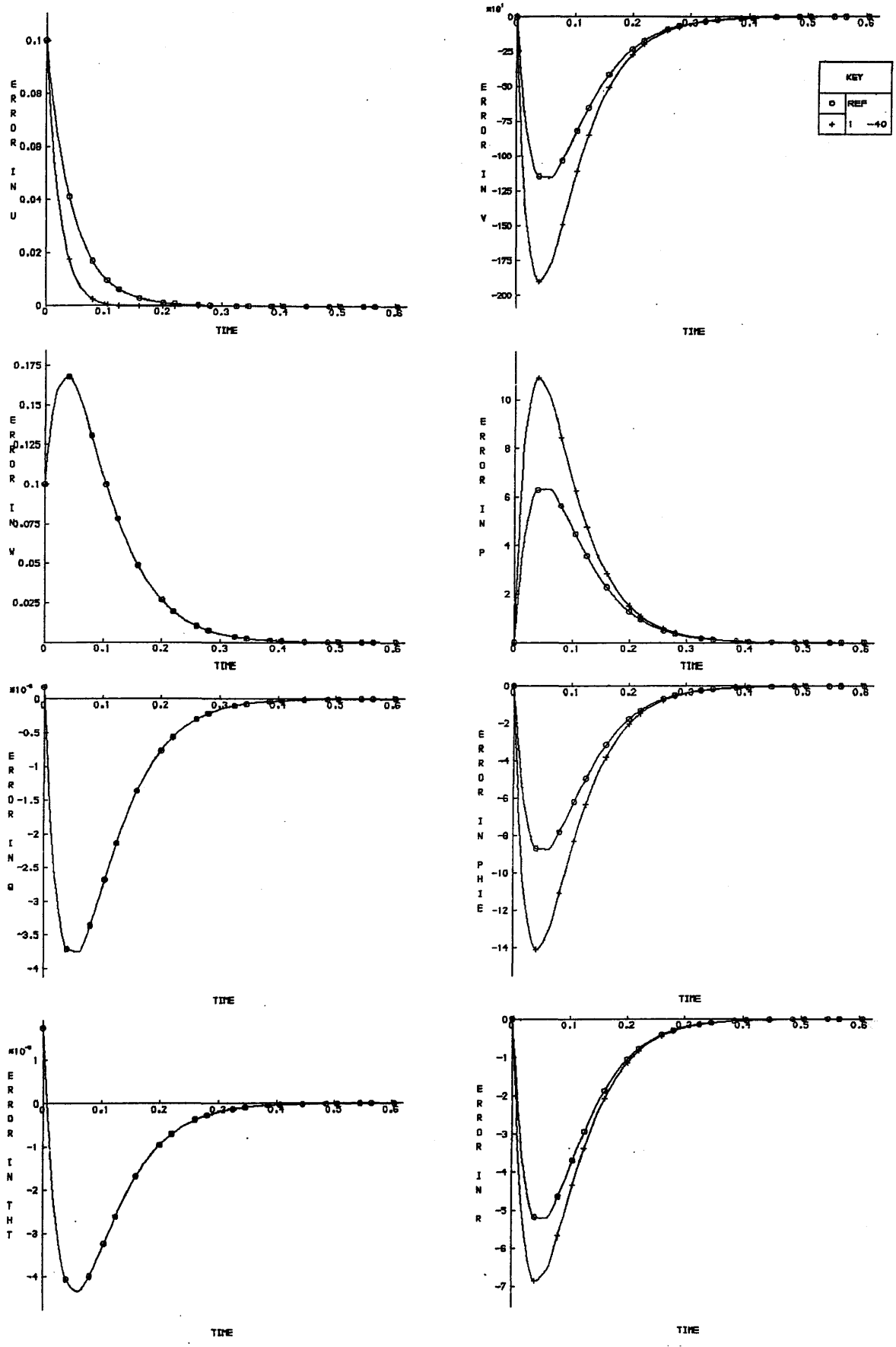

FIG 5.21 EFFECT ON OBSERVER ESTIMATE OF CHANGING EIGENVALUE ONE

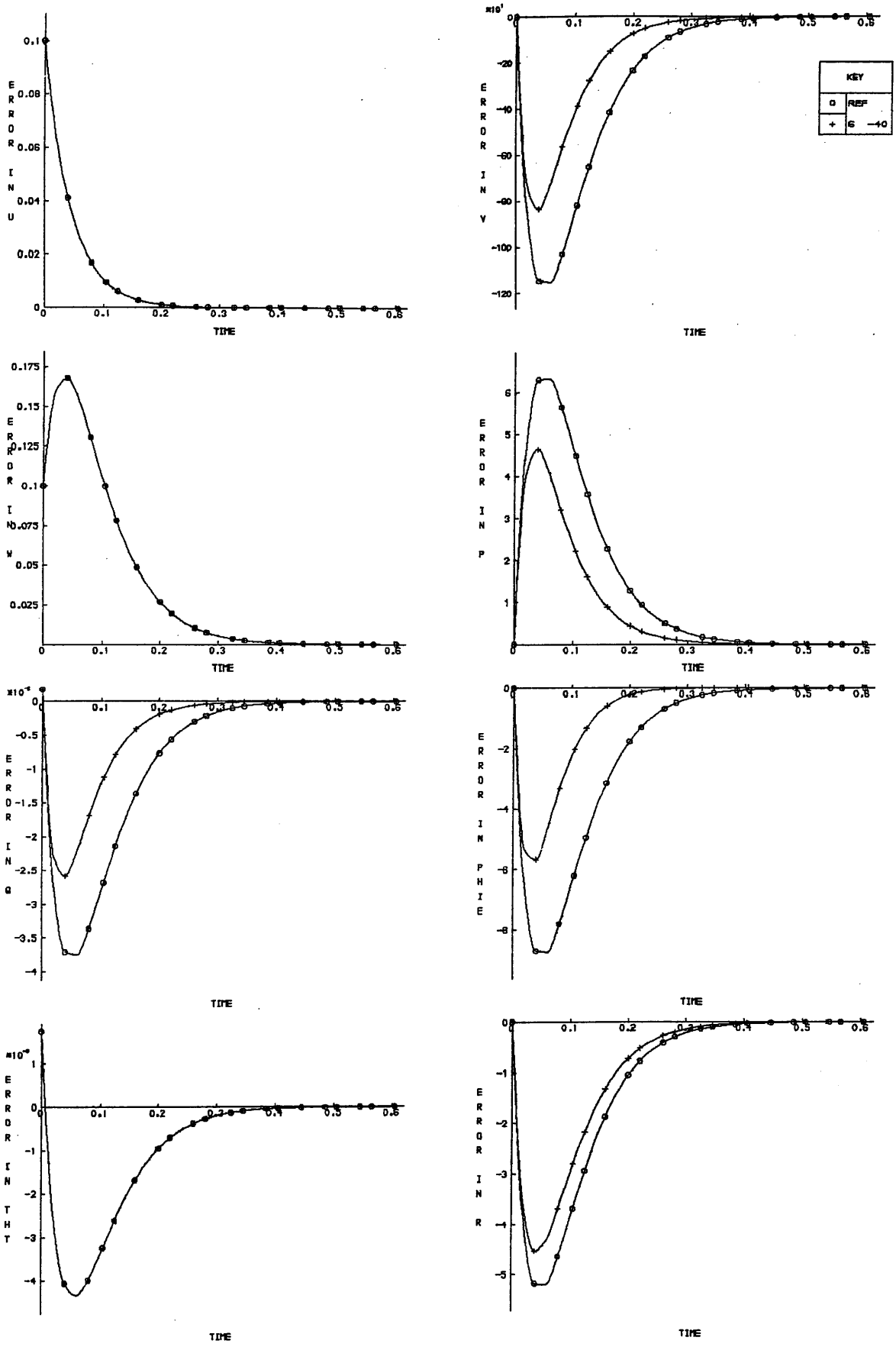

FIG 5.22 EFFECT ON OBSERVER ESTIMATE OF CHANGING EIGENVALUE SIX

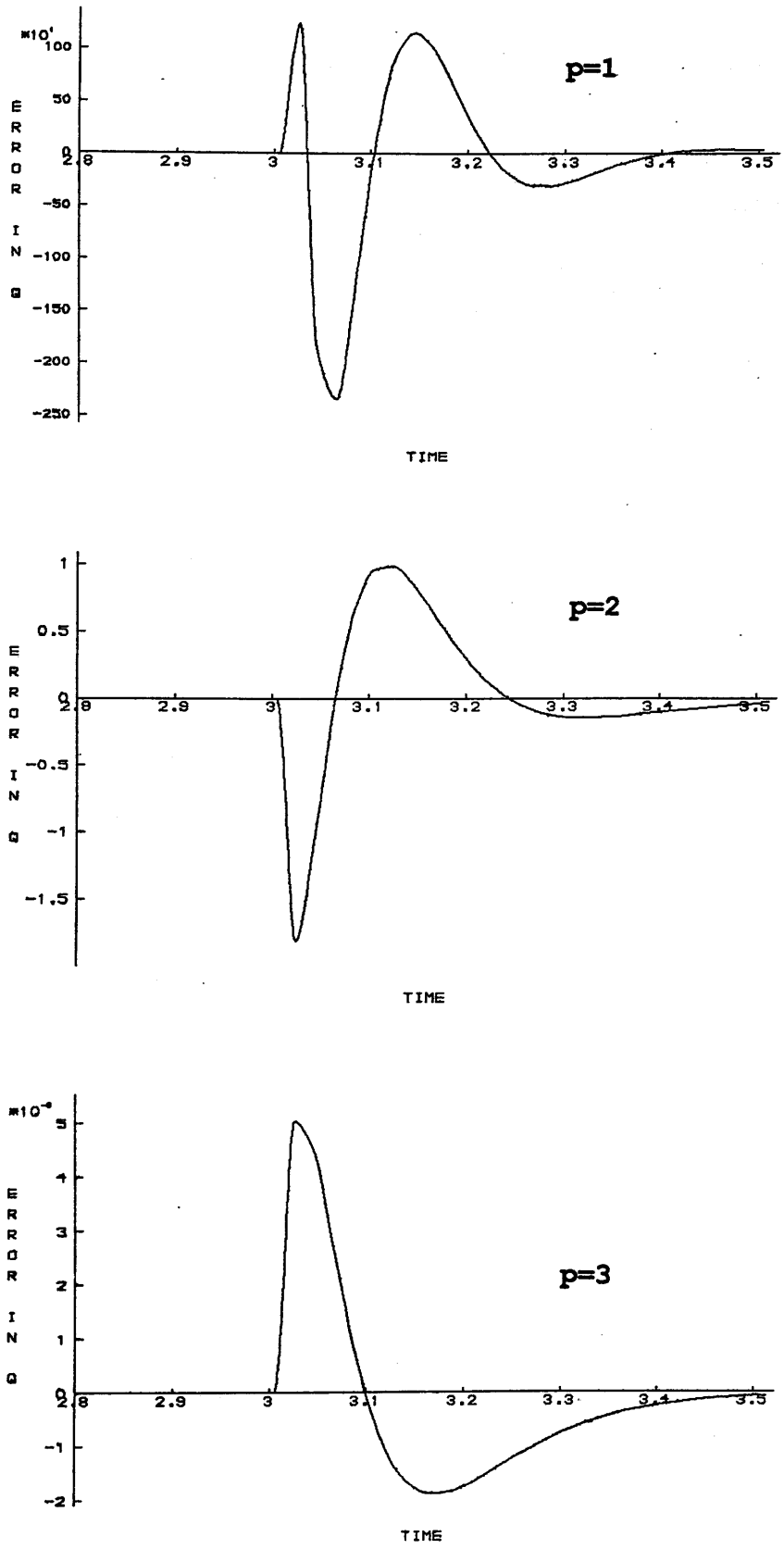

FIG 5.23 EFFECT OF VARYING p ON MAGNITUDE OF OVERSHOOT

in magnitude of overshoot – as p decreases, the magnitude of overshoot increases.

An explanation for this behaviour can be deduced from Chen, 1984, who states that for state feedback using a canonical form of order n and distinct eigenvalues, the largest magnitude in transient is approximately proportional to,

$$(\ |\lambda_{max}| \ )^{\mu_i - 1}$$

where $|\lambda_{max}|$ is the largest eigenvalue in magnitude and μ_i the order of the block. The magnitude of feedback gains is also proportional to n. Thus small feedback gains and small transients are achieved by the largest observable canonical form block being kept as small as possible.

CHAPTER 6

EVALUATION OF THE PERFORMANCE OF OBSERVABLE CANONICAL FORM OBSERVERS

6.1 INTRODUCTION

In the previous chapter the software implementation of the design of observable canonical form observers, including the observability test, transformation to canonical form, choice of full or reduced order observer, selection of eigenvalues and the choice of treating the system as one entity or as a set of p subsystems, was discussed. Observer accuracy was considered only in terms of the eigenvalues: how close were the eigenvalues of the designed observer to those requested.

This chapter examines observer accuracy in terms of performance: how faithful is the estimated state $\hat{\underset{\sim}{x}}$ to the actual state $\underset{\sim}{x}$. A quantitative measure of performance is provided by the correlation test described in section 5.2.6. Numerical problems with the observability test and the canonical transformation (and hence with observer performance) are investigated, and in particular the importance of the choice of C matrix (in other words, which system state variable(s) are used to reconstruct an estimate of the remaining state variables) is examined in detail.

Differences between eighth and fourteenth order models, and between reduced order and full order observers, are examined and the choice of suitable eigenvalues for the observer is appraised with regard to performance. Finally a new form of observer is developed: the *Twin Observer*, which provides a simple, but effective method of alleviating the problem of noise corrupted states.

6.2 OBSERVER PERFORMANCE WITH A 14th ORDER MODEL

The fourteenth order (eleven degrees of freedom) model can be partitioned into longitudinal, lateral and rotor dynamics; the rotor dynamics consisting of coning angle (β_0), longitudinal and lateral flapping (β_{1C} and β_{1S}) and the derivatives $\dot{\beta}_0$, $\dot{\beta}_{1C}$ and $\dot{\beta}_{1S}$ (section 3.10). These six rotor states have much faster dynamics than the eight fuselage states (ie. longitudinal and lateral states). For example, consider the eigenvalues of a Puma at one hundred knots,

Fuselage	Rotor
-2.17	-12.4 ± j51.1
-1.05 ± j1.03	-12.6 ± j24.3
-0.06 ± j0.94	-11.4 ± j 3.7
-0.01 ± j0.20	
-0.12	

It can be seen that even the smallest rotor eigenvalue is more than five times the magnitude of the largest fuselage eigenvalue. This creates difficulties in selecting suitable observer eigenvalues since appropriate eigenvalues for the rotor states (say approximately -25 in the above example) would be unsuitable for the fuselage states (for which -5 would be more applicable). The problem arises because the observer tends to act like a differentiator as the eigenvalues are increased towards minus infinity, and as such becomes highly sensitive to noise.

To illustrate this consider *fig 6.1* which shows two different reduced order observers designed for the Puma at one hundred knots. The control input was a doublet on θ_{1S} (Appendix six), observer C matrix C(3,6) and the observer in *fig 6.1a* had eigenvalues placed for the rotor states whilst the observer in *fig 6.1b* had them placed for the fuselage states.

It is apparent that with 'rotor eigenvalues' the observer follows the rotor states, but has excessive noise on the fuselage states due to the fast eigenvalues. Conversely, with 'fuselage eigenvalues' the observer accurately estimates the fuselage states, but no longer follows the rotor states since the observer dynamics are now slower than the rotor dynamics.

The probable solution to this problem would therefore involve two sets of observers: one set for the fuselage states and a second set for the rotor states, each set having appropriate eigenvalues. However this was not investigated further since, at that time, there were no plans for the rotor states to be utilised or controlled by an automatic flight control system. Consequently further analysis of the fourteenth order model only considered the fidelity of the eight fuselage states and the eigenvalues were selected accordingly.

Nevertheless, it should be noted that the design of observers for estimating rotor state variables is currently a topic of active research. See, for example, McKillip, Jr, 1984,85,86; DuVal, 1980; Fuller, 1981; Hall, Gupta and Hansen, 1980 and Molusis, Warmbrodt and Bar–Shalom, 1983.

Most of these designs use a Kalman filter type structure, although a full Kalman filter is rarely used as it requires an *a–priori* knowledge of the random processes perturbing the rotor system, a knowledge of the structure of the noise corrupting the measurements and an exact model of the plant dynamics. Given the complex dynamic and aerodynamic environment of most helicopter rotors, this proves to be too great a demand on mathematical modelling ability.

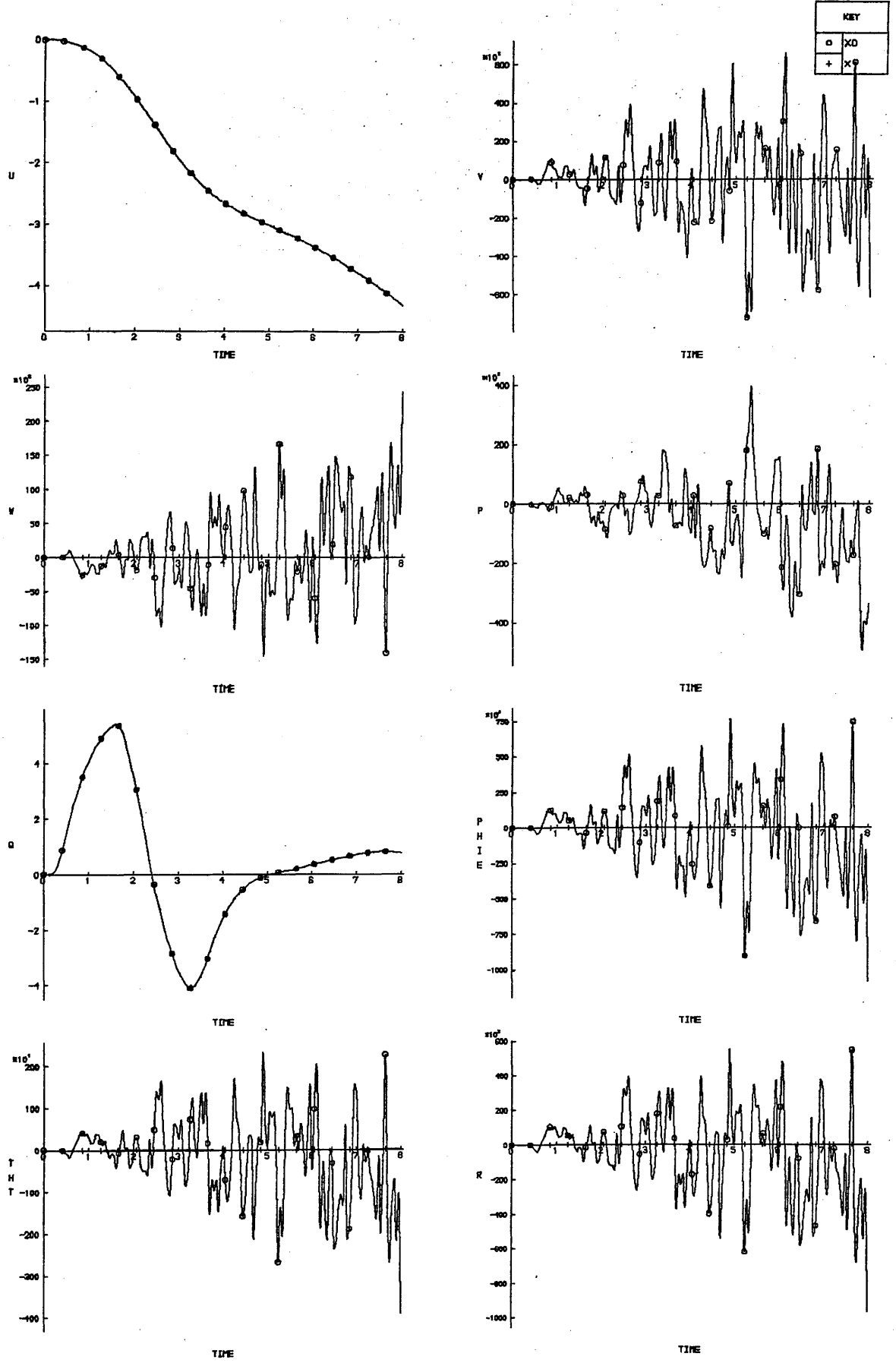

FIG 6.1 EIGENVALUE SELECTION PROBLEMS WITH 14th ORDER MODEL

(a) ROTOR EIGENVALUES

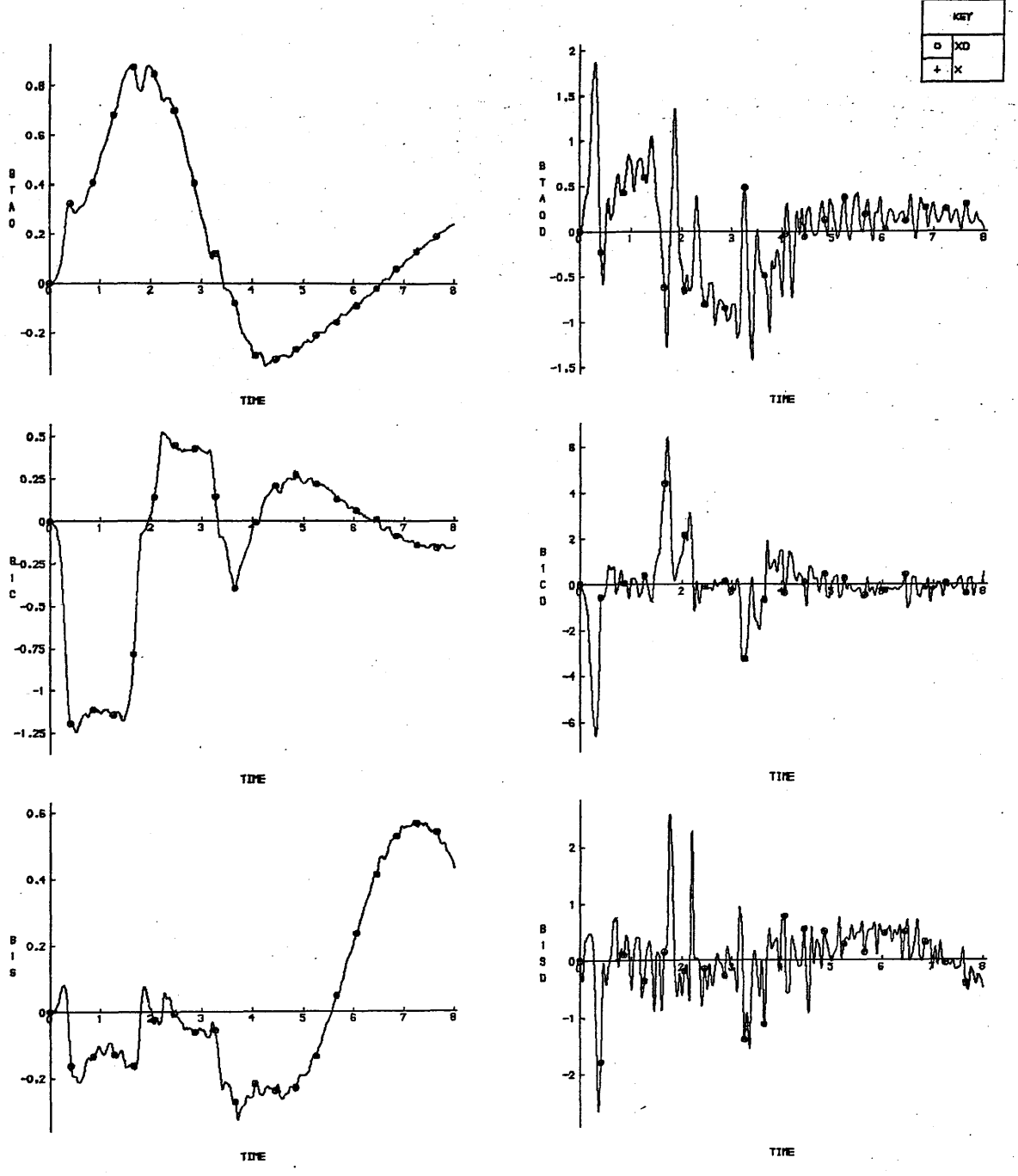

FIG 6.1 EIGENVALUE SELECTION PROBLEMS WITH 14th ORDER MODEL

(a) ROTOR EIGENVALUES

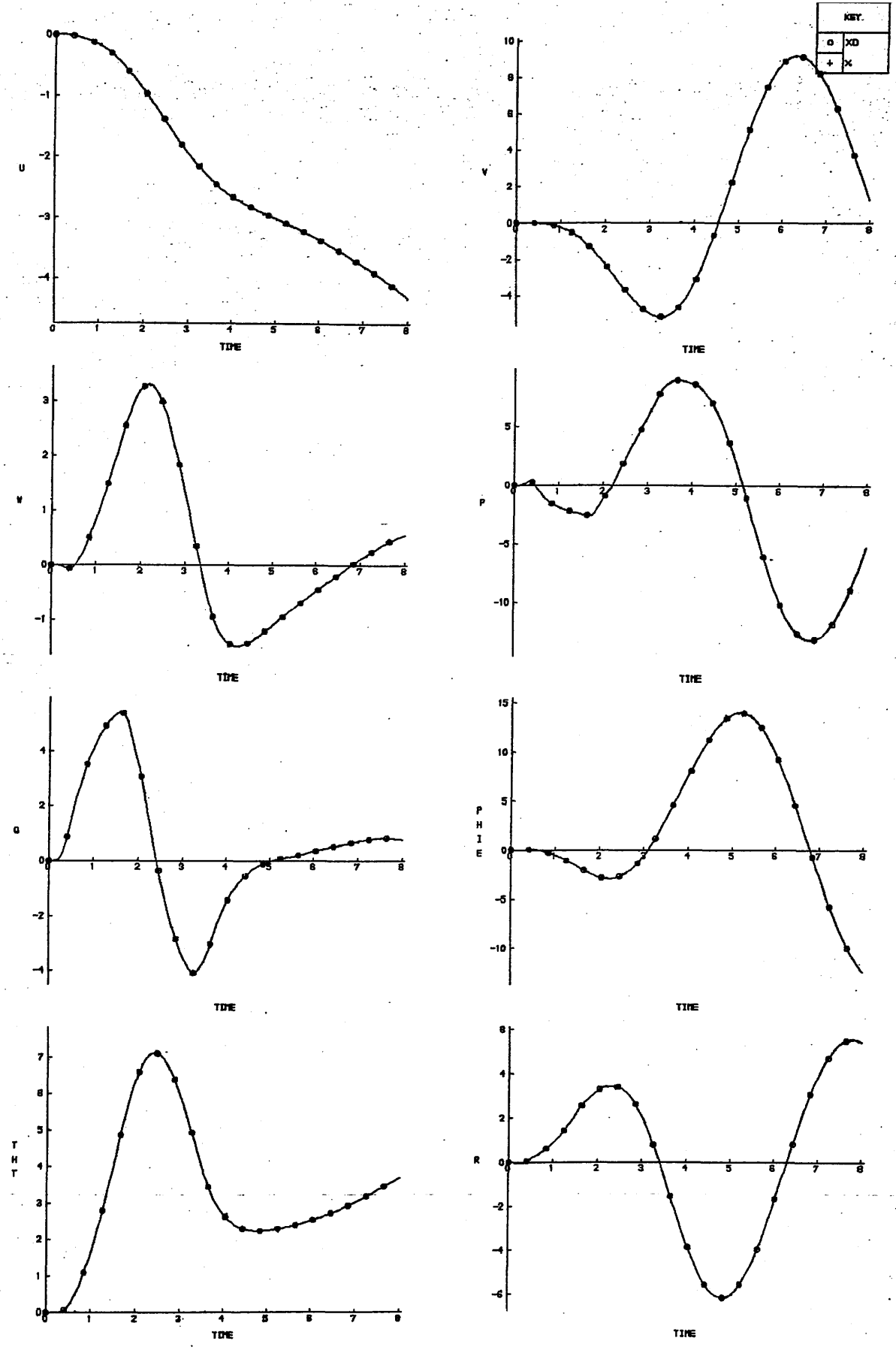

FIG 6.1 EIGENVALUE SELECTION PROBLEMS WITH 14th ORDER MODEL

(b) FUSELAGE EIGENVALUES

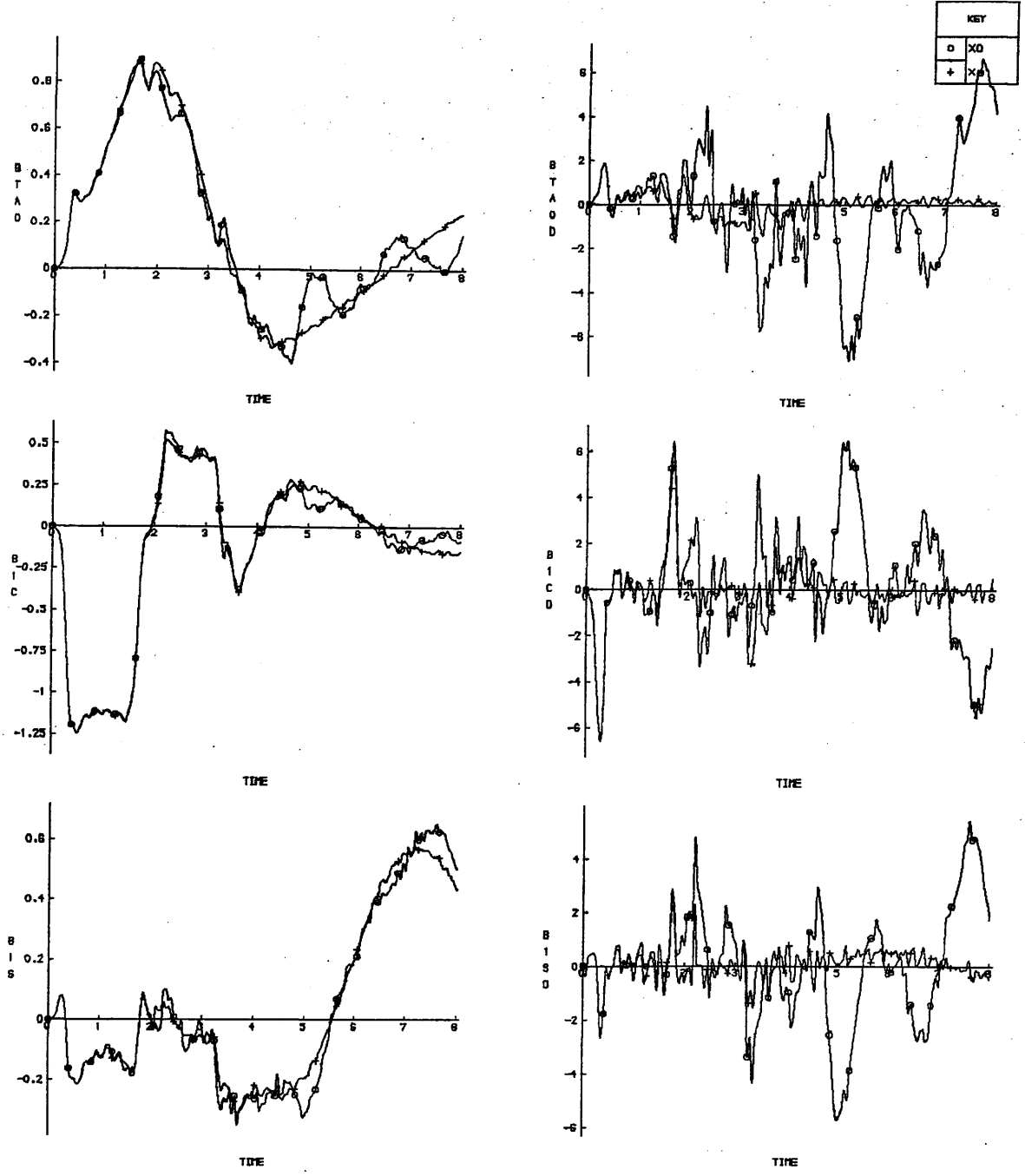

FIG 6.1 EIGENVALUE SELECTION PROBLEMS WITH 14th ORDER MODEL

(b) FUSELAGE EIGENVALUES

6.2.1 EFFECTS OF DIFFERENT C MATRICES

In section 4.5.5 it was demonstrated that different C matrices produced large variations in the transient response of the observer and in section 5.2.3 it was shown that the accuracy of the observer design increases as p (ie. the number of rows of C) increases. It is therefore not surprising to discover that observer performance is also affected by the choice of C matrix. With p= 1 the fourteenth order system was unobservable and therefore only C matrices with p≥2 were considered.

To illustrate the effect of different C matrices, consider Table 6.1 which gives the results obtained for a doublet input on θ_{1S} (Appendix six) to the Puma at one hundred knots. For each of the fifty six permutations of C matrix a reduced order observer was designed, with the two subobservers having eigenvalues of [−4, −3.8, −3.6, −3.4, −3.2, −3].

The eight−second time histories of the state estimates were evaluated using the correlation program: an 'x' indicates that all failed (eg. C(1,3) has an 'x' in the lateral column, thus the estimates of the lateral states v, p, φ and r were unsatisfactory); and numbers indicate the only satisfactory estimates (eg. C(5,7) has 2,3 in the longitudinal column and therefore the estimates of states two and three (w and q) were acceptable, whilst the estimates of states one and four (u and θ) were unacceptable). Note that estimates of the rotor states are still generated, but they are not inspected for the reasons given in the previous section.

The first thing to notice is that the results for C(i,j) are identical to those for C(j,i). In general, this was found to be true, but from examination of how the observer is designed through the selection of linearly independent vectors (section 3.7), it is obvious that this cannot be guaranteed. However, since it was true in most cases, and in order to reduce the amount of data to be analysed, it was decided to subsequently only consider the twenty eight C(i,j) matrices indicated by a '*' in Table 6.1.

The second feature which is apparent is that all the fails occur when the observer is being driven by two lateral or two longitudinal states. There are no fails involving one lateral / one longitudinal state. It is also noticeable that there are fewer fails in the half (ie. longitudinal or lateral) driving the observer. For example C(7,5) uses the lateral states v and φ to estimate the remaining two lateral states p and r (one fail: p) and the longitudinal states u, w, q and θ (two fails: u and θ). This was generally found to be the case: using longitudinal/lateral states to drive the observer gave better estimates of longitudinal/lateral states.

C MATRIX	LONG	LAT
* 1,2		8
* 1,3	X	X
* 1,4		5,6,8
* 1,5		
* 1,6		
* 1,7		
* 1,8		
2,1		8
* 2,3		
* 2,4		
* 2,5		
* 2,6		
* 2,7		
* 2,8		
3,1	X	X
3,2		
* 3,4	2	8
* 3,5		
* 3,6		
* 3,7		
* 3,8		
4,1		5,6,8
4,2		
4,3	2	8
* 4,5		
* 4,6		
* 4,7		
* 4,8		

C MATRIX	LONG	LAT
5,1		
5,2		
5,3		
5,4		
* 5,6		
* 5,7	2,3	8
* 5,8		
6,1		
6,2		
6,3		
6,4		
6,5		
* 6,7		
* 6,8		
7,1		
7,2		
7,3		
7,4		
7,5	2,3	8
7,6		
* 7,8		
8,1		
8,2		
8,3		
8,4		
8,5		
8,6		
8,7		

TABLE 6.1 EFFECT OF C MATRIX ON OBSERVER PERFORMANCE

6.2.2 OTHER FACTORS AFFECTING OBSERVER PERFORMANCE

In the above example, each of the fifty six C matrices passed the observability test (as described in sections 3.3 and 5.2.1) and thus should have provided perfect estimates. Obviously this is not the case and therefore either the observability test, the design of the observer, or some other factor, is at fault.

In order to examine the effect of different eigenvalues, two of the problem cases were selected for further investigation. These were C(1,2) which failed on lateral states only and C(1,3) which failed on both longitudinal and lateral states. Now the largest system eigenvalue is -2.17, so the smallest observer eigenvalue was varied from -2.17 to -6.51 (ie. $1\times$ to $3\times$) in steps of $0.1\times$. At each step the remaining observer eigenvalues were separated by 10% of the smallest eigenvalue. Thus the last set of the twenty one sets of eigenvalues tested was,

$$[\ -6.51,\ -7.16,\ -7.81,\ -8.46,\ -9.11,\ -9.76\ ]$$

No improvement was noted and from the correlation results it was apparent that as the eigenvalues increased in magnitude, the correlation decreased. This was because the larger eigenvalues made the observer more susceptible to noise.

The next area to be investigated was the effect of different control inputs and as a first step the test of section 6.2.1 was repeated using a $3-2-1-1$ input on θ_{1S} (Appendix six). This produced identical results, in so far as the same C matrices failed on the same states, which indicates that the *form* of input is not significant.

In order to examine the effect of noisy control inputs the four control inputs which form the doublet sequence (ie. doublet on θ_{1S} plus the simultaneous inputs on θ_{0e}, θ_{1C} and θ_{0t}) were approximated by a series of steps (*fig 6.2a*) and a series of ramps (*fig 6.2b*). The state response of the system to the noisy input was compared to that obtained using the series of ramps and, apart from small variations in the shape, there were no discernible differences.

The single case of a reduced order observer designed using C(1,2) and the same eigenvalues as previously (ie. $[\ -4,\ -3.8,\ -3.6,\ -3.4,\ -3.2,\ -3\ ]$ was used for the test. In addition to exploring the consequences of noisy inputs, the test was devised to determine whether the minor control inputs had an influence on the observer's performance. This was accomplished by stimulating the system and observer with a subset of the control vector. The combinations used for the test are shown in Table 6.2.

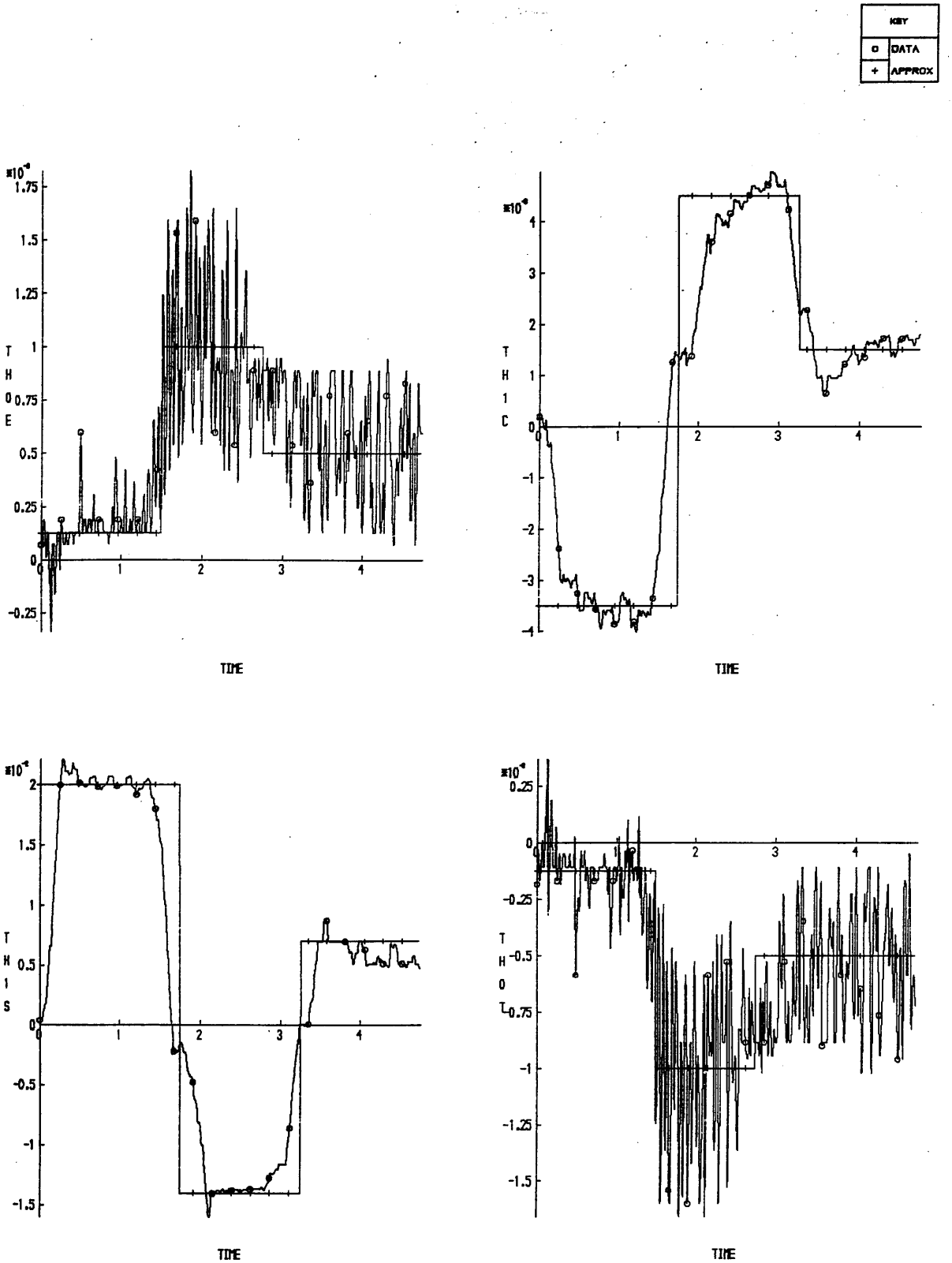

FIG 6.2A DOUBLET INPUT ON θ_{1s} APPROXIMATED BY STEPS

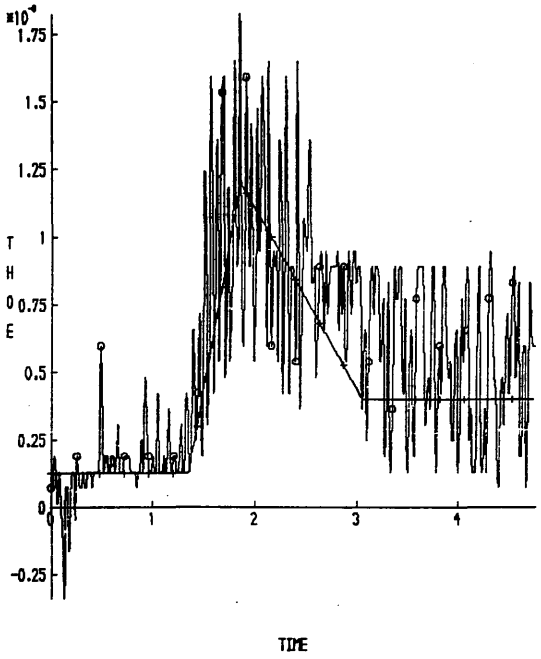

FIG 6.2B DOUBLET INPUT ON θ_{1s} APPROXIMATED BY RAMPS

θ_{0e}	θ_{1s}	θ_{1c}	θ_{0t}
X	X	X	X
	X		
X	X		
	X	X	
	X		X
X	X	X	
X	X		X
	X	X	X

TABLE 6.2

CONTROL INPUT COMBINATIONS

Each of the eight combinations were formed from each of the three forms of control vector: normal, steps or ramps, giving a total of twenty four different input vectors. Every run produced identical results to the original test: the longitudinal states were being estimated accurately whereas the lateral states were not. The test was repeated using a full order observer (the additional eigenvalue being placed at -3.5) with the same results. Thus it was concluded that neither noisy control inputs or the combination of inputs has any significant effect on observer performance.

6.3 CAN PERFORMANCE PROBLEMS BE IDENTIFIED AT THE DESIGN PHASE?

It is possible that for any given flight condition there will be several C matrices (or, in other words, combinations of sensors) which produce observers that cannot accurately follow the state of the system. It would clearly be advantageous to be able to identify and discard such cases at the observer design phase rather than having to conduct tests to eliminate them.

Since the tests of the preceding sections had failed to produce any indication of a deficient design procedure and had shown that the input was not significant, it was decided to examine the observability test. The principle of the observability test was introduced in section 3.3 and its computer implementation was discussed in section 5.2.1.

The crucial step in the determination of observability is the calculation of the rank of a matrix by NAG routine F04JDF, [N4]. The rank is determined by factorising

the real m×n (m⩽n) matrix A (nb. not the system matrix) as the *singular value decomposition* (SVD),

$$A = Q \begin{bmatrix} D & | & 0 \end{bmatrix} P^T \qquad (6.1)$$

where Q is an m×m orthogonal matrix, P is an n×n orthogonal matrix and D is the m×m diagonal matrix,

$$D = \mathrm{diag}\ (\ sv_1,\ sv_2,\ \ldots\ ,\ sv_m\ ) \qquad (6.2)$$

with

$$sv_1 \geqslant sv_2 \geqslant \ldots \geqslant sv_m \geqslant 0$$

these being the singular values of A. If the singular values $sv_{k+1},\ldots,sv_m$ are negligible, but sv_k is not negligible, relative to the data errors in A, then the rank of A is taken to be k. In practice, due to rounding and/or experimental errors, it is often difficult to decide what constitutes a negligible value and hence which singular values should be considered zero. To illustrate this consider the following two examples taken from the NAG manual.

In exact arithmetic, the rank of the (5×8) matrix

$$\begin{bmatrix} 22 & 14 & -1 & -3 & 9 & 9 & 2 & 4 \\ 10 & 7 & 13 & -2 & 8 & 1 & -6 & 5 \\ 2 & 10 & -1 & 13 & 1 & -7 & 6 & 0 \\ 3 & 0 & -11 & -2 & -2 & 5 & 5 & -2 \\ 7 & 8 & 3 & 4 & 4 & -1 & 1 & 2 \end{bmatrix}$$

is three. On a computer with seven decimal digits of precision the computed singular values would be,

$$3.5 \times 10^{1} \quad 2.0 \times 10^{1} \quad 2.0 \times 10^{1} \quad 1.3 \times 10^{-6} \quad 5.5 \times 10^{-7}$$

and the rank would be correctly taken to be three. However, the (7×7) *Hilbert matrix*, where $a_{ij} = 1/(i+j-1)$ has singular values of

$$1.7 \times 10^{0} \quad 2.7 \times 10^{-1} \quad 2.1 \times 10^{-2} \quad 1.0 \times 10^{-3}$$
$$2.9 \times 10^{-5} \quad 4.9 \times 10^{-7} \quad 3.5 \times 10^{-9}$$

and there is no clear cut–off between small and large values. In exact arithmetic the matrix is known to have full rank and none of its singular values are zero (with seven digit precision it would be taken to be singular). A further complication is that rank determination can be sensitive to the scaling of the matrix.

It is thus impossible to give a perfect rule, but in general the rank can reasonably be assumed to be the number of singular values which are neither zero nor very small compared with other singular values.

The NAG routine requires a user supplied relative tolerance (TOL) which is used to determine which singular values are insignificant. This is done by defining the rank of A (ie. k) to be the largest integer such that

$$sv_k > TOL * sv_1 \tag{6.3}$$

Alternatively, if sv_1 is the largest singular value then any singular value sv_i is taken to be zero if

$$sv_i \leqslant TOL * sv_1 \tag{6.4}$$

The recommended value for TOL is given as approximately the largest relative error in the elements of A, eg. if the elements of A are correct to four significant figures then TOL should be set to about 5×10^{-4}. The default value, which was being used, is *eps*, the machine accuracy (ie. the smallest value the computer holds such that 1+ eps= 1; on the VAX–750, eps= 0.27755576e–16).

Table 6.3 shows the singular values returned by the NAG routine for the Puma at one hundred knots, with three different C matrices: C(6,2) which produced good estimates, C(1,2) which only produced good longitudinal estimates and C(1,3) which failed on both longitudinal and lateral estimates. These values are independent of TOL – it is the choice of TOL which determines which, if any, of these singular values should be considered to be zero.

It can be seen that there are no obvious differences between the good and bad cases and that the largest decrease in magnitude, between one singular value and the next, is of the order of 10^2. If TOL was increased then at TOL = sv_{14} / sv_1

sv	C(6,2)	C(1,2)	C(1,3)
1	0.366 E+10	0.367 E+10	0.365 E+10
2	0.328 E+09	0.219 E+10	0.671 E+08
3	0.133 E+08	0.322 E+07	0.174 E+06
4	0.201 E+06	0.132 E+05	0.649 E+03
5	0.119 E+05	0.145 E+04	0.536 E+02
6	0.237 E+04	0.385 E+03	0.452 E+02
7	0.317 E+03	0.257 E+03	0.318 E+02
8	0.168 E+03	0.115 E+03	0.905 E+01
9	0.829 E+01	0.321 E+02	0.216 E+01
10	0.200 E+01	0.472 E+01	0.100 E+01
11	0.996 E+00	0.100 E+01	0.484 E+00
12	0.160 E+00	0.997 E+00	0.620 E-02
13	0.214 E-01	0.977 E-01	0.501 E-03
14	0.761 E-02	0.449 E-03	0.105 E-03
eps*sv_1	0.102 E-06	0.102 E-06	0.101 E-06

TABLE 6.3

SINGULAR VALUES

PRODUCED BY

OBSERVABILITY TEST

FOR THREE

DIFFERENT C MATRICES

C	1	2	3	4	5	6	7	8
1		+	+	+	*	*	*	*
2	+		-	-	*	*	*	*
3	+	-		+	*	-	*	*
4	+	-	+		*	*	*	*
5	*	*	*	-		-	+	-
6	*	*	-	-	-		-	*
7	*	*	*	*	+	-		*
8	*	*	*	*	-	*	*	

* Pass / Good

\- Fail / Good

\+ Fail / Bad

TOL = 0.27×10^{-12}

TABLE 6.4

OBSERVABILITY TEST RESULTS

(= 2.079×10^{-12} for C(6,2), for example), sv_{14}, the smallest singular value, would be treated as zero and the [A,C] pair would be defined as unobservable.

The value of TOL at which all the known bad cases would fail the observability test was determined to be 0.27×10^{-12}. Using this value, the observability test was run on all fifty six C matrices and the results are summarized in Table 6.4. The entry in row i and column j is the result for C(i,j). A '*' indicates that the [A,C] pair passed the observability test and that the designed observer produced acceptable estimates. Similarly a '–' or a '+' indicates that the observability test was failed, and that the estimates were good or bad, respectively.

Clearly setting TOL at a value which fails the known bad combinations has also caused several of the good cases to fail and, except for two entries, C(4,5)/C(5,4); C(4,6)/C(6,4), there is perfect symmetry about the main diagonal. Thus if these two entries are ignored, the remaining unique combinations are,

C(1,5)	C(2,5)	C(3,5)	C(4,7)	C(6,8)	C(7,8)
C(1,6)	C(2,6)	C(3,7)	C(4,6)		
C(1,7)	C(2,7)	C(3,8)			
C(1,8)	C(2,8)				

This provides sufficient redundancy for estimation purposes, but does it provide enough information for a sensor fault detection, logic scheme? This question is dealt with in chapter seven which considers the design and implementation of observer–based sensor fault detection schemes.

6.3.1 FURTHER INVESTIGATION OF THE OBSERVABILITY TEST

The observability tests in the preceding sections have all involved C matrices whose non–zero elements are unity. The effect of using values other than unity can be seen from Table 6.5. In all cases TOL = 0.27×10^{-12} and C_1 and C_2 refer to the non–zero element in rows one and two of C, respectively. A pass is indicated by a '*' and the ratio $C_1 : C_2$ is indicated.

Several effects are apparent: firstly for a given ratio $C_1 : C_2$, the results are the same, regardless of the magnitudes of C_1 and C_2. This was found to be the case with each combination of the magnitudes considered (.01, .1, 1, 10, 100, 1000) and is illustrated by the case $C_1 : C_2 = 1 : 1$. Secondly, as the ratio increases the number of passes decreases and thirdly, for given magnitudes x and y, {$C_1 = x$,

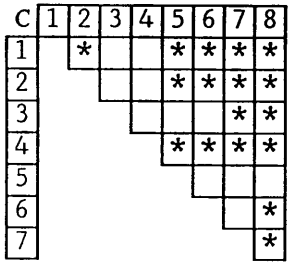

$C_1 = 0.01$
$C_2 = 0.01$
Ratio = 1:1

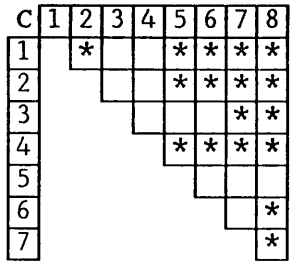

$C_1 = 0.1$
$C_2 = 0.1$
Ratio = 1:1

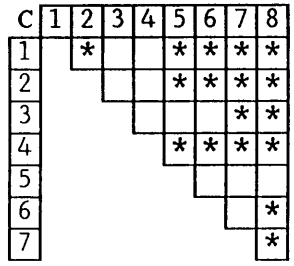

$C_1 = 1$
$C_2 = 1$
Ratio = 1:1

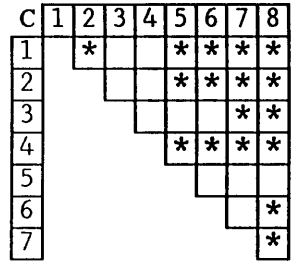

$C_1 = 10$
$C_2 = 10$
Ratio = 1:1

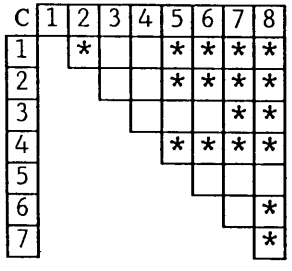

$C_1 = 100$
$C_2 = 100$
Ratio = 1:1

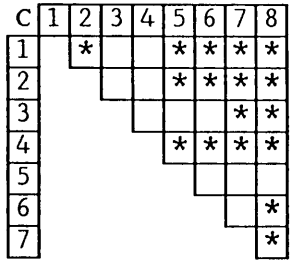

$C_1 = 1000$
$C_2 = 1000$
Ratio = 1:1

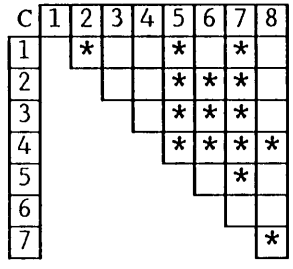

$C_1 = 10$
$C_2 = 1$
Ratio = 10:1

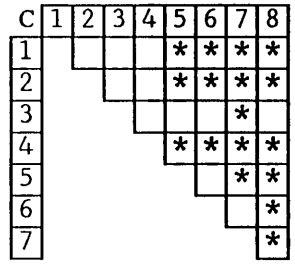

$C_1 = 1$
$C_2 = 10$
Ratio = 1:10

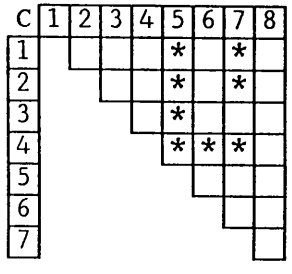

$C_1 = 100$
$C_2 = 1$
Ratio = 100:1

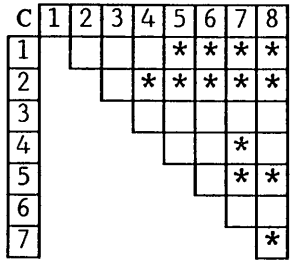

$C_1 = 1$
$C_2 = 100$
Ratio = 1:100

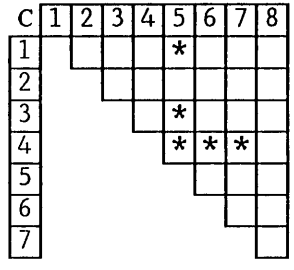

$C_1 = 1000$
$C_2 = 1$
Ratio = 1000:1

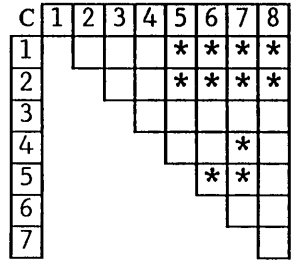

$C_1 = 1$
$C_2 = 1000$
Ratio = 1:1000

TABLE 6.5

EFFECT OF VARYING THE MAGNITUDE OF C MATRIX ELEMENTS

$C_2 = y\}$ gives different results than for $\{C_1 = y,\ C_2 = x\}$. Thus the initial arbitrary choice of unity, non–zero elements was extremely fortunate.

It is evident that there are numerical problems involved with this form of observability test and the fundamental reasons for this can be explained as follows (this analysis follows from Chen, 1984, who develops a similar argument for the controllability test, which as indicated in section 3.3, is dual to the observability test).

The computation of the (np×n) observability matrix (section 3.3)

$$V_2 = [\ C \quad CA \quad CA^2 \ . \ . \ . \ CA^{n-1}\ ]^T \tag{6.5}$$

is a relatively simple task. As discussed in section 5.2.1 there can be at most n linearly independent vectors (rows) in V_2 and therefore the complete matrix may not have to be evaluated. Furthermore, in order to minimize the powers of A involved, V_2 is examined row by row in the sequence,

$$C_1,\ C_2,\ \ldots\ ,C_p,\ C_1A,\ C_2A,\ \ldots\ ,C_pA,\ C_1A^2,\ \ldots\ ,C_pA^{n-1} \tag{6.6}$$

As each row is added the linear independence of the rows is determined by calculating the rank of the composite matrix using NAG routine F04JDF, [N4], which is a numerically stable method. However, if the dimension n of the equation is large, CA^j must be evaluated for large j, and in general this tends to transform the problem into a less well conditioned one.

A quantitative explanation for this can be determined by considering the *condition numbers* of matrices A^j, where the condition number of a matrix A is defined as,

$$\text{Cond}(A) \triangleq \frac{sv_1}{sv_s} \tag{6.7}$$

sv_1 and sv_s are the largest and smallest singular values and it can be shown that they are related to the eigenvalues by,

$$sv_s \leqslant |\lambda_n| < |\lambda_1| \leqslant sv_1 \tag{6.8}$$

Therefore, if $|\lambda_n| \gg |\lambda_1|$, Cond(A) is a very large number and in terms of computer computation, the multiplication of a matrix with a large condition number will introduce large computational errors and should thus be avoided if possible. Looking back to Table 6.3 the condition numbers of the composite matrix are

4.81×10^{11} for C(6,2); 8.17×10^{12} for C(1,2) and 3.48×10^{13} for C(1,3). It is interesting to note that the performance of these three observers was good, bad and very bad, respectively: ie. performance decreased as condition number increased.

To illustrate the rapid increase in Cond(A^j) as j increases, consider Table 6.6 which gives λ_1, λ_n and λ_1/λ_n ($\leq$Cond(A), from equation 6.8) for A^j, where $j=1\rightarrow6$. If the eigenvalues of A are $\{ \lambda_1, \lambda_2, .., \lambda_n \}$ then the eigenvalues of A^j are $\{ (\lambda_1)^j, (\lambda_2)^j, .., (\lambda_n)^j \}$. From the sequence of 6.6, and with n=14 and p=2, it is clear that the smallest power of A would be at least A^6 since rows thirteen and fourteen would be C_1A^6 and C_2A^6, respectively.

A^j	λ_n	λ_1	λ_1/λ_n
A	1.44 E-02	5.26 E+01	3.65 E+03
A^2	2.07 E-04	2.76 E+03	1.33 E+07
A^3	2.99 E-06	1.45 E+05	4.85 E+10
A^4	4.30 E-08	7.64 E+06	1.78 E+14
A^5	6.19 E-10	4.02 E+08	6.49 E+17
A^6	8.92 E-12	2.11 E+10	2.37 E+21

TABLE 6.6

EIGENVALUES OF A^j

6.4 OBSERVABILITY TEST AND OBSERVER PERFORMANCE AT DIFFERENT FLIGHT CONDITIONS

So far only the one flight condition has been considered: the Puma at one hundred knots level flight, and from the preceding sections it is apparent that there are problems with both the observability test and the performance of some of the designed observers. In order to determine whether these problems occur at other flight conditions a further eleven flight conditions of the Puma were examined.

These were 40, 60, 80, 120, 140 and 160 knots and 40 knots with descent angles of $-3°$, $-6°$, $-9°$, $-12°$ and $-15°$. The A and B matrices and the system eigenvalues are shown in Appendix five. For each flight condition the twenty eight C matrices were tested for observability (with $TOL=0.27\times10^{-12}$) and then used to design reduced and full order observers. The reduced order observers consisted of two subobservers with eigenvalues of [−4, −3.8, −3.6, −3.4, −3.2, −3] and the full order observers had the additional eigenvalue at −3.5. The performance of each was then evaluated for a doublet input on θ_{1S} (Appendix six). The results of the observability tests are shown in Table 6.7 (with respect to the reduced order results)

TABLE 6.7

OBSERVABILITY TEST

RESULTS

40 KNOTS

C	1	2	3	4	5	6	7	8
1		o	+	+	*	*	*	-
2			o	o	*	*	*	*
3				+	*	-	*	*
4					*	-	+	-
5						+	*	*
6							-	-
7								*

60 KNOTS

C	1	2	3	4	5	6	7	8
1		*	+	+	*	*	*	*
2			-	-	*	*	*	*
3				+	*	-	-	*
4					*	*	*	*
5						-	*	-
6							-	-
7								*

80 KNOTS

C	1	2	3	4	5	6	7	8
1		*	+	+	*	*	*	*
2			-	-	*	*	*	*
3				+	*	-	-	*
4					*	*	*	*
5						-	-	-
6							-	*
7								*

120 KNOTS

C	1	2	3	4	5	6	7	8
1		*	+	+	*	*	*	*
2			-	-	*	*	*	*
3				+	-	-	*	*
4					*	*	*	*
5						-	+	-
6							-	*
7								*

140 KNOTS

C	1	2	3	4	5	6	7	8
1		*	+	+	*	*	*	-
2			-	-	*	*	*	-
3				-	-	-	*	-
4					*	*	*	-
5						-	-	-
6							-	*
7								*

160 KNOTS

C	1	2	3	4	5	6	7	8
1		*	+	-	*	*	*	-
2			-	-	*	*	*	*
3				-	-	-	*	*
4					*	*	*	*
5						-	*	-
6							+	*
7								*

40 KNOTS -3°

C	1	2	3	4	5	6	7	8
1		*	+	+	*	-	+	-
2			o	*	*	*	*	*
3				+	*	-	*	-
4					*	-	*	*
5						+	*	*
6							-	-
7								*

40 KNOTS -6°

C	1	2	3	4	5	6	7	8
1		*	+	+	*	-	*	-
2			o	*	o	*	*	*
3				-	*	-	*	*
4					*	-	*	*
5						-	*	*
6							-	-
7								*

40 KNOTS -9°

C	1	2	3	4	5	6	7	8
1		*	+	+	*	-	*	+
2			-	*	*	*	*	*
3				-	*	-	*	*
4					*	+	*	o
5						+	*	*
6							-	-
7								*

40 KNOTS -12°

C	1	2	3	4	5	6	7	8
1		*	+	+	*	*	*	*
2			o	-	*	*	*	*
3				+	-	-	*	*
4					*	-	*	*
5						+	*	*
6							-	-
7								*

40 KNOTS -15°

C	1	2	3	4	5	6	7	8
1		*	+	+	-	*	*	*
2			o	-	*	*	*	*
3				-	-	-	*	*
4					-	*	*	*
5						+	*	-
6							-	-
7								*

*** Pass / Good**

- Fail / Good

+ Fail / Bad

o Pass / Bad

Comparison is with the performance of the reduced order observer. Results for 100 knots are in Table 6.4

	40	60	80	100	120	140	160	40 -3°	40 -6°	40 -9°	40 -12°	40 -15°
1,2	X O	O	O	X O	O			O	O	O	O	O
1,3	X O	X O	X O	X O	X O	X O	X O	X O	X O	X O	X O	X O
1,4	X O	X O	X O	X O	X O	X O	O	X O	X O	X O	X O	X O
1,5												
1,6												
1,7								X O				
1,8										X O		
2,3	X O							X O	X		X	O
2,4	X O	O				O		O	O	O	O	O
2,5									X O			
2,6												
2,7												
2,8												
3,4	X O	X O	X O	X O	X O			X O	O	O	X O	O
3,5												
3,6												
3,7												
3,8												
4,5												
4,6										X O		
4,7	X O											
4,8							O			X O		
5,6	X							X		X	X	X
5,7				X	X							
5,8												
6,7			O			O	X O					
6,8												
7,8												

TABLE 6.8 OBSERVER PERFORMANCE O - FULL ORDER, X - REDUCED ORDER

and the performance of the observers are summarized in Table 6.8.

It is clear that the problems with the observability test and observer performance are discernible at each flight condition, the main difficulty being the inability to identify which C matrices produce unacceptable estimates. The question remains as to whether the problem is with the observability test, the design of the observer, or both.

Considering the observer design procedure it is feasible that a particular [A,C] pair could be 'just' observable (ie. a small percentage change to one (or more) elements in either matrix would make the pair unobservable) and that the small numerical errors introduced by the design procedure and the simulation of the system/observer, were sufficient to produce an effectively unstable observer. (Note that it is not possible to design an observer to estimate the full state of an unobservable system since the design procedure requires n linearly independent vectors (section 5.2.1)). Similarly, particular combinations, although observable, may produce observers which are very sensitive to the numerical errors inherent in the computer simulation of the system.

With the observability test, the inability to categorically determine which singular values are zero (section 6.3.1) means that the results obtained by this particular method will always be suspect.

Comparing the full order results with those for reduced order it can be seen that except for at forty and one hundred knots, the performance of the reduced order observer was the same or superior to that of the full order observer, though the differences are slight. For example, the greatest difference is at 40 knots $-15°$, where there are three fails with the reduced order observer and six fails with the full order observer. The reason for the generally better performance by the reduced order observer is the reduction in computation and magnitude of numbers involved. Also, in its computer implementation the reduced order observer requires fewer integrators.

However, in terms of noise rejection it is the full order observer which should theoretically give superior performance. This can be explained by reference to *fig 3.3* (full order) and *fig 3.5* (reduced order). In the case of the reduced order observer q_2 (a partition of $\underline{y}$) is fed through the constant gain matrix H to the output of the estimator. Hence if q is corrupted by noise, the noise will appear in the output of the observer. In the full order observer $\underline{y}$ is integrated (or filtered) and thus high frequency noise in $\underline{y}$ will be suppressed.

6.5 THREE INSTRUMENTS PER OBSERVER

In an effort to determine the effect of using three instruments per observer (ie. p= 3), and in particular to ascertain whether the problems encountered with certain C matrices could be rectified by the use of more than two instruments, the following two tests were conducted.

The first test looked specifically at the C matrix C(1,3) which, as can be seen from Table 6.8, gave a fail for each of the flight conditions examined. One flight condition was considered: 40 knots $-15°$, and the designed reduced order observers consisted of three subobservers with eigenvalues at [-4, -3.6, -3.3, -3] and [-4, -3.5, -3] (ie. $n-p = 11$; $n_1 = n_2 = 4$, $n_3 = 3$). Thirty six observers (one for each of the combinations of instruments 1, 3 and j) were evaluated for the doublet input on θ_{1S} and the results are shown in Table 6.9. A '*' indicates a pass.

It can be seen that the addition of a third instrument made an improvement in twenty four cases: fourteen of which pass on both longitudinal and lateral states. Note that the cases (1,3,j) and (3,1,j) produced no improvement or less improvement than the other four permutations. A possible explanation for this can be found by considering the sequence in which n linearly independent rows of V_2 are selected (Equation 6.6).

If the first fourteen vectors of the sequence are linearly independent then vectors thirteen and fourteen will be C_1A^5 and C_2A^5. In the above two cases these will therefore be $C(1)A^5$ and $C(3)A^5$, whereas the other four permutations will only involve $C(1)A^5$ *or* $C(3)A^5$. However, the reason(s) why this produces differences in performance is unclear. From earlier work it would be reasonable to suggest that any improvement in performance must be due, at least in part, to the reduction in order of the canonical blocks, ie. 4,4,3 instead of 6,6.

The second test considered every possible combination of three instruments, rather than just those involving one and three. This gave a total of 336 permutations $-$ 56 combinations of 3$-$out$-$of$-$8: each of which can be ordered in six different ways. The flight condition examined was the Puma at one hundred knots, with the same control input and observer eigenvalues as in the first test. Results are tabulated in Table 6.10, the passes being underlined.

It is apparent that for any given pair of instruments the effect of adding a third is unpredictable. The first experiment showed that one particular bad combination *may* be improved by a third instrument and this can be seen to be generally true from

the results of the second test, eg. compare the results of C(5,7) with those of Table 6.8. Unfortunately the contrary is also true: good pairs may fail when a third instrument is added. For example, consider C(1,5): when C(3) is added two permutations fail and when C(2) is added four permutations fail.

The explanation for this is relatively simple – adding a third instrument can result in a previously determined bad combination, eg. if C(3) is added to C(1,5) then two of the permutations are C(1,3,5) and C(3,1,5) which, as demonstrated by test one, will produce bad results. Thus it would appear that there is no major advantage to be gained by using three instruments per observer and therefore this line of investigation was not pursued any further.

C MATRIX	LON	LAT
1,3,2		
1,3,4		
1,3,5		
1,3,6		
1,3,7		
1,3,8		
1,2,3	*	
1,4,3	*	
1,5,3	*	*
1,6,3	*	*
1,7,3	*	*
1,8,3	*	
3,1,2		
3,1,4		
3,1,5		
3,1,6		
3,1,7		
3,1,8		

C MATRIX	LON	LAT
2,1,3	*	
4,1,3	*	
5,1,3	*	*
6,1,3	*	*
7,1,3	*	*
8,1,3	*	
3,2,1	*	
3,4,1	*	
3,5,1	*	*
3,6,1	*	*
3,7,1	*	*
3,8,1	*	*
2,3,1	*	
4,3,1	*	
5,3,1	*	*
6,3,1	*	*
7,3,1	*	*
8,3,1	*	*

* = PASS

TABLE 6.9 THREE INSTRUMENTS (INCLUDING 1 AND 3) PER OBSERVER

1,2,3	1,3,2	2,1,3	2,3,1	3,1,2	3,2,1
1,2,4	1,4,2	2,1,4	2,4,1	4,1,2	4,2,1
1,2,5	1,5,2	2,1,5	2,5,1	5,1,2	5,2,1
1,2,6	1,6,2	2,1,6	2,6,1	6,1,2	6,2,1
1,2,7	1,7,2	2,1,7	2,7,1	7,1,2	7,2,1
1,2,8	1,8,2	2,1,8	2,8,1	8,1,2	8,2,1
1,3,4	1,4,3	3,1,4	3,4,1	4,1,3	4,3,1
1,3,5	1,5,3	3,1,5	3,5,1	5,1,3	5,3,1
1,3,6	1,6,3	3,1,6	3,6,1	6,1,3	6,3,1
1,3,7	1,7,3	3,1,7	3,7,1	7,1,3	7,3,1
1,3,8	1,8,3	3,1,8	3,8,1	8,1,3	8,3,1
1,4,5	1,5,4	4,1,5	4,5,1	5,1,4	5,4,1
1,4,6	1,6,4	4,1,6	4,6,1	6,1,4	6,4,1
1,4,7	1,7,4	4,1,7	4,7,1	7,1,4	7,4,1
1,4,8	1,8,4	4,1,8	4,8,1	8,1,4	8,4,1
1,5,6	1,6,5	5,1,6	5,6,1	6,1,5	6,5,1
1,5,7	1,7,5	5,1,7	5,7,1	7,1,5	7,5,1
1,5,8	1,8,5	5,1,8	5,8,1	8,1,5	8,5,1
1,6,7	1,7,6	6,1,7	6,7,1	7,1,6	7,6,1
1,6,8	1,8,6	6,1,8	6,8,1	8,1,6	8,6,1
1,7,8	1,8,7	7,1,8	7,8,1	8,1,7	8,7,1
2,3,4	2,4,3	3,2,4	3,4,2	4,2,3	4,3,2
2,3,5	2,5,3	3,2,5	3,5,2	5,2,3	5,3,2
2,3,6	2,6,3	3,2,6	3,6,2	6,2,3	6,3,2
2,3,7	2,7,3	3,2,7	3,7,2	7,2,3	7,3,2
2,3,8	2,8,3	3,2,8	3,8,2	8,2,3	8,3,2
2,4,5	2,5,4	4,2,5	4,5,2	5,2,4	5,4,2
2,4,6	2,6,4	4,2,6	4,6,2	6,2,4	6,4,2
2,4,7	2,7,4	4,2,7	4,7,2	7,2,4	7,4,2
2,4,8	2,8,4	4,2,8	4,8,2	8,2,4	8,4,2
2,5,6	2,6,5	5,2,6	5,6,2	6,2,5	6,5,2
2,5,7	2,7,5	5,2,7	5,7,2	7,2,5	7,5,2
2,5,8	2,8,5	5,2,8	5,8,2	8,2,5	8,5,2
2,6,7	2,7,6	6,2,7	6,7,2	7,2,6	7,6,2
2,6,8	2,8,6	6,2,8	6,8,2	8,2,6	8,6,2
2,7,8	2,8,7	7,2,8	7,8,2	8,2,7	8,7,2
3,4,5	3,5,4	4,3,5	4,5,3	5,3,4	5,4,3
3,4,6	3,6,4	4,3,6	4,6,3	6,3,4	6,4,3
3,4,7	3,7,4	4,3,7	4,7,3	7,3,4	7,4,3
3,4,8	3,8,4	4,3,8	4,8,3	8,3,4	8,4,3
3,5,6	3,6,5	5,3,6	5,6,3	6,3,5	6,5,3
3,5,7	3,7,5	5,3,7	5,7,3	7,3,5	7,5,3
3,5,8	3,8,5	5,3,8	5,8,3	8,3,5	8,5,3
3,6,7	3,7,6	6,3,7	6,7,3	7,3,6	7,6,3
3,6,8	3,8,6	6,3,8	6,8,3	8,3,6	8,6,3
3,7,8	3,8,7	7,3,8	7,8,3	8,3,7	8,7,3
4,5,6	4,6,5	5,4,6	5,6,4	6,4,5	6,5,4
4,5,7	4,7,5	5,4,7	5,7,4	7,4,5	7,5,4
4,5,8	4,8,5	5,4,8	5,8,4	8,4,5	8,5,4
4,6,7	4,7,6	6,4,7	6,7,4	7,4,6	7,6,4
4,6,8	4,8,6	6,4,8	6,8,4	8,4,6	8,6,4
4,7,8	4,8,7	7,4,8	7,8,4	8,4,7	8,7,4
5,6,7	5,7,6	6,5,7	6,7,5	7,5,6	7,6,5
5,6,8	5,8,6	6,5,8	6,8,5	8,5,6	8,6,5
5,7,8	5,8,7	7,5,8	7,8,5	8,5,7	8,7,5
6,7,8	6,8,7	7,6,8	7,8,6	8,6,7	8,7,6

TABLE 6.10 THREE INSTRUMENTS PER OBSERVER - EVERY PERMUTATION

6.6 OBSERVER PERFORMANCE WITH AN 8th ORDER MODEL

From the previous sections it is evident that there are many problems involved in designing a fourteenth order observer which has the desired eigenvalues and performance. It was shown that even although an observer had the required eigenvalues and that the [A,C] pair used to construct the observer had passed the observability test, there was no guarantee that the observer estimate would be of the required degree of fidelity.

It was also noted that the rotor states are not presently measured or necessary for control purposes and therefore do not require to be estimated. Thus the next step was to consider the eighth order model: do the same design and performance problems arise and is the model sufficiently accurate to produce a faithful estimate of the state?

The assumptions used to derive the eighth order model were established in section 2.6.1: the main premiss being that quasi–steady flapping and coning are used in the derivation of the reaction forces and moments on the fuselage. Consequently interaction of disc tilt modes with fuselage modes is neglected and β_0, β_{1S} and β_{1C} are determined solely through algebraic relationships. To illustrate the differences between the fourteenth and eighth order models consider *fig 6.3* which shows the response of eighth and fourteenth order models to the doublet input on θ_{1S} (Appendix six), at two different flight conditions.

The longitudinal responses are very similar: only minor differences between them, but there are significant differences in p and φ at 40 knots, $-3°$. However, the fourteenth order model contains many approximations and is therefore not accurate over the whole flight envelope (see chapter 2) and it is thus unwise to use it as a reference against which the eighth order model is judged. Both models should only be assessed against flight data.

6.6.1 RESULTS

Twelve flight conditions were considered: 20, 40, 60, 80, 100, 120 and 140 knots and 40 knots with descent angles of $-3°$, $-6°$, $-9°$, $-12°$ and $-15°$. A and B matrices and system eigenvalues are given in Appendix five. For each flight condition eight reduced order and eight full order observers were designed. Since p= 2 the reduced order observers consisted of two subobservers, each of which were assigned eigenvalues of [−4, −3.5, −3]. The full order observers had eigenvalues of

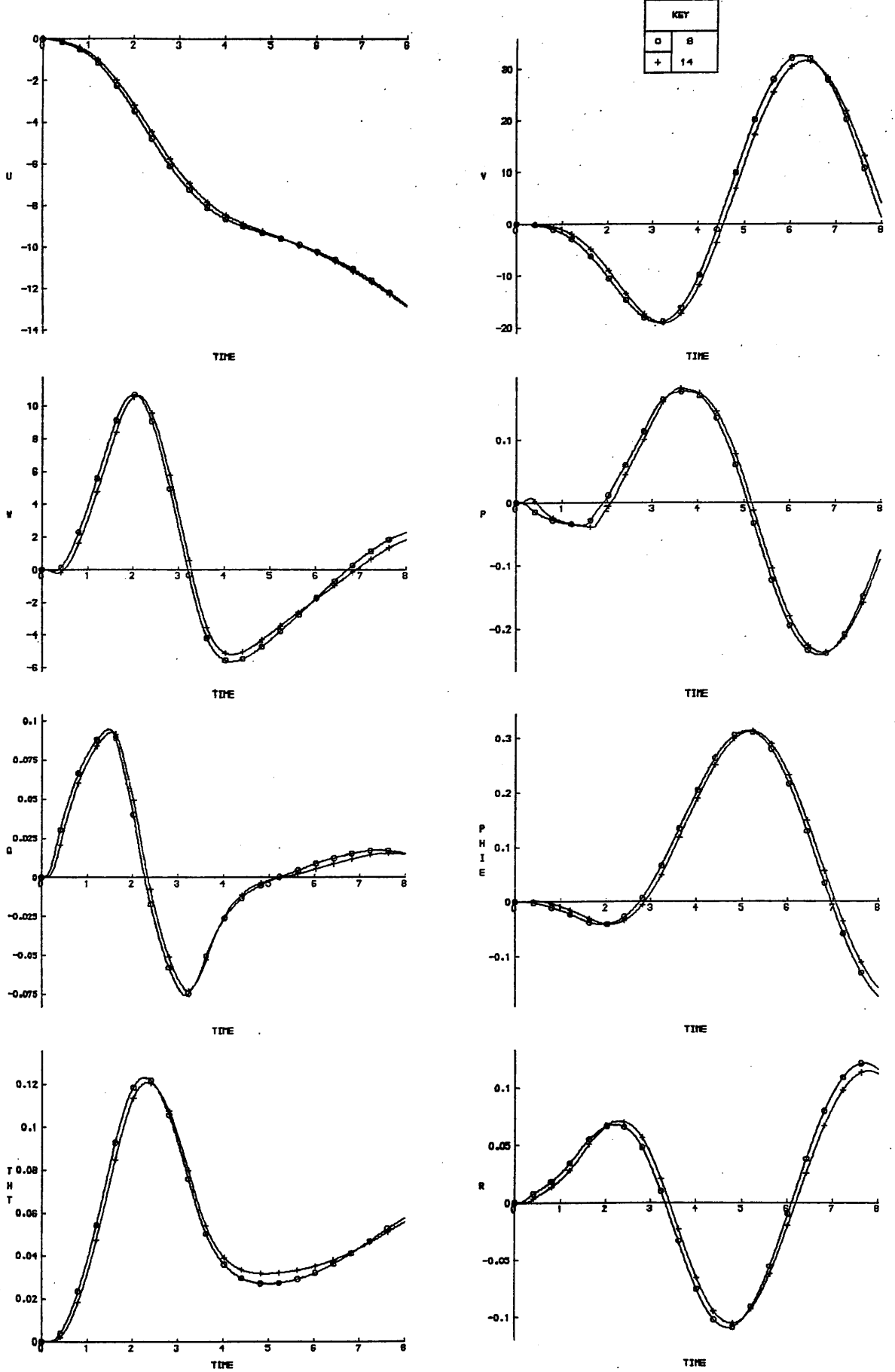

FIG 6.3A COMPARISON OF 8th AND 14th ORDER MODELS AT 100 KNOTS

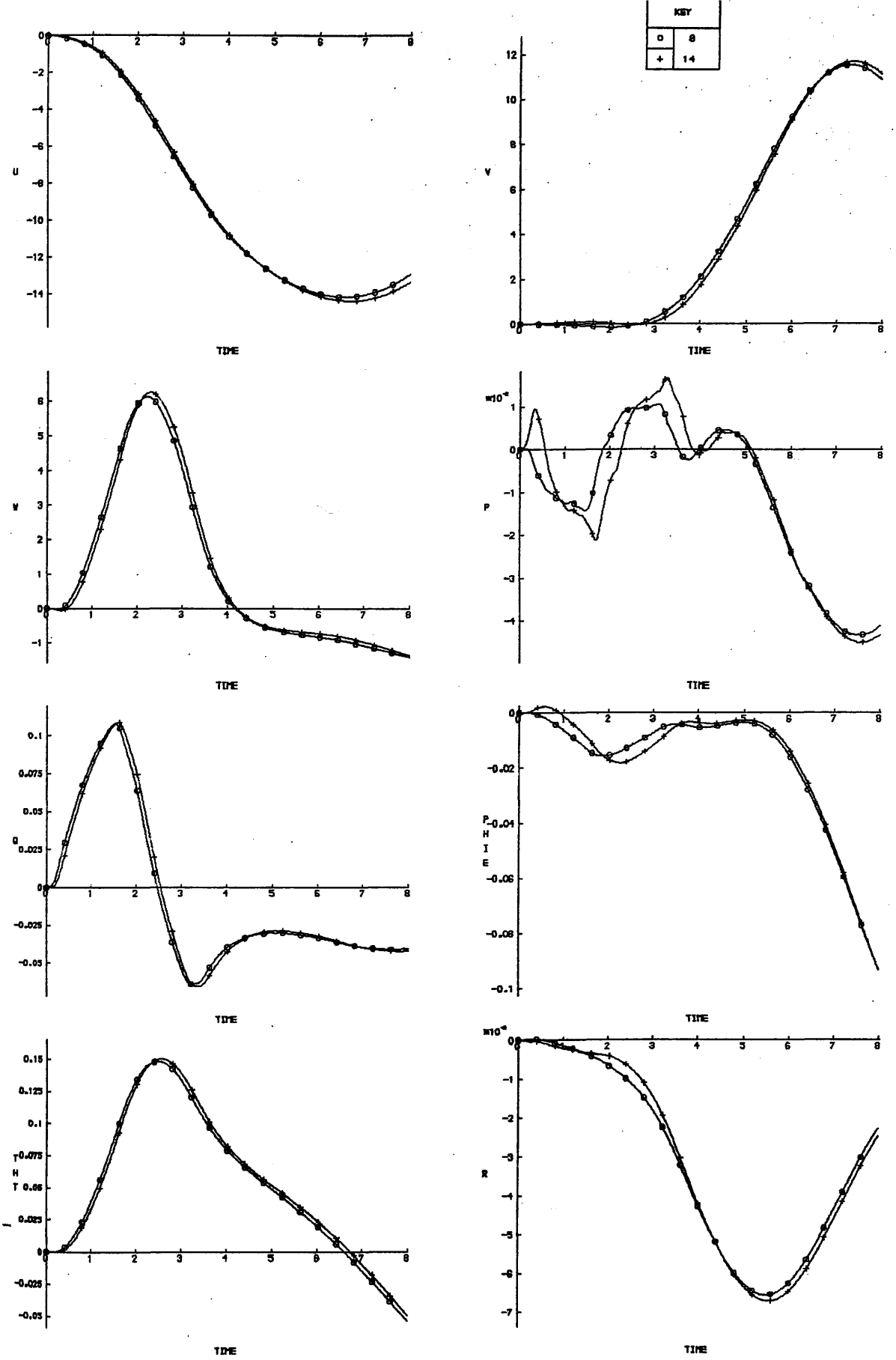

FIG 6.3B COMPARISON OF 8th AND 14th ORDER MODELS AT 40 KNOTS -3°

[−4, −3.6, −3.3, −3] for each of the two canonical blocks. The largest system eigenvalue at any of the flight conditions was −2.35. A doublet on θ_{1S} (Appendix six) was used as the control input. The results, in terms of the fails, are shown in Table 6.11.

	20	40	60	140	40 -9	40 -15
1,3	X O					
1,4		X	X O			
1,6					X O	
1,8					O	
2,4				X O		
3,4		X O				
4,6						X O
4,7		O				
5,8	X					

TABLE 6.11

FAILS WITH TWO

INSTRUMENTS PER OBSERVER

O - FULL ORDER

X - REDUCED ORDER

Comparing these results with those for the fourteenth order model (Table 6.8) it is obvious that the eighth order model gives superior results. For example, there are only eight reduced order fails with the eighth order model against fifty one with the fourteenth order model. This allows a greater degree of freedom in designing a logic scheme for sensor fault detection. The reduction in fails can be accounted for by the decrease in observer order: fourteen to eight for the full order case and six to three for the reduced order. Note that the order of the reduced order observer has decreased by 50%, whereas the figure for the full order observer is only 43%.

Having determined that good results could be obtained by using eighth order, two instrument observers, the next stage was to determine the maximum size of eigenvalues which could be used. In order to gauge the range over which fails started to occur the initial test covered four flight conditions in detail: 100 and 120 knots, and 40 knots with descent angles of −9° and −12°.

At each flight condition the eigenvalues were based on a percentage of the largest system eigenvalue: the smallest observer eigenvalue was increased from 0% to 200% in 10% steps, whilst at each step the remaining eigenvalues were in steps of 2% of this smallest eigenvalue, eg. if the largest system eigenvalue was −2, then at 100%

the full order observer eigenvalues would be [−4.0, −4.08, −4.16,..., −4.56]. The fails, and the percentage eigenvalues at which they failed, are shown in Table 6.12. All other C matrices passed with each set of eigenvalues. It would appear that a fail will occur almost immediately (eg. C(4,6), 40 knots, −12°) or in the range 150% to 200%. Those which still pass at 200% will fail at some greater value, but this was not investigated because eigenvalues greater than 200% were not considered necessary.

	100	120	40 -9	40 -12
1,2	150		170	
1,3	150			
1,4	160		150	
1,6			0	190
1,8			10	
2,4	200	200	190	150
4,6			150	10
6,7	120	130		

TABLE 6.12

% EIGENVALUES AT WHICH FAILS OCCUR

To illustrate the difference in error responses between eigenvalues of 100% and 200%, consider *fig 6.4* which demonstrates this for the 100 knots flight condition with C(1,7) and a scale factor fault of 0.8 on instrument seven from 0.5 to 1.5 seconds. Naturally the larger eigenvalues result in greatly increased overshoots and a faster return to zero error, but the smaller eigenvalues have the advantage of smaller overshoots which means that the error is less until approximately the last 25% of the respective responses. At this point the error is negligible. For these reasons it was decided to subsequently consider observer eigenvalues of approximately 100%: ie. two times faster than those of the system being observed.

The full set of twelve flight conditions were then tested with eigenvalues of 90%, 100% and 110%. Eigenvalues at ±10% of 100% were considered because from the previous experiment it was noted that occasionally a pass at x% failed at (x±10%). The C matrix was considered to fail if any of the three failed. Fails are shown in Table 6.13. Thus, even over this broad range of flight conditions, there is sufficient freedom of choice to allow the design of a state estimator / instrument fault detection scheme.

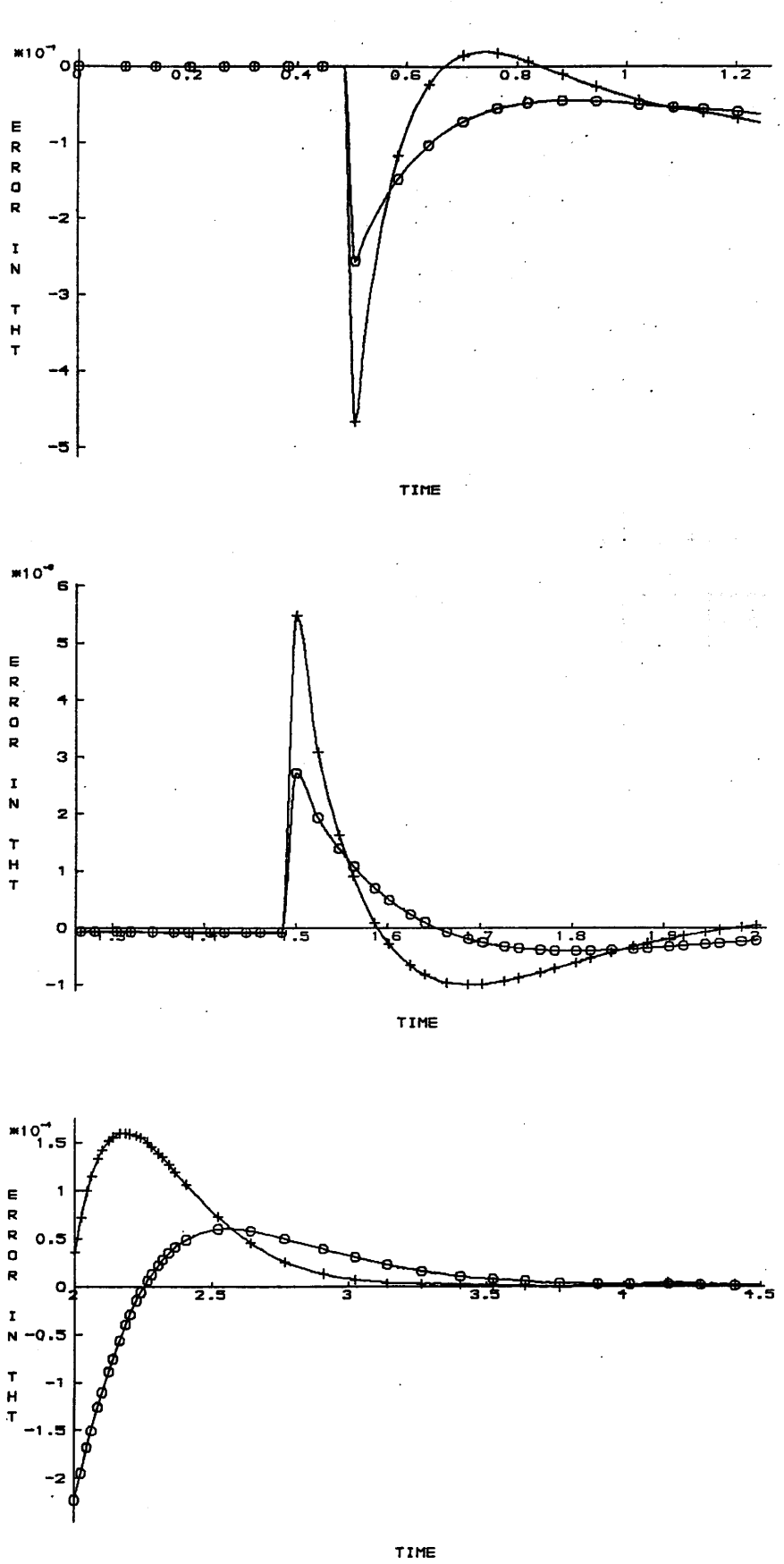

FIG 6.4 COMPARISON OF RESPONSE BETWEEN EIGENVALUES OF 100% AND 200%

	20	40	60	80	140	40 -3	40 -6	40 -9°	40 -12	40 -15
1,2		X		X		X				
1,3	X			X						
1,4		X	X			X	X			
1,6						X	X	X		
1,8								X		
2,4					X					X
3,4		X								
4,6		X							X	
5,8	X									
6,7					X					

TABLE 6.13 FAILS WITH EIGENVALUES OF 100%

6.7 VARIATION OF OBSERVER PARAMETERS WITH C MATRIX AND FLIGHT CONDITION

It has been demonstrated that by using two instruments per observer and eigenvalues twice as fast as those of the system, it is possible to determine an adequate number of observers to accurately estimate the system. However, with either the eighth or fourteenth order models the observability test was not able to accurately predict which observers do not meet the required performance criteria. In an effort to determine the reasons why some observers (ie. combinations of instruments perform so badly, it was decided to look at whether there was a correlation between the variation in observer parameters and the C matrices which failed).

The flight conditions examined were 80, 90, 100, 110 and 120 knots, and 100 knots with descent angles of $-9°$, $-6°$, $-3°$, $+3°$, $+6°$ and $+9°$. A and B matrices and system eigenvalues are given in Appendix five. An eighth order model was used and both reduced order and full order observers were considered. With the full order observer the H matrix is of dimension (8×2), but as shown in section 3.9, the reduced order observer consists of two reduced order subobservers, with equation (3.74),

$$\dot{\underset{\sim}{z}} = [A_{11}-HA_{21}]\underset{\sim}{z} + [A_{12}-HA_{22} + (A_{11}-HA_{21})H]q_2 + [B_1-HB_2]\underset{\sim}{u} + [\underset{\sim}{d}_1 - Hd_2] \quad (6.9)$$

which, to simplify, can be written as

$$\dot{z} = T_1\underset{\sim}{z} + T_2q_2 + T_3\underset{\sim}{u} + A_{ij} \quad (6.10)$$

The H matrix and T_1 are constant due to the partitioned form of $\tilde{A}$ (ie. in observable canonical form), but the remaining three terms are variable. Eigenvalues for the full order observer were [−3.5, −3.45, −3.4, −3.35, −3.3, −3.25, −3.2, −3.15] whilst the reduced order subobservers each had eigenvalues of [−3.4, −3.35, −3.3]. The control input was a doublet on θ_{1S} (Appendix six).

At each flight condition twenty eight reduced order and twenty eight full order observers were designed. The elements of each H matrix (for the full order observer) and matrices T_2, T_3 and A_{ij} (for the reduced order observer) were stored in data files for comparison and the performance of each observer was ascertained in order to determine which C matrices failed. To facilitate the evaluation of the elements of the matrices, they are visually presented in an isometric form: the base axes are flight condition and C matrix and the vertical axis is the value of the element.

First consider *fig 6.5 (a)* to *(d)*, which are the results for four of the elements of the full order H matrix in the range 80 to 120 knots. The performance results indicated that the only fail was with C(6,7) at 80 knots and looking at *fig 6.5 (a)* and *(b)* this corresponds to a very large peak. In *fig 6.5 (c)*, C(1,3) is highlighted (which didn't fail) although to a much lesser extent than C(6,7) in (a) and (b). However, if the performance results are examined more closely a correlation can be seen. For example, the correlation figures for state φ are,

80	.99949
90	.99809
100	.99641
110	.99828
120	.99776

Thus as the peak increases, the correlation decreases. Finally study *fig 6.5(d)* where the elements show a fair amount of variation with no apparent correlation to the performance results. In fact this was the case with the majority of the elements. However, for each case examined there were three elements which always indicated

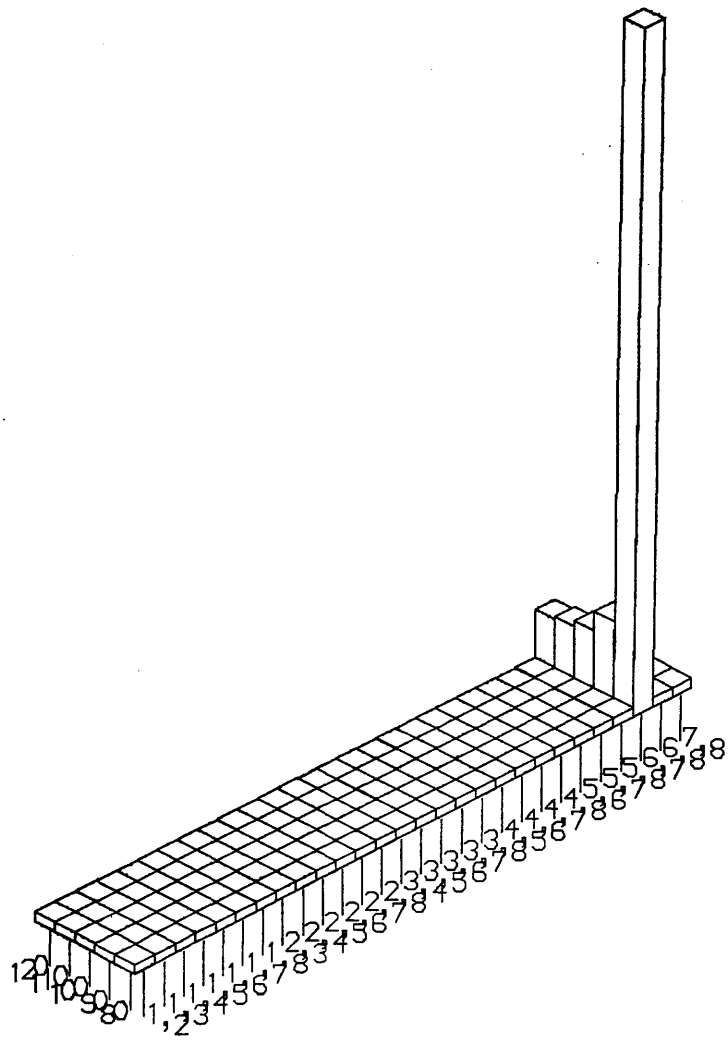

FIG 6.5A COMPARISON OF MAGNITUDE OF ELEMENT H(1,1) AS FLIGHT CONDITION AND C MATRIX VARY

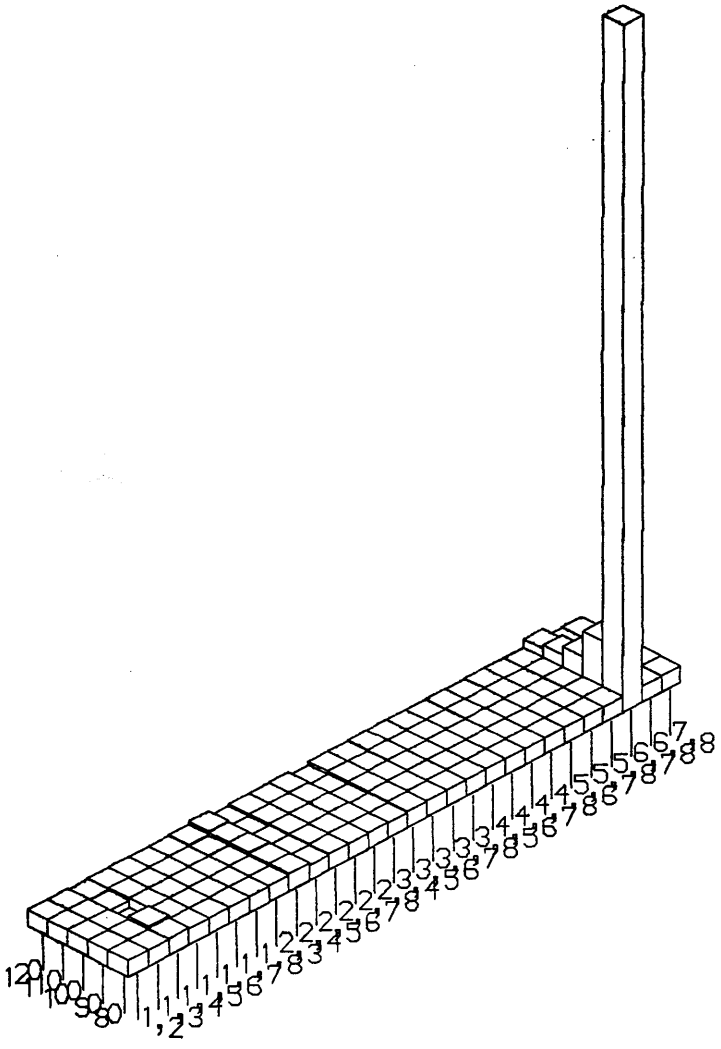

FIG 6.5B COMPARISON OF MAGNITUDE OF ELEMENT H(3,1) AS FLIGHT CONDITION AND C MATRIX VARY

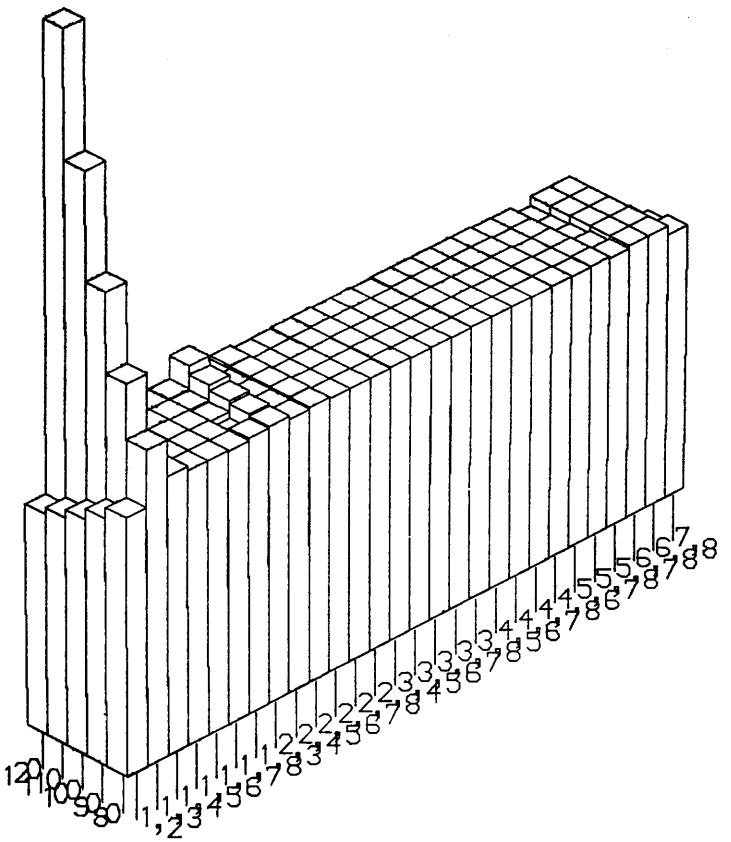

FIG 6.5C COMPARISON OF MAGNITUDE OF ELEMENT H(2,2) AS FLIGHT CONDITION AND C MATRIX VARY

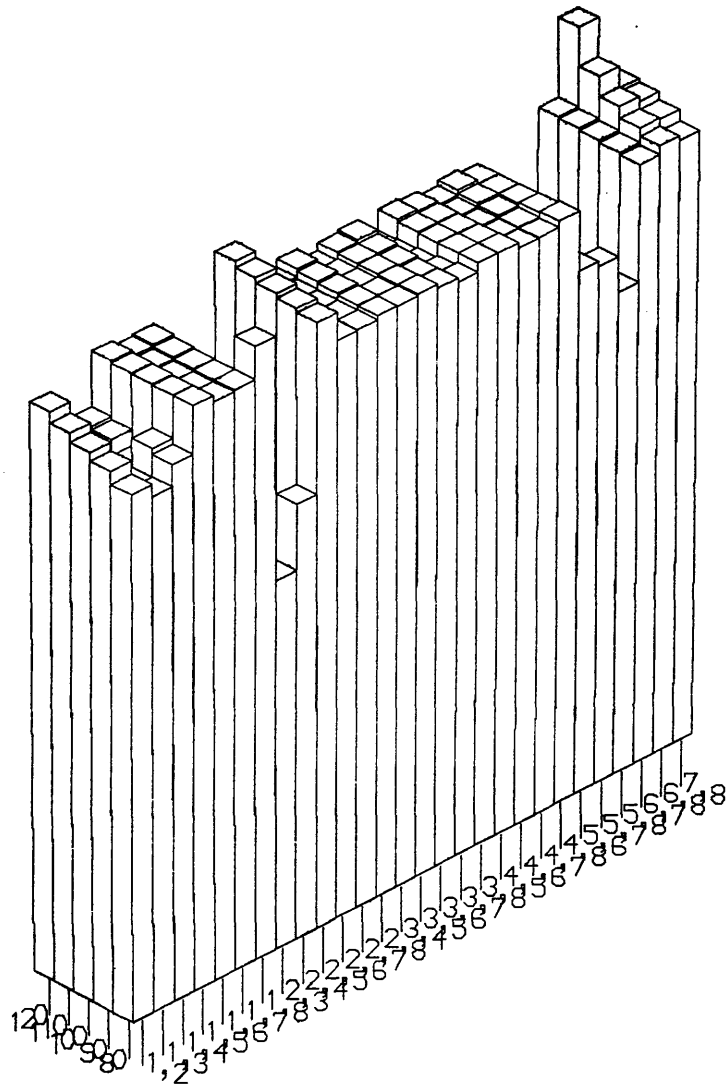

FIG 6.5D COMPARISON OF MAGNITUDE OF ELEMENT H(6.2) AS FLIGHT CONDITION AND C MATRIX VARY

at least some of the fails: these were H(1,1), H(3,1) and H(2,2). *Fig 6.6(a)* is a particularly good example: performance results indicated C(1,3) failing at $-6°$, $-3°$ and $+9°$. In some cases H(4,2), H(6,2) and H(8,2) also gave strong indications of possible fails. Note that it is not only a greatly increased magnitude which can indicate problems, but also a substantial reduction eg. C(3,4) in *fig 6.6(b)*.

With the reduced order observer only three elements gave a good correlation in every instance: $T_2(1)$, $T_2(2)$ and $T_2(3)$. For example, see *fig 6.7(a)* where C(1,3) failed at $-6°$, $-3°$ and $+9°$; C(6,7) failed every case and C(7,8) failed at $+9°$. It was also noted that many interesting 'patterns' were evident with elements $T_3(i,j)$, eg. *fig 6.7(b)*.

6.8 OBSERVER PERFORMANCE WITH NOISY STATES

From the preceding sections it is apparent that at any given flight condition in a noise free system it is possible, despite the problems in identifying which observers produce accurate estimates, to produce a sufficient number of observers to provide redundancy in state estimation and adequate freedom in the design of sensor fault detection logic. Unfortunately the helicopter is an extremely noisy environment, particularly due to mechanical vibration from the main and tail rotors resulting in electrical disturbances.

The classic solution to such noise corrupted measurements is to employ a Kalman filter (Kalman, 1960; Kalman and Bucy, 1961) which provides optimal noise rejection, but has the disadvantages of requiring a-priori information about the structure of the noise and a filter of the same order as the system being observed. The utilisation of the observable canonical form of the system, and hence the ability to treat the system as a set of subsystems, would alleviate the second problem, but this still leaves the complication of obtaining knowledge of the noise.

Because of this, and because the application of the Kalman filter in a noisy environment is well documented, whereas the Luenberger observer is not (since it is generally thought to be unsuitable for such applications), it was felt that it would be worthwhile to investigate whether or not the Luenberger observer could be adapted to provide noise free estimates.

A fourth order longitudinal model of the Puma at 100 Knots, level was used: the A and B matrices being,

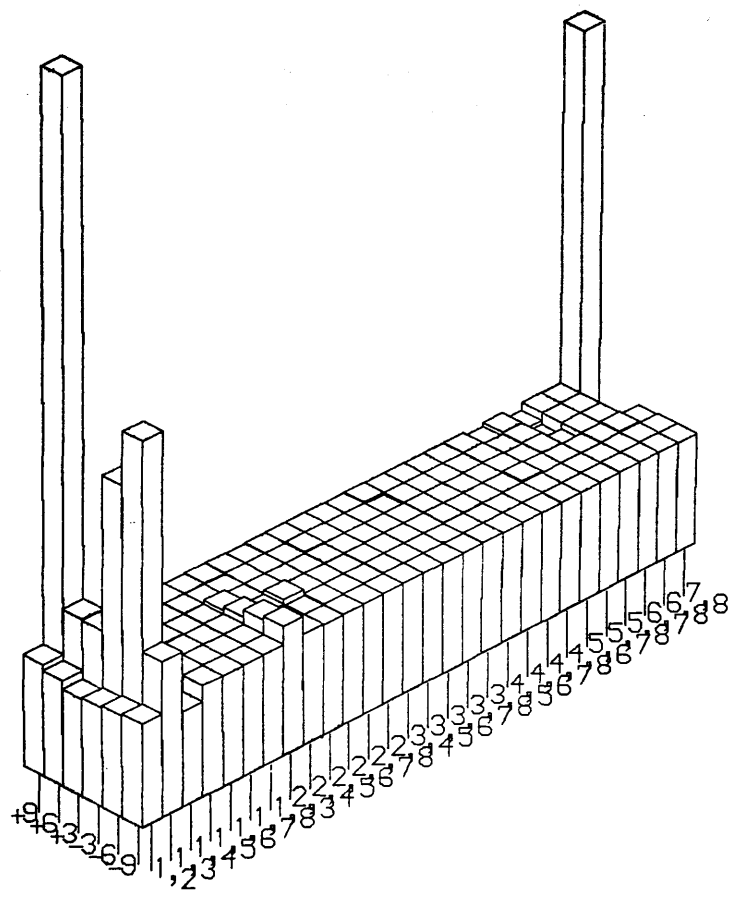

FIG 6.6A COMPARISON OF MAGNITUDE OF ELEMENT H(2,2) AS FLIGHT CONDITION AND C MATRIX VARY

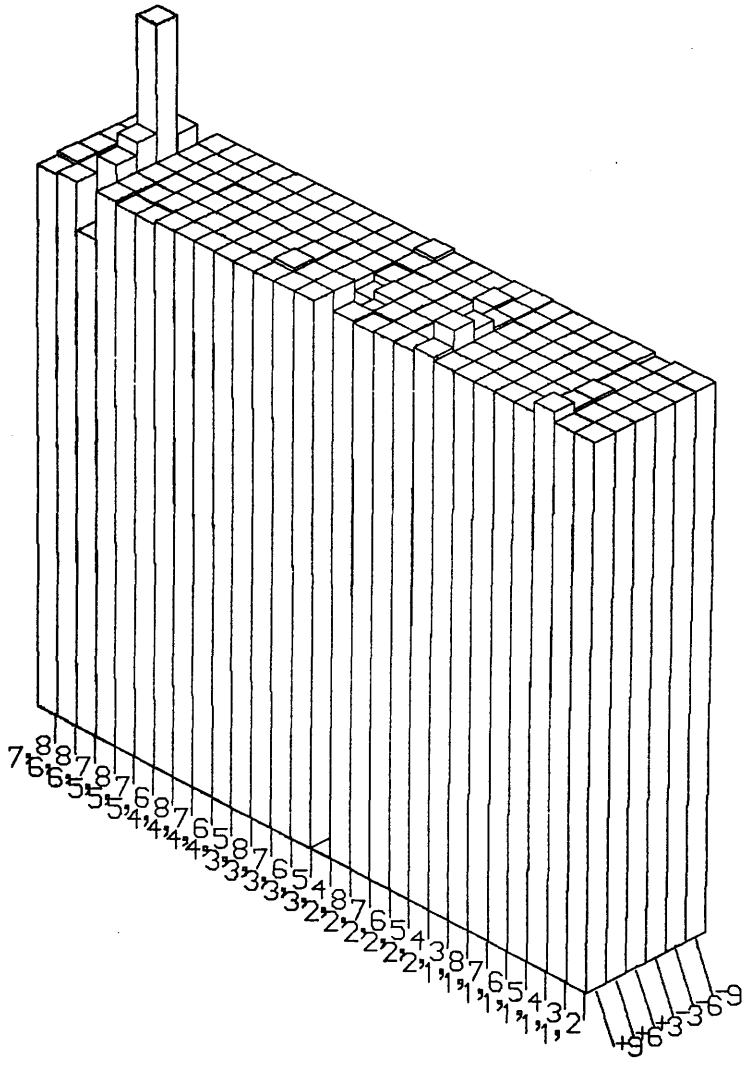

FIG 6.6B COMPARISON OF MAGNITUDE OF ELEMENT H(3,1) AS FLIGHT CONDITION AND C MATRIX VARY

FIG 6.7A COMPARISON OF MAGNITUDE OF ELEMENT T2(1) AS FLIGHT CONDITION AND C MATRIX VARY

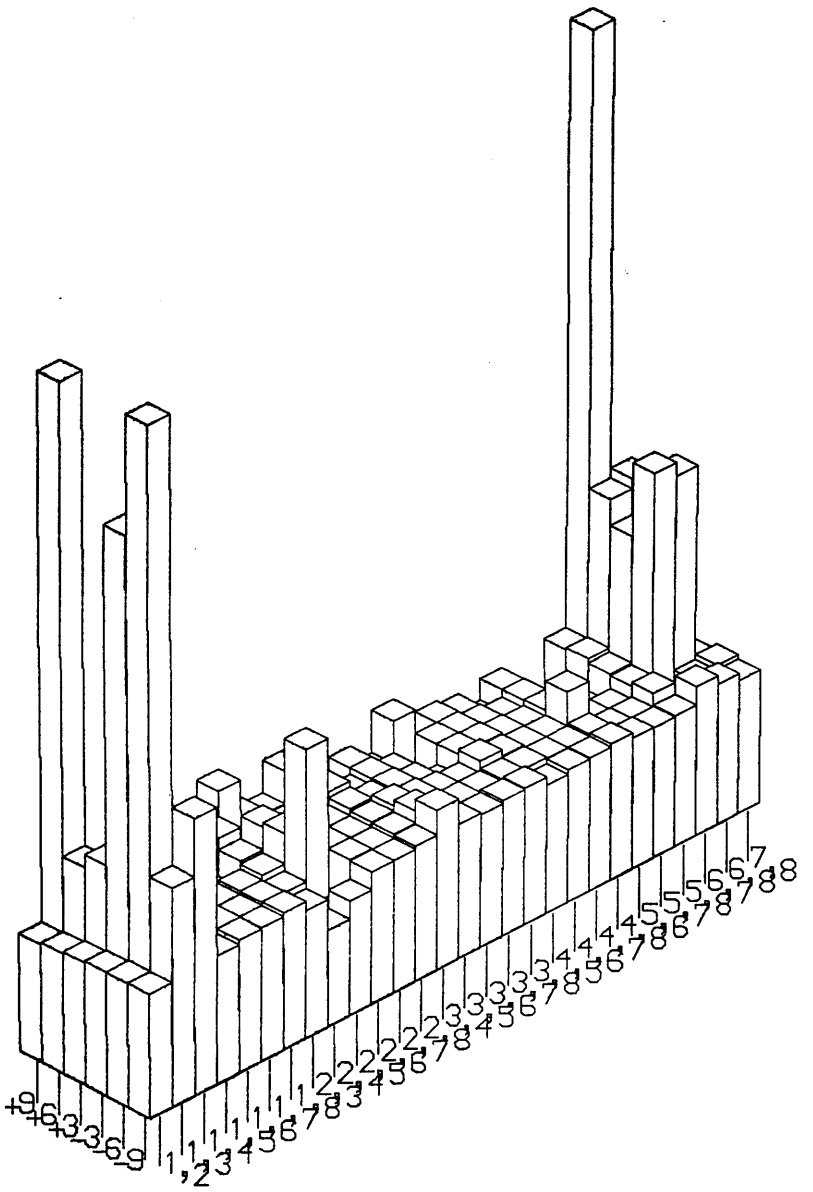

FIG 6.7B COMPARISON OF MAGNITUDE OF ELEMENT T3(1,4) AS FLIGHT CONDITION AND C MATRIX VARY

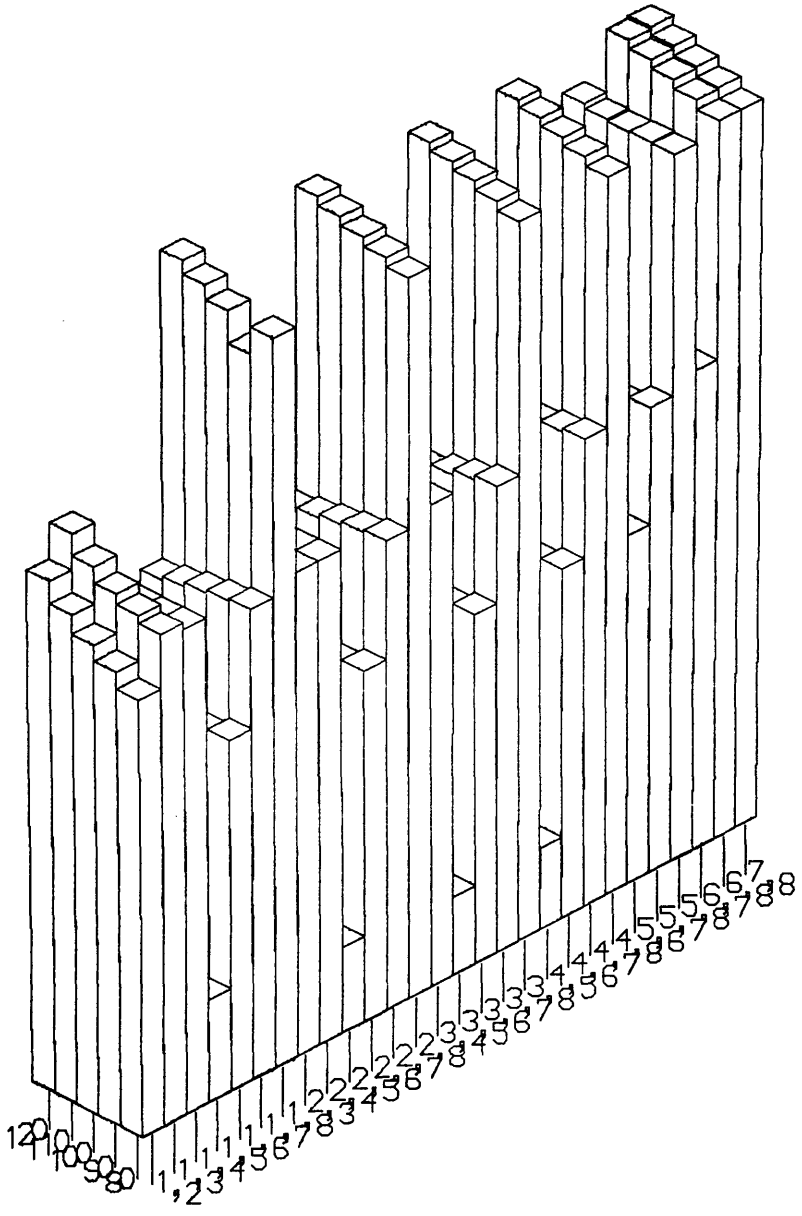

$$A = \begin{bmatrix} -0.027 & 0.004 & 4.653 & -32.183 \\ -0.030 & -0.857 & 168.220 & 0.466 \\ 0.002 & -0.008 & -0.801 & 0.000 \\ 0.000 & 0.000 & 1.000 & 0.000 \end{bmatrix} \qquad B = \begin{bmatrix} -7.818 & -30.938 \\ -377.693 & -130.775 \\ 2.139 & 6.386 \\ 0.000 & 0.000 \end{bmatrix}$$

and the eigenvalues of A are complex conjugate pairs:

$-0.83 \pm j1.12$

$-0.02 \pm j0.18$

Two sets of observer eigenvalues were initially used for comparison: 2× and 4× the largest system eigenvalue with 2% steps, ie.

EV1 : [-1.66, -1.69, -1.72, -1.76]

EV2 : [-3.31, -3.38, -3.44, -3.51]

and noise obtained from the flight data states (see Section 5.2.5) was added to the model generated states at full noise power. Each experiment was carried out with ten C matrices,

C(1)	C(1,2)	C(2,3)	C(3,4)
C(2)	C(1,3)	C(2,4)	
C(3)	C(1,4)		
C(4)			

but the results are illustrated by considering only two of these: C(1,4) and C(3,4). Initial errors in the observer estimates are introduced by setting the observer states to non− zero values at t= 0, specifically,

$\hat{u}(t_0) = -1 \qquad \hat{q}(t_0) = 0.0165$

$\hat{w}(t_0) = 1 \qquad \hat{\theta}(t_0) = 0.001125$

The control input was a doublet on θ_{1S} (Appendix six).

6.8.1 RESULTS

The first experiment was simply to establish the response of the observer in the absence of noise and the results are shown in *fig 6.8*. Two characteristics, which have been previously discussed, are immediately apparent – the faster reduction in error with larger eigenvalues coupled (in most, but not all instances) with an increased overshoot: eg. compare $\hat{w}$ in *figs (a)* and *(b)*; and the difference in estimates between the two C matrices: C(1,4) being more 'sensitive' than C(3,4).

When noise is added to the states, *fig 6.9*, the responses of the two observers are markedly different, *fig 6.10*. The estimates produced from C(3,4) are the same as previously, but with the addition of noise, whereas the greater 'sensitivity' of the observer using C(1,4) has resulted in poorly correlated results. Also, the use of larger eigenvalues increases the amount of noise appearing on the estimates from C(3,4) and exacerbates the problems with C(1,4). Ignoring the noise content of the estimates, out of the ten C matrices examined, only C(1) and C(1,4) didn't accurately follow the system state.

The next step was to determine whether a simple filter could be used to provide signals clean enough to allow the observer to produce a noise free estimate of the state. A basic first order *Low Pass* (or *Lag*) filter was used,

$$W(s) = \frac{Y(s)}{u(s)} = \frac{1}{1 + s\tau} \qquad (6.11)$$

and its effect on the noisy states (*fig 6.9*) can be seen in *fig 6.11*. A diagram of the system, with noise being added to $\underset{\sim}{x}$: giving noise corrupted state $\underset{\sim}{x}_n$; and a low pass filter on the output of the system: giving filtered output $\underset{\sim}{y}_f$, is shown in *fig 6.12*.

Two tests were then conducted – no noise added to the system state (*fig 6.13*) and noise added (*fig 6.14*). Both cases were with $\tau = 0.2$ and observer eigenvalues EV2. Considering the 'no–noise' case first, it is clear that the filter has introduced three effects: the magnitude of the overshoots have increased (eg. compare $\hat{u}$ in *fig 6.13b* with $\hat{u}$ in *fig 6.8d*); the number of overshoots has increased (eg. compare $\hat{w}$ in *fig 6.13a* with $\hat{w}$ in *fig 6.8b*) and the observer estimate 'lags' the system state (eg. $\hat{q}$ and $\hat{\theta}$ in *fig 6.13b*).

When noise is added, the response of C(3,4) is virtually identical to the no–noise, filtered responses, ie. the noise on the observer output has been reduced to a

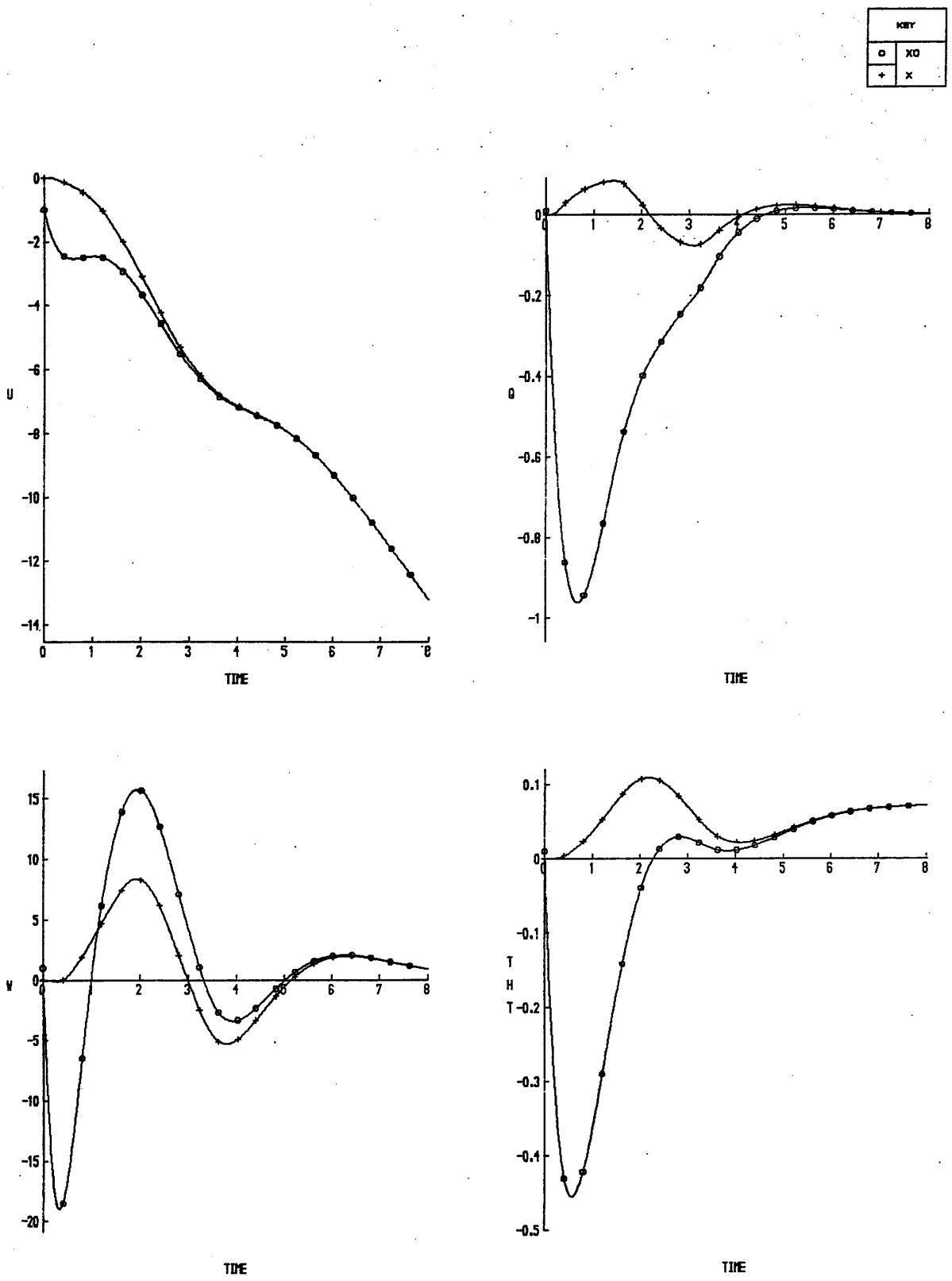

FIG 6.8A OBSERVER RESPONSE TO CLEAN INPUTS: C(1,4), EV1

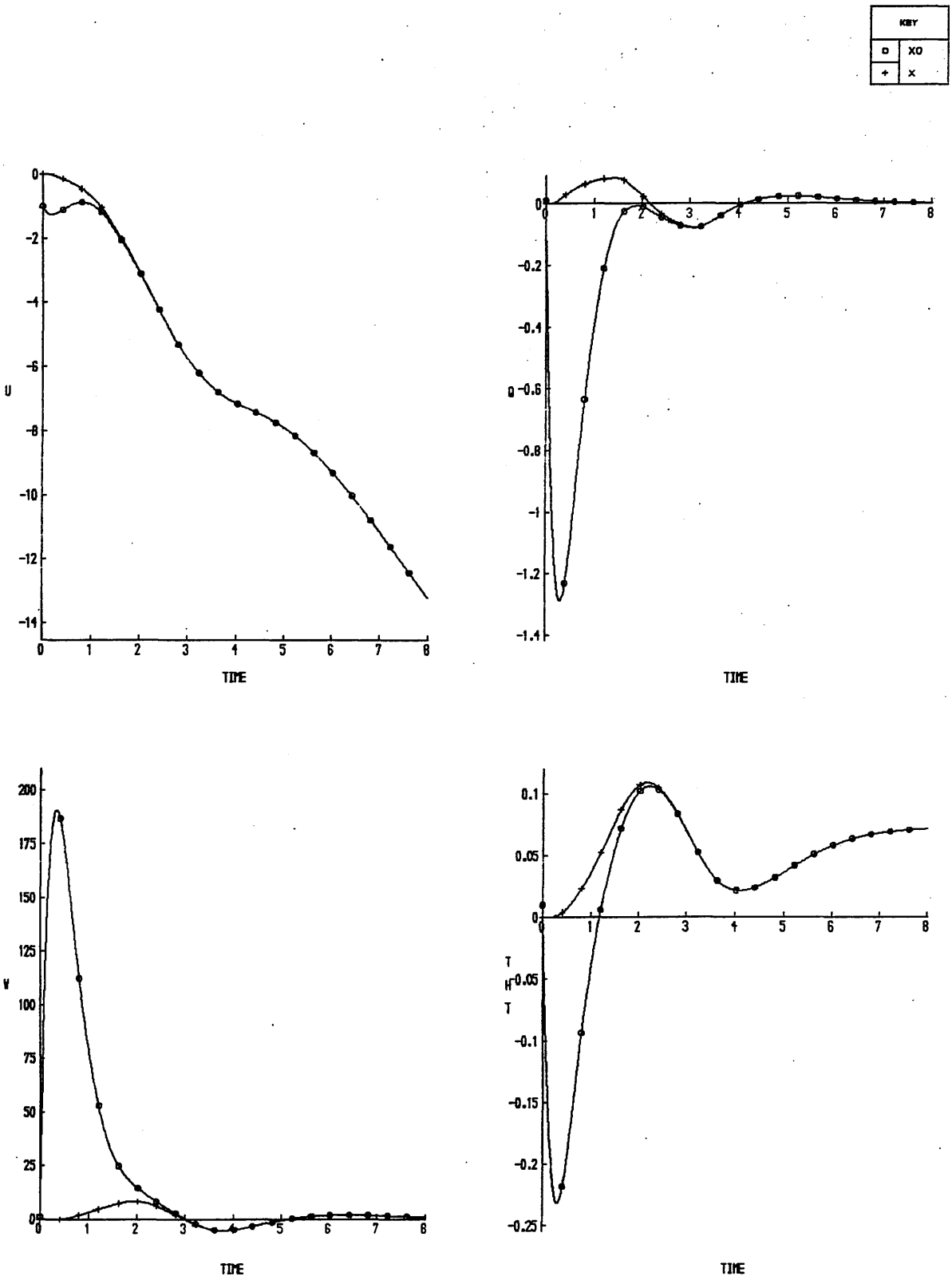

FIG 6.8B OBSERVER RESPONSE TO CLEAN INPUTS: C(1,4), EV2

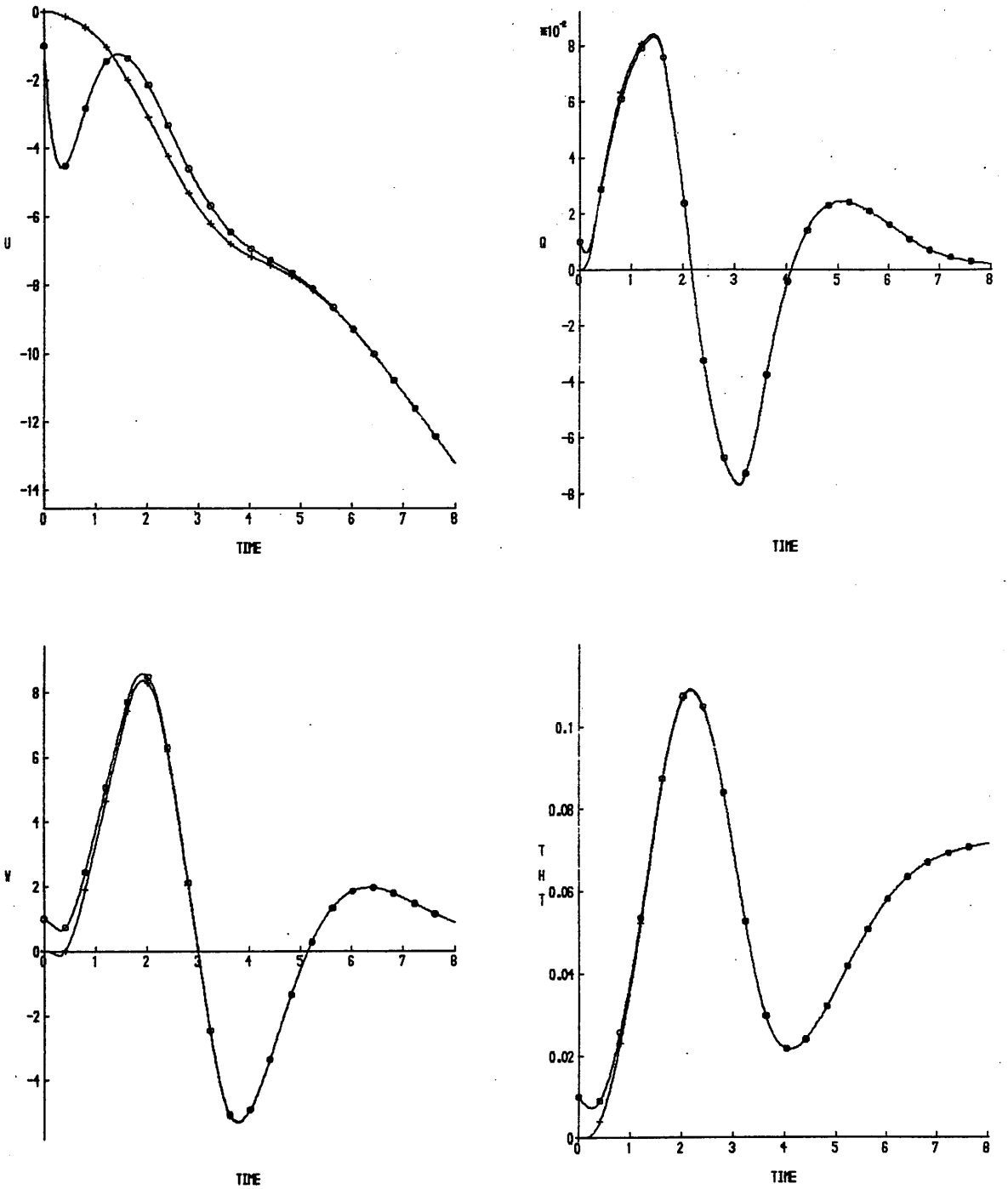

FIG 6.8C OBSERVER RESPONSE TO CLEAN INPUTS: C(3,4), EV1

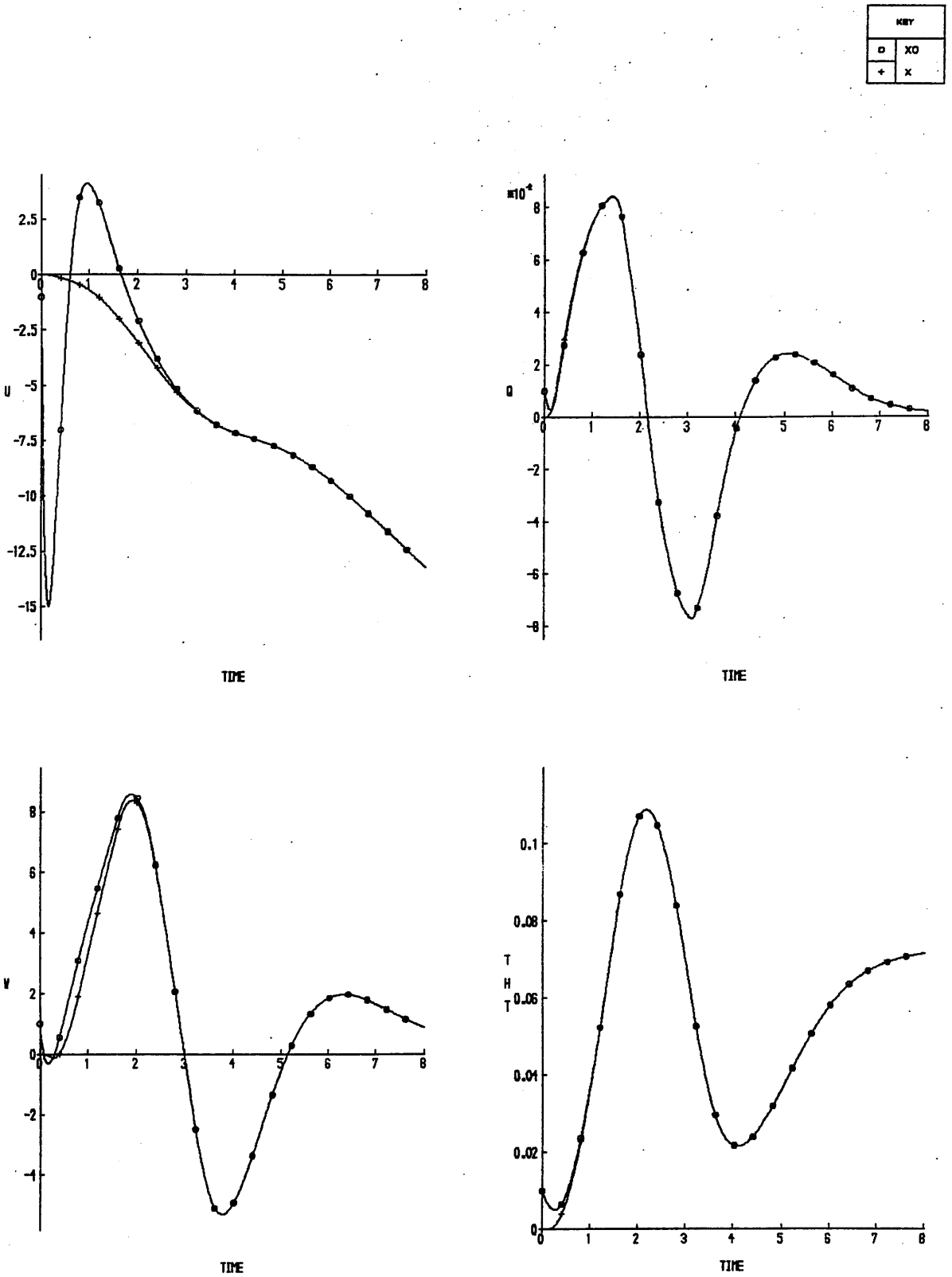

FIG 6.8D OBSERVER RESPONSE TO CLEAN INPUTS: C(3,4), EV2

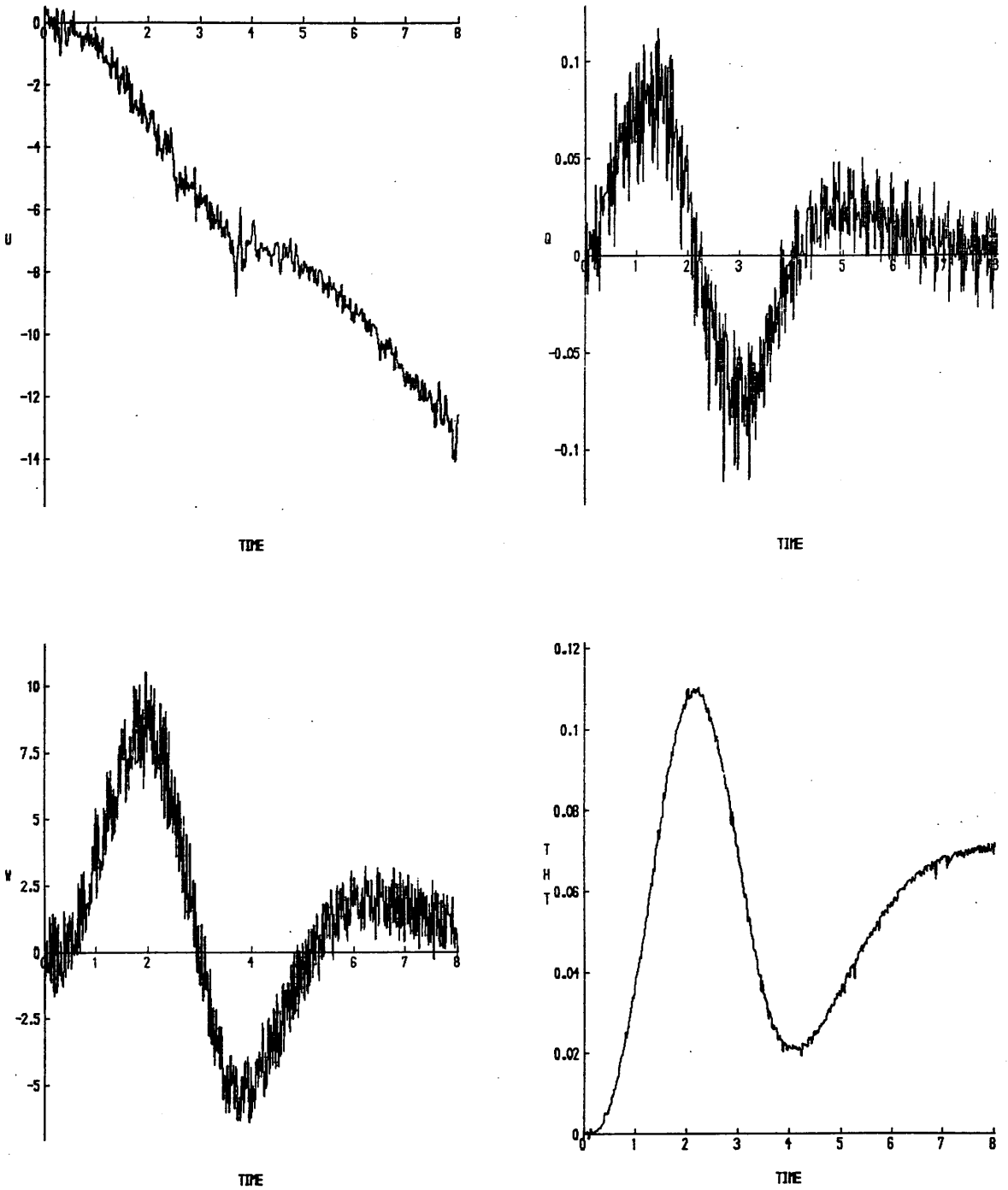

FIG 6.9 NOISE ADDED TO STATES

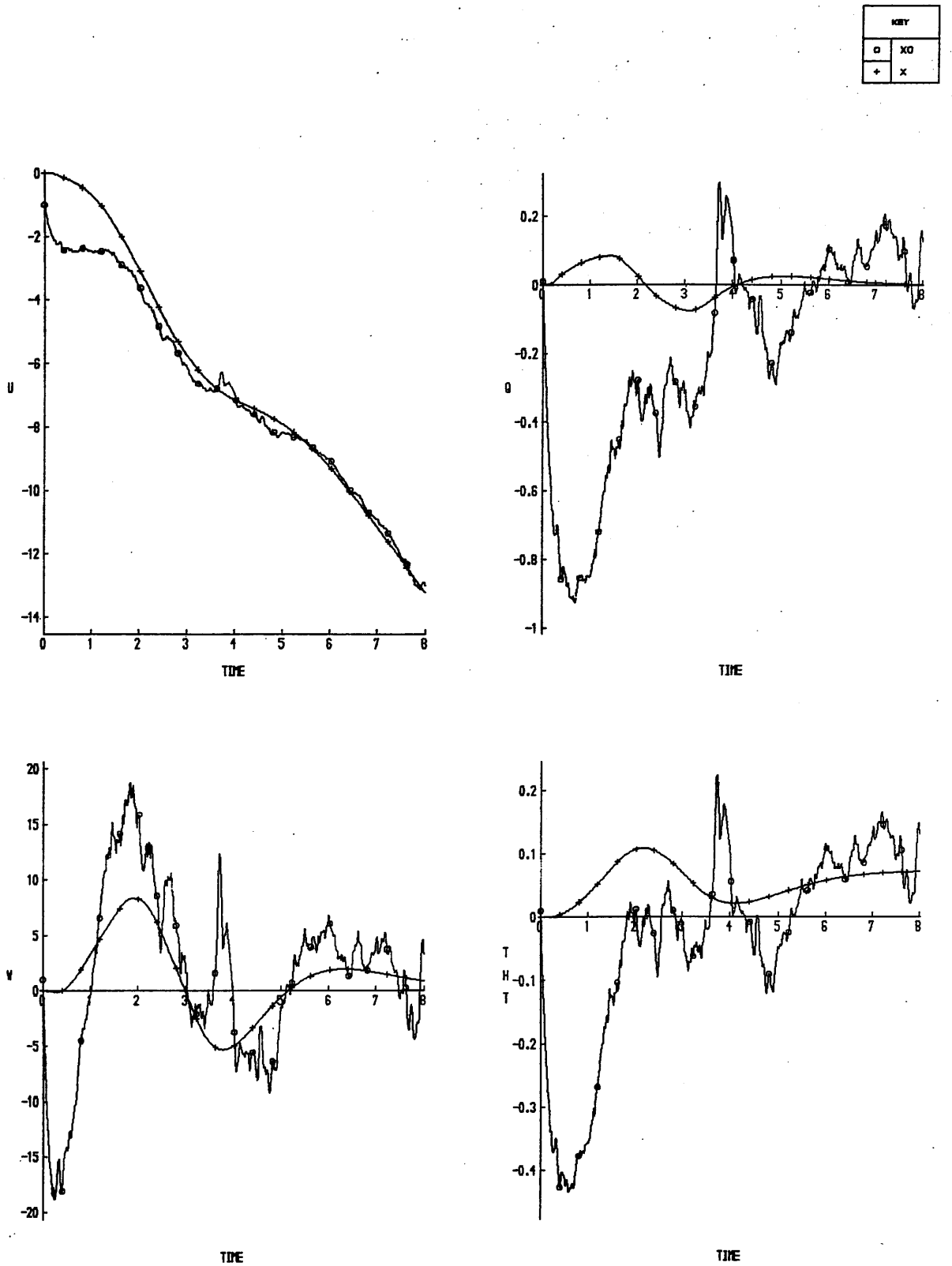

FIG 6.10A OBSERVER RESPONSE TO NOISY STATES: C(1,4), EV1

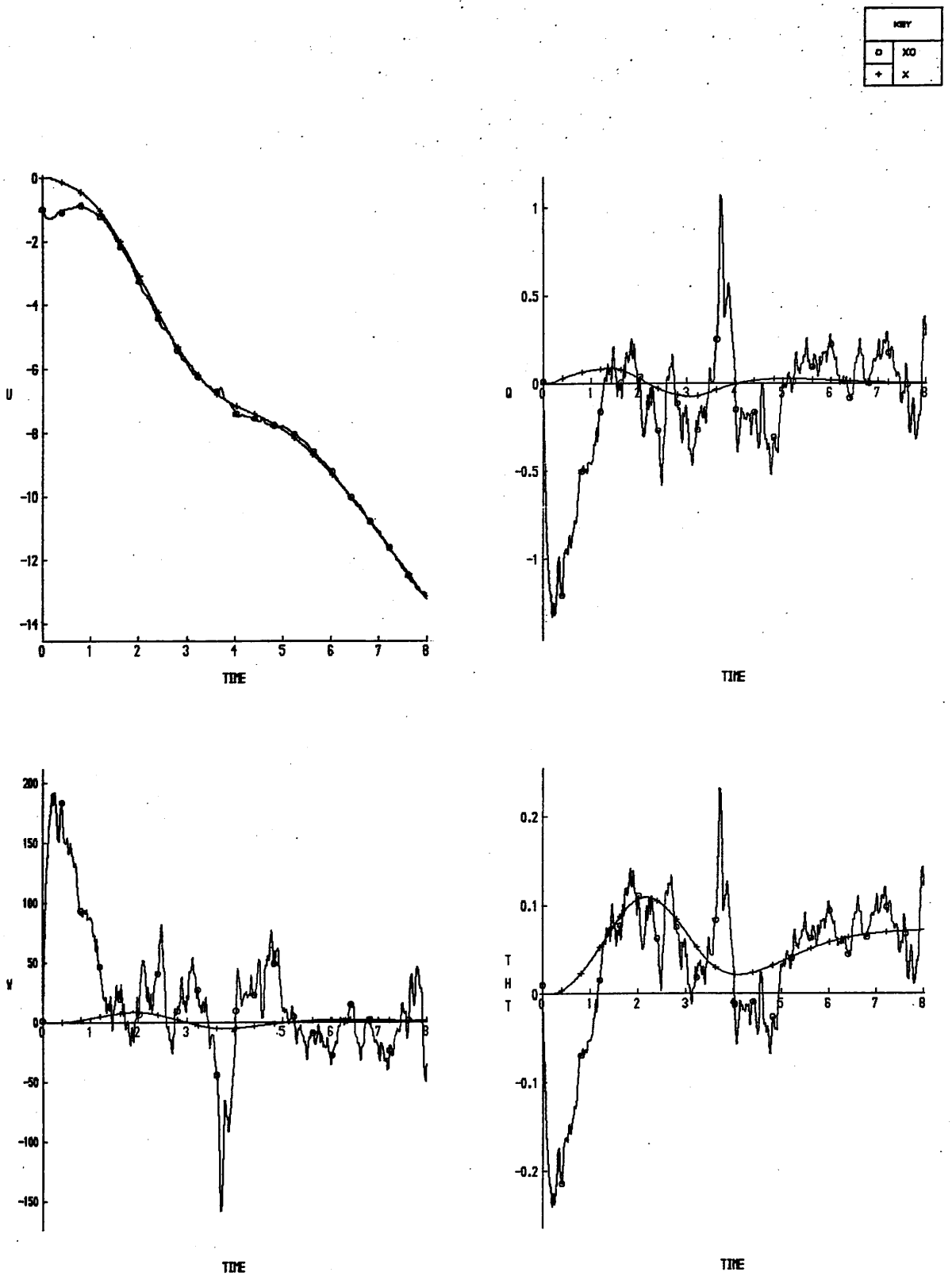

FIG 6.10B OBSERVER RESPONSE TO NOISY STATES: C(1.4), EV2

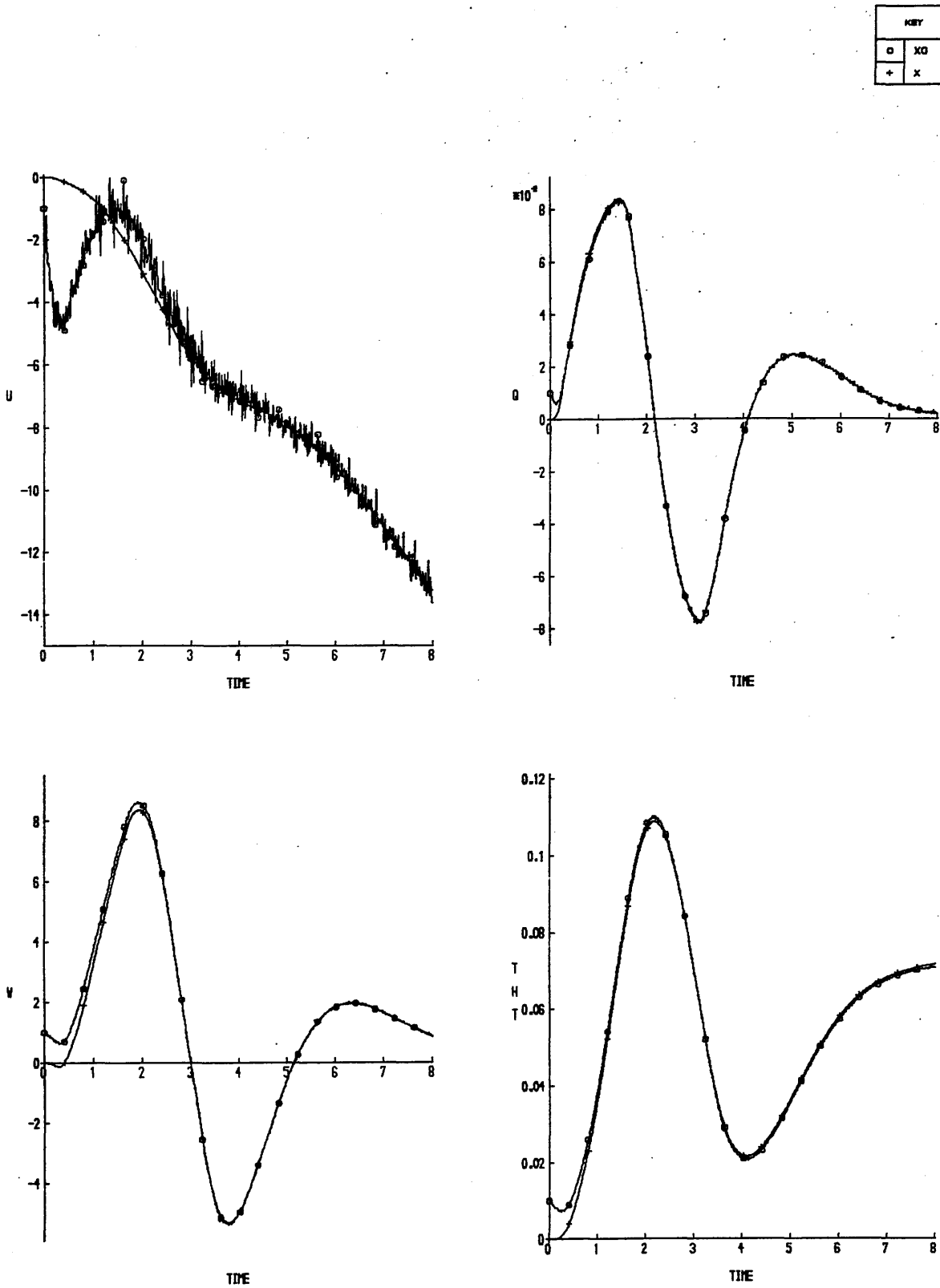

FIG 6.10C OBSERVER RESPONSE TO NOISY STATES: C(3,4), EV1

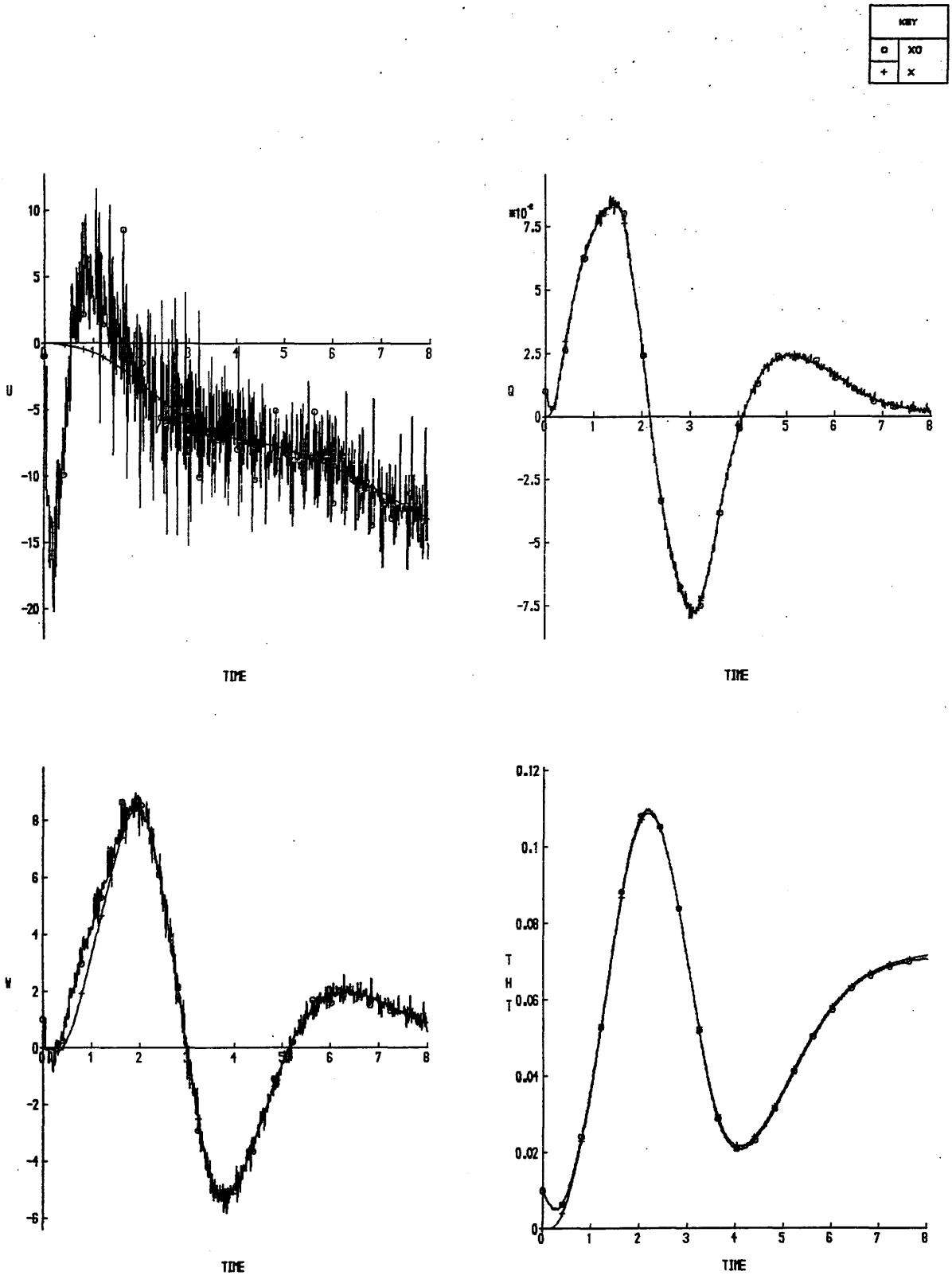

FIG 6.10D OBSERVER RESPONSE TO NOISY STATES: C(3,4), EV2

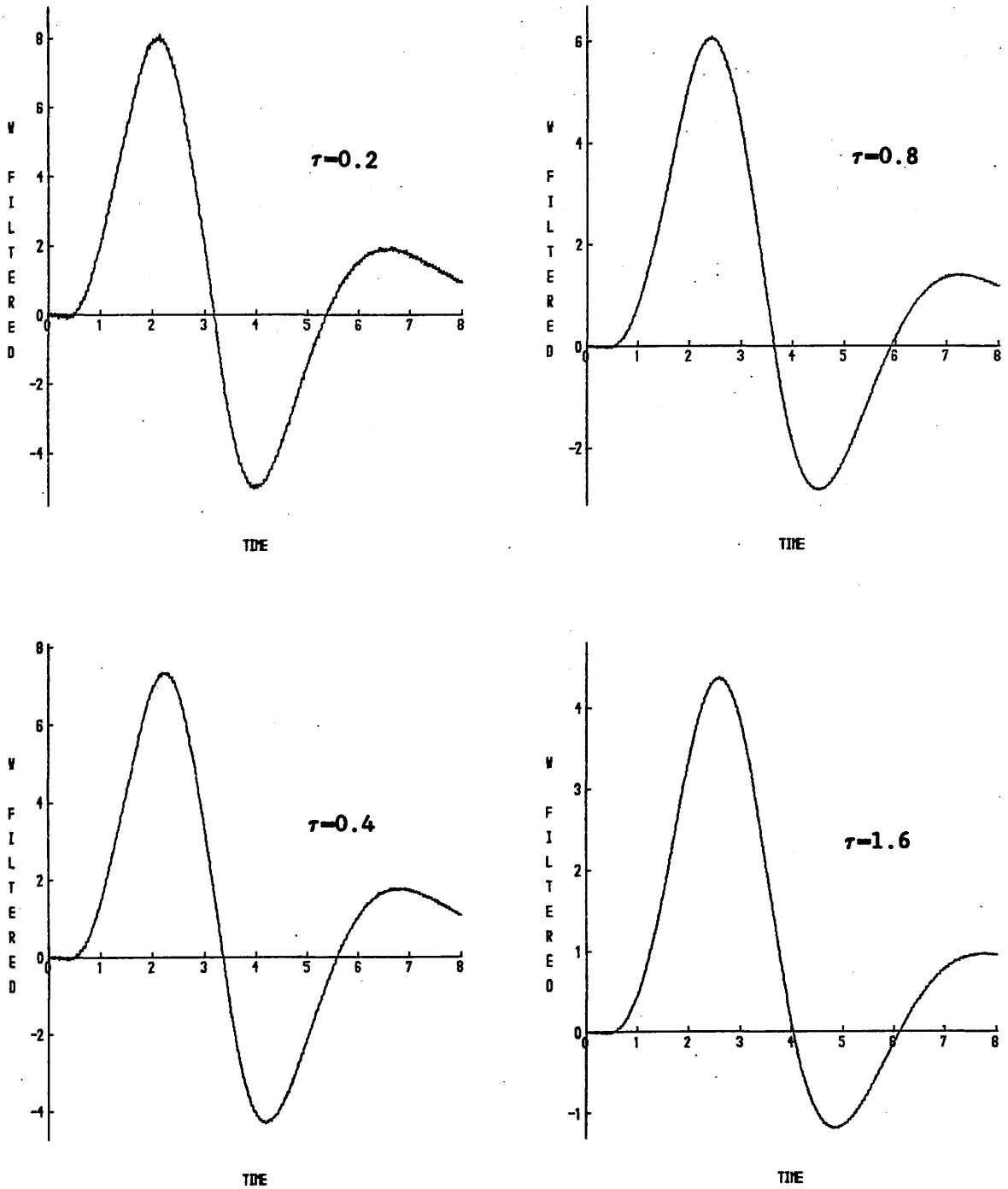

FIG 6.11 STATE w. LOW PASS FILTERED

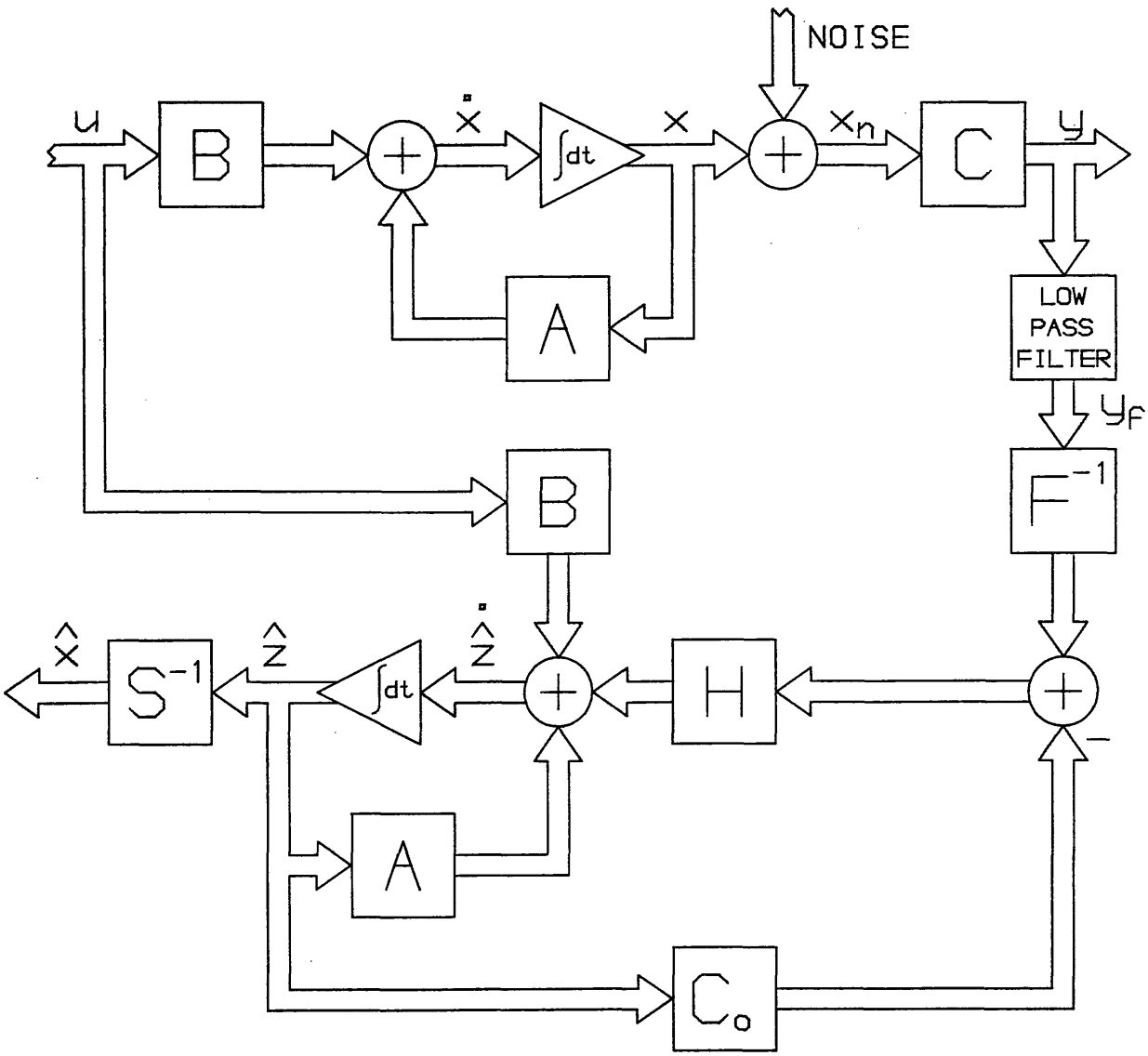

FIG 6.12 LOW PASS FILTER ON SYSTEM OUTPUT

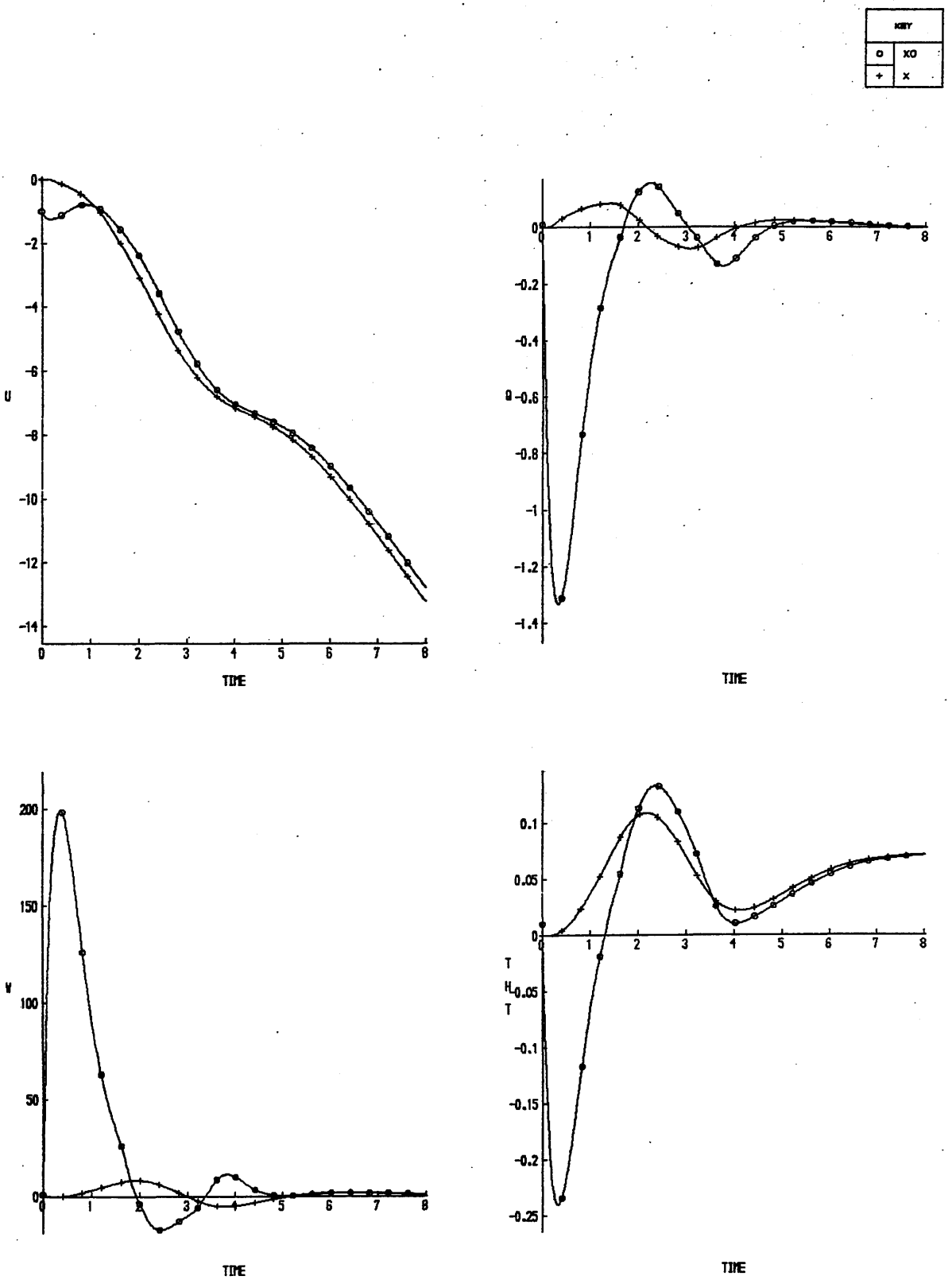

FIG 6.13A OBSERVER RESPONSE TO CLEAN, FILTERED STATES: C(1,4)

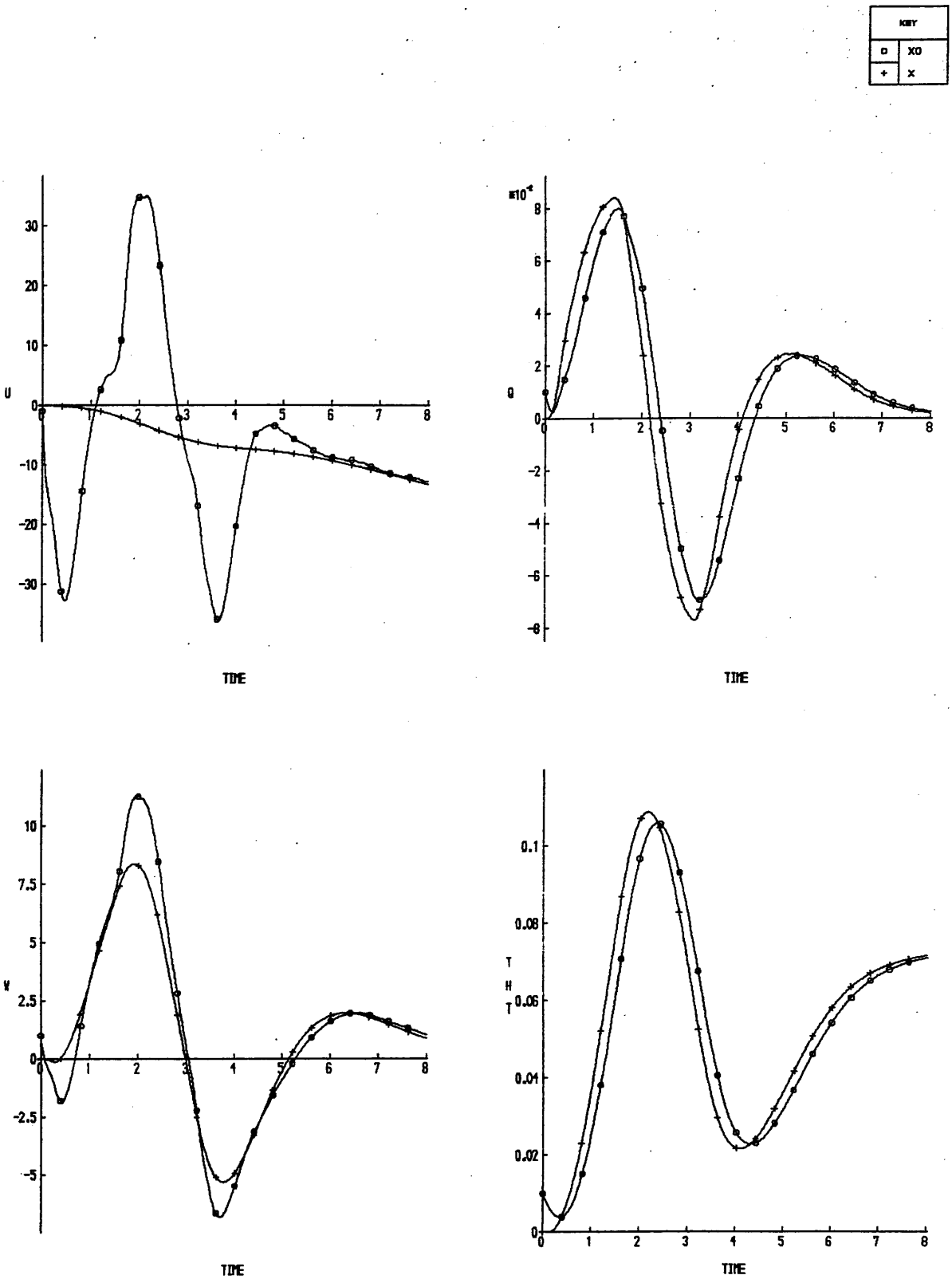

FIG 6.13B OBSERVER RESPONSE TO CLEAN, FILTERED STATES: C(3,4)

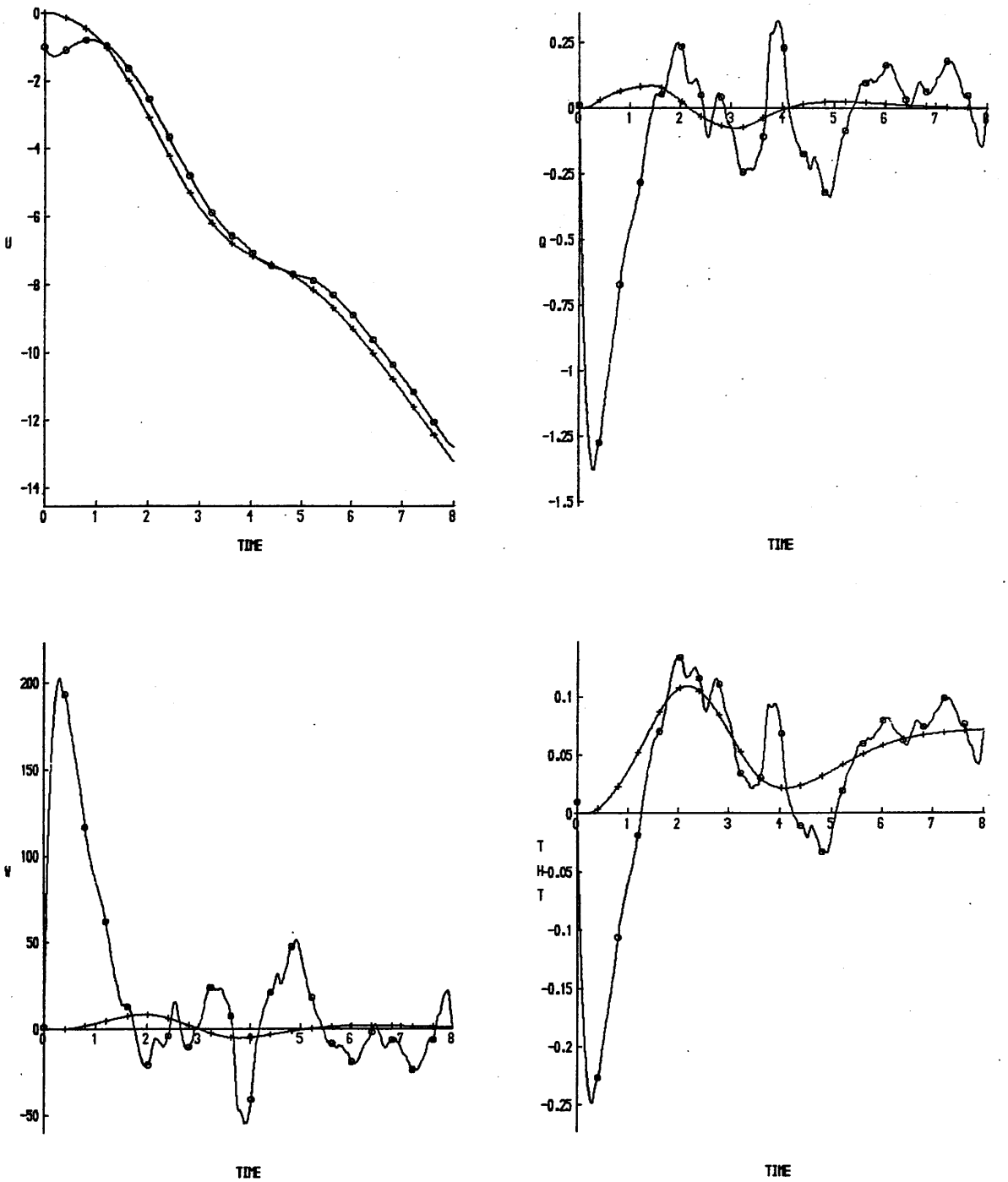

FIG 6.14A OBSERVER RESPONSE TO NOISY, FILTERED STATES: C(1,4)

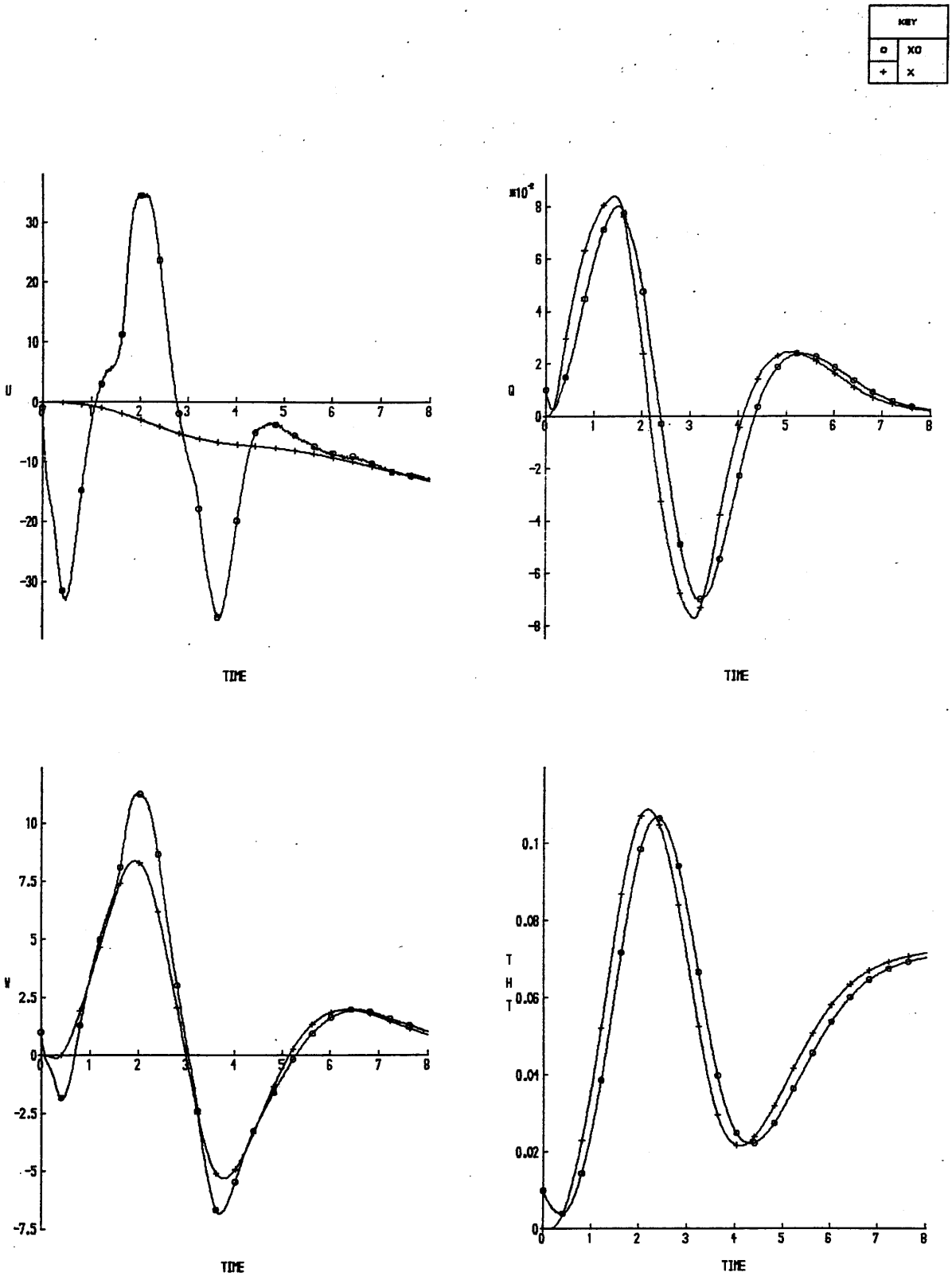

FIG 6.14B OBSERVER RESPONSE TO NOISY, FILTERED STATES: C(3,4)

negligible level. Compare $\hat{u}$ in *fig 6.10d* with *fig 6.13b* and *fig 6.14b*, for example. With C(1,4), the addition of noise has again resulted in poor results, however they are an improvement over the 'no filter' case, eg. compare *fig 6.10b* with *fig 6.14a*. As previously, the only unacceptable estimates were produced using C(1) and C(1,4); all other C matrices produced clean, lagged inputs.

Thus, despite its simplicity, these tests have demonstrated that a low pass filter can output signals clean enough to allow a virtually noise free estimate of the state. However, this estimate lags the system state and as the value of τ increases, the lag increases. Obviously, unless this lag can be eliminated, the estimates will be inadequate for control purposes, although possibly sufficient for instrument fault detection.

The first attempt at solving the problem was to add an identical low pass filter in the feedback loop of the observer: *fig 6.15*, in order to lag the feedback of the observer state $\hat{z}$ by an identical amount. For each C matrix, four cases were run: $\tau = 0.1$ and 0.2 for observer eigenvalues EV1 and EV2. No noise was added to the states.

The results are tabulated in *Table 6.14* and *fig 6.16* gives four examples from three of the four categories: good, minor, oscillatory and unstable. *Fig 6.16a* illustrates the 'minor' category, with one estimate ($\hat{u}$) being more oscillatory than in the no-filter case; *(b)* and *(c)* are both examples of the oscillatory category: the larger eigenvalues resulting in less damping; and *(d)* shows an unstable estimate.

The reasons for the differences can be seen from examining the eigenvalues of the complete system – ie. observed system, observer and the two low pass filters. For example, consider the system which includes an observer designed with C(1,4) and EV2. The eigenvalues of this composite system, without filters, are,

SYSTEM	-0.828 ± j1.1185	ξ=0.595
	-0.015 ± j0.1797	ξ=0.083
OBSERVER	-3.510	
	-3.444	
	-3.378	
	-3.312	

where ξ is the *Damping Factor*. As was shown in section 3.5, the eigenvalues are the union of those of the system and those of the state estimator (*Separation*

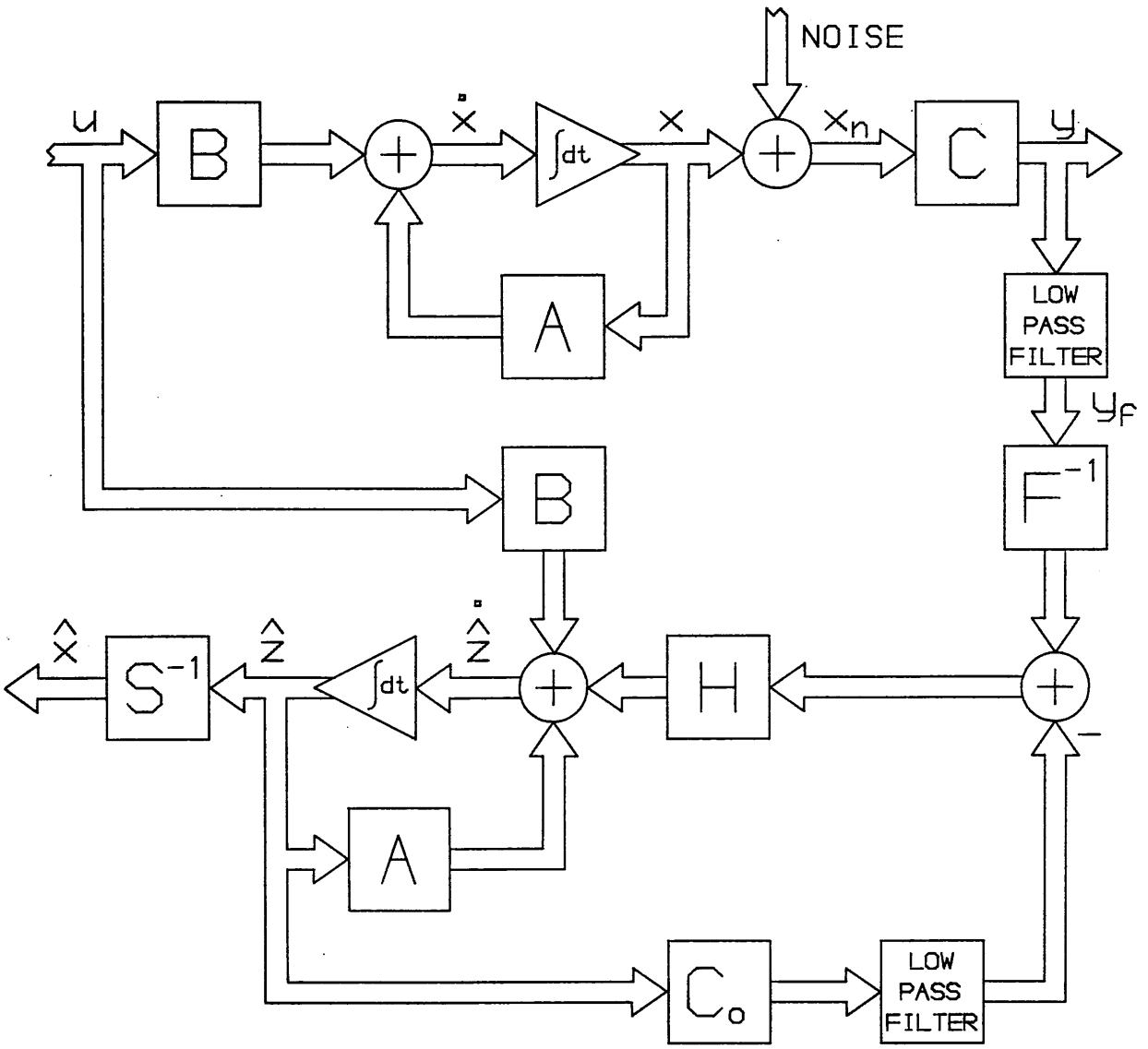

FIG 6.15 LOW PASS FILTER IN OBSERVER FEEDBACK LOOP

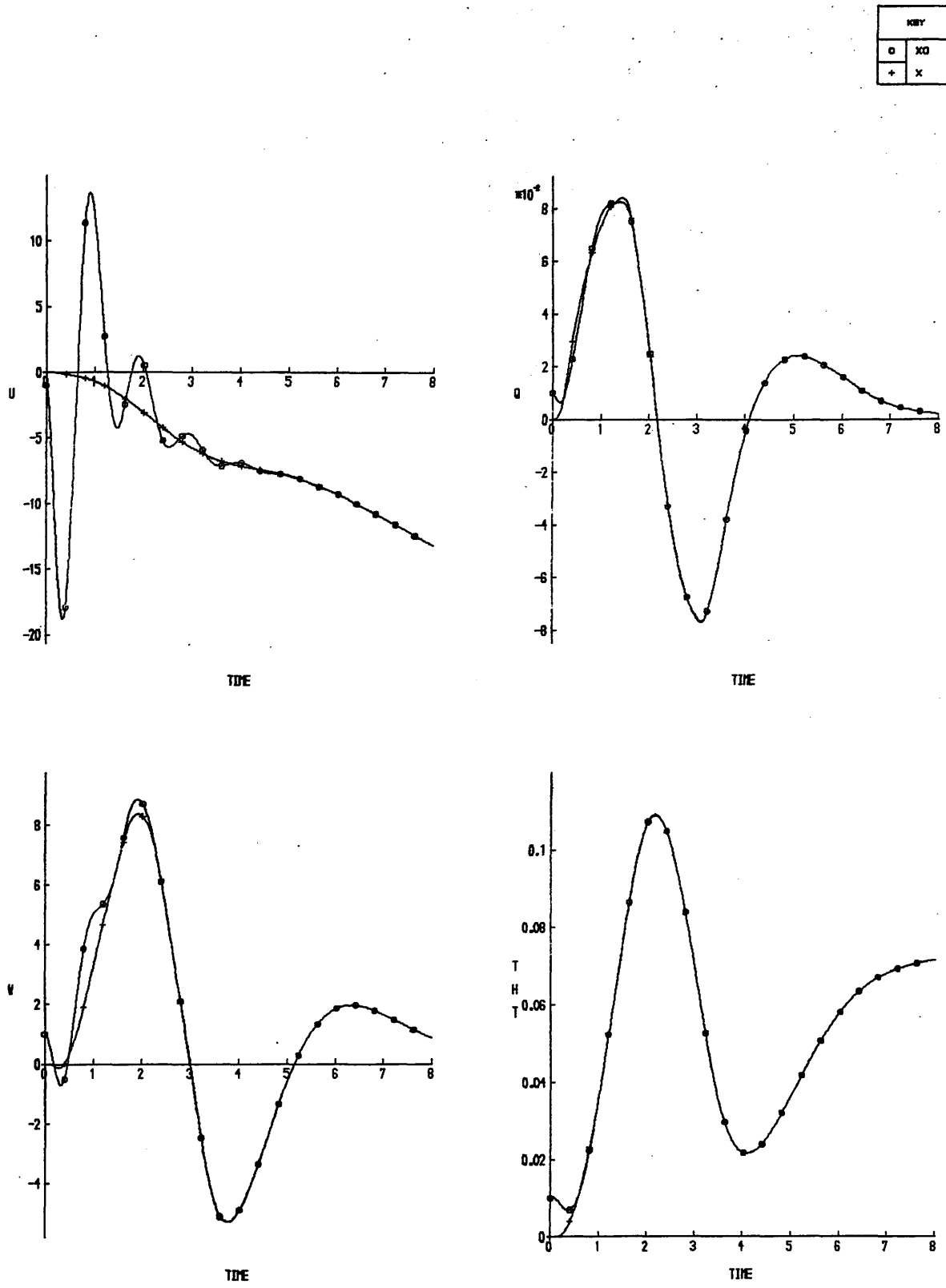

FIG 6.16A OBSERVER RESPONSE WITH FILTER IN FEEDBACK LOOP

τ=0.2, EV2, C(3,4)

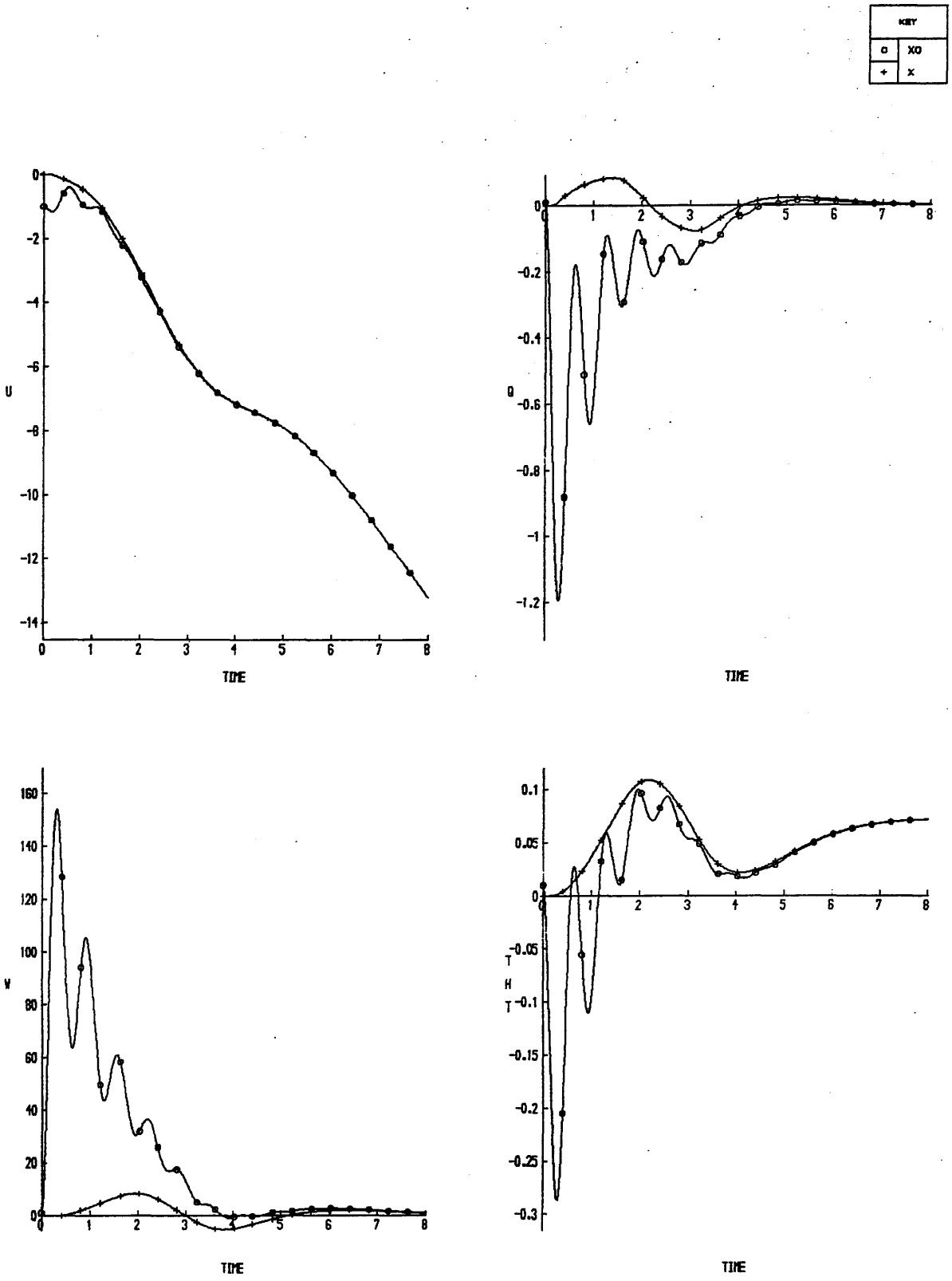

FIG 6.16B OBSERVER RESPONSE WITH FILTER IN FEEDBACK LOOP

τ=0.1, EV2, C(1.4)

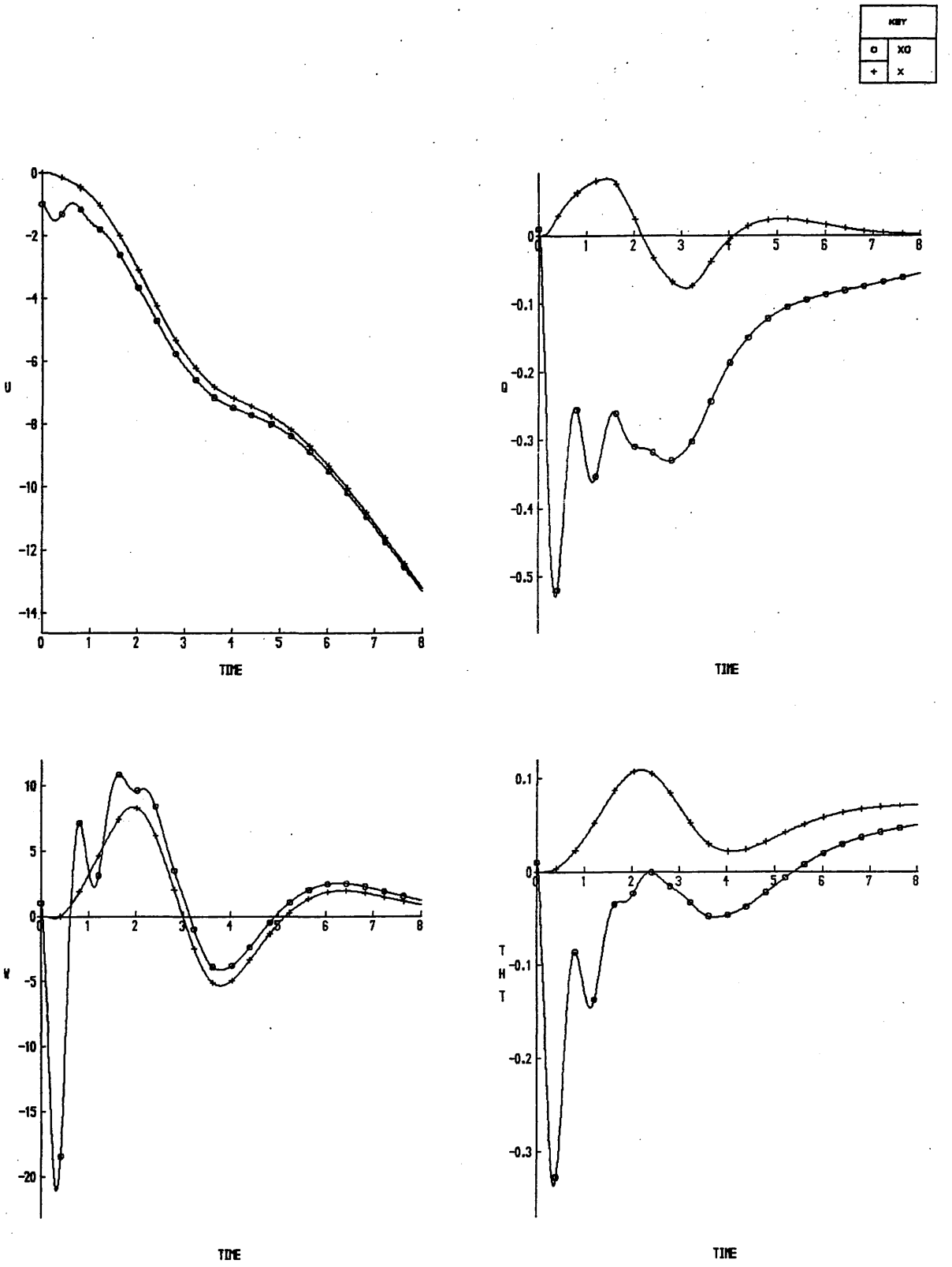

FIG 6.16C OBSERVER RESPONSE WITH FILTER IN FEEDBACK LOOP

τ=0.1, EV1, C(1,4)

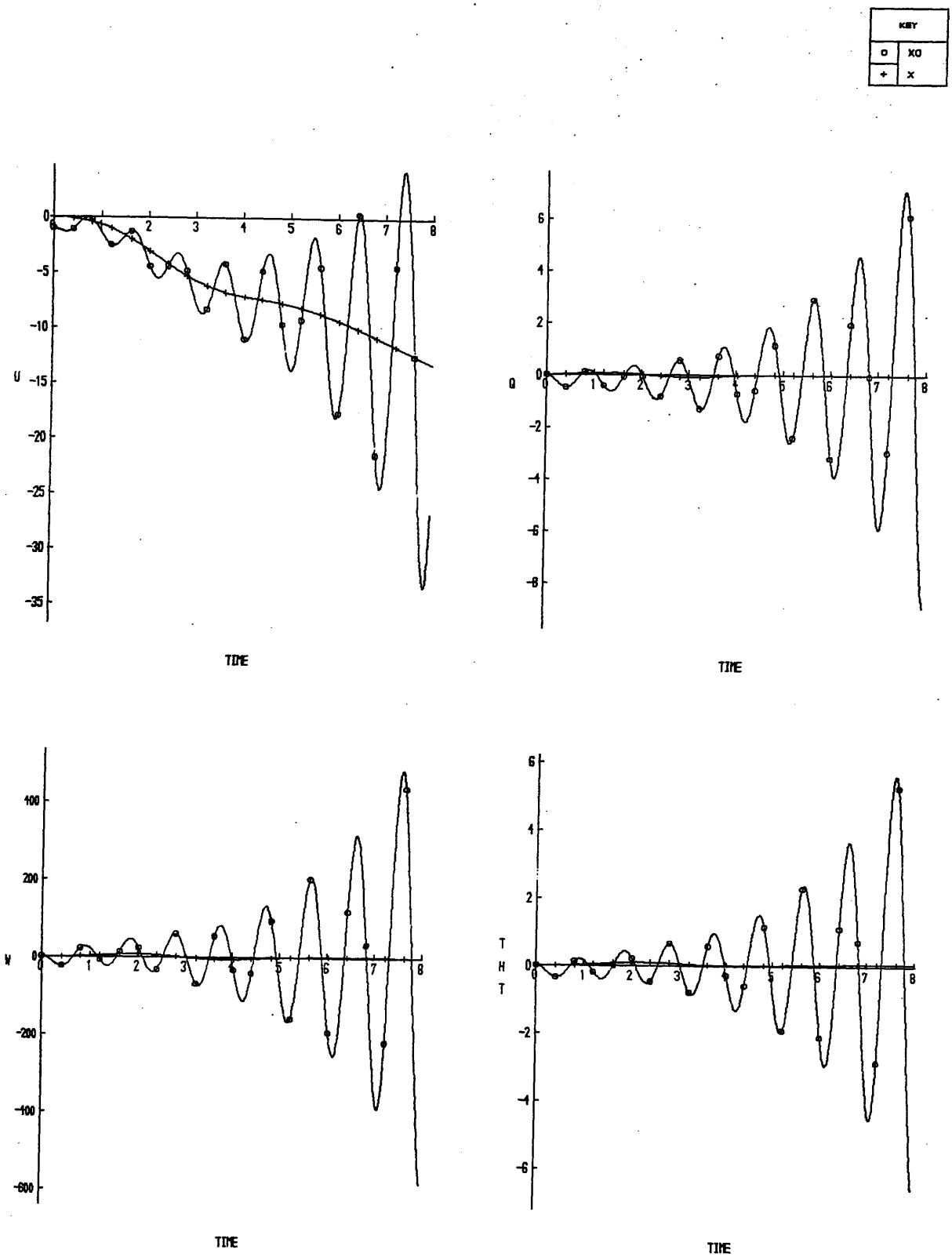

FIG 6.16D OBSERVER RESPONSE WITH FILTER IN FEEDBACK LOOP

τ=0.2, EV1, C(1,4)

		EV1				EV2			
C MTX	τ	good	min	osc	unst	good	min	osc	unst
C(1)	0.1	*					*		
	0.2	*						*	
C(2)	0.1	*					*		
	0.2	*						*	
C(3)	0.1	*					*		
	0.2	*						*	
C(4)	0.1	*					*		
	0.2	*						*	
C(1,2)	0.1	*				*			
	0.2	*				*			
C(1,3)	0.1	*				*			
	0.2	*				*			
C(1,4)	0.1			*				*	
	0.2				*				*
C(2,3)	0.1			*				*	
	0.2				*				*
C(2,4)	0.1	*				*			
	0.2		*				*		
C(3,4)	0.1	*				*			
	0.2		*				*		

GOOD - Estimates almost identical to no-filter case

MINOR - At least one estimate more oscillatory than no-filter case

OSCILLATORY - Highly oscillatory estimate, but still stable

UNSTABLE - Estimate unstable

TABLE 6.14 RESULTS WITH FILTERED STATES AND FILTER IN FEEDBACK LOOP

Property). Using a low pass filter on the output of the system adds four eigenvalues at -10 with $\tau = 0.1$ or four eigenvalues at -5 with $\tau = 0.2$, but the system and observer eigenvalues are unaltered. Unfortunately this is not the case when a low pass filter is also used in the feedback loop of the observer. With both filters having $\tau = 0.1$ or $\tau = 0.2$, the eigenvalues are,

	τ = 0.1	τ = 0.2
SYSTEM	-0.828 ± j1.118 ξ=0.595	-0.828 ± j1.118 ξ=0.595
	-0.015 ± j0.180 ξ=0.083	-0.015 ± j0.180 ξ=0.083
O/P FILTER	-10.0	-5.0
	-10.0	-5.0
	-10.0	-5.0
	-10.0	-5.0
F/B FILTER	-10.364	-5.112 ± j2.550 ξ=0.895
	-10.0	-5.0
	-10.0	-5.0
	- 5.071	
OBSERVER	-3.040	-2.913
	-1.157 ± j9.649 ξ=0.119	-0.578
	-0.896	+1.015 ± j7.776 ξ=-0.129

and clearly the eigenvalues of the observer and the filter are not independent – the addition of the filter has altered the observer eigenvalues and also the eigenvalues of the filter itself. With $\tau = 0.2$ the result is an unstable estimate due to the positive complex conjugate eigenvalue, whilst with $\tau = 0.1$ the estimate is underdamped with $\xi = 0.119$.

When noise is added to the states, those observers which provided good estimates in the absence of noise, produced almost identical estimates (eg. *fig 6.17a*: C(3,4), EV2, $\tau = 0.2$), whereas if the estimate was originally poor, the addition of noise aggravated the problem (eg. *fig 6.17b*: C(1,4), EV2, $\tau = 0.1$). Thus, although adequate, relatively noise free estimates can be produced by this method, it is unacceptable because the observer and filter eigenvalues are altered. It is of course feasible that an observer design method could be developed to allow the independent selection of observer and filter eigenvalues, however this was not investigated since a simpler solution was discovered.

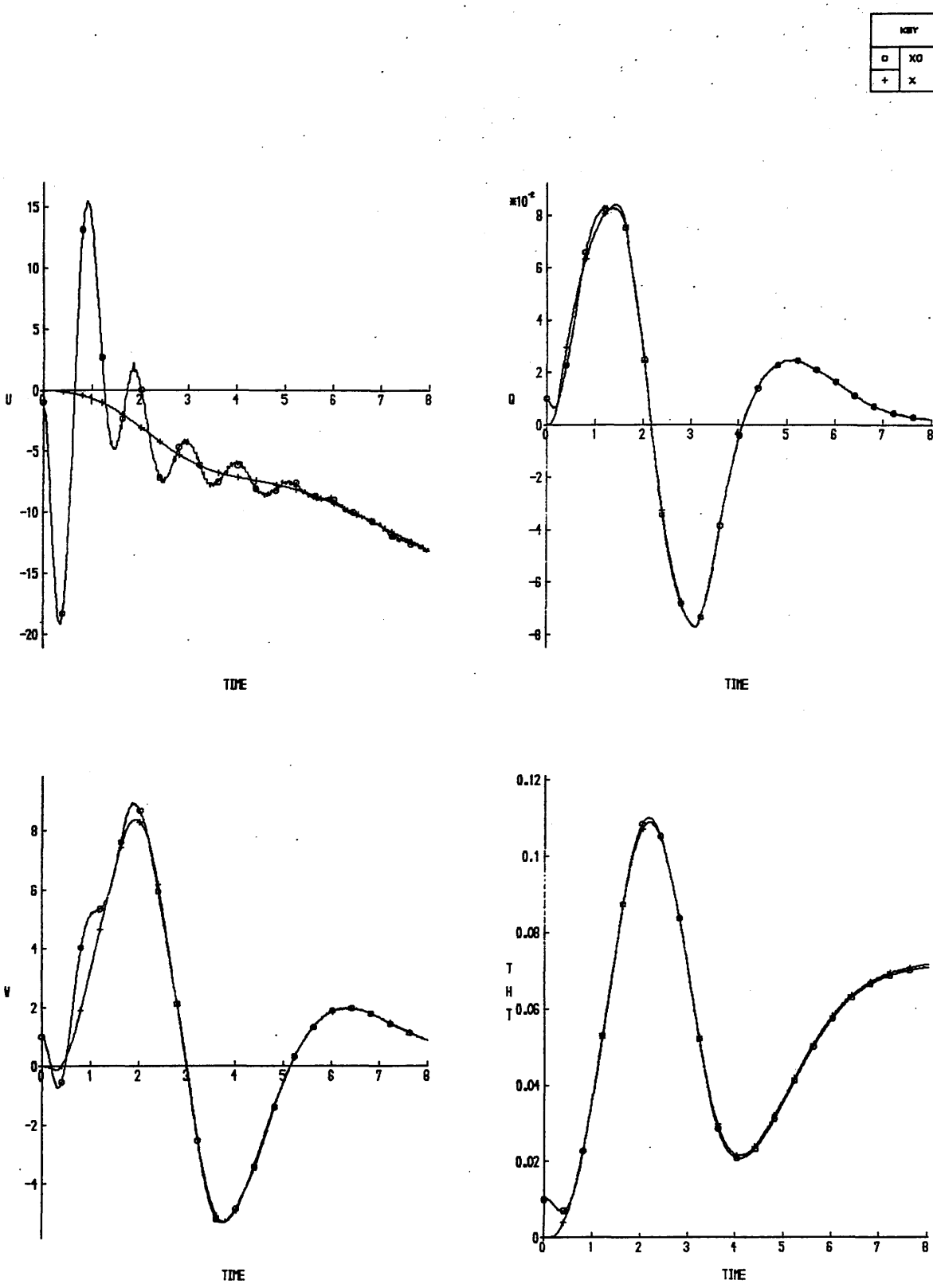

FIG 6.17A OBSERVER RESPONSE TO NOISY STATES WITH FILTER IN FEEDBACK LOOP: C(3,4)

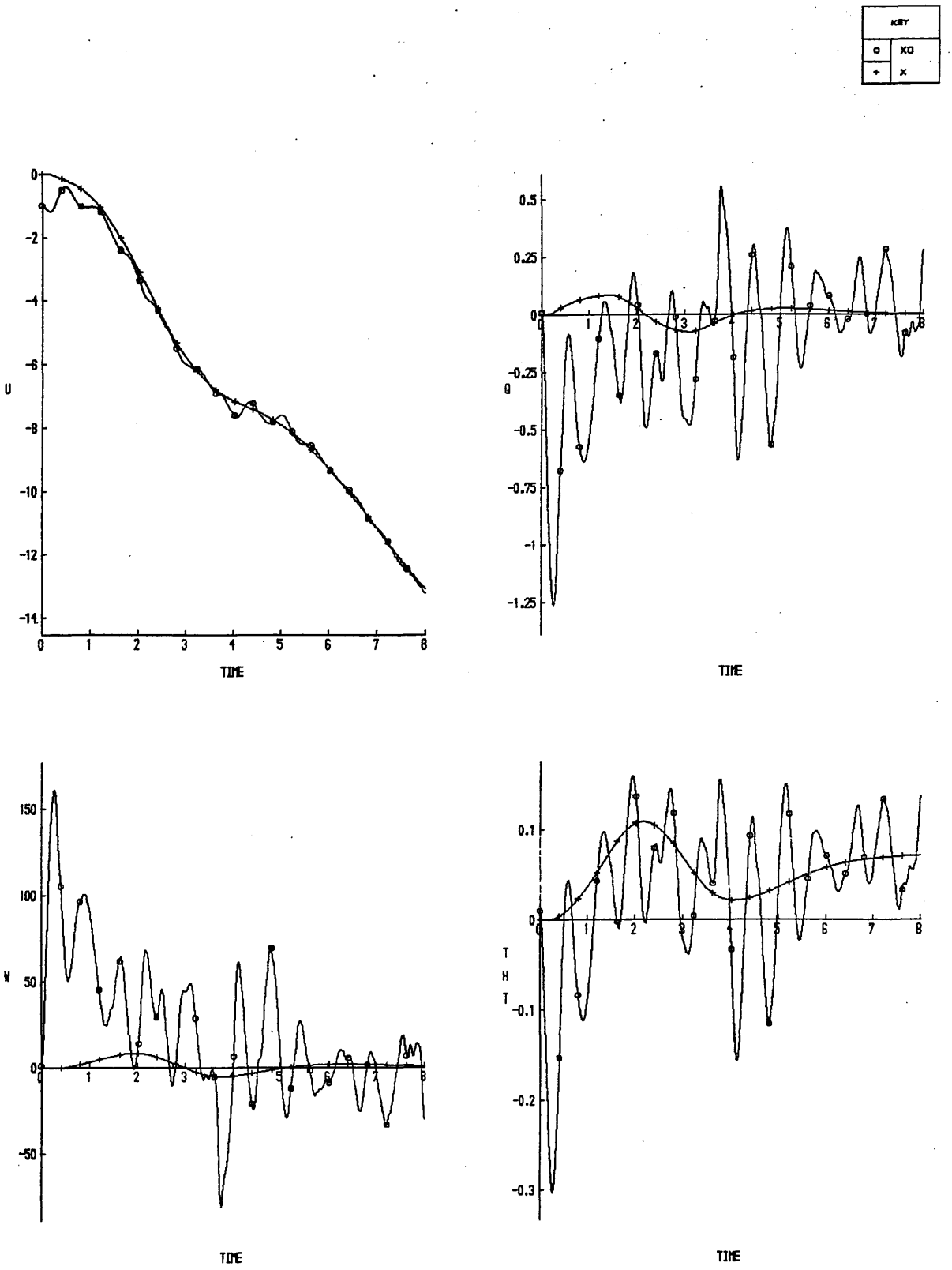

FIG 6.17B OBSERVER RESPONSE TO NOISY STATES WITH FILTER IN FEEDBACK LOOP: C(1,4)

6.9 THE TWIN OBSERVER

The system and observer are both linear and thus the outputs of the following are identical, ie. $\underset{\sim}{x}_f = \underset{\sim}{x}'$.

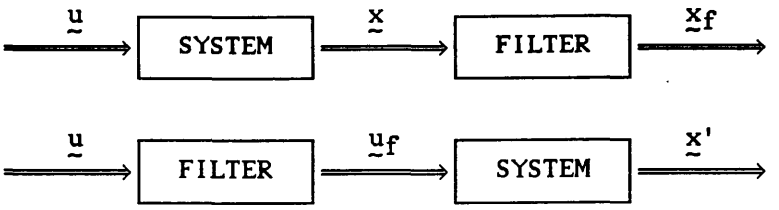

Therefore instead of having the filter in the feedback loop of the observer (*fig 6.15*), it was used to filter the input (*fig 6.18*). With this filter, but no filter on the system output, the observer estimate lags the system state. With a filter added to the system output the result is the same, but the observer estimate $\hat{\underset{\sim}{x}}$ and the filtered output of the system, $\underset{\sim}{x}_f$, are in phase.

The importance of this is that the error term is therefore zero, whereas when only one filter is used (either on the observer input or the system output) the error term is non–zero due to the lag introduced by the filter. It is the lag on this non–zero error vector which causes the observer estimate to lag the state of the system.

The solution is simple, but effective: use the *in–phase* error term produced by an observer using two filters, to drive a second observer with no filters, *fig 6.19*. The equations of the system and observers are thus,

$$\dot{\underset{\sim}{x}} = \underset{\sim}{A}\underset{\sim}{x} + \underset{\sim}{B}\underset{\sim}{u} \tag{6.12}$$

$$\dot{\hat{\underset{\sim}{z}}}_1 = \tilde{A}\hat{\underset{\sim}{z}}_1 + \tilde{B}\underset{\sim}{u}_f + H(F^{-1}C\underset{\sim}{x}_n - C_o\hat{\underset{\sim}{z}}_1) \tag{6.13}$$

$$\dot{\hat{\underset{\sim}{z}}}_2 = \tilde{A}\hat{\underset{\sim}{z}}_2 + \tilde{B}\underset{\sim}{u} + \underset{\sim}{e}_{z1} \tag{6.14}$$

Where e_{z1}, the error term driving observer 1, is,

$$\underset{\sim}{e}_{z1} = H(F^{-1}C\underset{\sim}{x}_n - C_o\hat{\underset{\sim}{z}}_1) \tag{6.15}$$

and the estimate of the system state $\underset{\sim}{x}$ is obtained from observer 2,

$$\hat{\underset{\sim}{x}} = S^{-1}\hat{\underset{\sim}{z}}_2 \tag{6.16}$$

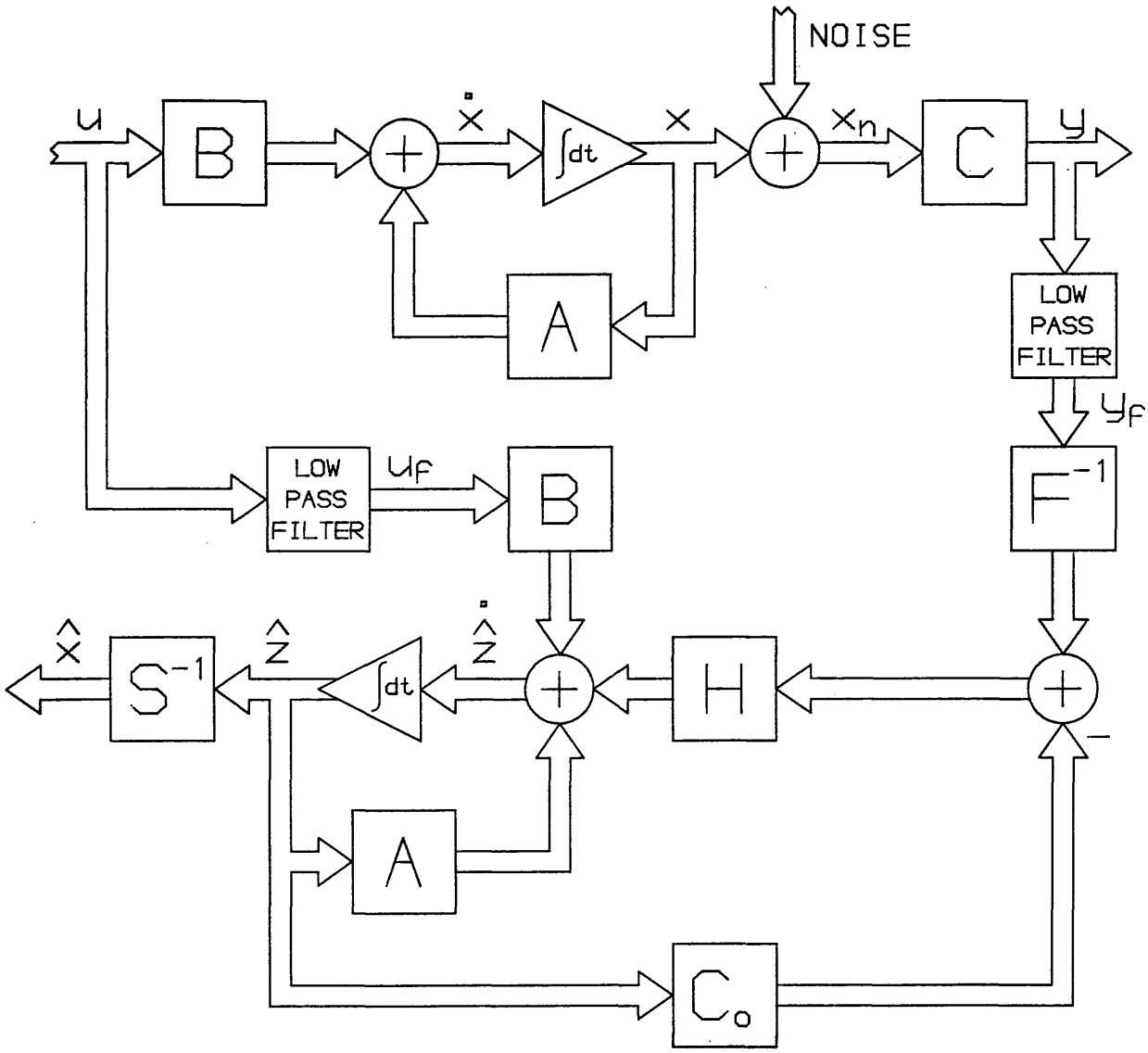

FIG 6.18 LOW PASS FILTER ON OBSERVER INPUT

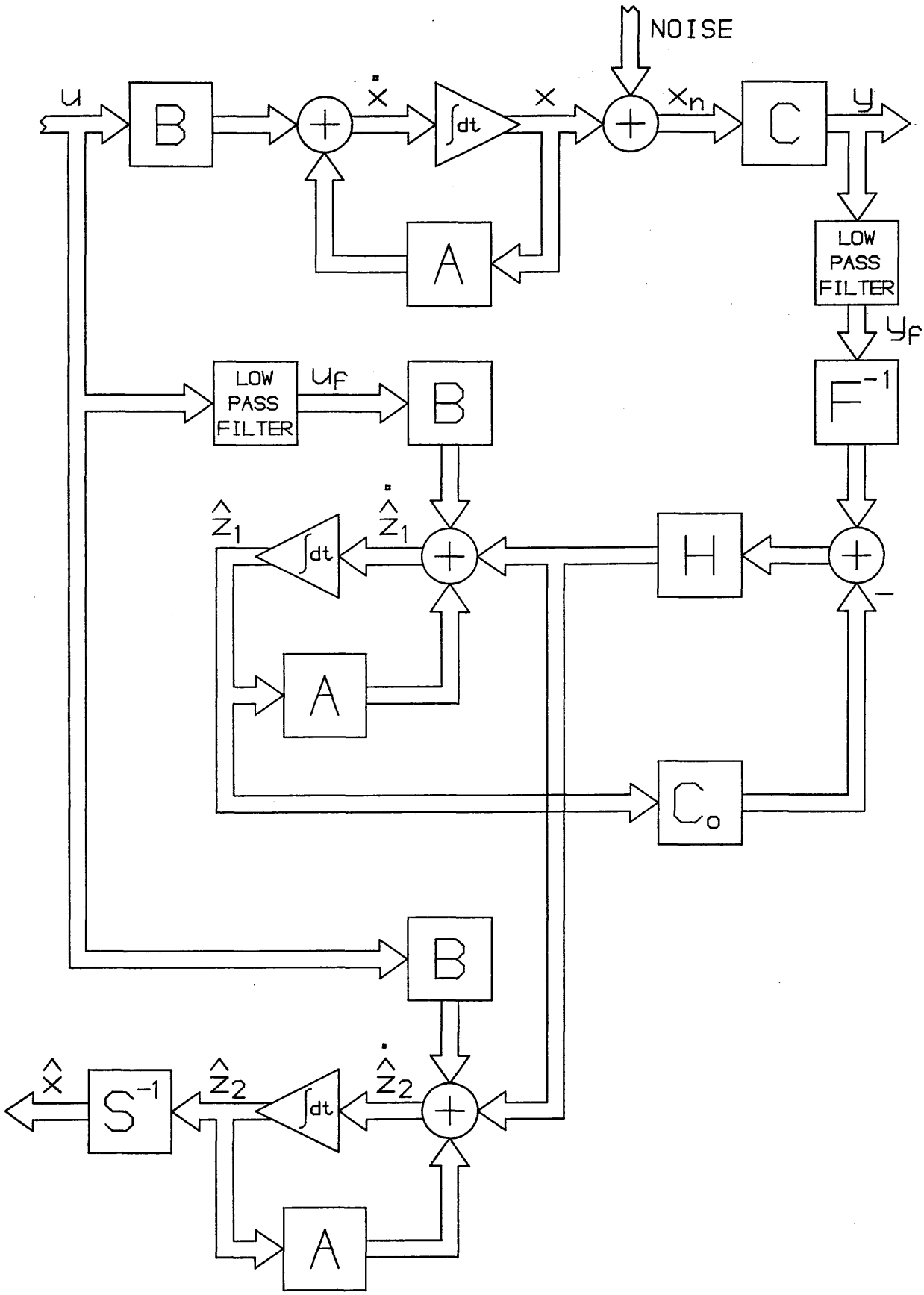

FIG 6.19 THE TWIN OBSERVER

6.9.1 RESULTS

The simulations were run using the same flight condition and input as in the previous cases and the observer eigenvalues were EV2. Both low pass filters had the same value of τ and this was varied from 0.2 to 1.6 in steps of 0.2. At every step a simulation was run for each of the ten C matrices.

Fig 6.20 shows the results for $\tau = 0.2$, 0.8 and 1.6 for C(3,4) and C(1,4). It can be seen that the observer estimate and system state are in phase and that any noise on the estimates is reduced as τ increases. *Fig 6.20(g)* demonstrates the reduction in error as τ increases, in the estimation of state q produced from C(1,4). Also note that as τ increases any overshoots remain the same. With $\tau = 1.6$ the only observer estimate which would fail the correlation test was that produced by C(1,4).

The test was repeated with a fourth order lateral model of the Puma at 100 Knots, level, for which the A and B matrices and system eigenvalues are,

$$A = \begin{bmatrix} -0.158 & -4.650 & 32.172 & -167.804 \\ -0.021 & -1.636 & 0.000 & 0.355 \\ 0.000 & 1.000 & 0.000 & -0.145 \\ 0.006 & -0.028 & 0.000 & -0.637 \end{bmatrix} \qquad B = \begin{bmatrix} 31.673 & 16.157 \\ 25.349 & 5.329 \\ 0.000 & 0.000 \\ 0.516 & -9.542 \end{bmatrix}$$

-1.86

$-0.21 \pm j1.1$

-0.16

Observer eigenvalues of 2X and 4X the largest system eigenvalue, with 2% steps, were thus,

EV3 : [-3.72, -3.79, -3.87, -3.94]

EV4 : [-7.44, -7.59, -7.74, -7.89]

The control input was a doublet on θ_{0t} (Appendix six) and initial errors in the observer estimates were established by setting

$\hat{v}(t_0) = 2.0 \qquad \hat{\varphi}(t_0) = 0.04$

$\hat{p}(t_0) = 0.02 \qquad \hat{r}(t_0) = -0.015$

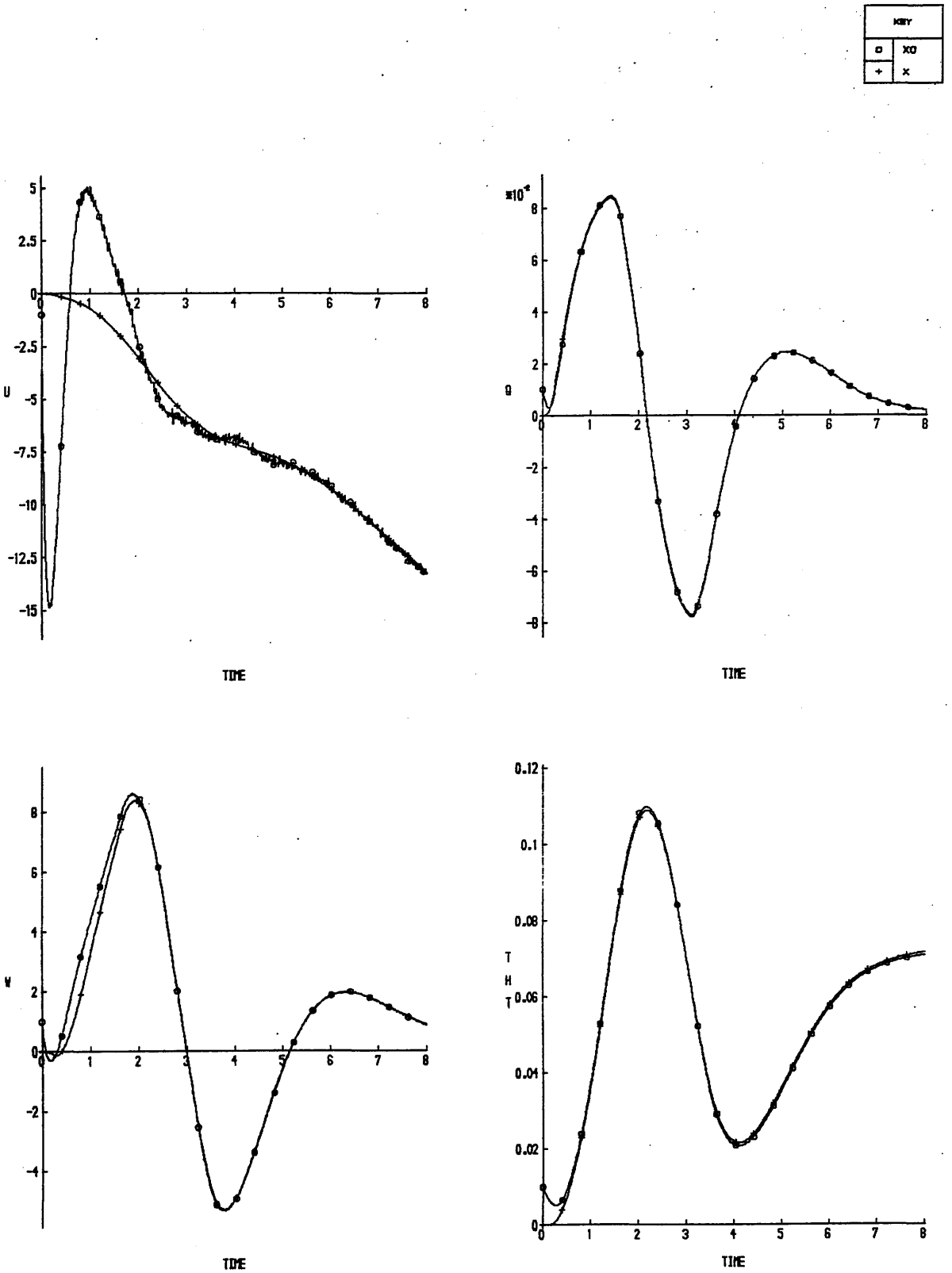

FIG 6.20A RESULTS USING THE TWIN OBSERVER; C(3,4), τ=0.2

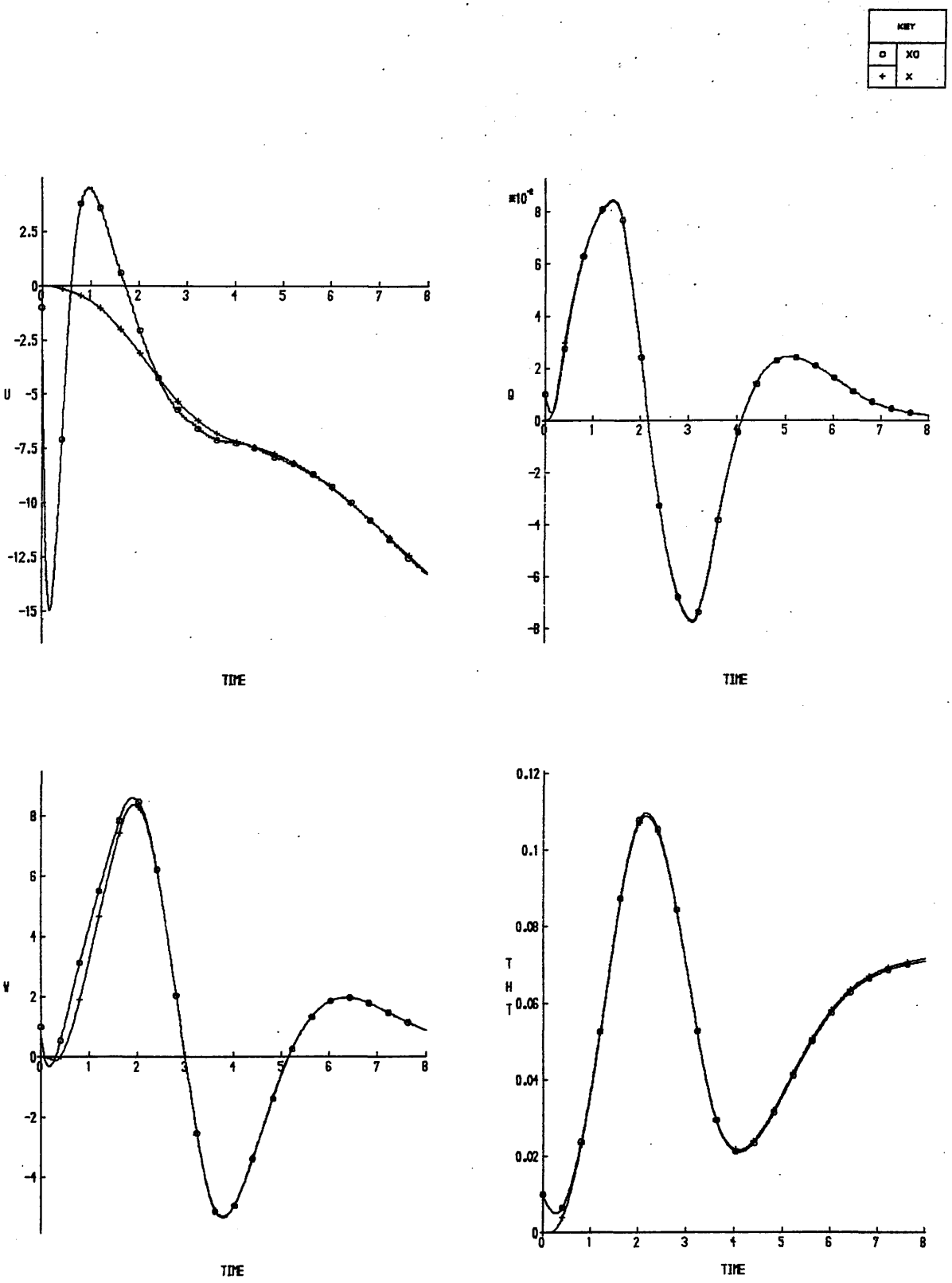

FIG 6.20B RESULTS USING THE TWIN OBSERVER: C(3,4), τ=0.8

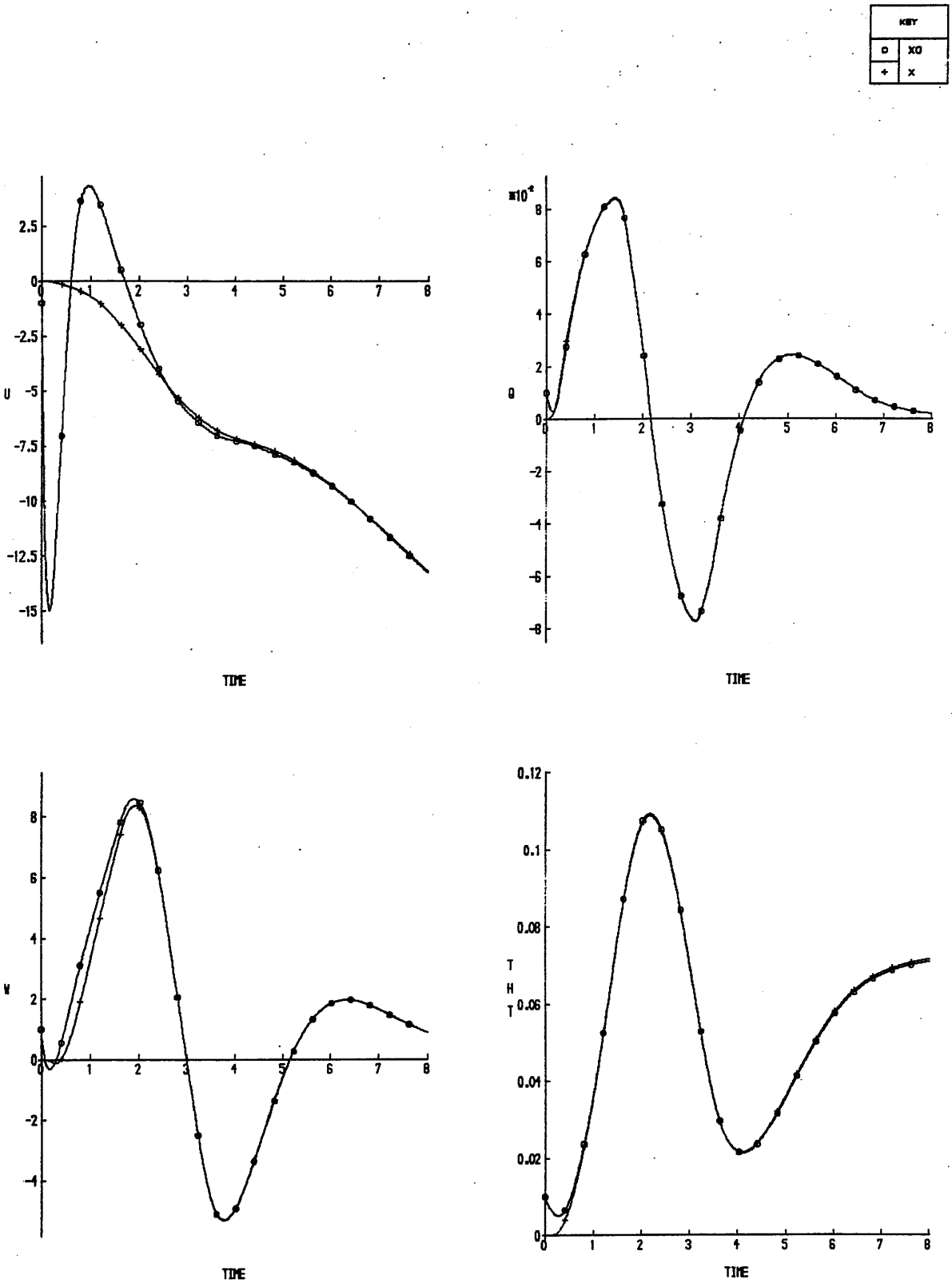

FIG 6.20C RESULTS USING THE TWIN OBSERVER: C(3.4), τ=1.6

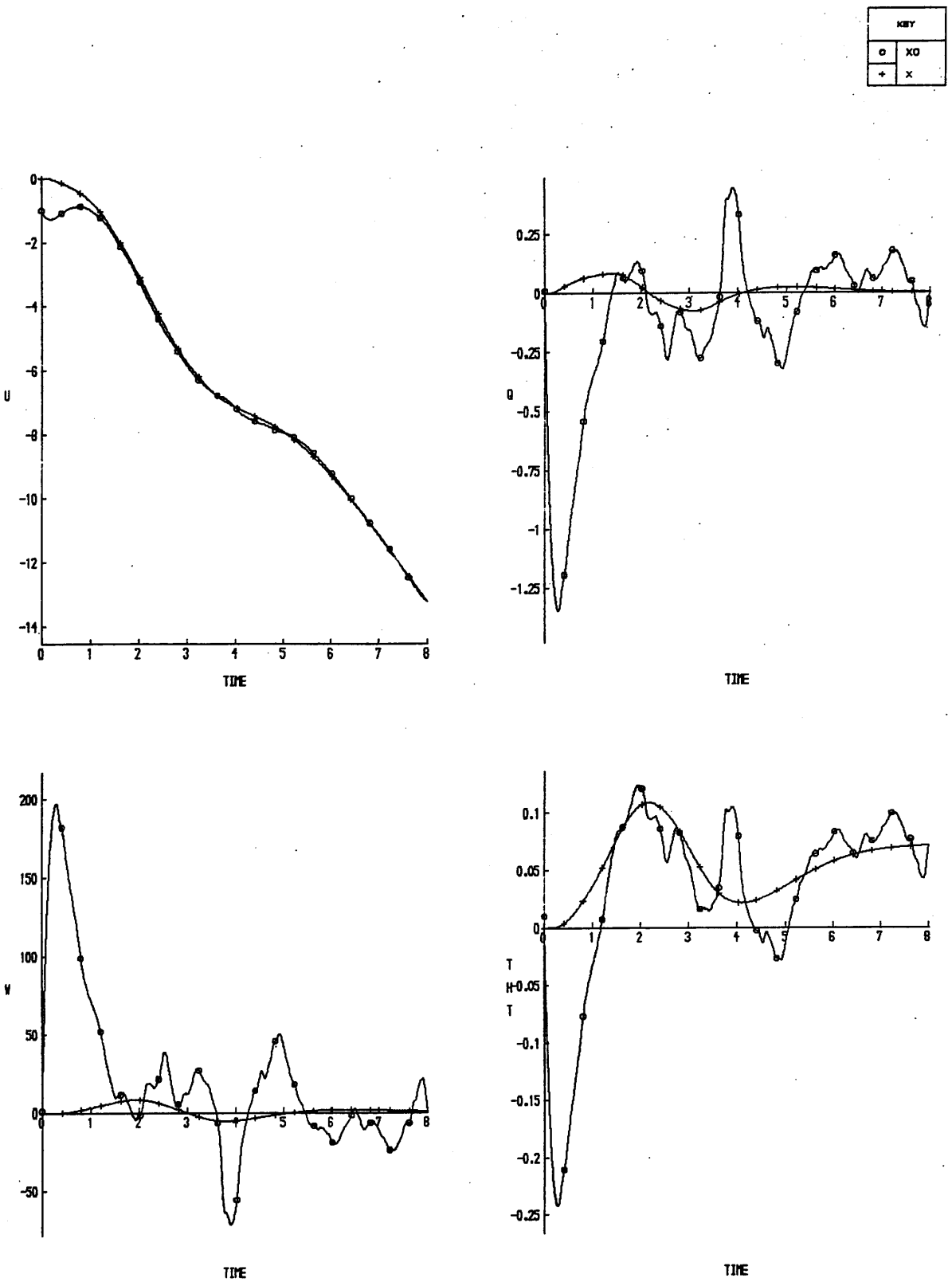

FIG 6.20D RESULTS USING THE TWIN OBSERVER: C(1,4), τ=0.2

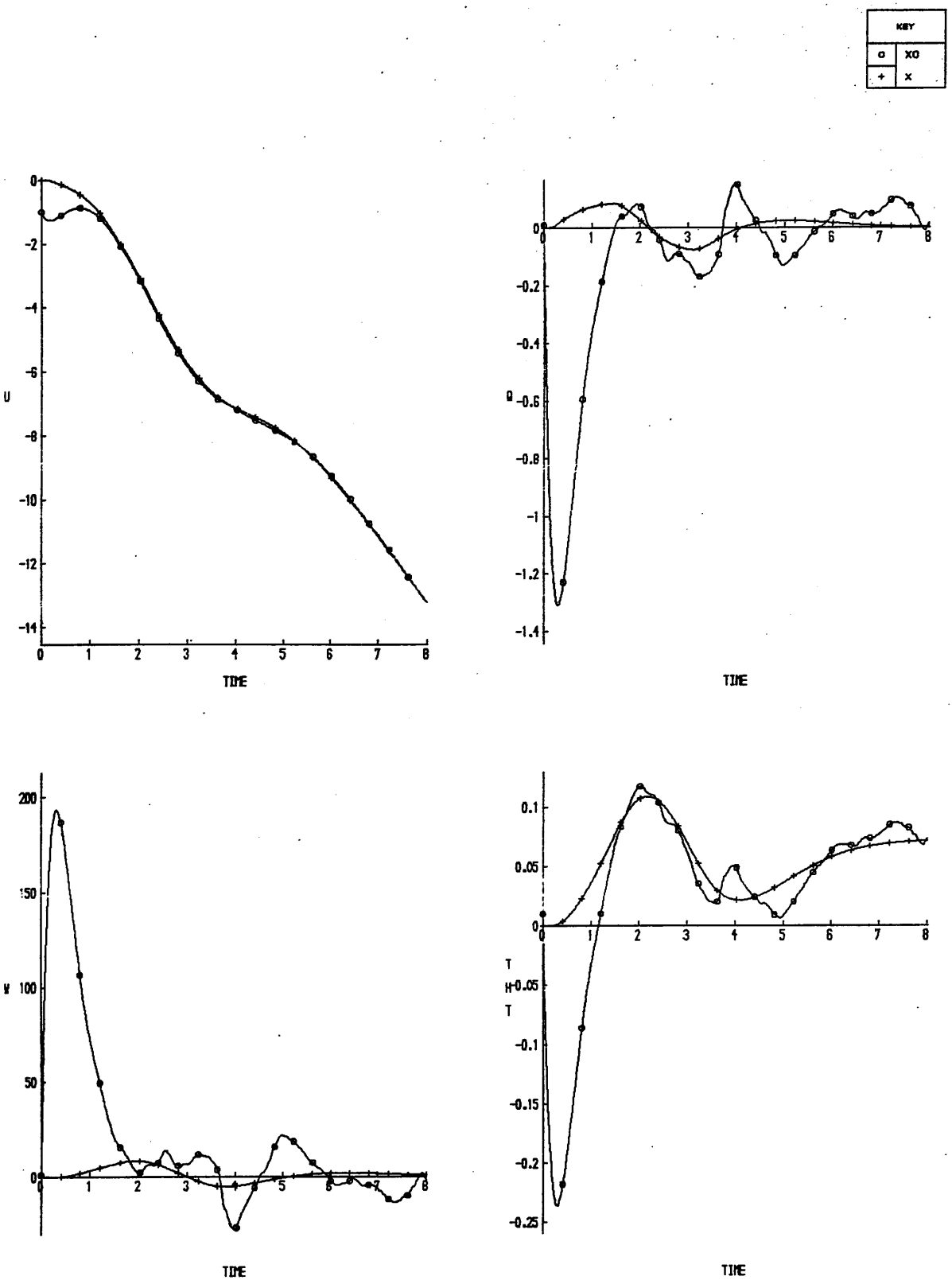

FIG 6.20E RESULTS USING THE TWIN OBSERVER: C(1.4), τ=0.8

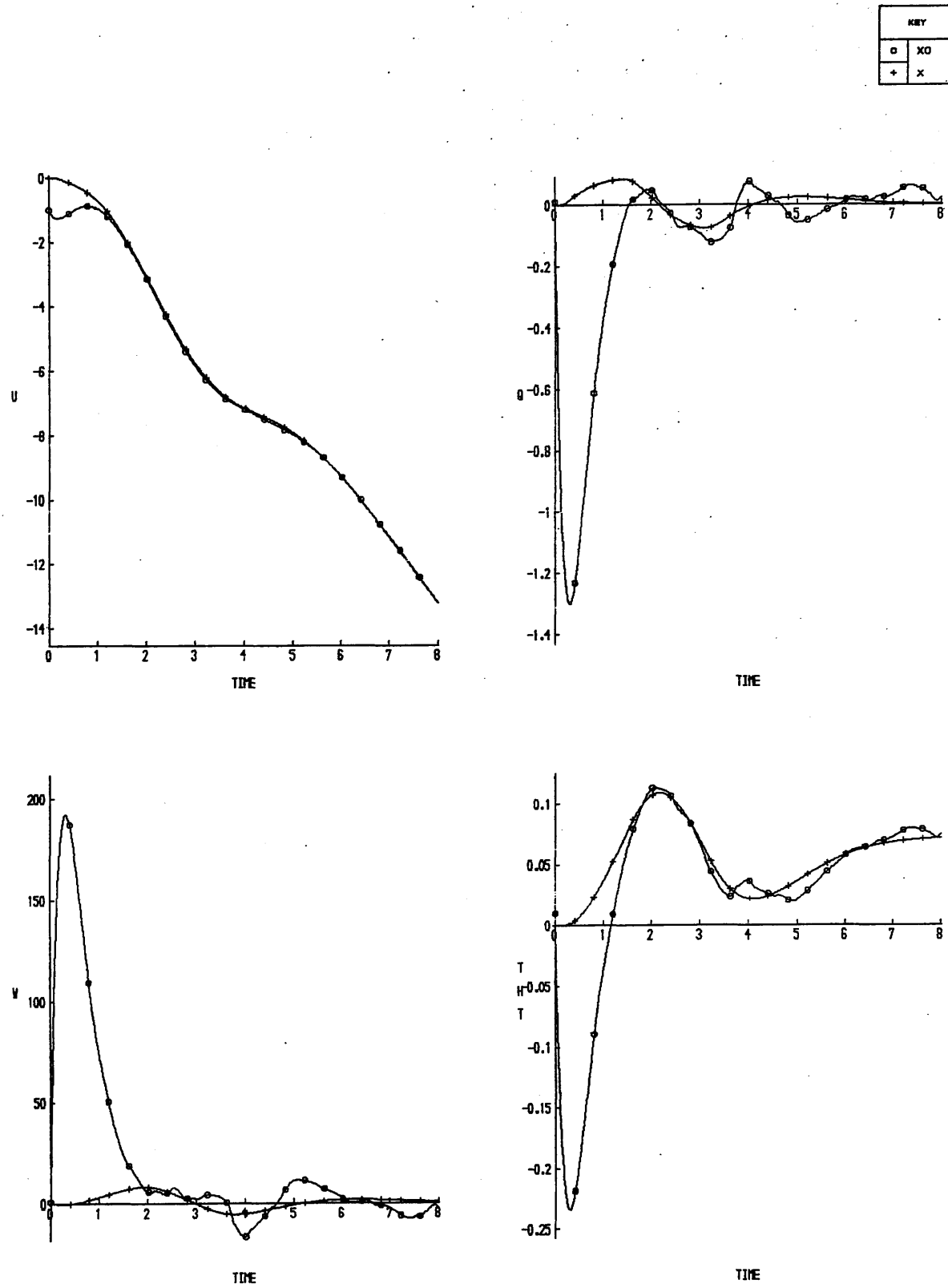

FIG 6.20F RESULTS USING THE TWIN OBSERVER: C(1.4), τ=1.6

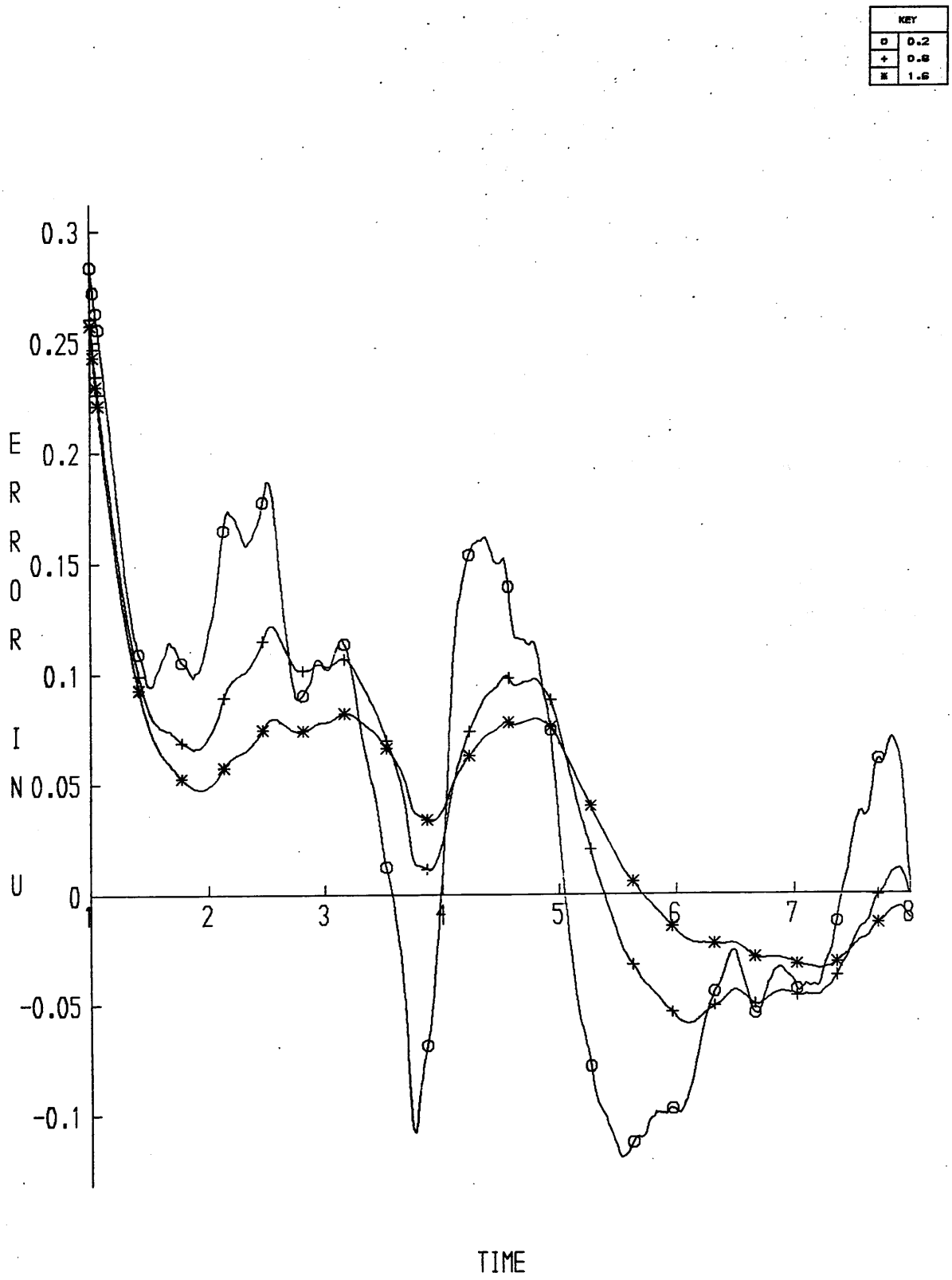

FIG 6.20G ERROR IN u AS τ VARIES

Noise was added to the model generated states at full noise power (*fig 6.21*). Each experiment was carried out with ten C matrices,

C(5)	C(5,6)	C(6,7)	C(7,8)
C(6)	C(5,7)	C(6,8)	
C(7)	C(5,8)		
C(8)			

The results were very similar to those obtained with the longitudinal model, but with one important exception. With the longitudinal model there was no apparent difference in performance between the use of one or two instruments, ie. C(i) or C(i,j), however with the lateral model the use of two instruments generally provided the better performance.

For example, consider *fig 6.22* which gives the results obtained for C(5), C(7) and C(5,7), with $\tau = 0.2$ and observer eigenvalues EV4. It can clearly be seen that by combining the two instruments both the noise content and magnitude of overshoot have been significantly reduced.

Thus with either a longitudinal or a lateral model, the use of the twin observer has alleviated the problem of noise on the instrument signals. Time did not permit further investigation of this solution, however the obvious areas for further research are the evaluation of a more sophisticated filter and the implementation of the twin observer on an eighth or fourteenth order model.

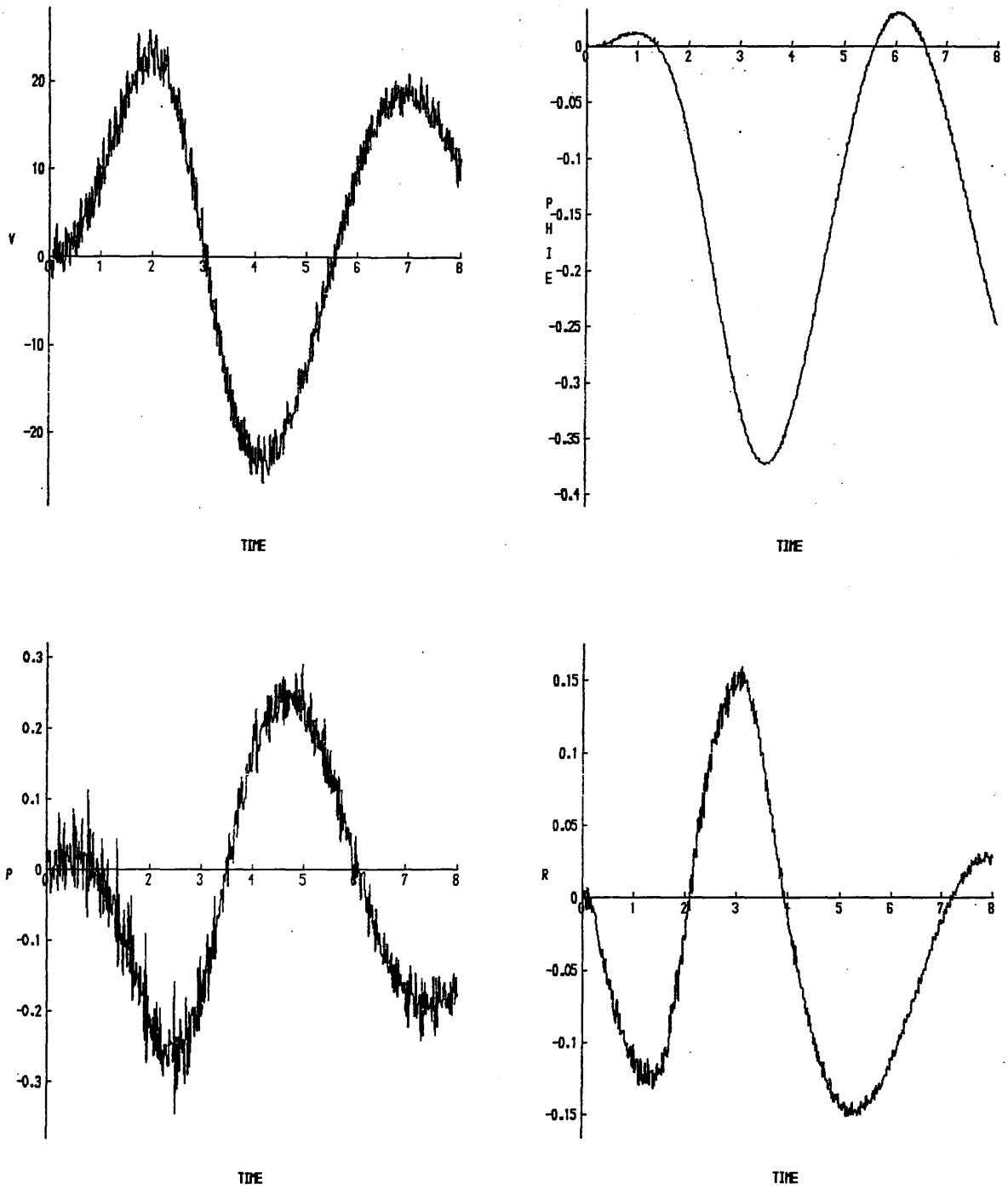

FIG 6.21 NOISE ADDED TO LATERAL STATES

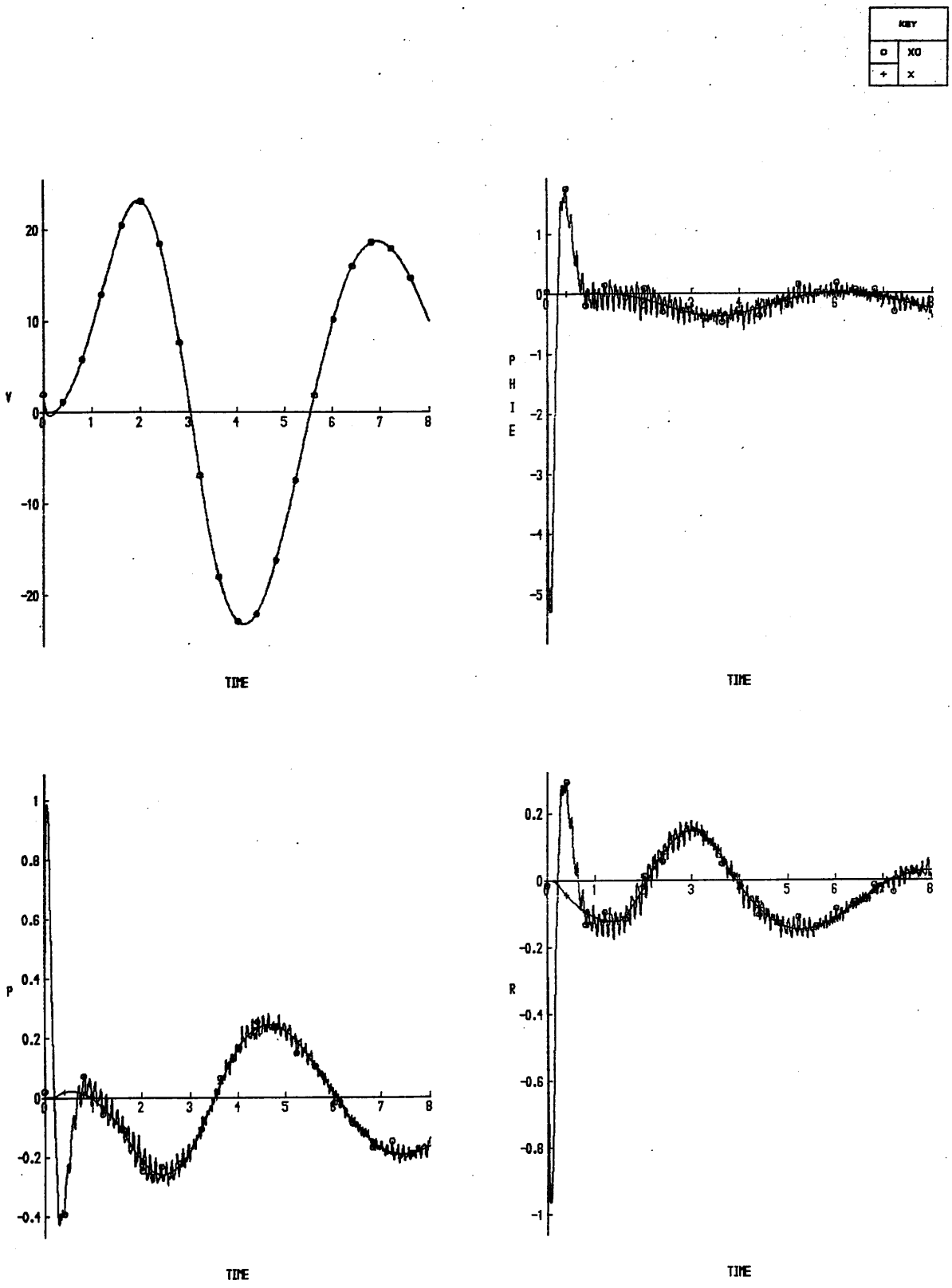

FIG 6.22A THE TWIN OBSERVER WITH A LATERAL MODEL: C(5)

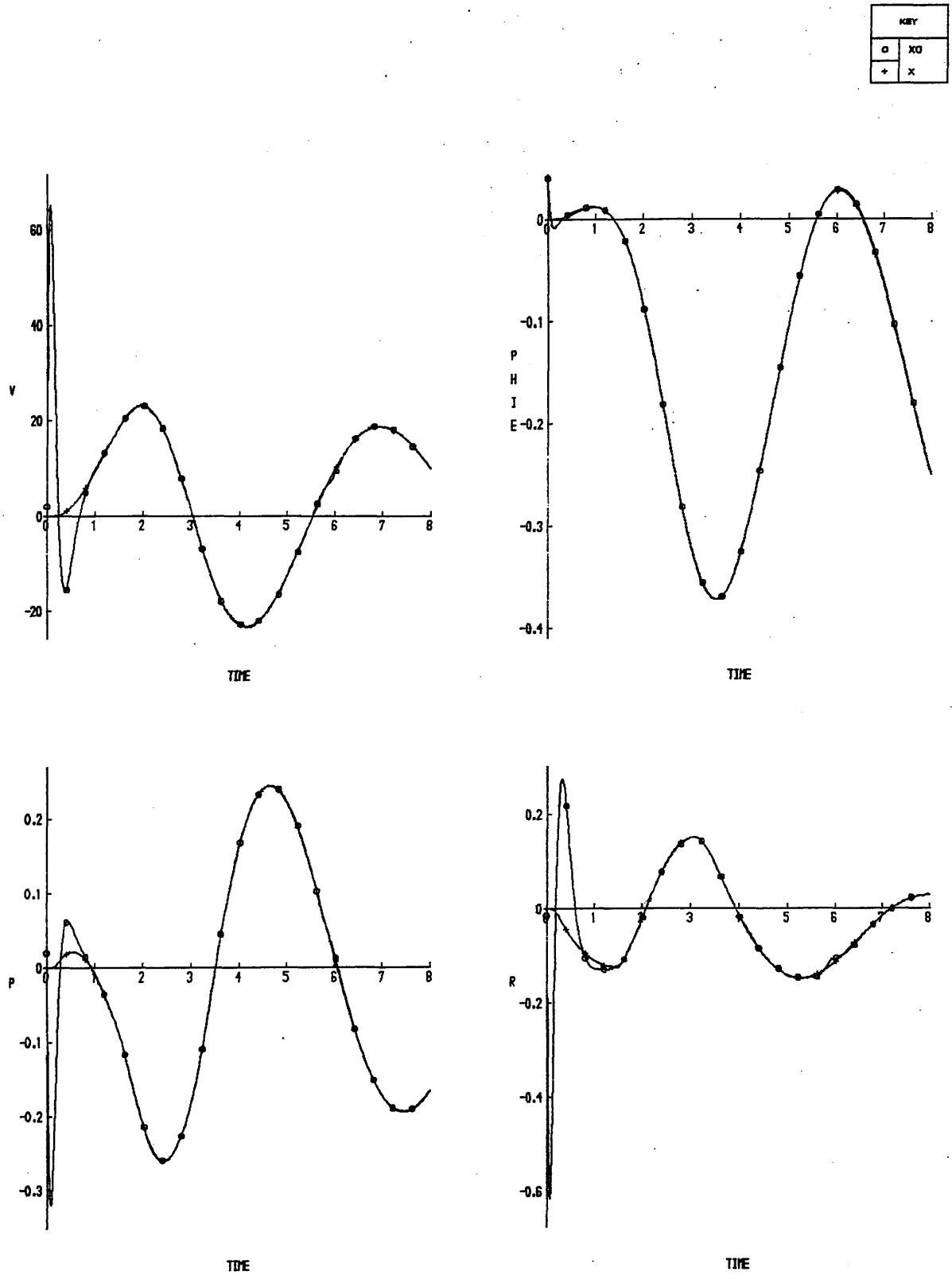

FIG 6.22B THE TWIN OBSERVER WITH A LATERAL MODEL: C(7)

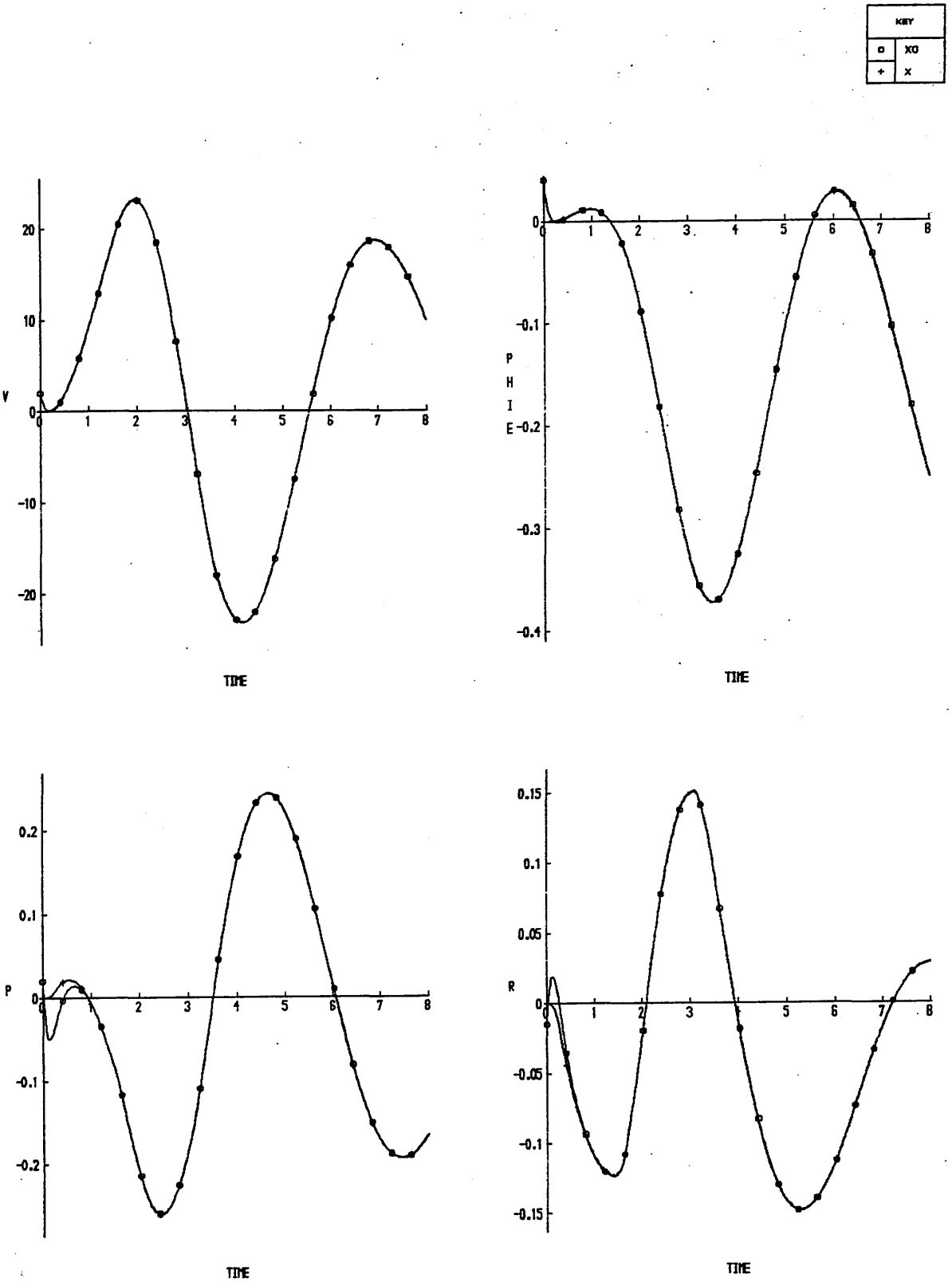

FIG 6.22C THE TWIN OBSERVER WITH A LATERAL MODEL: C(5,7)

CHAPTER SEVEN

INSTRUMENT FAULT DETECTION

7.1 INSTRUMENT FAULT DETECTION TECHNIQUES

The idea that an instrument failure in a dynamical system can be identified from the readings of other, dissimilar, instruments in the same system is as old as the art of flying aircraft 'by instruments'. However, the idea of so detecting instrument failures in automatic control systems, on line, so that corrective action can be taken in time to prevent loss of control, is relatively recent and mainly due to the introduction of *Active Control Technology systems* (ACT), eg. Wyatt, 1984; Richards. W; Winter, Padfield and Buckingham, 1984). Failure of these systems, particularly in aerospace applications, may have catastrophic consequences and therefore the problem of failure detection and accommodation has become of critical concern.

Hardware is often the main problem: processors may compute erroneous results or stop altogether, memory and sensors may return incorrect values; communication lines may corrupt information or lose it and actuators may stop working or become inaccurate. A single component might fail or an entire computer with its memory and communication lines might be disabled, as in an onboard fire or a strike by anti–aircraft guns, shrapnel, etc. Even if the computing system itself is flawless, it may still fail because of environmental effects such as power fluctuations or excessive heat.

If a system is to be reliable, it should therefore tolerate the faults that still arise in spite of all efforts to eliminate them. Redundancy in many forms is the means of keeping such faults from interfering with the systems planned reliability. Initially *Hardware Redundancy* was used on fixed–wing aircraft with *fly–by–wire* (FBW) systems: usually four lane (*Quadruplex*), eg. Korte, 1984, or three lane (*Triplex*) with self–monitoring, eg. Wyatt, 1984.

This provides an accurate and robust method: failure detection being decided by a simple *majority vote* logic system, but has the disadvantages of increased weight (with obvious impact on performance), utilisation of valuable space, increase in electromagnetic radiation and, perhaps most importantly, increased expense due to the high cost of avionics.

In recent years attention has therefore concentrated on *Software Redundancy*, which has been given many different names: *Functional Redundancy*, *Analytical Redundancy*, *Inherent Redundancy* and *Artificial Redundancy*, being the most common. The advantages of software redundancy lie in the trade–off of redundant hardware against computer processing of signals from dissimilar (non–redundant) sensors.

The techniques of software redundancy can be divided into two categories – time series analysis and state estimation. With time series analysis (see for example, Willsky and Jones, 1976; Madiwale and Friedland, 1983; Bonnice, Motyka, Wagner and Hall, 1976) the length of time sequence required for analysis results in large delays between the occurrence and detection of a fault and is therefore impracticable for the majority of aerospace applications. State estimation on the other hand, allows detection of even small faults, almost instantaneously.

Under the heading of state estimation four main methods of instrument fault detection have emerged: the *Dedicated Observer Scheme* (DOS), the *Failure Detection Filter*, the *Unknown Input Observer* and the *Disturbance Rejection Filter*. These are described below.

An unusual method involving the use of observer theory and predictive techniques is presented by McLean and Al–Khatib, 1984. This method uses a prediction technique based on information received from state measurements to provide the necessary analytical redundancy for the failure detection scheme.

THE DEDICATED OBSERVER SCHEME

The dedicated observer scheme was introduced by Clark, Fosth and Walton, 1975 and is the simplest of the four instrument fault detection methods. A DOS requires only one set of instruments, since the redundancy provided by multiple sets of instruments in the traditional scheme is provided, artificially, in the control computer, by a subsystem of multiple observers.

Assuming that the single set of instruments consists of three or more individual sensors, the output signal from each sensor is used to drive an observer which is especially designed for that sensor. Since each observer estimates the state vector of the system, there is redundancy in state vector estimates and these can be compared in a logical voting manner. If all the sensors are perfect, and if the dynamic parameters of the system are known exactly, then all the estimated state vectors will converge quickly to the real state.

However, if one of the sensors is in error, then the state vector estimated by its observer will also be in error, and so a comparison among the estimated states will identify the faulty sensor. A fault is indicated when the difference between two estimates exceeds some predetermined, non–zero, threshold value.

Since 1975 Clark has published a number of papers describing his DOS and its applications: a hydrofoil boat ([C5]–[C7], [C9]), inverted pendulum ([C10]), an A7 jet aircraft ([C11]) and a Boeing 737 ([C12]). In [C5] a simple majority voting scheme was used to identify any single fault. A simplified version of this, in which only one observer is required, is investigated in [C6]. In this scheme detection of a failure is accomplished by a logic circuit which simply compares the estimated instrument outputs to the actual instrument outputs.

In [C13] this scheme is expanded to include a random disturbance entering as an additive augmentation to the control inputs. In addition, a Kalman filter (driven by a single instrument) is used as the dedicated observer. A dedicated observer scheme using multiple Kalman filters was successfully tested on an altimeter in [C12]. Similarly, Kitamura, 1980, used Kalman filters for an instrument fault detection scheme in a nuclear plant.

More recently, Frank *et al* have expanded the basic dedicated observer scheme in an effort to reduce the detrimental effects of parameter variations and noisy inputs, whilst maximising the sensitivity to instrument faults. For example, in Frank and Keller, 1980, duplication of observers allows distinction between parameter variations and instrument faults. The first observer of the pair is designed to be insensitive to parameter variations and instrument faults, whereas the second one is made insensitive to parameter variations only, but sensitive to instrument failures.

Thus the difference of the outputs of the two observers is only sensitive to instrument faults. The observer designs are optimised for their specific purpose by the use of quadratic cost functionals and it is shown that this form of scheme can deal with parameter variations of up to 50%. Robustness tests carried out by Clark in [C5] and [C6], indicate that the 'standard' dedicated observer scheme can only accommodate parameter changes of up to 10%. Other papers by Frank on this topic are: Frank, 1986; Hengy and Frank; Wunnenberg and Frank; and Madbouly and Frank.

THE FAILURE DETECTION FILTER AND THE UNKNOWN INPUT OBSERVER

Failure detection filters were first developed by Beard, 1971 and Jones, 1973. They have an identical structure to the Luenberger observer and in the absence of faults the estimation error vector will reduce to zero. This difference between this type of observer and the Luenberger observer is in the behaviour of the estimation error vector in the presence of a fault.

With the Luenberger observer the error vector will have some unpredictable direction, however in the failure detection filter the error vector is fixed for a particular sensor fault. Thus by examination of the direction of the estimation error vector, the faulty sensor can be identified. The association between the direction of the error vector and the corresponding faulty sensor is fixed during the design of the observer gain matrix, H, and is accomplished using complex eigenstructure assignment (see Section 4.1.2).

Another technique proposed recently is that of the unknown input observer (Wunnenberg and Frank). The fundamental concept behind this form of observer is that the estimation error vector should be independent of the effects due to parameter variations and disturbance inputs. In the design of the observer the disturbances acting on the system need not be modelled, however a well defined disturbance distribution matrix must be established. Unfortunately, for most real systems this constraint makes the unknown input observer extremely difficult, if not impossible, to design and implement.

THE DISTURBANCE REJECTION FILTER

The major problem with the above state estimation techniques for instrument fault detection, is that they all require an accurate linear model of the system for their correct operation. It is also assumed that system disturbances are well modelled or else have an insignificant effect on plant parameter variations.

When these assumptions are not valid, which is the case in most real applications, the observer error vectors will be non-zero, even in the absence of a fault, and this may result in false triggering of alarms. The fault detection logic which processes the redundant state estimate vectors must therefore allow for this and the solution is often to simply increase and/or vary the threshold value.

However, a new robust approach – the *Disturbance Rejection Filter* – has recently been advanced by Patton, Willcox and Winter, 1987 and Willcox, 1988, which utilises the fact that in the non-ideal situation, the observer error signal contains all the information about parameter variations and disturbance inputs. Thus, by using a weighting of the observer error as a parity signal, it is possible to identify faults without the need to generate the complete state vector.

The *Parity Space* approach has previously been used by other authors, eg. Beard, 1971; Deckert, Desai, Deyst and Willsky, 1977; Chow and Willsky, 1984, but with

this method two new features have been developed. These are the application of the *Output Zeroing problem* (McFarlane and Karcanias, 1976; El–Ghezawi, Billings and Zinober, 1983) to the estimation error space (ie. the eigenstructure of each observer is designed such that a weighted combination of the error signals of each observer gives a 'null signal' in the no–fault condition) and the consideration of frequency domain parameter sensitivity to construct frequency discriminating properties into the observer error space dynamics.

In many applications the required frequency domain information about parameter variations and disturbance inputs is already available. Alternatively, the information may be obtained from the desired control characteristics and/or from frequency domain identification techniques, eg. Andry, Shapiro and Chung, 1984; Juang and Suzuki, 1986; Black, Murray–Smith and Padfield, 1986.

In Willcox 1988, the disturbance rejection filter was successfully tested on an inverted pendulum servo mechanism and an unmanned aircraft. It was shown that the robustness of the design allowed low threshold values to be used and consequently the rapid detection of faults.

7.2 THE DEDICATED OBSERVER SCHEME

In chapter six a new form of observer – the twin observer – was developed and successfully tested. It was demonstrated that with an accurate model of the system, the twin observer could produce an accurate relatively noise free estimate of the system state, even when the inputs to the observer were corrupted by noise. The next step was therefore to determine whether this form of observer was suitable for instrument fault detection. From section 7.1 it is apparent that the only applicable technique is that of the dedicated observer scheme, since the other three methods all involve specific observer designs.

The dedicated observer scheme (*fig 7.1*) only requires a single set of instruments, each of which drives an observer specifically designed for that instrument. Since each observer estimates the complete state vector there is redundancy in the state vector estimates and these are processed by a logic scheme to allow detection of instrument faults. The logic scheme proposed by Clark is relatively simple and best illustrated by example.

Consider a fourth order, noise free, longitudinal model being monitored by four instruments, each of which drives an observer. There are therefore four estimates of

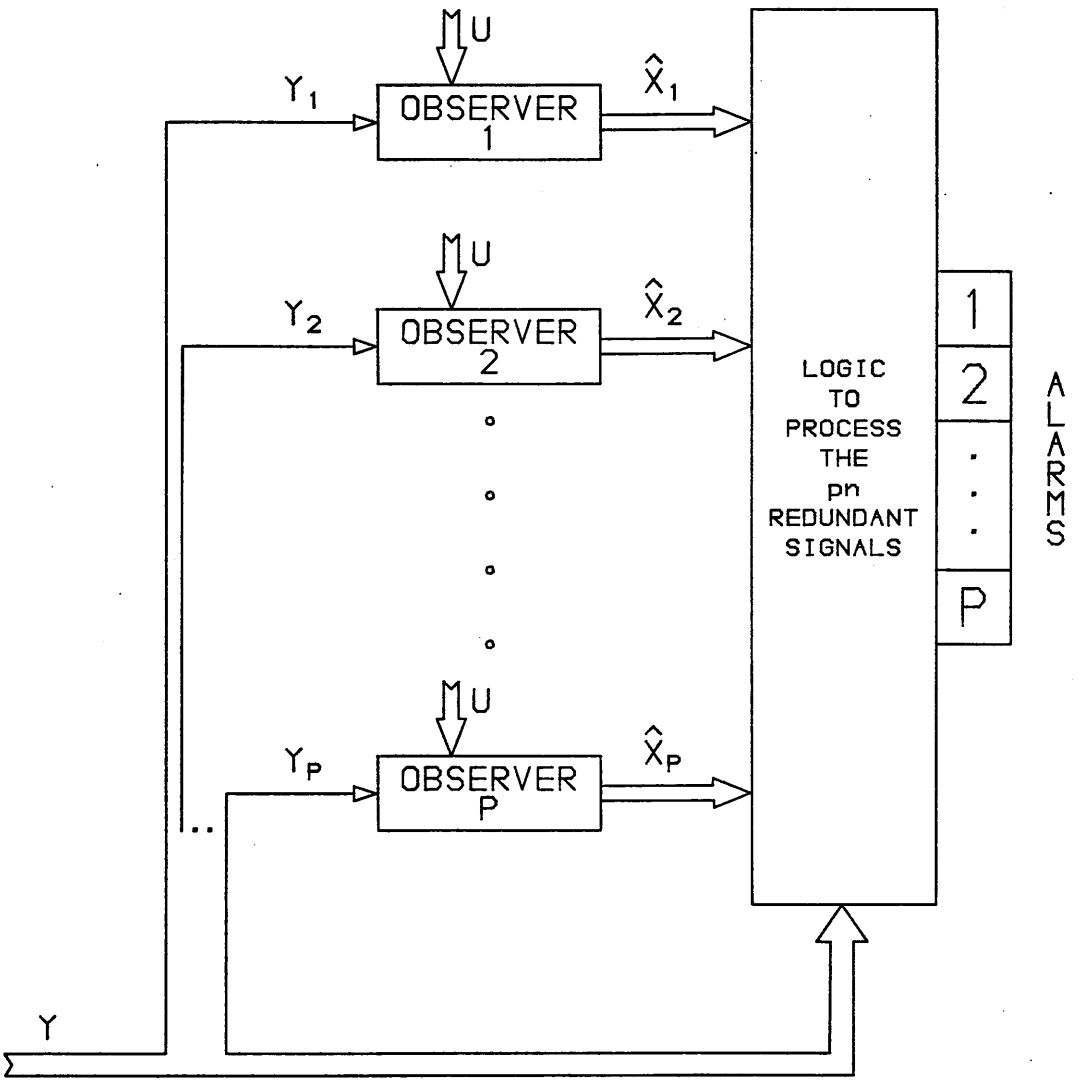

FIG 7.1 THE DEDICATED OBSERVER SCHEME

the system state: $\hat{\underset{\sim}{x}}_1$, $\hat{\underset{\sim}{x}}_2$, $\hat{\underset{\sim}{x}}_3$ and $\hat{\underset{\sim}{x}}_4$; where each $\hat{\underset{\sim}{x}}_i = [u, w, q, \theta]^T$ If six difference equations, $\underset{\sim}{a}_i$, are defined as,

$$\left.\begin{aligned} \underset{\sim}{a}_1 &= | \hat{\underset{\sim}{x}}_1 - \hat{\underset{\sim}{x}}_2 | & \underset{\sim}{a}_4 &= | \hat{\underset{\sim}{x}}_2 - \hat{\underset{\sim}{x}}_3 | \\ \underset{\sim}{a}_2 &= | \hat{\underset{\sim}{x}}_1 - \hat{\underset{\sim}{x}}_3 | & \underset{\sim}{a}_5 &= | \hat{\underset{\sim}{x}}_2 - \hat{\underset{\sim}{x}}_4 | \\ \underset{\sim}{a}_3 &= | \hat{\underset{\sim}{x}}_1 - \hat{\underset{\sim}{x}}_4 | & \underset{\sim}{a}_6 &= | \hat{\underset{\sim}{x}}_3 - \hat{\underset{\sim}{x}}_4 | \end{aligned}\right\} \qquad (7.1)$$

then in the absence of a fault all $\underset{\sim}{a}_i$'s will be zero. However, if one, or two, instruments develop a fault then several of the $\underset{\sim}{a}_i$'s will become non-zero: Table 7.1. Note that the non-zero $\underset{\sim}{a}_i$'s for two faults is simply the union of those for the individual faults.

	NON-ZERO $\underset{\sim}{a}_i$'s					
FAULT	1	2	3	4	5	6
1	X	X	X			
2	X			X	X	
3		X		X		X
4			X		X	X
1,2	X	X	X	X	X	
1,3	X	X	X	X		X
1,4	X	X	X		X	X
2,3	X	X		X	X	X
2,4	X		X	X	X	X
3,4		X	X	X	X	X

TABLE 7.1

NON-ZERO $\underset{\sim}{a}_i$'s FOR FAULTS ON ONE OR TWO INSTRUMENTS

If the four products, $\underset{\sim}{b}_i$, are defined as,

$$\left.\begin{aligned} \underset{\sim}{b}_1 &= \underset{\sim}{a}_1 \cdot \underset{\sim}{a}_2 \cdot \underset{\sim}{a}_3 & \underset{\sim}{b}_3 &= \underset{\sim}{a}_2 \cdot \underset{\sim}{a}_4 \cdot \underset{\sim}{a}_6 \\ \underset{\sim}{b}_2 &= \underset{\sim}{a}_1 \cdot \underset{\sim}{a}_4 \cdot \underset{\sim}{a}_5 & \underset{\sim}{b}_4 &= \underset{\sim}{a}_3 \cdot \underset{\sim}{a}_5 \cdot \underset{\sim}{a}_6 \end{aligned}\right\} \qquad (7.2)$$

then the non−zero $\underset{\sim}{b}_i$'s will indicate a fault on the corresponding instruments. This logic will identify a simultaneous fault on two instruments, but cannot accommodate three simultaneous faults.

When noise exists on the instrument signals and when small errors are present in the model and introduced in the design of the observer, the $\underset{\sim}{a}_i$'s, and hence the $\underset{\sim}{b}_i$'s, will all be non−zero in the absence of a fault. Consequently the resolution of an instrument fault will not be perfectly sharp. In particular, all $\underset{\sim}{b}_i$'s will increase for a fault on any instrument, although the $\underset{\sim}{b}_i$'s corresponding to the faulty instruments should increase the most.

For this reason and since all pertinent information can be obtained directly from the $\underset{\sim}{a}_i$'s, the four products, $\underset{\sim}{b}_i$'s, were not used. Specific details of the implementation of a logic scheme using the six difference equations, $\underset{\sim}{a}_i$'s, are given in section 7.4.

7.3 SIMULATION OF INSTRUMENT FAULTS

In order to investigate and assess observer performance in the presence of one or more instrument faults, and to subsequently evaluate instrument fault detection logic schemes, it was necessary to simulate various types of instrument fault. Four categories of fault were selected: *scale factor, scale factor ramp, threshold* or *dead−zone* and *bias*. These are explained below.

(1) SCALE FACTOR

Scale factor faults (*fig 7.2a)* were implemented as an (n×n) matrix K_{sf} with scale factor coefficients $K_i(t)$ on the main diagonal.

$$K_{sf}(t) = \begin{bmatrix} K_1(t) & & & \\ & K_2(t) & & \\ & & \ddots & \\ & & & K_n(t) \end{bmatrix} \qquad (7.3)$$

If the instrument vector is defined as $Y_I(t)$ then

$$\underset{\sim}{Y}_I(t) = K_{sf}(t) * \underset{\sim}{Y}(t) \qquad (7.4)$$

The coefficients have a nominal value of 1.0 and therefore a fault on instrument i between time t_1 and t_2 can be simulated by setting $K_i(t_1 \rightarrow t_2)$ to a value other than

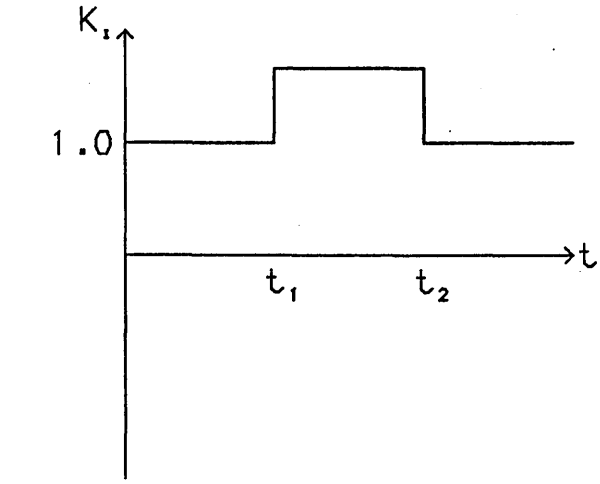

(A) SCALE FACTOR

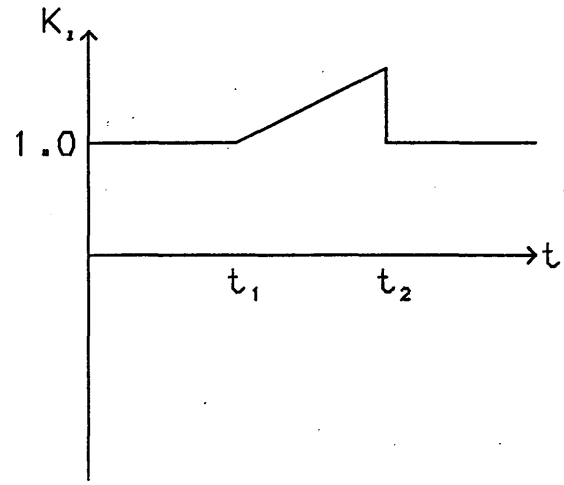

(B) SCALE FACTOR RAMP

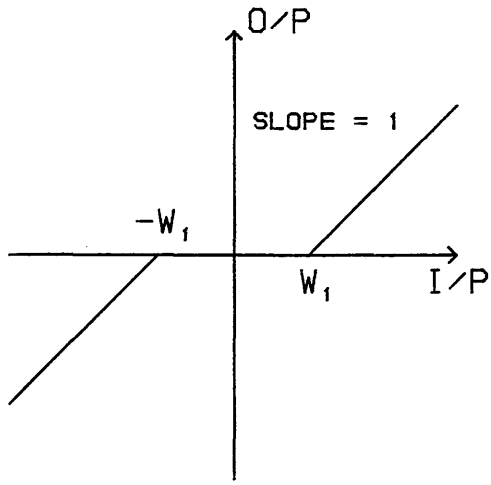

(C) THRESHOLD/DEAD-ZONE

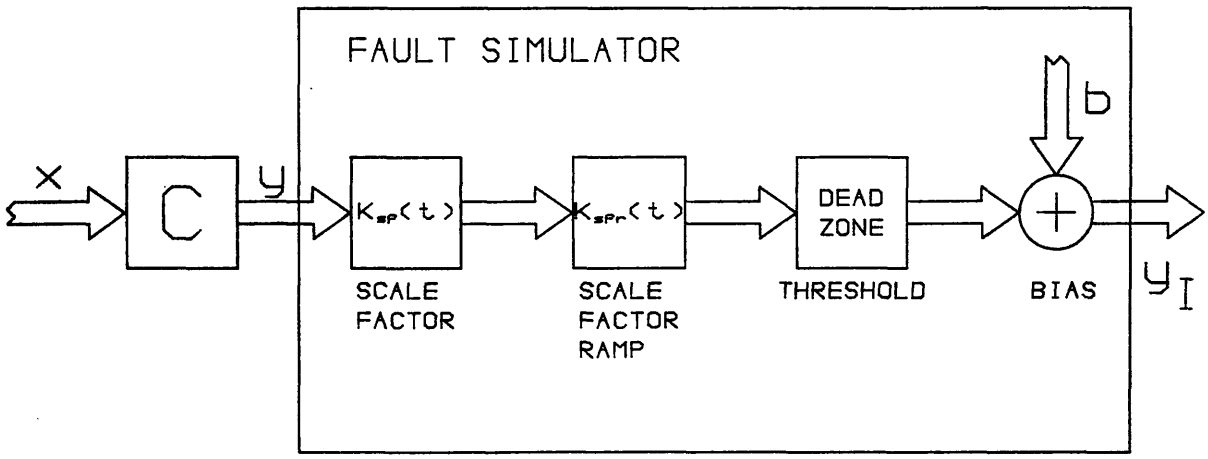

(D) IMPLEMENTATION

FIG 7.2 TYPES OF INSTRUMENT FAULT AND THEIR IMPLEMENTATION

1.0. This value is a constant between t_1 and t_2. An instrument failing completely can be simulated by setting $K_i(t_1 \rightarrow t_2) = 0$.

(2) SCALE FACTOR RAMP

Identical to scale factor except that between time t_1 and t_2 the value of K_i increases/decreases linearly from 1.0 to the specified fault level (*fig 7.2b*). This allows the simulation of an instrument which is gradually deteriorating.

$$\underset{\sim}{Y}_I(t) = K_{sfr}(t) * \underset{\sim}{Y}(t) \tag{7.5}$$

(3) THRESHOLD/DEAD–ZONE

Dead–zone element of gradient=1 (*fig 7.2c*) inserted in series with the scale factor coefficients in each instrument channel.

$$\left.\begin{array}{ll} Y_I(t) = Y(t) & Y(t) < -w \\ Y_I(t) = 0 & -w \leq Y(t) \leq w \\ Y_I(t) = Y(t) & Y(t) > w \end{array}\right\} \tag{7.6}$$

(4) BIAS

Bias errors are introduced additively and take the form of a vector $\underset{\sim}{b}$, with default value for element $b_i = 0$.

$$\underset{\sim}{b} = \begin{bmatrix} b_1(t) \\ \vdots \\ b_n(t) \end{bmatrix} \tag{7.7}$$

A bias of constant value can thus be applied between times t_1 and t_2.

$$\underset{\sim}{Y}_I(t) = \underset{\sim}{Y}(t) + \underset{\sim}{b}(t) \tag{7.8}$$

The software implementation of the various faults (*fig 7.2d*) allows complete freedom of selection: faults can occur simultaneously, overlap, on any instrument, at any time and for any duration.

7.4 INITIAL CONSIDERATIONS

In the preceding chapters the problem of observer design and their performance in noise free and noise corrupted systems, were examined and the twin observer was proposed as a solution to noise corrupted signals. The selection of eigenvalues and a value for τ were evaluated with respect to state estimation criteria, ie. rapid convergence to the system state and the fidelity of the estimate; the question is whether these criteria are compatible with instrument fault detection.

To investigate this question the fourth order longitudinal model of the Puma at 100 Knots was used (section 6.8) with observer eigenvalues EV1 and EV2: 2× and 4× the largest system eigenvalue with 2% steps. The observers were designed with C(3) and a temporary total failure of instrument three was simulated by a scale factor fault of 0 from 2 to 3 seconds. The control input was a doublet input on θ_{1S} (Appendix six) and noise was added at full noise power.

The first parameter to be examined was the eigenvalues: *fig 7.3* shows the observer response for EV1 and EV2. As would be expected from the no-fault case, the larger eigenvalues have resulted in an increase in the magnitude of error and the noise appearing on the estimate; and a reduction in the damping and the time to 'zero' error after the fault is removed. Note also, that in both cases, and for each of the four states, the initial overshoot at the time of application of the fault is much smaller than the subsequent overshoot. Furthermore, the removal of the fault can give rise to a larger error than the fault itself, eg. the error in w.

Next for consideration was the filter parameter τ and time histories were recorded for τ= 0.2, 0.4 and 0.8. These are plotted together in *fig 7.4*. It is apparent that the effect of an increase in τ is the opposite to that of an increase in eigenvalues: in other words a decrease in the magnitude of error and noise and an increase in the damping and the time to zero error.

The final variable to be assessed was the order of the low pass filters. So far a first order low pass filter has been employed,

$$\frac{Y(s)}{u(s)} = \frac{1}{1 + s\tau} \tag{7.9}$$

which has a slope of 20db/decade on a magnitude/frequency Bode plot. A second order low pass filter

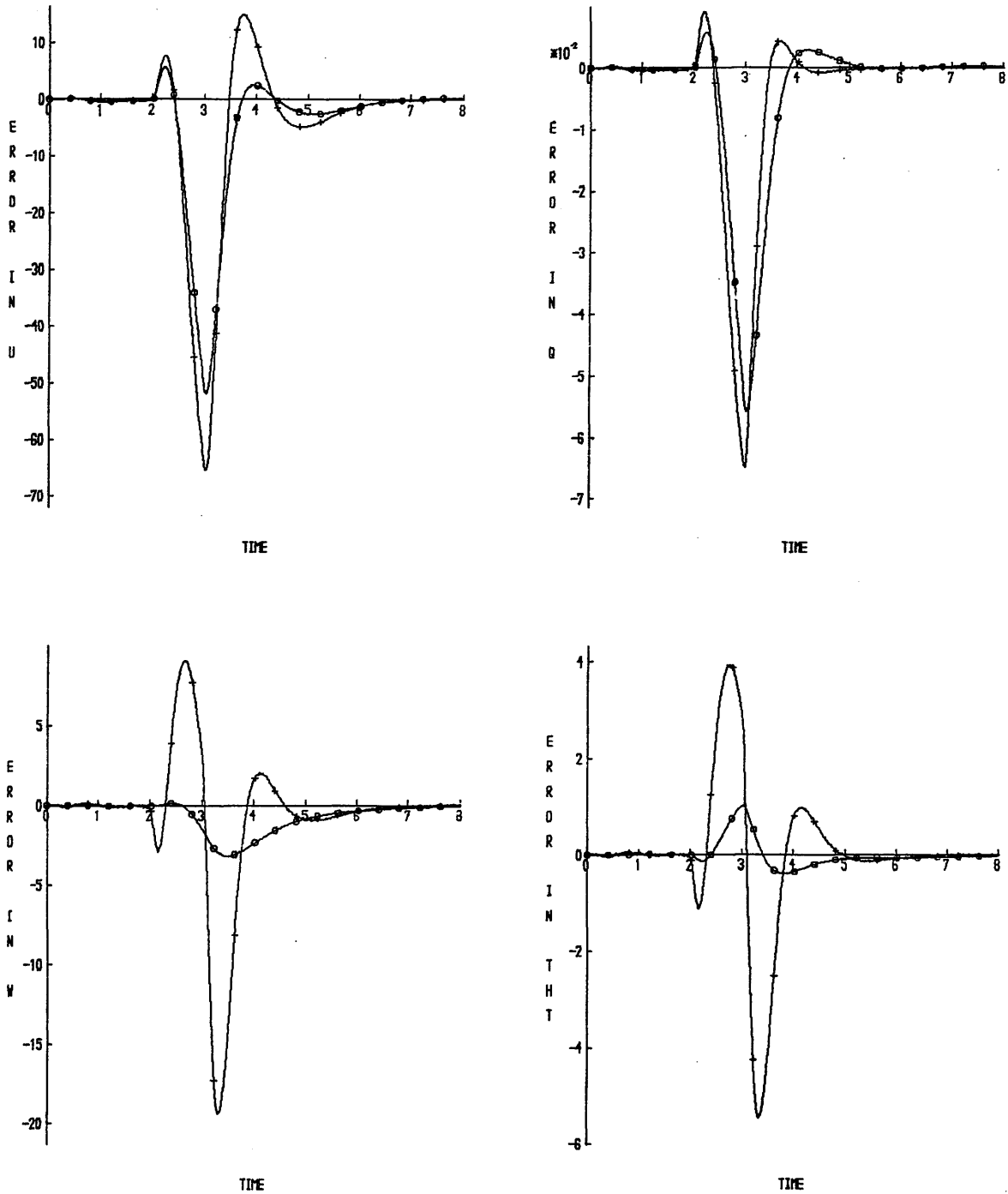

FIG 7.3 EFFECT OF EIGENVALUES ON OBSERVER RESPONSE TO AN INSTRUMENT FAULT

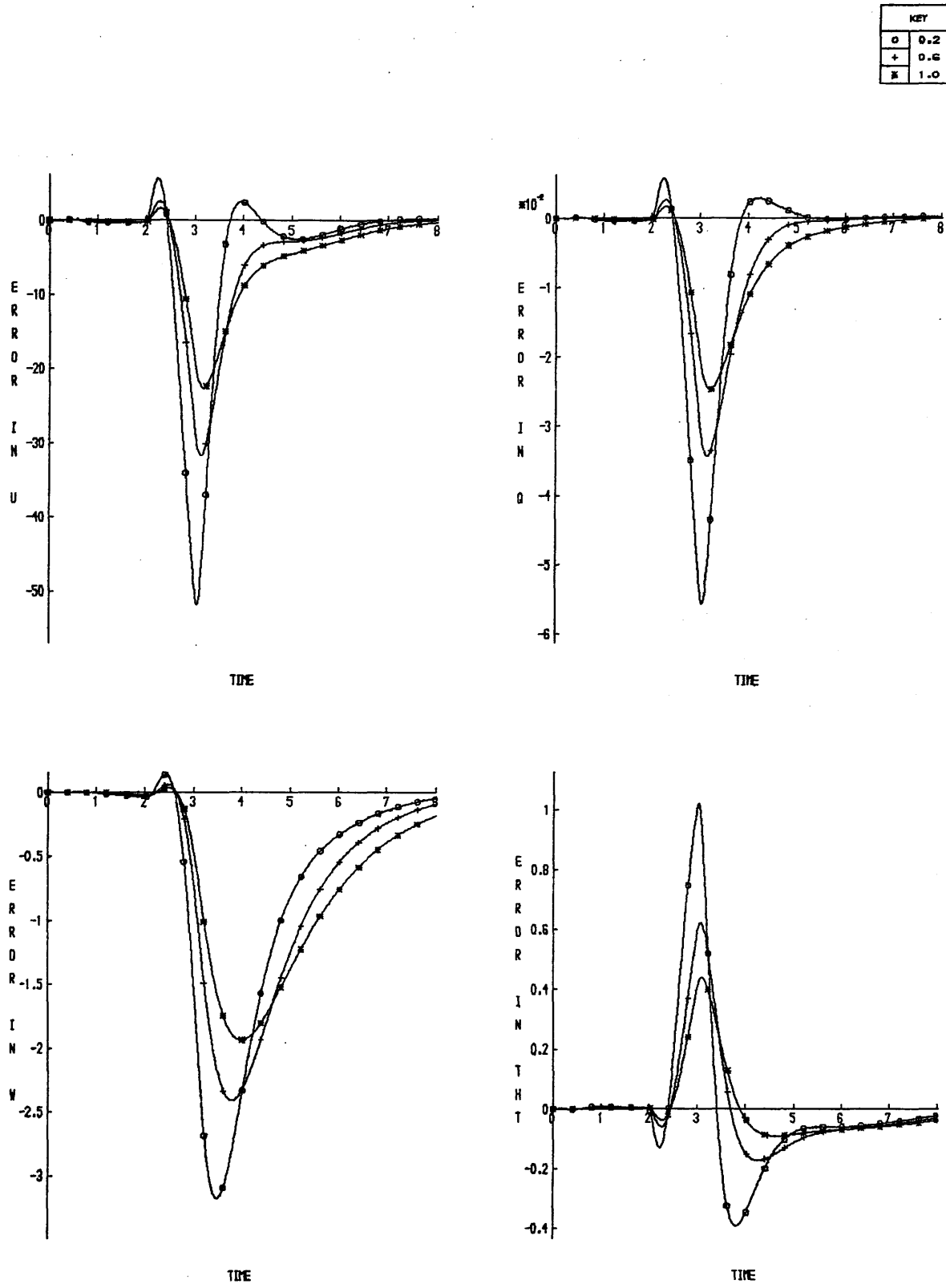

FIG 7.4 EFFECT OF τ ON OBSERVER RESPONSE TO AN INSTRUMENT FAULT

$$\frac{Y(s)}{u(s)} = \frac{1}{(1 + s\tau)^2} \qquad (7.10)$$

has a slope of 40db/decade and therefore for a given value of τ will reduce noise more effectively than the first order filter. This is clearly demonstrated in *fig 7.5* which compares the error responses of two observers designed with EV1 and $\tau = 0.2$: one with first order filters and the other with second order filters. Their responses to the fault are plotted in *fig 7.6* and it is evident that increasing the order of the filters has an identical effect to increasing the value of τ.

Having now determined the effects of varying the eigenvalues, τ and the order of the filters, the question is what are the optimum values of these parameters for instrument fault detection. To answer this it is first necessary to reconsider the proposed logic for the dedicated observer scheme.

It was demonstrated in section 7.2 that an instrument fault, or two simultaneous faults, could be identified from the six difference equations, $\underset{\sim}{a}_i$'s (equations 7.1, Table 7.1). Since there is noise on the instrument signals these will be non-zero even when there is no fault and therefore some *threshold* value must be set for each $\underset{\sim}{a}_i$. To avoid false triggering these thresholds must be sufficiently above the no-fault level.

Now the values of each $\underset{\sim}{a}_i$ depend on the estimates $\hat{\underset{\sim}{x}}_i$ and hence on the three parameters investigated above: eigenvalues, τ and filter order. In the case where there are no instrument faults, increasing τ or the order of the filters will decrease the noise on the estimates and therefore decrease the magnitudes of the $\underset{\sim}{a}_i$'s. Increasing the eigenvalues has the opposite effect – noise increases on the estimates and consequently the $\underset{\sim}{a}_i$'s increase in magnitude.

When an instrument develops a fault the errors, and hence $\underset{\sim}{a}_i$'s, will increase with increasing eigenvalues and decrease with increasing τ or system order. Thus by increasing τ or the system order a lower threshold can be set, but the rate the $\underset{\sim}{a}_i$'s increase will be reduced. Conversely, increasing the eigenvalues will result in a higher threshold and an increased rate.

In order to evaluate the effect of these factors on the time to detect an instrument fault, a series of tests were conducted with the logic scheme introduced earlier. Each of the six $\underset{\sim}{a}_i$'s (equations 7.1) are of form,

$$\underset{\sim}{a}_i = | \hat{\underset{\sim}{x}}_j - \hat{\underset{\sim}{x}}_k | \qquad (7.11)$$

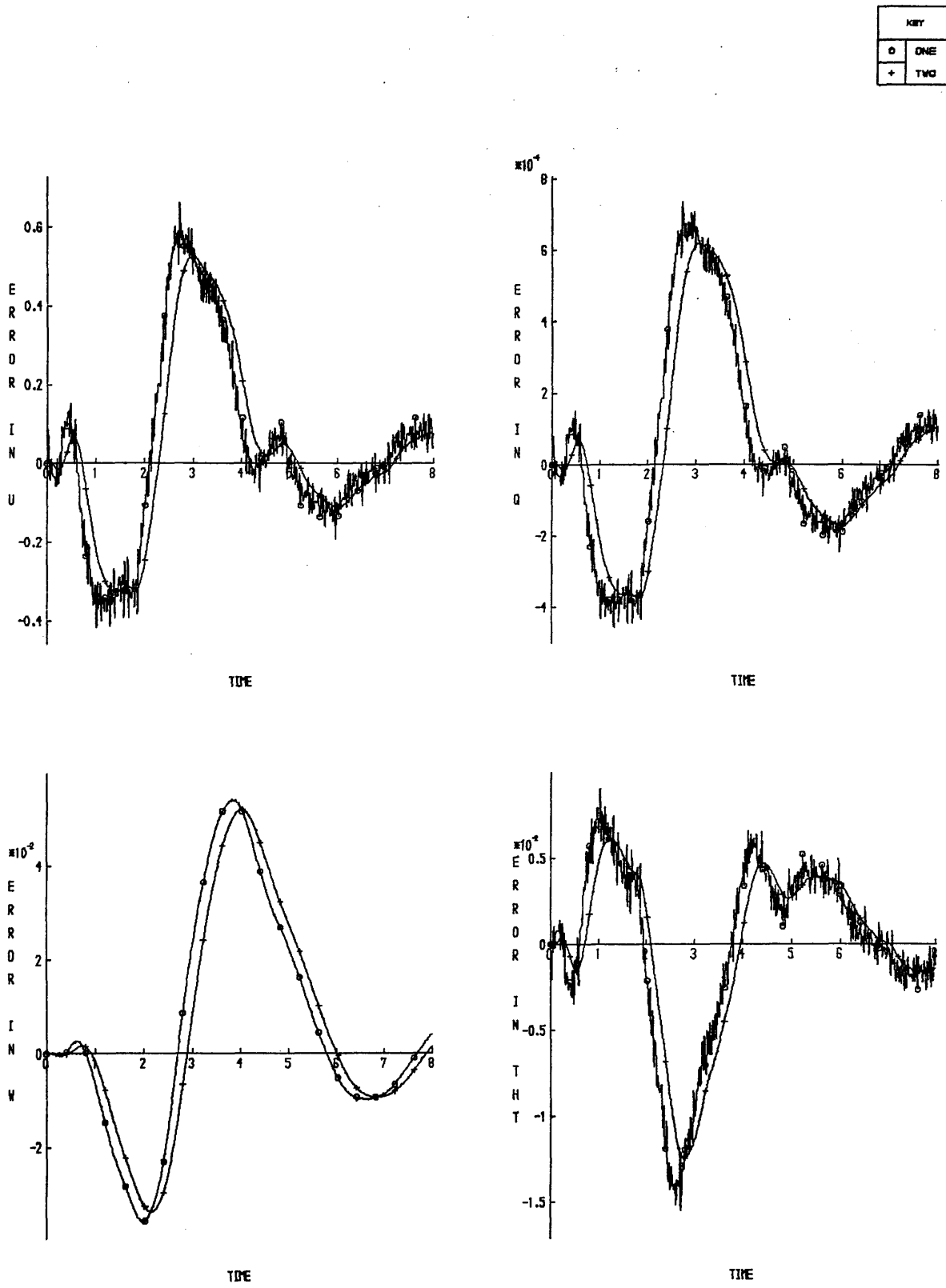

FIG 7.5 EFFECT OF FILTER ORDER ON OBSERVER RESPONSE TO NOISY STATES

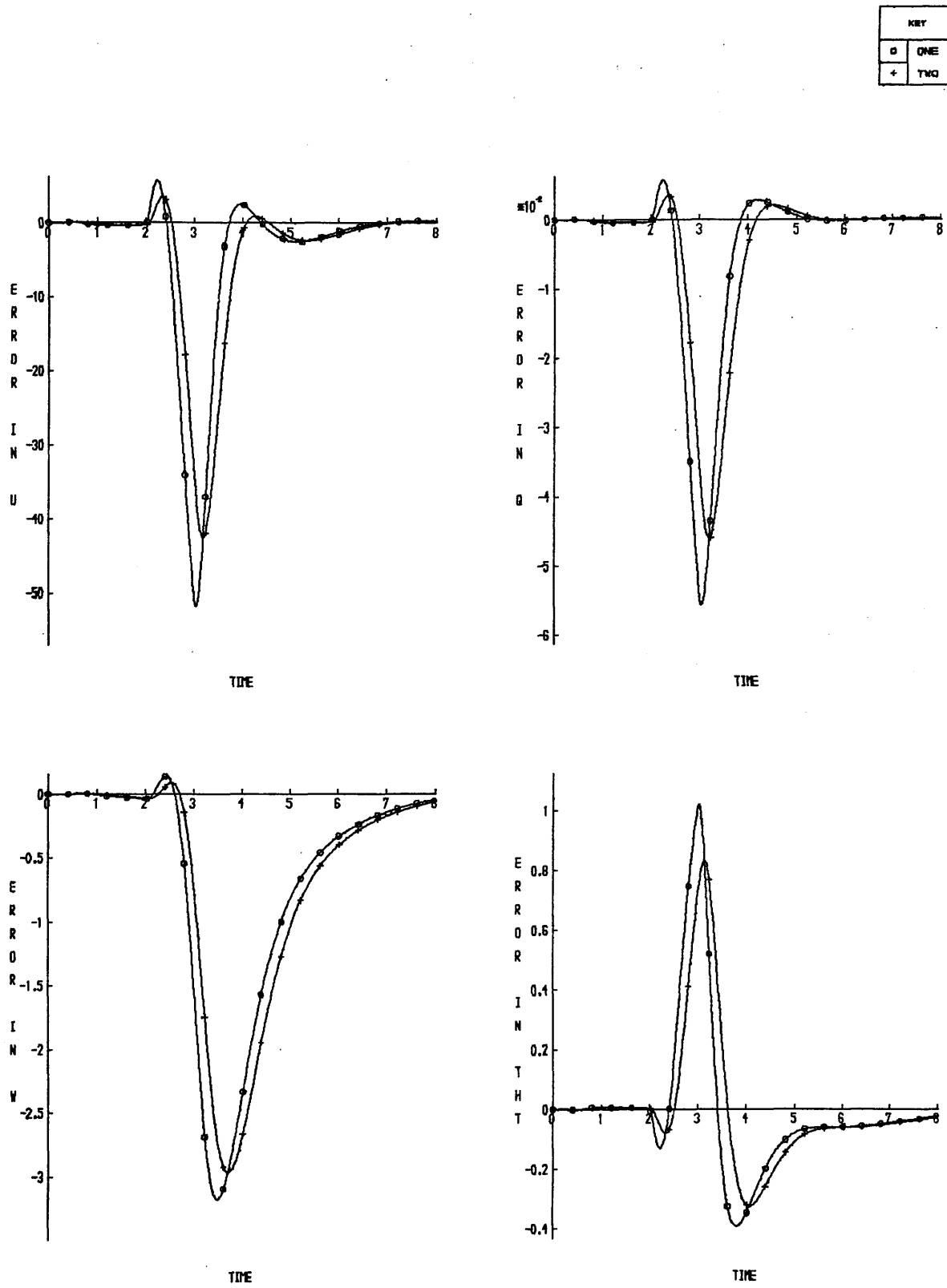

FIG 7.6 EFFECT OF FILTER ORDER ON OBSERVER RESPONSE TO AN INSTRUMENT FAULT

where $\hat{\underset{\sim}{x}}_j$ and $\hat{\underset{\sim}{x}}_k = [\ u,\ w,\ q,\ \theta\ ]^T$. Thus each $\underset{\sim}{a}_i$ consists of four elements which will be referred to as a_{iu}, a_{iw}, a_{iq} and $a_{i\theta}$; each of which require a different threshold.

The logic scheme used for these tests therefore consisted of thirty logic flags: A_i ($i=1\rightarrow6$) and A_{ij} ($i=1\rightarrow6$; $j=u,\ w,\ q,\ \theta$). If a_{iu}, a_{iw}, a_{iq} or $a_{i\theta}$ exceed their threshold then the corresponding logic flag A_{ij} is *latched* true. In an attempt to prevent false alarms, but also to make allowance for the fact that the four a_{ij}'s have different sensitivities to different types of faults and to faults occurring at different times, A_i is only set true when two or more of the four A_{ij} are true.

For the first test the threshold for each of the twenty four a_{ij}'s was simply set at 20% above the maximum value of a_{ij} recorded *with no fault present*, whilst for the second test the thresholds were set as follows.

It was shown earlier that the value of a_{ij} is dependent on the filter order, the eigenvalues and τ. Consequently the percentage increase in a_{ij},

$$\frac{[\text{Max } a_{ij} \text{ during fault}] - [\text{Max } a_{ij} \text{ with no fault}]}{[\text{Max } a_{ij} \text{ with no fault}]} * 100\% \qquad (7.12)$$

will also vary with these three parameters. This relationship is illustrated by Table 7.2 which gives the values of equation 7.12 for a zero scale factor fault on instrument one from 2 to 3 seconds. The longitudinal model was again used and the eigenvalues: EV1, EV2 and EV3 were 2×, 4× and 8× the largest system eigenvalue, respectively. Results are shown for a_{1u}, a_{1w}, a_{1q} and $a_{1\theta}$ for the three observers previously considered: no filters and first and second order filters.

It can be seen that as τ or the order of the filters increases the percentage increases, whereas an increase in the eigenvalues results in a decrease in the percentage. The explanation for this is that increasing eigenvalues or decreasing the filter order and τ, results in increasing noise on the estimates and hence a reduction in the resolution of a fault. Thus for the second test the threshold values were determined as,

$$\text{Max no fault } a_{ij} + 0.2*[\text{Max fault } a_{ij} - \text{Max no fault } a_{ij}] \qquad (7.13)$$

For each test the longitudinal model was used and a zero scale factor fault was applied to each instrument in turn, between two and three seconds. The parameters varied were the filters: no filters, first order, second order; the eigenvalues: EV1,

EV2, EV3; and where filters were used, τ was varied from 0.2 to 2.0 in steps of 0.2. Thus a total of sixty three combinations of parameters were tested for each of the four faults.

			a_{1u}	a_{1w}	a_{1q}	$a_{1\theta}$
EV1	NO FILTER		251	344	385	290
	1	0.2	624	684	736	586
		2.0	501	1117	1039	791
	2	0.2	636	816	823	700
		2.0	548	1096	1009	624
EV2	NO FILTER		40	250	208	172
	1	0.2	269	518	432	349
		2.0	433	711	529	542
	2	0.2	401	684	643	484
		2.0	496	1117	960	785
EV3	NO FILTER		-3.9	61	101	1.7
	1	0.2	66	189	242	170
		2.0	187	256	285	163
	2	0.2	199	181	309	429
		2.0	542	593	446	670

TABLE 7.2

VALUES OF EQUATION 7.12

FOR A ZERO SCALE FACTOR

FAULT ON INSTRUMENT ONE

FROM TWO TO THREE SECONDS

It should be noted that these tests represent the 'ideal' case since the thresholds are calculated using the time history of the fault to be detected. In addition the same noise is added to both the time histories, ie. fault/no fault time histories. A summary of results is given in Table 7.3 – only the results for $\tau = 0.2$ and $\tau = 2.0$ are shown. The first row of each pair are the results obtained with the thresholds set 20% above the no fault level whilst the second row are the results obtained with the thresholds set as per equation 7.13.

The first thing to be learned from these results is that identical fault times can be the product of different intermediate times. For example, the results for the first order filter with C(1) and EV3 are identical: 2.086 seconds, however the complete sequence of times given in Table 7.4 reveals the variations.

		FIRST ORDER FILTER			SECOND ORDER FILTER		
	τ	EV1	EV2	EV3	EV1	EV2	EV3
C1	0.2	2.164	2.125	2.086	2.266	2.188	2.141
		2.188	2.125	2.086	2.305	2.227	2.141
	2.0	2.266	2.141	2.086	2.586	2.344	2.164
		2.320	2.188	2.086	2.664	2.422	2.188
C2	0.2	2.047	2.023	2.023	2.125	2.062	2.047
		2.086	2.047	2.047	2.188	2.125	2.086
	2.0	2.086	2.047	2.023	2.266	2.141	2.062
		2.164	2.086	2.047	2.445	2.242	2.125
C3	0.2	2.062	2.062	2.023	2.164	2.141	2.047
		2.523	2.227	2.062	2.641	2.625	2.141
	2.0	2.164	2.141	2.023	2.688	2.688	2.062
		2.625	2.562	2.086	2.945	2.781	2.461
C4	0.2	2.086	2.086	2.047	2.164	2.141	2.102
		2.125	2.086	2.047	2.227	2.164	2.102
	2.0	2.125	2.086	2.062	2.242	2.164	2.125
		2.188	2.102	2.062	2.461	2.266	2.141

	NO FILTERS		
	EV1	EV2	EV3
C1	2.086	2.086	2.062
	2.086	2.086	2.047
C2	2.023	2.023	2.023
	2.023	2.023	2.023
C3	2.047	2.023	2.047
	2.086	2.086	2.047
C4	2.047	2.023	2.023
	2.023	2.023	2.023

Note - First rows correspond to method one of setting the threshold values.

TABLE 7.3

TIME AT WHICH ZERO SCALE FACTOR FAULT FROM 2-3 SECONDS, IS INDICATED

a	u	w	q	θ	A_i	
1	2.523	2.062	2.086	2.062	2.062	METHOD 1
2	2.703	2.086	2.086	2.164	2.086	τ = 0.2
3	2.484	2.062	2.086	2.086	2.086	
4	0.000	0.000	0.000	0.000	0.000	
5	0.000	0.000	0.000	0.000	0.000	
6	0.000	0.000	0.000	0.000	0.000	
1	2.523	2.086	2.086	2.125	2.086	METHOD 1
2	2.703	2.086	2.086	2.102	2.086	τ = 2.0
3	2.406	2.086	2.086	2.102	2.086	
4	0.000	0.000	0.000	0.000	0.000	
5	0.000	0.000	0.000	0.000	0.000	
6	0.000	0.000	0.000	0.000	0.000	
1	2.406	2.062	2.086	2.062	2.062	METHOD 2
2	2.703	2.062	2.086	2.164	2.086	τ = 0.2
3	2.461	2.062	2.086	2.086	2.086	
4	0.000	0.000	0.000	0.000	0.000	
5	0.000	0.000	0.000	0.000	0.000	
6	0.000	0.000	0.000	0.000	0.000	
1	2.523	2.086	2.086	2.125	2.086	METHOD 2
2	2.641	2.086	2.086	2.102	2.086	τ = 2.0
3	2.406	2.086	2.086	2.086	2.086	
4	0.000	0.000	0.000	0.000	0.000	
5	0.000	0.000	0.000	0.000	0.000	
6	0.000	0.000	0.000	0.000	0.000	

TABLE 7.4 INDIVIDUAL LOGIC FLAG TIMES

The second point is that for a fixed method of setting the thresholds, the time to detect a fault increases as the filter order and τ increases or as the eigenvalues decrease. Thirdly, the second method of setting the thresholds (ie. equation 7.13), except for the two cases with no filters, increased the time to detect a fault. This is simply because the second method results in higher thresholds.

Finally, consider *figs 7.7a–c*, which are the time histories of the fault/no fault a_{2j}'s for no filters, EV1 (*fig 7.7a*); first order filters, $\tau = 0.2$, EV1 (*fig 7.7b*) and first order filters, $\tau = 0.2$, EV3 (*fig 7.7c*). Undoubtedly of these three the best resolution of the fault is produced with first order filters, $\tau = 0.2$ and EV1.

After consideration of these results the decision was made to select this combination for further evaluation. The reason this combination was selected was because it was felt that this provided the best compromise between the need to prevent false alarms and the speed at which a fault can be identified.

7.5 THE EFFECT OF VARIATIONS IN FAULT PARAMETERS

Before investigating the selection of suitable thresholds it is necessary to first examine the effects of variations in the

- Type of fault
- Magnitude of fault
- Instrument with fault
- Time of fault
- Simultaneous faults
- Manoeuvre

Once again the longitudinal model of the Puma was used with a doublet input on θ_{1S} and noise added to the states at full noise power. The noise corrupted state time history is shown in *fig 7.8*. Faults were applied to instrument two (w) and instrument four (θ), which were chosen to allow comparison between a very noisy state (w) and a state relatively unaffected by noise (θ). In addition w will be affected by a dead–zone fault.

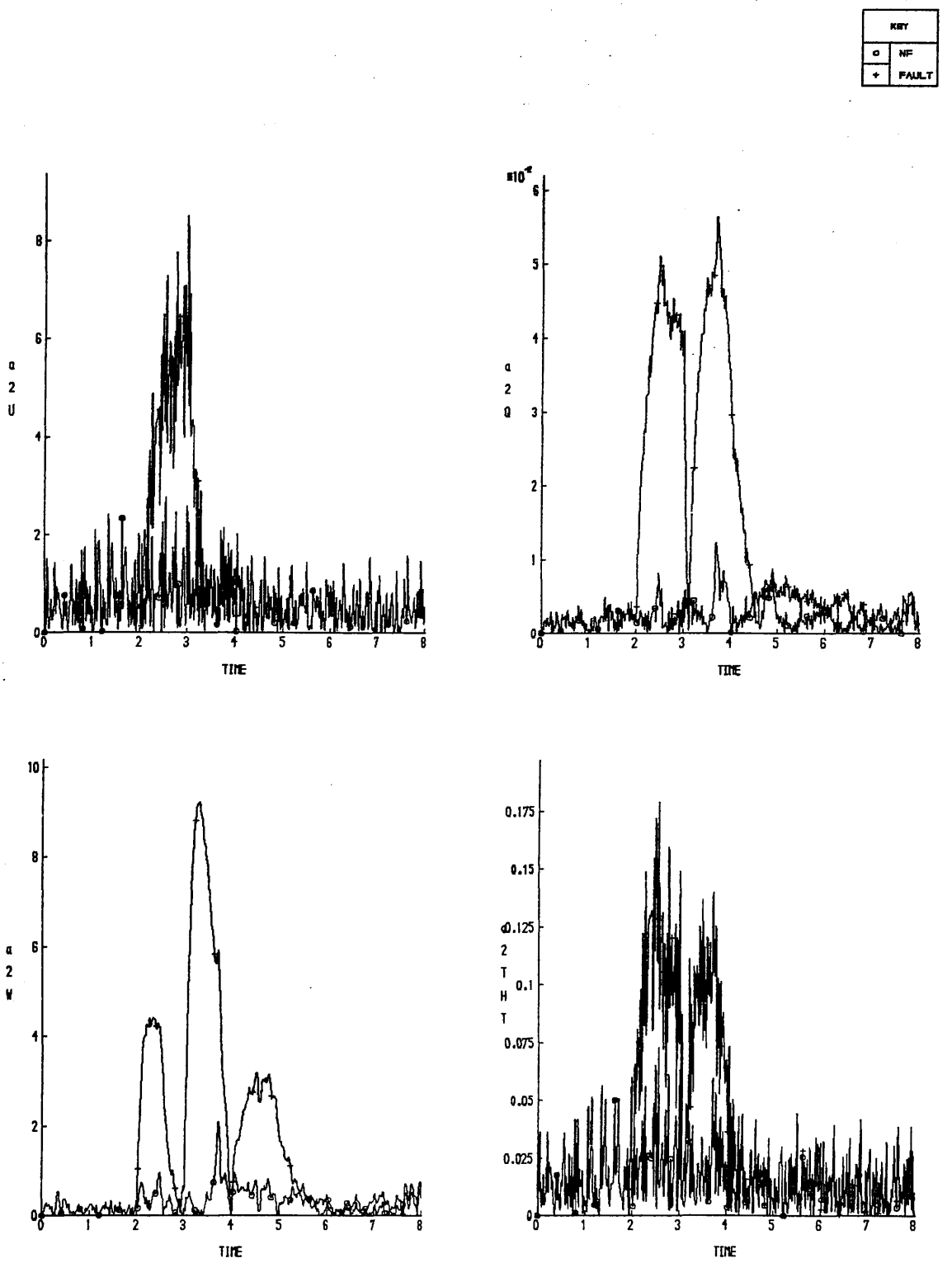

FIG 7.7A FAULT/NO-FAULT a_{2j} FOR ZERO SCALE FACTOR FAULT ON INSTRUMENT ONE FROM 2-3 SECS; EV1, NO FILTERS

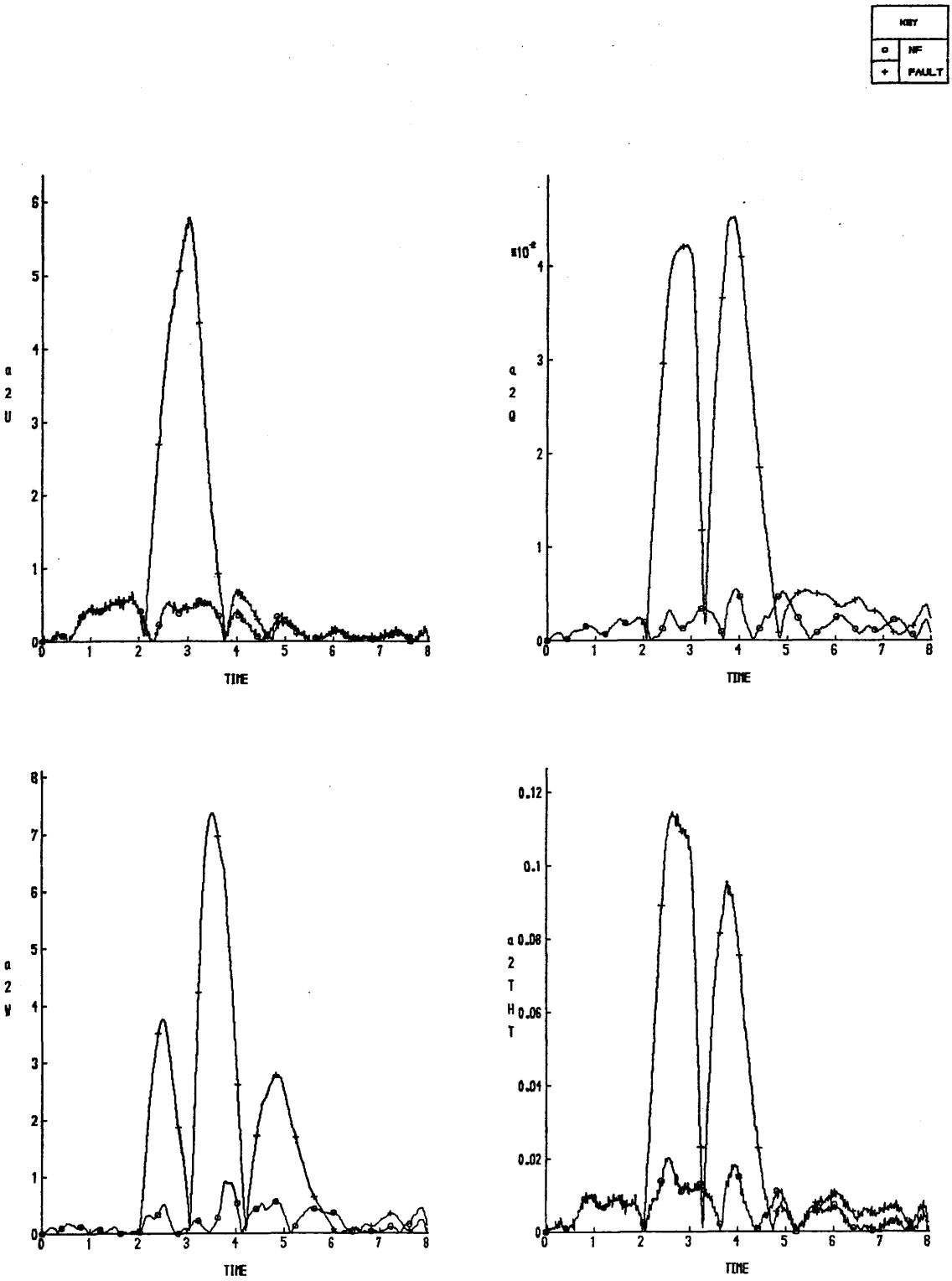

FIG 7.7B FAULT/NO-FAULT a_{2j} FOR ZERO SCALE FACTOR FAULT ON INSTRUMENT ONE FROM 2-3 SECS; EV1, 1st ORDER FILTERS, τ=0.2

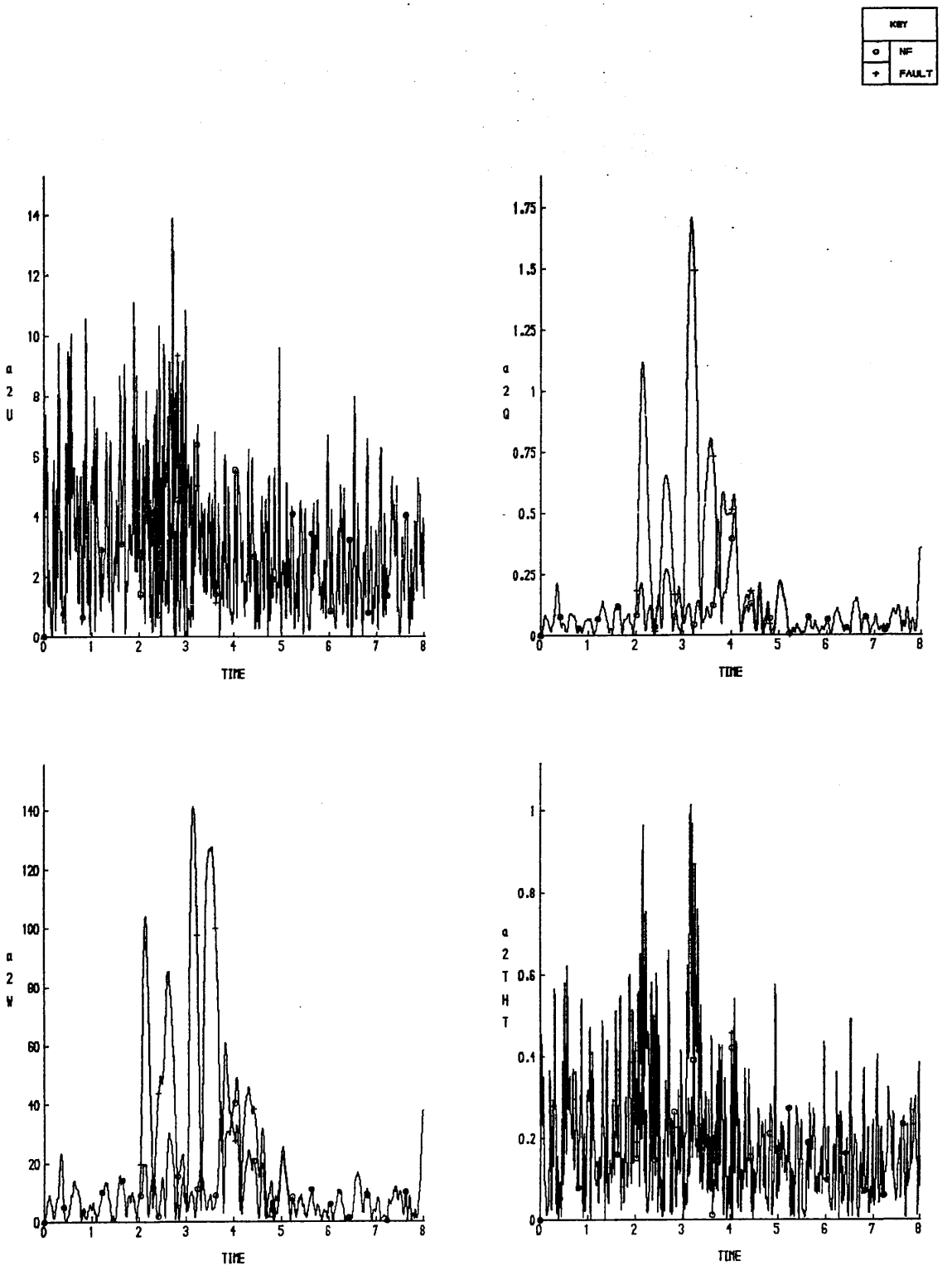

FIG 7.7C FAULT/NO-FAULT a_{2j} FOR ZERO SCALE FACTOR FAULT ON INSTRUMENT ONE FROM 2-3 SECS; EV3, 1st ORDER FILTERS, τ=0.2

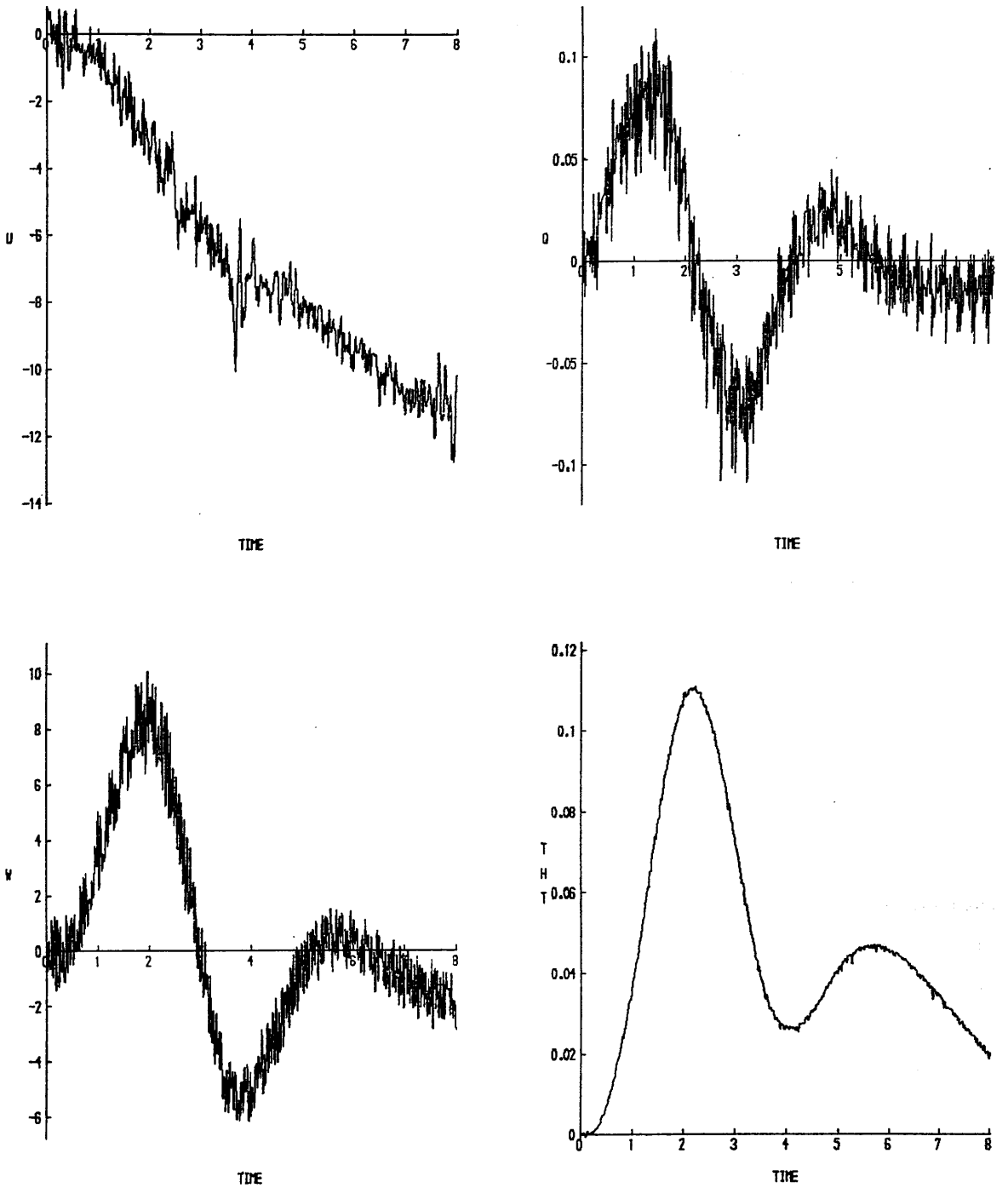

FIG 7.8 STATE TIME-HISTORY FOR DOUBLET INPUT ON θ_{1s}

TYPES OF FAULT

A comparison of observer error responses for the four different types of fault described in section 7.3 (scale factor, SF; scale factor ramp, SFR; bias, B and dead−zone, DZ) is shown in *fig 7.9*. The faults were applied from two to four seconds and each was of magnitude 0.8. The major difference between the responses is their magnitudes and this is easily explained by reference to the equations describing the four faults (equations 7.3− 7.8).

Clearly the actual magnitude of the fault varies with the type of fault, eg. the magnitude of a scale factor fault will depend on the value of the state whereas a bias fault is independent of the state. Note also that during the period of the fault the observer attempts to drive the error term to zero − this is best illustrated by the response to the bias fault − and that after the fault is removed the errors take a finite time to return to zero, the length of time being determined by the dynamics of the observer.

MAGNITUDE AND INSTRUMENT

Consider *fig 7.10* which gives the error responses for scale factor faults of 0.7, 0.8, 1.2 and 1.3 on instrument four, between two and four seconds. Since the observer is linear an increase in the magnitude of the fault results in a corresponding increase in the error. Similarly the response for a fault of magnitude x, is the negative of that for a fault of magnitude $-x$, eg. the responses for 1.2 $(+0.2\theta)$ and 0.8 (-0.2θ).

In earlier chapters it was demonstrated that different C matrices effect the accuracy of observer design and the fidelity of the estimate. The variations in observer response were explained by the modal expansion theory (section 4.5.5), which can also be used to interpret the differences between the responses shown in *fig 7.11*. This shows the error responses for scale factor faults of 1.1 on instruments two and four, from two to four seconds and as expected there are substantial differences in magnitude and shape between the the responses of the two observers.

TIME OF FAULT AND MANOEUVRE

The response of an observer to the time, or in other words the magnitude of the state, at which a fault occurs, varies with the type of fault. With a bias fault (equations 7.7/7.8) the error (ie. $\underset{\sim}{x}-\underset{\sim}{\hat{x}}$) is a constant and therefore there are only very minor differences due to the variation in magnitude of observer error at the

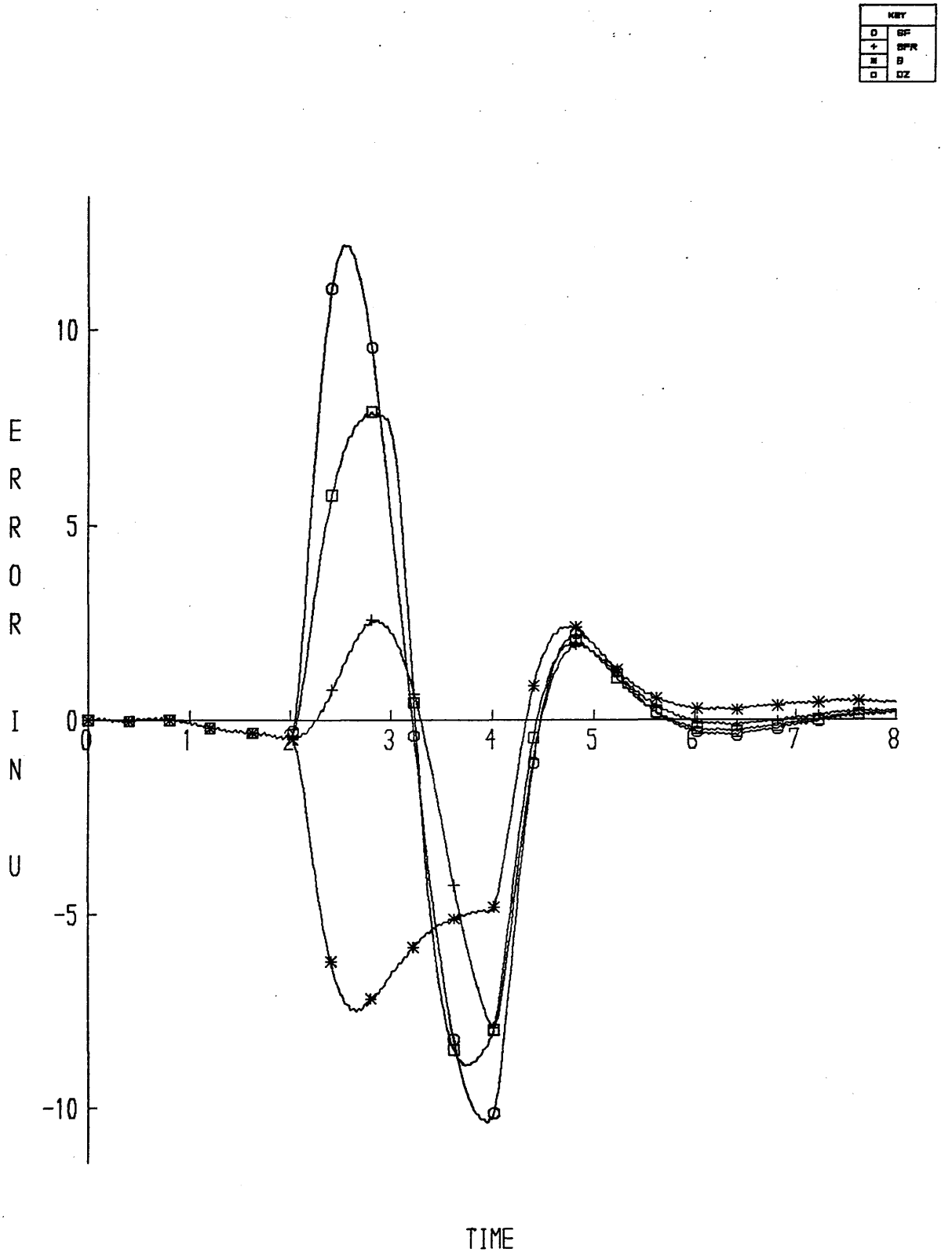

FIG 7.9 EFFECT OF TYPE OF FAULT ON OBSERVER RESPONSE TO AN INSTRUMENT FAULT

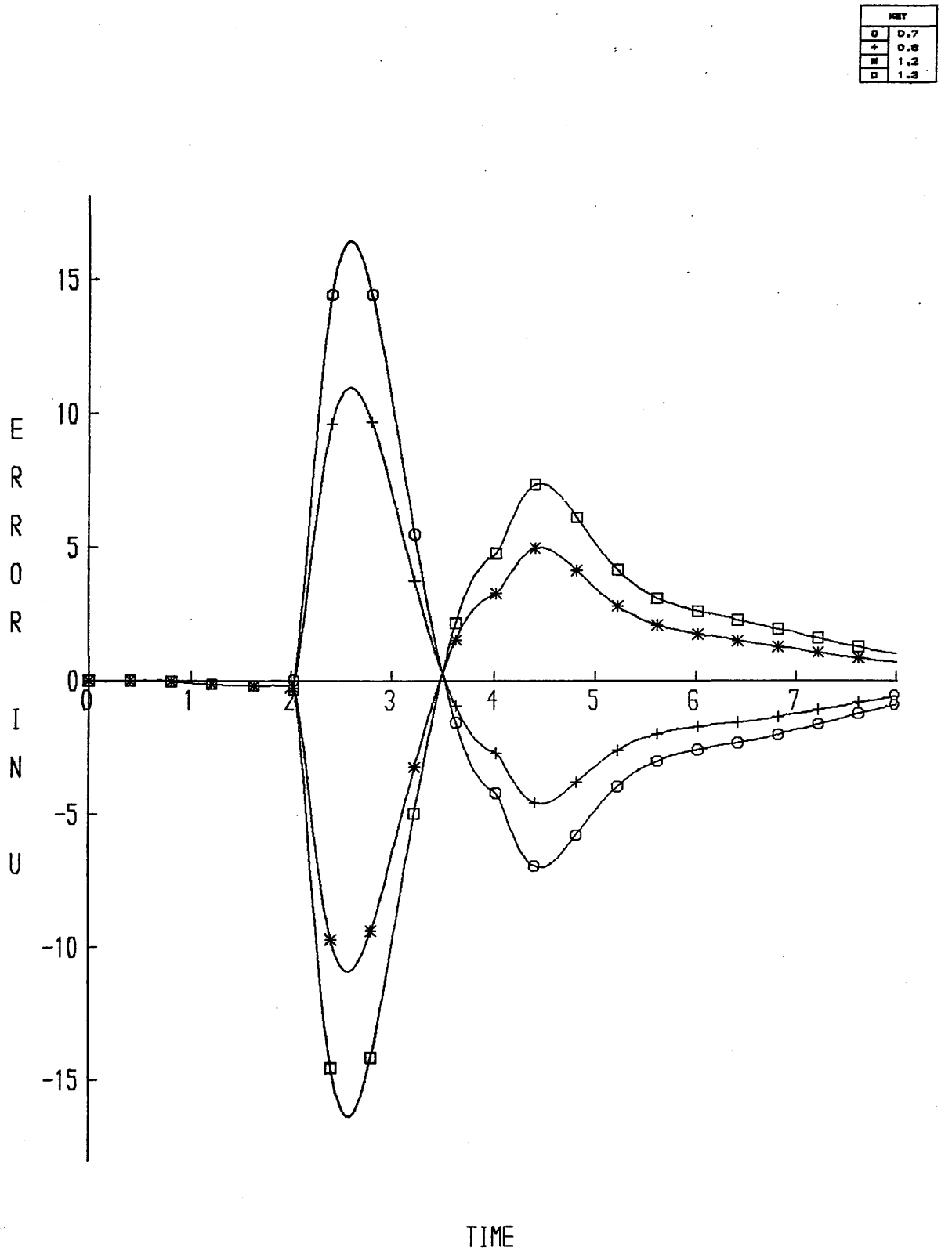

FIG 7.10 EFFECT OF MAGNITUDE OF FAULT ON OBSERVER RESPONSE TO AN INSTRUMENT FAULT

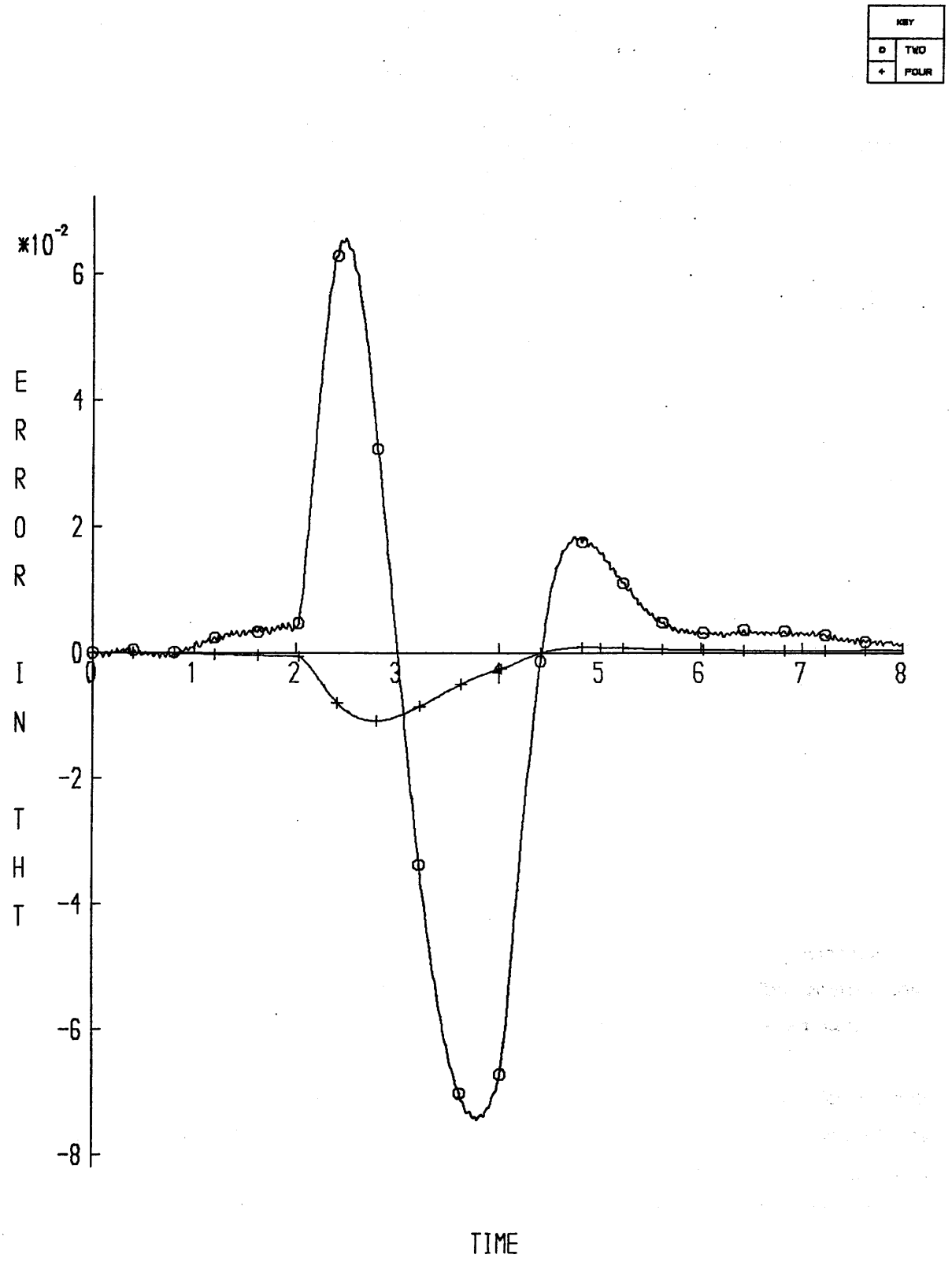

FIG 7.11 EFFECT OF C MATRIX ON OBSERVER RESPONSE TO AN INSTRUMENT FAULT

time the fault occurs. *Fig 7.12a* illustrates this for a bias fault of 1.0 on instrument two, with the time of fault varied from 0–1 to 7–8 seconds.

A dead–zone fault (equation 7.6) only occurs when the signal is within the limits of the dead–zone and therefore the time of fault will obviously determine whether or not the instrument output is zero. If the signal is within the dead–zone then the magnitude of the error will vary with the magnitude of the signal, the maximum error occurring at the limits of the dead–zone and zero error at $y=0$. Thus the observer response will vary, but the magnitude of the errors are constrained by the dead–zone limits.

With a scale factor or scale factor ramp fault (equations 7.3/7.4 and 7.5) the time of fault has a major influence on the observer response. Consider *fig 7.12b* which shows the variation in errors for a scale factor fault of 0.8 on instrument two at fault times between 0 and 8 seconds. It is clear that the magnitude of the error varies with the magnitude and sign of the signal (*fig 7.8*). In particular, between 0–1 and 5–7 seconds where the signal is close to zero the fault is almost imperceptible.

Finally since different manoeuvres result in different state time histories, the manoeuvre being flown at the time the fault occurs will also have an effect on the observer estimation error.

SIMULTANEOUS FAULTS

It was shown earlier that the proposed logic scheme was capable of detecting two simultaneous faults. To check this tests were conducted for all possible combinations of fault type and at varying fault times, two examples of which are given here.

First examine *fig 7.13a* which shows the fault/no fault a_{ij}'s for a scale factor fault of 0.8 on instrument two and a bias fault of 0.8 on instrument four, both faults occurring between two and four seconds. From Table 7.1 the a_{ij}'s changing for a fault on instrument two are a_{1j}, a_{4j} and a_{5j} and for a fault on instrument four – a_{3j}, a_{5j} and a_{6j}; a_{2j} does not change and is therefore not shown. With the exception of a_{1q} and a_{1w}, the resolution of the two faults is clear, although the immediate effect of the faults does not always result in an increase in all the a_{ij}'s, eg. a_{1q} initially decreases to almost zero.

If two faults occur at different, but overlapping time intervals the faults are still distinct. *Fig7.13b* illustrates this for bias faults of 0.8 on instrument two from one

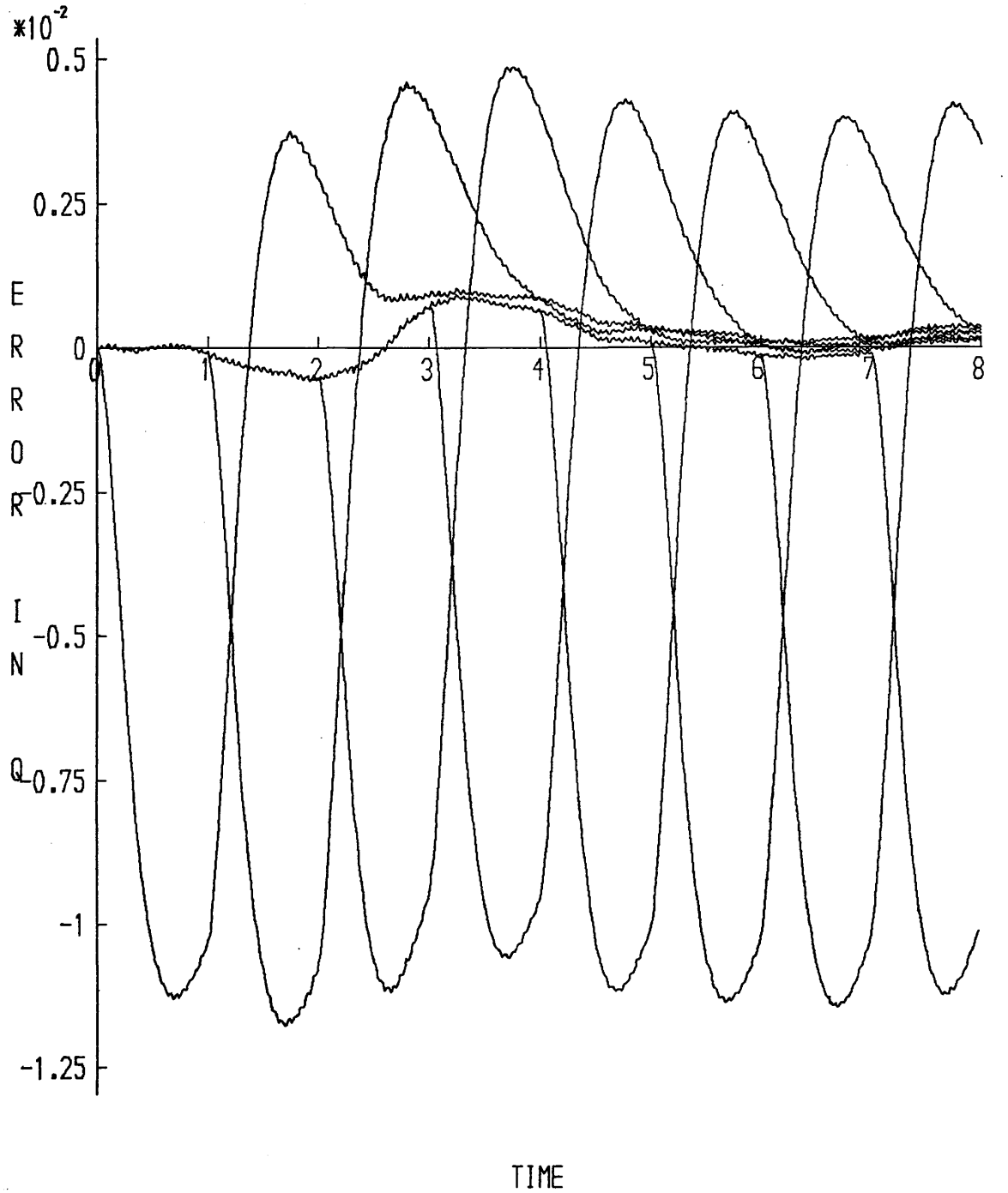

FIG 7.12A EFFECT OF TIME OF FAULT ON OBSERVER RESPONSE TO A BIAS FAULT

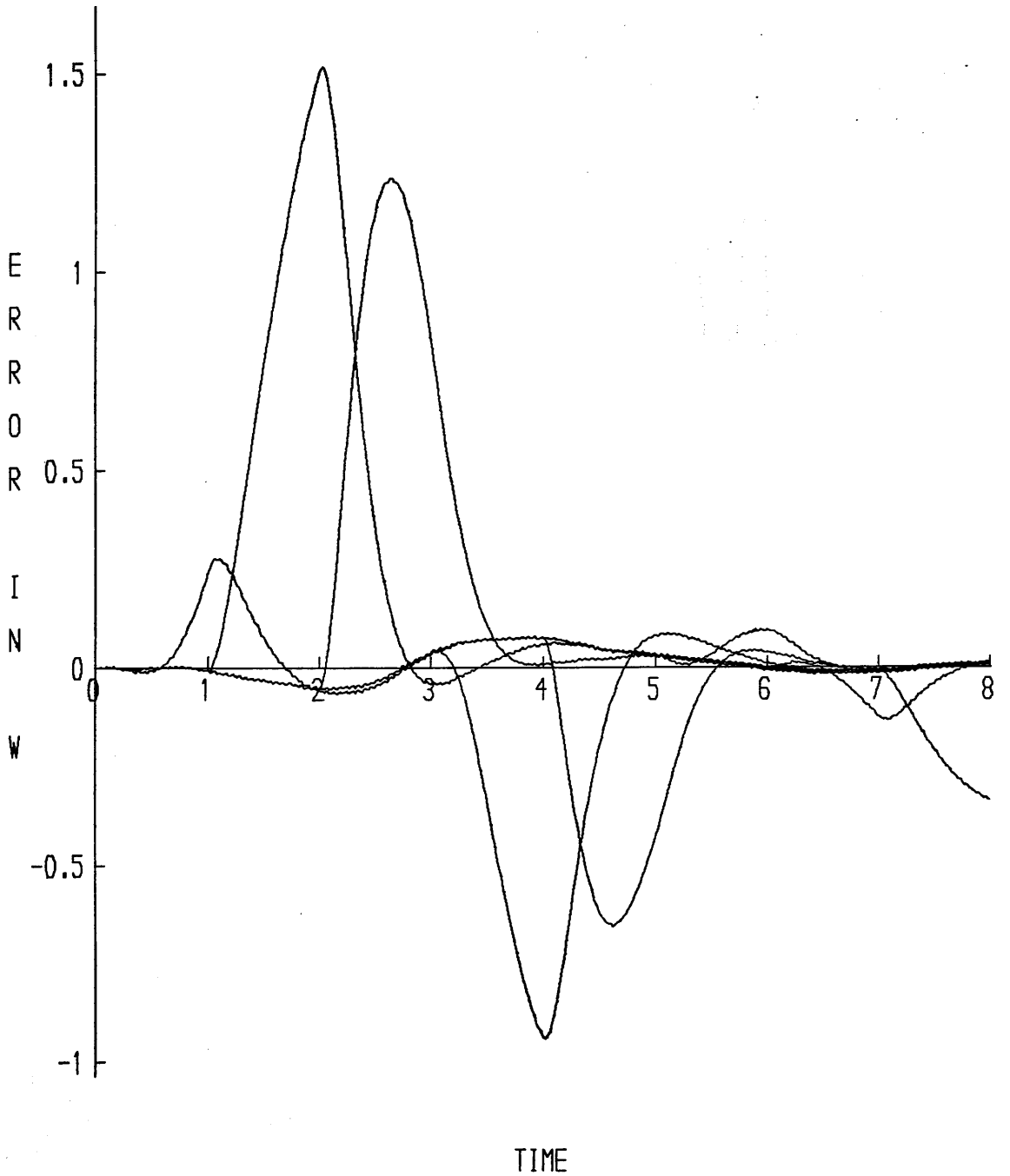

FIG 7.12B EFFECT OF TIME OF FAULT ON OBSERVER RESPONSE TO A SCALE FACTOR FAULT

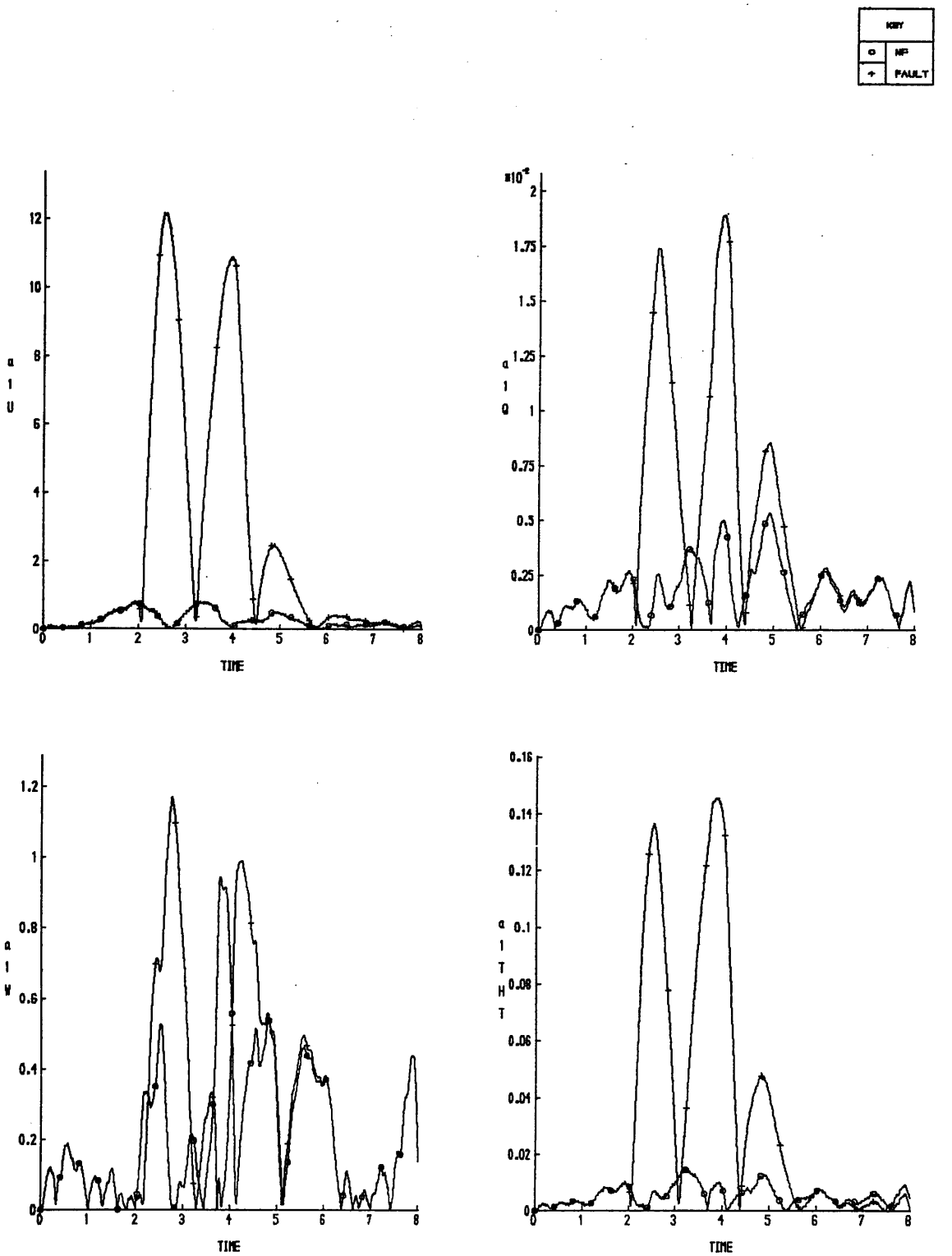

FIG 7.13A a_{ij}'s FOR SIMULTANEOUS FAULTS

SF 0.8 I2 / B 0.013 I4 2-4 SECS

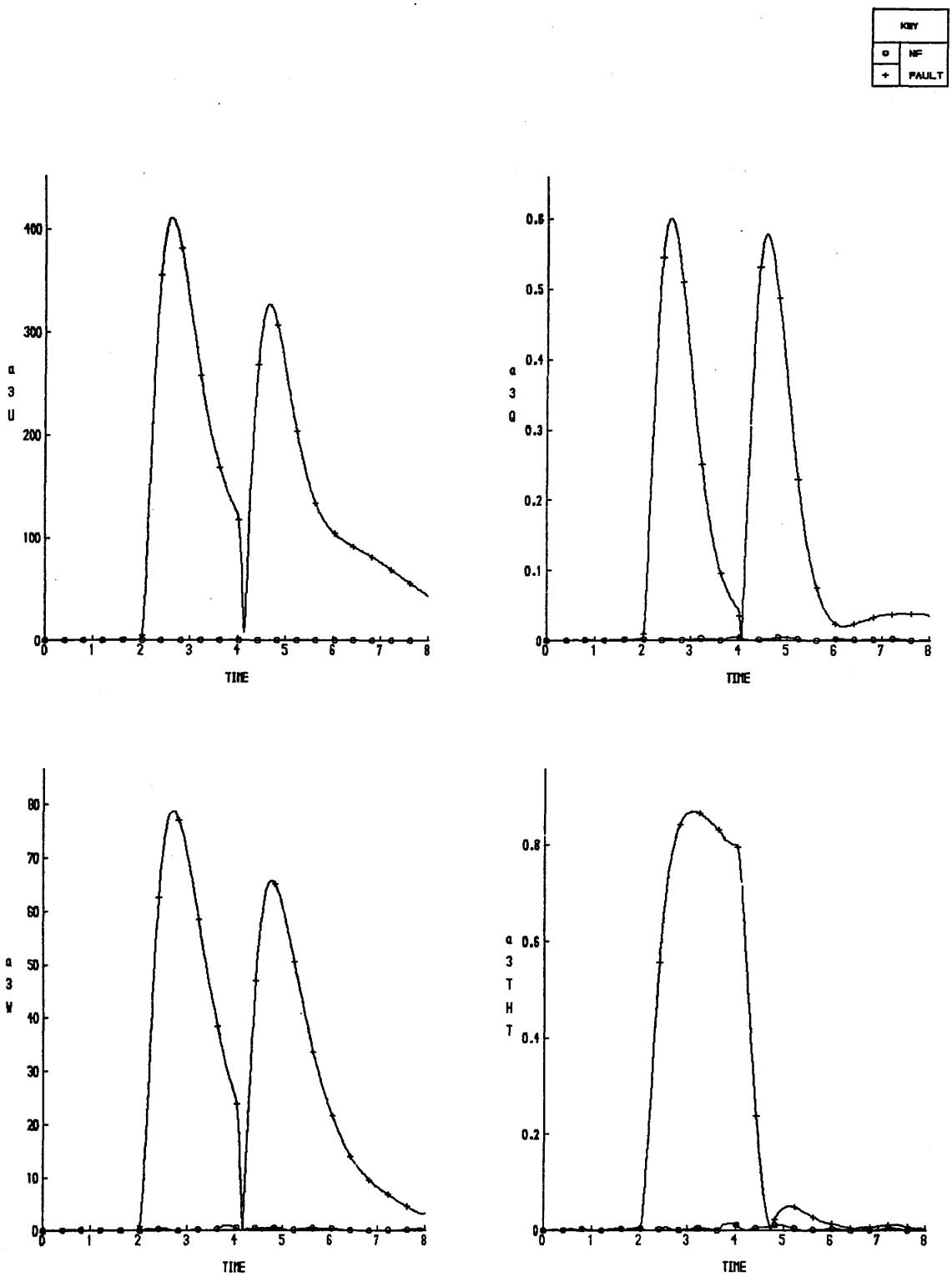

FIG 7.13A a_{ij}'s FOR SIMULTANEOUS FAULTS

SF 0.8 I2 / B 0.013 I4 2-4 SECS

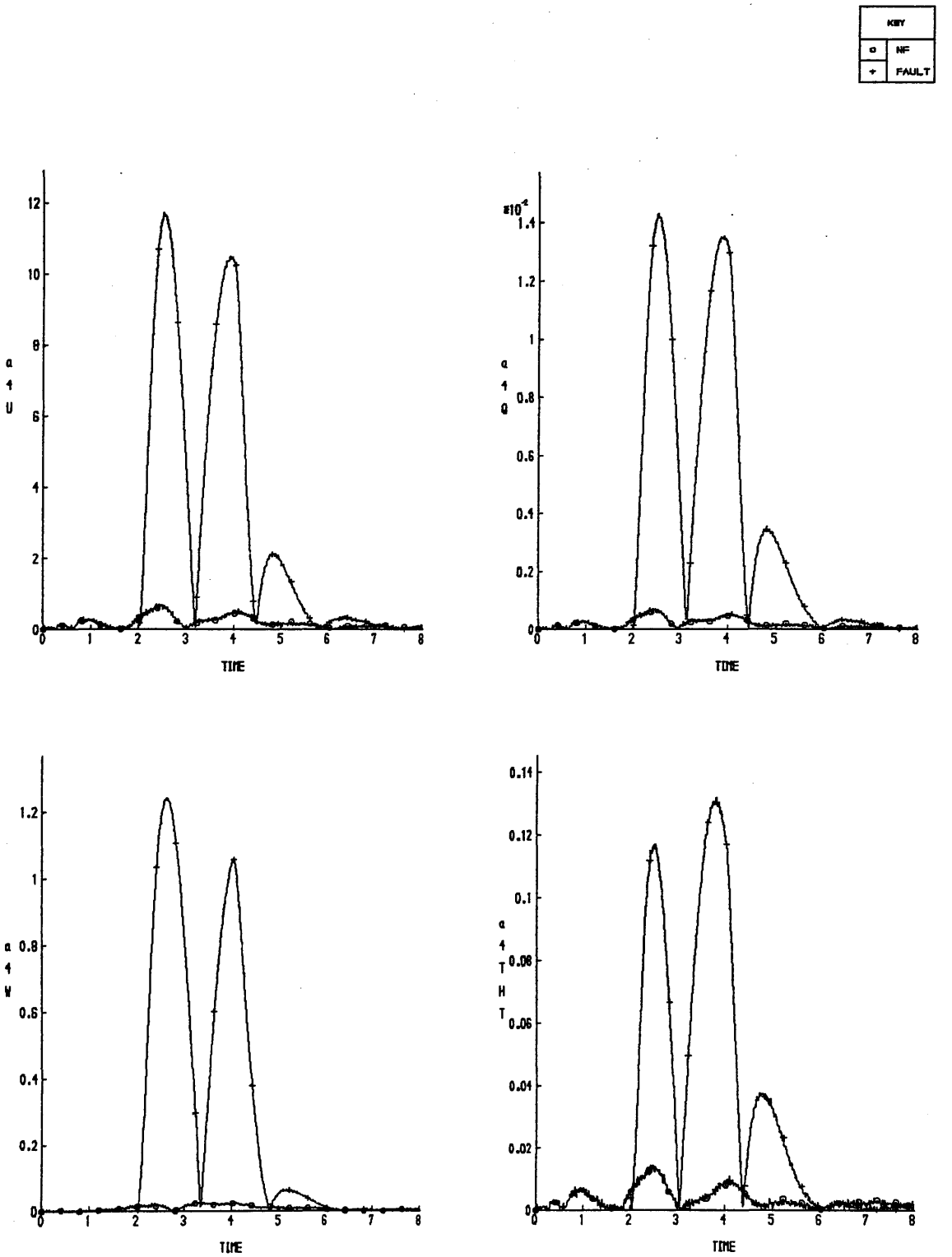

FIG 7.13A a_{ij}'s FOR SIMULTANEOUS FAULTS

SF 0.8 I2 / B 0.013 I4 2-4 SECS

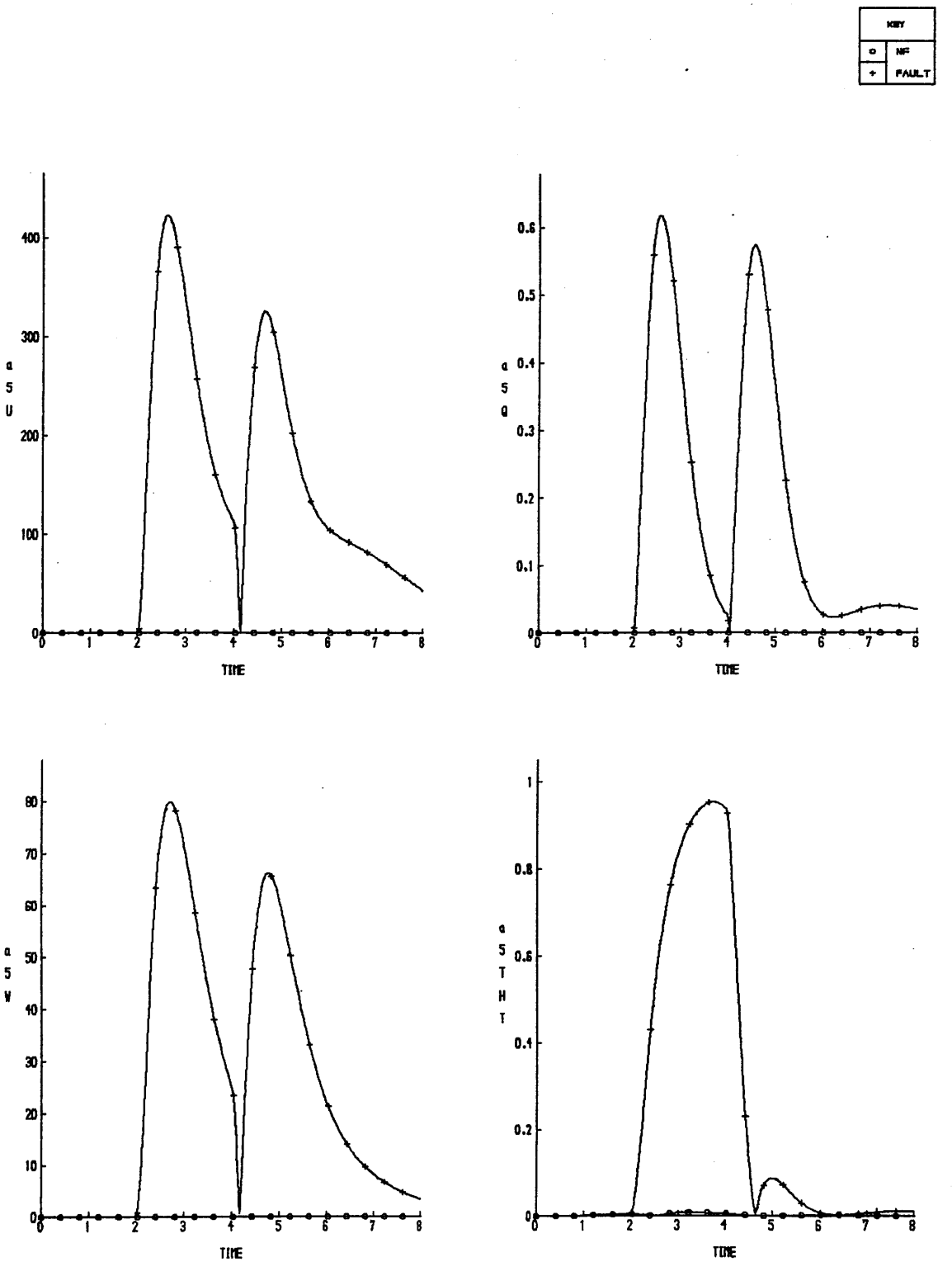

FIG 7.13A a_{ij}'s FOR SIMULTANEOUS FAULTS

SF 0.8 I2 / B 0.013 I4 2-4 SECS

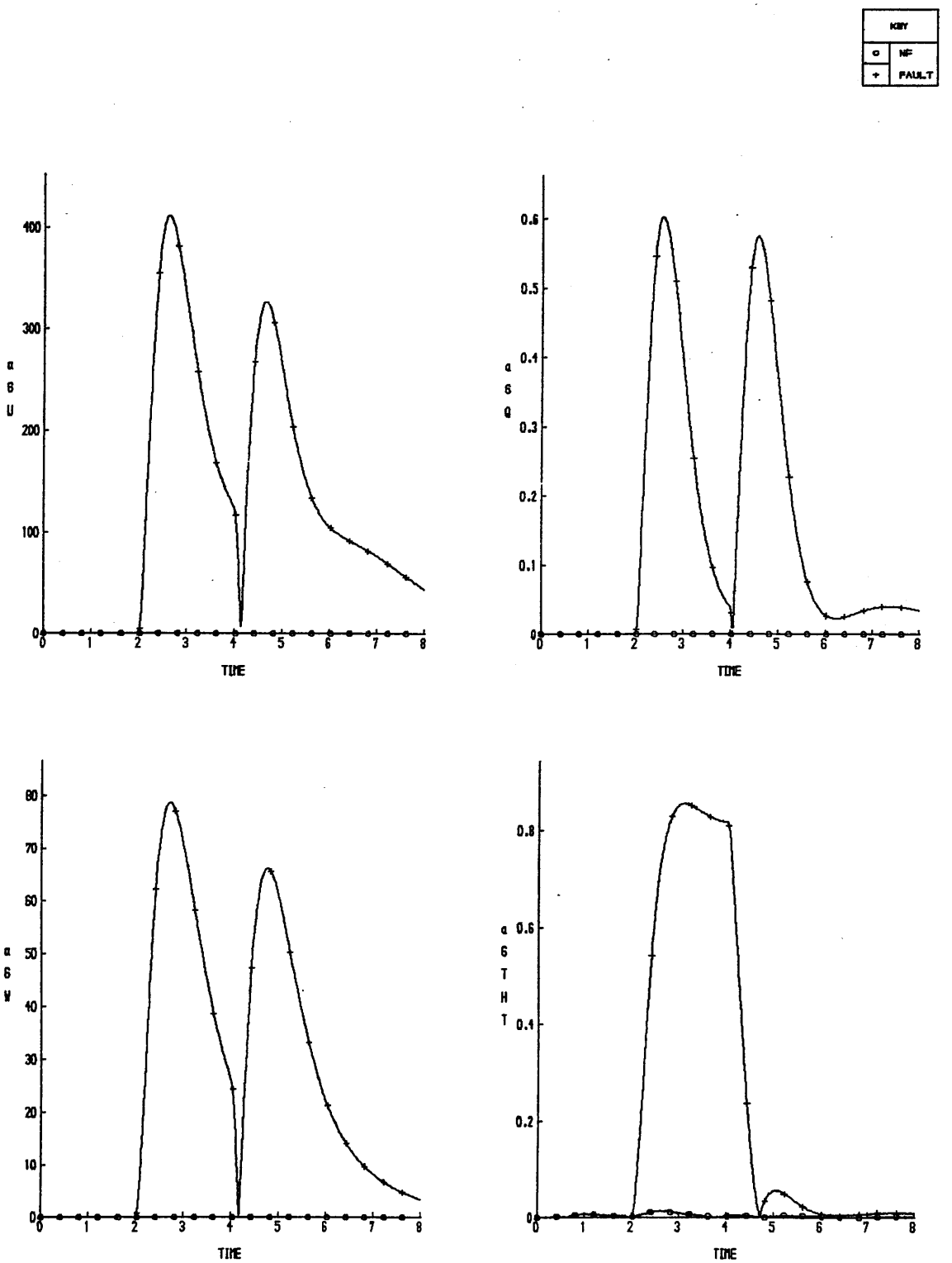

FIG 7.13A a_{ij}'s FOR SIMULTANEOUS FAULTS

SF 0.8 I2 / B 0.013 I4 2-4 SECS

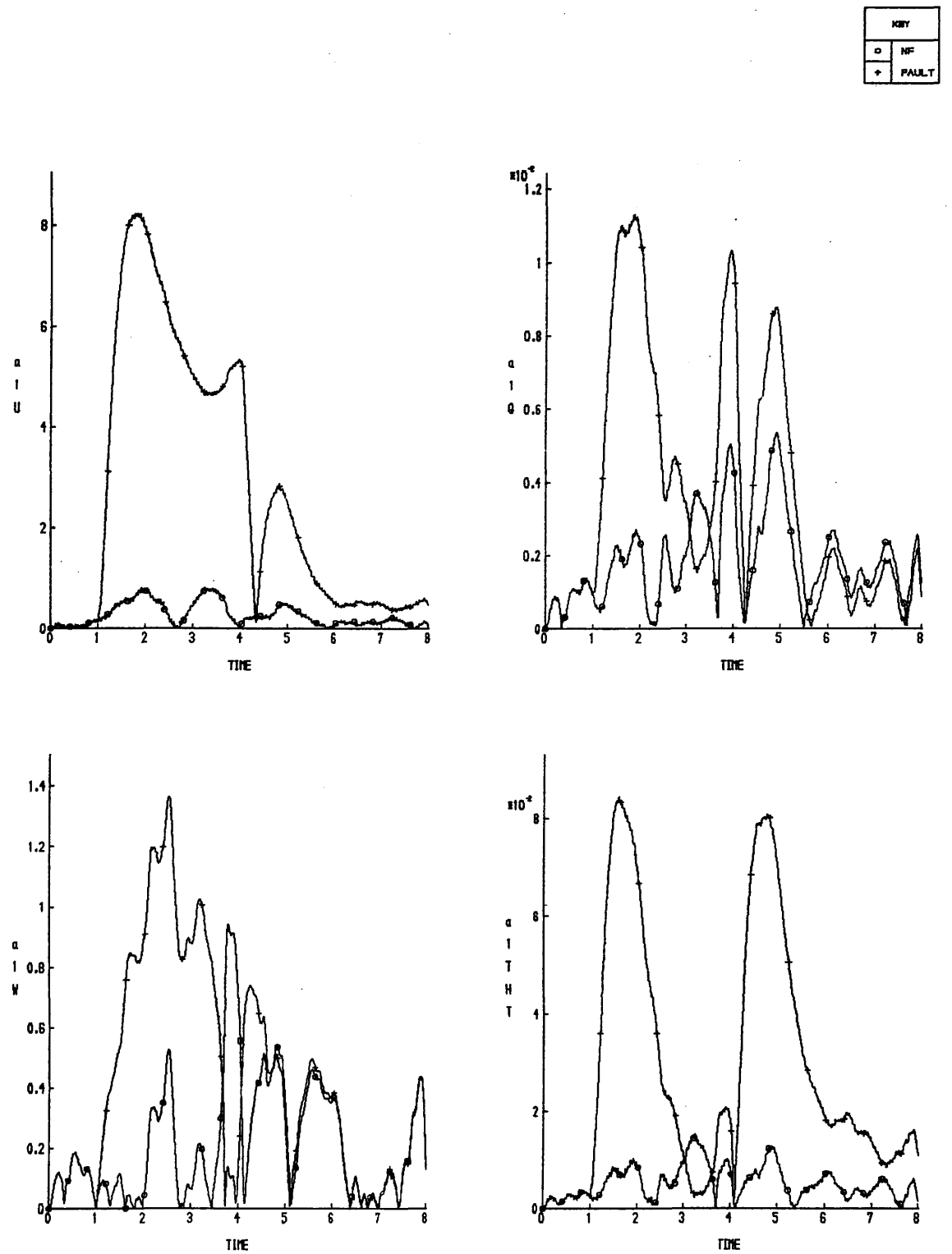

FIG 7.13B a_{ij}'s FOR SIMULTANEOUS FAULTS

B 0.8 I2 1-4 SECS / B 0.013 I4 2-5 SECS

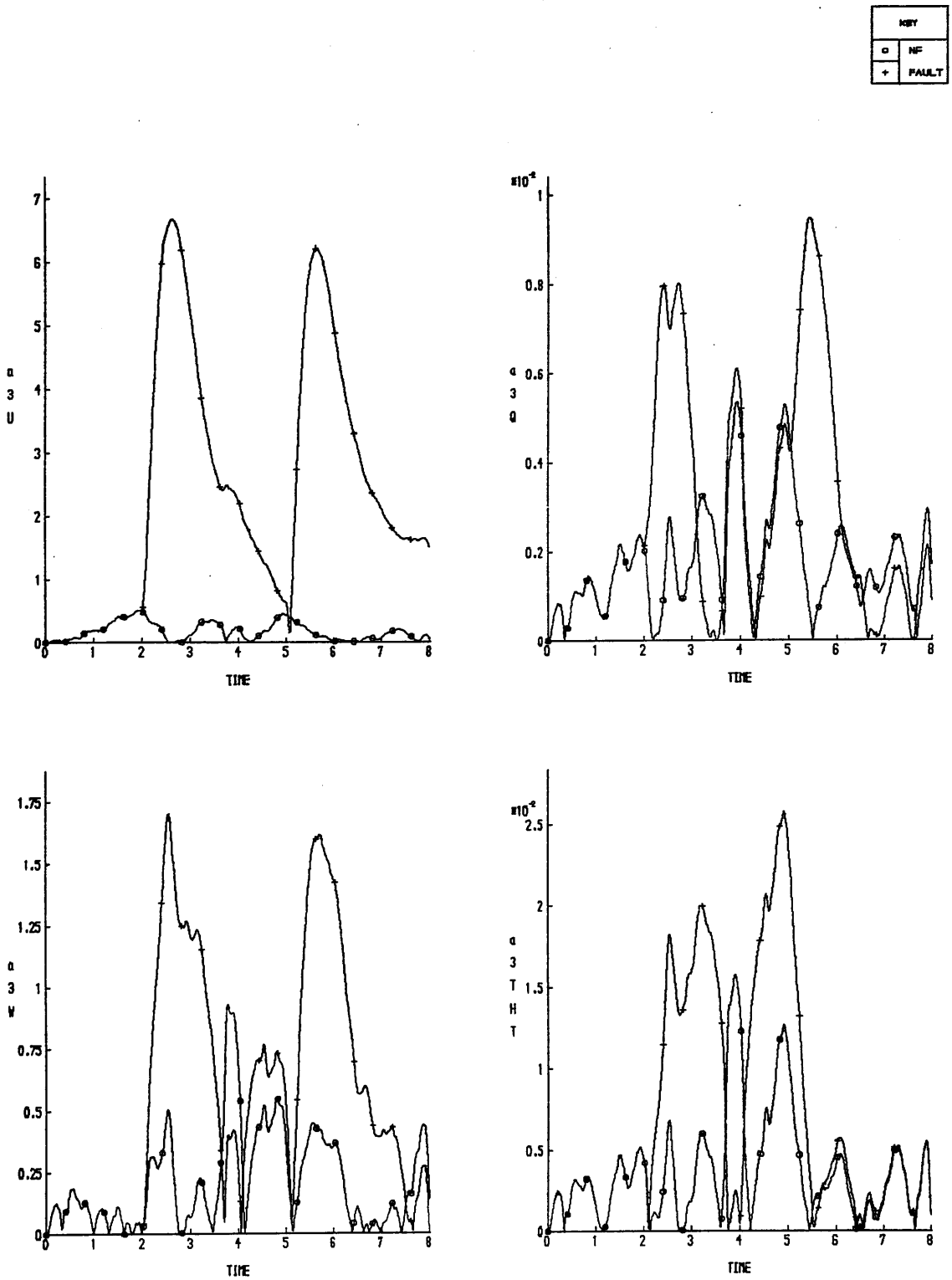

FIG 7.13B a_{ij}'s FOR SIMULTANEOUS FAULTS

B 0.8 I2 1-4 SECS / B 0.013 I4 2-5 SECS

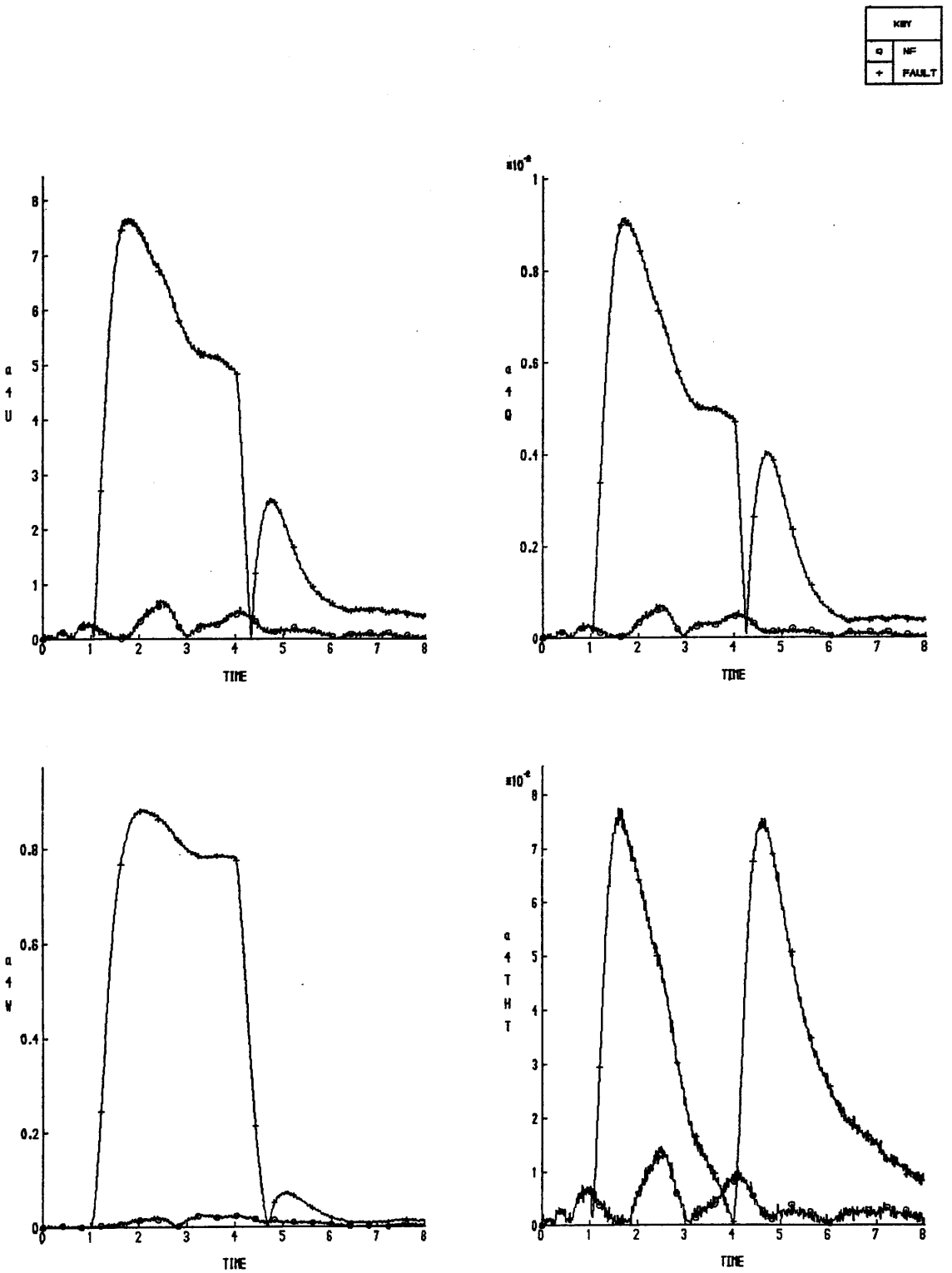

FIG 7.13B a_{ij}'s FOR SIMULTANEOUS FAULTS

B 0.8 I2 1-4 SECS / B 0.013 I4 2-5 SECS

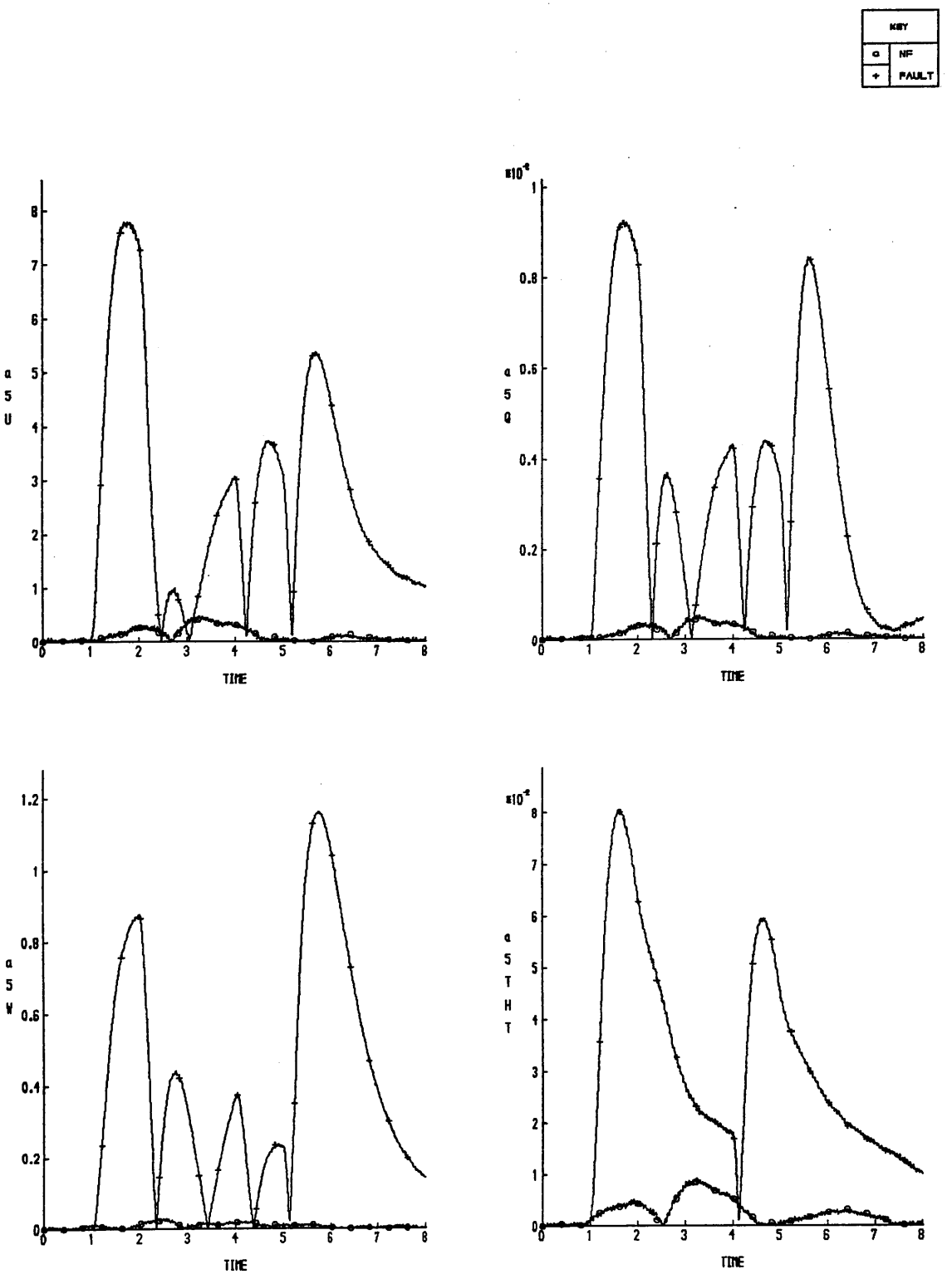

FIG 7.13B a_{ij}'s FOR SIMULTANEOUS FAULTS

B 0.8 I2 1-4 SECS / B 0.013 I4 2-5 SECS

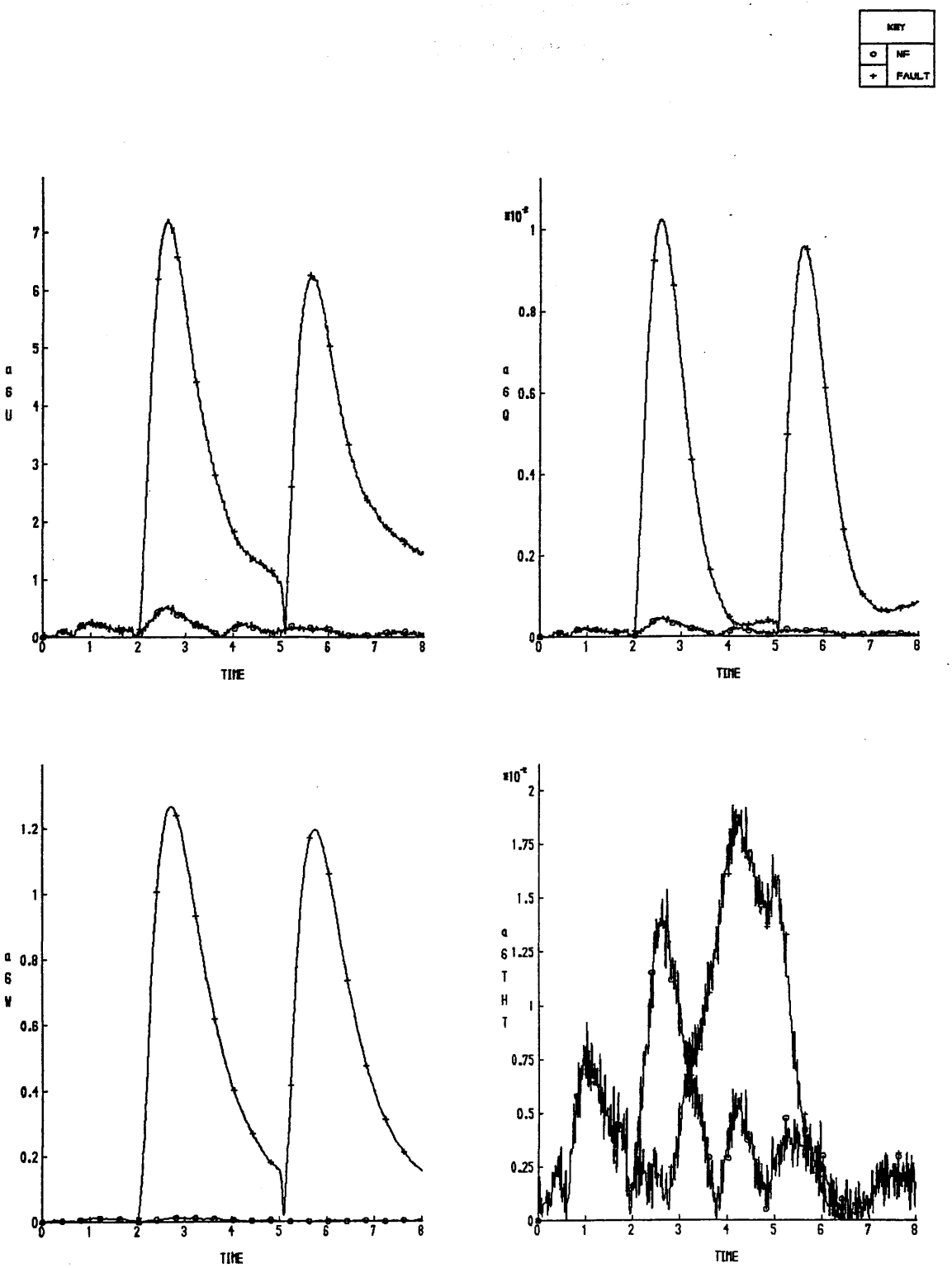

FIG 7.13B a_{ij}'s FOR SIMULTANEOUS FAULTS

B 0.8 I2 1-4 SECS / B 0.013 I4 2-5 SECS

to four seconds and 0.013 on instrument two from two to five seconds. a_{1j}, a_{4j} and a_{5j} increase at t=1 seconds to indicate a fault on instrument two and a_{3j}, (a_{5j}) and a_{6j} at t=2 seconds to indicate a fault on instrument four.

One last point to note is the variations in sensitivities of the a_{ij}'s. A good example of this can be seen with a_{6j} in *fig 7.13b*, where a_{6u}, a_{6w} and a_{6q} patently signal a fault whilst $a_{6\theta}$ shows comparably little change over the no fault case. However, since the fault detection logic only requires two out of four A_{ij}'s to be set true, this would not cause a problem.

7.6 SELECTION OF FAULT DETECTION THRESHOLDS

The simplest way to determine appropriate thresholds for each a_{ij} would be to select the worst possible case and set the thresholds accordingly. This would obviously minimise false alarms, but it would also increase the time to detect a fault and may result in less severe faults being missed. A more sophisticated method, considered by Clark, 1984, which takes account of the relationship between the magnitude of the states and the magnitude of observer errors, is to use thresholds which vary in proportion to the value of input and state. A simple realisation of this is,

$$L(t) = L_{ss} + W_1\underset{\sim}{x}(t) + W_2\underset{\sim}{u}(t) \qquad (7.13)$$

where L(t) is the time varying threshold, L_{ss} is the steady state threshold, $\underset{\sim}{x}(t)$ and $\underset{\sim}{u}(t)$ are perturbations from their trim values and W_1 and W_2 are weightings for the state and control variations, respectively. A more elaborate approach for L(t) could be a non−linear function of the states and inputs, eg.

$$L(t) = L_{ss} + W_1 f_1(\underset{\sim}{x}(t)) + W_2 f_2(\underset{\sim}{u}(t)) \qquad (7.14)$$

With simple functions such as e^x, L(t) could be made relatively constant for small perturbations of the state, whilst larger variations would result in increasingly higher thresholds.

If the fault detection logic is based on the observer error signals $\underset{\sim}{e}$ (note, *not* $\underset{\sim}{x}-\hat{\underset{\sim}{x}}$), instead of the state estimates $\hat{\underset{\sim}{x}}$, then the problem is further complicated by the differences in magnitude of $\underset{\sim}{e}$ between observers. For example, *fig 7.14* shows $\underset{\sim}{e}_1$ for two observers, C(1) and C(4), during the same manoeuvre. Although both produce an accurate, relatively noise free estimate of the state, the difference in magnitude between their error signals is approximately 10^3. Thus before comparing

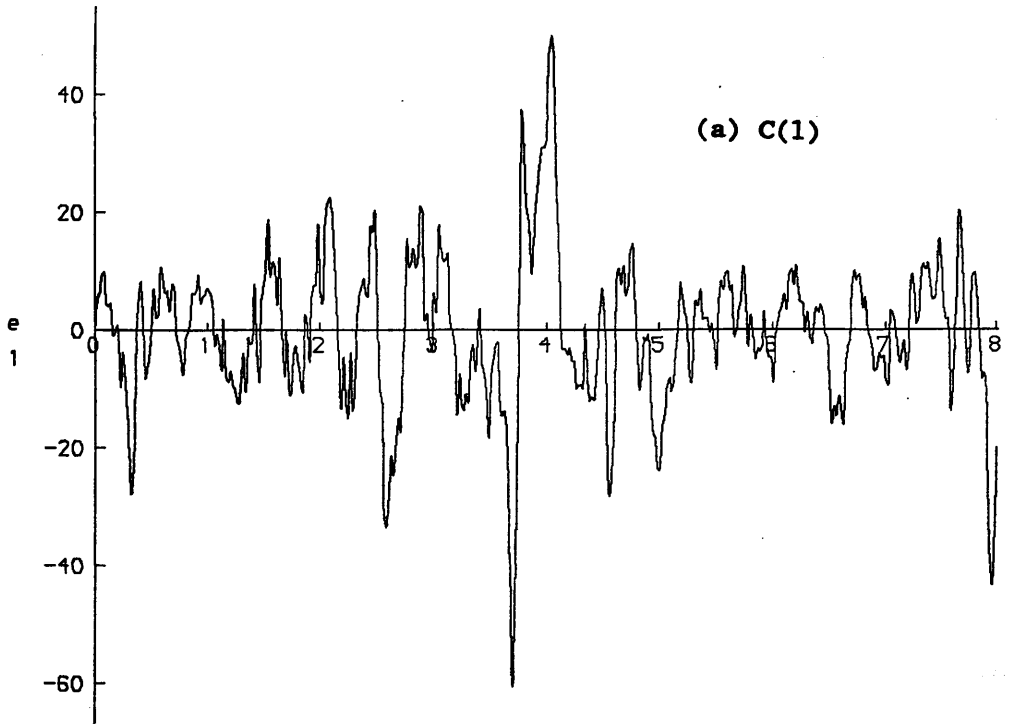

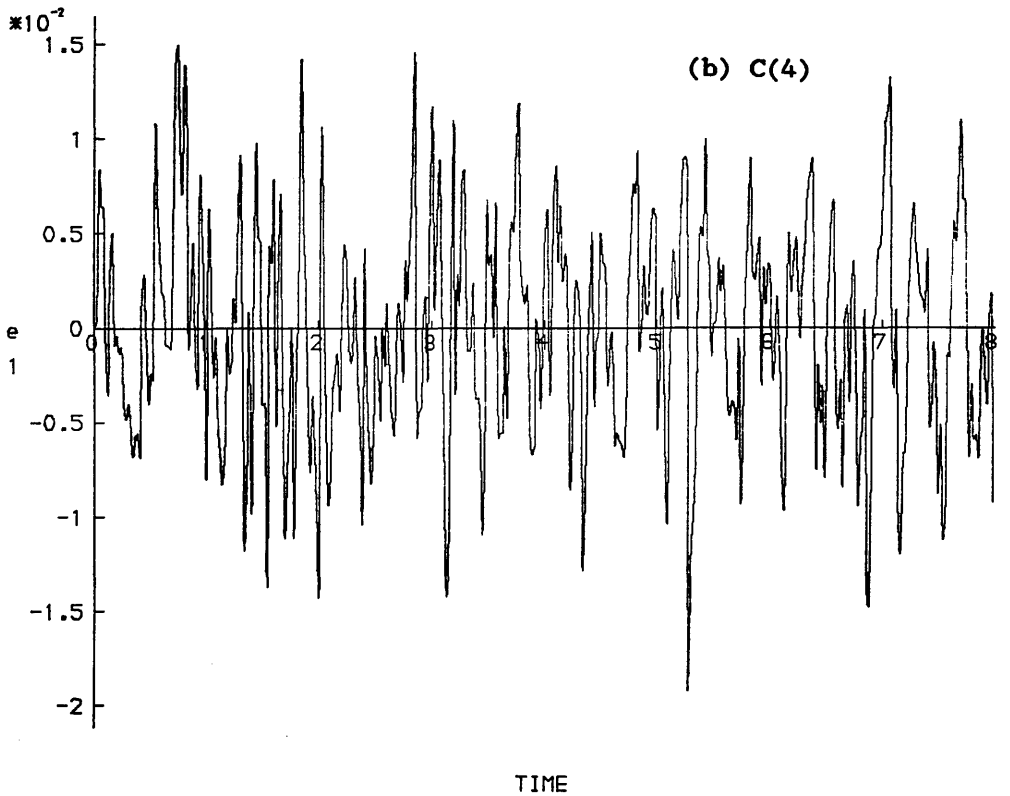

FIG 7.14 OBSERVER ERROR SIGNAL

error signals it would be essential to normalise them, but this is not easy due to the signals being extremely sensitive to noise.

When state estimates are compared, it was found that normalising and squaring the a_{ij}'s resulted in an improvement in the speed of detection of a fault. This is accomplished by first determining, as previously, the maximum no fault a_{ij}. Then, on subsequent tests with a fault introduced, each a_{ij} is initially normalised with respect to its corresponding maximum no fault value before being squared and compared to its fault threshold. The advantage of this method is that it increases the resolution of a fault since $(a_{ij})^2 < a_{ij}$ for $a_{ij} < 1.0$..

This improvement in detection rate can be seen in Table 7.5 which compares the detection times of the two logic schemes (ie. one as before, one with normalised and squared a_{ij}'s) for faults occurring at 1.0 and 7.0 seconds. At 1.0 second the improvement is 12.5% whilst at 7.0 seconds the figure is 27.7%.

In the above, and in the analysis of state estimation in earlier chapters, it has been assumed that the observer designs were based on an accurate linear model of the system. This was achieved by using the same A and B matrices produced by the mathematical model, Helistab, for both system and observer. Helistab, however, does not yet completely portray the helicopter's dynamic and aerodynamic characteristics and therefore in a real application parameter variations must be assumed.

With the observer designs considered in this thesis, these parameter variations will result in inaccurate estimates of the system state. This is obviously unacceptable for flight control system purposes, but is this also the case with instrument fault detection? Providing each observer produced the same wrong estimate then they could still be compared to detect faults.

Several tests were therefore run with a longitudinal system model of the Puma at 100 knots and observers designed with flight conditions of 80, 90, 110 and 120 knots, and 100 knots with descent angles of $-6°$, $-3°$, $+3°$ and $+6°$. For each flight condition four observers were designed: C(1), C(2), C(3) and C(4), and the time response of the system and observers to a doublet input on θ_{1S} (Appendix six) was recorded. Typical results are shown in *fig 7.15*. Results for u and q are comparable to those for θ and w, respectively.

The reasonable agreement between observers, of the estimates for q and w, would perhaps allow their use in a fault detection scheme, but unfortunately the estimates of u are too dissimilar. With θ it would be possible to use the estimates generated

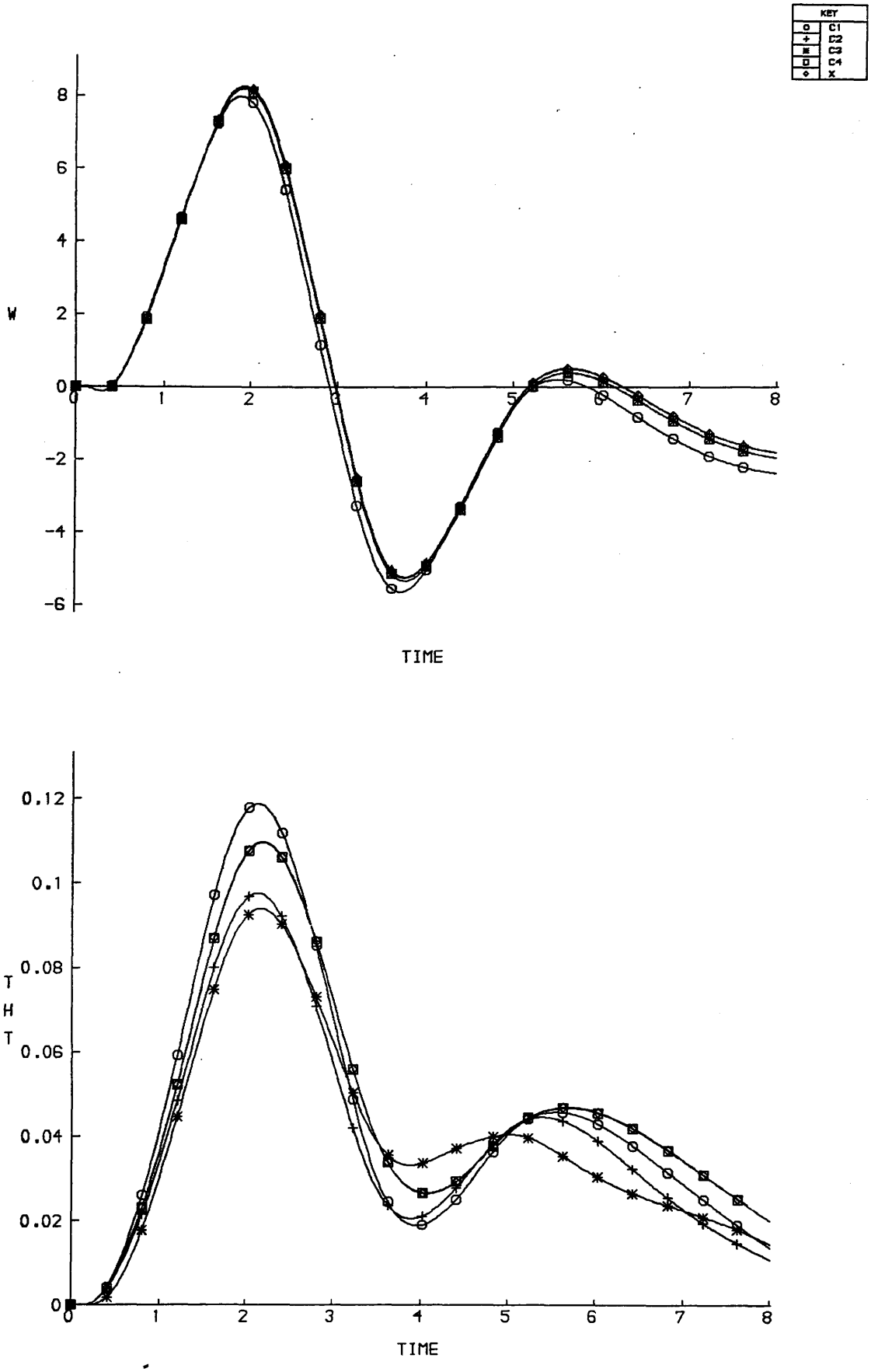

FIG 7.15A EFFECT OF INACCURATE OBSERVER MODEL ON OBSERVER RESPONSE SYSTEM 100 KNOTS, OBSERVER 90 KNOTS

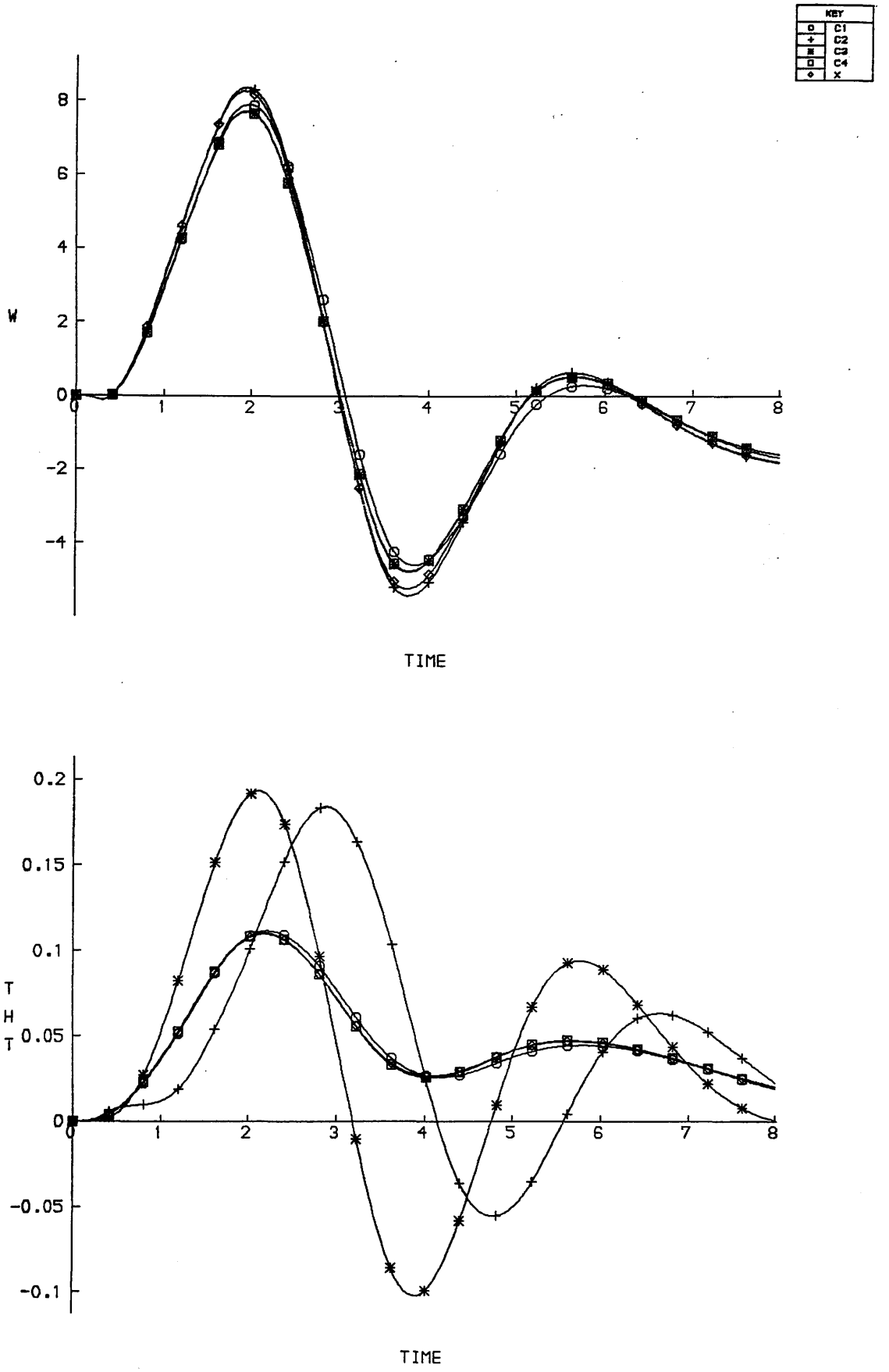

FIG 7.15B EFFECT OF INACCURATE OBSERVER MODEL ON OBSERVER RESPONSE SYSTEM 100 KNOTS, OBSERVER 100 KNOTS, -3°

a	u	w	q	θ	A_i	
1	1.141	1.867	1.500	1.188	1.188	FAULT AT 1.0 SECOND
2	0.000	0.000	0.000	0.000	0.000	
3	0.000	0.000	0.000	0.000	0.000	
4	1.125	1.086	1.102	1.164	1.102	
5	1.102	1.062	1.086	1.141	1.086	
6	0.000	0.000	0.000	0.000	0.000	
1	1.125	1.727	1.422	1.164	1.164	FAULT AT 1.0 SECOND
2	0.000	0.000	0.000	0.000	0.000	NORMALISED/SQUARED
3	0.000	0.000	0.000	0.000	0.000	
4	1.102	1.086	1.086	1.125	1.086	
5	1.086	1.062	1.086	1.125	1.086	
6	0.000	0.000	0.000	0.000	0.000	
1	7.266	0.000	0.000	7.367	7.367	FAULT AT 7.0 SECOND
2	0.000	0.000	0.000	0.000	0.000	
3	0.000	0.000	0.000	0.000	0.000	
4	7.242	7.164	7.227	7.383	7.227	
5	7.188	7.164	7.188	7.266	7.188	
6	0.000	0.000	0.000	0.000	0.000	
1	7.203	0.000	0.000	7.266	7.266	FAULT AT 7.0 SECOND
2	0.000	0.000	0.000	0.000	0.000	NORMALISED/SQUARED
3	0.000	0.000	0.000	0.000	0.000	
4	7.203	7.141	7.188	7.320	7.188	
5	7.164	7.164	7.164	7.227	7.164	
6	0.000	0.000	0.000	0.000	0.000	

TABLE 7.5 COMPARISON OF LOGIC SCHEMES

by C(1) and C(4), but not those from C(2) and C(3). An improvement in the correlation of estimates between observers might be achieved by designing the observers using eigenstructure assignment such that each observer had common eigenvectors as well as common eigenvalues. The benefit of this is that each observer response should then have the same decay rate (due to the eigenvalues) and the same shape (due to the eigenvectors). Thus even although the estimates would not be suitable for control use, they would be sufficient for instrument fault detection.

Unfortunately time precluded any further investigation of instrument fault detection and therefore the problems and possible solutions discussed in this chapter remain subjects for future work.

CHAPTER EIGHT

CONCLUSIONS AND FUTURE WORK

8.1 SUMMARY AND CONCLUSIONS

In general terms, the work described in this thesis demonstrates that deterministic, continuous–time, linear, time–invariant system theory can be used to design 'Luenberger' state observers for state estimation and instrument fault detection in the single rotor helicopter.

For accurate state estimation a precise linear model of the system is required. Unfortunately, the only available mathematical model was not capable of fully portraying the helicopter's aerodynamic and dynamic characteristics over the complete flight envelope. A detailed description of the model, its limitations and work currently being carried out on improvements was given in Chapter two. It was also shown that an exact model of the system could be simulated by using the same A and B matrices produced by the mathematical model, for computer simulation of both system and observer.

In Chapter three observer theory was presented for the observability test, full order and reduced order observers and in particular, an algorithm for the transformation of the system into observable canonical form. An important consequence of this transformation is that the transformed system can be considered as a set of subsystems, each being coupled to each other only through their outputs. It was shown that this was a relatively simple procedure and the resulting changes to the observer equations were explained.

A review of observer design techniques were given in Chapter four and two design methods were initially selected for consideration : a method proposed by Gopinath and an observable canonical form method. From the tests conducted it was apparent that the Gopinath dyadic observer design algorithm was unsuitable for the order of system under consideration (ie. $n=8$ and $n=14$).

The reasons for this were twofold. Firstly the system (A), distribution (B) and output (C) matrices were often ill–conditioned, or tended to produce an ill–conditioned problem; and secondly the digital computer implementation of the algorithm was numerically unstable. This method was therefore rejected.

The canonical form method involves the use of the observable canonical transformation defined in Chapter three and it was demonstrated that with the system in this form the determination of the observer matrix, H, is a trivial calculation. In Chapter five, the computer implementation of this algorithm was described and the significant numerical benefits illustrated.

The main advantage of the method is that it allows observers to be designed for each subsystem rather than for the whole system. Since the number of subsystems is determined by the dimensions of the output matrix, the accuracy of the observer design can be improved by increasing the magnitude of p. An observer designed using the canonical transformation was successfully tested with a feedback controller utilising modal control.

Observer performance with eighth and fourteenth order system models was considered in Chapter six and several numerical problems were examined. In particular, it proved extremely difficult to predict which combinations of system and output matrix give a satisfactory estimate. In an attempt to solve this problem the numerical methods used in the observability test were examined, but unfortunately this did not produce any answers.

It was shown that canonical form observers can produce accurate estimates if the system states are 'clean', but that noise corrupted states (achieved by adding noise obtained from flight data to the model generated states) result in noise corrupted estimates. To solve this problem a new form of observer – the twin observer – was introduced and it was demonstrated that with a good model of the system the twin observer can produce accurate, relatively noise free estimates of the system state.

Having thus established that it is possible to use a Luenberger observer to estimate the state of a stochastic system the final objective was to determine whether the twin observer was suitable for use in an observer based instrument fault detection scheme. This question was considered in Chapter seven, which included a literature review of current fault detection techniques. From this review it was apparent that the most appropriate technique to use with the twin observer was a software redundancy method known as the dedicated observer scheme.

The advantages of software redundancy lie in the trade–off of redundant hardware against computer processing of signals from dissimilar (non–redundant) sensors, however designing a reliable, robust scheme is extremely difficult. The problems with this method were examined in detail, particularly the problem of selecting suitable threshold values for the fault detection logic.

It was shown that with this type of observer an inaccurate model of the system has severe implications for the viability of a fault detection scheme. This was because different observers produced differing (wrong) estimates of the state. A possible solution to the problem would be to design the observer using eigenstructure

assignment (such that each observer had common eigenvectors as well as common eigenvalues) then each observer response should have the same decay rate and shape. Thus even although the estimates would not be suitable for control use, they could be compared by a logic scheme to detect faults.

8.2 FUTURE WORK

Throughout this thesis it has clearly been stated and proved that a precise, linear model of the system is required for accurate state estimation with the 'Luenberger' form of observer. The present work on improvements to the model is therefore of vital importance if state observer techniques are to be used for helicopter flight control.

However, due to the complexity of the dynamic and aerodynamic effects, it is reasonable to assume that the model will never be 100% accurate and therefore any future work must consider techniques of designing observers to be insensitive (or *robust*) to parameter variations. Robust observer design methods have already been published and thus the first step would be to review these and determine whether the techniques are compatible with the observable canonical form method. If they were not, then techniques of making the canonical form method robust should be investigated and a comparison made to decide which method produced the best results.

Further investigation of the twin observer is required, in particular the use of a more sophisticated filter and the implementation with an eighth and fourteenth order model. Note that since this form of observer is basically two observers connected together, any technique to improve the robustness of the standard observer will be applicable to the twin observer.

The utilization of the twin observer in a dedicated observer scheme and other observer–based fault detection schemes also requires attention. From the work carried out so far, it would appear that observer design criterion for fault detection are incompatible with those for state estimation and therefore the methods should be considered independently.

A good example of this is the suggestion in the previous section that eigenstructure assignment could be used to design observers for fault detection; the idea being that each observer would produce the same estimate, even when the model was inaccurate. An investigation of this is obviously a priority. An examination of

different logic schemes and variable thresholds should also prove beneficial. It is also suggested that a more theoretical consideration should be given to the numerical methods used for the observability test and the transformation of the system state equation to observable canonical form, in an effort to predict the 'sensitivity' and performance of different combinations of A and C matrices.

Finally, since the observers are based on linear models it would be necessary to employ some form of *scheduling* to ensure that the correct observers are used throughout the flight envelope.

REFERENCES

[A1] ANDRY Jr, A. N, SHAPIRO, E. Y and CHUNG, J. C
Eigenstructure Assignment For Linear Systems
IEEE Trans on Aerosp and Electronic Sys, Vol–19, No 5, 1983, 711–728

[A2] –
Modalized Observers
IEEE Trans on Autom Contr, Vol AC–29, No 7, July 1984

[A3] AOKI, M. L and HUDDLE, J. R
Stochastic System With A Constrained Estimator
Trans IEEE, Vol AC–12, 1967, 432–433

[A4] APLEVICH, J. D
Direct Computation Of Canonical Forms For Linear Systems By Elementary Matrix Operations
IEEE Trans on Autom Cont, Vol–19, 1974, 124–126

[A5] ARBEL, A and TSE, E
Observer Design For Large–Scale Linear Systems
IEEE Trans on Autom Cont, Vol AC–24, No 3, 1979, 469–476

[A6] ASTROM, K. J and EYKHOFF, P
System Identification – A Survey
Automatica 7, 1971, 123

[B1] BAILLIE, S. W
Vertical Axis Control Systems for 4+0 Sidearm Controller Implementations in Rotorcraft
Helicopter Handling Qualities and Control, Royal Aeronautics Society, London, 1988

[B2] BAKKEN, J. T
Implementation of Fly–by–Wire/ Fly–by–Light Experimental Flight Control Systems in Helicopters
National Specialists Meeting on Flight Controls and Avionics, AHS, Cherry Hill, N.J, 1987

[B3] BASS, R. W and GURA, I
High Order System Design via State–Space Considerations
Preprints Joint Autom Cont Conf, Atlanta, Georgia, June 1965

[B4] **BEARD, R. V**
Failure Accomodation in Linear Systems Through Self–Reorganization
Report No MVT–71–1 MAN Vehicle Laboratory, MIT, Cambridge, Mass, Sept 1971

[B5] **BLACK, C. G**
Consideration Of Trends In Stability And Control Derivatives From Helicopter System Identification
13th European Rotorcraft Forum, Arles, France, 1987

[B6] **– and MURRAY–SMITH, D. J**
A Frequency–Domain System Identification Approach to Helicopter Flight Mechanics Model Validation
Vertica, Vol–13, No. 3, 1989, 343–368

[B7] **–, MURRAY–SMITH, D. J and PADFIELD, G. D**
Experience With Frequency–Domain Methods In Helicopter System Identification
12th European Rotorcraft Forum, Garmish, FRG, 1986

[B8] **BLANVILLAIN, P and JOHNSON, T. L**
Specific–Optimal Control with a Dual Minimal Order Observer–Base Compensator
Int J Cont, Vol–28, 1978, 277–294

[B9] **BONGIORNO Jr, J. J**
On The Design Of Observers For Insensitivity To Plant Parameter Variations
Int J Cont, Vol–18, No 3, 1973, 597–605

[B10] **BONGIORNO Jr, J. J and YOULA, D. C**
On Observers In Multivariable Control Systems
Int J Cont, Vol–8, 1968, 221–243

[B11] **BONNICE, W. F, MOTYKA, P, WAGNER, E and HALL, S. R**
Aircraft Control Surface Failure detection and Isolation using the OSGLR Test
Proc AIAA Conf Guidance and Contr, 1986

[B12] **BRONSON, R**
Matrix Methods – An Introduction
Academic Press, 1969

[C1] **CHARLTON, M. T and HOUSTON, S. S**
Flight Test and Analysis Procedures for New Handling criteria
Helicopter Handling Qualities and Control, Royal Aeronautical Society, London, 1988

[C2] **CHARLTON, M. T, PADFIELD, G. D and HORTON, R. I**
Helicopter Agility in Low Speed Manoeuvres
Proc of the 13th European Rotorcraft Forum, Arles, France, 1987

[C3] **CHEN, C. T**
Linear System Theory And Design
Holt, Rinehart and Winston, N.Y, 1984

[C4] **CHOW, E. Y and WILLSKY A. S**
Analytical Redundancy and the Design of Robust Failure Detection Systems
IEEE Trans on Autom Contr, Vol–29, July 1984, 689–691

[C5] **CLARK, R. N**
Instrument Fault Detection
IEEE Trans on Aerosp and Elect Sys, Vol–14, No 3, 1978, 456–465

[C6] –
A Simplified Instrument Failure Detection Scheme
IEEE Trans on Aerosp and Elect Sys, Vol–14, No 4, 1978, 558–563

[C7] –
The Dedicated Observer Approach To Instrument Failure Detection
Proc of the 18th Conf, Ft Lauderdale, 1979, 237–241

[C8] –
Instrument Fault Models
IEEE Trans. AES, Mar 1984

[C9] –, **FOSTH, D. C, and WALTON, V. M**
Detecting Instrument Malfunctions In Control Systems
IEEE Trans on Aerosp and Elect Sys, Vol–11, No 4, 1975, 465–473

[C10] –, FRANK, P. M and WUNNENBERG, J
An Application of Instrument Fault Detection
IFAC Identification and System Parameter Estimation, York, 1985, 699–704

[C11] – and HERTEL, J. E
Instrument Failure Detection In Partially Observable Systems
IEEE Trans on Aerosp and Elect Sys, Vol–18, No 3, 1982, 310–317

[C12] –, MASRELIEZ, C. J and BURROWS, J. W
A Functionally Redundant Altimeter
IEEE Trans on Aerosp and Elect Sys, Vol–12, No 4, 1976, 459–462

[C13] – and SETZER, W
Sensor Fault Detection In A System With Random Disturbances
IEEE Trans on Aerosp and Elect Sys, Vol–16, No 14, 1980, 468–473

[C14] CROSSLEY and PORTER
Eigenvalue and Eigenvector Sensitivities in Linear Systems Theory
Int J Cont, Vol–10, No 2, 1969, 163–170

[C15] CUMMING, S. D. G
Design Of Observers Of Reduced Dynamics
Electron Lett, Vol–5, 1969, 213–214

[C16] CURTISS Jr, H. C and PRICE, G
Studies Of Rotorcraft Agility And Manoeuverability
10th European Rotorcraft Forum, The Hague, Sept 1984, Paper No 69

[D1] DAS, G and GHOSHAL, T. K
Reduced Order Observer Construction by Generalized Matrix Inverse
Int J Cont, Vol–33, 1981, 371–378

[D2] DAVISON, E. J and WANG, S. H
On Pole Assignment in Linear Multivariable Systems
IEEE Trans Autom Cont, Vol AC–20, 1975, 516–518

[D3] DECKERT, J. C, DESAI, M. N, DEYST, J. J and WILLSKY, A. S
F–8 DFBW Sensor Failure Identification Using Analytical Redundancy
IEEE Trans on Autom Contr, Vol–22, Oct 1977, 795–803

[D4] DEKLEVA, J and ROZIC, N
Forecasting : Kalman Models
IFAC Identification and System Parameter Estimation, York, 1985, 649–656

[D5] DELLON, F and SARACHIK, P. E
Optimal Control of Unstable Linear Plants with Inaccessible States
IEEE Trans Autom Cont, Vol AC–13, 1968, 491–495

[D6] DJAFERIS, T. E
Generic Pole Assignment Using Dynamic Output Feedback
Int J Cont, Vol–37, No.1, 1983, 127–144

[D7] DUNCAN, W. J
The Principles Of The Control And Stability Of Aircraft
Cambridge University Press, 1952

[D8] DuVAL, R
Use of Multiblade Sensors for On–Line Rotor Tip–Path–Plane Estimation
J. of the AHS, 1980, 25 (4), 13–21

[E1] EL–GHEZAWI, O. M. E, BILLINGS, S. A and ZINOBER, A. S. I
Variable Structure Systems and System Zeros
Proc IEEE, Part D, Vol–130, Jan 1983, 1–5

[E2] ELLIS, J. K and WHITE, G. W. T
An Introduction to Modal Analysis and Control
Control, Vol–9, 1965, 193–197

[F1] FAIRMAN, F. W and GUPTA, R. D
Design of Multi–Functional Reduced Order Observers
INT J SYS Science, Vol–11, 1980, 1083–1094

[F2] FORTMANN, T. E and WILLIAMSON, D
Design Of Low–Order Observers For Linear Feedback Control Laws
IEEE Trans on Autom Cont, Vol AC–17, No 3, 1972, 301–308

[F3] FRANK, P. M
Fault Diagnosis in Dynamic Systems via State Estimation – A Survey
Proc 1st European Workshop on Fault Diagnosis, Relaibility and Related Knowledge–based approaches, Sept 1986, Rhodes, Greece

[F4] – and KELLER, L
Sensitivity Discriminating Observer Design For Instrument Failure Detection
IEEE Trans on Aerosp and Elect Sys, Vol–16, No 4, 1980, 460–467

[F5] FULLER, J
Rotor State Estimation for Rotorcraft
Proc AHS National Specialists Meeting on Helicopter Vibration, Hartford, Connecticut, 1981

[G1] GILBERT, E. G
Controllability And Observability In Multivariable Control Systems
J.S.I.A.M Cont, Ser A, Vol–2, No 1, 1963, 128–151

[G2] GOKNAR, I. C and DERVISOGLU, A
An Algorithm To Determine The Controllability And Observability Of Linear Time–Invariant Systems Using Zero–State Algebraic Equations
IEEE Trans on Autom Cont, June 1977, Tech notes and corresp, 495–498

[G3] GOPINATH, B
On The Control Of Linear Multiple Input–Output Systems
Bell Sys Tech Jour, Vol–50, No 3, March 1971, 1063–1081

[H1] HALL Jr, W, GUPTA, N and HANSEN, R
Rotorcraft System Identification Techniques for Handling Qualities and Stability and Control Evaluation
Proc 34th AHS National Specialists Meeting on Helicopter Vibration, Hartford, Connecticut, 1981

[H2] HAM, N. D
Helicopter Individual Blade Control and its Applications
Proc 39th AHS National Forum, May 1983

[H3] – and McKILLIP Jr, R. M
A simple System for Helicopter Individual Blade Control and its Application to Gust Alleviation
Proc 36th AHS National Forum, May 1980

[H4] HENGY, D and FRANK, P. M
Component Failure Detection via Non–Linear State Observers
Dept of Elect Eng, Univ of Duisburg, FRG, 1983

[H5] HOPKIN, H. R
A Scheme Of Notation And Nomenclature For Aircraft Dynamics And Associated Aerodynamics
RAE Tech Report 66200, Parts 1–5, 1966
ARC R&M No 3562, Parts 1–5, 1970

[I1] ISERMANN, R
Process Fault Detection Based On Modelling And Estimation Methods – A Survey
Automatica, Vol–20, No 4, 1984, 387–404

[J1] JAMESON, A and ROTHSCHILD, D
A Direct Approach to the Design of Asymptotically Optimal Controllers
Int J Cont, Vol–13, 1971, 1041–1050

[J2] JOHNSON, G. W
A Deterministic Theory of Estimation and Control
IEEE Trans Autom Cont, Vol AC–14, 1969, 380–384

[J3] JONES, H. L
Failure Detection in Linear Systems
PhD Thesis, Dept of Aeronautics and Astronautics, MIT, Cambr, Mass, 1973

[J4] JORDAN, D and SRIDHAR, B
An Efficient Algorithm For Calculation Of The Luenberger Canonical Form
IEEE Trans on Autom Cont, Vol–18, 1973, 292–295

[J5] JUANG, J. N and SUZUKI, H
An Eigensystem Realization Algorithm in Frequency Domain for Modal Parameter Identification
Proc AIAA Conf Guidance and Contr, 1986

[K1] KALMAN, R. E
A New Approach To Linear Filtering And Prediction Problems
J Basic Eng, Vol–82, 1960, 35

[K2] –
On the General Theory of Control Systems
Proc 1st IFAC Cong, Vol–1, Butterworth's, London, 1960(b), 481–493

[K3] –
Mathematical Description Of Linear Dynamical Systems
J.S.I.A.M Control, Vol–1, 1963, 152

[K4] – and BERTRAM, J. E
General Synthesis Procedure for Computer Control of Single and Multiloop Linear Systems
Trans AIEE, Vol–77, 1959, 602–609

[K5] – and BUCY, R. S
New Results in Linear Filtering and Prediction Theory
IEEE Trans ASME, J. Basic Eng, Ser D, March 1961, 95–108

[K6] KITAMURA, M
Detection of Sensor Failures in a Nuclear Plant using Analytical Redundancy
J. American Nuclear Society, Vol–34, 1980

[K7] KLEIN, G and MOORE, B. C
Eigenvalue – Generalized Eigenvector Assignment With State Feedback
IEEE Trans on Autom Cont, Vol AC–22, 1977, 140–141

[K8] KORTE, U
Some Flight Test Results With Redundant Digital Flight Control Systems
Messerschmitt–Bolkow–Blohm GMBH Aircraft Division, 1984

[K9] KRETZ, M
Research in Multicyclic and Active Control of Rotary Wings
Vertica, 1976, 1 (2)

[L1] LUENBERGER, D. G
Observing The State Of A Linear System
IEEE Trans on Mil Elect, Vol Mil–8, Apr 1964, 74–80

[L2] –
Invertible Solutions to the Operator Equation $TA - BT = C$
Proc Am Math Soc, Vol–16, 1965, 1226–1229

[L3] –
Observers For Multivariable Systems
Trans IEEE, Vol AC–11, 1966, 190–197

[L4] –
Canonical Forms For Linear Multivariable Systems
IEEE Trans on Autom Cont, Vol AC–12, June 1967, 290–293

[L5] –
An Introduction To Observers
Trans IEEE, Vol AC–16, 1971, 596–602

[M1] MacFARLANE, A. G. J and KARCANIAS, N
Poles and Zeros of Linear Multivariable Systems: A survey of Algebraic, Geometric and Complex Variable Theory
Int J Cont, Vol–24, July 1976, 33–74

[M2] McKILLIP Jr, R. M
Periodic Control of the Individual Blade Control Helicopter Rotor
Proc of 10th European Rotorcraft Forum, The Hague, The Netherlands, 1984

[M3] –
Kinematic Observers for Rotor Control
Proc Int Conf on Rotorcraft Basic Research, Research Triangle Park, NC, 1985

[M4] –
Kinematic Observers For Active Control Of Helicopter Rotor Vibrations
12th European Rotorcraft Forum, Garmish, FRG, 1986

[M5] McLEAN, D and AL–KHATIB, K
Simulation Study Of An Analytically–Redundant Flight Control System
Dept of Transport Tech, Univ of Tech, Loughborough, 1984.

[M6] MADBOULY, E. El and FRANK, P. M
Robust Instrument Failure Detection via Luenberger Observers in Nuclear Power Plants
Univ of Duisburg, FRG, 1983

[M7] MADIWALE, A and FRIEDLAND, B
Comparison of Innovations–Based Analytical Redundancy Methods
Proc ACC, June 1983

[M8] MIMINIS, G. S and PAIGE, C. C
An Algorithm For Pole Assignment Of Time–Invariant Linear Systems
Int J Cont, Vol–35, No 2, 1982, 341–354

[M9] MITA, T
Design Of A Zero–Sensitive Observer
Int J Cont, Vol–22, No 2, 1975, 215–227

[M10] MOLUSIS, J, WARMBRODT, W and BAR–SHALOM, Y
Identification of Helicopter Rotor Dynamic Models
Proc 24th AIAA Structures, Dynamics and Materials Conf, Lake Tahoe, Nevada, 1983

[M11] MOORE, B. C
On The Flexibility Offered By State Feedback In Multivariable Systems Beyond Closed Loop Eigenvalue Assignment
IEEE Trans On Autom Cont, Vol AC–21, 1976, 689–692

[M12] MOORE, J. B
A Note on Minimal Order Observers
IEEE Trans Autom Cont, Vol AC–17, 1972, 255–256

[M13] – and LEDWICH, G. F
Minimal Order Observers for Estimating Linear Functions of a State Vector
IEEE Trans Autom Cont, Vol AC–20, 1975, 623–632

[M14] MORSE, A. S, WOLOVICH, W. A and ANDERSON, B. D. O
Generic Pole Assignment : Preliminary Results
IEEE Trans Autom Cont, Vol AC–28, No.4, 1983, 503–506

[M15] MUNRO, N
A Systematic Design Procedure for Reduced–Order Observers
Report No 178, Control Systems Centre, UMIST, Manchester, 1971

[M16] –
Computer–Aided Design Procedure for Reduced Order Observers
Proc IEE, Vol–120, 1973, 319–324

[M17] –
Pole Assignment
Proc Instn Elect Engs, Vol–126, 1979, 549–554

[M18] – and VARDULAKIS, A. I
Pole–Shifting Using Output Feedback
IBID, Vol–18, 1973, 1267–1273

[N1] NEWMANN, M. M
Design Algorithms for Minimal Order Luenberger Observers
Electron Lett, Vol–5, 1969, 390–392

[N2] –
A Continuous–Time, Reduced Order Filter For Estimating The State Vector Of A Linear Stochastic System
Int J Cont, Vol–11, No 2, 1970, 229–239

[N3] –
Specific Optimal Control of the Linear Regulator Using a Dynamical Controller Based on the Minimal order Observer
Int J Cont, Vol–12, 1970(b), 33–48

[N4] NUMERICAL ALGORITHMS GROUP Ltd
NAG Fortran Mark–11
NAG Central Office, Oxford, OX2 7DE, 1987

[O1] O'REILLY, J
Observers For Linear Systems
Mathematics In Science And Engineering, Vol–170, Academic Press, 1983

[O2] – and NEWMANN, M. M
Minimal order Observer–Estimators for Continuous–Time Linear Systems
Int J Cont, Vol–22, 1975, 573–590

[P1] PADFIELD, G. D
A Theoretical Model Of Helicopter Flight Mechanics For Application To Piloted Simulation
TR 81048, Royal Aerospace Establishment, Bedford, 1981

[P2] –
Helicopter Handling Qualities and Control: Is the Helicopter Community Prepared for Change
Conf Helicopter Handling Qualities and Control, Nov 1988, Royal Aero Soc.

[P3] PARRY, D. L. K and MURRAY–SMITH, D. J
The Application Of Modal Control Theory To The Single Rotor Helicopter
11th European Rotorcraft Forum, 1985, 78.1–78.18

[P4] PATTON, R. J and WILLCOX, S. W
Comparison Of Two Techniques Of I.F.D Based On A Non–Linear Stochastic Model Of An Aircraft
IFAC Identification And System Parameter Estimation, York, 1985, 711–717

[P5] –, – and WINTER, J. S
Parameter–Insensitive Technique For Aircraft Sensor Fault Analysis
J Guidance, Vol–10, No 4, 1987, 359–367

[P6] PORTER, B and CROSSLEY, T. R
Modal Control : Theory and Applications
Taylor and Francis, London, 1972

[R1] RETALLACK, D. G and MacFARLANE, A. G. J
Pole Shifting Techniques for Multivariable Feedback Systems
Proc IEE, Vol–117(5), 1970, 1037–1038

[R2] RICHARDS, R. J
An Introduction To Dynamics And Control
Longman Inc, London, 1979

[R3] RICHARDS, W. R
ACT Applied To Helicopter Flight Control
Smiths Industries Aerospace And Defence Systems, Cheltenham, 1983

[R4] ROMAN, J. R and BULLOCK, T. E
Design of Minimal Order State Observers for Linear Functions of the State via Realization Theory
IEEE Trans Autom Cont, Vol AC–20, 1975, 613–622

[R5] ROMAN, J. R, JONES, L. E and BULLOCK, T. E
Observing a Function of the State
Proc IEEE Decision and Cont Conf, San Diego, California, Dec 1973

[R6] ROSENBROCK, H. H
Chem Eng Prog, Vol–58, 1962, 43
Distinctive Problems of Process Control

[R7] –
State Space And Multivariable Theory
New York, Wiley–Interscience, 1970

[R8] ROY, S. D
Helicopter Controls And Displays – Future Concepts
Westland Helicopters Ltd, Yeovil, Somerset, 1984.

[S1] SARMA, I. G and JAYARAJ, C
On The Use Of Observers In Finite–Time Optimal Regulator Problems
Int J Cont, Vol–11, No 3, 1970, 489–497

[S2] SHAPIRO, E. Y and CHUNG, J. C
Constrained Eigenvalue/Eigenvector Assignment – Application to Flight Control Systems
Proc 19th Annual Allerton Conf Communication, Control and Computing, Univ Illinois, 1981, 320–328

[S3] SHAW, J and ALBION, N
Active Control of Rotor Blade Pitch for Vibration Reduction: A Wind Tunnel Demonstartion
Vertica, 1980, 4 (1)

[S4] SIRISENA, H. R
Minimal Order Observers for Linear Functions of a State Vector
Int J Cont, Vol–29, 1979, 235–254

[S5] SMITH, J
An Analysis Of Helicopter Flight Mechanics Part 1. Users Guide To The Software Package Helistab
TM FS(B)569, Royal Aerospace Establishment, Bedford, 1984

[S6] SRINATHKUMAR, S
Eigenvalue/ Eigenvector Assignment Using Output Feedback
IEEE Trans Autom Cont, Vol AC–23, 1978, 79–81

[S7] STUCKENBERG, N
Sensor Failure Detection in Flight Control Systems using Deterministic Observers
IFAC Identification and System Parameter Estimation, York, 1985

[S8] SUNDARESWARAN, K. K, McLANE, P. J and BAYOUMI, M. M
Observers For Linear Systems With Arbitrary Plant Disturbances
IEEE Trans On Autom Cont, Vol AC–22, No 5, 1977, 870–871

[T1] TISCHLER, M. B
Digital Control of Highly Augmented Combat Aircraft
NASA Technical Memorandum 88346, 1987

[T2] TSE, E
Observer–Estimators for Discrete–Time Systems
IEEE Trans Autom Cont, Vol AC–18, 1973, 10–16

[T3] – and ATHANS, M
Optimal Minimal Order Observer–Estimators for Discrete Linear Time–Varying Systems
IEEE Trans Autom cont, Vol AC–15, 1970, 416–426

[T4] – and –
Observer Theory for Continuous–Time Systems
Information and cont, Vol–22, 1973, 405–434

[T5] TSIM Nonlinear Dynamics Simulation Package – Users Reference Manual And Users Guide
Cambridge Controls Ltd, Cambridge, CB3 0HB, 1986

[T6] TUEL Jr, W. G, CHIDAMBARA, M. R, RANE, D. S, MUFTI, I. H and JOHNSON, C. D
Five Letters Of Correspondence on *The Transformation To (Phase–Variable) Canonical Form*
IEEE Trans On Autom Cont, Vol–11, 1966, 607–610

[W1] WANG, S. H and DAVISON, E. J
Canonical Forms of Linear Multivariable Systems
SIAM J Cont, Vol–14, 1976, 236–250

[W2] WILLCOX, S. W
Robust Sensor Fault Diagnosis for Aircraft Based on Analytical Redundancy
PhD Thesis, Dept of Electronics, Univ of York, June 1988

[W3] WILLSKY, A. S
A Survey Of Design Methods For Failure Detection In Dynamic Systems
Automatica, Vol–12, 1976, 601–611

[W4] –
Failure Detection In Dynamic Systems
AGARD LS–109, 1980

[W5] – and JONES, H. L
A Generalized Likelihood Ratio Approach to the Detection and Estimation of Jumps in Linear Systems
IEEE Trans on Autom Contr, Vol–21, Feb 1976

[W6] WINTER, J. S, CORBIN, M. J and LESLEY, M. M
Description of TSIM2: A Software Package for Coputer Aided Design of Flight Control Systems
RAE Tech Report No 83007, Jan 1983

[W7] WINTER, J. S, PADFIELD, G. D and BUCKINGHAM, S. L
The Evolution Of ACS For Helicopters – Conceptual Simulation To Preliminary Design
AGARD Flight Mechs Panel Symp On Active Cont Sys, Toronto, 1984

[W8] WOLOVICH, W. A
On State Estimation of Observable Systems
Proc Joint Autom Cont Conf, 1968, 210–220

[W9] –
Linear Multivariable Systems
Springer– Verlag, New York, 1974

[W10] **WONHAM, W. M**
On Pole Assignment In Multi–input, Controllable Linear Systems
IEEE Trans On Autom Cont, Vol AC–12, 1967, 660–665

[W11] **– and MORSE, A. S**
Feedback Invariants of Linear Multivariable Systems
Automatica, Vol–8, 1972, 93–100

[W12] **WOOD, E. R**
Higher Harmonic Control for the Jet Smooth Ride
Vertiflite, 1983, 29 (4), 28–32

[W13] **WUNNENBERG, J, CLARK, R. N and FRANK, P. M**
An Application Of Instrument Fault Detection
IFAC Identification And System Parameter Estimation, York, 1985, 699–704

[W14] **WUNNENBERG, J and FRANK, P. M**
Sensor Fault Detection via Robust Observers
Dept of Elect Eng, Univ of Duisburg, FRG, 1984

[W15] **WYATT, G. C. F**
The Evolution Of Active Control Technology Systems For The 1990's Helicopter
Westlands Helicopters Ltd, Yeovil, Somerset, 1984

[W16] **YUKSEL, Y. O and BONGIORNO Jr, J. J**
Observers For Linear Multivariable Systems With Applications
IEEE Trans On Autom Cont, Vol AC–16, No 6, 1971, 603–613

APPENDICES

APPENDIX 1 LINEARIZING THE EQUATIONS OF MOTION

(1) $\dot{u} = vr - wq - g\sin\theta + \frac{X}{m}$

Replace total values by trim value, subscript '0', plus a perturbation

$$(\dot{u} + \dot{u}_0) = (v + v_0)r - (w + w_0)q - g\sin(\theta + \theta_0) + \frac{X}{m}$$

$\dot{u}_0 = 0$ by definition and discard products involving perturbations

$$\dot{u} = v_0 r - w_0 q - g(\sin\theta\cos\theta_0 + \cos\theta\sin\theta_0) + \frac{X}{m}$$

Expand as Taylor series and make small angle assumptions

$$\dot{u} = v_0 r - w_0 q - g\theta\cos\theta_0 - g\sin\theta_0 + \frac{1}{m}\left[X_0 + \frac{\partial X}{\partial u} u + \ldots + \frac{\partial X}{\partial \theta_{0t}} \theta_{0t} \right]$$

but

$$0 = -g\sin\theta_0 + \frac{X_0}{m}$$

hence

$$\dot{u} = \frac{\partial X}{\partial u} u + \frac{\partial X}{\partial w} w + \left[\frac{\partial X}{\partial q} - w_0 \right] q + \left[\frac{\partial X}{\partial \theta} - g\cos\theta_0 \right] \theta + \frac{\partial X}{\partial v} v + \frac{\partial X}{\partial p} p$$

$$+ \frac{\partial X}{\partial \varphi} \varphi + \left[\frac{\partial X}{\partial r} + v_0 \right] r + \frac{\partial X}{\partial \theta_{0e}} \theta_{0e} + \frac{\partial X}{\partial \theta_{1s}} \theta_{1s} + \frac{\partial X}{\partial \theta_{1c}} \theta_{1c} + \frac{\partial X}{\partial \theta_{0t}} \theta_{0t}$$

where all partial derivatives are multiplied by the factor : $\frac{1}{m}$

(2) $\dot{v} = wp - ur + g\sin\varphi\cos\theta + \frac{Y}{m}$

by analogy with (1)

$$\dot{v} = w_0 p - u_0 r + g\sin(\varphi_0 + \varphi)\cos(\theta_0 + \theta) + \frac{Y}{m}$$

$$\dot{v} = w_0 p - u_0 r + g(\sin\varphi_0\cos\varphi + \cos\varphi_0\sin\varphi)(\cos\theta_0\cos\theta - \sin\theta_0\sin\theta) + \frac{Y}{m}$$

Taylor expansion -

$$\dot{v} = w_0 p - u_0 r + g(\sin\varphi_0 + \varphi\cos\varphi_0)(\cos\theta_0 - \theta\sin\theta_0)$$

$$+ \frac{1}{m}\left[Y_0 + \frac{\partial Y}{\partial u} u + \ldots + \frac{\partial Y}{\partial \theta_{0t}} \theta_{0t} \right]$$

but

$$0 = g\sin\varphi_0\cos\theta_0 + \frac{Y_0}{m}$$

hence

$$\dot{v} = \frac{\partial Y}{\partial u}u + \frac{\partial Y}{\partial w}w + \frac{\partial Y}{\partial q}q + \left[\frac{\partial Y}{\partial \theta} - g\sin\varphi_0\sin\theta_0\right]\theta + \frac{\partial Y}{\partial v}v$$
$$+ \left[\frac{\partial Y}{\partial p} + w_0\right]p + \left[\frac{\partial Y}{\partial \varphi} + g\cos\varphi_0\cos\theta_0\right]\varphi + \left[\frac{\partial Y}{\partial r} - u_0\right]r + \frac{\partial Y}{\partial \theta_{0e}}\theta_{0e}$$
$$+ \frac{\partial Y}{\partial \theta_{1s}}\theta_{1s} + \frac{\partial Y}{\partial \theta_{1c}}\theta_{1c} + \frac{\partial Y}{\partial \theta_{0t}}\theta_{0t}$$

where all partial derivatives are multiplied by the factor : $\frac{1}{m}$

(3) $\dot{w} = uq - vp + g\cos\varphi\cos\theta + \frac{Z}{m}$

by analogy with (1) and (2)

$$\dot{w} = u_0q - v_0p + g\cos(\varphi_0 + \varphi)\cos(\theta_0 + \theta) + \frac{Z}{m}$$

$$\dot{w} = u_0q - v_0p + g(\cos\varphi_0\cos\varphi - \sin\varphi_0\sin\varphi)(\cos\theta_0\cos\theta - \sin\theta_0\sin\theta) + \frac{Z}{m}$$

Taylor expansion -

$$\dot{w} = u_0q - v_0p + g(\cos\varphi_0 - \varphi\sin\varphi_0)(\cos\theta_0 - \theta\sin\theta_0)$$
$$+ \frac{1}{m}\left[Z_0 + \frac{\partial Z}{\partial u}u + \ldots + \frac{\partial Z}{\partial \theta_{0t}}\theta_{0t}\right]$$

but

$$0 = g\cos\varphi_0\cos\theta_0 + \frac{Z_0}{m}$$

hence

$$\dot{w} = \frac{\partial Z}{\partial u}u + \frac{\partial Z}{\partial w}w + \left[\frac{\partial Z}{\partial q} + u_0\right]q + \left[\frac{\partial Z}{\partial \theta} - g\cos\varphi_0\sin\theta_0\right]\theta$$
$$+ \frac{\partial Z}{\partial v}v + \left[\frac{\partial Z}{\partial p} - v_0\right]p + \left[\frac{\partial Z}{\partial \varphi} - g\sin\varphi_0\cos\theta_0\right]\varphi + \frac{\partial Z}{\partial r}r$$
$$+ \frac{\partial Z}{\partial \theta_{0e}}\theta_{0e} + \frac{\partial Z}{\partial \theta_{1s}}\theta_{1s} + \frac{\partial Z}{\partial \theta_{1c}}\theta_{1c} + \frac{\partial Z}{\partial \theta_{0t}}\theta_{0t}$$

where all partial derivatives are multiplied by the factor : $\frac{1}{m}$

$$(4)\quad \dot{p} = qr\left[\frac{I_{yy} - I_{zz}}{I_{xx}}\right] + (pq + \dot{r})\frac{I_{xz}}{I_{xx}} + \frac{L}{I_{xx}}$$

$$(5)\quad \dot{r} = pq\left[\frac{I_{xx} - I_{yy}}{I_{zz}}\right] + (\dot{p} - rq)\frac{I_{xz}}{I_{zz}} + \frac{N}{I_{zz}}$$

$p_0 = q_0 = r_0$ and expand as a Taylor series

$$\dot{p} = \dot{r}\,\frac{I_{xz}}{I_{xx}} + \frac{1}{I_{xx}}\left[L_0 + \frac{\partial L}{\partial u}\,u + \ldots + \frac{\partial L}{\partial \theta_{0t}}\,\theta_{0t} \right]$$

$$\dot{r} = \dot{p}\,\frac{I_{xz}}{I_{zz}} + \frac{1}{I_{zz}}\left[N_0 + \frac{\partial N}{\partial u}\,u + \ldots + \frac{\partial N}{\partial \theta_{0t}}\,\theta_{0t} \right]$$

For trim $L_0 = N_0 = 0$

$$\dot{p} = \frac{I_{xz}}{I_{xx}}\left[\dot{p}\,\frac{I_{xz}}{I_{zz}} + \frac{1}{I_{zz}}\left[\frac{\partial N}{\partial u}\,u + \ldots + \frac{\partial N}{\partial \theta_{0t}}\,\theta_{0t} \right] \right] + \frac{1}{I_{xx}}\left[\frac{\partial L}{\partial u}\,u + \ldots + \frac{\partial L}{\partial \theta_{0t}}\,\theta_{0t} \right]$$

hence

$$\dot{p} = \frac{I_{zz}}{I_{xx}I_{zz} - I_{xz}^2}\left[\left[\frac{\partial L}{\partial u} + i\frac{\partial N}{\partial u} \right]u + \left[\frac{\partial L}{\partial w} + i\frac{\partial N}{\partial w} \right]w + \left[\frac{\partial L}{\partial q} + i\frac{\partial N}{\partial q} \right]q + \left[\frac{\partial L}{\partial \theta} + i\frac{\partial N}{\partial \theta} \right]\theta + \left[\frac{\partial L}{\partial v} + i\frac{\partial N}{\partial v} \right]v + \left[\frac{\partial L}{\partial p} + i\frac{\partial N}{\partial p} \right]p + \left[\frac{\partial L}{\partial \varphi} + i\frac{\partial N}{\partial \varphi} \right]\varphi + \left[\frac{\partial L}{\partial r} + i\frac{\partial N}{\partial r} \right]r + \left[\frac{\partial L}{\partial \theta_{0e}} + i\frac{\partial N}{\partial \theta_{0e}} \right]\theta_{0e} + \left[\frac{\partial L}{\partial \theta_{1s}} + i\frac{\partial N}{\partial \theta_{1s}} \right]\theta_{1s} + \left[\frac{\partial L}{\partial \theta_{1c}} + i\frac{\partial N}{\partial \theta_{1c}} \right]\theta_{1c} + \left[\frac{\partial L}{\partial \theta_{0t}} + i\frac{\partial N}{\partial \theta_{0t}} \right]\theta_{0t} \right]$$

where $i = \dfrac{I_{xz}}{Izz}$

and by analogy with $\dot{p}$

$$\dot{r} = \frac{I_{xx}}{I_{xx}I_{zz} - I_{xz}^2}\left[\left[\frac{\partial N}{\partial u} + j\frac{\partial L}{\partial u} \right]u + \left[\frac{\partial N}{\partial w} + j\frac{\partial L}{\partial w} \right]w + \left[\frac{\partial N}{\partial q} + j\frac{\partial L}{\partial q} \right]q + \left[\frac{\partial N}{\partial \theta} + j\frac{\partial L}{\partial \theta} \right]\theta + \left[\frac{\partial N}{\partial v} + j\frac{\partial L}{\partial v} \right]v + \left[\frac{\partial N}{\partial p} + j\frac{\partial L}{\partial p} \right]p + \left[\frac{\partial N}{\partial \varphi} + j\frac{\partial L}{\partial \varphi} \right]\varphi + \left[\frac{\partial N}{\partial r} + j\frac{\partial L}{\partial r} \right]r + \left[\frac{\partial N}{\partial \theta_{0e}} + j\frac{\partial L}{\partial \theta_{0e}} \right]\theta_{0e} + \left[\frac{\partial N}{\partial \theta_{1s}} + j\frac{\partial L}{\partial \theta_{1s}} \right]\theta_{1s} + \left[\frac{\partial N}{\partial \theta_{1c}} + j\frac{\partial L}{\partial \theta_{1c}} \right]\theta_{1c} + \left[\frac{\partial N}{\partial \theta_{0t}} + j\frac{\partial L}{\partial \theta_{0t}} \right]\theta_{0t} \right]$$

where $j = \dfrac{I_{xz}}{Ixx}$

$$(6)\ \dot{q} = pr\left[\frac{I_{zz} - I_{xx}}{I_{yy}}\right] + (r^2 - p^2)\frac{I_{xz}}{I_{yy}} + \frac{M}{I_{yy}}$$

Linearization follows immediately

$$\dot{q} = \frac{1}{I_{yy}}\left[\frac{\partial M}{\partial u}u + \frac{\partial M}{\partial w}w + \frac{\partial M}{\partial q}q + \frac{\partial M}{\partial \theta}\theta + \frac{\partial M}{\partial v}v + \frac{\partial M}{\partial p}p + \frac{\partial M}{\partial \varphi}\varphi + \frac{\partial M}{\partial r}r + \frac{\partial M}{\partial \theta_{0e}}\theta_{0e} + \frac{\partial M}{\partial \theta_{1s}}\theta_{1s} + \frac{\partial M}{\partial \theta_{1c}}\theta_{1c} + \frac{\partial M}{\partial \theta_{0t}}\theta_{0t}\right]$$

$$(7)\ \dot{\varphi} = p + (r\cos\varphi + q\sin\varphi)\tan\theta$$

$$(\dot{\varphi}_0 + \dot{\varphi}) = p + [r\cos(\varphi_0 + \varphi) + q\sin(\varphi_0 + \varphi)]\tan(\theta_0 + \theta)$$

$$\dot{\varphi} = p + (r\cos\varphi_0 - \varphi r\sin\varphi_0 + q\sin\varphi_0 + \varphi q\cos\varphi_0)\tan\theta_0$$

$$\dot{\varphi} = p + r\cos\varphi_0\tan\theta_0 + q\sin\varphi_0\tan\theta_0$$

$$(8)\ \dot{\theta} = q\cos\varphi - r\sin\varphi$$

$$(\dot{\theta}_0 + \dot{\theta}) = q\cos(\varphi_0 + \varphi) - r\sin(\varphi_0 + \varphi)$$

$$\dot{\theta} = q\cos\varphi_0 - \varphi\sin\varphi_0 - r\sin\varphi_0 - \varphi r\cos\varphi_0$$

$$\dot{\theta} = q\cos\varphi_0 - r\sin\varphi_0$$

$$(9)\ \dot{\psi} = r\cos\varphi\sec\theta + q\sin\varphi\sec\theta$$

$$(\dot{\psi}_0 + \dot{\psi}) = [r\cos(\varphi_0 + \varphi) + q\sin(\varphi_0 + \varphi)] / \cos(\theta_0 + \theta)$$

$$\dot{\psi} = (r\cos\varphi_0 - \varphi r\sin\varphi_0 + q\sin\varphi_0 + \varphi q\cos\varphi_0) / \cos\theta_0$$

$$\dot{\psi} = r\cos\varphi_0\sec\theta_0 + q\sin\varphi_0\sec\theta_0$$

APPENDIX 2

ALGORITHM TO CALCULATE TRANSFORMATION MATRICES R AND R^{-1}

```
C CALCULATION OF R
C
      DO 100 J=1,N
         IF(C(1,J).NE.0.0)GOTO 10
 100  CONTINUE
C
 10   K=N-J
      L=1
C
      DO 110 J=1,N
         R(N,J)=C(1,J)
 110  CONTINUE
C
      DO 130 I=N-1,1,-1
         IF(I.EQ.K)THEN L=L+1
         DO 120 J=1,N
              IF(J.EQ.L)THEN
                   R(I,J)=1.0
              ELSE
                   R(I,J)=0.0
              END IF
 120     CONTINUE
         L=L+1
 130  CONTINUE
C
C CALCULATION OF R-1
C
      K=N-K
      L=N-1
C
      DO 150 I=1,N
         IF(I.EQ.K)GOTO 160
         DO 140 J=1,N
              IF(J.EQ.L)THEN
                   RINV(I,J)=1.0
              ELSE
                   RINV(I,J)=0.0
              END IF
 140     CONTINUE
C
         L=L-1
C
 150  CONTINUE
C
      RINV(K,N)=1.0/C(1,K)
C
      L=1
C
      DO 160 I=N-1,1
         IF(I.EQ.N-K)THEN L=L+1
         RINV(K,I)=C(1,L)*(-RINV(K,N))
         L=L+1
 160  CONTINUE
C
      STOP
      END
```

APPENDIX 3

ALGORITHM TO CALCULATE A POLYNOMIAL FROM ITS ROOTS

```
C Real and Imag parts of the N eigenvalues passed in through AREAL and
C AIMAG. Coefficients (a_i) of the polynomial passed out as COF(i)
C
C
      SUBROUTINE CHAREQ(AREAL,AIMAG,COF,N)
      IMPLICIT REAL*16(A-H,O-U)
      IMPLICIT COMPLEX*16(W,X,Y,Z)
      DIMENSION AIMAG(20),AREAL(20),COF(20),W(20),X(20),Y(20),Z(20)
      REAL*8 V(20)
C
C
      DO 100 I=1,N
         W(I)=DCMPLX(-AREAL(I),AIMAG(I))
 100  CONTINUE
C
C
      X(1)=(0.0,0.0)
      X(2)=W(1)
      X(3)=(1.0,0.0)
      X(4)=(0.0,0.0)
C
C
      DO 130 I=1,N-1
C
         DO 110 J=2,I+3
              Y(J-1)=X(J)*W(I+1)
              Z(J-1)=X(J-1)
 110     CONTINUE
C
C
         DO 120 J=2,I+3
              X(J)=Y(J-1)+Z(J-1)
 120     CONTINUE
C
C
         X(I+4)=(0.0,0.0)
C
 130  CONTINUE
C
C
      DO 140 I=1,N
         V(I)=DREAL(X(I+1))
         COF(N+1-I)=QEXTD(V(I))
 140  CONTINUE
C
C
      RETURN
      END
```

APPENDIX 4 LIST OF SYMBOLS

The symbols listed below are those which appear in this thesis. Additional symbols which appear in *fig 2.12* can be obtained from Padfield, [P1].

Main Rotor

a_0 Blade lift curve slope

c Blade chord

h_R Negative z coordinate of rotor hub

I_β Blade flapping moment of inertia

K_β Blade flapping stiffness - spring constant

R Blade radius

s Rotor solidity ($=bc/\pi R$)

x_{cg} Centre of gravity location forward of fuselage reference point. Aircarft z axis aligned along shaft; hence CG at shaft base.

γ_s Rotor shaft forward tilt

θ_{tw} Linear blade twist

Tail Rotor

a_{0T} Blade lift curve slope

F_T Fin blockage factor

h_T Negative z coordinate of hub

$k_{\lambda T}$ Main rotor downwash factor

l_T Tail rotor location aft of fuselage reference point

R_T Blade radius

s_T Tail rotor solidity

Tailplane

l_{TP} Location aft of fuselage reference point

S_{TP} Tailplane area

Fin

h_{FN} Negative z component of fin centre of pressure

l_{FN} Location aft of fuselage reference point

S_{FN} Fin area

Fuselage

C_{YS} Aerodynamic sideforce coefficient
l_F Fuselage reference length
S_p Fuselage plan area
S_s Fuselage side area

Engine

G_{TR} Tail rotor gearing
I_R Moment of inertia of rotor and transmission system
K_3 Overall engine torque/rotorspeed gain
Ω_i Idling rotorspeed

Helicopter Inertias

I_{xx} Roll moment of inertia
I_{yy} Pitch moment of inertia
I_{zz} Yaw moment of inertia
I_{xz} Product of inertia
m Aircraft mass

Miscellaneous

C_{MF}	Fuselage pitching moment function
C_{NF}, C_{NFA}, C_{NFB}	Fuselage yawing moment functions
C_Q	Main rotor torque coefficient
C_T	Main rotor thrust coefficient
C_{TT}	Tail rotor thrust coefficient
C_X, C_Y, C_Z	Main rotor force coefficients in shaft axis
C_{XF}, C_{ZF}	Fuselage force functions
C_{YFN}	Fin sideforce function
C_{ZTP}	Tailplane force coefficient
g	Gravitational constant
L, M, N	Overall aircraft rolling, pitching, yawing moments
L_F, M_F, N_F	Fuselage aerodynamic rolling, pitching, yawing moments
L_{FN}, M_{FN}, N_{FN}	Fin aerodynamic rolling, pitching, yawing moments
L_R, M_R, N_R	Rotor moments in body reference axis
L_{TP}, M_{TP}, N_{TP}	Tailplane moments
L_T, M_T, N_T	Tail rotor moments

p, q, r	Aircraft roll, pitch, yaw rates about body reference axes
Q_E	Engine torque
Q_R	Main rotor torque
Q_{TR}	Tail rotor torque
u, v, w	Aircraft velocity components at CG
u_A, v_A, w_A	Aircraft *aerodynamic* velocities at CG
V_F	Fuselage total velocity
V_{FN}	Fin total velocity
V_T	Tailplane total velocity
X, Y, Z	Overall aircraft force components
X_F, Y_F, Z_F	Fuselage aerodynamic forces
X_{FN}, Y_{FN}, Z_{FN}	Fin aerodynamic forces
X_R, Y_R, Z_R	Rotor forces in body reference axes
X_{TP}, Y_{TP}, Z_{TP}	Tailplane forces
X_T, Y_T, Z_T	Tail rotor forces
α_F	Fuselage incidence angle
α_{TP}	Tailplane incidence angle
β_F	Fuselage sideslip angle
β_{FN}	Fin sideslip angle
β_0, β_{1C}, β_{1S}	Harmonics of flapping
λ_0	Rotor downwash component
μ	Normalized rotor velocity in xy plane
μ_x, μ_y, μ_z	Normalized rotor velocity components
ψ, θ, φ	Euler angles
Ω	Rotor speed
Ω_T	Tail rotor speed
b	Number of main rotor blades
γ	Blade lock number
ρ	Air density

APPENDIX 5 – MATRICES AND EIGENVALUES

The following pages list the eighth and fourteenth order system (A) and distribution (B) matrices and the system eigenvalues, for each flight condition examined during the course of this research.

$$A_{14} = \begin{bmatrix}
-0.02346186 & 0.05629925 & -2.92614627 & -32.17914963 & 0.00146664 & 0.11193927 & 0.00000000 & 0.00000000 & 0.00000000 & 32.02882385 & 0.00000000 & 0.00000000 & 0.00000000 & 0.00000000 \\
-0.00953863 & -0.80271620 & 134.81477356 & -0.69158614 & -0.01941474 & -1.48180497 & 1.05781341 & 0.00000000 & 0.00000000 & 0.00000000 & 0.00000000 & 0.00000000 & 0.00000000 & 0.00000000 \\
0.00065875 & -0.00501982 & -0.44104967 & 0.00000000 & 0.00005633 & 0.00429913 & 0.00000000 & 0.00000000 & 0.00000000 & -27.77480698 & 0.00000000 & 0.00000000 & 0.00000000 & 0.00000000 \\
0.00000000 & 0.00000000 & 0.99945956 & 0.00000000 & 0.00000000 & 0.00000000 & 0.00000000 & 0.03287238 & 0.00000000 & 0.00000000 & 0.00000000 & 0.00000000 & 0.00000000 & 0.00000000 \\
0.00629075 & -0.00134549 & 0.00278159 & 0.02274557 & -0.15681608 & 2.74039578 & 32.16175842 & -133.48402405 & -0.00168425 & -0.00001033 & -32.02885437 & -0.00001033 & -0.00001033 & -0.00001033 \\
-0.00099786 & -0.00599013 & 0.00163304 & 0.00000000 & 0.00020575 & 0.02190930 & 0.00000000 & -0.28667676 & 0.00010906 & 1.93801916 & -160.91217041 & -0.00000227 & -0.00000227 & -0.00000227 \\
0.00000000 & 0.00000000 & -0.00070685 & 0.00000000 & 0.00000000 & 1.00000000 & 0.00000000 & 0.02149118 & 0.00000000 & 0.00000000 & 0.00000000 & 0.00000000 & 0.00000000 & 0.00000000 \\
-0.00490917 & -0.01125400 & 0.00121135 & 0.00000000 & 0.04039855 & 0.16909410 & 0.00000000 & -1.35012507 & 0.00138464 & 4.30222988 & -29.02689362 & 0.00000504 & 0.00000504 & 0.00000504 \\
0.00000000 & 0.00000000 & 0.00000000 & 0.00000000 & 0.00000000 & 0.00000000 & 0.00000000 & 0.00000000 & 0.00000000 & 0.00000000 & 0.00000000 & 1.00000000 & 0.00000000 & 0.00000000 \\
0.00000000 & 0.00000000 & 0.00000000 & 0.00000000 & 0.00000000 & 0.00000000 & 0.00000000 & 0.00000000 & 0.00000000 & 0.00000000 & 0.00000000 & 0.00000000 & 1.00000000 & 0.00000000 \\
0.00000000 & 0.00000000 & 0.00000000 & 0.00000000 & 0.00000000 & 0.00000000 & 0.00000000 & 0.00000000 & 0.00000000 & 0.00000000 & 0.00000000 & 0.00000000 & 0.00000000 & 1.00000000 \\
-0.01963501 & 1.51640630 & -0.54809570 & 0.00000000 & 0.04012299 & 3.06274414 & 0.00000000 & 0.00000000 & -1514.8037109 & 0.00000000 & 0.00000000 & -31.72782135 & 0.00000000 & -3.81547332 \\
-0.00016851 & -0.40948763 & 31.89879417 & 0.00000000 & 0.33471489 & 72.09477234 & 0.00000000 & 0.00000000 & -271.87033081 & -245.30659485 & -1148.8522949 & 0.00000000 & -31.72782135 & -71.26000214 \\
0.31903443 & 0.43297729 & -72.77062988 & 0.00000000 & 0.19995566 & 32.31328964 & 0.00000000 & 0.00000000 & 0.00000000 & 1112.07226562 & -245.30664062 & -7.63037539 & 71.26000214 & -31.72782135
\end{bmatrix}$$

$$B_{14} = \begin{bmatrix}
29.22977448 & 7.54111910 & 0.00000000 & 0.00000000 \\
-386.93383789 & -99.82666779 & 0.00000000 & 0.00000000 \\
1.12262952 & 0.28963271 & 0.00000000 & 0.00000000 \\
0.00000000 & 0.00000000 & 0.00000000 & 0.00000000 \\
-0.77974343 & -0.20115878 & 0.00001033 & 22.04103279 \\
4.36361694 & 1.12580502 & 0.00000227 & -1.34352684 \\
0.00000000 & 0.00000000 & 0.00000000 & 0.00000000 \\
10.79339123 & 2.78466535 & -0.00000504 & -18.09545326 \\
0.00000000 & 0.00000000 & 0.00000000 & 0.00000000 \\
0.00000000 & 0.00000000 & 0.00000000 & 0.00000000 \\
0.00000000 & 0.00000000 & 0.00000000 & 0.00000000 \\
913.14318848 & 206.31256104 & 0.00000000 & 0.00000000 \\
-154.98075867 & -39.98403549 & 1148.85205078 & 0.00000000 \\
475.00903320 & 1167.89501953 & 0.00000000 & 0.00000000
\end{bmatrix}$$

-15.859 ± j35.352
-15.470 ± j69.568
-12.207
-8.709 ± j10.238
-4.188
-0.651 ± j 2.257
-0.401
-0.030
0.134 ± j 0.372

$$A_{8} = \begin{bmatrix}
-0.03221484 & 0.04037539 & -0.73662990 & -32.17914963 & -0.00211328 & -0.35667557 & 0.00000000 & 0.00000000 \\
-0.00953863 & -0.80271620 & 134.81477356 & -0.69158614 & -0.01941474 & -1.48180497 & 1.05781341 & 0.00000000 \\
0.00825047 & 0.00878071 & -2.33975840 & 0.00000000 & 0.00316003 & 0.41067171 & 0.00000000 & 0.00000000 \\
0.00000000 & 0.00000000 & 0.99945956 & 0.00000000 & 0.00000000 & 0.00000000 & 0.00000000 & 0.03287238 \\
0.00433443 & 0.01429716 & -0.42178351 & 0.02274557 & -0.16671012 & 0.64605570 & 32.16175842 & -133.48403931 \\
-0.01135805 & 0.07147910 & -1.99888182 & 0.00000000 & -0.04970622 & -10.52839470 & 0.00000000 & -0.28667676 \\
0.00000000 & 0.00000000 & -0.00070685 & 0.00000000 & 0.00000000 & 1.00000000 & 0.00000000 & 0.02149118 \\
-0.00785809 & 0.00075491 & -0.08945623 & 0.00000000 & 0.03095283 & -1.79190302 & 0.00000000 & -1.35012507
\end{bmatrix}$$

$$B_{8} = \begin{bmatrix}
14.29285431 & -25.03465843 & 6.74729204 & 0.00000000 \\
-386.93383789 & -99.82666779 & 0.00000000 & 0.00000000 \\
14.07609844 & 28.53879738 & -5.85112238 & 0.00000000 \\
0.00000000 & 0.00000000 & 0.00000000 & 0.00000000 \\
4.92125034 & -5.00933743 & -30.58004189 & 22.04103279 \\
32.09765244 & -25.00374794 & -153.22517395 & -1.34352684 \\
0.00000000 & 0.00000000 & 0.00000000 & 0.00000000 \\
13.95298004 & -5.94896317 & -26.80756569 & -18.09545326
\end{bmatrix}$$

-10.545
-3.199
-0.654 ± j 2.255
-0.406
-0.031
0.134 ± j 0.376

Helicopter : Lynx

Forward Velocity : 80 Kts

Descent Angle : 0 Deg

$$A_{14} = \begin{bmatrix}
0.00128119 & 0.01093704 & -1.01701641 & -32.17276001 & -0.00054596 & -0.01391087 & 0.00000000 & -0.00000230 & -0.00002303 & 32.11809540 & -0.00002303 & -0.00002303 & -0.00002303 & -0.00002303 \\
-0.15751356 & -0.35984263 & 34.71664810 & -0.94235224 & 0.01718879 & 0.43792510 & -1.37646949 & 0.00007370 & 0.00073700 & 0.00073700 & 0.00073700 & 0.00073700 & 0.00073700 & 0.00073700 \\
-0.00072662 & -0.00280944 & -0.05398383 & 0.00000000 & 0.00008334 & 0.00212336 & 0.00000000 & 0.00000022 & 0.00000225 & -6.33186483 & 0.00000225 & 0.00000225 & 0.00000225 & 0.00000225 \\
0.00000000 & 0.00000000 & 0.99908423 & 0.00000000 & 0.00000000 & 0.00000000 & 0.00000000 & -0.04278596 & 0.00000000 & 0.00000000 & 0.00000000 & 0.00000000 & 0.00000000 & 0.00000000 \\
-0.00627847 & 0.00363814 & -0.01558140 & -0.03944483 & -0.03576628 & 0.89463454 & 32.14270782 & -33.29760742 & 0.00649481 & 0.00033779 & 32.11810303 & 0.00000000 & 0.00000000 & 0.00000000 \\
-0.00078371 & 0.00164977 & -0.00598364 & 0.00000000 & -0.00423187 & -0.02289924 & 0.00000000 & 0.08998281 & 0.00125269 & 0.03712244 & 25.88650131 & -0.00000262 & -0.00000262 & -0.00000262 \\
0.00000000 & 0.00000000 & 0.00125483 & 0.00000000 & 0.00000000 & 1.00000000 & 0.00000000 & 0.02930132 & 0.00000000 & 0.00000000 & 0.00000000 & 0.00000000 & 0.00000000 & 0.00000000 \\
0.00496104 & 0.00128791 & -0.00084535 & 0.00000000 & 0.00757042 & 0.06363150 & 0.00000000 & -0.26513940 & -0.00363547 & -0.78368288 & 2.57701039 & 0.00003833 & 0.00003833 & 0.00003833 \\
0.00000000 & 0.00000000 & 0.00000000 & 0.00000000 & 0.00000000 & 0.00000000 & 0.00000000 & 0.00000000 & 0.00000000 & 0.00000000 & 0.00000000 & 1.00000000 & 0.00000000 & 0.00000000 \\
0.00000000 & 0.00000000 & 0.00000000 & 0.00000000 & 0.00000000 & 0.00000000 & 0.00000000 & 0.00000000 & 0.00000000 & 0.00000000 & 0.00000000 & 0.00000000 & 1.00000000 & 0.00000000 \\
0.00000000 & 0.00000000 & 0.00000000 & 0.00000000 & 0.00000000 & 0.00000000 & 0.00000000 & 0.00000000 & 0.00000000 & 0.00000000 & 0.00000000 & 0.00000000 & 0.00000000 & 1.00000000 \\
0.25968629 & 0.59832382 & -1.79439545 & -0.00007629 & -0.02968559 & -0.75393677 & 0.00007629 & 0.00007629 & -766.61529541 & 0.00076294 & 0.00076294 & -25.25598145 & 0.00076294 & -0.85418338 \\
-0.36656123 & -0.38060945 & 27.81490707 & 0.00001907 & -0.35888377 & -56.51078033 & -0.00001907 & -0.00001907 & -46.16384506 & -37.61663437 & -682.81115723 & -0.00019073 & -25.25693512 & -54.00018692 \\
0.37717360 & 0.07683716 & -56.66202545 & 0.00000000 & -0.52695501 & -28.97113800 & 0.00000000 & 0.00000000 & 0.00000000 & 681.05316162 & -37.61634827 & -1.70976448 & 53.99999619 & -25.25674438
\end{bmatrix}$$

$$B_{14} = \begin{bmatrix}
7.12097454 & 0.54058146 & -0.00008445 & -0.00002303 \\
-224.18641663 & -17.01879311 & 0.00270233 & 0.00073700 \\
-1.08700395 & -0.08251761 & 0.00001343 & 0.00000225 \\
0.00000000 & 0.00000000 & 0.00000000 & 0.00000000 \\
2.48000336 & 0.18844156 & 0.00003071 & 10.01611519 \\
1.57854056 & 0.11985885 & -0.00000425 & 1.93632627 \\
0.00000000 & 0.00000000 & 0.00000000 & 0.00000000 \\
-9.55432701 & -0.72525358 & 0.00004784 & -5.67566490 \\
0.00000000 & 0.00000000 & 0.00000000 & 0.00000000 \\
0.00000000 & 0.00000000 & 0.00000000 & 0.00000000 \\
0.00000000 & 0.00000000 & 0.00000000 & 0.00000000 \\
462.27380371 & 29.36515808 & 0.00076294 & 0.00076294 \\
-19.14329529 & -1.45158768 & 682.81097412 & -0.00019073 \\
75.46768188 & 683.28936768 & 0.00000000 & 0.00000000
\end{bmatrix}$$

-12.628 ± j24.626
-12.525 ± j51.241
-11.200 ± j 3.501
-2.275
-1.221
-0.355
-0.093
-0.067 ± j 0.681
0.139 ± j 0.446

$$A_{8} = \begin{bmatrix}
-0.01745634 & 0.00624719 & 1.71935856 & -32.17276001 & 0.02335937 & 1.20197558 & 0.00000000 & -0.00000230 \\
-0.15751356 & -0.35984263 & 34.71664810 & -0.94235224 & 0.01718879 & 0.43792510 & -1.37646949 & 0.00007370 \\
0.00296607 & -0.00188470 & -0.59344083 & 0.00000000 & -0.00462544 & -0.23757932 & 0.00000000 & 0.00000034 \\
0.00000000 & 0.00000000 & 0.99908423 & 0.00000000 & 0.00000000 & 0.00000000 & 0.00000000 & -0.04278596 \\
-0.02321447 & -0.01573463 & 1.14712596 & -0.03944329 & -0.05391302 & -1.82838988 & 32.14271164 & -33.29760742 \\
-0.01446049 & -0.01395783 & 0.93428701 & 0.00000000 & -0.01881734 & -2.21618652 & 0.00000000 & 0.08998236 \\
0.00000000 & 0.00000000 & 0.00125483 & 0.00000000 & 0.00000000 & 1.00000000 & 0.00000000 & 0.02930132 \\
0.00406064 & -0.00015078 & 0.02568956 & 0.00000000 & 0.00553085 & -0.18451065 & 0.00000000 & -0.26514134
\end{bmatrix}$$

$$B_{8} = \begin{bmatrix}
3.45203662 & -31.59356689 & 1.76850712 & -0.00002303 \\
-224.18641663 & -17.01879311 & 0.00270233 & 0.00073700 \\
-0.36362800 & 6.25251150 & -0.34865320 & 0.00000335 \\
0.00000000 & 0.00000000 & 0.00000000 & 0.00000000 \\
0.47281590 & 1.80727637 & 32.02063370 & 10.01609993 \\
-0.04360127 & 1.38752365 & 25.80997849 & 1.93632185 \\
0.00000000 & 0.00000000 & 0.00000000 & 0.00000000 \\
-9.62589645 & 0.18854862 & 2.52606225 & -5.67568445
\end{bmatrix}$$

-2.120
-1.072
-0.358
-0.093
-0.066 ± j 0.676
0.135 ± j 0.450

Helicopter : Puma

Forward Velocity : 20 Kts

Descent Angle : 0 Deg

$$A_{14} = \begin{bmatrix}
-0.00240522 & 0.01624559 & 15.51678944 & -32.17201996 & -0.00076084 & -0.02871765 & 0.00000000 & 0.00000000 & 0.00000000 & 32.46026993 & 0.00000000 & 0.00000000 & 0.00000000 & 0.00000000 \\
-0.09798764 & -0.49532971 & 66.37725830 & -0.96706623 & 0.02075563 & 0.78343052 & -1.56828582 & 0.00000000 & 0.00000000 & 0.00000000 & 0.00000000 & 0.00000000 & 0.00000000 & 0.00000000 \\
0.00022017 & -0.00330445 & -0.02187307 & 0.00000000 & 0.00011185 & 0.00422176 & 0.00000000 & 0.00000000 & 0.00000000 & -6.36962938 & 0.00000000 & 0.00000000 & 0.00000000 & 0.00000000 \\
0.00000000 & 0.00000000 & 0.99881119 & 0.00000000 & 0.00000000 & 0.00000000 & 0.00000000 & -0.04874650 & 0.00000000 & 0.00000000 & 0.00000000 & 0.00000000 & 0.00000000 & 0.00000000 \\
-0.00767717 & 0.00803068 & 0.05249126 & -0.04821052 & -0.05862395 & -15.66331577 & 32.13336182 & -65.11766052 & 0.00571175 & 0.00024567 & 32.46026993 & 0.00000000 & 0.00000000 & 0.00000000 \\
-0.00113905 & 0.00309754 & 0.00783335 & 0.00000000 & -0.00589457 & -0.03140476 & 0.00000000 & 0.12179190 & 0.00110648 & 0.07129875 & 26.04090500 & 0.00000000 & 0.00000000 & 0.00000000 \\
0.00000000 & 0.00000000 & 0.00146714 & 0.00000000 & 0.00000000 & 1.00000000 & 0.00000000 & 0.03006159 & 0.00000000 & 0.00000000 & 0.00000000 & 0.00000000 & 0.00000000 & 0.00000000 \\
0.00481298 & -0.00135794 & -0.03274219 & 0.00000000 & 0.00823497 & 0.09536476 & 0.00000000 & -0.35838616 & -0.00324167 & -1.50633729 & 2.59234095 & 0.00000000 & 0.00000000 & 0.00000000 \\
0.00000000 & 0.00000000 & 0.00000000 & 0.00000000 & 0.00000000 & 0.00000000 & 0.00000000 & 0.00000000 & 0.00000000 & 0.00000000 & 0.00000000 & 1.00000000 & 0.00000000 & 0.00000000 \\
0.00000000 & 0.00000000 & 0.00000000 & 0.00000000 & 0.00000000 & 0.00000000 & 0.00000000 & 0.00000000 & 0.00000000 & 0.00000000 & 0.00000000 & 0.00000000 & 1.00000000 & 0.00000000 \\
0.00000000 & 0.00000000 & 0.00000000 & 0.00000000 & 0.00000000 & 0.00000000 & 0.00000000 & 0.00000000 & 0.00000000 & 0.00000000 & 0.00000000 & 0.00000000 & 0.00000000 & 1.00000000 \\
0.15662308 & 0.80948794 & -1.03988647 & 0.00000000 & -0.03583755 & -1.35215759 & 0.00000000 & 0.00000000 & -766.61572266 & 0.00000000 & 0.00000000 & -25.25674438 & 0.00000000 & -1.62620032 \\
-0.14819440 & -0.33368769 & 26.27331734 & 0.00000000 & -0.37691125 & -56.51933670 & 0.00000000 & 0.00000000 & -87.80822754 & -37.61634827 & -685.11212158 & 0.00000000 & -25.25674438 & -53.99999619 \\
0.39712754 & 0.15004043 & -56.79719925 & 0.00000000 & -0.31096077 & -27.38319397 & 0.00000000 & 0.00000000 & 0.00000000 & 678.75213623 & -37.61634827 & -3.25215626 & 53.99999619 & -25.25674438
\end{bmatrix}$$

$$B_{14} = \begin{bmatrix}
8.81707096 & 1.25536358 & -0.00004606 & 0.00000000 \\
-240.52349854 & -34.24591446 & 0.00147400 & 0.00000000 \\
-1.29613400 & -0.18454255 & 0.00000671 & 0.00000000 \\
0.00000000 & 0.00000000 & 0.00000000 & 0.00000000 \\
3.02315664 & 0.43077624 & -0.00003071 & 10.31582928 \\
1.87325263 & 0.26686949 & -0.00001366 & 1.99427295 \\
0.00000000 & 0.00000000 & 0.00000000 & 0.00000000 \\
-10.60576153 & -1.51199007 & 0.00005678 & -5.84554005 \\
0.00000000 & 0.00000000 & 0.00000000 & 0.00000000 \\
0.00000000 & 0.00000000 & 0.00000000 & 0.00000000 \\
0.00000000 & 0.00000000 & 0.00000000 & 0.00000000 \\
488.94119263 & 59.32540894 & 0.00000000 & 0.00000000 \\
-55.46312332 & -7.92322159 & 685.11218262 & 0.00000000 \\
146.74415588 & 687.34686279 & 0.00000000 & 0.00000000
\end{bmatrix}$$

$$\begin{matrix}
-12.628 \pm j24.589 \\
-12.516 \pm j51.221 \\
-11.184 \pm j\ 3.519 \\
-2.499 \\
-1.189 \\
-0.503 \\
-0.097 \\
-0.019 \pm j\ 0.813 \\
0.123 \pm j\ 0.386
\end{matrix}$$

$$A_{8} = \begin{bmatrix}
-0.02177080 & 0.00797774 & 18.29386139 & -32.17201996 & 0.01310478 & 1.12932193 & 0.00000000 & 0.00000000 \\
-0.09798764 & -0.49532971 & 66.37725830 & -0.96706623 & 0.02075563 & 0.78343052 & -1.56828582 & 0.00000000 \\
0.00402049 & -0.00168189 & -0.56681424 & 0.00000000 & -0.00260802 & -0.22301881 & 0.00000000 & 0.00000000 \\
0.00000000 & 0.00000000 & 0.99881119 & 0.00000000 & 0.00000000 & 0.00000000 & 0.00000000 & -0.04874650 \\
-0.01448014 & -0.01175682 & 1.15048850 & -0.04820898 & -0.07706287 & -18.39738083 & 32.13336182 & -65.11766052 \\
-0.00664136 & -0.01278147 & 0.89478624 & 0.00000000 & -0.02065102 & -2.22223306 & 0.00000000 & 0.12179190 \\
0.00000000 & 0.00000000 & 0.00146714 & 0.00000000 & 0.00000000 & 1.00000000 & 0.00000000 & 0.03006159 \\
0.00516916 & -0.00255305 & -0.07391384 & 0.00000000 & 0.00611854 & -0.17671917 & 0.00000000 & -0.35838616
\end{bmatrix}$$

$$B_{8} = \begin{bmatrix}
1.53008008 & -31.55520439 & 1.79341924 & 0.00000000 \\
-240.52349854 & -34.24591446 & 0.00147400 & 0.00000000 \\
0.13386634 & 6.25378275 & -0.35192400 & 0.00000000 \\
0.00000000 & 0.00000000 & 0.00000000 & 0.00000000 \\
-1.85685492 & 1.53493977 & 32.36106491 & 10.31582928 \\
-2.05802488 & 1.08062899 & 25.96527672 & 1.99427295 \\
0.00000000 & 0.00000000 & 0.00000000 & 0.00000000 \\
-10.65737438 & 0.09865202 & 2.50127459 & -5.84554005
\end{bmatrix}$$

$$\begin{matrix}
-2.302 \\
-1.024 \\
-0.518 \\
-0.097 \\
-0.022 \pm j\ 0.810 \\
0.121 \pm j\ 0.388
\end{matrix}$$

Helicopter : Puma

Forward Velocity : 40 Kts

Descent Angle : -15 Deg

$$A_{14} = \begin{bmatrix}
-0.00227507 & 0.01639349 & 12.09988022 & -32.17281723 & -0.00075083 & -0.02854107 & 0.00000000 & -0.00000230 & -0.00002303 & 32.38080978 & -0.00002303 & -0.00002303 & -0.00002303 & -0.00002303 \\
-0.10465020 & -0.49624324 & 67.05806732 & -0.94048518 & 0.02078093 & 0.78991610 & -1.46279669 & 0.00007370 & 0.00073700 & 0.00073700 & 0.00073700 & 0.00073700 & 0.00073700 & 0.00073700 \\
-0.00002027 & -0.00403556 & -0.05459211 & 0.00000000 & 0.00011077 & 0.00421093 & 0.00000000 & 0.00000034 & 0.00000335 & -6.36085701 & 0.00000335 & 0.00000335 & 0.00000335 & 0.00000335 \\
0.00000000 & 0.00000000 & 0.99896574 & 0.00000000 & 0.00000000 & 0.00000000 & 0.00000000 & -0.04546941 & 0.00000000 & 0.00000000 & 0.00000000 & 0.00000000 & 0.00000000 & 0.00000000 \\
-0.00748682 & 0.00712599 & 0.03751634 & -0.04357971 & -0.05872848 & -12.24753094 & 32.13911057 & -65.82837677 & 0.00612631 & 0.00033779 & 32.38080978 & -0.00001535 & -0.00001535 & -0.00001535 \\
-0.00111964 & 0.00277316 & 0.00504911 & 0.00000000 & -0.00590921 & -0.03122063 & 0.00000000 & 0.12250274 & 0.00117732 & 0.07225463 & 26.00505638 & -0.00000651 & -0.00000651 & -0.00000651 \\
0.00000000 & 0.00000000 & 0.00133062 & 0.00000000 & 0.00000000 & 1.00000000 & 0.00000000 & 0.02923387 & 0.00000000 & 0.00000000 & 0.00000000 & 0.00000000 & 0.00000000 & 0.00000000 \\
0.00493694 & -0.00001610 & -0.02582663 & 0.00000000 & 0.00828220 & 0.09454907 & 0.00000000 & -0.36046734 & -0.00344836 & -1.52633536 & 2.58881903 & 0.00003804 & 0.00003804 & 0.00003804 \\
0.00000000 & 0.00000000 & 0.00000000 & 0.00000000 & 0.00000000 & 0.00000000 & 0.00000000 & 0.00000000 & 0.00000000 & 0.00000000 & 0.00000000 & 1.00000000 & 0.00000000 & 0.00000000 \\
0.00000000 & 0.00000000 & 0.00000000 & 0.00000000 & 0.00000000 & 0.00000000 & 0.00000000 & 0.00000000 & 0.00000000 & 0.00000000 & 0.00000000 & 0.00000000 & 1.00000000 & 0.00000000 \\
0.00000000 & 0.00000000 & 0.00000000 & 0.00000000 & 0.00000000 & 0.00000000 & 0.00000000 & 0.00000000 & 0.00000000 & 0.00000000 & 0.00000000 & 0.00000000 & 0.00000000 & 1.00000000 \\
0.16597137 & 0.81053239 & -1.10511780 & 0.00000000 & -0.03587876 & -1.36344910 & 0.00000000 & 0.00000000 & -766.61645508 & 0.00000000 & 0.00000000 & -25.25674438 & 0.00000000 & -1.65179265 \\
-0.13861370 & -0.35089988 & 26.20372772 & 0.00000954 & -0.36611852 & -56.43269348 & 0.00000954 & 0.00000954 & -89.19001007 & -37.61634827 & -685.21289062 & 0.00009537 & -25.25664902 & -53.99990082 \\
0.38842812 & 0.15112686 & -56.73553467 & 0.00000000 & -0.31796035 & -27.42950439 & 0.00000000 & 0.00000000 & 0.00000000 & 678.65124512 & -37.61634827 & -3.30333757 & 53.99999619 & -25.25674438
\end{bmatrix}$$

$$B_{14} = \begin{bmatrix}
8.64528084 & 1.25005865 & -0.00007677 & -0.00002303 \\
-239.27648926 & -34.59795380 & 0.00221100 & 0.00073700 \\
-1.27549922 & -0.18442950 & 0.00001198 & 0.00000335 \\
0.00000000 & 0.00000000 & 0.00000000 & 0.00000000 \\
2.80810642 & 0.40637848 & -0.00004606 & 10.20917892 \\
1.74962091 & 0.25313357 & -0.00001691 & 1.97365117 \\
0.00000000 & 0.00000000 & 0.00000000 & 0.00000000 \\
-10.05271435 & -1.45542467 & 0.00007580 & -5.78507471 \\
0.00000000 & 0.00000000 & 0.00000000 & 0.00000000 \\
0.00000000 & 0.00000000 & 0.00000000 & 0.00000000 \\
0.00000000 & 0.00000000 & 0.00000000 & 0.00000000 \\
486.72296143 & 59.92050171 & 0.00000000 & 0.00000000 \\
-58.45651627 & -8.47845078 & 685.21350098 & 0.00009537 \\
148.69651794 & 687.46813965 & 0.00000000 & 0.00000000
\end{bmatrix}$$

$$-12.628 \pm j24.587$$
$$-12.515 \pm j51.221$$
$$-11.194 \pm j\ 3.516$$
$$-2.442$$
$$-1.137$$
$$-0.550$$
$$-0.091$$
$$-0.038 \pm j\ 0.823$$
$$0.099 \pm j\ 0.379$$

$$A_{8} = \begin{bmatrix}
-0.02115966 & 0.00804332 & 14.86746979 & -32.17281723 & 0.01344515 & 1.12930524 & 0.00000000 & -0.00000230 \\
-0.10465020 & -0.49624324 & 67.05806732 & -0.94048518 & 0.02078093 & 0.78991610 & -1.46279669 & 0.00007370 \\
0.00368974 & -0.00239516 & -0.59825546 & 0.00000000 & -0.00267685 & -0.22323534 & 0.00000000 & 0.00000024 \\
0.00000000 & 0.00000000 & 0.99896574 & 0.00000000 & 0.00000000 & 0.00000000 & 0.00000000 & -0.04546941 \\
-0.01390698 & -0.01349546 & 1.12997699 & -0.04357817 & -0.07662627 & -14.97037315 & 32.13911057 & -65.82836914 \\
-0.00632023 & -0.01379212 & 0.88857543 & 0.00000000 & -0.02024575 & -2.21535110 & 0.00000000 & 0.12250307 \\
0.00000000 & 0.00000000 & 0.00133062 & 0.00000000 & 0.00000000 & 1.00000000 & 0.00000000 & 0.02923387 \\
0.00531458 & -0.00126957 & -0.06892874 & 0.00000000 & 0.00618166 & -0.17770934 & 0.00000000 & -0.36046928
\end{bmatrix}$$

$$B_{8} = \begin{bmatrix}
1.27275217 & -31.49275208 & 1.78928900 & -0.00002303 \\
-239.27648926 & -34.59795380 & 0.00221100 & 0.00073700 \\
0.17283897 & 6.24749994 & -0.35149094 & 0.00000240 \\
0.00000000 & 0.00000000 & 0.00000000 & 0.00000000 \\
-2.22440267 & 1.47378409 & 32.28183746 & 10.20919418 \\
-2.30879879 & 1.03734815 & 25.92956734 & 1.97365439 \\
0.00000000 & 0.00000000 & 0.00000000 & 0.00000000 \\
-10.10759354 & 0.17314620 & 2.49660754 & -5.78509426
\end{bmatrix}$$

$$-2.260$$
$$-0.950$$
$$-0.581$$
$$-0.092$$
$$-0.040 \pm j\ 0.819$$
$$0.097 \pm j\ 0.381$$

Helicopter : Puma

Forward Velocity : 40 Kts

Descent Angle : -12 Deg

$$A_{14} = \begin{bmatrix}
-0.00218851 & 0.01626775 & 8.68012047 & -32.17387390 & -0.00073219 & -0.02797450 & 0.00000000 & 0.00000307 & -0.00003071 & 32.29917145 & 0.00003071 & -0.00003071 & 0.00000000 & 0.00003071 \\
-0.11154456 & -0.49704787 & 67.57440948 & -0.90375805 & 0.02078830 & 0.79426444 & -1.35701263 & -0.00012283 & 0.00122833 & 0.00000000 & -0.00122833 & 0.00122833 & 0.00000000 & -0.00122833 \\
-0.00021866 & -0.00453351 & -0.08030041 & 0.00000000 & 0.00010873 & 0.00415405 & 0.00000000 & -0.00000055 & 0.00000551 & -6.35184813 & -0.00000551 & 0.00000551 & 0.00000000 & -0.00000551 \\
0.00000000 & 0.00000000 & 0.99911010 & 0.00000000 & 0.00000000 & 0.00000000 & 0.00000000 & -0.04217774 & 0.00000000 & 0.00000000 & 0.00000000 & 0.00000000 & 0.00000000 & 0.00000000 \\
-0.00723678 & 0.00623638 & 0.02227427 & -0.03867251 & -0.05883664 & -8.82858276 & 32.14479828 & -66.35897827 & 0.00651016 & 0.00035315 & 32.29922104 & -0.00001535 & 0.00000000 & 0.00001535 \\
-0.00109170 & 0.00245049 & 0.00223466 & 0.00000000 & -0.00592442 & -0.03101417 & 0.00000000 & 0.12301511 & 0.00125595 & 0.07299784 & 25.96822548 & -0.00000651 & 0.00000000 & 0.00000651 \\
0.00000000 & 0.00000000 & 0.00118580 & 0.00000000 & 0.00000000 & 1.00000000 & 0.00000000 & 0.02808941 & 0.00000000 & 0.00000000 & 0.00000000 & 0.00000000 & 0.00000000 & 0.00000000 \\
0.00505059 & 0.00132577 & -0.01893253 & 0.00000000 & 0.00833081 & 0.09362137 & 0.00000000 & -0.36197370 & -0.00365449 & -1.54189050 & 2.58505273 & 0.00003804 & 0.00000000 & -0.00003804 \\
0.00000000 & 0.00000000 & 0.00000000 & 0.00000000 & 0.00000000 & 0.00000000 & 0.00000000 & 0.00000000 & 0.00000000 & 0.00000000 & 0.00000000 & 1.00000000 & 0.00000000 & 0.00000000 \\
0.00000000 & 0.00000000 & 0.00000000 & 0.00000000 & 0.00000000 & 0.00000000 & 0.00000000 & 0.00000000 & 0.00000000 & 0.00000000 & 0.00000000 & 0.00000000 & 1.00000000 & 0.00000000 \\
0.00000000 & 0.00000000 & 0.00000000 & 0.00000000 & 0.00000000 & 0.00000000 & 0.00000000 & 0.00000000 & 0.00000000 & 0.00000000 & 0.00000000 & 0.00000000 & 0.00000000 & 1.00000000 \\
0.17582855 & 0.81164819 & -1.17492676 & 0.00000000 & -0.03589249 & -1.37115479 & -0.00003815 & 0.00000000 & -766.61529541 & -0.00038147 & 0.00000000 & -25.25636292 & -0.00038147 & -1.67281783 \\
-0.12847432 & -0.36866274 & 26.13012314 & -0.00001907 & -0.35521573 & -56.34529877 & -0.00000954 & -0.00001907 & -90.32516479 & -37.61644363 & -685.29742432 & 0.00028610 & -25.25683975 & -54.00018692 \\
0.37971458 & 0.15189476 & -56.67388916 & -0.00003815 & -0.32569352 & -27.48149872 & 0.00000000 & -0.00003815 & 0.00038147 & 678.56713867 & -37.61672974 & -3.34500265 & 53.99999619 & -25.25712585
\end{bmatrix}$$

$$B_{14} = \begin{bmatrix}
8.38019180 & 1.22705817 & -0.00006142 & 0.00003071 \\
-237.93046570 & -34.83895111 & 0.00147400 & -0.00122833 \\
-1.24443388 & -0.18221544 & 0.00000910 & -0.00000551 \\
0.00000000 & 0.00000000 & 0.00000000 & 0.00000000 \\
2.59293318 & 0.38004610 & -0.00001535 & 10.11220169 \\
1.62596774 & 0.23823261 & -0.00000878 & 1.95491314 \\
0.00000000 & 0.00000000 & 0.00000000 & 0.00000000 \\
-9.50042057 & -1.39285815 & 0.00002825 & -5.73018312 \\
0.00000000 & 0.00000000 & 0.00000000 & 0.00000000 \\
0.00000000 & 0.00000000 & 0.00000000 & 0.00000000 \\
0.00000000 & 0.00000000 & 0.00000000 & 0.00000000 \\
484.34335327 & 60.32104492 & -0.00038147 & 0.00000000 \\
-61.50693893 & -9.03158188 & 685.29711914 & -0.00019073 \\
150.21057129 & 687.55609131 & 0.00000000 & -0.00038147
\end{bmatrix}$$

-12.628 ± j24.586
-12.515 ± j51.221
-11.203 ± j 3.513
-2.384
-1.104
-0.584
-0.086
-0.057 ± j 0.832
0.082 ± j 0.373

$$A_{8} = \begin{bmatrix}
-0.02059030 & 0.00785068 & 11.43797112 & -32.17387390 & 0.01382609 & 1.12981188 & 0.00000000 & 0.00000461 \\
-0.11154456 & -0.49704787 & 67.57440948 & -0.90375805 & 0.02078830 & 0.79426444 & -1.35701263 & -0.00012283 \\
0.00340062 & -0.00287821 & -0.62265092 & 0.00000000 & -0.00275319 & -0.22353232 & 0.00000000 & -0.00000057 \\
0.00000000 & 0.00000000 & 0.99911010 & 0.00000000 & 0.00000000 & 0.00000000 & 0.00000000 & -0.04217774 \\
-0.01325134 & -0.01522870 & 1.10898924 & -0.03867251 & -0.07619256 & -11.54012680 & 32.14479828 & -66.35897827 \\
-0.00597159 & -0.01481077 & 0.88216996 & 0.00000000 & -0.01984000 & -2.20844865 & 0.00000000 & 0.12301432 \\
0.00000000 & 0.00000000 & 0.00118580 & 0.00000000 & 0.00000000 & 1.00000000 & 0.00000000 & 0.02808941 \\
0.00544843 & 0.00001129 & -0.06359286 & 0.00000000 & 0.00624615 & -0.17866431 & 0.00000000 & -0.36197376
\end{bmatrix}$$

$$B_{8} = \begin{bmatrix}
0.94445723 & -31.44312668 & 1.78502822 & 0.00004606 \\
-237.93046570 & -34.83895111 & 0.00147400 & -0.00122833 \\
0.21794005 & 6.24255991 & -0.35103995 & -0.00000575 \\
0.00000000 & 0.00000000 & 0.00000000 & 0.00000000 \\
-2.58625412 & 1.41270530 & 32.20038605 & 10.11220169 \\
-2.55523276 & 0.99469692 & 25.89282799 & 1.95490527 \\
0.00000000 & 0.00000000 & 0.00000000 & 0.00000000 \\
-9.56007767 & 0.24918835 & 2.49203873 & -5.73018360
\end{bmatrix}$$

-2.217
-0.885
-0.640
-0.087
-0.058 ± j 0.828
0.079 ± j 0.375

Helicopter : Puma

Forward Velocity : 40 Kts

Descent Angle : -9 Deg

$$A_{14} = \begin{bmatrix}
-0.00213378 & 0.01593042 & 5.24593449 & -32.17506790 & -0.00070772 & -0.02711928 & 0.00000000 & 0.00000000 & 0.00000000 & 32.21580124 & 0.00000000 & 0.00000000 & 0.00000000 & 0.00000000 \\
-0.11866216 & -0.49775106 & 67.93151093 & -0.86037326 & 0.02078683 & 0.79654902 & -1.25081098 & 0.00000000 & 0.00000000 & 0.00000000 & 0.00000000 & 0.00000000 & 0.00000000 & 0.00000000 \\
-0.00038816 & -0.00481414 & -0.09889039 & 0.00000000 & 0.00010602 & 0.00406279 & 0.00000000 & 0.00000000 & 0.00000000 & -6.34264708 & 0.00000000 & 0.00000000 & 0.00000000 & 0.00000000 \\
0.00000000 & 0.00000000 & 0.99924409 & 0.00000000 & 0.00000000 & 0.00000000 & 0.00000000 & -0.03887529 & 0.00000000 & 0.00000000 & 0.00000000 & 0.00000000 & 0.00000000 & 0.00000000 \\
-0.00692686 & 0.00538745 & 0.00863057 & -0.03375765 & -0.05894754 & -5.39499140 & 32.15029144 & -66.71199799 & 0.00698614 & 0.00038385 & 32.21584702 & 0.00000000 & 0.00000000 & 0.00000000 \\
-0.00105552 & 0.00213439 & -0.00024707 & 0.00000000 & -0.00594010 & -0.03079599 & 0.00000000 & 0.12375589 & 0.00135085 & 0.07353759 & 25.93060684 & 0.00000000 & 0.00000000 & 0.00000000 \\
0.00000000 & 0.00000000 & 0.00104031 & 0.00000000 & 0.00000000 & 1.00000000 & 0.00000000 & 0.02673996 & 0.00000000 & 0.00000000 & 0.00000000 & 0.00000000 & 0.00000000 & 0.00000000 \\
0.00515516 & 0.00265416 & -0.01311680 & 0.00000000 & 0.00838074 & 0.09261362 & 0.00000000 & -0.36414227 & -0.00395573 & -1.55319464 & 2.58135390 & 0.00000000 & 0.00000000 & 0.00000000 \\
0.00000000 & 0.00000000 & 0.00000000 & 0.00000000 & 0.00000000 & 0.00000000 & 0.00000000 & 0.00000000 & 0.00000000 & 0.00000000 & 1.00000000 & 0.00000000 & 0.00000000 & 0.00000000 \\
0.00000000 & 0.00000000 & 0.00000000 & 0.00000000 & 0.00000000 & 0.00000000 & 0.00000000 & 0.00000000 & 0.00000000 & 0.00000000 & 0.00000000 & 0.00000000 & 1.00000000 & 0.00000000 \\
0.00000000 & 0.00000000 & 0.00000000 & 0.00000000 & 0.00000000 & 0.00000000 & 0.00000000 & 0.00000000 & 0.00000000 & 0.00000000 & 0.00000000 & 0.00000000 & 0.00000000 & 1.00000000 \\
0.18615036 & 0.81284142 & -1.24767303 & -0.00003815 & -0.03589020 & -1.37500763 & 0.00000000 & 0.00000000 & -766.61572266 & 0.00000000 & 0.00000000 & -25.25674438 & 0.00000000 & -1.68942010 \\
-0.11765852 & -0.38714200 & 26.05167389 & -0.00000954 & -0.34420052 & -56.25720978 & 0.00000000 & 0.00000000 & -91.22180939 & -37.61634827 & -685.36425781 & 0.00000000 & -25.25674438 & -53.99999619 \\
0.37097320 & 0.15235367 & -56.61201477 & 0.00000000 & -0.33430251 & -27.53997803 & 0.00000000 & 0.00000000 & 0.00000000 & 678.50000000 & -37.61596680 & -3.37858653 & 53.99999619 & -25.25674438
\end{bmatrix}$$

$$B_{14} = \begin{bmatrix}
8.05127430 & 1.19059205 & -0.00005374 & 0.00000000 \\
-236.47589111 & -34.96915817 & 0.00147400 & 0.00000000 \\
-1.20618117 & -0.17836455 & 0.00000766 & 0.00000000 \\
0.00000000 & 0.00000000 & 0.00000000 & 0.00000000 \\
2.37774467 & 0.35197869 & -0.00001535 & 10.01395035 \\
1.50237584 & 0.22230858 & -0.00000878 & 1.93591499 \\
0.00000000 & 0.00000000 & 0.00000000 & 0.00000000 \\
-8.94956589 & -1.32505059 & 0.00002825 & -5.67448139 \\
0.00000000 & 0.00000000 & 0.00000000 & 0.00000000 \\
0.00000000 & 0.00000000 & 0.00000000 & 0.00000000 \\
0.00000000 & 0.00000000 & 0.00000000 & 0.00000000 \\
481.78750610 & 60.52665710 & -0.00038147 & 0.00000000 \\
-64.63222504 & -9.58156586 & 685.36419678 & 0.00000000 \\
151.29585266 & 687.60913086 & 0.00000000 & 0.00000000
\end{bmatrix}$$

-12.629 ± j24.585
-12.514 ± j51.222
-11.213 ± j 3.509
-2.324
-1.098
-0.592
-0.082
-0.077 ± j 0.840
0.069 ± j 0.367

$$A_8 = \begin{bmatrix}
-0.02005051 & 0.00746109 & 7.99382591 & -32.17506790 & 0.01425163 & 1.13081133 & 0.00000000 & 0.00000000 \\
-0.11866216 & -0.49775106 & 67.93151093 & -0.86037326 & 0.02078683 & 0.79654902 & -1.25081098 & 0.00000000 \\
0.00313984 & -0.00314674 & -0.63989598 & 0.00000000 & -0.00283804 & -0.22391045 & 0.00000000 & 0.00000000 \\
0.00000000 & 0.00000000 & 0.99924409 & 0.00000000 & 0.00000000 & 0.00000000 & 0.00000000 & -0.03887529 \\
-0.01250734 & -0.01693920 & 1.08937132 & -0.03375765 & -0.07576138 & -8.09520245 & 32.15029144 & -66.71199799 \\
-0.00559105 & -0.01583914 & 0.87591207 & 0.00000000 & -0.01943393 & -2.20156002 & 0.00000000 & 0.12375589 \\
0.00000000 & 0.00000000 & 0.00104031 & 0.00000000 & 0.00000000 & 1.00000000 & 0.00000000 & 0.02673996 \\
0.00557256 & 0.00127529 & -0.05898193 & 0.00000000 & 0.00631165 & -0.17956541 & 0.00000000 & -0.36414227
\end{bmatrix}$$

$$B_8 = \begin{bmatrix}
0.57383090 & -31.40264511 & 1.78059089 & 0.00000000 \\
-236.47589111 & -34.96915817 & 0.00147400 & 0.00000000 \\
0.26606280 & 6.23856163 & -0.35056400 & 0.00000000 \\
0.00000000 & 0.00000000 & 0.00000000 & 0.00000000 \\
-2.94334579 & 1.35197961 & 32.11724472 & 10.01395035 \\
-2.79806757 & 0.95286685 & 25.85532379 & 1.93591499 \\
0.00000000 & 0.00000000 & 0.00000000 & 0.00000000 \\
-9.01551628 & 0.32623389 & 2.48765516 & -5.67448139
\end{bmatrix}$$

-2.173
-0.854
-0.666
-0.082
-0.078 ± j 0.835
0.066 ± j 0.370

Helicopter : Puma

Forward Velocity : 40 Kts

Descent Angle : -6 Deg

$$A_{14} = \begin{bmatrix}
-0.00209811 & 0.01544213 & 1.81190717 & -32.17627716 & -0.00068034 & -0.02607289 & 0.00000000 & 0.00000000 & 0.00000000 & 32.13194275 & 0.00000000 & 0.00000000 & 0.00000000 & 0.00000000 \\
-0.12594581 & -0.49835345 & 68.12965393 & -0.81401604 & 0.02078683 & 0.79659826 & -1.14500237 & 0.00000000 & 0.00000000 & 0.00000000 & 0.00000000 & 0.00000000 & 0.00000000 & 0.00000000 \\
-0.00053953 & -0.00488694 & -0.11013834 & 0.00000000 & 0.00010300 & 0.00394738 & 0.00000000 & 0.00000000 & 0.00000000 & -6.33339405 & 0.00000000 & 0.00000000 & 0.00000000 & 0.00000000 \\
0.00000000 & 0.00000000 & 0.99936664 & 0.00000000 & 0.00000000 & 0.00000000 & 0.00000000 & -0.03558540 & 0.00000000 & 0.00000000 & 0.00000000 & 0.00000000 & 0.00000000 & 0.00000000 \\
-0.00655913 & 0.00456927 & -0.00303705 & -0.02922971 & -0.05905968 & -1.96135688 & 32.15543747 & -66.88875580 & 0.00733929 & 0.00041456 & 32.13200378 & 0.00000000 & 0.00000000 & 0.00000000 \\
-0.00101157 & 0.00182400 & -0.00232273 & 0.00000000 & -0.00595603 & -0.03056326 & 0.00000000 & 0.12450346 & 0.00141780 & 0.07387748 & 25.89277649 & 0.00000000 & 0.00000000 & 0.00000000 \\
0.00000000 & 0.00000000 & 0.00090093 & 0.00000000 & 0.00000000 & 1.00000000 & 0.00000000 & 0.02530138 & 0.00000000 & 0.00000000 & 0.00000000 & 0.00000000 & 0.00000000 & 0.00000000 \\
0.00525067 & 0.00396895 & -0.00858691 & 0.00000000 & 0.00843168 & 0.09153473 & 0.00000000 & -0.36633444 & -0.00416271 & -1.56031489 & 2.57756305 & 0.00000000 & 0.00000000 & 0.00000000 \\
0.00000000 & 0.00000000 & 0.00000000 & 0.00000000 & 0.00000000 & 0.00000000 & 0.00000000 & 0.00000000 & 0.00000000 & 0.00000000 & 1.00000000 & 0.00000000 & 0.00000000 & 0.00000000 \\
0.00000000 & 0.00000000 & 0.00000000 & 0.00000000 & 0.00000000 & 0.00000000 & 0.00000000 & 0.00000000 & 0.00000000 & 0.00000000 & 0.00000000 & 0.00000000 & 1.00000000 & 0.00000000 \\
0.00000000 & 0.00000000 & 0.00000000 & 0.00000000 & 0.00000000 & 0.00000000 & 0.00000000 & 0.00000000 & 0.00000000 & 0.00000000 & 0.00000000 & 0.00000000 & 0.00000000 & 1.00000000 \\
0.19682464 & 0.81410599 & -1.32308960 & 0.00003815 & -0.03588829 & -1.37519836 & 0.00000000 & 0.00000000 & -766.61608887 & 0.00000000 & 0.00000000 & -25.25674438 & 0.00000000 & -1.70157170 \\
-0.10611276 & -0.40637502 & 25.96795082 & -0.00000954 & -0.33315191 & -56.16888046 & 0.00000000 & 0.00000000 & -91.87784576 & -37.61644363 & -685.41387939 & 0.00000000 & -25.25674438 & -53.99999619 \\
0.36225358 & 0.15250358 & -56.55036926 & 0.00000000 & -0.34389228 & -27.60570526 & 0.00000000 & 0.00000000 & 0.00000000 & 678.45080566 & -37.61672974 & -3.40288782 & 53.99999619 & -25.25674438
\end{bmatrix}$$

$$B_{14} = \begin{bmatrix}
7.68259048 & 1.14520514 & -0.00004606 & 0.00000000 \\
-234.72993469 & -34.99003601 & 0.00147400 & 0.00000000 \\
-1.16314626 & -0.17338400 & 0.00000778 & 0.00000000 \\
0.00000000 & 0.00000000 & 0.00000000 & 0.00000000 \\
2.16272521 & 0.32277510 & 0.00000000 & 9.91602135 \\
1.37896943 & 0.20567214 & -0.00000326 & 1.91697955 \\
0.00000000 & 0.00000000 & 0.00000000 & 0.00000000 \\
-8.40156746 & -1.25347209 & 0.00001902 & -5.61898708 \\
0.00000000 & 0.00000000 & 0.00000000 & 0.00000000 \\
0.00000000 & 0.00000000 & 0.00000000 & 0.00000000 \\
0.00000000 & 0.00000000 & 0.00000000 & 0.00000000 \\
479.04397583 & 60.54725647 & 0.00000000 & 0.00000000 \\
-67.82484436 & -10.12477875 & 685.41387939 & 0.00000000 \\
151.95350647 & 687.62817383 & 0.00000000 & 0.00000000
\end{bmatrix}$$

$$\begin{matrix}
-12.629 \pm j24.584 \\
-12.514 \pm j51.222 \\
-11.222 \pm j\ 3.505 \\
-2.262 \\
-1.126 \\
-0.569 \\
-0.097 \pm j\ 0.848 \\
-0.077 \\
0.060 \pm j\ 0.363
\end{matrix}$$

$$A_8 = \begin{bmatrix}
-0.01953041 & 0.00693428 & 4.54972982 & -32.17627716 & 0.01472367 & 1.13226998 & 0.00000000 & 0.00000000 \\
-0.12594581 & -0.49835345 & 68.12965393 & -0.81401604 & 0.02078683 & 0.79659826 & -1.14500237 & 0.00000000 \\
0.00289713 & -0.00321011 & -0.64978015 & 0.00000000 & -0.00293201 & -0.22436875 & 0.00000000 & 0.00000000 \\
0.00000000 & 0.00000000 & 0.99936664 & 0.00000000 & 0.00000000 & 0.00000000 & 0.00000000 & -0.03558540 \\
-0.01167406 & -0.01863916 & 1.07152367 & -0.02922971 & -0.07533574 & -4.65033579 & 32.15543747 & -66.88875580 \\
-0.00517648 & -0.01687975 & 0.86987513 & 0.00000000 & -0.01903076 & -2.19474745 & 0.00000000 & 0.12450346 \\
0.00000000 & 0.00000000 & 0.00090093 & 0.00000000 & 0.00000000 & 1.00000000 & 0.00000000 & 0.02530138 \\
0.00568763 & 0.00252222 & -0.05531402 & 0.00000000 & 0.00637730 & -0.18041331 & 0.00000000 & -0.36633444
\end{bmatrix}$$

$$B_8 = \begin{bmatrix}
0.18438040 & -31.36791992 & 1.77608442 & 0.00000000 \\
-234.72993469 & -34.99003601 & 0.00147400 & 0.00000000 \\
0.31486493 & 6.23511648 & -0.35007924 & 0.00000000 \\
0.00000000 & 0.00000000 & 0.00000000 & 0.00000000 \\
-3.29555488 & 1.29232872 & 32.03363037 & 9.91602135 \\
-3.03711033 & 0.91228372 & 25.81760406 & 1.91697955 \\
0.00000000 & 0.00000000 & 0.00000000 & 0.00000000 \\
-8.47540760 & 0.40287900 & 2.48349667 & -5.61898708
\end{bmatrix}$$

$$\begin{matrix}
-2.129 \\
-0.888 \\
-0.628 \\
-0.098 \pm j\ 0.843 \\
-0.077 \\
0.057 \pm j\ 0.365
\end{matrix}$$

Helicopter : Puma

Forward Velocity : 40 Kts

Descent Angle : -3 Deg

$$A_{14} = \begin{bmatrix}
-0.00206633 & 0.01485434 & -1.63363469 & -32.17741013 & -0.00065256 & -0.02494360 & 0.00000000 & -0.00000230 & -0.00002303 & 32.04809570 & -0.00002303 & -0.00002303 & -0.00002303 & -0.00002303 \\
-0.13339770 & -0.49871656 & 68.16987610 & -0.76817459 & 0.02079616 & 0.79492772 & -1.03953779 & 0.00007370 & 0.00073700 & 0.00073700 & 0.00073700 & 0.00073700 & 0.00073700 & 0.00073700 \\
-0.00068443 & -0.00475906 & -0.11398140 & 0.00000000 & 0.00009995 & 0.00382055 & 0.00000000 & 0.00000045 & 0.00000449 & -6.32413816 & 0.00000449 & 0.00000449 & 0.00000449 & 0.00000449 \\
0.00000000 & 0.00000000 & 0.99947792 & 0.00000000 & 0.00000000 & 0.00000000 & 0.00000000 & -0.03230828 & 0.00000000 & 0.00000000 & 0.00000000 & 0.00000000 & 0.00000000 & 0.00000000 \\
-0.00613453 & 0.00381580 & -0.01035945 & -0.02428106 & -0.05916056 & 1.48485518 & 32.16012955 & -66.89041138 & 0.00783062 & 0.00039921 & 32.04811096 & 0.00000000 & 0.00000000 & 0.00000000 \\
-0.00096021 & 0.00152540 & -0.00353316 & 0.00000000 & -0.00596987 & -0.03013825 & 0.00000000 & 0.12525038 & 0.00151121 & 0.07401285 & 25.85493088 & -0.00000326 & -0.00000326 & -0.00000326 \\
0.00000000 & 0.00000000 & 0.00077181 & 0.00000000 & 0.00000000 & 1.00000000 & 0.00000000 & 0.02387640 & 0.00000000 & 0.00000000 & 0.00000000 & 0.00000000 & 0.00000000 & 0.00000000 \\
0.00533857 & 0.00525358 & -0.00669032 & 0.00000000 & 0.00847683 & 0.08987568 & 0.00000000 & -0.36852279 & -0.00442072 & -1.56330454 & 2.57385755 & 0.00001902 & 0.00001902 & 0.00001902 \\
0.00000000 & 0.00000000 & 0.00000000 & 0.00000000 & 0.00000000 & 0.00000000 & 0.00000000 & 0.00000000 & 0.00000000 & 0.00000000 & 0.00000000 & 1.00000000 & 0.00000000 & 0.00000000 \\
0.00000000 & 0.00000000 & 0.00000000 & 0.00000000 & 0.00000000 & 0.00000000 & 0.00000000 & 0.00000000 & 0.00000000 & 0.00000000 & 0.00000000 & 0.00000000 & 1.00000000 & 0.00000000 \\
0.00000000 & 0.00000000 & 0.00000000 & 0.00000000 & 0.00000000 & 0.00000000 & 0.00000000 & 0.00000000 & 0.00000000 & 0.00000000 & 0.00000000 & 0.00000000 & 0.00000000 & 1.00000000 \\
0.20783845 & 0.81544381 & -1.40010834 & 0.00007629 & -0.03590546 & -1.37199402 & 0.00007629 & 0.00007629 & -766.61572266 & 0.00076294 & 0.00076294 & -25.25598145 & 0.00076294 & -1.70856404 \\
-0.09367752 & -0.42655906 & 25.87790489 & 0.00001907 & -0.32206860 & -56.08048248 & 0.00001907 & 0.00001907 & -92.29660034 & -37.61615753 & -685.44555664 & 0.00019073 & -25.25655365 & -53.99980545 \\
0.35354385 & 0.15234908 & -56.48876190 & 0.00000000 & -0.35466233 & -27.68032074 & 0.00000000 & 0.00000000 & 0.00000000 & 678.41876221 & -37.61634827 & -3.41839719 & 53.99999619 & -25.25674438
\end{bmatrix}$$

$$B_{14} = \begin{bmatrix}
7.31346130 & 1.09521973 & -0.00004606 & -0.00002303 \\
-233.06774902 & -34.90331650 & 0.00147400 & 0.00073700 \\
-1.12017429 & -0.16775094 & 0.00000784 & 0.00000449 \\
0.00000000 & 0.00000000 & 0.00000000 & 0.00000000 \\
1.95159006 & 0.29260418 & -0.00003071 & 9.81940556 \\
1.25789857 & 0.18848258 & -0.00000927 & 1.89830089 \\
0.00000000 & 0.00000000 & 0.00000000 & 0.00000000 \\
-7.86546516 & -1.17885697 & 0.00004266 & -5.56422091 \\
0.00000000 & 0.00000000 & 0.00000000 & 0.00000000 \\
0.00000000 & 0.00000000 & 0.00000000 & 0.00000000 \\
0.00000000 & 0.00000000 & 0.00000000 & 0.00000000 \\
476.08834839 & 60.37483215 & 0.00076294 & 0.00076294 \\
-71.10157013 & -10.66055298 & 685.44592285 & 0.00019073 \\
152.18582153 & 687.61138916 & 0.00000000 & 0.00000000
\end{bmatrix}$$

-12.628 ± j24.584
-12.513 ± j51.223
-11.231 ± j 3.501
-2.196
-1.181
-0.521
-0.118 ± j 0.856
-0.072
0.054 ± j 0.359

$$A_{8} = \begin{bmatrix}
-0.01901411 & 0.00632066 & 1.09406817 & -32.17741013 & 0.01524904 & 1.13418090 & 0.00000000 & -0.00000230 \\
-0.13339770 & -0.49871656 & 68.16987610 & -0.76817459 & 0.02079616 & 0.79492772 & -1.03953779 & 0.00007370 \\
0.00266068 & -0.00307530 & -0.65224725 & 0.00000000 & -0.00303667 & -0.22491260 & 0.00000000 & 0.00000034 \\
0.00000000 & 0.00000000 & 0.99947792 & 0.00000000 & 0.00000000 & 0.00000000 & 0.00000000 & -0.03230828 \\
-0.01074482 & -0.02030457 & 1.05777013 & -0.02428106 & -0.07490384 & -1.19304335 & 32.16012955 & -66.89041901 \\
-0.00472196 & -0.01793429 & 0.86447901 & 0.00000000 & -0.01862850 & -2.18786430 & 0.00000000 & 0.12525088 \\
0.00000000 & 0.00000000 & 0.00077181 & 0.00000000 & 0.00000000 & 1.00000000 & 0.00000000 & 0.02387640 \\
0.00579581 & 0.00373478 & -0.05394570 & 0.00000000 & 0.00643593 & -0.18172546 & 0.00000000 & -0.36852229
\end{bmatrix}$$

$$B_{8} = \begin{bmatrix}
-0.18463373 & -31.33517075 & 1.77153957 & -0.00002303 \\
-233.06774902 & -34.90331650 & 0.00147400 & 0.00073700 \\
0.35951853 & 6.23180819 & -0.34958568 & 0.00000335 \\
0.00000000 & 0.00000000 & 0.00000000 & 0.00000000 \\
-3.63979506 & 1.23407495 & 31.95001984 & 9.81940556 \\
-3.27073908 & 0.87319410 & 25.77989769 & 1.89830589 \\
0.00000000 & 0.00000000 & 0.00000000 & 0.00000000 \\
-7.94885826 & 0.47848684 & 2.47959423 & -5.56421566
\end{bmatrix}$$

-2.083
-0.956
-0.556
-0.118 ± j 0.851
-0.072
0.051 ± j 0.362

Helicopter : Puma

Forward Velocity : 40 Kts

Descent Angle : 0 Deg

$$A_{14} = \begin{bmatrix}
-0.00637121 & 0.01712303 & -1.59038782 & -32.18264771 & -0.00068310 & -0.03741501 & 0.00000000 & 0.00000000 & 0.00000000 & 31.94095230 & 0.00000000 & 0.00000000 & 0.00000000 & 0.00000000 \\
-0.07798027 & -0.59109068 & 101.42609406 & -0.50307590 & 0.02215789 & 1.21359253 & -0.84769690 & 0.00000000 & 0.00000000 & 0.00000000 & 0.00000000 & 0.00000000 & 0.00000000 & 0.00000000 \\
-0.00046971 & -0.00644689 & -0.17460731 & 0.00000000 & 0.00010515 & 0.00575932 & 0.00000000 & 0.00000000 & 0.00000000 & -6.31231499 & 0.00000000 & 0.00000000 & 0.00000000 & 0.00000000 \\
0.00000000 & 0.00000000 & 0.99965304 & 0.00000000 & 0.00000000 & 0.00000000 & 0.00000000 & -0.02634018 & 0.00000000 & 0.00000000 & 0.00000000 & 0.00000000 & 0.00000000 & 0.00000000 \\
-0.00341797 & 0.00373017 & -0.00453024 & -0.01309019 & -0.08078483 & 1.43137515 & 32.17123413 & -100.55419159 & 0.00413795 & 0.00019960 & 31.94096947 & 0.00000000 & 0.00000000 & 0.00000000 \\
-0.00057047 & 0.00130907 & -0.00147460 & 0.00000000 & -0.00730344 & -0.03526331 & 0.00000000 & 0.14895399 & 0.00080005 & 0.11051631 & 25.80658531 & 0.00000000 & 0.00000000 & 0.00000000 \\
0.00000000 & 0.00000000 & 0.00041190 & 0.00000000 & 0.00000000 & 1.00000000 & 0.00000000 & 0.01563244 & 0.00000000 & 0.00000000 & 0.00000000 & 0.00000000 & 0.00000000 & 0.00000000 \\
0.00309410 & 0.00841471 & -0.00467011 & 0.00000000 & 0.00826897 & 0.10671548 & 0.00000000 & -0.43831158 & -0.00234916 & -2.33561206 & 2.56900811 & 0.00000000 & 0.00000000 & 0.00000000 \\
0.00000000 & 0.00000000 & 0.00000000 & 0.00000000 & 0.00000000 & 0.00000000 & 0.00000000 & 0.00000000 & 0.00000000 & 0.00000000 & 0.00000000 & 1.00000000 & 0.00000000 & 0.00000000 \\
0.00000000 & 0.00000000 & 0.00000000 & 0.00000000 & 0.00000000 & 0.00000000 & 0.00000000 & 0.00000000 & 0.00000000 & 0.00000000 & 0.00000000 & 0.00000000 & 1.00000000 & 0.00000000 \\
0.00000000 & 0.00000000 & 0.00000000 & 0.00000000 & 0.00000000 & 0.00000000 & 0.00000000 & 0.00000000 & 0.00000000 & 0.00000000 & 0.00000000 & 0.00000000 & 0.00000000 & 1.00000000 \\
0.10243988 & 0.95185471 & -0.64201355 & 0.00000000 & -0.03825226 & -2.09529877 & 0.00000000 & 0.00000000 & -766.61608887 & 0.00000000 & 0.00000000 & -25.25674438 & 0.00000000 & -2.56255674 \\
-0.04118223 & -0.34974355 & 25.51716805 & 0.00000000 & -0.30357465 & -55.78182220 & 0.00000000 & 0.00000000 & -138.36775208 & -37.61634827 & -689.82861328 & 0.00000000 & -25.25674438 & -53.99999619 \\
0.32276344 & 0.24349785 & -56.26285553 & 0.00000000 & -0.24525757 & -26.82495117 & 0.00000000 & 0.00000000 & 0.00000000 & 674.03564453 & -37.61634827 & -5.12472916 & 53.99999619 & -25.25674438
\end{bmatrix}$$

$$B_{14} = \begin{bmatrix}
7.97440434 & 1.75909507 & 0.00000000 & 0.00000000 \\
-258.66619873 & -57.05997849 & 0.00000000 & 0.00000000 \\
-1.22749972 & -0.27077797 & 0.00000000 & 0.00000000 \\
0.00000000 & 0.00000000 & 0.00000000 & 0.00000000 \\
1.77064133 & 0.39090148 & -0.00000768 & 10.98530769 \\
1.11784911 & 0.24664995 & 0.00000000 & 2.12369943 \\
0.00000000 & 0.00000000 & 0.00000000 & 0.00000000 \\
-6.65200233 & -1.46771145 & 0.00000000 & -6.22490406 \\
0.00000000 & 0.00000000 & 0.00000000 & 0.00000000 \\
0.00000000 & 0.00000000 & 0.00000000 & 0.00000000 \\
0.00000000 & 0.00000000 & 0.00000000 & 0.00000000 \\
517.11883545 & 98.51989746 & -0.00076294 & 0.00000000 \\
-89.50529480 & -19.74706650 & 689.82867432 & 0.00000000 \\
235.51712036 & 696.52557373 & 0.00000000 & 0.00000000
\end{bmatrix}$$

-12.627 ± j24.513
-12.482 ± j51.188
-11.287 ± j 3.549
-2.137
-0.899 ± j 0.332
-0.154 ± j 0.966
-0.089
0.014 ± j 0.295

$$A_{8} = \begin{bmatrix}
-0.02176709 & 0.00427222 & 1.13372374 & -32.18264771 & 0.01014831 & 1.08717477 & 0.00000000 & 0.00000000 \\
-0.07798027 & -0.59109068 & 101.42609406 & -0.50307590 & 0.02215789 & 1.21359253 & -0.84769690 & 0.00000000 \\
0.00257338 & -0.00390756 & -0.71295732 & 0.00000000 & -0.00203497 & -0.21648766 & 0.00000000 & 0.00000000 \\
0.00000000 & 0.00000000 & 0.99965304 & 0.00000000 & 0.00000000 & 0.00000000 & 0.00000000 & -0.02634018 \\
-0.00534612 & -0.01976465 & 1.03386068 & -0.01309019 & -0.09511849 & -1.19503319 & 32.17123413 & -100.55419159 \\
-0.00218171 & -0.01770179 & 0.84690934 & 0.00000000 & -0.01884429 & -2.15337086 & 0.00000000 & 0.14895399 \\
0.00000000 & 0.00000000 & 0.00041190 & 0.00000000 & 0.00000000 & 1.00000000 & 0.00000000 & 0.01563244 \\
0.00406520 & 0.00746662 & -0.12033623 & 0.00000000 & 0.00632361 & -0.18675783 & 0.00000000 & -0.43831158
\end{bmatrix}$$

$$B_{8} = \begin{bmatrix}
-3.62120891 & -31.24379730 & 1.77714384 & 0.00000000 \\
-258.66619873 & -57.05997849 & 0.00000000 & 0.00000000 \\
1.06421876 & 6.25143433 & -0.35120556 & 0.00000000 \\
0.00000000 & 0.00000000 & 0.00000000 & 0.00000000 \\
-6.06281185 & 0.45268661 & 31.83974838 & 10.98530769 \\
-5.25129080 & 0.18249722 & 25.73097038 & 2.12369943 \\
0.00000000 & 0.00000000 & 0.00000000 & 0.00000000 \\
-6.43419790 & 0.95041126 & 2.43093204 & -6.22490406
\end{bmatrix}$$

-2.072
-0.781 ± j 0.410
-0.155 ± j 0.961
-0.089
0.010 ± j 0.297

Helicopter : Puma

Forward Velocity : 60 Kts

Descent Angle : 0 Deg

$$A_{14} = \begin{bmatrix}
-0.00984132 & 0.01854823 & -0.69516408 & -32.18615723 & -0.00072670 & -0.05128826 & 0.00000000 & 0.00000000 & 0.00000000 & 31.83354568 & 0.00000000 & 0.00000000 & 0.00000000 & 0.00000000 \\
-0.04727987 & -0.65129316 & 134.86125183 & -0.16575120 & 0.02370092 & 1.67276788 & -0.78313571 & 0.00000000 & 0.00000000 & 0.00000000 & 0.00000000 & 0.00000000 & 0.00000000 & 0.00000000 \\
-0.00034779 & -0.00800881 & -0.23355857 & 0.00000000 & 0.00011203 & 0.00790707 & 0.00000000 & 0.00000000 & 0.00000000 & -6.30045938 & 0.00000000 & 0.00000000 & 0.00000000 & 0.00000000 \\
0.00000000 & 0.00000000 & 0.99970394 & 0.00000000 & 0.00000000 & 0.00000000 & 0.00000000 & -0.02433149 & 0.00000000 & 0.00000000 & 0.00000000 & 0.00000000 & 0.00000000 & 0.00000000 \\
-0.00232278 & 0.00379176 & -0.00142563 & -0.00384622 & -0.10054988 & 0.53013605 & 32.17649460 & -134.27914429 & 0.00207281 & 0.00008445 & 31.83354568 & 0.00000000 & 0.00000000 & 0.00000000 \\
-0.00039657 & 0.00125130 & -0.00060635 & 0.00000000 & -0.00826902 & -0.03863081 & 0.00000000 & 0.16151436 & 0.00040197 & 0.14670998 & 25.75812149 & 0.00000000 & 0.00000000 & 0.00000000 \\
0.00000000 & 0.00000000 & 0.00012535 & 0.00000000 & 0.00000000 & 1.00000000 & 0.00000000 & 0.00515038 & 0.00000000 & 0.00000000 & 0.00000000 & 0.00000000 & 0.00000000 & 0.00000000 \\
0.00183056 & 0.00995118 & -0.00177690 & 0.00000000 & 0.00704704 & 0.11775959 & 0.00000000 & -0.47551221 & -0.00117444 & -3.10106659 & 2.56419349 & 0.00000000 & 0.00000000 & 0.00000000 \\
0.00000000 & 0.00000000 & 0.00000000 & 0.00000000 & 0.00000000 & 0.00000000 & 0.00000000 & 0.00000000 & 0.00000000 & 0.00000000 & 0.00000000 & 1.00000000 & 0.00000000 & 0.00000000 \\
0.00000000 & 0.00000000 & 0.00000000 & 0.00000000 & 0.00000000 & 0.00000000 & 0.00000000 & 0.00000000 & 0.00000000 & 0.00000000 & 0.00000000 & 0.00000000 & 1.00000000 & 0.00000000 \\
0.00000000 & 0.00000000 & 0.00000000 & 0.00000000 & 0.00000000 & 0.00000000 & 0.00000000 & 0.00000000 & 0.00000000 & 0.00000000 & 0.00000000 & 0.00000000 & 0.00000000 & 1.00000000 \\
0.03998375 & 1.03264165 & -0.19367218 & 0.00000000 & -0.04091644 & -2.88803101 & 0.00000000 & 0.00000000 & -766.61645508 & 0.00000000 & 0.00000000 & -25.25674438 & 0.00000000 & -3.41398454 \\
-0.04542103 & -0.28149766 & 25.55381775 & 0.00000000 & -0.29976910 & -55.65605927 & 0.00000000 & 0.00000000 & -184.34133911 & -37.61653900 & -695.94793701 & 0.00000000 & -25.25674438 & -53.99999619 \\
0.29951018 & 0.33920670 & -56.09004974 & 0.00000000 & -0.19128036 & -26.36268616 & 0.00000000 & 0.00000000 & 0.00000000 & 667.91613770 & -37.61672974 & -6.82745647 & 53.99999619 & -25.25674438
\end{bmatrix}$$

$$B_{14} = \begin{bmatrix}
8.69861317 & 2.49194121 & 0.00000000 & 0.00000000 \\
-283.69985962 & -81.27312469 & 0.00000000 & 0.00000000 \\
-1.34104967 & -0.38417754 & 0.00000000 & 0.00000000 \\
0.00000000 & 0.00000000 & 0.00000000 & 0.00000000 \\
1.79771841 & 0.51519340 & 0.00000000 & 12.13455963 \\
1.10407901 & 0.31633431 & 0.00000000 & 2.34587169 \\
0.00000000 & 0.00000000 & 0.00000000 & 0.00000000 \\
-6.10730267 & -1.74974358 & 0.00000000 & -6.87613583 \\
0.00000000 & 0.00000000 & 0.00000000 & 0.00000000 \\
0.00000000 & 0.00000000 & 0.00000000 & 0.00000000 \\
0.00000000 & 0.00000000 & 0.00000000 & 0.00000000 \\
556.25842285 & 140.30647278 & 0.00000000 & 0.00000000 \\
-87.58268738 & -25.09078979 & 695.94805908 & 0.00000000 \\
321.94976807 & 710.58734131 & 0.00000000 & 0.00000000
\end{bmatrix}$$

-12.622 ± j24.414
-12.434 ± j51.135
-11.363 ± j 3.629
-2.128
-0.962 ± j 0.721
-0.138 ± j 0.979
-0.102
-0.006 ± j 0.245

$$A_{8} = \begin{bmatrix}
-0.02421116 & 0.00106699 & 2.03576803 & -32.18615723 & 0.00762527 & 1.06022441 & 0.00000000 & 0.00000000 \\
-0.04727987 & -0.65129316 & 134.86125183 & -0.16575120 & 0.02370092 & 1.67276788 & -0.78313571 & 0.00000000 \\
0.00249648 & -0.00454918 & -0.77406144 & 0.00000000 & -0.00154078 & -0.21208352 & 0.00000000 & 0.00000000 \\
0.00000000 & 0.00000000 & 0.99970394 & 0.00000000 & 0.00000000 & 0.00000000 & 0.00000000 & -0.02433149 \\
-0.00407922 & -0.01954121 & 1.02208018 & -0.00384622 & -0.11426551 & -2.04313993 & 32.17649460 & -134.27914429 \\
-0.00188379 & -0.01769429 & 0.84014726 & 0.00000000 & -0.01932718 & -2.11568427 & 0.00000000 & 0.16151436 \\
0.00000000 & 0.00000000 & 0.00012535 & 0.00000000 & 0.00000000 & 1.00000000 & 0.00000000 & 0.00515038 \\
0.00308897 & 0.00977661 & -0.18536209 & 0.00000000 & 0.00512860 & -0.19779542 & 0.00000000 & -0.47551221
\end{bmatrix}$$

$$B_{8} = \begin{bmatrix}
-7.16467237 & -31.42292786 & 1.78740048 & 0.00000000 \\
-283.69985962 & -81.27312469 & 0.00000000 & 0.00000000 \\
1.79880357 & 6.32827902 & -0.35376009 & 0.00000000 \\
0.00000000 & 0.00000000 & 0.00000000 & 0.00000000 \\
-7.47272253 & -0.34377956 & 31.72352982 & 12.13455963 \\
-6.46888494 & -0.53454471 & 25.67734337 & 2.34587169 \\
0.00000000 & 0.00000000 & 0.00000000 & 0.00000000 \\
-5.30859470 & 1.48488367 & 2.38122058 & -6.87613583
\end{bmatrix}$$

-2.096
-0.830 ± j 0.728
-0.138 ± j 0.976
-0.103
-0.010 ± j 0.246

Helicopter : Puma

Forward Velocity : 80 Kts

Descent Angle : 0 Deg

$$A_{14} = \begin{bmatrix}
-0.01423722 & 0.02433046 & 1.12514579 & -32.18571091 & -0.00092014 & -0.07419967 & 0.00000000 & 0.00000000 & 0.00000000 & 31.77183914 & 0.00000000 & 0.00000000 & 0.00000000 & 0.00000000 \\
-0.03700800 & -0.83178502 & 151.46595764 & 0.23713216 & 0.02901578 & 2.33982301 & -0.80598843 & 0.00000000 & 0.00000000 & 0.00000000 & 0.00000000 & 0.00000000 & 0.00000000 & 0.00000000 \\
-0.00029309 & -0.01109028 & -0.32722086 & 0.00000000 & 0.00014291 & 0.01152451 & 0.00000000 & 0.00000000 & 0.00000000 & -6.35337162 & 0.00000000 & 0.00000000 & 0.00000000 & 0.00000000 \\
0.00000000 & 0.00000000 & 0.99968642 & 0.00000000 & 0.00000000 & 0.00000000 & 0.00000000 & -0.02504191 & 0.00000000 & 0.00000000 & 0.00000000 & 0.00000000 & 0.00000000 & 0.00000000 \\
-0.00215552 & 0.00503085 & -0.00074428 & 0.00594144 & -0.13553706 & -1.33067000 & 32.17549133 & -150.94616699 & 0.00187958 & 0.00007549 & 31.77184868 & 0.00001510 & 0.00001510 & 0.00001510 \\
-0.00065882 & -0.00026449 & -0.00078714 & 0.00000000 & -0.01264989 & -0.08442712 & 0.00000000 & 0.34860966 & 0.00061992 & 0.98513418 & 25.37663269 & 0.00000765 & 0.00000765 & 0.00000765 \\
0.00000000 & 0.00000000 & -0.00018457 & 0.00000000 & 0.00000000 & 1.00000000 & 0.00000000 & -0.00736814 & 0.00000000 & 0.00000000 & 0.00000000 & 0.00000000 & 0.00000000 & 0.00000000 \\
0.00129493 & 0.00912192 & 0.00133656 & 0.00000000 & 0.00854880 & 0.15193748 & 0.00000000 & -0.62587529 & -0.00110738 & -3.54947233 & 0.69683415 & -0.00000963 & -0.00000963 & -0.00000963 \\
0.00000000 & 0.00000000 & 0.00000000 & 0.00000000 & 0.00000000 & 0.00000000 & 0.00000000 & 0.00000000 & 0.00000000 & 0.00000000 & 0.00000000 & 1.00000000 & 0.00000000 & 0.00000000 \\
0.00000000 & 0.00000000 & 0.00000000 & 0.00000000 & 0.00000000 & 0.00000000 & 0.00000000 & 0.00000000 & 0.00000000 & 0.00000000 & 0.00000000 & 0.00000000 & 1.00000000 & 0.00000000 \\
0.00000000 & 0.00000000 & 0.00000000 & 0.00000000 & 0.00000000 & 0.00000000 & 0.00000000 & 0.00000000 & 0.00000000 & 0.00000000 & 0.00000000 & 0.00000000 & 0.00000000 & 1.00000000 \\
0.01180153 & 1.33115125 & 0.03150940 & 0.00000000 & -0.05094337 & -4.10842896 & 0.00000000 & 0.00000000 & -766.61608887 & 0.00000000 & 0.00000000 & -31.63739777 & 0.00000000 & -4.80568743 \\
-0.07094307 & -0.30904809 & 32.11278915 & 0.00000000 & -0.31090182 & -55.56167603 & 0.00000000 & 0.00000000 & -259.48773193 & -37.61653900 & -876.38073730 & 0.00000000 & -31.63739777 & -53.99999619 \\
0.29704896 & 0.48058739 & -56.06025696 & 0.00000000 & -0.20418243 & -32.72087097 & 0.00000000 & 0.00000000 & 0.00000000 & 832.03851318 & -37.61634827 & -9.61065388 & 53.99999619 & -31.63739777
\end{bmatrix}$$

$$B_{14} = \begin{bmatrix}
11.52756882 & 3.65522623 & 0.00000000 & 0.00000000 \\
-363.51293945 & -115.26479340 & 0.00000000 & 0.00000000 \\
-1.79044485 & -0.56772256 & 0.00000000 & 0.00000000 \\
0.00000000 & 0.00000000 & 0.00000000 & 0.00000000 \\
2.39567304 & 0.75981867 & 0.00001510 & 15.56764030 \\
2.97173285 & 0.94236749 & 0.00000765 & 5.13501024 \\
0.00000000 & 0.00000000 & 0.00000000 & 0.00000000 \\
-6.80750179 & -2.15872169 & -0.00000963 & -9.19434834 \\
0.00000000 & 0.00000000 & 0.00000000 & 0.00000000 \\
0.00000000 & 0.00000000 & 0.00000000 & 0.00000000 \\
0.00000000 & 0.00000000 & 0.00000000 & 0.00000000 \\
718.44903564 & 202.37693787 & 0.00000000 & 0.00000000 \\
-108.62808228 & -34.44557190 & 876.38073730 & 0.00000000 \\
457.44171143 & 901.20281982 & 0.00000000 & 0.00000000
\end{bmatrix}$$

-15.780 ± j22.083
-15.400 ± j49.074
-15.233 ± j 5.872
-1.467
-1.077 ± j 1.238
-0.163 ± j 1.042
-0.143
-0.008 ± j 0.194

$$A_{8} = \begin{bmatrix}
-0.02567884 & 0.00476966 & 3.31420159 & -32.18571091 & 0.00638966 & 1.08425248 & 0.00000000 & 0.00000000 \\
-0.03700800 & -0.83178502 & 151.46595764 & 0.23713216 & 0.02901578 & 2.33982301 & -0.80598843 & 0.00000000 \\
0.00199497 & -0.00717893 & -0.76496315 & 0.00000000 & -0.00131866 & -0.22013099 & 0.00000000 & 0.00000000 \\
0.00000000 & 0.00000000 & 0.99968642 & 0.00000000 & 0.00000000 & 0.00000000 & 0.00000000 & -0.02504191 \\
-0.00440340 & -0.02172636 & 1.06927025 & 0.00594144 & -0.14649823 & -3.34265351 & 32.17549133 & -150.94616699 \\
-0.00280868 & -0.02222334 & 0.92171943 & 0.00000000 & -0.02117736 & -1.65552902 & 0.00000000 & 0.34860966 \\
0.00000000 & 0.00000000 & -0.00018457 & 0.00000000 & 0.00000000 & 1.00000000 & 0.00000000 & -0.00736814 \\
0.00252372 & 0.01072160 & -0.21974607 & 0.00000000 & 0.00749200 & -0.02160734 & 0.00000000 & -0.62587529
\end{bmatrix}$$

$$B_{8} = \begin{bmatrix}
-6.47775316 & -30.85840797 & 1.43361449 & 0.00000000 \\
-363.51293945 & -115.26479340 & 0.00000000 & 0.00000000 \\
1.81033969 & 6.33400869 & -0.28667769 & 0.00000000 \\
0.00000000 & 0.00000000 & 0.00000000 & 0.00000000 \\
-9.59411335 & -1.49376106 & 31.68893623 & 15.56764030 \\
-7.15997696 & -1.92670572 & 25.35485840 & 5.13501024 \\
0.00000000 & 0.00000000 & 0.00000000 & 0.00000000 \\
-5.05890989 & 1.64760923 & 0.53486335 & -9.19434834
\end{bmatrix}$$

-1.559
-1.003 ± j 1.149
-0.161 ± j 1.045
-0.143
-0.010 ± j 0.194

Helicopter : Puma

Forward Velocity : 90 Kts

Descent Angle : 0 Deg

$$A_{14} = \begin{bmatrix}
-0.01588393 & 0.04294569 & 24.28590012 & -32.18383789 & -0.00218526 & -0.15024947 & 0.00000000 & 0.00000000 & 0.00000000 & 33.47454071 & 0.00000000 & 0.00000000 & 0.00000000 & 0.00000000 \\
-0.01019891 & -0.85368007 & 166.67478943 & -0.41996330 & 0.03852039 & 2.64845490 & -1.72470951 & 0.00000000 & 0.00000000 & 0.00000000 & 0.00000000 & 0.00000000 & 0.00000000 & 0.00000000 \\
0.00095291 & -0.01223030 & -0.24067171 & 0.00000000 & 0.00029790 & 0.02048221 & 0.00000000 & 0.00000000 & 0.00000000 & -6.54448605 & 0.00000000 & 0.00000000 & 0.00000000 & 0.00000000 \\
0.00000000 & 0.00000000 & 0.99856305 & 0.00000000 & 0.00000000 & 0.00000000 & 0.00000000 & -0.05358947 & 0.00000000 & 0.00000000 & 0.00000000 & 0.00000000 & 0.00000000 & 0.00000000 \\
-0.00432690 & 0.01132110 & 0.01817834 & -0.02264706 & -0.14725834 & -24.51261902 & 32.13697815 & -166.07023621 & 0.00135873 & 0.00001510 & 33.47452164 & 0.00000000 & 0.00000000 & 0.00000000 \\
-0.00114458 & 0.00650206 & 0.00420396 & 0.00000000 & -0.01318314 & -0.11060565 & 0.00000000 & 0.35381868 & 0.00045155 & 1.12750113 & 26.13998795 & 0.00000000 & 0.00000000 & 0.00000000 \\
0.00000000 & 0.00000000 & 0.00070033 & 0.00000000 & 0.00000000 & 1.00000000 & 0.00000000 & 0.01304966 & 0.00000000 & 0.00000000 & 0.00000000 & 0.00000000 & 0.00000000 & 0.00000000 \\
0.00174239 & -0.00568083 & -0.00483202 & 0.00000000 & 0.00813598 & 0.21019083 & 0.00000000 & -0.63535637 & -0.00079924 & -4.06247711 & 0.71781170 & 0.00000000 & 0.00000000 & 0.00000000 \\
0.00000000 & 0.00000000 & 0.00000000 & 0.00000000 & 0.00000000 & 0.00000000 & 0.00000000 & 0.00000000 & 0.00000000 & 0.00000000 & 1.00000000 & 0.00000000 & 0.00000000 & 0.00000000 \\
0.00000000 & 0.00000000 & 0.00000000 & 0.00000000 & 0.00000000 & 0.00000000 & 0.00000000 & 0.00000000 & 0.00000000 & 0.00000000 & 0.00000000 & 1.00000000 & 0.00000000 & 0.00000000 \\
0.00000000 & 0.00000000 & 0.00000000 & 0.00000000 & 0.00000000 & 0.00000000 & 0.00000000 & 0.00000000 & 0.00000000 & 0.00000000 & 0.00000000 & 0.00000000 & 1.00000000 & 0.00000000 \\
-0.03542404 & 1.35323906 & 0.36712646 & 0.00000000 & -0.06762924 & -4.65049744 & 0.00000000 & 0.00000000 & -766.61645508 & 0.00000000 & 0.00000000 & -31.63739777 & 0.00000000 & -5.22053385 \\
-0.10209350 & -0.25388527 & 32.33779907 & 0.00000000 & -0.43030167 & -56.48303986 & 0.00000000 & 0.00000000 & -281.88781738 & -37.61672974 & -880.37322998 & 0.00000000 & -31.63739777 & -53.99999619 \\
0.37853774 & 0.53669471 & -56.63213730 & 0.00000000 & -0.21109352 & -32.74179459 & 0.00000000 & 0.00000000 & 0.00000000 & 828.04608154 & -37.61653900 & -10.44028378 & 53.99999619 & -31.63739777
\end{bmatrix}$$

$$B_{14} = \begin{bmatrix}
21.40458298 & 7.27812290 & -0.00006039 & 0.00000000 \\
-377.30731201 & -128.29460144 & 0.00096621 & 0.00000000 \\
-2.91791892 & -0.99216729 & 0.00000766 & 0.00000000 \\
0.00000000 & 0.00000000 & 0.00000000 & 0.00000000 \\
5.19227839 & 1.76713824 & -0.00001510 & 16.18483734 \\
6.36757803 & 2.16569567 & -0.00001531 & 5.33859062 \\
0.00000000 & 0.00000000 & 0.00000000 & 0.00000000 \\
-14.48619270 & -4.92670298 & 0.00002889 & -9.55886364 \\
0.00000000 & 0.00000000 & 0.00000000 & 0.00000000 \\
0.00000000 & 0.00000000 & 0.00000000 & 0.00000000 \\
0.00000000 & 0.00000000 & 0.00000000 & 0.00000000 \\
740.01123047 & 225.26092529 & 0.00000000 & 0.00000000 \\
-89.12582397 & -30.30662537 & 880.37396240 & 0.00000000 \\
501.97048950 & 911.67852783 & 0.00000000 & 0.00000000
\end{bmatrix}$$

-15.763 ± j21.963
-15.340 ± j49.015
-15.254 ± j 6.021
-1.490
-1.077 ± j 0.970
-0.230
-0.185 ± j 1.005
0.020 ± j 0.264

$$A_{8} = \begin{bmatrix}
-0.03130971 & 0.01999618 & 26.62638855 & -32.18383789 & 0.00564577 & 1.07642686 & 0.00000000 & 0.00000000 \\
-0.01019891 & -0.85368007 & 166.67478943 & -0.41996330 & 0.03852039 & 2.64845490 & -1.72470951 & 0.00000000 \\
0.00396871 & -0.00774350 & -0.69825041 & 0.00000000 & -0.00123293 & -0.21934199 & 0.00000000 & 0.00000000 \\
0.00000000 & 0.00000000 & 0.99856305 & 0.00000000 & 0.00000000 & 0.00000000 & 0.00000000 & -0.05358947 \\
-0.00709318 & -0.01633921 & 1.14289391 & -0.02264706 & -0.16300032 & -26.64518547 & 32.13698578 & -166.07023621 \\
-0.00382396 & -0.01584993 & 0.96131557 & 0.00000000 & -0.02521138 & -1.73462868 & 0.00000000 & 0.35381868 \\
0.00000000 & 0.00000000 & 0.00070033 & 0.00000000 & 0.00000000 & 1.00000000 & 0.00000000 & 0.01304966 \\
0.00355486 & -0.00348739 & -0.26475468 & 0.00000000 & 0.00684873 & 0.01559765 & 0.00000000 & -0.63535637
\end{bmatrix}$$

$$B_{8} = \begin{bmatrix}
0.53223091 & -29.69995308 & 1.51769745 & 0.00000000 \\
-377.30731201 & -128.29460144 & 0.00096621 & 0.00000000 \\
1.16300154 & 6.23736906 & -0.29672241 & 0.00000000 \\
0.00000000 & 0.00000000 & 0.00000000 & 0.00000000 \\
-7.66737652 & -0.96036774 & 33.37832642 & 16.18483734 \\
-4.37192345 & -1.20775378 & 26.11598206 & 5.33859062 \\
0.00000000 & 0.00000000 & 0.00000000 & 0.00000000 \\
-12.22871208 & -0.49749175 & 0.53157008 & -9.55886364
\end{bmatrix}$$

-1.709
-0.907 ± j 0.925
-0.231
-0.198 ± j 0.999
0.017 ± j 0.266

Helicopter : Puma

Forward Velocity : 100 Kts

Descent Angle : -9 Deg

$$A_{14} = \begin{bmatrix}
-0.01587738 & 0.03820115 & 16.95075989 & -32.18628693 & -0.00179108 & -0.13188316 & 0.00000000 & 0.00000000 & 0.00000000 & 32.90822220 & 0.00000000 & 0.00000000 & 0.00000000 & 0.00000000 \\
-0.01646157 & -0.85515469 & 167.47352600 & -0.13898934 & 0.03599688 & 2.65055585 & -1.42798591 & 0.00000000 & 0.00000000 & 0.00000000 & 0.00000000 & 0.00000000 & 0.00000000 & 0.00000000 \\
0.00050977 & -0.01273818 & -0.29785156 & 0.00000000 & 0.00025021 & 0.01842336 & 0.00000000 & 0.00000000 & 0.00000000 & -6.48092175 & 0.00000000 & 0.00000000 & 0.00000000 & 0.00000000 \\
0.00000000 & 0.00000000 & 0.99901533 & 0.00000000 & 0.00000000 & 0.00000000 & 0.00000000 & -0.04436687 & 0.00000000 & 0.00000000 & 0.00000000 & 0.00000000 & 0.00000000 & 0.00000000 \\
-0.00357135 & 0.00928916 & 0.01017087 & -0.00654607 & -0.14717931 & -17.17235756 & 32.15448761 & -166.97137451 & 0.00140402 & -0.00003019 & 32.90819931 & -0.00001510 & -0.00001510 & -0.00001510 \\
-0.00094353 & 0.00435443 & 0.00178743 & 0.00000000 & -0.01306886 & -0.10340656 & 0.00000000 & 0.35408887 & 0.00046303 & 1.11878014 & 25.88608360 & -0.00000383 & -0.00000383 & -0.00000383 \\
0.00000000 & 0.00000000 & 0.00019175 & 0.00000000 & 0.00000000 & 1.00000000 & 0.00000000 & 0.00431773 & 0.00000000 & 0.00000000 & 0.00000000 & 0.00000000 & 0.00000000 & 0.00000000 \\
0.00146807 & -0.00095974 & -0.00104190 & 0.00000000 & 0.00789437 & 0.19393165 & 0.00000000 & -0.63584173 & -0.00082813 & -4.03107548 & 0.71084005 & 0.00000963 & 0.00000963 & 0.00000963 \\
0.00000000 & 0.00000000 & 0.00000000 & 0.00000000 & 0.00000000 & 0.00000000 & 0.00000000 & 0.00000000 & 0.00000000 & 0.00000000 & 0.00000000 & 1.00000000 & 0.00000000 & 0.00000000 \\
0.00000000 & 0.00000000 & 0.00000000 & 0.00000000 & 0.00000000 & 0.00000000 & 0.00000000 & 0.00000000 & 0.00000000 & 0.00000000 & 0.00000000 & 0.00000000 & 1.00000000 & 0.00000000 \\
0.00000000 & 0.00000000 & 0.00000000 & 0.00000000 & 0.00000000 & 0.00000000 & 0.00000000 & 0.00000000 & 0.00000000 & 0.00000000 & 0.00000000 & 0.00000000 & 0.00000000 & 1.00000000 \\
-0.02665482 & 1.35585141 & 0.30578613 & 0.00000000 & -0.06320000 & -4.65396881 & 0.00000000 & 0.00000000 & -766.61608887 & 0.00000000 & 0.00000000 & -31.63739777 & 0.00000000 & -5.26937532 \\
-0.09300079 & -0.26293373 & 32.27277756 & 0.00000000 & -0.39300632 & -56.18501663 & 0.00000000 & 0.00000000 & -284.52493286 & -37.61634827 & -880.86529541 & 0.00000000 & -31.63739777 & -53.99999619 \\
0.34858647 & 0.53947639 & -56.41984940 & 0.00000000 & -0.20488396 & -32.68892288 & 0.00000000 & 0.00000000 & 0.00000000 & 827.55432129 & -37.61653900 & -10.53796101 & 53.99999619 & -31.63739777
\end{bmatrix}$$

$$B_{14} = \begin{bmatrix}
18.78592110 & 6.43734598 & -0.00003019 & 0.00000000 \\
-377.55511475 & -129.37677002 & 0.00072466 & 0.00000000 \\
-2.62432933 & -0.89927638 & 0.00000575 & 0.00000000 \\
0.00000000 & 0.00000000 & 0.00000000 & 0.00000000 \\
4.33562708 & 1.48708820 & -0.00001510 & 16.17451096 \\
5.31442118 & 1.82156456 & -0.00001148 & 5.33518791 \\
0.00000000 & 0.00000000 & 0.00000000 & 0.00000000 \\
-12.08678436 & -4.14266062 & 0.00001926 & -9.55276775 \\
0.00000000 & 0.00000000 & 0.00000000 & 0.00000000 \\
0.00000000 & 0.00000000 & 0.00000000 & 0.00000000 \\
0.00000000 & 0.00000000 & 0.00000000 & 0.00000000 \\
740.11614990 & 227.15568542 & 0.00000000 & 0.00000000 \\
-93.82362366 & -32.15179443 & 880.86566162 & 0.00000000 \\
506.33871460 & 912.67950439 & 0.00000000 & 0.00000000
\end{bmatrix}$$

-15.761 ± j21.949
-15.335 ± j49.017
-15.283 ± j 6.004
-1.559
-1.079 ± j 1.197
-0.199
-0.150 ± j 1.007
0.003 ± j 0.225

$$A_{8} = \begin{bmatrix}
-0.02985206 & 0.01549117 & 19.24448204 & -32.18628693 & 0.00572628 & 1.07324231 & 0.00000000 & 0.00000000 \\
-0.01646157 & -0.85515469 & 167.47352600 & -0.13898934 & 0.03599688 & 2.65055585 & -1.42798591 & 0.00000000 \\
0.00326193 & -0.00826572 & -0.74957484 & 0.00000000 & -0.00123009 & -0.21891470 & 0.00000000 & 0.00000000 \\
0.00000000 & 0.00000000 & 0.99901533 & 0.00000000 & 0.00000000 & 0.00000000 & 0.00000000 & -0.04436687 \\
-0.00611598 & -0.01843128 & 1.11391664 & -0.00654607 & -0.16129991 & -19.25578690 & 32.15448761 & -166.97135925 \\
-0.00341990 & -0.01820176 & 0.94798845 & 0.00000000 & -0.02392015 & -1.70133209 & 0.00000000 & 0.35408887 \\
0.00000000 & 0.00000000 & 0.00019175 & 0.00000000 & 0.00000000 & 1.00000000 & 0.00000000 & 0.00431773 \\
0.00312466 & 0.00122481 & -0.25816724 & 0.00000000 & 0.00666920 & 0.00131056 & 0.00000000 & -0.63584173
\end{bmatrix}$$

$$B_{8} = \begin{bmatrix}
-1.93051827 & -29.98188400 & 1.49288535 & 0.00000000 \\
-377.55511475 & -129.37677002 & 0.00072466 & 0.00000000 \\
1.45581710 & 6.27319622 & -0.29400921 & 0.00000000 \\
0.00000000 & 0.00000000 & 0.00000000 & 0.00000000 \\
-8.56291771 & -1.31407619 & 32.81242371 & 16.17451096 \\
-5.53058863 & -1.61810136 & 25.86151505 & 5.33518791 \\
0.00000000 & 0.00000000 & 0.00000000 & 0.00000000 \\
-9.82756138 & 0.25805748 & 0.52590799 & -9.55276775
\end{bmatrix}$$

-1.684
-0.970 ± j 1.125
-0.200
-0.155 ± j 1.007
0.001 ± j 0.225

Helicopter : Puma

Forward Velocity : 100 Kts

Descent Angle : -6 Deg

$$A_{14} = \begin{bmatrix}
-0.01589629 & 0.03238866 & 9.70262718 & -32.18618393 & -0.00139137 & -0.11033970 & 0.00000000 & -0.00000302 & -0.00003019 & 32.34016800 & -0.00003019 & -0.00003019 & -0.00003019 & -0.00003019 \\
-0.02325082 & -0.85635316 & 167.98461914 & 0.16113971 & 0.03338257 & 2.64729524 & -1.13522458 & 0.00004831 & 0.00048311 & 0.00048311 & 0.00048311 & 0.00048311 & 0.00048311 & 0.00048311 \\
0.00012010 & -0.01268064 & -0.33789939 & 0.00000000 & 0.00020177 & 0.01600083 & 0.00000000 & 0.00000038 & 0.00000383 & -6.41716051 & 0.00000383 & 0.00000383 & 0.00000383 & 0.00000383 \\
0.00000000 & 0.00000000 & 0.99937773 & 0.00000000 & 0.00000000 & 0.00000000 & 0.00000000 & -0.03527213 & 0.00000000 & 0.00000000 & 0.00000000 & 0.00000000 & 0.00000000 & 0.00000000 \\
-0.00281691 & 0.00732596 & 0.00384069 & 0.00552853 & -0.14710817 & -9.91883087 & 32.16604996 & -167.54374695 & 0.00140402 & 0.00001510 & 32.34017563 & 0.00000000 & 0.00000000 & 0.00000000 \\
-0.00075474 & 0.00220298 & 0.00000344 & 0.00000000 & -0.01296530 & -0.09603949 & 0.00000000 & 0.35445660 & 0.00045537 & 1.10744941 & 25.63142204 & -0.00000765 & -0.00000765 & -0.00000765 \\
0.00000000 & 0.00000000 & -0.00017665 & 0.00000000 & 0.00000000 & 1.00000000 & 0.00000000 & -0.00500509 & 0.00000000 & 0.00000000 & 0.00000000 & 0.00000000 & 0.00000000 & 0.00000000 \\
0.00122998 & 0.00380783 & 0.00151855 & 0.00000000 & 0.00767578 & 0.17719772 & 0.00000000 & -0.63649744 & -0.00080887 & -3.99023747 & 0.70386839 & 0.00001926 & 0.00001926 & 0.00001926 \\
0.00000000 & 0.00000000 & 0.00000000 & 0.00000000 & 0.00000000 & 0.00000000 & 0.00000000 & 0.00000000 & 0.00000000 & 0.00000000 & 0.00000000 & 1.00000000 & 0.00000000 & 0.00000000 \\
0.00000000 & 0.00000000 & 0.00000000 & 0.00000000 & 0.00000000 & 0.00000000 & 0.00000000 & 0.00000000 & 0.00000000 & 0.00000000 & 0.00000000 & 0.00000000 & 1.00000000 & 0.00000000 \\
0.00000000 & 0.00000000 & 0.00000000 & 0.00000000 & 0.00000000 & 0.00000000 & 0.00000000 & 0.00000000 & 0.00000000 & 0.00000000 & 0.00000000 & 0.00000000 & 0.00000000 & 1.00000000 \\
-0.01657295 & 1.35853159 & 0.23418427 & 0.00000000 & -0.05860977 & -4.64828491 & 0.00000000 & 0.00000000 & -766.61608887 & 0.00000000 & 0.00000000 & -31.63739777 & 0.00000000 & -5.30758572 \\
-0.08421688 & -0.27211952 & 32.20979691 & 0.00000000 & -0.35524693 & -55.88367462 & 0.00000000 & 0.00000000 & -286.58792114 & -37.61634827 & -881.25347900 & 0.00000000 & -31.63739777 & -53.99999619 \\
0.31909370 & 0.54126513 & -56.21120453 & 0.00000000 & -0.19865951 & -32.63755798 & 0.00000000 & 0.00000000 & 0.00000000 & 827.16601562 & -37.61672974 & -10.61437511 & 53.99999619 & -31.63739777
\end{bmatrix}$$

$$B_{14} = \begin{bmatrix}
15.74192047 & 5.42665958 & -0.00004529 & -0.00003019 \\
-377.68191528 & -130.19709778 & 0.00096621 & 0.00048311 \\
-2.28283143 & -0.78695619 & 0.00000766 & 0.00000383 \\
0.00000000 & 0.00000000 & 0.00000000 & 0.00000000 \\
3.47554898 & 1.19927824 & -0.00001510 & 16.16623878 \\
4.24727392 & 1.46453762 & -0.00001148 & 5.33245230 \\
0.00000000 & 0.00000000 & 0.00000000 & 0.00000000 \\
-9.64264393 & -3.32479978 & 0.00002889 & -9.54786205 \\
0.00000000 & 0.00000000 & 0.00000000 & 0.00000000 \\
0.00000000 & 0.00000000 & 0.00000000 & 0.00000000 \\
0.00000000 & 0.00000000 & 0.00000000 & 0.00000000 \\
740.07611084 & 228.59458923 & 0.00000000 & 0.00000000 \\
-98.62194061 & -33.99925232 & 881.25366211 & 0.00000000 \\
509.70117188 & 913.45104980 & 0.00000000 & 0.00000000
\end{bmatrix}$$

-15.759 ± j21.938
-15.331 ± j49.021
-15.310 ± j 5.986
-1.557
-1.096 ± j 1.311
-0.178
-0.132 ± j 1.017
-0.005 ± j 0.199

$$A_{8} = \begin{bmatrix}
-0.02847659 & 0.00996740 & 11.94958019 & -32.18619156 & 0.00581671 & 1.07309651 & 0.00000000 & -0.00000302 \\
-0.02325082 & -0.85635316 & 167.98461914 & 0.16113971 & 0.03338257 & 2.64729524 & -1.13522458 & 0.00004831 \\
0.00261639 & -0.00823174 & -0.78375548 & 0.00000000 & -0.00122835 & -0.21882638 & 0.00000000 & 0.00000038 \\
0.00000000 & 0.00000000 & 0.99937773 & 0.00000000 & 0.00000000 & 0.00000000 & 0.00000000 & -0.03527213 \\
-0.00517741 & -0.02040825 & 1.08698809 & 0.00552853 & -0.15964462 & -11.95386791 & 32.16604996 & -167.54374695 \\
-0.00305598 & -0.02052422 & 0.93540299 & 0.00000000 & -0.02265386 & -1.66843510 & 0.00000000 & 0.35445699 \\
0.00000000 & 0.00000000 & -0.00017665 & 0.00000000 & 0.00000000 & 1.00000000 & 0.00000000 & -0.00500509 \\
0.00273059 & 0.00597212 & -0.25214407 & 0.00000000 & 0.00651422 & -0.01310557 & 0.00000000 & -0.63649845
\end{bmatrix}$$

$$B_{8} = \begin{bmatrix}
-4.76840591 & -30.41562653 & 1.46779418 & -0.00003019 \\
-377.68191528 & -130.19709778 & 0.00096621 & 0.00048311 \\
1.78725922 & 6.32522249 & -0.29125383 & 0.00000383 \\
0.00000000 & 0.00000000 & 0.00000000 & 0.00000000 \\
-9.43649292 & -1.65997934 & 32.24510956 & 16.16623878 \\
-6.68326902 & -2.02706361 & 25.60634995 & 5.33245611 \\
0.00000000 & 0.00000000 & 0.00000000 & 0.00000000 \\
-7.39287138 & 1.03535938 & 0.52067924 & -9.54787159
\end{bmatrix}$$

-1.647
-1.014 ± j 1.223
-0.179
-0.133 ± j 1.021
-0.007 ± j 0.199

Helicopter : Puma

Forward Velocity : 100 Kts

Descent Angle : -3 Deg

$$A_{14} = \begin{bmatrix}
-0.01280432 & 0.02010237 & 1.17044580 & -32.18581772 & -0.00081317 & -0.06779935 & 0.00000000 & 0.00000000 & -0.00003839 & 31.76651382 & 0.00003839 & -0.00003839 & 0.00000000 & 0.00003839 \\
-0.03165318 & -0.69573241 & 168.40040588 & 0.22222991 & 0.02580579 & 2.15159655 & -0.80566335 & 0.00000000 & 0.00098267 & 0.00000000 & -0.00098267 & 0.00098267 & 0.00000000 & -0.00098267 \\
-0.00026499 & -0.00956516 & -0.29034618 & 0.00000000 & 0.00012440 & 0.01037241 & 0.00000000 & 0.00000000 & 0.00000527 & -6.29306364 & -0.00000527 & 0.00000527 & 0.00000000 & -0.00000527 \\
0.00000000 & 0.00000000 & 0.99968660 & 0.00000000 & 0.00000000 & 0.00000000 & 0.00000000 & -0.02503427 & 0.00000000 & 0.00000000 & 0.00000000 & 0.00000000 & 0.00000000 & 0.00000000 \\
-0.00195911 & 0.00413724 & -0.00042301 & 0.00556972 & -0.11939450 & -1.34173000 & 32.17565536 & -168.02061462 & 0.00110550 & 0.00003839 & 31.76651382 & -0.00000768 & 0.00000000 & 0.00000768 \\
-0.00033205 & 0.00139115 & -0.00036413 & 0.00000000 & -0.00905763 & -0.04175617 & 0.00000000 & 0.16839679 & 0.00021203 & 0.18279135 & 25.72787857 & -0.00000488 & 0.00000050 & 0.00000439 \\
0.00000000 & 0.00000000 & -0.00017292 & 0.00000000 & 0.00000000 & 1.00000000 & 0.00000000 & -0.00690501 & 0.00000000 & 0.00000000 & 0.00000000 & 0.00000000 & 0.00000000 & 0.00000000 \\
0.00115763 & 0.01014433 & 0.00098557 & 0.00000000 & 0.00534748 & 0.12872548 & 0.00000000 & -0.49610192 & -0.00060568 & -3.86401153 & 2.56117558 & 0.00002853 & -0.00001441 & -0.00001412 \\
0.00000000 & 0.00000000 & 0.00000000 & 0.00000000 & 0.00000000 & 0.00000000 & 0.00000000 & 0.00000000 & 0.00000000 & 0.00000000 & 0.00000000 & 1.00000000 & 0.00000000 & 0.00000000 \\
0.00000000 & 0.00000000 & 0.00000000 & 0.00000000 & 0.00000000 & 0.00000000 & 0.00000000 & 0.00000000 & 0.00000000 & 0.00000000 & 0.00000000 & 0.00000000 & 1.00000000 & 0.00000000 \\
0.00000000 & 0.00000000 & 0.00000000 & 0.00000000 & 0.00000000 & 0.00000000 & 0.00000000 & 0.00000000 & 0.00000000 & 0.00000000 & 0.00000000 & 0.00000000 & 0.00000000 & 1.00000000 \\
0.00313225 & 1.08605194 & 0.07156372 & 0.00000000 & -0.04454689 & -3.71475220 & 0.00007629 & -0.00007629 & -766.61608887 & -0.00076294 & 0.00000000 & -25.25598145 & -0.00076294 & -4.26293516 \\
-0.05401020 & -0.23208770 & 25.61897278 & 0.00000000 & -0.30505791 & -55.63705444 & 0.00001907 & -0.00001907 & -230.18112183 & -37.61653900 & -703.78515625 & 0.00019073 & -25.25693512 & -53.99999619 \\
0.28202859 & 0.43701515 & -55.95787048 & 0.00000000 & -0.16371307 & -26.08722687 & 0.00003815 & -0.00003815 & 0.00038147 & 660.07879639 & -37.61672974 & -8.52484989 & 53.99961472 & -25.25674438
\end{bmatrix}$$

$$B_{14} = \begin{bmatrix}
9.67063141 & 3.35055351 & 0.00000000 & 0.00003839 \\
-306.89178467 & -106.32766724 & 0.00000000 & -0.00098267 \\
-1.47947419 & -0.51258802 & 0.00000000 & -0.00000527 \\
0.00000000 & 0.00000000 & 0.00000000 & 0.00000000 \\
2.00118399 & 0.69414610 & -0.00000768 & 13.12285995 \\
1.20098352 & 0.41626006 & -0.00000226 & 2.53693628 \\
0.00000000 & 0.00000000 & 0.00000000 & 0.00000000 \\
-6.19534111 & -2.14696336 & -0.00000979 & -7.43618011 \\
0.00000000 & 0.00000000 & 0.00000000 & 0.00000000 \\
0.00000000 & 0.00000000 & 0.00000000 & 0.00000000 \\
0.00000000 & 0.00000000 & 0.00000000 & 0.00000000 \\
591.06787109 & 183.55751038 & -0.00076294 & 0.00000000 \\
-81.22673035 & -28.14254761 & 703.78533936 & 0.00000000 \\
409.27581787 & 729.78515625 & -0.00038147 & 0.00000000
\end{bmatrix}$$

-12.611 ± j24.287
-12.371 ± j51.067
-11.455 ± j 3.721
-2.176
-1.054 ± j 1.027
-0.124
-0.060 ± j 0.941
-0.012 ± j 0.204

$$A_{8} = \begin{bmatrix}
-0.02647511 & -0.00229819 & 3.92088509 & -32.18581772 & 0.00630414 & 1.04407048 & 0.00000000 & 0.00000000 \\
-0.03165318 & -0.69573241 & 168.40040588 & 0.22222991 & 0.02580579 & 2.15159655 & -0.80566335 & 0.00000000 \\
0.00244330 & -0.00512766 & -0.83521855 & 0.00000000 & -0.00128543 & -0.20989464 & 0.00000000 & 0.00000000 \\
0.00000000 & 0.00000000 & 0.99968660 & 0.00000000 & 0.00000000 & 0.00000000 & 0.00000000 & -0.02503427 \\
-0.00374148 & -0.01991448 & 1.00818467 & 0.00556972 & -0.13293758 & -3.86006427 & 32.17565155 & -168.02061462 \\
-0.00185384 & -0.01819919 & 0.83233613 & 0.00000000 & -0.01998456 & -2.07500339 & 0.00000000 & 0.16839702 \\
0.00000000 & 0.00000000 & -0.00017292 & 0.00000000 & 0.00000000 & 1.00000000 & 0.00000000 & -0.00690501 \\
0.00267667 & 0.01093241 & -0.25224999 & 0.00000000 & 0.00339046 & -0.20955987 & 0.00000000 & -0.49610096
\end{bmatrix}$$

$$B_{8} = \begin{bmatrix}
-10.62556744 & -31.87635994 & 1.80480433 & 0.00004606 \\
-306.89178467 & -106.32766724 & 0.00000000 & -0.00098267 \\
2.54155254 & 6.46608829 & -0.35753915 & -0.00000766 \\
0.00000000 & 0.00000000 & 0.00000000 & 0.00000000 \\
-8.60273457 & -1.18522573 & 31.63750267 & 13.12285995 \\
-7.49961090 & -1.30697823 & 25.63377762 & 2.53692961 \\
0.00000000 & 0.00000000 & 0.00000000 & 0.00000000 \\
-4.58108187 & 1.98657930 & 2.33125854 & -7.43619061
\end{bmatrix}$$

-2.154
-0.920 ± j 0.986
-0.125
-0.057 ± j 0.942
-0.014 ± j 0.204

Helicopter : Puma

Forward Velocity : 100 Kts

Descent Angle : 0 Deg

$$A_{14} = \begin{bmatrix}
-0.01606388 & 0.01896820 & -4.84609604 & -32.17756653 & -0.00067099 & -0.06297275 & 0.00000000 & 0.00000000 & 0.00000000 & 31.19113350 & 0.00000000 & 0.00000000 & 0.00000000 & 0.00000000 \\
-0.03732666 & -0.85785872 & 168.17805481 & 0.76180851 & 0.02798097 & 2.62603879 & -0.56293827 & 0.00000000 & 0.00000000 & 0.00000000 & 0.00000000 & 0.00000000 & 0.00000000 & 0.00000000 \\
-0.00058334 & -0.01109264 & -0.36850804 & 0.00000000 & 0.00011354 & 0.01065542 & 0.00000000 & 0.00000000 & 0.00000000 & -6.28818655 & 0.00000000 & 0.00000000 & 0.00000000 & 0.00000000 \\
0.00000000 & 0.00000000 & 0.99984694 & 0.00000000 & 0.00000000 & 0.00000000 & 0.00000000 & -0.01749436 & 0.00000000 & 0.00000000 & 0.00000000 & 0.00000000 & 0.00000000 & 0.00000000 \\
-0.00135980 & 0.00357620 & -0.00171955 & 0.01337899 & -0.14697129 & 4.64239645 & 32.17254257 & -167.75125122 & 0.00139648 & 0.00005284 & 31.19112015 & -0.00000755 & -0.00000755 & -0.00000755 \\
-0.00043863 & -0.00211977 & -0.00092509 & 0.00000000 & -0.01278795 & -0.08088651 & 0.00000000 & 0.35487142 & 0.00045920 & 1.07755947 & 25.11628342 & -0.00000191 & -0.00000191 & -0.00000191 \\
0.00000000 & 0.00000000 & -0.00041425 & 0.00000000 & 0.00000000 & 1.00000000 & 0.00000000 & -0.02367538 & 0.00000000 & 0.00000000 & 0.00000000 & 0.00000000 & 0.00000000 & 0.00000000 \\
0.00089946 & 0.01350028 & 0.00168129 & 0.00000000 & 0.00730649 & 0.14255318 & 0.00000000 & -0.63724083 & -0.00082331 & -3.88250399 & 0.68969876 & 0.00000481 & 0.00000481 & 0.00000481 \\
0.00000000 & 0.00000000 & 0.00000000 & 0.00000000 & 0.00000000 & 0.00000000 & 0.00000000 & 0.00000000 & 0.00000000 & 0.00000000 & 0.00000000 & 1.00000000 & 0.00000000 & 0.00000000 \\
0.00000000 & 0.00000000 & 0.00000000 & 0.00000000 & 0.00000000 & 0.00000000 & 0.00000000 & 0.00000000 & 0.00000000 & 0.00000000 & 0.00000000 & 0.00000000 & 1.00000000 & 0.00000000 \\
0.00000000 & 0.00000000 & 0.00000000 & 0.00000000 & 0.00000000 & 0.00000000 & 0.00000000 & 0.00000000 & 0.00000000 & 0.00000000 & 0.00000000 & 0.00000000 & 0.00000000 & 1.00000000 \\
0.00520363 & 1.36398578 & 0.08113861 & 0.00000000 & -0.04912644 & -4.61090088 & 0.00000000 & 0.00000000 & -766.61608887 & 0.00000000 & 0.00000000 & -31.63739777 & 0.00000000 & -5.35447407 \\
-0.06701241 & -0.29147816 & 32.08652496 & 0.00000000 & -0.27823582 & -55.26885986 & 0.00000000 & 0.00000000 & -289.11990356 & -37.61634827 & -881.73315430 & 0.00000000 & -31.63739777 & -53.99999619 \\
0.26020545 & 0.54199982 & -55.79429626 & 0.00000000 & -0.18627167 & -32.53982544 & 0.00000000 & 0.00000000 & 0.00000000 & 826.68609619 & -37.61672974 & -10.70814419 & 53.99999619 & -31.63739777
\end{bmatrix}$$

$$B_{14} = \begin{bmatrix}
9.05446243 & 3.14415383 & 0.00000000 & 0.00000000 \\
-377.58459473 & -131.11546326 & 0.00000000 & 0.00000000 \\
-1.53207517 & -0.53200966 & 0.00000000 & 0.00000000 \\
0.00000000 & 0.00000000 & 0.00000000 & 0.00000000 \\
1.75117314 & 0.60865211 & -0.00000755 & 16.15269279 \\
2.07644105 & 0.72123080 & -0.00000383 & 5.32799053 \\
0.00000000 & 0.00000000 & 0.00000000 & 0.00000000 \\
-4.62944460 & -1.60790730 & 0.00000481 & -9.53987980 \\
0.00000000 & 0.00000000 & 0.00000000 & 0.00000000 \\
0.00000000 & 0.00000000 & 0.00000000 & 0.00000000 \\
0.00000000 & 0.00000000 & 0.00000000 & 0.00000000 \\
739.59045410 & 230.20324707 & 0.00000000 & 0.00000000 \\
-108.78524780 & -37.77561188 & 881.73297119 & 0.00000000 \\
513.65393066 & 914.34631348 & 0.00000000 & 0.00000000
\end{bmatrix}$$

-15.758 ± j21.926
-15.357 ± j 5.946
-15.328 ± j49.030
-1.495
-1.115 ± j 1.386
-0.146
-0.122 ± j 1.008
-0.010 ± j 0.160

$$A_{8} = \begin{bmatrix}
-0.02597176 & -0.00273871 & -2.69354653 & -32.17757034 & 0.00593564 & 1.07642007 & 0.00000000 & 0.00000000 \\
-0.03732666 & -0.85785872 & 168.17805481 & 0.76180851 & 0.02798097 & 2.62603879 & -0.56293827 & 0.00000000 \\
0.00141417 & -0.00671668 & -0.80246592 & 0.00000000 & -0.00121825 & -0.21905059 & 0.00000000 & 0.00000000 \\
0.00000000 & 0.00000000 & 0.99984694 & 0.00000000 & 0.00000000 & 0.00000000 & 0.00000000 & -0.01749436 \\
-0.00340585 & -0.02407142 & 1.04062653 & 0.01337899 & -0.15644194 & 2.70263958 & 32.17254257 & -167.75128174 \\
-0.00242803 & -0.02511076 & 0.91277218 & 0.00000000 & -0.02018558 & -1.60352623 & 0.00000000 & 0.35487142 \\
0.00000000 & 0.00000000 & -0.00041425 & 0.00000000 & 0.00000000 & 1.00000000 & 0.00000000 & -0.02367538 \\
0.00208732 & 0.01559236 & -0.24320416 & 0.00000000 & 0.00627527 & -0.04215930 & 0.00000000 & -0.63724083
\end{bmatrix}$$

$$B_{8} = \begin{bmatrix}
-10.90643120 & -31.48629570 & 1.41652465 & 0.00000000 \\
-377.58459473 & -131.11546326 & 0.00000000 & 0.00000000 \\
2.49243236 & 6.44967556 & -0.28557211 & 0.00000000 \\
0.00000000 & 0.00000000 & 0.00000000 & 0.00000000 \\
-11.12573719 & -2.32621908 & 31.09832764 & 16.15269279 \\
-8.97728252 & -2.83664608 & 25.09049225 & 5.32799053 \\
0.00000000 & 0.00000000 & 0.00000000 & 0.00000000 \\
-2.42943692 & 2.63782620 & 0.51132917 & -9.53987980
\end{bmatrix}$$

-1.564
-1.057 ± j 1.281
-0.147
-0.117 ± j 1.017
-0.012 ± j 0.160

Helicopter : Puma

Forward Velocity : 100 Kts

Descent Angle : 3 Deg

$$A_{14} = \begin{bmatrix}
-0.01619651 & 0.01211335 & -12.24382591 & -32.16999817 & -0.00038703 & -0.03996034 & 0.00000000 & 0.00000000 & 0.00000000 & 30.61263847 & 0.00000000 & 0.00000000 & 0.00000000 & 0.00000000 \\
-0.04399857 & -0.85808671 & 167.84631348 & 1.03312027 & 0.02526543 & 2.60855031 & -0.28631225 & 0.00000000 & 0.00000000 & 0.00000000 & 0.00000000 & 0.00000000 & 0.00000000 & 0.00000000 \\
-0.00093839 & -0.00962762 & -0.35848248 & 0.00000000 & 0.00007795 & 0.00804851 & 0.00000000 & 0.00000000 & 0.00000000 & -6.22325706 & 0.00000000 & 0.00000000 & 0.00000000 & 0.00000000 \\
0.00000000 & 0.00000000 & 0.99996042 & 0.00000000 & 0.00000000 & 0.00000000 & 0.00000000 & -0.00889986 & 0.00000000 & 0.00000000 & 0.00000000 & 0.00000000 & 0.00000000 & 0.00000000 \\
-0.00067939 & 0.00180527 & -0.00191732 & 0.00925448 & -0.14691040 & 12.04703617 & 32.16862869 & -167.37574768 & 0.00023400 & 0.00000377 & 30.61264801 & 0.00000000 & 0.00000000 & 0.00000000 \\
-0.00031584 & -0.00427114 & -0.00040582 & 0.00000000 & -0.01271739 & -0.07330542 & 0.00000000 & 0.35498583 & 0.00007749 & 1.05926037 & 24.85693741 & 0.00000000 & 0.00000000 & 0.00000000 \\
0.00000000 & 0.00000000 & -0.00028582 & 0.00000000 & 0.00000000 & 1.00000000 & 0.00000000 & -0.03211426 & 0.00000000 & 0.00000000 & 0.00000000 & 0.00000000 & 0.00000000 & 0.00000000 \\
0.00080677 & 0.01838228 & -0.00005802 & 0.00000000 & 0.00716290 & 0.12507829 & 0.00000000 & -0.63744628 & -0.00013722 & -3.81659818 & 0.68257546 & 0.00000000 & 0.00000000 & 0.00000000 \\
0.00000000 & 0.00000000 & 0.00000000 & 0.00000000 & 0.00000000 & 0.00000000 & 0.00000000 & 0.00000000 & 0.00000000 & 0.00000000 & 0.00000000 & 1.00000000 & 0.00000000 & 0.00000000 \\
0.00000000 & 0.00000000 & 0.00000000 & 0.00000000 & 0.00000000 & 0.00000000 & 0.00000000 & 0.00000000 & 0.00000000 & 0.00000000 & 0.00000000 & 0.00000000 & 1.00000000 & 0.00000000 \\
0.00000000 & 0.00000000 & 0.00000000 & 0.00000000 & 0.00000000 & 0.00000000 & 0.00000000 & 0.00000000 & 0.00000000 & 0.00000000 & 0.00000000 & 0.00000000 & 0.00000000 & 1.00000000 \\
0.01562119 & 1.36666417 & 0.00759125 & 0.00000000 & -0.04435768 & -4.58034515 & 0.00000000 & 0.00000000 & -766.61608887 & 0.00000000 & 0.00000000 & -31.63739777 & 0.00000000 & -5.36308956 \\
-0.05833702 & -0.30190295 & 32.02430725 & 0.00000000 & -0.23928356 & -54.95708466 & 0.00000000 & 0.00000000 & -289.58511353 & -37.61634827 & -881.82183838 & 0.00000000 & -31.63739777 & -53.99999619 \\
0.23043518 & 0.54090345 & -55.58387756 & 0.00000000 & -0.18023948 & -32.49450684 & 0.00000000 & 0.00000000 & 0.00000000 & 826.59759521 & -37.61672974 & -10.72537518 & 53.99999619 & -31.63739777
\end{bmatrix}$$

$$B_{14} = \begin{bmatrix}
5.78062439 & 2.01001930 & 0.00000000 & 0.00000000 \\
-377.35317993 & -131.21183777 & 0.00000000 & 0.00000000 \\
-1.16429293 & -0.40484250 & 0.00000000 & 0.00000000 \\
0.00000000 & 0.00000000 & 0.00000000 & 0.00000000 \\
0.89782447 & 0.31247845 & 0.00000000 & 16.14870834 \\
0.98522222 & 0.34267318 & 0.00000000 & 5.32667589 \\
0.00000000 & 0.00000000 & 0.00000000 & 0.00000000 \\
-2.08755827 & -0.72604722 & 0.00000000 & -9.53752995 \\
0.00000000 & 0.00000000 & 0.00000000 & 0.00000000 \\
0.00000000 & 0.00000000 & 0.00000000 & 0.00000000 \\
0.00000000 & 0.00000000 & 0.00000000 & 0.00000000 \\
739.13043213 & 230.36842346 & 0.00000000 & 0.00000000 \\
-114.26124573 & -39.72988129 & 881.82202148 & 0.00000000 \\
514.23913574 & 914.46075439 & 0.00000000 & 0.00000000
\end{bmatrix}$$

-15.757 ± j21.925
-15.377 ± j 5.924
-15.328 ± j49.037
-1.449
-1.112 ± j 1.374
-0.131
-0.127 ± j 0.980
-0.010 ± j 0.138

$$A_{8} = \begin{bmatrix}
-0.02481383 & -0.00917265 & -10.13880539 & -32.16999817 & 0.00593263 & 1.07722783 & 0.00000000 & 0.00000000 \\
-0.04399857 & -0.85808671 & 167.84631348 & 1.03312027 & 0.02526543 & 2.60855031 & -0.28631225 & 0.00000000 \\
0.00081350 & -0.00530064 & -0.78641319 & 0.00000000 & -0.00120667 & -0.21906742 & 0.00000000 & 0.00000000 \\
0.00000000 & 0.00000000 & 0.99996042 & 0.00000000 & 0.00000000 & 0.00000000 & 0.00000000 & -0.00889986 \\
-0.00256758 & -0.02575316 & 1.02010596 & 0.00925448 & -0.15490960 & 10.15399456 & 32.16862869 & -167.37574768 \\
-0.00214674 & -0.02736283 & 0.90229517 & 0.00000000 & -0.01899374 & -1.57179904 & 0.00000000 & 0.35498583 \\
0.00000000 & 0.00000000 & -0.00028582 & 0.00000000 & 0.00000000 & 1.00000000 & 0.00000000 & -0.03211426 \\
0.00183888 & 0.02042309 & -0.23970930 & 0.00000000 & 0.00619713 & -0.05641294 & 0.00000000 & -0.63744628
\end{bmatrix}$$

$$B_{8} = \begin{bmatrix}
-13.84233665 & -31.98937416 & 1.39043689 & 0.00000000 \\
-377.35317993 & -131.21183777 & 0.00000000 & 0.00000000 \\
2.82525396 & 6.50704002 & -0.28266105 & 0.00000000 \\
0.00000000 & 0.00000000 & 0.00000000 & 0.00000000 \\
-11.93627167 & -2.64174724 & 30.52137756 & 16.14870834 \\
-10.11035824 & -3.23091602 & 24.83094406 & 5.32667589 \\
0.00000000 & 0.00000000 & 0.00000000 & 0.00000000 \\
0.07286785 & 3.44696188 & 0.50719333 & -9.53752995
\end{bmatrix}$$

-1.524
-1.057 ± j 1.263
-0.132
-0.121 ± j 0.990
-0.011 ± j 0.138

Helicopter : Puma

Forward Velocity : 100 Kts

Descent Angle : 6 Deg

$$A_{14} = \begin{bmatrix}
-0.01631648 & 0.00571524 & -19.84015083 & -32.16172409 & -0.00016936 & -0.01940120 & 0.00000000 & 0.00000000 & 0.00000000 & 30.03127289 & 0.00000000 & 0.00000000 & 0.00000000 & 0.00000000 \\
-0.04997206 & -0.85787296 & 167.19764709 & 1.26489007 & 0.02257889 & 2.58649659 & -0.01686037 & 0.00000000 & 0.00000000 & 0.00000000 & 0.00000000 & 0.00000000 & 0.00000000 & 0.00000000 \\
-0.00133253 & -0.00772619 & -0.33023661 & 0.00000000 & 0.00004985 & 0.00571076 & 0.00000000 & 0.00000000 & 0.00000000 & -6.15800095 & 0.00000000 & 0.00000000 & 0.00000000 & 0.00000000 \\
0.00000000 & 0.00000000 & 0.99999988 & 0.00000000 & 0.00000000 & 0.00000000 & 0.00000000 & -0.00052430 & 0.00000000 & 0.00000000 & 0.00000000 & 0.00000000 & 0.00000000 & 0.00000000 \\
-0.00003701 & 0.00010684 & -0.00017442 & 0.00066889 & -0.14685415 & 19.65034866 & 32.16171265 & -166.65034485 & 0.00003798 & 0.00000118 & 30.03128433 & -0.00000024 & -0.00000024 & -0.00000024 \\
-0.00021181 & -0.00641123 & 0.00079431 & 0.00000000 & -0.01265906 & -0.06583156 & 0.00000000 & 0.35498464 & 0.00001256 & 1.03877127 & 24.59629631 & -0.00000012 & -0.00000012 & -0.00000012 \\
0.00000000 & 0.00000000 & -0.00002062 & 0.00000000 & 0.00000000 & 1.00000000 & 0.00000000 & -0.03932944 & 0.00000000 & 0.00000000 & 0.00000000 & 0.00000000 & 0.00000000 & 0.00000000 \\
0.00074461 & 0.02327895 & -0.00299109 & 0.00000000 & 0.00704741 & 0.10773164 & 0.00000000 & -0.63744408 & -0.00002242 & -3.74277830 & 0.67541784 & 0.00000000 & 0.00000000 & 0.00000000 \\
0.00000000 & 0.00000000 & 0.00000000 & 0.00000000 & 0.00000000 & 0.00000000 & 0.00000000 & 0.00000000 & 0.00000000 & 0.00000000 & 0.00000000 & 1.00000000 & 0.00000000 & 0.00000000 \\
0.00000000 & 0.00000000 & 0.00000000 & 0.00000000 & 0.00000000 & 0.00000000 & 0.00000000 & 0.00000000 & 0.00000000 & 0.00000000 & 0.00000000 & 0.00000000 & 1.00000000 & 0.00000000 \\
0.00000000 & 0.00000000 & 0.00000000 & 0.00000000 & 0.00000000 & 0.00000000 & 0.00000000 & 0.00000000 & 0.00000000 & 0.00000000 & 0.00000000 & 0.00000000 & 0.00000000 & 1.00000000 \\
0.02476959 & 1.36924291 & -0.05702972 & 0.00000000 & -0.03964233 & -4.54162598 & 0.00000000 & 0.00000000 & -766.61608887 & 0.00000000 & 0.00000000 & -31.63739777 & 0.00000000 & -5.36117601 \\
-0.04932280 & -0.29714519 & 31.95960045 & 0.00000000 & -0.20006856 & -54.64207458 & 0.00000000 & 0.00000000 & -289.48175049 & -37.61634827 & -881.80218506 & 0.00000000 & -31.63739777 & -53.99999619 \\
0.20001678 & 0.53873175 & -55.36876678 & 0.00000000 & -0.17440414 & -32.45201111 & 0.00000000 & 0.00000000 & 0.00000000 & 826.61669922 & -37.61672974 & -10.72154713 & 53.99999619 & -31.63739777
\end{bmatrix}$$

$$B_{14} = \begin{bmatrix}
2.82773519 & 0.98299062 & 0.00000000 & 0.00000000 \\
-376.98870850 & -131.04977417 & 0.00000000 & 0.00000000 \\
-0.83234870 & -0.28934348 & 0.00000000 & 0.00000000 \\
0.00000000 & 0.00000000 & 0.00000000 & 0.00000000 \\
0.05383839 & 0.01873306 & 0.00000000 & 16.14733505 \\
-0.10614724 & -0.03689984 & 0.00000000 & 5.32622290 \\
0.00000000 & 0.00000000 & 0.00000000 & 0.00000000 \\
0.47014377 & 0.16344531 & 0.00000000 & -9.53671837 \\
0.00000000 & 0.00000000 & 0.00000000 & 0.00000000 \\
0.00000000 & 0.00000000 & 0.00000000 & 0.00000000 \\
0.00000000 & 0.00000000 & 0.00000000 & 0.00000000 \\
738.50787354 & 230.07965088 & 0.00000000 & 0.00000000 \\
-120.13216400 & -41.75863266 & 881.80218506 & 0.00000000 \\
513.83093262 & 914.34020996 & 0.00000000 & 0.00000000
\end{bmatrix}$$

-15.758 ± j21.926
-15.394 ± j 5.900
-15.330 ± j49.044
-1.405
-1.092 ± j 1.335
-0.145 ± j 0.928
-0.112
-0.007 ± j 0.093

$$A_{8} = \begin{bmatrix}
-0.02365836 & -0.01507866 & -17.78303528 & -32.16172409 & 0.00587561 & 1.07546067 & 0.00000000 & 0.00000000 \\
-0.04997206 & -0.85787296 & 167.19764709 & 1.26489007 & 0.02257889 & 2.58649659 & -0.01686037 & 0.00000000 \\
0.00017303 & -0.00346236 & -0.75205469 & 0.00000000 & -0.00118960 & -0.21879649 & 0.00000000 & 0.00000000 \\
0.00000000 & 0.00000000 & 0.99999988 & 0.00000000 & 0.00000000 & 0.00000000 & 0.00000000 & -0.00052430 \\
-0.00174489 & -0.02672628 & 1.00140142 & 0.00066889 & -0.15342303 & 17.80344391 & 32.16171265 & -166.65034485 \\
-0.00186409 & -0.02911187 & 0.89226067 & 0.00000000 & -0.01782989 & -1.54064786 & 0.00000000 & 0.35498464 \\
0.00000000 & 0.00000000 & -0.00002062 & 0.00000000 & 0.00000000 & 1.00000000 & 0.00000000 & -0.03932944 \\
0.00162109 & 0.02526774 & -0.23684067 & 0.00000000 & 0.00614672 & -0.07025622 & 0.00000000 & -0.63744402
\end{bmatrix}$$

$$B_{8} = \begin{bmatrix}
-16.41568565 & -32.36833191 & 1.36398697 & 0.00000000 \\
-376.98870850 & -131.04977417 & 0.00000000 & 0.00000000 \\
3.11398625 & 6.54958200 & -0.27968821 & 0.00000000 \\
0.00000000 & 0.00000000 & 0.00000000 & 0.00000000 \\
-12.72457027 & -2.94353247 & 29.94178391 & 16.14733505 \\
-11.23349857 & -3.61516333 & 24.57017326 & 5.32622337 \\
0.00000000 & 0.00000000 & 0.00000000 & 0.00000000 \\
2.58115983 & 4.25341320 & 0.50341368 & -9.53671837
\end{bmatrix}$$

-1.493
-1.034 ± j 1.221
-0.138 ± j 0.938
-0.112
-0.008 ± j 0.093

Helicopter : Puma

Forward Velocity : 100 Kts

Descent Angle : 9 Deg

$$A_{14} = \begin{bmatrix}
-0.01761611 & 0.02780691 & 4.05537939 & -32.17895126 & -0.00113253 & -0.10224618 & 0.00000000 & 0.00000000 & 0.00000000 & 31.79409981 & 0.00000000 & 0.00000000 & 0.00000000 & 0.00000000 \\
-0.02543445 & -0.88017035 & 184.97813416 & 0.70064735 & 0.03257989 & 2.94136143 & -0.90661925 & 0.00000000 & 0.00000000 & 0.00000000 & 0.00000000 & 0.00000000 & 0.00000000 & 0.00000000 \\
-0.00017862 & -0.01318067 & -0.39462322 & 0.00000000 & 0.00017162 & 0.01549430 & 0.00000000 & 0.00000000 & 0.00000000 & -6.35586882 & 0.00000000 & 0.00000000 & 0.00000000 & 0.00000000 \\
0.00000000 & 0.00000000 & 0.99960303 & 0.00000000 & 0.00000000 & 0.00000000 & 0.00000000 & -0.02817401 & 0.00000000 & 0.00000000 & 0.00000000 & 0.00000000 & 0.00000000 & 0.00000000 \\
-0.00207423 & 0.00592207 & 0.00070579 & 0.01954387 & -0.15837127 & -4.27033567 & 32.16609955 & -184.65382385 & 0.00107944 & 0.00002265 & 31.79409218 & 0.00000000 & 0.00000000 & 0.00000000 \\
-0.00053766 & 0.00050890 & -0.00093447 & 0.00000000 & -0.01304215 & -0.09303518 & 0.00000000 & 0.35910943 & 0.00035588 & 1.20309663 & 25.38661385 & 0.00000000 & 0.00000000 & 0.00000000 \\
0.00000000 & 0.00000000 & -0.00061372 & 0.00000000 & 0.00000000 & 1.00000000 & 0.00000000 & -0.02177452 & 0.00000000 & 0.00000000 & 0.00000000 & 0.00000000 & 0.00000000 & 0.00000000 \\
0.00084428 & 0.00775740 & 0.00325425 & 0.00000000 & 0.00632362 & 0.16925350 & 0.00000000 & -0.64498675 & -0.00063554 & -4.33484840 & 0.69712299 & 0.00000000 & 0.00000000 & 0.00000000 \\
0.00000000 & 0.00000000 & 0.00000000 & 0.00000000 & 0.00000000 & 0.00000000 & 0.00000000 & 0.00000000 & 0.00000000 & 0.00000000 & 0.00000000 & 1.00000000 & 0.00000000 & 0.00000000 \\
0.00000000 & 0.00000000 & 0.00000000 & 0.00000000 & 0.00000000 & 0.00000000 & 0.00000000 & 0.00000000 & 0.00000000 & 0.00000000 & 0.00000000 & 0.00000000 & 1.00000000 & 0.00000000 \\
0.00000000 & 0.00000000 & 0.00000000 & 0.00000000 & 0.00000000 & 0.00000000 & 0.00000000 & 0.00000000 & 0.00000000 & 0.00000000 & 0.00000000 & 0.00000000 & 0.00000000 & 1.00000000 \\
-0.02039108 & 1.38679576 & 0.26382446 & 0.00000000 & -0.05720101 & -5.16456604 & 0.00000000 & 0.00000000 & -766.61608887 & 0.00000000 & 0.00000000 & -31.63739777 & 0.00000000 & -5.86496449 \\
-0.07916508 & -0.25820485 & 32.17538834 & 0.00000000 & -0.32528323 & -55.61702728 & 0.00000000 & 0.00000000 & -316.68395996 & -37.61653900 & -887.23144531 & 0.00000000 & -31.63739777 & -53.99999619 \\
0.28308144 & 0.60395014 & -55.95077515 & 0.00000000 & -0.18415527 & -32.47936249 & 0.00000000 & 0.00000000 & 0.00000000 & 821.18798828 & -37.61634827 & -11.72904778 & 53.99999619 & -31.63739777
\end{bmatrix}$$

$$B_{14} = \begin{bmatrix}
13.61432552 & 5.08859158 & 0.00000000 & 0.00000000 \\
-391.64660645 & -146.38473511 & 0.00000000 & 0.00000000 \\
-2.06309915 & -0.77111953 & 0.00000000 & 0.00000000 \\
0.00000000 & 0.00000000 & 0.00000000 & 0.00000000 \\
2.90097070 & 1.08505416 & 0.00000000 & 16.71898651 \\
3.45408869 & 1.29128957 & 0.00000000 & 5.51478052 \\
0.00000000 & 0.00000000 & 0.00000000 & 0.00000000 \\
-7.72130537 & -2.88645172 & 0.00000000 & -9.87434101 \\
0.00000000 & 0.00000000 & 0.00000000 & 0.00000000 \\
0.00000000 & 0.00000000 & 0.00000000 & 0.00000000 \\
0.00000000 & 0.00000000 & 0.00000000 & 0.00000000 \\
760.61022949 & 257.01333618 & 0.00000000 & 0.00000000 \\
-98.84986877 & -36.94725037 & 887.23187256 & 0.00000000 \\
566.80529785 & 928.38671875 & 0.00000000 & 0.00000000
\end{bmatrix}$$

-15.728 ± j21.763
-15.451 ± j 6.063
-15.251 ± j48.971
-1.598
-1.142 ± j 1.484
-0.187
-0.079 ± j 0.984
-0.008 ± j 0.166

$$A_{8} = \begin{bmatrix}
-0.02866981 & 0.00310665 & 6.26996326 & -32.17895126 & 0.00550245 & 1.06526041 & 0.00000000 & 0.00000000 \\
-0.02543445 & -0.88017035 & 184.97813416 & 0.70064735 & 0.03257989 & 2.94136143 & -0.90661925 & 0.00000000 \\
0.00203109 & -0.00824299 & -0.83733410 & 0.00000000 & -0.00115464 & -0.21790099 & 0.00000000 & 0.00000000 \\
0.00000000 & 0.00000000 & 0.99960303 & 0.00000000 & 0.00000000 & 0.00000000 & 0.00000000 & -0.02817401 \\
-0.00418445 & -0.02289436 & 1.05621886 & 0.01954387 & -0.16945724 & -6.23273420 & 32.16609955 & -184.65382385 \\
-0.00264034 & -0.02340820 & 0.92565840 & 0.00000000 & -0.02164299 & -1.61583531 & 0.00000000 & 0.35910943 \\
0.00000000 & 0.00000000 & -0.00061372 & 0.00000000 & 0.00000000 & 1.00000000 & 0.00000000 & -0.02177452 \\
0.00230480 & 0.01049494 & -0.27553862 & 0.00000000 & 0.00517705 & -0.03294689 & 0.00000000 & -0.64498675
\end{bmatrix}$$

$$B_{8} = \begin{bmatrix}
-8.95990944 & -31.01918602 & 1.45358789 & 0.00000000 \\
-391.64660645 & -146.38473511 & 0.00000000 & 0.00000000 \\
2.45001841 & 6.44722033 & -0.29058224 & 0.00000000 \\
0.00000000 & 0.00000000 & 0.00000000 & 0.00000000 \\
-10.96704483 & -2.52158213 & 31.68495750 & 16.71898651 \\
-8.46504498 & -2.95167542 & 25.35447693 & 5.51478052 \\
0.00000000 & 0.00000000 & 0.00000000 & 0.00000000 \\
-4.94735336 & 1.95751595 & 0.49654326 & -9.87434101
\end{bmatrix}$$

-1.656
-1.080 ± j 1.377
-0.188
-0.078 ± j 0.995
-0.009 ± j 0.166

Helicopter : Puma

Forward Velocity : 110 Kts

Descent Angle : 0 Deg

$$A_{14} = \begin{bmatrix}
-0.01549776 & 0.02247291 & 4.03682423 & -32.18022537 & -0.00096780 & -0.08980493 & 0.00000000 & 0.00000000 & 0.00000000 & 31.77906799 & 0.00000000 & 0.00000000 & 0.00000000 & 0.00000000 \\
-0.02388155 & -0.73145300 & 201.97067261 & 0.63961732 & 0.02846612 & 2.64140630 & -0.90115386 & 0.00000000 & 0.00000000 & 0.00000000 & 0.00000000 & 0.00000000 & 0.00000000 & 0.00000000 \\
-0.00018378 & -0.01118133 & -0.34432584 & 0.00000000 & 0.00014504 & 0.01345892 & 0.00000000 & 0.00000000 & 0.00000000 & -6.29444742 & 0.00000000 & 0.00000000 & 0.00000000 & 0.00000000 \\
0.00000000 & 0.00000000 & 0.99960780 & 0.00000000 & 0.00000000 & 0.00000000 & 0.00000000 & -0.02800356 & 0.00000000 & 0.00000000 & 0.00000000 & 0.00000000 & 0.00000000 & 0.00000000 \\
-0.00192720 & 0.00481475 & 0.00052204 & 0.01776092 & -0.13767965 & -4.21457148 & 32.16754913 & -201.74603271 & 0.00066023 & 0.00002303 & 31.77906799 & -0.00000768 & -0.00000768 & -0.00000768 \\
-0.00031860 & 0.00173769 & -0.00021510 & 0.00000000 & -0.00974271 & -0.04524849 & 0.00000000 & 0.17183030 & 0.00012739 & 0.21914041 & 25.73353386 & -0.00000276 & -0.00000276 & -0.00000276 \\
0.00000000 & 0.00000000 & -0.00055684 & 0.00000000 & 0.00000000 & 1.00000000 & 0.00000000 & -0.01987673 & 0.00000000 & 0.00000000 & 0.00000000 & 0.00000000 & 0.00000000 & 0.00000000 \\
0.00076053 & 0.00916443 & 0.00307683 & 0.00000000 & 0.00337196 & 0.14229254 & 0.00000000 & -0.50659573 & -0.00037591 & -4.63255072 & 2.56175542 & 0.00000461 & 0.00000461 & 0.00000461 \\
0.00000000 & 0.00000000 & 0.00000000 & 0.00000000 & 0.00000000 & 0.00000000 & 0.00000000 & 0.00000000 & 0.00000000 & 0.00000000 & 0.00000000 & 1.00000000 & 0.00000000 & 0.00000000 \\
0.00000000 & 0.00000000 & 0.00000000 & 0.00000000 & 0.00000000 & 0.00000000 & 0.00000000 & 0.00000000 & 0.00000000 & 0.00000000 & 0.00000000 & 0.00000000 & 1.00000000 & 0.00000000 \\
0.00000000 & 0.00000000 & 0.00000000 & 0.00000000 & 0.00000000 & 0.00000000 & 0.00000000 & 0.00000000 & 0.00000000 & 0.00000000 & 0.00000000 & 0.00000000 & 0.00000000 & 1.00000000 \\
-0.02102470 & 1.12421644 & 0.24562836 & 0.00000000 & -0.04913940 & -4.56016541 & 0.00000000 & 0.00000000 & -766.61608887 & 0.00000000 & -25.25674438 & 0.00000000 & -5.10881472 & \\
-0.05986824 & -0.19608727 & 25.66349030 & 0.00000000 & -0.31729907 & -55.69044113 & 0.00000000 & 0.00000000 & -275.85525513 & -37.61634827 & -713.31805420 & 0.00000000 & -25.25674438 & -53.99999619 \\
0.26704368 & 0.53585112 & -55.84320068 & 0.00000000 & -0.14905700 & -25.90339661 & 0.00000000 & 0.00000000 & 0.00000000 & 650.54626465 & -37.61634827 & -10.21686268 & 53.99999619 & -25.25674438
\end{bmatrix}$$

$$B_{14} = \begin{bmatrix}
11.20167255 & 4.47968292 & 0.00000000 & 0.00000000 \\
-329.47296143 & -131.76028442 & 0.00000000 & 0.00000000 \\
-1.67877603 & -0.67136234 & 0.00000000 & 0.00000000 \\
0.00000000 & 0.00000000 & 0.00000000 & 0.00000000 \\
2.40408468 & 0.96209145 & -0.00000768 & 14.01264191 \\
1.41788626 & 0.56715930 & -0.00000276 & 2.70894551 \\
0.00000000 & 0.00000000 & 0.00000000 & 0.00000000 \\
-6.92474127 & -2.76968431 & 0.00000461 & -7.94036913 \\
0.00000000 & 0.00000000 & 0.00000000 & 0.00000000 \\
0.00000000 & 0.00000000 & 0.00000000 & 0.00000000 \\
0.00000000 & 0.00000000 & 0.00000000 & 0.00000000 \\
623.69500732 & 227.46086121 & 0.00000000 & 0.00000000 \\
-74.85752106 & -29.93698120 & 713.31829834 & 0.00000000 \\
496.65985107 & 754.06536865 & 0.00000000 & 0.00000000
\end{bmatrix}$$

-12.593 ± j24.133
-12.295 ± j50.983
-11.564 ± j 3.811
-2.276
-1.147 ± j 1.266
-0.162
-0.007 ± j 0.172
0.050 ± j 0.875

$$A_{8} = \begin{bmatrix}
-0.02863670 & -0.00516640 & 6.82214117 & -32.18022537 & 0.00553860 & 1.03299379 & 0.00000000 & 0.00000000 \\
-0.02388155 & -0.73145300 & 201.97067261 & 0.63961732 & 0.02846612 & 2.64140630 & -0.90115386 & 0.00000000 \\
0.00241860 & -0.00570684 & -0.89601099 & 0.00000000 & -0.00114358 & -0.20893544 & 0.00000000 & 0.00000000 \\
0.00000000 & 0.00000000 & 0.99960780 & 0.00000000 & 0.00000000 & 0.00000000 & 0.00000000 & -0.02800356 \\
-0.00362479 & -0.02057191 & 0.99345922 & 0.01776092 & -0.15135656 & -6.67746544 & 32.16755295 & -201.74603271 \\
-0.00178317 & -0.01898156 & 0.82303351 & 0.00000000 & -0.02077295 & -2.03195477 & 0.00000000 & 0.17183030 \\
0.00000000 & 0.00000000 & -0.00055684 & 0.00000000 & 0.00000000 & 1.00000000 & 0.00000000 & -0.01987673 \\
0.00253873 & 0.01115078 & -0.32290357 & 0.00000000 & 0.00132276 & -0.21991430 & 0.00000000 & -0.50659573
\end{bmatrix}$$

$$B_{8} = \begin{bmatrix}
-13.74989319 & -32.52979279 & 1.83196592 & 0.00000000 \\
-329.47296143 & -131.76028442 & 0.00000000 & 0.00000000 \\
3.26371074 & 6.65921211 & -0.36285391 & 0.00000000 \\
0.00000000 & 0.00000000 & 0.00000000 & 0.00000000 \\
-9.64319324 & -2.07834625 & 31.61520004 & 14.01264191 \\
-8.49887562 & -2.14573479 & 25.61348534 & 2.70894551 \\
0.00000000 & 0.00000000 & 0.00000000 & 0.00000000 \\
-4.25754404 & 2.38064909 & 2.28149652 & -7.94036913
\end{bmatrix}$$

-2.243
-1.013 ± j 1.183
-0.163
-0.008 ± j 0.172
0.052 ± j 0.885

Helicopter : Puma

Forward Velocity : 120 Kts

Descent Angle : 0 Deg

$$A_{14} = \begin{bmatrix}
-0.01800673 & 0.02616496 & 7.85811329 & -32.16885376 & -0.00122110 & -0.12120879 & 0.00000000 & 0.00000000 & 0.00000000 & 31.90521812 & 0.00000000 & 0.00000000 & 0.00000000 & 0.00000000 \\
-0.02091243 & -0.76182884 & 235.53092957 & 1.06759298 & 0.03161237 & 3.13792276 & -1.06751919 & 0.00000000 & 0.00000000 & 0.00000000 & 0.00000000 & 0.00000000 & 0.00000000 & 0.00000000 \\
-0.00009156 & -0.01289559 & -0.39478603 & 0.00000000 & 0.00017722 & 0.01759177 & 0.00000000 & 0.00000000 & 0.00000000 & -6.30837059 & 0.00000000 & 0.00000000 & 0.00000000 & 0.00000000 \\
0.00000000 & 0.00000000 & 0.99944919 & 0.00000000 & 0.00000000 & 0.00000000 & 0.00000000 & -0.03318526 & 0.00000000 & 0.00000000 & 0.00000000 & 0.00000000 & 0.00000000 & 0.00000000 \\
-0.00208786 & 0.00586994 & 0.00148782 & 0.03520401 & -0.15557104 & -8.04395676 & 32.15089035 & -235.42958069 & 0.00047598 & 0.00003071 & 31.90523911 & 0.00001535 & 0.00001535 & 0.00001535 \\
-0.00033156 & 0.00230579 & -0.00012509 & 0.00000000 & -0.01035939 & -0.04981544 & 0.00000000 & 0.17287180 & 0.00009504 & 0.25628674 & 25.79046440 & 0.00000163 & 0.00000163 & 0.00000163 \\
0.00000000 & 0.00000000 & -0.00110194 & 0.00000000 & 0.00000000 & 1.00000000 & 0.00000000 & -0.03318743 & 0.00000000 & 0.00000000 & 0.00000000 & 0.00000000 & 0.00000000 & 0.00000000 \\
0.00047691 & 0.00705850 & 0.00505017 & 0.00000000 & 0.00121944 & 0.16140744 & 0.00000000 & -0.51008862 & -0.00026753 & -5.41783524 & 2.56740737 & -0.00000951 & -0.00000951 & -0.00000951 \\
0.00000000 & 0.00000000 & 0.00000000 & 0.00000000 & 0.00000000 & 0.00000000 & 0.00000000 & 0.00000000 & 0.00000000 & 0.00000000 & 0.00000000 & 1.00000000 & 0.00000000 & 0.00000000 \\
0.00000000 & 0.00000000 & 0.00000000 & 0.00000000 & 0.00000000 & 0.00000000 & 0.00000000 & 0.00000000 & 0.00000000 & 0.00000000 & 0.00000000 & 0.00000000 & 1.00000000 & 0.00000000 \\
0.00000000 & 0.00000000 & 0.00000000 & 0.00000000 & 0.00000000 & 0.00000000 & 0.00000000 & 0.00000000 & 0.00000000 & 0.00000000 & 0.00000000 & 0.00000000 & 0.00000000 & 1.00000000 \\
-0.03827972 & 1.15294683 & 0.37002563 & 0.00000000 & -0.05457344 & -5.41740417 & 0.00000000 & 0.00000000 & -766.61608887 & 0.00000000 & 0.00000000 & -25.25674438 & 0.00000000 & -5.95121050 \\
-0.06287632 & -0.16905078 & 25.68708420 & 0.00000000 & -0.33522034 & -55.79740524 & 0.00000000 & 0.00000000 & -321.34112549 & -37.61653900 & -724.52185059 & 0.00000000 & -25.25674438 & -53.99999619 \\
0.25131360 & 0.63500863 & -55.72340012 & 0.00000000 & -0.14143506 & -25.76986313 & 0.00000000 & 0.00000000 & 0.00000000 & 639.34234619 & -37.61634827 & -11.90152836 & 53.99999619 & -25.25674438
\end{bmatrix}$$

$$B_{14} = \begin{bmatrix}
13.61344147 & 6.07866478 & 0.00000000 & 0.00000000 \\
-352.43148804 & -157.36683655 & 0.00000000 & 0.00000000 \\
-1.97578299 & -0.88222492 & 0.00000000 & 0.00000000 \\
0.00000000 & 0.00000000 & 0.00000000 & 0.00000000 \\
3.04188871 & 1.35879683 & 0.00001535 & 14.85682774 \\
1.77482498 & 0.79259217 & 0.00000163 & 2.87214589 \\
0.00000000 & 0.00000000 & 0.00000000 & 0.00000000 \\
-8.36071968 & -3.73353148 & -0.00000951 & -8.41873264 \\
0.00000000 & 0.00000000 & 0.00000000 & 0.00000000 \\
0.00000000 & 0.00000000 & 0.00000000 & 0.00000000 \\
0.00000000 & 0.00000000 & 0.00000000 & 0.00000000 \\
655.85900879 & 271.66329956 & 0.00000000 & 0.00000000 \\
-69.44389343 & -31.00795746 & 724.52221680 & 0.00000000 \\
583.72821045 & 783.36621094 & 0.00000000 & 0.00000000
\end{bmatrix}$$

-12.563 ± j23.952
-12.206 ± j50.885
-11.689 ± j 3.880
-2.421
-1.228 ± j 1.464
-0.223
0.005 ± j 0.149
0.173 ± j 0.765

$$A_{8} = \begin{bmatrix}
-0.03063034 & -0.00711106 & 10.69635963 & -32.16885376 & 0.00503557 & 1.02274346 & 0.00000000 & 0.00000000 \\
-0.02091243 & -0.76182884 & 235.53092957 & 1.06759298 & 0.03161237 & 3.13792276 & -1.06751919 & 0.00000000 \\
0.00240433 & -0.00631606 & -0.95596987 & 0.00000000 & -0.00105977 & -0.20859724 & 0.00000000 & 0.00000000 \\
0.00000000 & 0.00000000 & 0.99944919 & 0.00000000 & 0.00000000 & 0.00000000 & 0.00000000 & -0.03318526 \\
-0.00359851 & -0.02127809 & 0.97918063 & 0.03520401 & -0.16961181 & -10.45234585 & 32.15089035 & -235.42958069 \\
-0.00165296 & -0.01985674 & 0.81298488 & 0.00000000 & -0.02166016 & -1.98764491 & 0.00000000 & 0.17287180 \\
0.00000000 & 0.00000000 & -0.00110194 & 0.00000000 & 0.00000000 & 1.00000000 & 0.00000000 & -0.03318743 \\
0.00249862 & 0.01053054 & -0.39823550 & 0.00000000 & -0.00096905 & -0.22664401 & 0.00000000 & -0.51008862
\end{bmatrix}$$

$$B_{8} = \begin{bmatrix}
-16.31096649 & -33.26667023 & 1.87145674 & 0.00000000 \\
-352.43148804 & -157.36683655 & 0.00000000 & 0.00000000 \\
3.94138575 & 6.89742184 & -0.37002876 & 0.00000000 \\
0.00000000 & 0.00000000 & 0.00000000 & 0.00000000 \\
-10.63311481 & -3.00726509 & 31.68354034 & 14.85682774 \\
-9.49658871 & -3.04239154 & 25.62627983 & 2.87214589 \\
0.00000000 & 0.00000000 & 0.00000000 & 0.00000000 \\
-4.37737894 & 2.59738612 & 2.23178101 & -8.41873264
\end{bmatrix}$$

-2.360
-1.089 ± j 1.343
-0.226
0.004 ± j 0.150
0.170 ± j 0.783

Helicopter : Puma

Forward Velocity : 140 Kts

Descent Angle : 0 Deg

$$A_{14} = \begin{bmatrix}
-0.02031604 & 0.03152253 & 12.54224014 & -32.15198898 & -0.00160764 & -0.16638686 & 0.00000000 & 0.00000000 & 0.00000000 & 32.17201233 & 0.00000000 & 0.00000000 & 0.00000000 & 0.00000000 \\
-0.02176830 & -0.78872138 & 269.05908203 & 1.49068010 & 0.03515439 & 3.63837051 & -1.30856752 & 0.00000000 & 0.00000000 & 0.00000000 & 0.00000000 & 0.00000000 & 0.00000000 & 0.00000000 \\
0.00000898 & -0.01472979 & -0.44115406 & 0.00000000 & 0.00022464 & 0.02324945 & 0.00000000 & 0.00000000 & 0.00000000 & -6.33781338 & 0.00000000 & 0.00000000 & 0.00000000 & 0.00000000 \\
0.00000000 & 0.00000000 & 0.99917144 & 0.00000000 & 0.00000000 & 0.00000000 & 0.00000000 & -0.04069930 & 0.00000000 & 0.00000000 & 0.00000000 & 0.00000000 & 0.00000000 & 0.00000000 \\
-0.00237443 & 0.00734242 & 0.00256721 & 0.06067963 & -0.17318256 & -12.73926544 & 32.12516403 & -269.05261230 & 0.00236454 & 0.00003071 & 32.17201233 & 0.00001535 & 0.00001535 & 0.00001535 \\
-0.00035262 & 0.00311383 & -0.00011406 & 0.00000000 & -0.01093297 & -0.05607455 & 0.00000000 & 0.17202824 & 0.00045462 & 0.29485214 & 25.91084862 & 0.00000552 & 0.00000552 & 0.00000552 \\
0.00000000 & 0.00000000 & -0.00188856 & 0.00000000 & 0.00000000 & 1.00000000 & 0.00000000 & -0.04636422 & 0.00000000 & 0.00000000 & 0.00000000 & 0.00000000 & 0.00000000 & 0.00000000 \\
0.00019010 & 0.00381776 & 0.00741017 & 0.00000000 & -0.00103516 & 0.18875514 & 0.00000000 & -0.50806326 & -0.00134394 & -6.23306465 & 2.57939696 & -0.00000923 & -0.00000923 & -0.00000923 \\
0.00000000 & 0.00000000 & 0.00000000 & 0.00000000 & 0.00000000 & 0.00000000 & 0.00000000 & 0.00000000 & 0.00000000 & 0.00000000 & 0.00000000 & 1.00000000 & 0.00000000 & 0.00000000 \\
0.00000000 & 0.00000000 & 0.00000000 & 0.00000000 & 0.00000000 & 0.00000000 & 0.00000000 & 0.00000000 & 0.00000000 & 0.00000000 & 0.00000000 & 0.00000000 & 1.00000000 & 0.00000000 \\
0.00000000 & 0.00000000 & 0.00000000 & 0.00000000 & 0.00000000 & 0.00000000 & 0.00000000 & 0.00000000 & 0.00000000 & 0.00000000 & 0.00000000 & 0.00000000 & 0.00000000 & 1.00000000 \\
-0.05079727 & 1.17544019 & 0.46062469 & 0.00000000 & -0.06068726 & -6.28170013 & 0.00000000 & 0.00000000 & -766.61608887 & 0.00000000 & 0.00000000 & -25.25674438 & 0.00000000 & -6.78992271 \\
-0.06364460 & -0.14813194 & 25.69429398 & 0.00000000 & -0.35724983 & -55.94152451 & 0.00000000 & 0.00000000 & -366.62808228 & -37.61672974 & -737.37225342 & 0.00000000 & -25.25674438 & -53.99999619 \\
0.23137531 & 0.73392487 & -55.57359695 & 0.00000000 & -0.13799191 & -25.66600800 & 0.00000000 & 0.00000000 & 0.00000000 & 626.49176025 & -37.61615753 & -13.57882786 & 53.99999619 & -25.25674438
\end{bmatrix}$$

$$B_{14} = \begin{bmatrix}
17.21317673 & 8.37062550 & 0.00000000 & 0.00000000 \\
-376.40219116 & -183.04119873 & 0.00000000 & 0.00000000 \\
-2.40525889 & -1.16965616 & 0.00000000 & 0.00000000 \\
0.00000000 & 0.00000000 & 0.00000000 & 0.00000000 \\
3.96826649 & 1.93023252 & 0.00001535 & 15.68582249 \\
2.30142665 & 1.11926413 & 0.00000552 & 3.03240657 \\
0.00000000 & 0.00000000 & 0.00000000 & 0.00000000 \\
-10.61664677 & -5.16307831 & -0.00000923 & -8.88848877 \\
0.00000000 & 0.00000000 & 0.00000000 & 0.00000000 \\
0.00000000 & 0.00000000 & 0.00000000 & 0.00000000 \\
0.00000000 & 0.00000000 & 0.00000000 & 0.00000000 \\
688.67419434 & 315.98815918 & 0.00000000 & 0.00000000 \\
-65.07072449 & -31.64367676 & 737.37243652 & 0.00000000 \\
670.29553223 & 817.62103271 & 0.00000000 & 0.00000000
\end{bmatrix}$$

-12.515 ± j23.745
-12.106 ± j50.774
-11.833 ± j 3.910
-2.602
-1.299 ± j 1.637
-0.308
0.019 ± j 0.136
0.310 ± j 0.585

$$A_{8} = \begin{bmatrix}
-0.03226393 & -0.00790352 & 15.45388985 & -32.15198898 & 0.00464261 & 1.00957572 & 0.00000000 & 0.00000000 \\
-0.02176830 & -0.78872138 & 269.05908203 & 1.49068010 & 0.03515439 & 3.63837051 & -1.30856752 & 0.00000000 \\
0.00236259 & -0.00696269 & -1.01474285 & 0.00000000 & -0.00100656 & -0.20841752 & 0.00000000 & 0.00000000 \\
0.00000000 & 0.00000000 & 0.99917144 & 0.00000000 & 0.00000000 & 0.00000000 & 0.00000000 & -0.04069930 \\
-0.00365332 & -0.02189898 & 0.96666396 & 0.06067963 & -0.18773715 & -15.09468460 & 32.12516403 & -269.05261230 \\
-0.00148993 & -0.02071064 & 0.80303079 & 0.00000000 & -0.02260129 & -1.94275844 & 0.00000000 & 0.17202824 \\
0.00000000 & 0.00000000 & -0.00188856 & 0.00000000 & 0.00000000 & 1.00000000 & 0.00000000 & -0.04636422 \\
0.00240201 & 0.00912181 & -0.47940022 & 0.00000000 & -0.00340570 & -0.22791573 & 0.00000000 & -0.50806326
\end{bmatrix}$$

$$B_{8} = \begin{bmatrix}
-18.12552071 & -33.96238327 & 1.92581046 & 0.00000000 \\
-376.40219116 & -183.04119873 & 0.00000000 & 0.00000000 \\
4.55693293 & 7.17012215 & -0.37937745 & 0.00000000 \\
0.00000000 & 0.00000000 & 0.00000000 & 0.00000000 \\
-11.56587315 & -3.94649434 & 31.86038399 & 15.68582249 \\
-10.48793983 & -3.97959542 & 25.67750359 & 3.03240657 \\
0.00000000 & 0.00000000 & 0.00000000 & 0.00000000 \\
-5.01099825 & 2.56961751 & 2.18131685 & -8.88848877
\end{bmatrix}$$

-2.501
-1.146 ± j 1.483
-0.320
0.019 ± j 0.138
0.301 ± j 0.607

Helicopter : Puma

Forward Velocity : 160 Kts

Descent Angle : 0 Deg

APPENDIX 6 – CONTROL INPUTS

This appendix shows the standard control inputs used throughout this thesis. They were obtained from flight data of the Lynx and are shown *trimmed* with a truncated time interval. This is the form in which they were used.

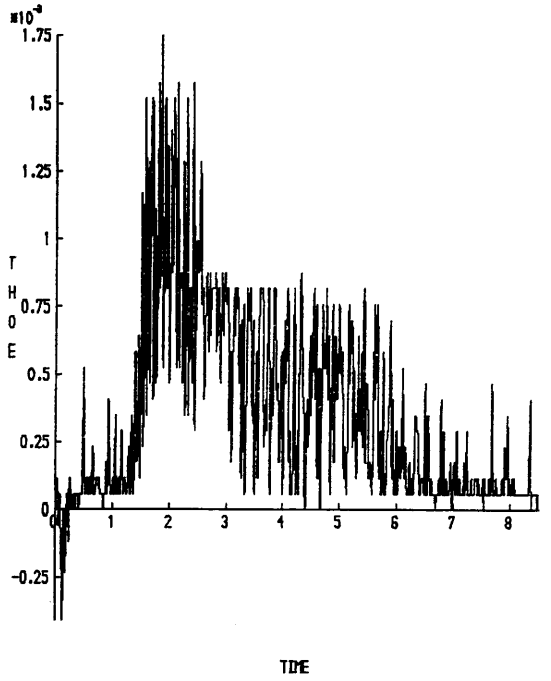

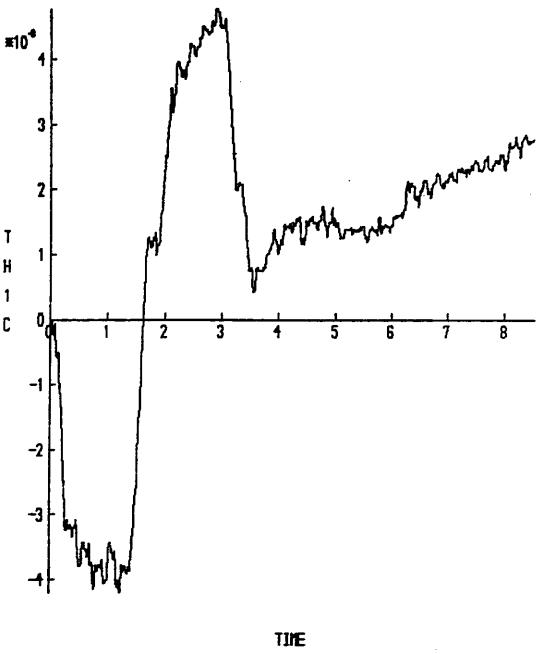

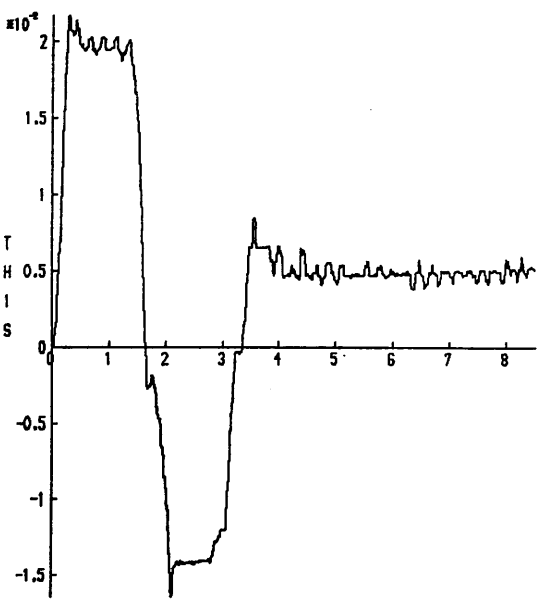

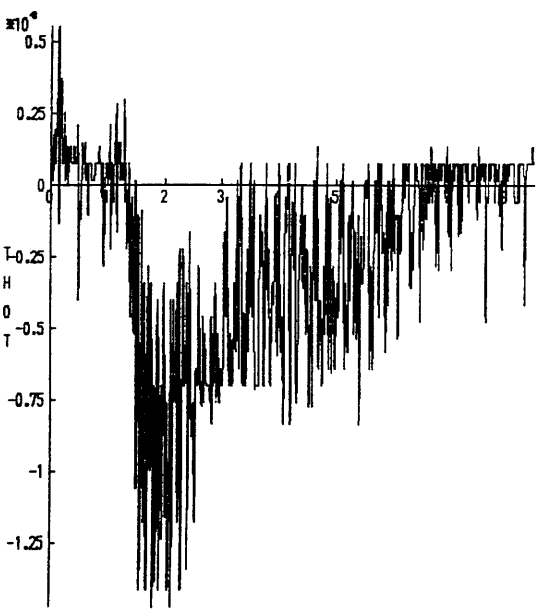

DOUBLET ON θ_{1S}

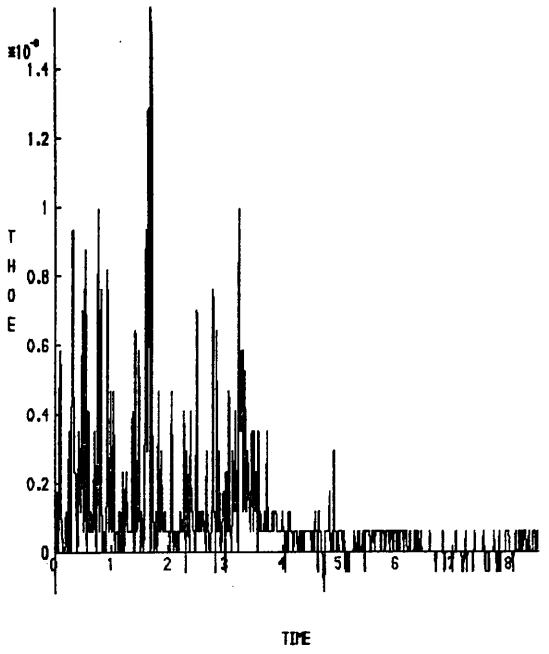

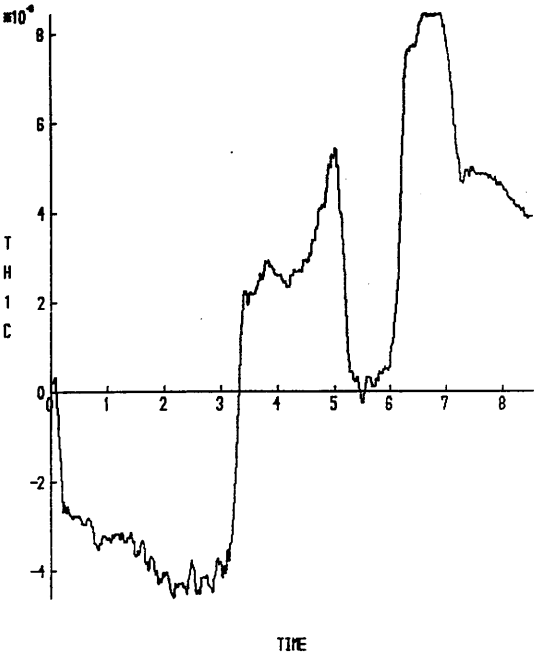

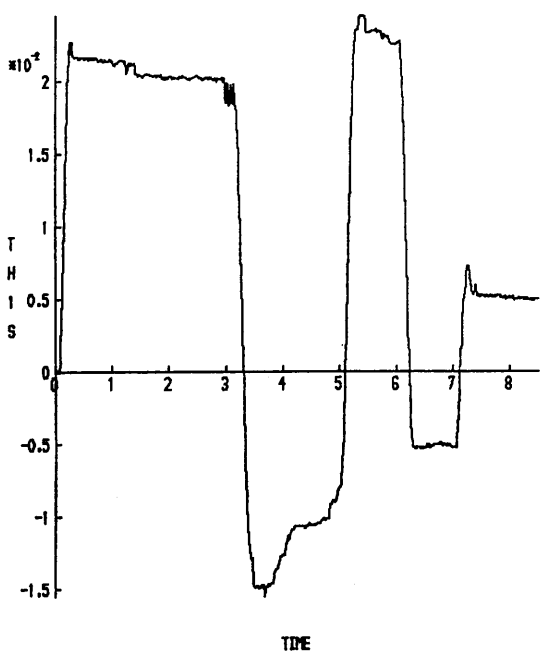

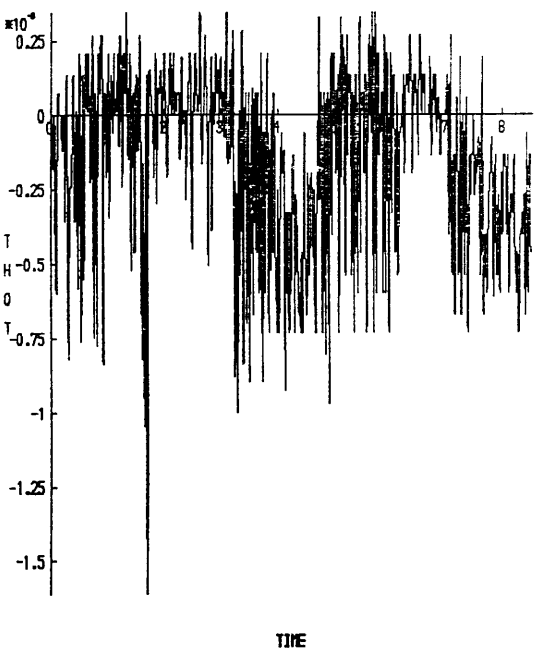

3-2-1-1 ON θ_{1S}

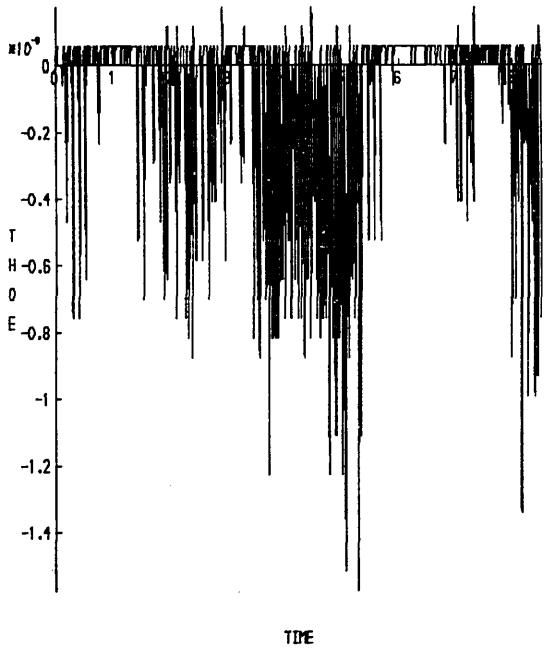

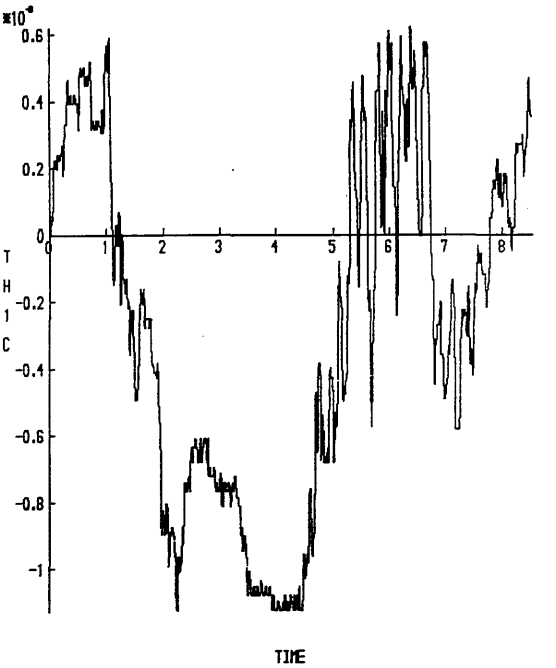

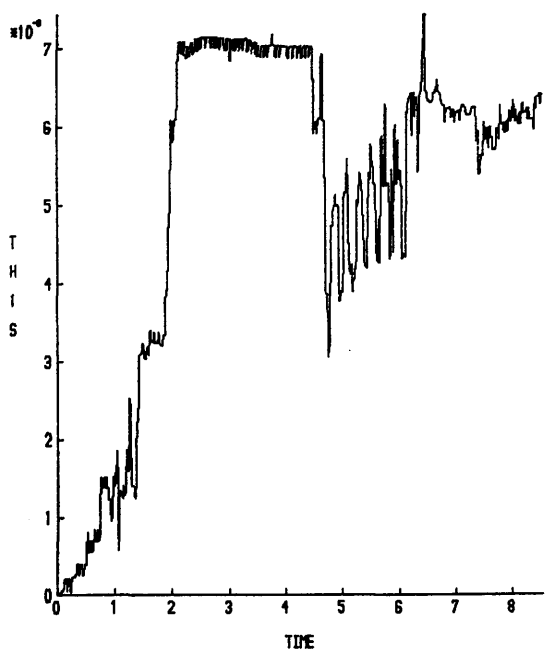

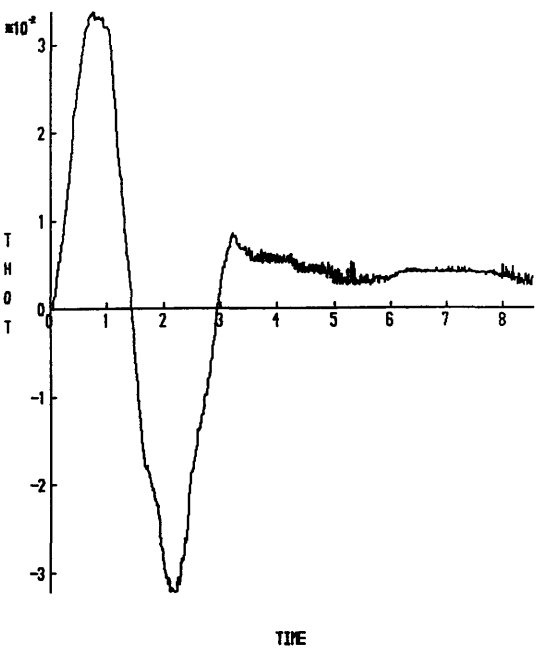

DOUBLET ON θ_{ot}